THE SILICA ISSUE IN THE LIMESTONE RESOURCE AT MCDONALD'S OPARURE LIME QUARRY

A thesis

submitted in partial fulfilment

of the requirements for the Degree

of

Master of Science in Earth and Ocean Sciences

at the

University of Waikato

by

ORLA HANSEN

THE UNIVERSITY OF
WAIKATO
Te Whare Wānanga o Waikato

University of Waikato
2008

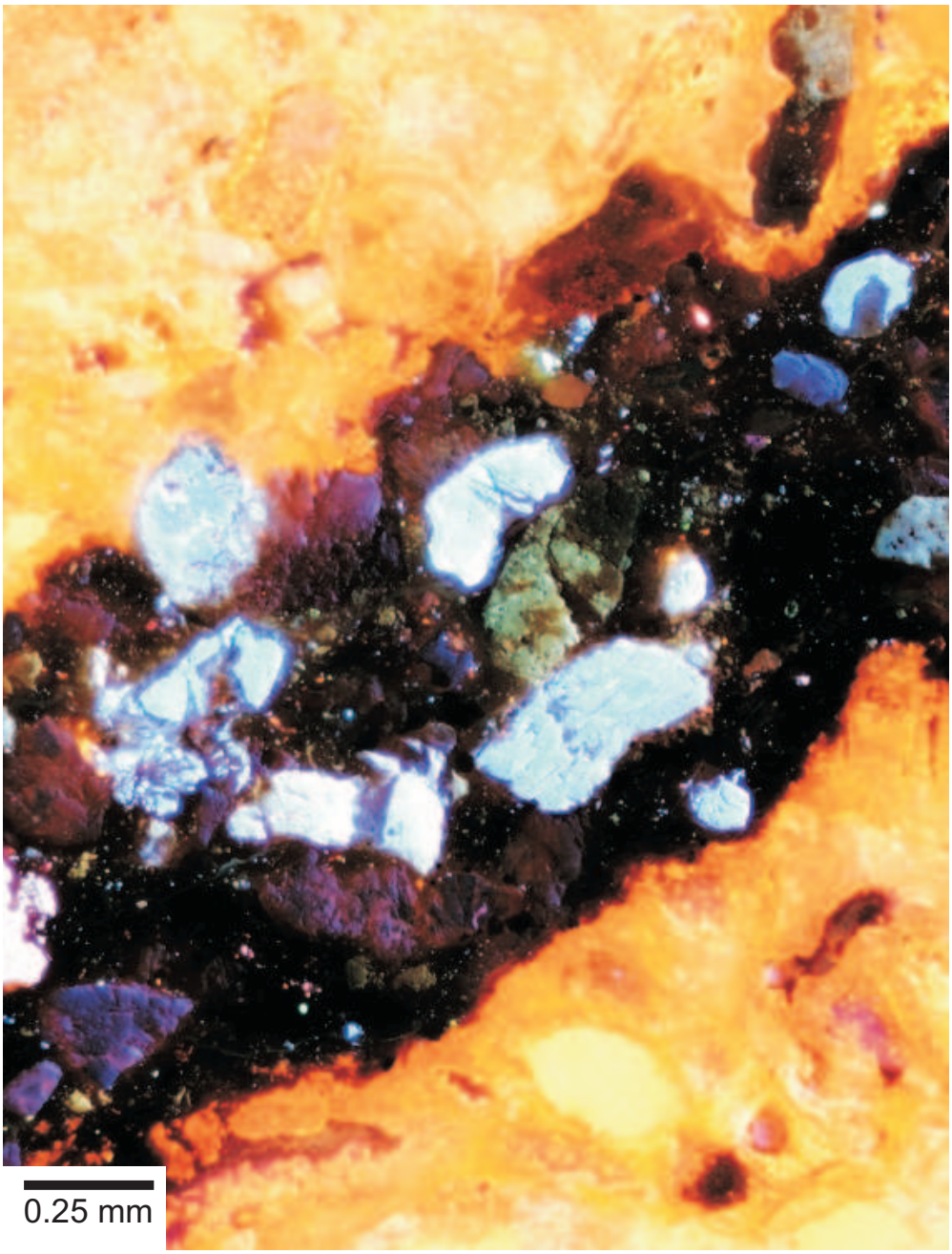

Photomicrograph under cathodoluminescent light (CL) of a silica-rich discrete dissolution seam (central feature) in the Lower Steel unit, McDonald's Oparure Lime Quarry. Silica minerals are blue, green, and black, and carbonate is orange. Refer to Chapter 5, Figure 5.24C for further details.

ABSTRACT

McDonald's Oparure Lime Quarry extracts limestone from the latest Oligocene to earliest Miocene aged Otorohanga Limestone formation of the Te Kuiti Group. The quarry produces a range of limestone grades that are utilised by various industries, including the iron and steel, agricultural, and roading construction industries. One of the most important aspects of production is quality control which is driven by quality restrictions on the chemical composition of the limestones imposed by the industrial end users. In steel manufacture, silica is highly undesirable as it has detrimental effects on downstream processes such as the ability of calcium oxide to remove impurities from the steel and its abrasiveness inside pipes transporting lime into the steel making vessel. A guideline of <1.7% silica content in the lime is required.

McDonald's Lime Ltd and major shareholders Holcim New Zealand Ltd are aware that silica levels vary across the Oparure limestone resource, and so hold some concerns about their ability to maintain quality guidelines on their limestone products. Consequently, it is relevant that knowledge be gained about the nature, distribution, and origin of silica-rich zones within the limestone resource so as to allow for greater certainty in quarry planning and operations.

The main aims of this study were to determine the chemical stratigraphy of the limestone units in the quarry so as to assess primary sources of silica in the intact limestone (host limestone); to use field methods to measure the nature and distribution of a variety of discontinuity features which separate the intact rock blocks within the limestone rock mass; to identify sources of secondary silica-rich materials and their characteristics; and to determine the overall distribution of silica within the limestone resource. Additionally, a ground penetrating radar (GPR) trial was undertaken to establish whether this geophysical technique is successful in detecting subsurface caves that may trap silica-rich materials.

The host limestone or intact rock mass of the quarry units contains variable amounts of calcium carbonate, as follows: Caprock (av. 89.5%), Upper Steel (av. 98.2%), Aglime (av. 94.5%), High Grade (av. 97.2%), Lower Steel (av. 97.3%), and Sub-economic (av. 95%). The remaining non-carbonate component largely resides in silica-bearing minerals such as clay minerals, quartz, feldspar, and glauconite, but also in authigenic minerals such as pyrite and gypsum.

In McDonald's Oparure Lime Quarry six main discontinuity types are identified, all of which are associated with silica-rich materials. The six discontinuity types are: (1) discrete seams; (2) diffuse seams; (3) subhorizontal stylolites; (4) subvertical stylolites; (5) joints; and (6) caves and other karst features. Types (1), (2), and (3) have formed as a result of burial of the carbonate-rich sediments during which pressure dissolution has preferentially dissolved skeletal fragments, leaving behind and concentrating insoluble residue (siliceous material). These are primary sources of silica. Types (4) and (5) are produced as a result of tectonic activity, including deformation and uplift. Subvertical stylolites formed by pressure dissolution associated with tectonic stresses during uplift of the limestones, and their contained silica also derives from a primary source inside the limestone strata. Type (6) discontinuities are produced by dissolution by fresh water of the subaerially exposed limestone. Joints, caves, and other karst features trap silica-rich materials sourced mainly from overlying overburden lithologies, including the Quaternary Kauroa Ash and the early Miocene Mahoenui Group mudstone; these are secondary sources of silica. A distinctive leathery clay mineral called palygorskite occurs commonly as a chemical precipitate in both joints and caves as an infill. A final source of silica identified that is not a discontinuity material, but is operation induced, involves the accumulation of blast and road dust coating rock surfaces, here referred to as surface accumulations.

The overburden units and discontinuity materials show a range of chemical compositions and some, such as cave infills, comprise greater than 60% SiO_2. The main siliceous minerals within overburden units and discontinuity materials are clays (smectite, palygorskite, gibbsite, vermiculite, halloysite, illite), quartz (and minor cristobalite), feldspar (oligoclase), and glauconite. Carbonate minerals including mainly calcite and minor dolomite.

GPR successfully detected cave structures to an effective penetration of about 10 m, but cave infills cannot be quantified using this method.

The knowledge gained in this study about the distribution, location, quantities, and nature of the silica materials in the limestone units, closely related to the different discontinuity types identified, has the potential to assist in determining appropriate processing techniques to minimise the silica issue at the Oparure Quarry.

ACKNOWLEDGEMENTS

I would like to thank the team at Holcim NZ for giving me the opportunity to research such an interesting project. Thanks to John Reeves for his support during the project and for making the time to discuss the project with me. I'd also like to show my gratitude to Bruce Garrick who discussed the silica issue with me and for giving me an extraordinary tour of the Otorohanga Plant. Holcim New Zealand's financial support and enthusiasm towards me has made this thesis a pleasure to work on. Also thanks to AusIMM and the University of Waikato for the scholarships I received from them.

Many thanks to McDonald's Quarry previous manager Chris Pilmer for instigating the project with the University of Waikato; without his involvement this project would have not been possible. Thanks to the current quarry Manager Darcy Maddern for always taking the time to chat with me, and being so helpful. Darcy's friendly personality made my trips to the quarry an enjoyable experience; I always looked forward to visiting onsite. To the other quarry staff members I met, including Dean and Neville, thanks for always acknowledging me and making me feel welcome. Thanks to Julie and Dawn on reception for also being welcoming and very friendly each time I arrived and departed. I had the opportunity to get a tour of the crushing plant. Thanks to Des who gave me a ride in the gigantic dump truck and for showing me around. Thanks to Peter for giving me a tour of the Aglime plant; he did a great job splitting the cores that I worked on!

Thank you to Ormiston Associates Ltd for happily providing me with a host of information including fantastic aerial photos and informative reports that were invaluable to getting my thesis underway. A special thanks to Trisha Simonson who was also responsible for instigating this project, and for always being friendly, encouraging, and helpful. Trisha's wealth of experience has pushed me even more to pursue a career as a geologist in the future. Thanks to Simon Carryer for encouraging the idea of this project to Holcim New Zealand Ltd.

Thanks to Connal Holmes from New Zealand Steel who gave me a fantastic tour of the plant, and some really helpful information. Connal's enthusiasm towards steel manufacturing made the tour an exciting expedition!

My greatest thanks go out to my supervisors Cam Nelson, Vicki Moon, and Steve Hood. Their guidance and support has been indispensable and greatly appreciated during the journey of this project. Cam and Vicki have been a huge part of improving my academic skills, not only during the course of my masters, but also in undergraduate studies. Steve has been a fantastic help in the field and in petrography, and his enthusiasm and 'always there to help' attitude are greatly appreciated.

I'd also like to thank my partner Daniel who became part of my life as I started my research, and for always being encouraging, loving, and a great friend. Thank you to my friends Danielle, Sanja, Alison, Michelle, Rachel, Stacey, Lisa, and Natalie for being supportive, and for being really good friends. Thanks to Kate who pulled me through to the end and worked alongside me. Thanks to my parents Mama and Papa, who have supported me financially throughout my years at university and especially Mama for being an inspiration, and for always being there for me.

Thanks to Jo Russell who kindly provided accommodation when I was core logging day after day. Thank you to the Department of Earth and Ocean Sciences technical support team for all their assistance, Annette Rodgers, Jacinta Parentzee, Renat Radosinsky, Xu Ganqing, and Chris McKinnon. Thanks to Annie Barker from the Department of Chemistry, and Kathleen Dabell from the Waikato Radiocarbon Dating Laboratory, who taught me a thing or two about acid titration. Thank you to Adam Vonk, my neighbour in the adjoining office, who was a wealth of knowledge, and was always happy to help with any issues that came along! Thanks to Spectrachem Analytical for running my samples. And finally thanks to Sydney Wright for office assistance in the course of this study.

TABLE OF CONTENTS

Appendices:

LIST OF FIGURES

LIST OF TABLES

CHAPTER ONE

Introduction

Limestone is a very important industrial mineral resource that can be quarried as a raw material and used in the production of a wide variety of end use products (Siegel, 1967; Naydowski et al., 2001). In 1968 Holcim New Zealand Ltd became the major shareholder of the McDonald's Lime company, who relocated (from Otago Peninsula where it was originally based, followed by moves to Totara, North Otago, and Kakanui near Oamaru) to their current locations in the Waitomo region. McDonald's Lime Ltd operates a limestone quarry in Oparure in the King Country region of western central North Island, New Zealand. The quarry produces a range of limestone qualities, including agricultural (>90%), high grade (>95%), and steel grade (>98%) lime. Stratigraphically, the limestone extracted comes from the Otorohanga Limestone of Waitakian age (25.2-21.7 million years), the topmost formation in the predominantly Oligocene age (33.7-23.8 million years, Cooper; 2004) Te Kuiti Group (Nelson, 1978a).

All the industrial limestone grades are $CaCO_3$ content dependent due to the presence of varying amounts of non-carbonate components. The latter are mainly siliceous minerals, largely insoluble with acid treatment, and are collectively labelled 'silica content' in this study. Throughout this thesis the word silica is synonymous with any of silica-bearing minerals, siliceous materials, insoluble residue, and siliciclasts (non-carbonate grains that have been eroded and transported to a depositional environment), such as quartz, feldspar, glauconite, and clay minerals. All non-carbonate components are also included as part of the 'silica issue' and include non-siliceous minerals such as pyrite (iron sulphide) and gypsum (calcium sulphate).

There are quality guidelines that must be met for each limestone unit including a $CaCO_3$ content of 90%+ for agricultural limestone, >95% for high grade limestone, and >98% for steel grade limestone. The most restricted grade is the steel grade limestone. Steel grade limestone is used in the manufacture of steel in

which the chemical composition (i.e. silica and sulphur) of the limestone must meet strict specifications. Silica in particular is an undesirable element if present at high levels due to the negative effects silica has on certain stages in the steel manufacturing process including mechanical wear caused by the abrasive properties of silica, and its negative effects on quality of the final steel product. It has become apparent to quarry management staff and Ormiston Associates Ltd (consultant geologists) that the limestone resource at McDonald's Oparure Lime Quarry is of variable quality because of variations in the content of silica in the limestone.

This study will show that the silica in the quarry limestone units is mainly in contained discontinuity features that are genetically associated with different periods of limestone evolution, namely:
(1) Diagenetic - discontinuities related to processes of burial and cementation (compaction, pressure-dissolution) of the limestone, such as dissolution seams and subhorizontal stylolites.
(2) Tectonic - discontinuities related to deformation and uplift of the limestone rock mass, such as subvertical stylolites, joints, and faults.
(3) Weathering - discontinuities resulting from dissolution of limestone by percolating fresh rain and ground water, such as runnels, caves, and collapse features.

Silica associated with type (1) discontinuities is inherited from within the host limestone itself, and so the silica minerals can be regarded as of primary origin. In contrast, the silica associated with types (2) and (3) discontinuities is mainly introduced from some external source to the limestone, typically from infiltration of fresh water carrying silica detritals down from overlying mudrock, volcanic ash, and/or soil horizons, or precipitating minerals *in situ*, and so the silica minerals can be regarded as secondary in origin.

Since it is crucial that the limestones follow quality guidelines, it is essential that the zones of high silica be identified and more knowledge gained about their distribution and origin to allow for greater certainty in quarry planning and operations.

1.1 Background

McDonald's Lime Quarry is located on Oparure Road near Oparure, about 6 km west of Te Kuiti (Figure 1.1). The quarry sits within a 67 hectare property, currently the largest single limestone quarry in the North Island, and has been operating since 1981 after initial exploratory drilling programmes in 1977 and 1981. A number of drilling programmes have been undertaken since the late 1970s to characterise the geology of the limestone deposit and to identify features such as fault patterns and displacements within the quarry, including the use of percussion, reverse circulation, and continuous drilling methods (Simonson, 2005). A series of four drilling programmes have been undertaken since the year 2000 and are named the 200, 300, 400, and 500 drill hole series. Chipped limestone samples and cores from drill holes have aided in determining the chemical composition of the deposit.

In June and July of 2005 Holcim New Zealand Ltd instigated the most recent drilling programme consisting of five continuous cores, 64.1 mm in diameter, collectively known as the 500 drill hole series. The drilling programme was undertaken to provide data on the potential for achieving expected quality restrictions for each limestone grade. Detailed logging was carried out by Ormiston Associates Ltd, including core descriptions, major element chemistry, and rock mass characteristics such as core recovery and defect (discontinuity) spacing on the 500 drill hole series. All five cores were sawn into two halves; one half was powdered for X-ray fluorescence (XRF) analysis of chemical composition, and the other half archived and stored inside two large shipping containers located on the quarry site.

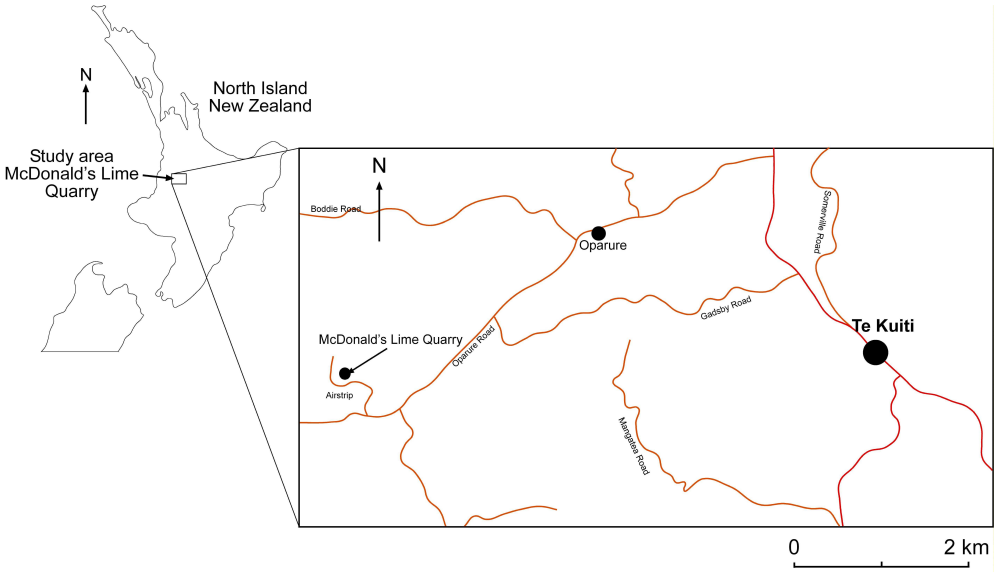

Figure 1.1 Location map of study area (McDonald's Lime Quarry), main roads and townships.

1.2 The silica issue

Due to concerns expressed by McDonald's Lime Ltd about the varied silica content in the Oparure deposit and their ability to maintain the required quality restrictions for the various lime markets, an investigation was carried out in 2005 to monitor the changes in silica content from drill hole material to the crushed product. These particular drill holes, known as 'shots', are drilled within the main quarry and produce pulverised rock unlike the continuous cores drilled from previous drilling programmes. A number of drill holes such as these are routinely drilled to either provide chemical composition information on the areas currently being extracted or used as an entry point for explosives to be inserted for blasting. The investigation involved measuring the silica content in raw materials sampled directly from drill hole shots, and materials sampled subsequent to blasting that were then crushed and fed to a kiln. Results from XRF analyses carried out on these rock samples indicated differences in silica percentages between samples from the drill hole, the blasted rock entering the kilns, and the finished lime product. This experimental work demonstrated that the silica content became reduced on average by 0.51% due to blasting, extracting, and crushing processes. The method used and results of this experiment are recorded in Appendix A-1.1.

1.3 Aims

The main aim of this research is to identify the nature, distribution, and origin of silica material within the limestone at McDonald's Oparure Lime Quarry, especially areas where the silica occurs in high concentrations. A secondary aim is to comment on any possible separation techniques for reducing the silica content in the crushed limestone. To achieve these aims, the following objectives are defined:

1. Determine the overall distribution of silica-bearing minerals within the four main quarry limestone units.

2. Measure the nature and distribution of discontinuities within the limestones and describe rock mass features.

3. Determine the mineralogical and chemical composition of the limestones to assess primary sources of silica.

4. Identify potential secondary sources of silica materials within discontinuities and determine their textural, mineralogical, and chemical composition.

5. Trial ground penetrating radar as a tool for identifying limestone cavities suspected of containing secondary sources of silica.

1.4 Study outline

Field work was largely based at the quarry and involved outcrop descriptions and measurements to describe rock mass characteristics so as to provide quantitative data on discontinuities. Sampling of limestones and materials containing silica was undertaken for analysis of chemical and mineral composition. Detailed descriptions of several drilled cores were carried out in two large ship containers located at the quarry followed by intensive sampling of one core to be used as a reference core for subsequent detailed chemical and mineral analysis.

1.5 Thesis structure

This thesis is divided into eight chapters followed by references and appendices. A sample catalogue is given in Appendix A-1.2.

Chapter 1 - Introduction: Briefly introduces the silica issue and the importance of the steel grade limestone to meet strict carbonate content specifications. It also covers background information about the quarry operation, study intentions, and main aims of the study.

Chapter 2 - Literature review: A literature review which covers the following:

(a) Geological history of the Te Kuiti district and wider King Country region
(b) Cenozoic limestones in New Zealand
(c) Economic importance of limestones worldwide and in New Zealand
(d) Site description and stratigraphy of McDonald's Lime Quarry, and end uses of their limestone products
(e) The role of lime in the steel manufacturing process and the silica issue.

Chapter 3 - Discontinuities in outcrop: Introduces the various discontinuity features in the quarry limestone units, how they are associated with siliceous materials, and discusses the characteristics and formation of these discontinuity types. Results are also presented for rock mass features such as joint spacing and joint infills for each of the exposed limestone units.

Chapter 4 – Discontinuities in cores: Describes discontinuities in continuously drilled limestone cores from the 500 series and presents results from detailed logging of three of these cores. This chapter especially focuses on the identification and description of discontinuity types in the cores since they commonly contain high concentrations of siliceous impurities. The frequency and total thickness for some of these discontinuities is also quantified.

Chapter 5 – Petrographic, mineral, and textural characteristics: This chapter covers the following:

(a) An introduction to carbonate rock terminology and limestone classification

(b) Results from detailed petrographic (microscopic) descriptions of quarry limestone units and of the siliceous materials occurring in some discontinuities
(c) Determination of the mineral composition for each of the quarry limestone units, discontinuity materials, and overburden units
(d) Determination of the textural characteristics for each of the quarry limestone units, discontinuity materials, and overburden units.

Chapter 6 – Chemical composition: Describes the chemical composition (e.g. $CaCO_3$ content) of the quarry limestone units, overburden units, and the siliceous materials contained in discontinuities. The differences between the composition of limestone units and discontinuity materials are also highlighted which involves comparing the composition of limestone excluding discontinuity materials versus limestone including discontinuity materials (bulk composition).

Chapter 7 – Ground penetrating radar: Briefly describes the ground penetrating radar (GPR) technique, the application of GPR in carbonate environments, and presents results from a trial undertaken in McDonald's Oparure Lime quarry. Recommendations are also given for future GPR studies.

Chapter 8 – Summary, conclusions, and recommendations: Summarises key points from each chapter, concludes the thesis, and offers some recommendations for future work.

CHAPTER TWO

Literature review

2.1 Introduction

This chapter summarises some relevant background information for this study. The material covered includes a general geological history of the wider King Country region and more specific geological information for the Te Kuiti district; some comments about New Zealand Cenozoic limestones and modern carbonate sediments, with particular reference to the Te Kuiti Group; and finally the economic importance of carbonate rocks, a description of the study site, the effects silica has on steel manufacture, and the silica issue at McDonald's Lime Quarry.

2.2 General geology of Te Kuiti district

A geological time scale is shown in Figure 2.1 introducing the geological age names that appear in the following account. A general map of the geology in the King Country region is shown in Figure 2.2, and a generalised stratigraphic diagram in Figure 2.3. Table 2.1 shows the main events that have shaped the landscape during geological development of the King Country region. Some supporting details are given in the following section.

2.2.1 Triassic-Jurassic (251 to 145.5 million years ago)

The oldest rocks in the Te Kuiti district and wider King Country region are late Triassic-Jurassic bluish-grey marine sandstones often greywackes and siltstones (sometimes argillites), collectively referred to as (Mesozoic) basement rocks (Figure 2.2). These rocks build the Rangitoto and Hauhungaroa Ranges to the east, and the Herangi Range to the west, as well as underlying at depth all younger rocks in the region (Nelson, 1993).

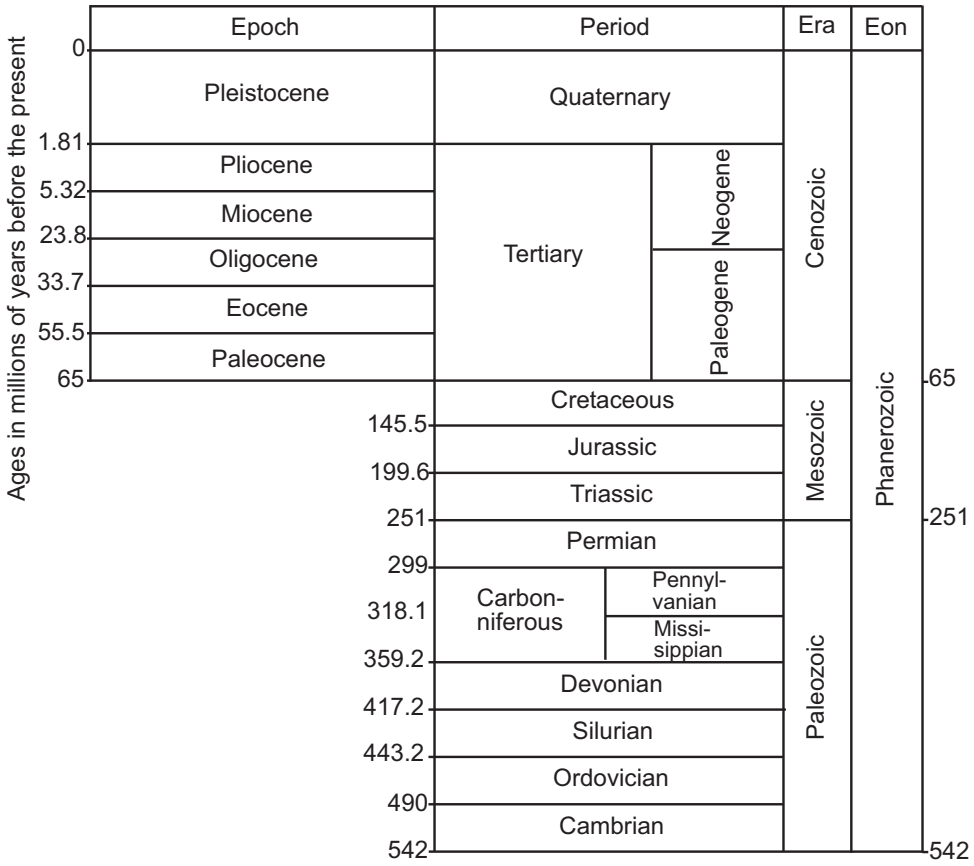

Figure 2.1 New Zealand geological timescale. Adapted from Cooper (2004).

The sediments were derived from the eastern margin of the combined Australia and Antarctica continents that formed part of the Gondwana supercontinent during the Triassic and Jurassic (about 251-145.5 million years ago) and were deposited in the deep seas bordering the supercontinent. The total thickness of the deeply buried basement rocks reaches up to 10 km or more (Nelson, 1993). West of a north-south lineament (corresponding to the Waipa Fault) through Te Kuiti, the basement rocks are fossiliferous and include interbedded volcanic ash layers derived from coeval volcanism along parts of the Gondwana coastline. The Waipa Fault marks the junction separating two contrasting deposits of Mesozoic sedimentary rocks that collided by sea-floor spreading about 100 million years ago, and uplifted to add new land to the Gondwana margin. This uplift event is known as the Rangitata Orogeny (Nelson, 1993). Between the two contrasting rocks, a slice of basaltic oceanic crust became caught up in the collision zone at the Waipa Fault, and is represented by serpentinite, which is mined at the Wairere Serpentinite Quarry near Piopio to the south.

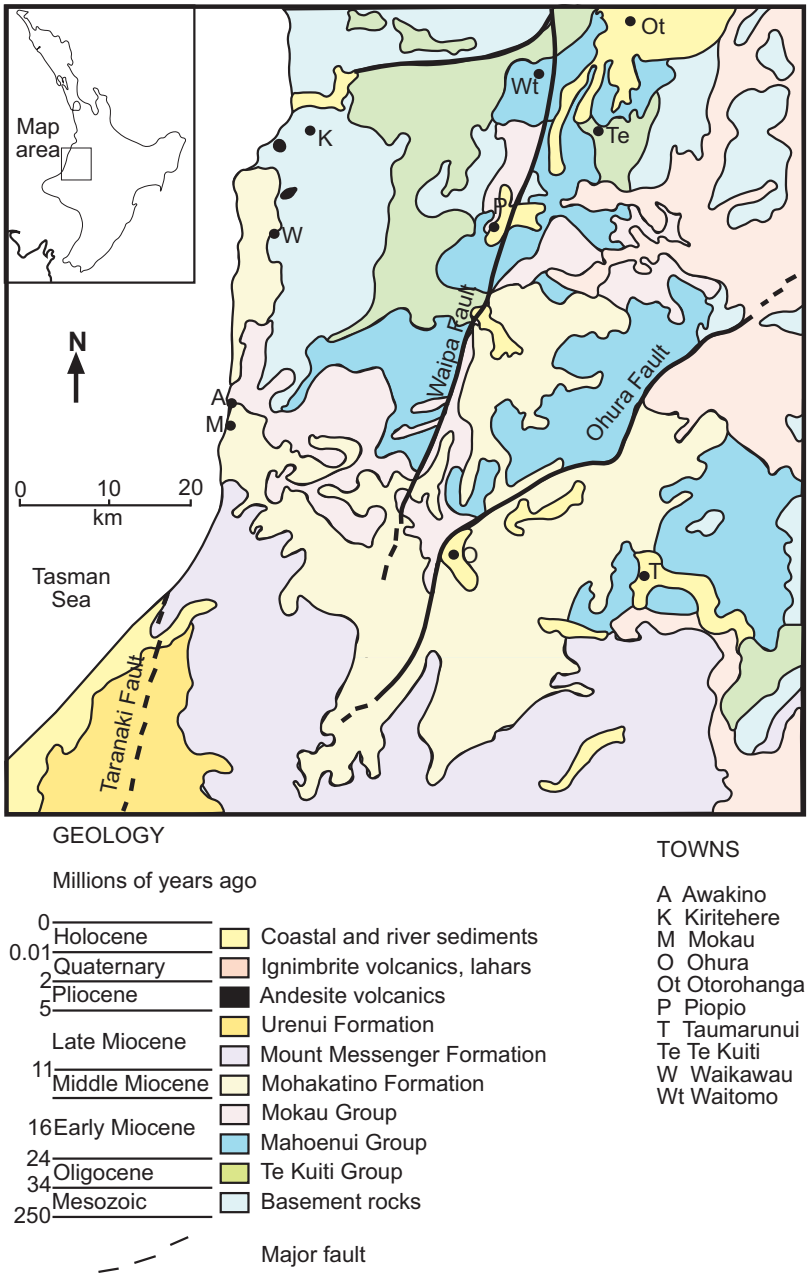

Figure 2.2 Geology of the King Country region, adapted from Nelson (1993). Inset shows the location of the King Country region in the North Island of New Zealand.

The serpentinite is a mainly subsurface feature, but is well exposed at the surface at Dun Mountain near Nelson in the South Island. Rocks west of the Waipa Fault form a broad north-south trending down warped fold known as the Kawhia Regional Syncline. The basement rocks east of the fault are structurally complex, jointed, sheared, and faulted (Nelson, 1993).

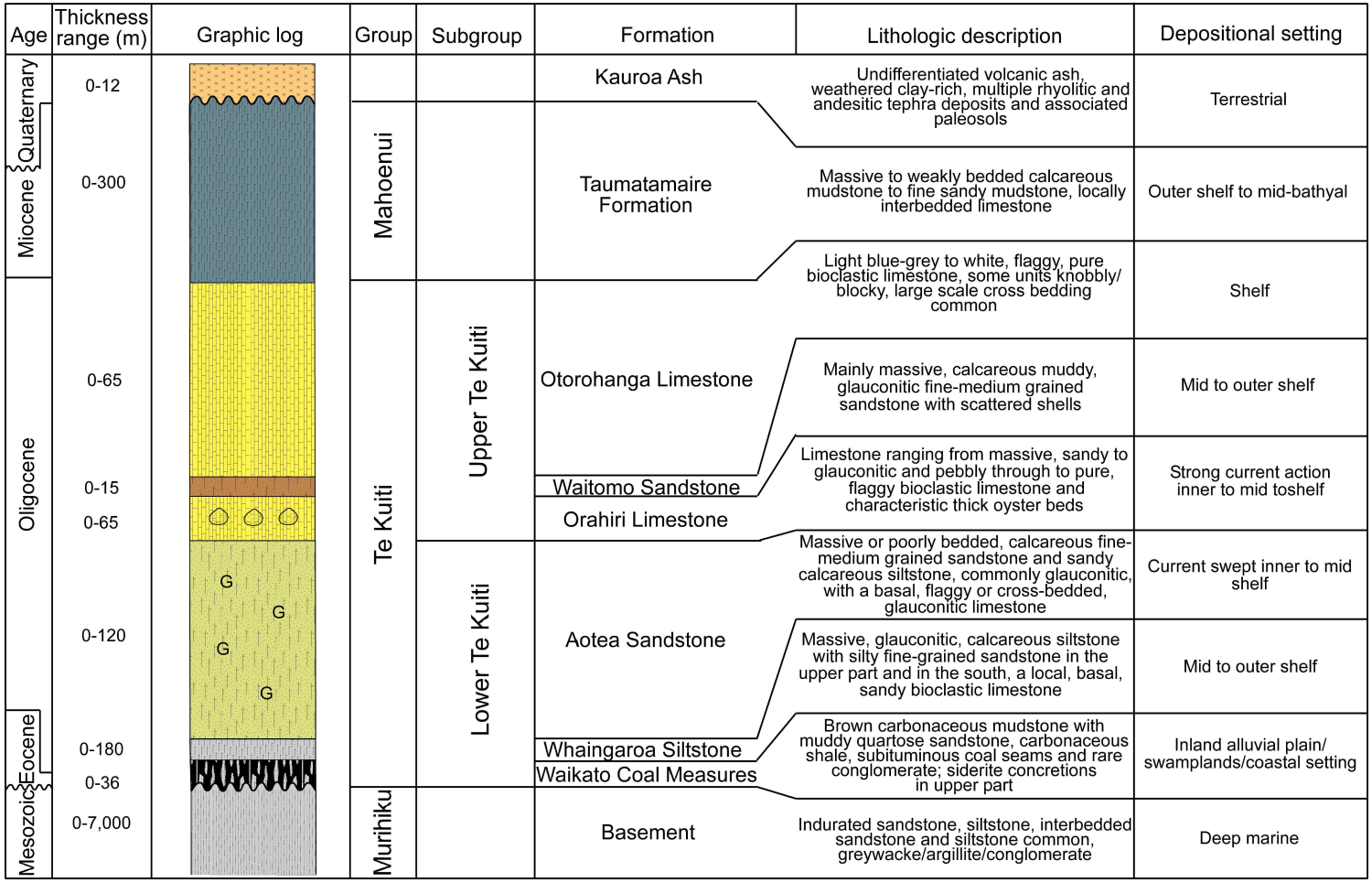

Figure 2.3 General geology of the Te Kuiti district. Data sourced from Nelson (1978a). G = glauconitic, and symbol in Orahiri Limestone (graphic log) = oysters.

Table 2.1 Geological history of the King Country region. Data sourced from Nelson (1993), and absolute ages from Cooper (2004).

Geological time	Main event
Quaternary (2.3 m.y. ago-present)	Volcanic ashes blanketed the King Country region sourced from Rotorua-Taupo, Tongariro, and Taranaki volcanoes.
Pliocene and Quaternary (since 5 m.y. ago)	Onshore volcanism depositing lava flows, pyroclastics flows, and widespread ashfall over the region. Deposits sourced from Pirongia, Karioi to the north, and Taranaki, and Rotorua-Taupo volcanic centres.
Late Miocene (11.2-7.12 m.y. ago)	The King Country region emerged out of the sea and marine sedimentation ceases. North-south trending faults through the King Country region become active including Taranaki, Manganui, Marokopa, Waipa, Ohura, and Hauhungaroa Faults. This active faulting was part of a New Zealand wide activity known as the Kaikoura Orogeny.
Middle Miocene (16.4-11.2 m.y. ago)	Deposition of sandstones and mudstones continues, but includes volcanic particles and ash layers to form volcanogenic mudstones and sandstones up to a few 100 metres thick known as the Mohakatino Formation.
Early Miocene (23.8-16.4 m.y. ago)	Limestone formation ceases and is replaced by the deposition of thick (200-500 m) blue-grey mudstones and alternating beds of mudstone and sandstone (flysch) as at Taumarunui referred to as the Mahoenui Group. During deposition, the marine basins were rapidly sinking (by 100s of metres) as a result of active faulting in the region. Alpine Fault forms initiating propagation of the present plate boundary between the Australian and Pacific crustal plates. Seas begin to shallow about 20 million years ago and the Mahoenui Group is overlain by sandstones of the Mokau Group; coal seams also formed as seas shallowed sufficiently to allow formation of coal seams.
Late Eocene-Oligocene (37-33.7 m.y. ago)	Coal deposits widespread and up to 100 m thick in the Waikato region to the north. Inundation of shallow seas, deposit calcareous siltstones, calcareous sandstones, and limestones accumulating from 33.7-23.8 m.y ago. These deposits are up to 100-200 m thick and are collectively known as the Te Kuiti Group.
Late Cretaceous-Eocene (99.6-55.5 m.y. ago)	Tectonic processes initiate the separation of the New Zealand subcontinent from the Gondwana landmass, New Zealand drifts away (from 80-55 m.y. ago) from Gondwana into the Pacific Ocean, opening up the Tasman Sea. Mountainous landscape (formed as a result of the earlier Rangitata Orogeny) becomes eventually reduced to a low-lying landscape.
Triassic-Jurassic (251-145.5 m.y. ago)	Oldest rocks in the Te Kuiti district and wider King Country region. Bluish-grey marine sandstones and siltstones (greywackes) that form the Rangitoto and Hauhungaroa Ranges (to west) and Herangi Range to the east. Sediments derived from the eastern margin of the Australia-Antarctica continents (joined at the time) that formed part of the Gondwana supercontinent. The Waipa Fault (trending north-south through the King Country region) marks the link separating two contrasting sedimentary deposits of Mesozoic rocks which collided as a result of seafloor spreading about 100 m.y. ago, and uplifted to add new land to the Gondwana margin. The collision event is known as the Rangitata Orogeny. Mesozoic rocks west of the Waipa Fault form a broad, north- south trending, down warped fold known as the Kawhia Syncline. Rocks east of the fault are folded, jointed, sheared, and faulted.

2.2.2 Late Cretaceous-Eocene (80 to 45 million years ago)

As a result of upwelling and diverging of the mantle beneath the Gondwana supercontinent, the New Zealand landmass (part of the Australia and Antarctic continent) rifted (broke away) from Gondwana drifting into the Pacific Ocean from 80-55 million years ago, forming the Tasman Sea. Drifting ceased at about 50 million years ago as the Antarctica continent separated from the Australia continent. No rocks were deposited in the King Country region from 100-45 million years ago as the landscape was subaerially exposed. The region was initially mountainous resulting from activities that had occurred during the Rangitata Orogeny, but with time the region was eventually reduced to a low-lying landscape (Nelson, 1993; Edbrooke, 2005).

2.2.3 Late Eocene-Oligocene (45 to 25 million years ago)

The low-lying landscape provided a setting to support swamps and coal deposition. Freshwater coal deposits are widespread throughout the region, including at Bennydale, Otewa near Te Kuiti, Okoko west of Otorohanga, and in the Waikato region to the north where there are up to 100 m thick (Nelson, 1993). After coal deposition, shallow seas inundated the area depositing calcareous siltstones, calcareous sandstones, and limestones from about 40-25 million years ago (Oligocene). The Oligocene was a period of relative tectonic quiescence accompanied by widespread regional subsidence and minor faulting (Edbrooke, 2005). The limestones are characterised by steep bluffs, sinkholes or tomos, and crags in the landscape. These deposits reach up to 100-200 m thick and are collectively known as the Te Kuiti Group (Nelson, 1993). These marine deposits unconformably overlie the Mesozoic basement rocks (Nelson, 1978a; Dodd and Nelson, 1998).

2.2.4 Early Miocene (25 to 15 million years ago)

In the early Miocene the Australian-Pacific plate boundary in its present location propagated through the New Zealand region (Dodd and Nelson, 1998). This is expressed as a major fracture lineament in the South Island known as the Alpine Fault. Deformation and strong differential uplift occurred along the plate margin resulting in widespread subsidence in the King Country region that continued into

the middle Miocene (Dodd and Nelson, 1998). Limestone formation ceased and was replaced by the deposition of thick (200-500 m) blue-grey mudstones and alternating beds of mudstone and sandstone (flysch), as at Taumarunui, referred to as the Mahoenui Group. Mahoenui Group is characterised by hummocky hills that are often susceptible to slumping in the landscape. During deposition of the mudstones, the marine basins were rapidly sinking (100s of metres) as a result of active faulting in the region. Parts of the landscape became uplifted and eroded, while others were depressed into troughs that accumulated sand and mud detritus (Nelson, 1993). Major movement of Mesozoic basement rocks overthrusting on the Taranaki Fault also occurred during the early Miocene (Edbrooke, 2005).

Seas began to shallow about 20 million years ago and the Mahoenui Group was overlain by porous sandstones of the Mokau Group (Figure 2.2) which form blocky bluffs in the landscape. Coal seams were also deposited as seas became sufficiently shallow for formation of brackish marine to terrestrial sediments. Some of these coal seams have been mined, as at Mahoenui, Ohura, and near Taumarunui (Nelson, 1993).

2.2.5 Middle Miocene (15 to 10 million years ago)

As the deposition of sandstones and mudstones continued, volcanic particles and ashes sourced from andesitic volcanoes 40 km offshore from Marokopa, were deposited over the Mokau Group forming volcanogenic mudstones and sandstones up to a few 100 metres known as the Mohakatino Formation (Figure 2.2).

2.2.6 Late Miocene (10 to 5 million years ago)

By the late Miocene the King Country region was most likely emerging out of the sea and marine sedimentation ceased, although marine deposition continued to the south in the inland Taranaki region and offshore Taranaki Basin (Nelson, 1993; King and Thrasher, 1996). North-south trending faults through the King Country region became active, including the Taranaki, Manganui, Marokopa, Waipa (Figure 2.2), Ohura (Figure 2.2), and Hauhungaroa Faults. This fault activity was part of New Zealand wide activity known as the Kaikoura Orogeny. All the rocks in the King Country region became exposed, and occur at different elevations due

to differential uplift. About 10 million years ago weathering, erosion, and rivers continued to shape the landscape forming, for example, rugged steeplands in greywackes (Nelson, 1993).

2.2.7 Pliocene-Quaternary (since 5 million years ago)

After complete emersion of the King Country region, products of volcanism have modified the landscape. This onshore volcanism continued spreading lava flows, pyroclastic flows, and widespread ashfall over the region. Deposits are sourced from Pirongia, Karioi to the north, and the Taranaki and Rotorua-Taupo volcanic centres (Nelson, 1993).

Coastal and river sediments also accumulated during the Pliocene-Holocene (Figure 2.2). During the Quaternary, caldera forming eruptions from the Taupo Volcanic Zone produced voluminous and widespread ignimbrites that accumulated particularly in topographic lows, and tephra deposits that mantled the surface in the King Country region (Edbrooke, 2005).

2.2.8 Quaternary (2.3 million years ago to present)

Volcanic ashes blanket the King Country region and can be divided into three ash ages that have been sourced from Taupo, Rotorua, Tongariro, and/or Taranaki (Nelson, 1993). Old ashes include the Kauroa Ash-Hamilton Ashes (2.3-0.1 million years old) that have weathered to reddish brown clays, sourced from Rotorua-Taupo volcanic centres. Middle (aged) ashes include the Rotoehu Ash (50,000 years old) sourced from Lake Rotoma, characterised by fine cream sands; Aokautere Ash (20,000 years old) erupted from near Wairakei, which are pumiceous and widespread; and Holocene Ashes that are brown, friable and the main parent soils for much of the King Country region. Several different thin ashes now mixed and combined are known as the Mairoa Ash, sourced from Taranaki, Tongariro, Rotorua, and Taupo centres. Young ashes include Taupo Pumice Lapilli erupted 1,800 years ago from the Horomatangi Reefs area in northeastern Lake Taupo (Nelson, 1993).

2.3 Cenozoic limestones in New Zealand

Cenozoic limestones are widely distributed in both islands of New Zealand, particularly in the Oligocene-Miocene. Three limestone megafacies occur in New Zealand (Figure 2.4) including mainly deepwater Amuri limestones of Paleocene-Eocene age, the temperate shelf Te Kuiti Group limestones of Oligocene age, and the shelfal Te Aute limestones of Pliocene-Pleistocene age (Dodd and Nelson, 1998). Figure 2.4 shows the timing of tectonic events and deposition of each limestone megafacies, along with the other main lithologies deposited during the Cenozoic.

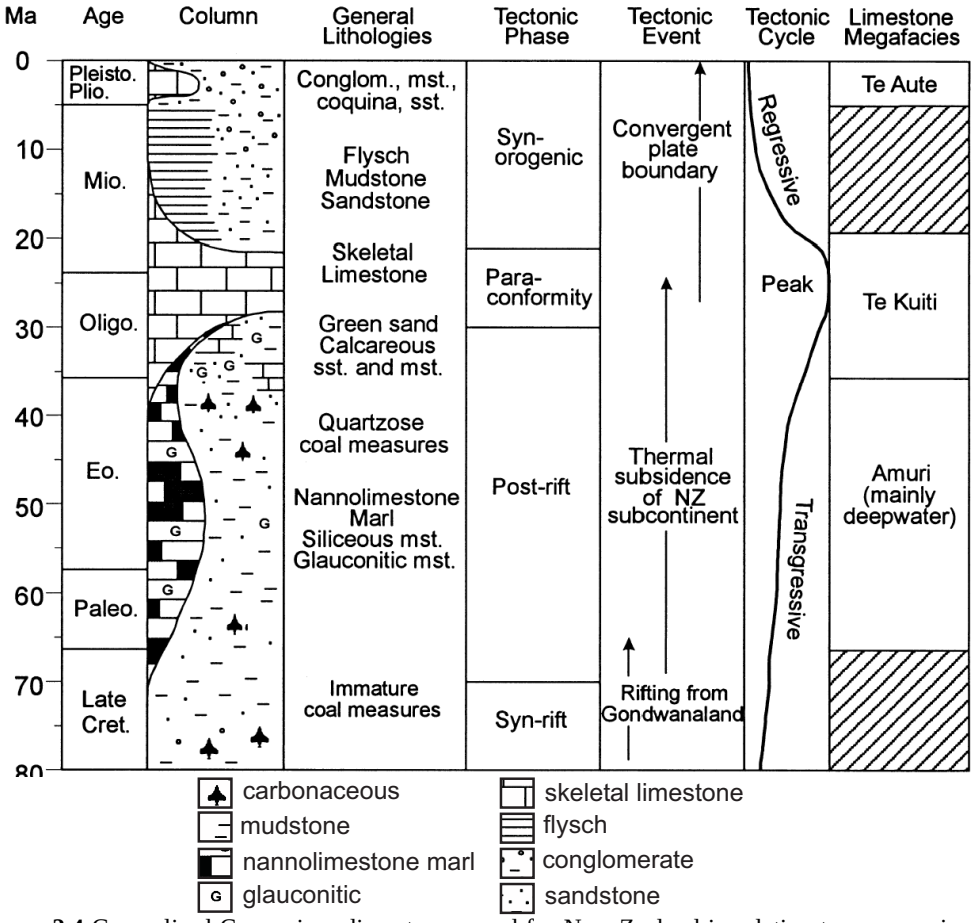

Figure 2.4 Generalised Cenozoic sedimentary record for New Zealand in relation to some major tectonic events. Note that shallow marine limestones completely dominate the Oligocene period (Te Kuiti Group megafacies), occur sporadically in the Pliocene-Pleistocene (Te Aute megafacies), and that limestones having deep marine characteristics occur locally in the Paleocene-Eocene part of the record (Amuri megafacies). Adapted from Dodd and Nelson (1998).

A spectrum of $CaCO_3$ contents (50-100%) exists in the New Zealand Cenozoic limestones (Nelson, 1978b). Most limestones are associated with terrigenous formations either below or above, and sometimes complexly interbedded with them. These Cenozoic limestones were mainly deposited in non-tropical, cool-

warm-temperate climatic conditions, in open marine shelf or ramp environments, between 60° and 35°S paleo-latitudes (Hayton et al., 1995). Evidence from oxygen isotope records indicates that the mean sea water temperature in New Zealand since the Eocene was cooler than 20°C (Nelson, 1978b). Based on the Te Kuiti Group megafacies, average sedimentation rates are 1-2 cm/1000 years (Nelson, 1978b). The sediments are mainly calcilutites (<0.063 mm) or calcarenites (0.063-2.0 mm) (Nelson, 1978b). The Paleocene to Eocene limestones are dominantly calcilutites, and are restricted to the far north and east coast of New Zealand. This is due to the landmass being subaerially exposed at the time, where coal swamps were forming (Nelson, 1978b). During the Oligocene, highly calcareous sediments were deposited over much of the country (>200 m thick) and include calcarenites and calcirudites (Nelson, 1978b). The Pliocene-Pleistocene limestones are dominantly coarse calcirudites and sometimes coquinites (whole shell), and occur mainly in eastern North Island (Hayton et al., 1995; Hood and Nelson, 1996).

The Te Kuiti Group (50-250 m thick) and Te Aute limestones (5-150 m thick) were deposited in high energy open platform, or tide influenced seaways at mid-outer shelf depths, in warm-cool temperate climatic conditions. New Zealand limestones show examples of both shallow burial (e.g. Te Aute megafacies, <700 m) and deeper burial (Te Kuiti Group megafacies, >2000 m) due to a tectonically complex setting at a convergent plate margin developed since the mid-Cenozoic. Relatively deep burial (1-5 km) has contributed to a series of diagenetic fabrics in New Zealand limestones (Dodd and Nelson, 1998). The Te Kuiti Group limestones are typically well cemented, hard limestones, whereas the Te Aute megafacies limestones are commonly differentially cemented, varying from dense well cemented limestones to soft friable, poorly cemented rocks (Hood and Nelson, 1996).

The framework of New Zealand Cenozoic limestones is practically entirely made up of the skeletal fragments of organisms (Nelson, 1978a). The main skeletal contributors to the New Zealand limestones are bryozoans, benthic and planktic foraminifera, echinoderms, calcareous red algae, barnacles, and bivalves. Minor contributors include brachiopods, solitary corals, gastropods, ostracods, and sponge spicules (Nelson, 1978b; Hayton et al., 1995; Dodd and Nelson, 1998).

Other skeletal material identified includes serpulids, coccolithophorids, radiolarians (siliceous), and diatoms (siliceous). The occurrence of these organisms is controlled by their preferred habitats, including a spectrum of environmental tolerances (Hayton et al., 1995). Non-skeletal grains such as ooids, pellets, and aggregates are generally absent in New Zealand Cenozoic limestones because of normal marine salinities and temperate climatic conditions during carbonate deposition (high temperatures and/or high salinities are required for formation and/or preservation of ooids, pellets, and aggregates) (Nelson, 1978b). The skeletal material is typically fragmented and abraded as a result of biological (e.g. boring by organisms) and physical processes (e.g. wave and current action), and is the reason why whole macrofossil specimens are scarce (Nelson, 1978a).

Initially the New Zealand Cenozoic limestones were generalised into one skeletal assemblage (foramol) using the scheme devised by Chave (1967) and Lees and Buller (1972). Subsequently, workers such as Hayton et al. (1995) have established some important distinctive differences in the limestones and generated 7 major skeletal assemblages: (1) barnamol = barnacle/bivalve dominated; (2) bimol = bivalve dominated; (3) bryomol = bryozoan/bivalve dominated; (4) echinofor = echinoid/benthic foraminifera dominated; (5) nannofor = nannofossil/planktic foraminifera dominated; (6) rhodalgal = calcareous red algal dominated; and (7) rhodechfor = calcareous red algal/echinoderm/benthic foraminifera dominated. The Paleocene-Eocene Amuri limestone megafacies are dominated by a nannofor assemblage (Hood and Nelson, 1996), bryomol and echinofor assemblages are typical in the Te Kuiti Group, and barnamol and bimol associations are typical in the Te Aute limestones (Dodd and Nelson, 1998). The primary mineralogy of these skeletons is calcitic, predominantly low to moderate-Mg calcite, although some local infaunal aragonitic bivalves occur in the Te Aute bimol and barnamol limestones (Dodd and Nelson, 1998).

The lithification of New Zealand carbonate sediments involves the precipitation of sparry calcite and/or ferroan calcite cement in pore spaces of original or modified sediment (Nelson, 1978b). The cements in New Zealand limestones are typically sparry calcite comprising 5-25% of Te Kuiti Group limestones, and 20-40% of Te Aute limestones (Dodd and Nelson, 1998; Hood and Nelson, 1996). The cement is dominantly coarsely (20-500 μm) to finely (<20 μm) crystalline equant cement. Up to 25% of the cement comprises rim (overgrowths) cements associated with

echinoderms (Dodd and Nelson, 1998). Other cements also occur in New Zealand Cenozoic limestones, such as marine cements (generally rare) occurring in *in situ* oyster and bryozoan mounds, or with unconformities and hardground development. Marine cements have been identified in McDonald's Oparure Quarry in the Otorohanga Limestone (Te Kuiti Group) within a bryozoan mound (Nelson, pers. comm., 2007). Marine (or sea floor) cements form under special conditions such as high hydrodynamic energy levels, and reduced or negative sedimentation rates, and form relatively early in the diagenetic history of a limestone (Dodd and Nelson, 1998). This early cement occurs in rocks with open fabrics, where porosities of up to 45% pore volume can be retained (as a result of the rock being made rigid by the marine cement). Other sources of cement come from pressure dissolution. The original porosity of carbonate sediment can be 40%; however, burial causes mechanical and chemical compaction which can reduce the porosity to close to 0% (Dodd and Nelson, 1998). Beneath 500 m of burial pressure dissolution is a major source of cement. Approximately 5-20% pore space is left in Cenozoic New Zealand limestones, which consequently becomes later filled by low-Mg calcite cement (Dodd and Nelson, 1998). Pre-Pliocene limestones are typically well cemented, and hard with low porosities, whereas Pliocene-Pleistocene limestones are partly/differentially cemented and retain high porosities (Nelson, 1978b).

2.3.1 Modern carbonates

Modern non-tropical carbonate sediments also occur in New Zealand and are good analogues for onshore New Zealand Cenozoic limestones (Nelson et al., 1988b). New Zealand modern carbonate sediments have been studied by several workers (e.g. Nelson et al., 1982; Nelson and Hancock, 1984); a useful compendium is Nelson (1982). New Zealand sits astride the Australian-Pacific convergent plate boundary and consequently the continent experiences active tectonism, volcanism, uplift, and high erosion rates that contribute to siliciclastic detritus (Nelson et al., 1988a). As a result, the majority of the continental shelf (ca. 250,000 km^2) is covered in siliciclastic sands and muds with relatively small amounts of carbonate (<10%) (Kamp and Nelson, 1988). However, carbonate content increases beyond the shelf as depth increases (Nelson et al., 1988a). Approximately 50,000 km^2 (20% of the New Zealand continental shelf) of shallow marine platforms in <250 m water depth are covered in modern and relict non-tropical skeletal carbonate

sediments comprising >70% $CaCO_3$. Surficial deposits are aged from 20,000 years B.P. to modern (Nelson et al., 1988a). The two main areas of modern carbonate sedimentation occur off the north and south of New Zealand, specifically on Three Kings platform (34ºS) and Snares platform (48ºS) (Nelson et al., 1988b). A further 6,000 km^2 involve local occurrences of carbonate sediments, such as off Wanganui and Otago, and on the Foveaux shelf (Nelson et al., 1988b).

Three main controls allow carbonate sediments to form on the New Zealand shelf: (1) terrigenous input from rivers and sedimentation rates are relatively low in these areas; (2) the locally rocky and gravelly nature of the seafloor provides firm hard substrates for epibenthos; and (3) high-energy levels on the open shelf brings in high contents of nutrients for organisms (Nelson et al., 1988a). New Zealand modern carbonate sediments are closely associated with siliciclastic deposits (adjacent), including mixed carbonate-siliciclastic sediment, and rapid facies transitions (Nelson et al., 1988b).

Modern carbonate sediments in New Zealand are typically coarse-grained sands and gravels that are whole or fragmented; carbonate mud is rare. Mineralogy of the sediments is a combination of mainly calcite (90%) and aragonite (<10%), the former being predominantly high-magnesium calcite off northern New Zealand and low-magnesium calcite in the south (Nelson et al., 1988a). Skeletal material is composed of bryozoans, molluscs, local foraminifera, barnacles, calcareous red algae, and echinoderms. The main skeletal assemblage that occurs is the bryomol association (Nelson et al., 1988b).

Physical processes such as wave and current action (storms in particular) cause skeletal breakage and fragmentation. The wave environment on these carbonate platforms is dominated by high energy waves and long period swells originating from west and southwest of New Zealand. Storm waves are generated from the north. Tidal flows play an important role in the dispersal of modern skeletal sediments (Nelson et al., 1988b). Carbonate sediments commonly experience bioerosion such as boring activity which also plays an important role in the degradation and fragmentation of skeletal material; for example, grazing of coralline red algae coated surfaces by echinoids forming skeletal detritus. Macro-

boring organisms include gastropods, polycheates, and sponges, and micro-boring ones include algae, bacteria, and fungi. The degradation of carbonate sediments is a source of carbonate mud; however, the seeming paucity of carbonate mud in the modern New Zealand carbonates probably relates to the low supply rates of bioeroded fine detritus and the flushing of mud from high energy open-water shelves (Nelson et al., 1988b).

2.3.2 Non-tropical carbonates in New Zealand

The shelf carbonate model developed by Irwin (1965) and Heckel (1972) is based on a theoretical model of shallow marine sedimentation largely developed for tropical carbonates. This depositional model is and has been used to interpret ancient shallow marine limestones such as the well known modern tropical deposits of the Bahamas, Persian Gulf, and the Great Barrier reef (Dodd and Nelson, 1998). The environmental controls and processes and products of Cenozoic carbonate sediments in New Zealand, however, are different to the tropical model. Traditionally, carbonate shelf sediments were viewed as a low latitude phenomenon (Nelson, 1978b). Chave (1967) was one of the first to collect information that showed that highly calcareous sediments are being deposited on many modern shelves beyond the tropics (Nelson, 1978b). Studies show that non-tropical carbonate sediments are widespread in areas such as New Zealand, southern Australia, British Columbia, and Ireland. Cenozoic non-tropical carbonates also have occurrences in New Zealand, southern Australia, and the Mediterranean (Dodd and Nelson, 1998).

Non-tropical limestones are distributed in temperate latitudes and are also referred to as cool water, temperate, or temperate latitude carbonates (Nelson, 1988). The facies characteristics of non-tropical carbonates show some fundamental differences with carbonates developed in warm subtropical or tropical conditions. Increased work on non-tropical limestones (e.g. Nelson, 1978a, 1988; Nelson et al., 1988b; Hayton et al., 1995; Hood and Nelson, 1996; James, 1997; Hood et al., 2003; Nelson et al., 2003; Hood et al., 2004) has emphasised key differences that occur between non-tropical and tropical sediments. A Table of differences for tropical shelf carbonates, modern New Zealand shelf carbonates, and New Zealand Cenozoic limestones are given in Appendix B-2.1. One of the major differences is that tropical carbonate sediments have a greater abundance of

aragonite (>50%), whereas non-tropical sediments rarely contain >50% aragonite, and typically <10%. Aragonite usually dissolves in non-tropical limestones before lithification (hardening) of the carbonate sediment during early diagenesis (all processes acting on a sediment after deposition, excluding metamorphism); therefore evidence of any original aragonitic component is usually absent (Dodd and Nelson, 1998). Grain textures are sand and mud dominated in tropical carbonates whereas gravel and sand textures dominate in non-tropical carbonates.

As mentioned earlier, non-tropical limestones in New Zealand are almost exclusively comprised of skeletal remains. These include bryozoans, bivalves, calcareous red algae, benthic foraminifera, and barnacles (Nelson, 1988). Non-skeletal grains such as ooids and aggregates are absent. In contrast, these non-skeletal grains are common in tropical carbonates (Nelson, 1988). Non-tropical shelves are typically dominated by the foramol skeletal assemblage (foraminifera and mollusc dominated). However, a skeletal classification comprising a spectrum of non-tropical foramol carbonates has now been developed (Hayton et al., 1995). In contrast, the tropical shelves are typically dominated by chlorozoan skeletal organisms such as calcareous green algae (*Chlorophyta*) and hermatypic coral (*Zooantharia*) (Hayton et al., 1995). This contrast in organism types is controlled by the different environmental conditions present, the waters being >20°C, and saturated to supersaturated in $CaCO_3$ in tropical carbonate environments, compared to waters <20°C and, saturated to undersaturated in nontropical carbonate environments (Hood and Nelson, 1996).

2.4 Te Kuiti Group

The Te Kuiti Group was first established by Kear and Schofield (1959) and has been studied subsequently by other workers, including Barrett (1967), Nelson (1973, 1978a), Nelson et al. (1988a, 1994), Hood and Nelson (1996), Dodd and Nelson (1998), and Tripathi (in prep.). The nomenclature of the group has also been revised several times, most recently by White and Waterhouse (1993).

2.4.1 Lithologies

The Te Kuiti Group is a transgressional sequence of shallow water predominantly marine beds of late Eocene to early Miocene age; most of the group falls largely within the Oligocene age (Barrett, 1967; Nelson, 1978a). These were deposited on a gently undulating erosional surface, as the sea transgressed from the north (Barrett, 1967). The group accumulated on an open platform or tide influenced seaway, in mid-outer shelf depths (Dodd and Nelson, 1998). The sedimentary lithologies of the Te Kuiti Group in the South Auckland area lie above a regional unconformity developed on Mesozoic basement rocks belonging to the Murihiku Supergroup and Manaia Hill Group (Nelson, 1978a). The group is generally conformably overlain by the Mahoenui Group mudstones and localised limestones (e.g. Cherry Crag Limestone), and its northerly equivalent Waitemata Group. Lithologies in the group include locally common non-marine to marginal marine coal measures, mudstones, and conglomerates, and more widespread calcareous sandstones, calcareous siltstones, and sandy and pure skeletal limestones. Muds and muddy sandstones are predominantly massive and bioturbated, and mud-poor sandstones and limestones are thinly bedded (3-10 cm thick) (Nelson, 1978a). Limestone beds are typically subhorizontal wavy and lenticularly stratified, and are occasionally cross-bedded (Nelson, 1978a).

2.4.2 Formations

The group is subdivided into Lower and Upper subgroups, shown in Figure 2.3. Nelson (1978a) has identified six formations, seven members, and named 30 beds as a result of lithologic variation within the formations in the group. The six formations are formally named Waikato Coal Measures, Whaingaroa Siltstone, Aotea Sandstone, Orahiri Limestone, Waitomo Sandstone, and Otorohanga Limestone. Boundaries between the formations are commonly unconformities, sharp, slightly irregular, often bored, pebbly, and/or glauconitic (Nelson, 1978a). The seven members are Awamarino, Waitetuna, Mangaotaki, Te Anga, Pakeho, Waitanguru, and Piopio members (Nelson, 1978a).

2.4.3 Distribution

The group reaches a combined thickness of 200-300 m (Kear and Schofield, 1959; Nelson, 1978a) and crops out throughout the South Auckland Land District between Papakura in the north and Taumarunui in the south (Nelson, 1978a). North of the latitude of approximately Mount Karioi, siltstones of the Te Kuiti Group predominate. Limestones occur both north and south of this latitude, particularly in the west, and thicken southward. Te Kuiti Group thins as a group to the south; however, limestones dominate the group south of Waitomo (Nelson, 1978a; White and Waterhouse, 1993).

2.4.4 Composition

The $CaCO_3$ content of the limestones ranges from 40-100% and is comprised almost entirely of low-Mg calcite (Nelson et al., 1988b). Some 80-90% of the calcite occurs as skeletal fragments, mainly bryozoans, echinoderms, benthic and planktic foraminifera, bivalves, barnacles, and coralline red algae, and the remaining 10-20% occurs as chemically precipitated inter- (between grains) and intra- (within grains) particle cement (Nelson et al., 1988b). The siliciclastic (non-carbonate) component comprises a sand fraction of quartz, plagioclase feldspar, and volcanic and sedimentary rock fragments, and a finer fraction of quartz, plagioclase, smectite, illite, and chlorite. Excluding smectite (probably authigenic), the siliciclastic minerals are sourced from Mesozoic basement rocks. Glauconite is common in most lithologies and is frequently concentrated near unconformities (Nelson, 1978b).

2.4.5 Otorohanga Limestone

The following section briefly summarises properties of the Otorohanga Limestone, as the quarry resource is located within this formation. Otorohanga Limestone may overlie Waitomo Sandstone, Orahiri Limestone, or Mesozoic basement rocks, and seldomly Lower Te Kuiti Group formations (Figure 2.3). It is commonly overlain conformably by Mahoenui Group, and locally by Pleistocene Pakaumanu Ignimbrites (Nelson, 1978a). Because of erosion, the upper boundary of the Otorohanga Limestone is nowhere found immediately north of Waitomo County (Nelson, 1978a), so it is not known if the formation was

more widespread beyond this direction. The Otorohanga Limestone passes north into calcareous siltstone (Te Akatea Siltstone), and is replaced by calcareous mudstones of the Mahoenui Group in the Mangapehi region (Nelson, 1978a).

The Otorohanga Limestone is characterised by vertical cliffs in outcrop and forms extensive karst topography (e.g. Waitomo Caves), particularly in Waitomo County. Otorohanga Limestone is characteristically a blue-grey to white, flaggy pure limestone (seldomly exceeding 10% terrigenous material, except near Kawhia) in which three members have been established by Nelson (1978a). The most characteristic macrofossil in the Otorohanga Limestone is the large pecten *Athlopecten athleta* of Waitakian (latest Oligocene) age, which is also the age for the entire limestone (Nelson, 1978a). Starting with the basal limestone the three members and associated abbreviations are known as Pakeho Limestone (OtA), Waitanguru Limestone (OtB), and Piopio Limestone (OtC). Figure 2.5 gives some details of these members. The topmost member (Piopio Limestone) is a pure, flaggy limestone, is blue-grey when fresh, and pale cream when weathered. Two beds occur within the Piopio Member (OtC): (1) upper flaggy limestone beds that occur in the lower part of the member and are distinguished from the flaggy beds in the Pakeho Limestone Member as being purer, having a greater variation in flag thicknesses (2.5-20 cm), and more shaley interflag seams; and (2) argillaceous limestone beds that occur near the top part of the member which have shaley interflag seams >1 cm or more thick, and become progressively more argillaceous as the member rapidly passes into the overlying Mahoenui Group mudstones. Pyrite grains and nodules are also dispersed throughout the limestones. The Waitanguru Limestone Member (developed mainly in the central part of Waitomo) is characteristically white, and appears blocky, or knobbly, and/or cavernous in outcrop. The member is very pure with >98% $CaCO_3$ content, and seams are present but not always obvious due to the knobbly appearance. Three beds occur in the Waitanguru Limestone Member (OtB): (1) blocky limestone beds which are thickly flagged (7-20 cm). Accelerated weathering along vertical joints gives the outcrop a blocky or slabby appearance. Knobbly characteristics are not well developed; (2) packed knobbly limestone beds which are white, very pure, , typically tightly packed with coarse bryozoan fragments; and (3) open knobbly limestone beds which are coarse to very coarse grained.

Age	NZ stage	Group	Subgroup	Formation	Member	Description	Photo
latest Oligocene -earliest Miocene	Waitakian	Te Kuiti	Upper Te Kuiti	Otorohanga Limestone (Ot)	Piopio Limestone (OtC)	The OtC member of the Otorohanga Limestone is pure and flaggy which is typically blue-grey unweathered, and pale cream oxidised. Upper flaggy beds occur within the OtC member and possess higher calcium carbonate content compared to the lower OtA member which is also flaggy. Interflag seams are considerably more shaley than the other members, and cross bedding is common regionally. Upper limestone beds of OtC become increasingly argillaceous towards the upper boundary and overlying Mahoenui Group mudstones. Furthermore, interflag thickness increases, and flags become richer in fine-grained siliciclastic material. Scattered pyrite nodules and grains are also common.	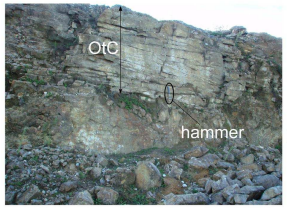 Piopio Limestone (OtC) McDonald's Oparure Lime Quarry (2007)
					Waitanguru Limestone (OtB)	Typically white high purity beds that occur particularly in the central Waitomo County region. The OtB member outcrops weather to blocky/ knobbly cavernous rock faces. Due to the knobbly appearance, developing seams are less obvious but present nonetheless. Where vertical joints have been exploited by weathering, beds appear blocky or slabby. There are also two types of knobbly limestone beds that occur within the OtB member including packed knobbly limestone beds which are very white, pure, and contain tightly packed bryozoans, and open knobbly limestone beds which are characteristically coarse-grained and possess a more open fabric	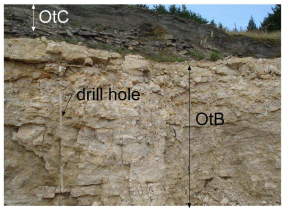 Waitanguru Limestone (OtB) McDonald's Oparure Lime Quarry (2007)
					Pakeho Limestone (OtA)	Thickest and most widespread member of the Otorohanga Limestone. Contact with overlying OtB may be sharp or gradational. Several beds occur within the member and range from basal conglomerates containing glauconite commonly found directly on Mesozoic basement, well developed flaggy limestone beds and sometimes cross-bedding with local concentrations of pectinid valves, and irregularly seamed limestone beds which appear dull and porcellanous, and contain rare oysters and disseminated Mesozoic basement pebbles	 Pakeho Limestone (OtA) McDonald's Oparure Lime Quarry (2007)

Figure 2.5 Lithostratigraphy of Otorohanga Limestone in Waitomo County. Note the use of abbreviations e.g. Ot = Otorohanga Limestone. Adapted from Nelson (1978a).

The Pakeho Limestone Member (OtA) (lowest member) is the most widespread and thickest of the three members of the Otorohanga Limestone. Three beds occur within the member and they are: (1) basal beds that are thin, gritty, glauconitic limestones that have developed where the Otorohanga Limestone rests on Mesozoic basement rocks; (2) lower flaggy limestone beds which are well developed, pure, and range from 5-10 cm thick; and (3) irregularly seamed limestone beds (Nelson, 1978a).

2.4.6 Distinguishing quarry units from geological units

McDonald's Oparure Quarry uses geological and economic names for the stratigraphic sequence in the quarry. The sequence is subdivided on the basis of the end uses of each unit, that is Kauroa Ash (overburden), Mahoenui Group mudstones (overburden), Caprock (overburden), Upper Steel (steel manufacture), Aglime (agriculture), High Grade (road stabilisation), and Lower Steel (steel manufacture). Because there are geological units in the quarry as well as economic units, Table 2.2 distinguishes the lithostratigraphic units from the economic units. Using descriptions of the three members of the Otorohanga Limestone from Nelson (1978a), the economic quarry units are correlated against members in the Table.

2.5 Economic importance of limestones

Limestone and other carbonate rocks are undoubtedly a source of one of the most useful raw materials on Earth. For example, the production of $CaCO_3$ minerals each year is of huge economic importance. Lime is used for steel making, flue gas desulphurisation, mining, construction, pulp and paper, precipitation of calcium carbonate, and water treatment. In 2006 world lime production totalled 130 million metric tons (Willet, 2007). Figure 2.6 shows the production of lime from various countries for 2006. The quarrying of carbonate rocks has dominated industrial mineral economies at certain times, for example in the early 1960s more than 70% of the total rock quarried in the United States was either limestone, dolomite, or marble (Siegel, 1967).

Table 2.2 Geological units beside the corresponding quarry unit. Ot = Otorohanga Limestone, and the following letter is equivalent to one of the members from the Otorohanga Limestone named by Nelson (1978a). They are OtC = Piopio Limestone Member, OtB = Waitanguru Limestone Member, and OtA = Pakeho Limestone Member.

Geological unit	Quarry unit
Kauroa Ash	Kauroa Ash
Mahoenui Group mudstones	Mahoenui Group mudstones
OtC	Caprock
OtB	Upper Steel
OtA	Aglime
OtA	High Grade
OtA	Lower Steel

Carbonate rocks are an important commodity as they can form permeable and porous rock units that act as storage for water aquifers (Ben-Itzhak and Gvirtzman, 2005; Kaufmann and Romanov, 2008; Beddows et al., 2007), natural gas, and petroleum products (Matavelli et al., 1992; Hood et al., 2003; Aali et al., 2006). Greater than 50% of the world's known petroleum and natural gas reservoirs are in carbonate rocks, and have been known to host past and existing metalliferous reserves (Han et al., 2007; Höll et al., 2007; Misi et al., 2007). As well as the economic importance of carbonate rocks, there is the academic aspect which in turn can often lead to the economic development and successful exploitation of carbonate rocks (Siegel, 1967).

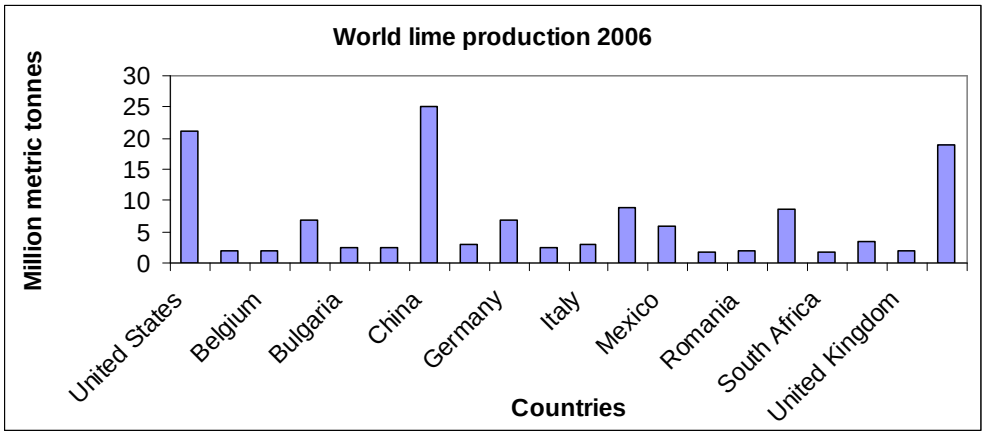

Figure 2.6 World lime production for a range of countries. Data sourced from Willett (2007).

2.5.1 Uses of carbonate rocks

The uses of carbonate rocks as a raw material have become indispensable on a global level in many industries. Their importance has led to the industrial development of specifically limestone, dolomite, and marble (Naydowski et al., 2001). The list of uses is impressive, amounting to several hundred. Figure 2.7 shows a selection of the many uses of limestone. To a greater or lesser extent limestone is involved in almost every industry (Naydowski et al., 2001). Global production of carbonate rocks is principally driven by this industrial demand. Industries especially dependent on limestone include the steel, building, and road construction industries.

2.5.2 Limestones in New Zealand

New Zealand has prospective mineral deposits and is well known for gold, silver, coal, iron sand, aggregate, limestone, clay, dolomite, pumice, salt, serpentinite, and zeolite production (Crowns Minerals, 2001). In the five years since 1999, the value of coal, metals, and industrial minerals has increased by 47% due to the production of strong aggregates and construction materials and rises in commodity prices. Figure 2.8 shows the relative contribution of carbonate rock to industrial mineral production. Aggregate products such as limestone underpins infrastructure and building development, and limestone used as a fertiliser supports the agriculture industry. In particular, cement is one of the most important materials, having an end value greater than $100 million per year (Christie and Barker, 2007).

A strong growth in construction in 2004 led to an 11% increase from 2003 in the production of limestone for marl and cement (Crowns Minerals, 2005). An annual report on mineral commodities from 2005/2006 shows that the production of agricultural limestone has increased by 35.6% to 2.59 million tonnes (Crowns Minerals, 2007b). A total of 4.1 million tonnes of limestone for industry boosts New Zealand's mineral economy by greater than $70 million each year (Crowns Minerals, 2007a). Figure 2.9 shows the percentage of limestone produced that is used by four main industry sectors.

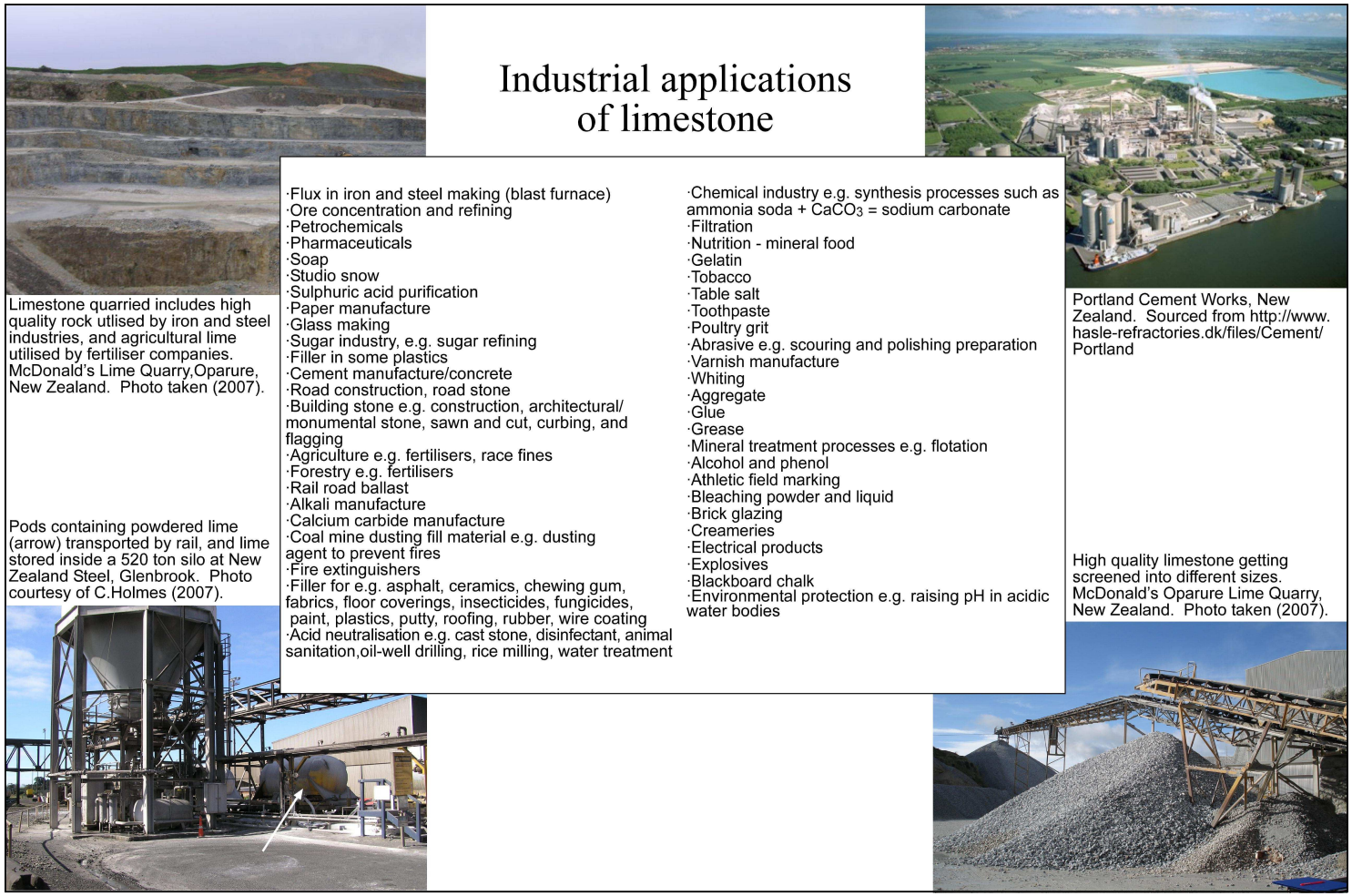

Figure 2.7 Industrial uses of limestone as a raw material. Data adapted from Siegel (1967) and Rohleder and Huwald (2001).

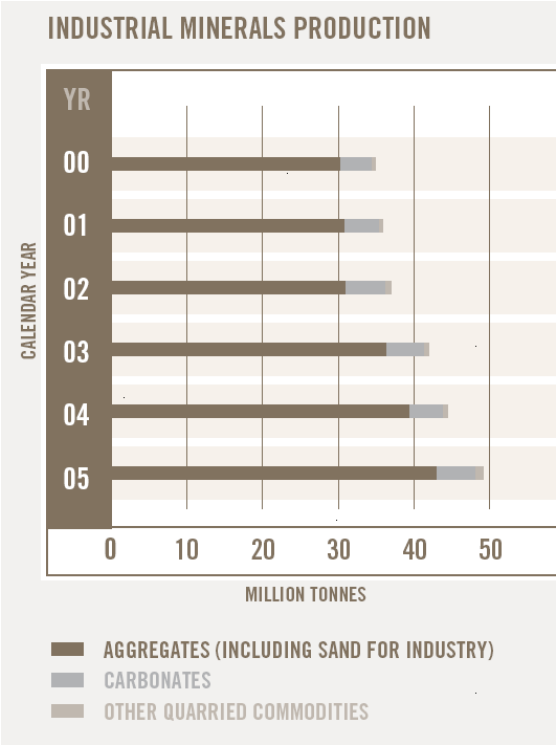

Figure 2.8 The contribution of aggregates, carbonates, and other quarried commodities to industrial mineral production in New Zealand. Sourced from Crowns Minerals (2007b).

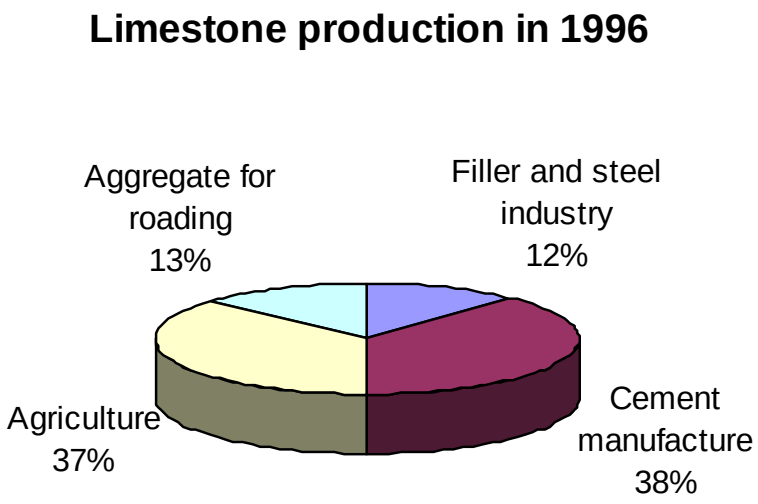

Figure 2.9 Limestone production in the four main industry sectors. Values sourced from Christie and Brathwaite (1999).

Though the limestone resource in New Zealand has not yet been quantified, it is estimated to be large (in the tens of millions of tonnes or more in known limestone areas), and sufficient to meet demands of the foreseeable future of local demand in New Zealand (Christie and Barker, 2007).

The main areas that produce limestone in New Zealand are Northland, Waikato, southern Hawkes Bay, Wairarapa, North West Nelson, Westland, Canterbury, and Southland (Thompson et al., 1995). Marble (metamorphosed limestone) is also produced, including formations of Ordovician age in North West Nelson and Fiordland. Figure 2.10 shows the occurrence of limestone, marble, and dolomite deposits and locations of production. The best quality large tonnage deposit in New Zealand is in the South Waikato where $CaCO_3$ contents of 95-100% commonly occur (Christie et al., 2001). These deposits are generally produced for fertiliser, roading aggregate, steel production, and hydrated lime manufacture.

There are four main commercial end products for limestone in New Zealand, namely limestone, lime/quicklime, slaked lime, and hydraulic lime. Table 2.3 defines each limestone type, their associated uses, and the properties of each type.

In addition to the extraction of limestone for various uses, limestone caves in New Zealand are a major attraction for the tourism industry with some, like the Waitomo Caves and Ruakuri Caves, having international appeal. Other attractive limestone outcrops include the Mangapahoe Natural Bridge near Waitomo, and Pancake Rocks at Punakaiki (Figure 2.11) on the West Coast of the South Island (Christie et al., 2001).

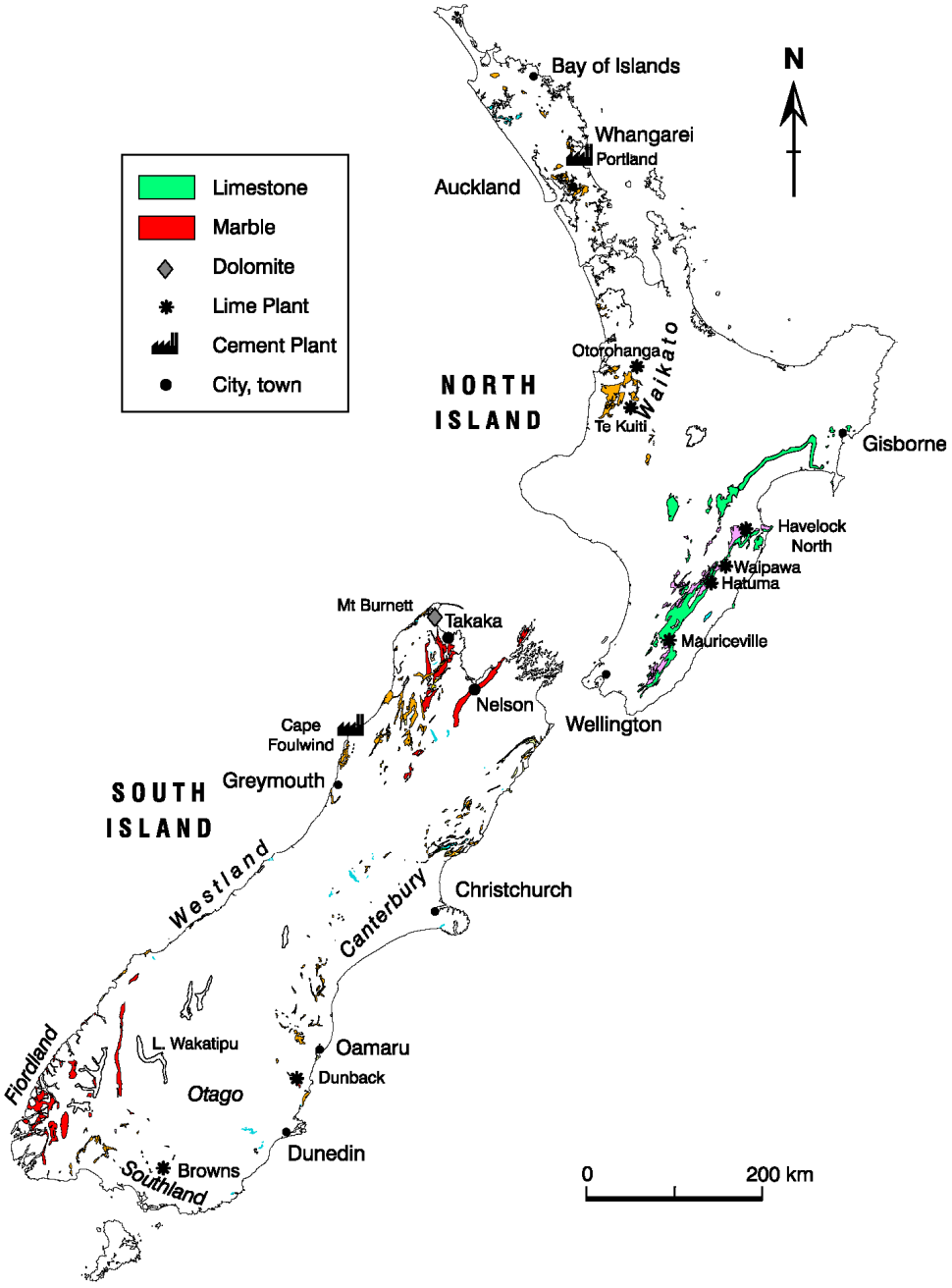

Figure 2.10 Locations of limestone, marble, and dolomite deposits, and their production plants in New Zealand. Sourced from Christie et al. (2001).

Table 2.3 Commercial types of limestone used in New Zealand. Adapted from Christie et al. (2001).

Commerical type	Composition	Formation	Uses
Limestone	$CaCO_3$	Deposition of shells in seawater that have experienced burial forming a sedimentary rock	Filler for carpet backings, surface coatings for paper, plastics, paint, rubber and glass, aggregate, agriculture, roading, building stone, cement manufacture
Lime/quicklime	CaO	Produced by heating 'calcining' to 1000°C to expel carbon dioxide and water	Steel manufacture, paper pulp manufacture, or mortar, soil stabilisation, sugar industry, water treatment, and in the cyanide process in gold and silver mining
Slaked lime	$Ca(OH)_2$	Quicklime converted to stable slake lime to form calcium hydroxide by the addition of water; easily transported	Sugar industry, water treatment and leather tanning
Hydraulic lime	Impure limestone containing silica and alumina, clay sized commonly	Forms a cement under water; produced by heating	Cement for concrete emplaced under water

Figure 2.11 Pancake Rocks, Punakaiki, West Coast, South Island, New Zealand. Photo courtesy of Bowman (2008).

2.6 McDonald's Oparure Lime Quarry

2.6.1 Site description

Figure 2.12 shows the layout of the study site. Topography of the study area includes a broad west-east trending ridge crest where the quarry occupies the eastern reaches of the ridge. Steep gullies incise the ridge to the north and south. In the Were Block a long narrow tomo has been identified (Figure 2.12).

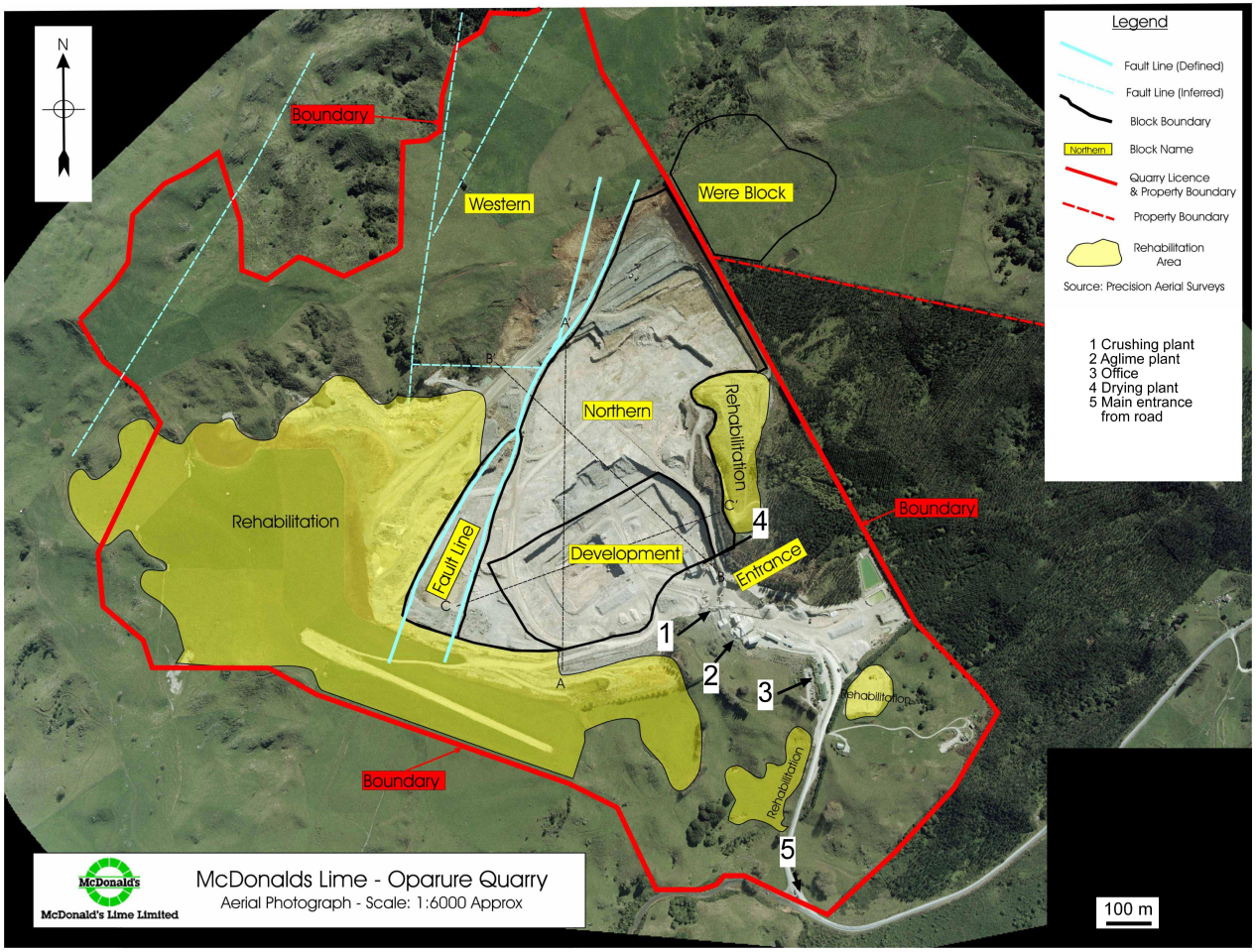

Figure 2.12 Aerial photo site map of McDonald's Oparure Lime Quarry. Map (adapted) courtesy of Ormiston Associates Ltd (2002).

The main excavated area occurs in the Development Block, shown on Figure 2.12. It comprises several working floors and has been developed in a northwesterly direction up to the current boundary. A large area has been rehabilitated, including the construction of an airstrip to the south of the quarry within the rehabilitation area. A crushing plant, Aglime plant, drying plant, administrative office, and entrance are situated towards the eastern side of the site.

2.6.2 Quarry geology

The geology at McDonald's Oparure Lime Quarry is similar to the geology of the Te Kuiti district (Figure 2.3). Quaternary undifferentiated ashes of the Kauroa Ash are underlain by early Miocene Mahoenui Group mudstones. Together the Kauroa Ash and Mahoenui Group mudstones comprise the overburden units at the quarry. Underlying the soft calcareous mudstones of the Mahoenui Group is the latest Oligocene-earliest Miocene aged Otorohanga Limestone from the Te Kuiti Group where the contact is generally conformable, showing a gradual increase in the mud component in the top lithologies of the Otorohanga Limestone. The Otorohanga Limestone is the target geological unit. In view of the fact that the Otorohanga Limestone is itself internally variable, it has been further subdivided by the quarry operators into different grades of limestone according to their chemical composition and end uses. From the bottom upwards these grades are as follows: Lower Steel, High Grade, Aglime, Upper Steel, and Caprock (Figure 2.13). Being thin and of relatively low quality, the Caprock is also treated as overburden. Beneath the Lower Steel grade unit there is more limestone belonging to the Otorohanga Limestone, but currently it holds no interest to the quarry as it is not yet economic to exploit. It is named the Sub-economic unit in this study.

Figure 2.13 shows a generalised stratigraphic sequence at the quarry derived from a combination of drill core and field observations. The Otorohanga Limestone is exposed within the excavated area of the quarry and commonly in outcrop in surrounding farmland. Drill cores taken within and outside the quarry show that Aotea Sandstone (oldest), Orahiri Limestone, and an equivalent of Waitomo Sandstone occur beneath the quarry. The Waitomo Sandstone equivalent is a sandy limestone in this location.

Geological unit	Geological group	Quarry unit	Description	Thickness (m)	Depositional setting	Age
Kauroa Ash		Over burden	Extremely weathered tephra deposits and paleosols. Unconformably overlies Taumatamarie Formation	8-12	Terrestrial	Quaternary
Taumatamarie Formation	Mahoenui Group	Over burden	Weakly bedded to massive, calcareous fine to sandy mudstone, gradational contact with underlying Otorohanga Limestone	10-25	Marine	Early Miocene
Otorohanga Limestone	Te Kuiti Group	Caprock (overburden)	Capping limestone, medium strength, light grey flaggy limestone. Irregular contact with underlying Upper Steel unit	2-5	Marine	Latest Oligocene-earliest Miocene
		Upper Steel	Strong, yellow to white limestone, flaggy or knobbly/blocky. Lacks jointing. Wavy contact with underlying Aglime unit	~ 10		
		Aglime	Strong, bluish grey, light orange brown limestone. Flaggy, joint sets well developed (parallel fault). Wavy bedding surfaces. Contact with underlying High Grade is not obvious. Dissolution staining common, lenses of higher quality rock	10-20		
		High Grade	Lenses of higher and lower quality rock, gradual changes in chemical composition. Flaggy, wavy discontinuous bedding surfaces. Joint sets well developed. Contact with underlying Lower Steel not obvious	15-25		
		Lower Steel	Light yellow to white, flaggy, cross bedded, well developed joint sets although fewer sets than High Grade and Aglime units	10-15		
		Subeconomic	Blue-grey rock, slightly sandy limestone, bivalves common	15-20		
*Waitomo Sandstone Equivalent		-	Massive, brown grey, calcareous glauconitic fine-medium grained sandy limestone	5-15		Late-Oligocene
Orahiri Limestone		-	Grey, flaggy limestone with oyster beds	5-14		
Aotea Sandstone		-	Massive calcareous, glauconitic fine-medium grained sandstone	70+		Latest Eocene-late-Oligocene

Figure 2.13 Generalised stratigraphic sequence at McDonald's Oparure Lime Quarry. Note thicknesses are based on drill hole data.

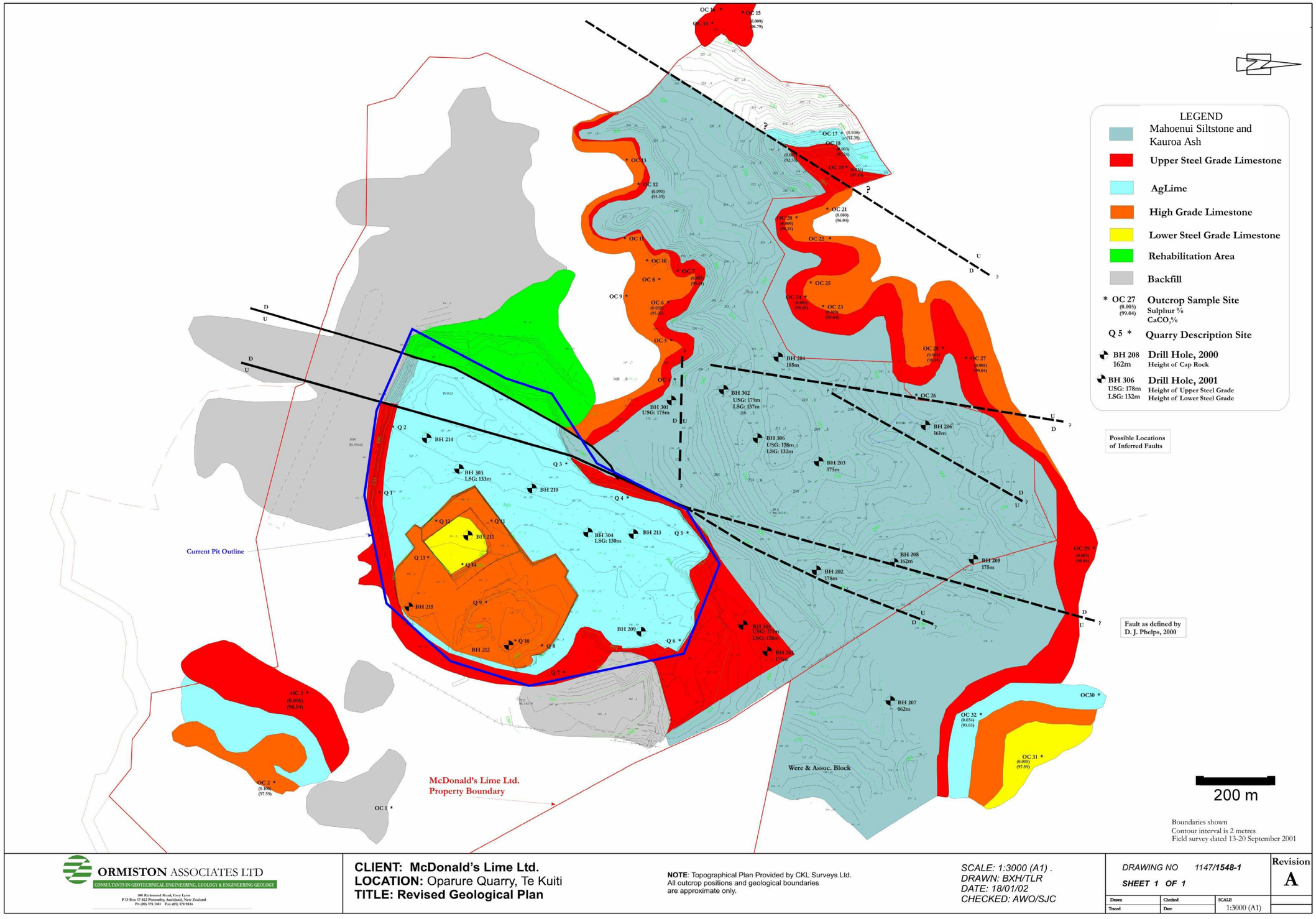

Figure 2.14 Mapped geology of quarry units at McDonald's Oparure Lime Quarry. Map (adapted) courtesy of Ormiston Associates Ltd (2002).

Unfortunately previous drilling programmes have not drilled deep enough to confirm whether the Whaingaroa Siltstone or any other Lower Te Kuiti Group formations are present. Mesozoic basement rocks of the Murihiku Supergroup certainly underlie the quarry at depth.

Along the western side of the quarry, a single fault trending north-south splits into two separate normal faults towards the south. The faults are significant and downthrow the main limestone resource to the west by approximately 20 m. There appears to have been limited lateral movement along the faults.

Several other faults have been inferred further west of the main fault and are shown on Figure 2.14. Figure 2.14 shows the mapped distribution of the quarry units in the Otorohanga Limestone and the overlying Mahoenui Group and Kauroa Ash as in 2002. Although the area within the McDonald's Lime property boundary is subject to change due to quarry operations, the mapped area outside the property boundary at present holds true. Locations of past drill holes and sampling areas are also shown (Figure 2.14).

2.6.3 End-uses of quarried limestones

McDonald's Lime Ltd produces mainly agricultural limestone (Aglime), high grade limestone (High Grade), and steel quality limestone (Upper and Lower Steel). The end use applications are many across a range of industries, including steel manufacturing, gold mining, roading, pulp and paper, water treatment, mortar and planters, asphalt and manufacture, fellmongery, tanning, aerial application, fillers and extenders, farm races, animal feeds, and landscapes.

Each quarry limestone unit has a broadly unique chemical composition which typically dictates its end usage. The major industries that use the limestones generally require the purchased limestone to meet their particular specifications (Figure 2.15). Consequently, it is necessary for McDonald's Lime Ltd to maintain a strict quality (chemical) control on the quarried limestone resource. Particularly stringent requirements on the elemental composition of raw materials are imposed by the iron and steel industry.

Quarry unit	Chemical constituents				Approx. thickness (m)	Product end use
	$CaCO_3$	CaO	SO_3	SiO_2		
Caprock	>95%	variable	variable	variable	2-5	
Upper Steel	>95%	>53.48%	<0.09%	<1.7%	~10	Steel manufacture
Aglime	90%+	50.40%+	No limit	No limit	10-20	Fertiliser, aggregate, industrial filler
High Grade	94-98%	52.64-53.48%	<1.5%	No limit	15-25	Pulp manufacture, wastewater treatment, soil stabilisation,
Lower Steel	>95%	>53.48%	<0.09%	<1.7%	10-15	Steel manufacture

Note: Caprock is regarded as overburden and is not kiln fed.

Figure 2.15 Quarry limestone units and their quality limits for kiln feed. Adapted from Simonson (2005).

2.7 Steel manufacture at New Zealand Steel, Glenbrook

There are several main phases involved in the process of changing iron into steel. They are iron manufacture, steel manufacture, and post-slab casting processing. How they relate is shown in Figure 2.16. Figure 2.17 shows a flow diagram of the processes involved in the first two phases. Given that this study is limestone based, the green circles in Figure 2.16 represent the locations in which burnt lime and limestone is used. Green circle 1 shows where high grade limestone chip (High Grade unit from McDonald's Oparure Lime Quarry) is added, and green circle 2 shows where steel grade burnt lime (derived from Upper and Lower Steel limestone units from McDonald's Oparure Lime Quarry which has been burnt (limestone that has been heated to ~1000ºC to expel H_2O and CO_2) at the Otorohanga Plant in Otorohanga and added by means of a blowing phase.

2.7.1 Use of limestone as a flux in steel manufacture

In general, the principal role of limestone in the steel manufacturing process is to act as a fluxing agent. Carbonate rock is commonly used as a fluxing agent for removal of silica, alumina, and other undesirable impurities from ore rock. Limestone is therefore an essential material for purifying ore rock.

Limestone as a fluxing agent is used in production of pig iron from iron ore in the blast furnace process where a fluid slag is formed. Impurities such as silica, aluminium, and sulphur dissolve leaving the iron relatively pure (Christie et al.,

2001). The slag floats to the top of the molten iron and is scooped off. Ideally the limestone should contain less than 1.5% silica and <0.1% of sulphur and phosphorous. However, due to logistics in individual operations, more silica and up to 0.5% sulphur may be tolerated (Siegel, 1967). Some operations may use limestone with 4-15% $MgCO_3$ as a flux; however, a purer limestone, if available at the same cost, would contribute to a more efficient process.

In open hearth smelting, limestone flux is ideally 98% $CaCO_3$ with 2% impurities such as alumina, silica, and traces of phosphorous. However, areas where purer material is not available, flux may contain 5-10% $MgCO_3$, 1.5% alumina, and 1% silica. The capacity for phosphorous removal is lessened by higher $MgCO_3$ content and, as a consequence, more flux must be used. In some instances if transportation costs for acquiring purer fluxing agent are significant, a less efficient material will be employed (Siegel, 1967). Nonetheless, the concentrations of each element present are all part of a unique balance that needs to be perfected to achieve success in the art of steel manufacture.

2.7.2 Negative effects of silica at New Zealand Steel - "The silica issue"

The chemical composition and temperature of the slag determines the chemistry and hence quality of the steel. It is crucial for the slag to form as it removes undesirable elements (e.g. silica, titanium, and sulphur). Phosphorous is also undesirable and can be fixed by CaO (burnt lime). The relative amounts of each element determine the physical property of the molten slag, such as its melting temperature, viscosity, and fluidity, which in turn determines the ability to remove impurities from the iron. An important slag parameter is the basicity index which involves the ratio of basic elements (i.e. CaO, MgO) to acidic elements (i.e. SiO_2, TiO_2, and Al_2O_3).

At the New Zealand Steel plant, to achieve maximum impurity removal the ratio of burnt lime to impurities is generally 3.2:1. This is important as elements such as silica have a major effect on the ability of CaO to fix phosphorous. As shown in Figures 2.16 and 2.17, burnt lime, natural gas, and oxygen are blown into the floor of the Kombiniert/Combined Oxygen Blowing Maxhuette (KOBM) vessel to assist the fluxing process (Figure 2.18).

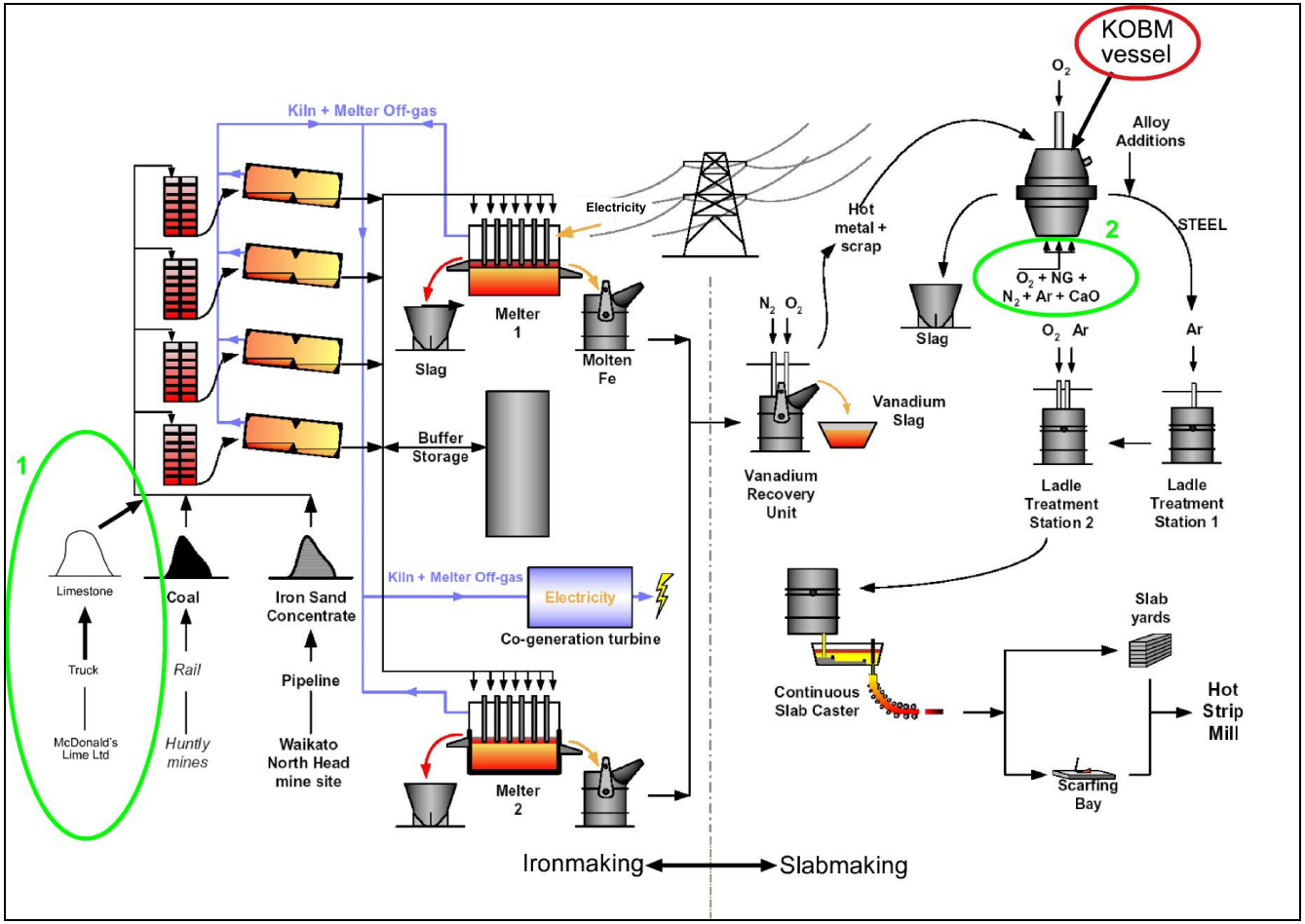

Figure 2.16 Flow diagram of the iron-steel making process. NG = natural gas. Green circle 1 = addition of High Grade limestone chip to coal stockpile, green circle 2 = addition of steel grade burnt lime to steel making vessel (KOBM). Adapted from Williams (2004a).

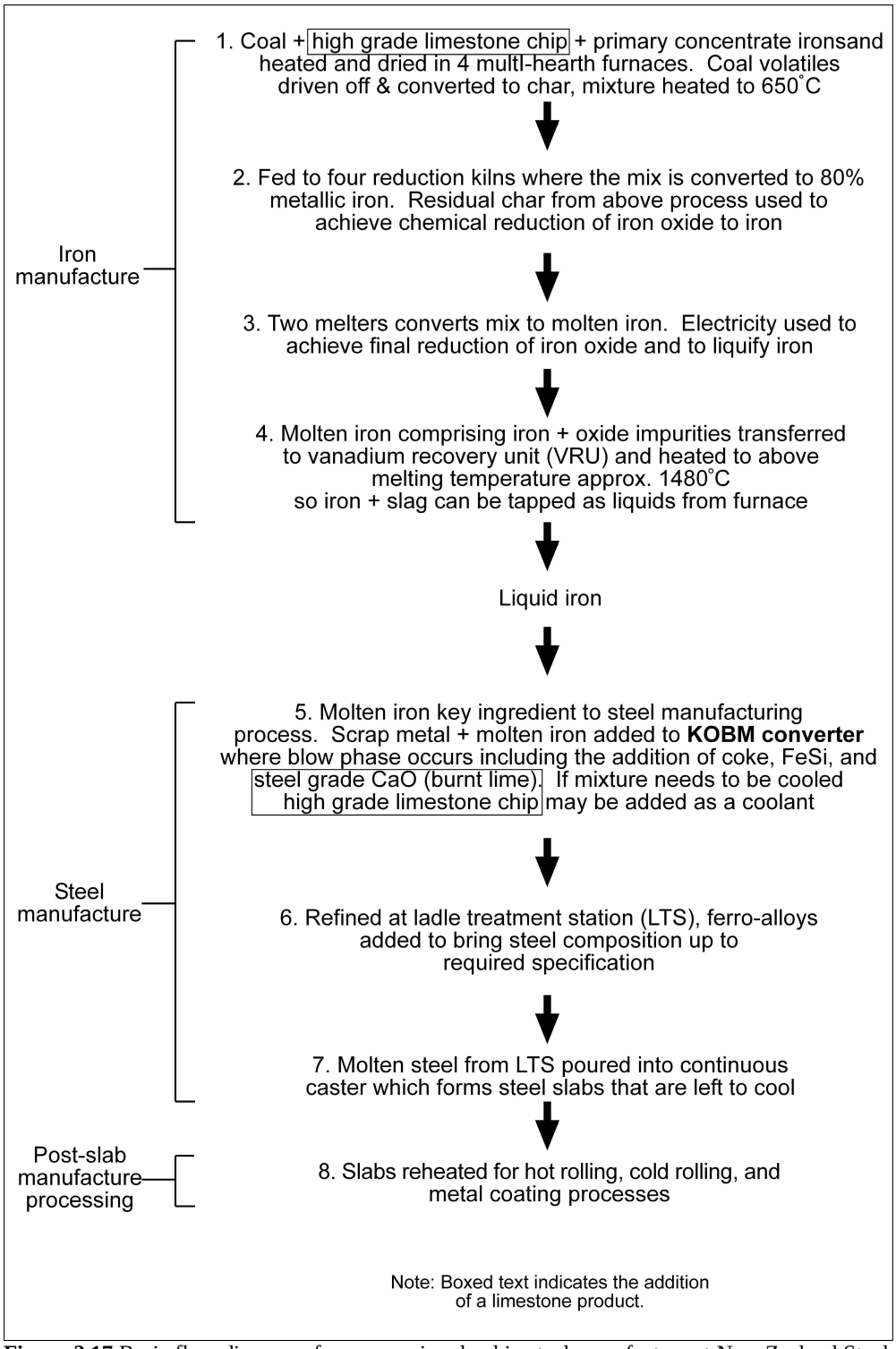

Figure 2.17 Basic flow diagram of processes involved in steel manufacture at New Zealand Steel, Glenbrook. Adapted from Williams (2004a).

The burnt lime, along with natural gas and oxygen, are blown through six injection ports known as tuyeres (stainless steel pipes) at extremely high pressures of approximately 20 bars. The tuyeres are located at the base of the KOBM vessel and feed the burnt lime into the vessel. The high pressure ensures that the molten iron does not fall out the bottom of the KOBM vessel and prevents blockages (Holmes, pers. comm., 2007).

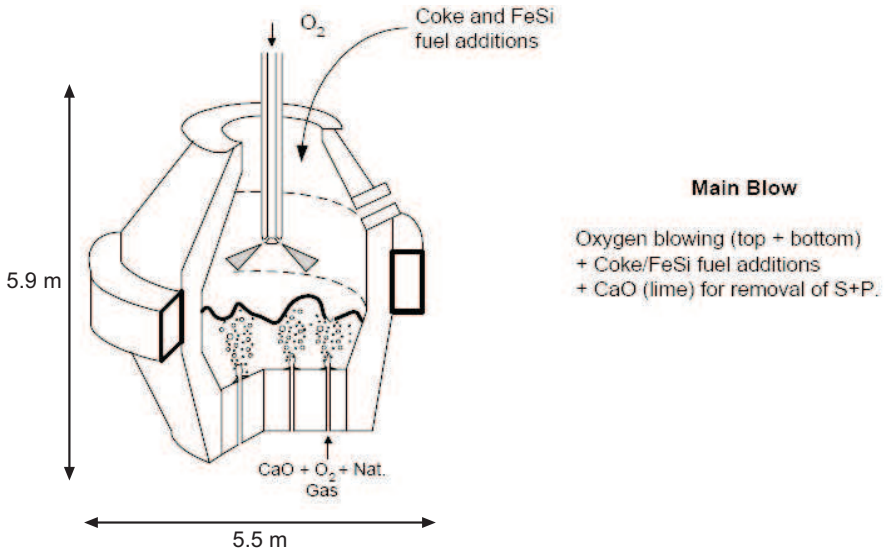

Figure 2.18 Schematic of Kombiniert/combined Oxygen Blowing Maxhette (KOBM) vessel and entry point for blowing phase. Adapted from Williams (2004a).

The necessary high pressure in the pipes, however, poses an additional problem. It has been identified that any silica present in the burnt lime causes mechanical wear to the tuyeres leading to the KOBM vessel. The silica has an abrasive effect, abrading the tuyeres over time (Figure 2.19). A silica content of 2.2% in the burnt lime has a noticeable effect on the tuyeres (Holmes, pers. comm., 2007).

In addition to burnt lime passing through the tuyeres, burnt lime is transported through pipes elsewhere in the steel manufacturing plant by compressed air. Any silica in the burnt lime creates internal wear inside these pipes as well, particularly at bends in the profile.

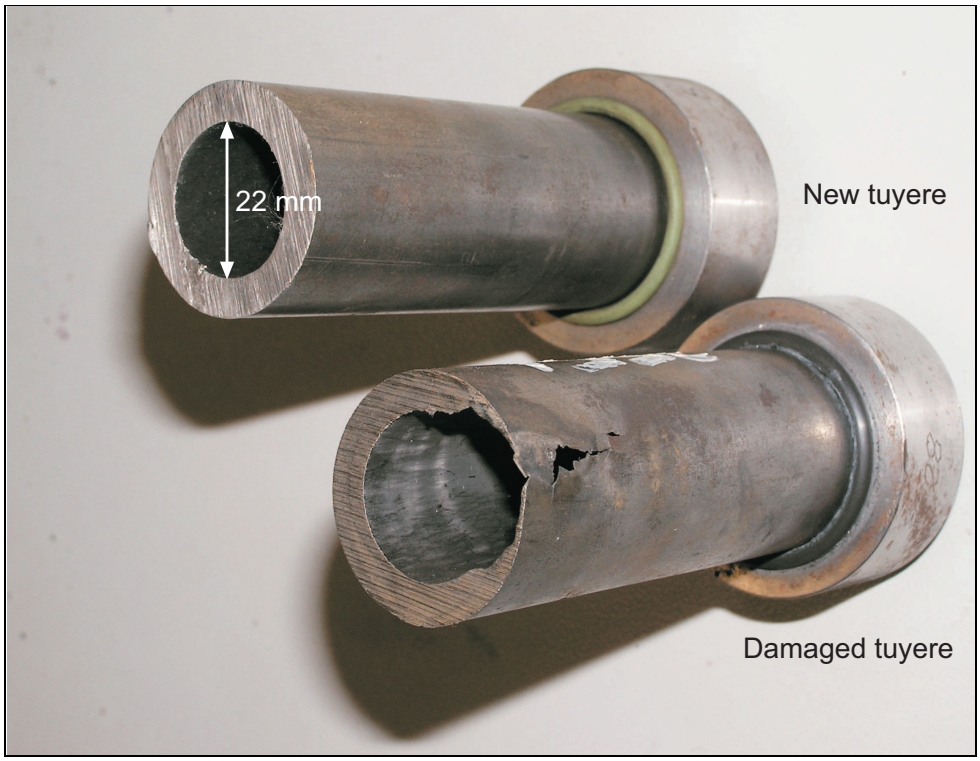

Figure 2.19 Injection ports (tuyeres) from KOBM. Photo courtesy of Holmes (2007).

The above information concerning the steel manufacturing process provides good insight to the validity of the stringent quality restrictions that McDonald's Lime Quarry must adhere to in order to maintain and fulfil their customers requirements. Each economic unit is not entirely uniform in composition, with lenses or layers of other rock quality commonly occurring within the dominant rock type. Furthermore, the continuity of units is not consistent, and can be further complicated by faulting within the quarry. All of these issues add further challenges to maintaining quality restrictions for all the quarry limestone units.

CHAPTER THREE

Discontinuities in outcrop

3.1 Introduction

The quarry limestone units are fundamentally made up of host rock and discontinuities. Discontinuities comprise any naturally occurring feature that separates the intact rock blocks within a rock mass, such as joints, faults, or bedding planes (Wyllie and Mah, 2004). The host rock is therefore the intact rock blocks between the discontinuities. Four types of discontinuity have been identified within the limestone resource, namely dissolution seams, stylolites, joints, and caves. All are associated with silica. This chapter discusses the characteristics and formation of these discontinuity types. Results from rock mass description and discontinuities found in the quarry limestones (i.e. Upper Steel, Aglime, High Grade, and Lower Steel) are also presented, along with the methods used and the rock parameters measured.

3.1.1 Pressure dissolution

As carbonate sediments are buried they undergo changes in fabric, composition, rigidity, and porosity (Wanless, 1981). Elastic strain increases at grain contacts during sediment burial, leading to an increase in solubility at grain contacts (chemical reaction) (Moore, 2001). Ions released in solution from the dissolution at grain contacts are then carried (diffused) away to a place of less elastic strain, and precipitated as a cement on an unstrained grain (Moore, 2001). Precipitation of the new cement occurs in nearby pore space, either as interparticle (between grains), or as intraparticle (within grains, commonly inside the chambers of skeletal material) cement (Nelson, 1978a). These events occur as a result of pressure dissolution. Pressure dissolution is a chemical compaction process responsible for the formation of diagenetic (all processes that affect a sediment after deposition, excluding metamorphism) dissolution seams and stylolites. It is a phenomenon that has been studied by many workers, including Barrett (1964),

Bathurst (1971), Buxton and Sibley (1981), Wanless (1981), and Evans and Elmore (2006). It is also responsible for porosity reduction in carbonate sequences, and can be an important source of cement below burial depths of 500 m (Dodd and Nelson, 1998). Figure 3.1 shows some sketches of typical pressure dissolution features (stylolites, wispy seams, and solution seams) encountered in limestones in the subsurface.

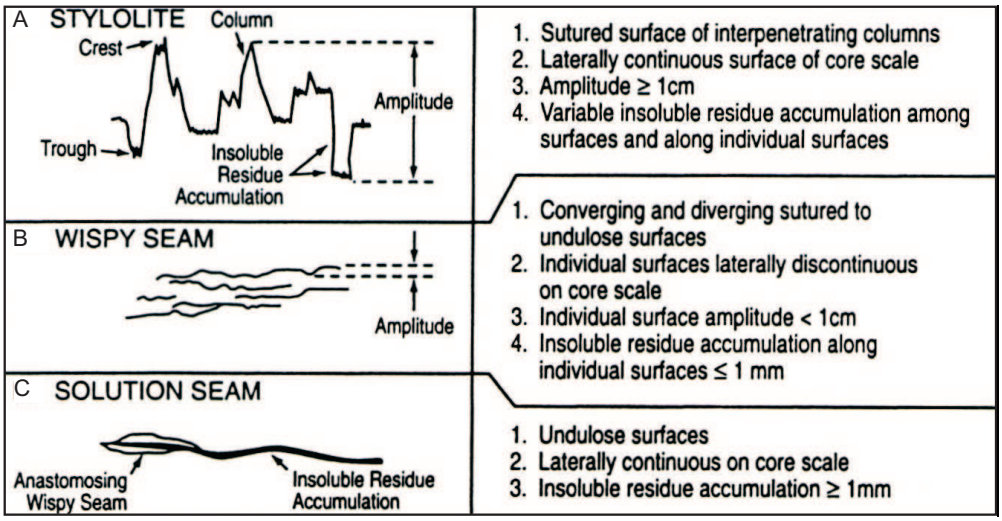

Figure 3.1 Pressure dissolution features commonly found in limestones that have undergone burial diagenesis. Sketches of a stylolite (A), wispy dissolution seam, referred to as a diffuse seam in this study (B), and a solution seam (C) which is referred to as a discrete seam in this study. A list of key characteristics for each feature is shown on the right. Adapted from Moore (2001).

3.1.2 Dissolution seams

In limestones, preferential dissolution of calcitic skeletal fragments can occur at levels in a deposit that are relatively enriched in terrigenous or silica materials. These levels of dissolution often relate closely to a primary sedimentary control, such as the alternation of carbonate sediments (e.g. storm emplaced) and siliceous/siliciclastic sediments (e.g. background sedimentation between the deposition of carbonate sediments). The influence of siliceous (silica) sediments promotes accelerated pressure dissolution in carbonate sediments, and is a well known phenomenon (Dodd and Nelson, 1998; Tada and Siever, 1989; Hood et al., 2003). Pressure dissolution of these deposits can result in a sedimentary layering of two characteristic bed types, namely thicker limestone beds relatively poor in silica (flags), and thinner beds relatively enriched in silica materials involving quartz, feldspar, clay, and glauconite minerals, called dissolution seams (Dodd and Nelson, 1998). Solution or dissolution seams can occur in limestones

containing clay or silt sized particles where pressure dissolution removes $CaCO_3$ and leaves behind and concentrates the insoluble material (Barrett, 1964). These burial features have been recorded as beginning to develop at subsurface depths of about 190 m (in marly lithologies) but are better developed at approximately 340 m (Nicolaides and Wallace, 1997). The flags are hard, well cemented, diagenetically modified limestone beds commonly 5-20 cm thick, and are bound by dissolution seams which are smoothly undulating surfaces that preferentially weather upon subaerial exposure, producing a flaggy appearance in outcrop (flaggy limestones). Flaggy limestones are common in the Te Kuiti Group limestones in the Waitomo-Te Anga area (Barrett, 1964). The thin dissolution seams are approximately 0.5-15 mm thick and generally separate the limestone flags (Dodd and Nelson, 1998). Thinner seams (<1 mm) can occur close together, merging and diverging irregularly, while thicker seams (>1 mm) are characterised by gently undulating surfaces with low relief (Barrett, 1964). Skeletal material near seams does not cross the seams, but is truncated by them; the truncated material has been removed by dissolution. Penetration of skeletal fragments (due to compaction) also results in the concentration of insoluble material at the surfaces of these contacts.

The relatively silica enriched dissolution seams (cement donor beds) are thought to supply the majority of $CaCO_3$ cement precipitated in the limestone flags (cement receptor beds) (Nelson, 1978b). The alternation of flags and dissolution seam represents stratification that is partly post-depositional in origin that can reflect original primary sediment characteristics. Lithologic differences and sedimentary structures such as cross bedding in primary sediments for example, are emphasised and modified by selective interparticle solution, also producing rhythmic alternation of two contrasting, differentially cemented sedimentary fabrics (Nelson, 1978b).

3.1.3 Stylolites

Stylolites are also a product of burial diagenesis, forming as a result of pressure dissolution. Like dissolution seams these features contain insoluble residue concentrated along surfaces. However, the key difference is that stylolites are characterised by a serrated or sutured surface and are much thinner (<1 mm thick),

and therefore, contain less siliceous material than dissolution seams. In 3D, it is observed as a column of one rock mass that fits into sockets in the other rock mass (Bathurst, 1995). The suture amplitude is typically greater than the local grain diameter. Stylolites die out laterally as the suture amplitude diminishes (Bathurst, 1995). Surface relief can range from 1 mm – decimetres, and in outcrop appears as planar to interweaving sutured surfaces (Wanless, 1981). Stylolites cut through grains and matrix indiscriminately. They form in pure limestones that contain low clay content (Bathurst, 1995). Stylolites occur perpendicular to the axis of maximum principal stress (e.g. burial stresses form subhorizontal stylolites), and grow in intact rock which has been made rigid by some degree of cementation but also retains some porosity and permeability (Bathurst, 1995). Previous studies indicate that depths of 800-1000 m are required for the formation of stylolites (Nicolaides and Wallace, 1997).

Some subhorizontal stylolites correspond with depositional bedding planes, and others mark lithological changes (Bathurst, 1995). However, other occurrences are unrelated to bedding and are roughly parallel or oblique to bedding planes. This is evident in cross cutting relationships of contrasting lithologies (Bathurst, 1995).

Subvertical stylolites can also occur and sometimes in the same limestone that contains subhorizontal stylolites (as observed in the quarry limestones). Subvertical stylolites form as a result of compressive tectonic stresses. The formation of these tectonic stylolites is controlled by deformation forces other than simple burial forces (Bathurst, 1995). With the exception of orientation, the characteristics of stylolites of both subhorizontal and subvertical orientations are generally the same.

3.1.4 Vertical joints

Sedimentary rocks such as limestones experience a long history of modification over time. A typical sequence of sedimentary rock formation involves deposition in some surface sedimentary environment (e.g. seafloor) followed by burial of up to several kilometres, heat and pressure, and subsequent uplift to the surface again (Wyllie and Mah, 2004). As a result of these events the rock mass is often

affected by deformation processes such as folding and faulting. These strains can exceed the rock strength and consequently cause the rock to fracture thereby forming discontinuities (Wyllie and Mah, 2004). These fractures can contain infills, either chemically precipitated minerals such as calcite or material that has washed in from an external source. Joints are simple fractures that do not show evidence of shear (no observable relative movement) or mineralisation, typically occurring perpendicular to bedding of sedimentary rocks (e.g. limestones) (Odonne et al., 2007). They can intersect or terminate at primary surfaces such as bedding, whereas faults show observable displacement (Wyllie and Mah, 2004). Joints are commonly found in deformed areas, but also in regions that are undeformed (Gillespie et al., 2001). They are the most common brittle structures found in the Earth's upper crust (Becker and Gross, 1996).

A joint set refers to a series of parallel joints, and two or more intersecting sets produce a joint system (Wylie and Mah, 2004). Joint sets are characterised by consistency of orientations over wide areas (Arlegui and Simon, 2001).

There are many reasons why joints are studied. They can be used to map regional stress trajectories to help identify regions of stress. Joints occur in shallow tectonic environments, sometimes in relatively undeformed basins and platforms, and as a consequence, are often the only available structures for mapping orientation of paleostress (Arlegui and Simon, 2001). Joints also play a dominant role in the failure process of a rock mass; low strength areas in the rock mass are caused by the presence and arrangement of rock joints (Gehle and Kutter, 2003). This influence of joints in a rock mass is the reason why they are often studied in detail in rock mechanics research (Gehle and Kutter, 2003). Joints also play an important role for subsurface flow of fluids such as hydrocarbons and ground water (Becker and Gross, 1996). Joints can also act as migration pathways for overlying materials such as Kauroa Ash and Mahoenui Group mudstones (overburden quarry units), to wash down into underlying limestone units. Their quantification becomes important and applicable to a range of societal needs (e.g. oil production, and the assessment of environmental problems such as groundwater contamination). Fluid flow is influenced by fracture or joint density and orientation, and therefore factors that control joint spacing are often studied (Becker and Gross, 1996).

3.1.5 Caves

By definition, caves are natural holes in the ground large enough for human entry (Waltham et al., 2005). Caves are a weathering feature resulting from the dissolution of $CaCO_3$, which occurs as a result of acidic waters penetrating limestones. Caves and associated karst (landscapes created on soluble rock with efficient underground drainage; Waltham et al., 2005) are widespread in the western central North Island of New Zealand centred on the King Country region, and particularly Waitomo County (Williams, 2004b). The following account gives details on the origin of these caves and karst landscapes, based on the work by Williams (2004b).

As discussed in Chapter 2, Section 2.2 carbonate sediments were deposited during the Oligocene (33.7-23.8 million years ago) and early Miocene (23.8-16.4 million years ago), followed by deposition of thick calcareous mudstones (Mahoenui Group) and sandstones (Mokau Group and Mohakatino Formation) in the King Country region (Nelson, 1993). Uplift initiated in the Miocene (as a result of tectonic deformation along the Pacific-Australian plate boundary) resulted in widespread erosion decreasing the formerly extensive limestone outcrop to discontinuous patches (Williams, 2004b). By the Pliocene, stripping of the overlying clastic sediments was well advanced in the western North Island, and karst evolved on limestone outcrops about 1-3 million years after the limestones became exposed. In the King Country region karst is predominantly a doline or sinkhole (closed depression in karst) landscape with dendritic cave systems with well developed passages. This karst evolved since the Pliocene in rocks of about 100 m in stratigraphic thickness (karst support rocks).

Karst evolution has been intermittently interrupted by burial with thick sheets of welded ignimbrites (Coromandel Volcanic Zone from early Miocene to Pliocene, and Taupo Volcanic Zone from the mid Pleistocene), and ashfall deposits from North Island volcanics, decoupling karst from the hydrogeochemical system for a period of several hundred thousand years. The welded ignimbrites provided a relatively impermeable cover that prohibited percolation. Karst in the King Country region remained buried until exhumed and re-exposed by late Quaternary erosion.

The main karst supporting rocks are the Orahiri and Otorohanga Limestones in the Te Kuiti Group. Williams (2004b) explains that the limestones have closely spaced joints and therefore have a very high fissure frequency. Fissures are defined as cavities opened by dissolution along a rock discontinuity (e.g. joint), but are smaller than a cave passage (Waltham et al., 2005). Fissures in the limestones have been exploited by hydrogeological processes, and together with other discontinuities such as faults permit doline initiation by providing a preferred drainage path for infiltrating water (Williams, 2004b).

The overlying Mahoenui Group mudstones (overburden at the quarry) contain pyrite nodules which yield acidic percolation that interacts with limestone to form gypsum. 100 years ago the landscape was entirely covered in dense evergreen forest (80% cleared at present) (Williams, 2004b). Forested, mild, humid conditions together with acidic solution from the pyrite nodules further aided karstification, the formation of percolation pathways, and cave initiation during the Miocene (Williams, 2004b).

Due to Upper Tertiary and Quaternary tectonic and erosional processes, limestone outcrop in the King Country is a fragmented mosaic covering 400 km^2. Karstified limestone connected to a hydrogeochemical system beneath the surface further extends the karstified area to 800 km^2 (Williams, 2004b).

3.2 Methods for describing rock mass properties

3.2.1 Selection criteria for choosing rock mass sites

Rock mass work was carried out on four limestone quarry units, namely Upper Steel, Aglime, High Grade, and Lower Steel. Figure 3.2 shows the locations of the faces measured. The Caprock unit, located stratigraphically above the Upper Steel, is not included in the rock mass description as it is thin, difficult to access, and is treated as overburden by the quarry operations. Each face was selected based on availability, accessibility, safety, orientation, and most importantly freshness.

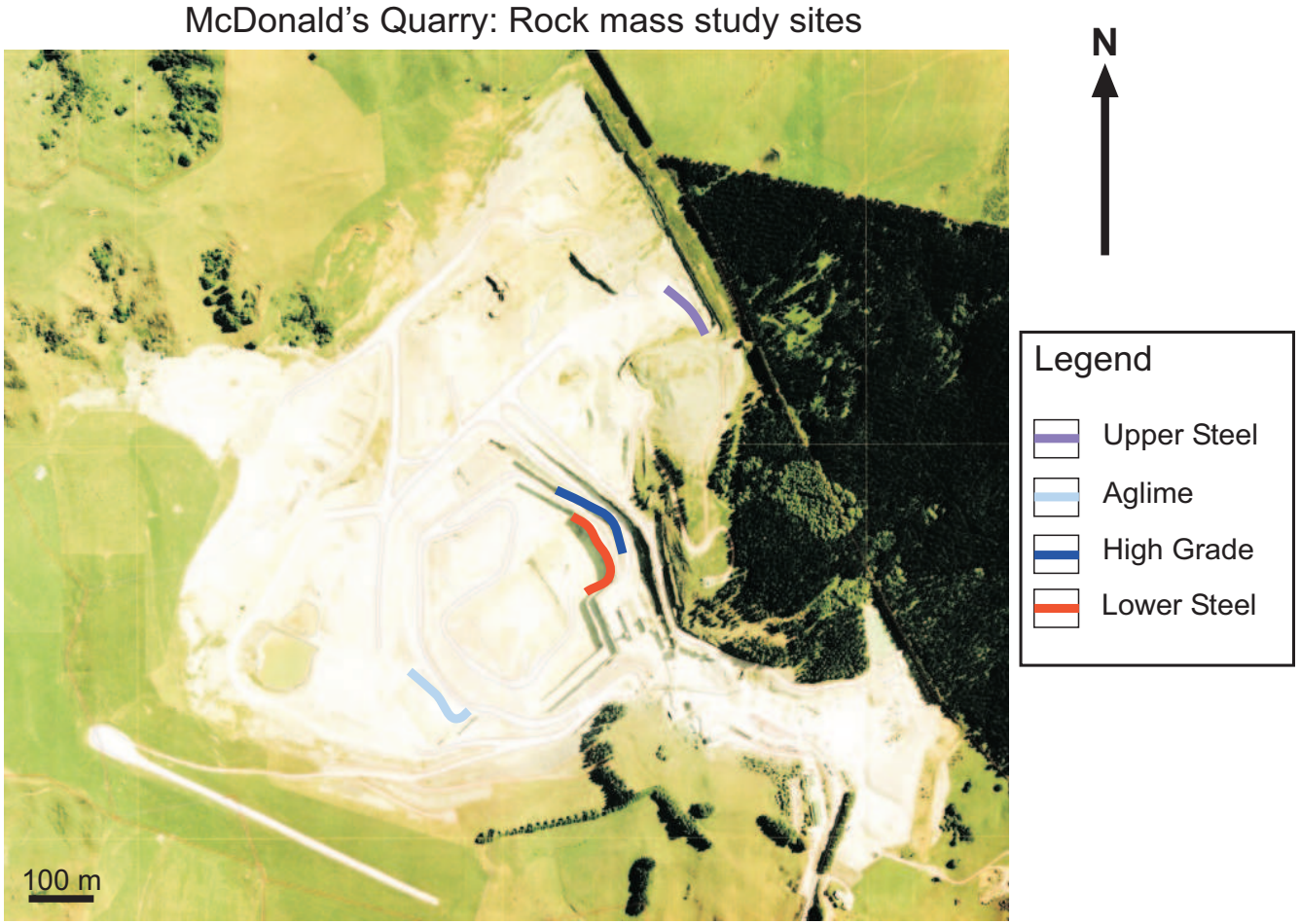

Figure 3.2 Aerial photo of McDonald's Oparure Lime Quarry showing rock mass study sites within various exposed limestone units (i.e. Upper Steel, Aglime, High Grade, and Lower Steel). Aerial photo taken February 2007. Courtesy of McDonald's Lime Ltd.

Consequently the selection criteria used to choose the sites have the following characteristics: 1) faces trending perpendicular (roughly east-west) to the main joint sets in the quarry; 2) faces that were not being actively worked at the time of data collection; 3) faces that were relatively fresh, such as faces that ideally had recently been blasted or had not experienced long term weathering; and 4) safe areas that could be accessed on foot. Criteria 3 emphasises the fact that some faces located particularly along high traffic areas appear significantly different to freshly blasted faces. This makes it difficult to fully assess weathering features such as discolouration on faces. Due to traffic from large machinery (e.g. diggers and dump trucks), older faces commonly possess surface accumulations including quarry dust that has accumulated over time. Discontinuity infills are also likely to be compromised and washed away over time due to weathering processes.

In addition, joints or fractures become more relaxed (e.g. from vibrations of heavy vehicles and blasting) and open compared to freshly blasted faces due to long periods of exposure. Fresh faces are therefore the best to describe as they represent better original characteristics.

Rock mass description was used to determine the rock mass and discontinuities present in each quarry unit. Discontinuities such as joints were measured using the scanline mapping method to determine joint spacing and orientation (Wylie and Mah, 2004). This, together with other rock mass parameters described and calculations used are discussed below. The procedures are more fully defined by Wylie and Mah (2004).

3.2.2 Scanline mapping

All field measurements and descriptions were recorded onto data sheets (e.g. Figure 3.3). Scanlines, sometimes referred to as line mapping, were used to collect statistical data of geological features (e.g. joint spacing, joint orientation), and to describe infills, to create a representative data set for each quarry limestone unit. Horizontal scanlines involved stretching a tape measure horizontally across a face to map discontinuities that intersect the line.

Date	30.03.07
Location:	McDonald's Quarry, Lower Steel Grade, northern face
Joint type:	Master joint
Northing	N6316251
Easting	E2691507
Elevation (m)	118
Orient. of face	85/302
Line No.	1

Flag No.	Flag thick. (mm)	Joint No.	Distance (m)	App. joint spac. (m)	No. of joints	Dip°	Dip direction°	Aperture Width (mm)	Infill	Moisture
		1	0.0	0.0	3-4	75	184	40	yes	moist
		2	11.7	11.7	5	85	152	2-5	yes	seepage
		3	22.3	10.5	1	85	332	5-10	none	dry
		4	26.8	4.5	1-2	86	164	3-6	none	wet
		5	31.2	4.4	3-4	90	148	3-5	none	dry-sl. Moist
		6	40.2	9.0	3-6	86	133	20	yes	dry
		7	47.1	6.9	1-4	86	136	10-30	none	dry
		8	51.9	4.9	3	85	334	10-20	none	dry

Comments e.g. colour, infill material, weathering, discolouration

black discolouration near bottom, infill light brown clay
joints closely spaced, clay infill
aperture tight higher up
raining on the day
thin brown lining on joint surface

Figure 3.3 Example of a field data sheet used to record rock mass data for master joints in the Lower Steel, unit, northern face. App = Apparent, spac. = spacing, sl. = slightly. Joint zones involve more than one joint. Other field data sheets can be found in Appendix C-3.1.

Line lengths were usually between 50 and 100 m. The line length was based both on the size of the exposure (face) and the number of master joints which ranged from approximately 10-20.

After initial field observations it was decided that there were two distinct joint types in the quarry. These were at different scales including: (1) large vertical 'master' joints that appeared to be continuous throughout the rock mass typically terminating at the top of the quarry benches. These joints are accentuated by zones (typically 0.3 m either side of joint) of discolouration (oxidation) along joint surfaces, and appear more relaxed (open) than small joints (other type); and (2) small vertical joints which are much smaller in vertical length than master joints and terminate over much shorter distances, typically being persistent across several or more limestone flags. These joints have tighter apertures, and oxidation and infills are less common or rarer than the master joints. In this study, small joints represent the joints between master joints. Every master joint was measured on a horizontal scanline for each site exposure, whilst two horizontal scanlines for small joints were measured for each quarry unit exposure. Each scanline for small joints started at one of the master joints chosen at random, and finished at the neighbouring master joint (e.g. between master joints 3 and 4).

Some vertical scanlines were also measured where the tape was hung vertically. These scanlines measured the vertical spacing between flags. Vertical scanlines were also measured at two sites for each quarry unit exposure, again a location (usually midway) between two master joints chosen at random.

Rock mass parameters

The **dip and dip direction** (perpendicular to strike) indicates orientation of a discontinuity surface. If the dip of a surface is 88° and dip direction 132°, the orientation is expressed as 88/132. Orientation was measured using a Freiberger Präzision smechanik geological compass. The compass lid is placed against the surface and moved until it is level, which is indicated when the centring bubble is within the circle. The needle is then released to indicate dip direction, and the dip simply read off the scale on the hinge (Wylie and Mah, 2004). Magnetic readings are adjusted, for example for a magnetic declination of 20° east, 20° is added to

the dip direction reading to obtain true north (Wylie and Mah, 2004). The estimated value of magnetic declination for the location of the quarry is 20° 11' E (National Geophysical Data Center, 2007).

Dip and dip direction were plotted onto equatorial equal-area contoured stereonet plots in the Rockware software program (RW2002) to indicate dominant joint set(s), which shows as a cluster of poles (points or measurements) on the stereonet. To determine the average orientation in each cluster, a series of bearing and distance measurements were undertaken. This was achieved by using the measuring tools in the Rockware software.

A bearing was measured for each cluster to give the direction to the pole cluster and 180° was added or subtracted to find the dip direction of the plane(s).

A distance was also measured for each cluster, and later converted to a dip value using the following equation (707 is the default stereonet size):

$$\alpha = 2 \times \sin^{-1} (\text{distance}/ 707)$$

Rock type includes features such as origin of the rock, colour, and mineralogy. The rock type of each limestone unit in this study has been described as being either sparry (dominant cement in the limestone is spar) defined as a mosaic of calcite crystals, coarsely crystalline to appear transparent in thin section; or micritic (dominant cement type in the limestone is micrite) defined as microcrystalline calcite, defined as having crystals 1-4 μm in diameter and is formed as organic or inorganic precipitates or as a product of the breakdown of coarser carbonate grains (Scholle and Ulmer-Scholle, 2003).

Discontinuity types include joints, faults, bedding, and other discontinuities identified at the quarry (i.e. dissolution seams, stylolites, joints, and caves).

Discontinuity spacing is the distance separating adjacent discontinuities. Direct measurements of the distance from the start of the scanline to each discontinuity are recorded, and apparent spacings can be calculated from these. In order to account for the relative orientation between the face and the discontinuities an

average true spacing is calculated for each discontinuity set which gives the perpendicular distance between joints based on the average orientation for that set. This is determined from the following equation:

$S = S_{app}\sin\theta$

S_{app} is the measured apparent spacing, and θ is the angle between the face and strike of discontinuities (Wylie and Mah, 2004). An average true spacing is calculated for each joint set identified.

Persistence is the measure of the continuous length of the discontinuity. This is estimated for master and small joints.

Aperture is the perpendicular distance separating the adjacent rock walls of an open discontinuity that is air or water filled.

Seepage is locations of water flow, and areas where there is evidence of water flow (e.g. iron oxidation staining; orange or yellow in colour).

Infilling/width is the perpendicular distance between adjacent rock walls or the width of a filled discontinuity. Any infill materials are described, and are sampled for mineralogical, textural, and chemical composition analyses (discussed later in Chapter 5, Section 5.4).

Weathering is the reduction of rock strength due to disintegration and decomposition of the rock mass. Features of decomposition weathering include rocks that contain iron which oxidises to produce a yellow or orange discolouration, or carbonation involving the dissolution of limestone. Weathering is important in terms of the formation of clay minerals which are often associated with joints.

3.3 Upper Steel rock mass results

Field data sheets containing rock mass information about the Upper Steel limestone are given in Appendix C-3.1.

Weathering, rock type, and bedding: The Upper Steel limestone unit is predominantly an oxidised, moderately weathered, creamy white to light yellow sparry limestone. Water was observed seeping and dripping from the unit at the time of observation. The rock mass shows two different bedding features. Moving down the stratigraphy, the upper rock mass has a knobbly appearance (Figure 3.4D) equivalent to the Waitanguru Limestone member (OtB) of the Otorohanga Limestone (Nelson, 1978a). From a distance it appears to be slightly flaggy, however, on closer inspection, the limestone is stylolitised which is often referred to as pseudo-bedding. The knobbly limestone is lensoidal and comes and goes across the Upper Steel unit in the quarry; however, it maintains a similar stratigraphic level where observed. The lower rock mass is flaggy and dominated by predominantly subhorizontal flags.

Dip and dip direction data are plotted on stereonets for the limestone flags (Appendix C-3.2). Bearing and distance measurements used to calculate dip and dip direction from the stereonets are summarised in Appendix C-3.3. The lower rock mass is characterised by large, irregular, approximately horizontal flags (0° dip) ranging from 100-560 mm thick, with an average thickness of 240 mm (Figure 3.4C). These flags occupy the lower two or three metres of the unit, comparable to the Piopio Limestone member (OtA) of the Otorohanga Limestone (Nelson, 1978a).

Discontinuities: Discontinuities in the Upper Steel unit include dissolution seams (Figure 3.5), subvertical and subhorizontal (Figure 3.6) stylolites, and karst features. Seams are typically discrete and concentrated, moist to wet, and comprise rusty brown silt, ranging from <2-3 mm in thickness, although thicknesses up to 15 mm were recorded on other site visits but are not typical. Stylolites of both orientations have similar characteristics (i.e. contain rusty orange clay and are typically <1 mm in thickness). No intact caves were observed, however, there are many collapsed dolines and fissures (Waltham et al., 2005) trending north-south along the northwestern face (Figure 3.4A, B, E). Collapsed dolines are defined as sinkholes which have formed by collapse of rock into a cave passage or chamber (Waltham et al., 2005). The faces are concave and smoothly curved, and share characteristics typical of karst features. The features are 1 m high by 1 m or more wide.

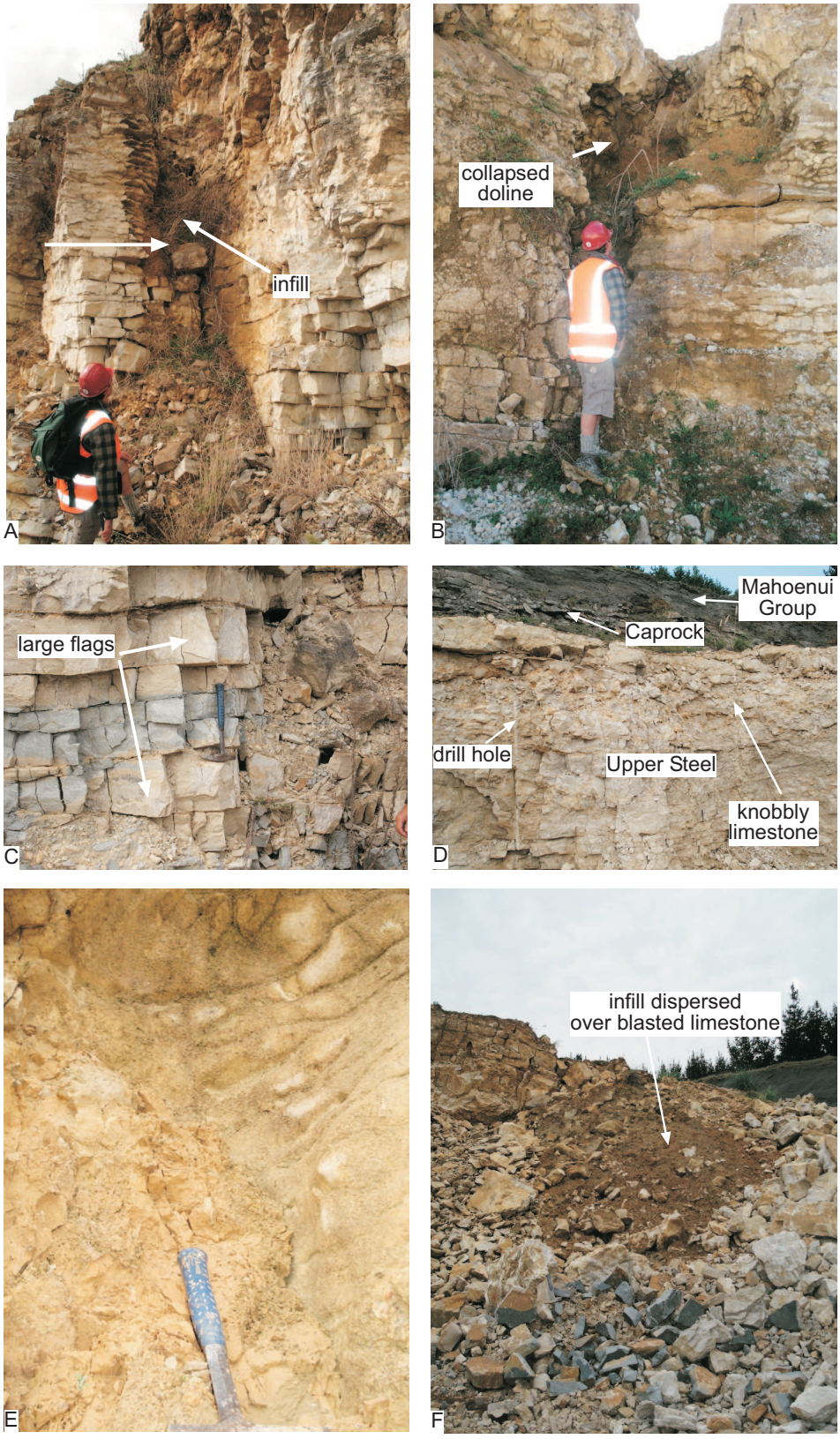

Figure 3.4 Rock mass characteristics of the Upper Steel limestone unit: (A) Infill material washed into a fissure in the limestone, eastern face, north end. (B) Collapsed doline (karst feature), eastern face, north end. (C) Thick limestone flags (modified beds), eastern face, north end. (D) Knobbly, massive limestone, northern face, north end. (E) Infill washed into cave feature, western face, north end. (F) Infill probably sourced from overburden units (Mahoenui Group mudstone or Kauroa Ash) on blasted Upper Steel limestone, north end.

Blasting has likely removed the main cave structures and 'left over' a portion of the caves. Infills are found inside or outside these features (Figure 3.4A, E, and F) and have been sampled for textural and chemical analysis. The infills are moist to wet, orange brown clays, and are about 0.3 m thick, although thickness is difficult to determine. The Upper Steel unit appears to have no master joint systems.

Non-discontinuity features: Porous zones ranging from 10-40 mm thick are common in the Upper Steel unit where calcite cement has been leached from the limestone along discrete horizons. The porous areas consist of brownish leached friable material (Figure 3.5) often associated with dissolution seams (e.g. the porous zones typically occur equally either side of a seam).

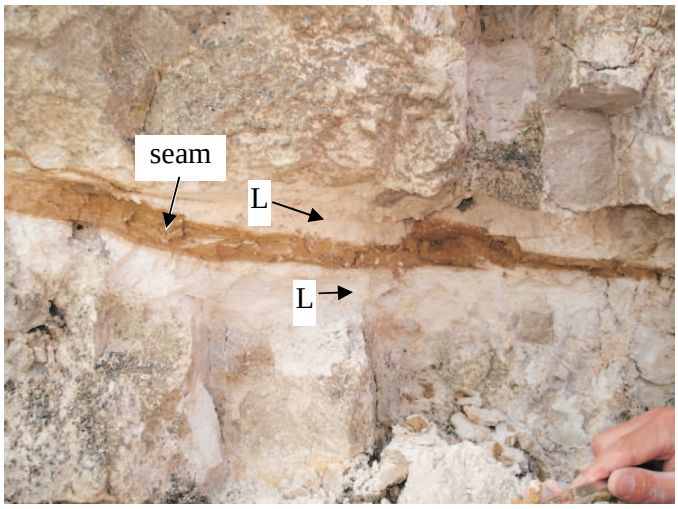

Figure 3.5 Discrete dissolution seam (arrowed) in the Upper Steel limestone unit with leached limestone (L) either side. The seam is rusty brown, containing silt and clay sized grains.

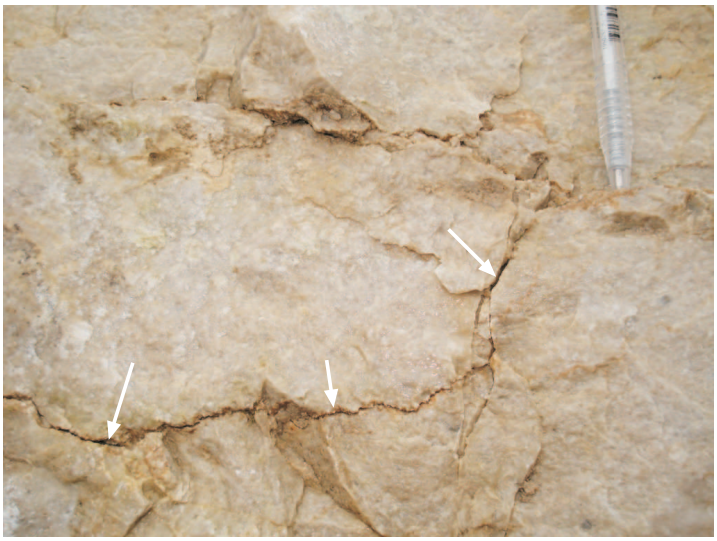

Figure 3.6 A subhorizontal stylolite in the Upper Steel limestone unit. The stylolite (see white arrows) is a thin feature (<1 mm thick), and contains clay mineral.

3.4 Aglime rock mass results

Field data sheets containing rock mass information about the Aglime limestone unit are given in Appendix C-3.1.

Weathering, rock type, and bedding: The Aglime unit is typically an unoxidised, fresh, blue-grey micritic limestone. The unit was dry at the time of observation. Oxidised zones of orange to light brown rock are common, particularly along vertical master joint (Figure 3.8A and B) surfaces and occasionally on small joints. These discolouration zones occur on both sides of a master joint surface, and are typically 0.30 m wide (approximately). Because this width is an apparent width, the true width perpendicular to joints is likely to be smaller. Aglime has flaggy bedding characteristics which are variable across the quarry ranging from approximately horizontal (0-10° dip) to wavy lozenge shaped flags occurring with a range of thicknesses (i.e. 20-200 mm), and an average thickness of 100 mm. Both flag types (horizontal and wavy lozenge shaped) usually occur at the same site close to each other, or appear as disorganised bedding where a mixture of the two flag types occurs together.

Discontinuities: Discontinuities in the Aglime unit include dissolution seams and joints. Seams are mainly discrete (Figure 3.7), condensed, dry to damp, medium brown or rusty orange or grey clay, ranging from 2-10 mm in thickness. Diffuse wispy seams (Figure 3.8D) are observed at one location, within large blasted boulders up to 1 m or more in size. No stylolites or caves were identified in the Aglime unit. Some surface coatings/accumulations were sampled in the Aglime limestone unit that were not joint infills. These accumulations comprise quarry dust sourced from blasting and vehicular traffic (see Chapter 5, Section 5.4.7 for results for mineral composition, and Chapter 6, Section 6.6.6 for results for chemical composition).

Joints: To identify joint sets, dip and dip direction data are plotted on stereonets for master and small joints (Appendix C-3.2). Bearing and distance measurements used to calculate dip and dip direction from the stereonets are summarised in Appendix C-3.3. Using apparent spacing, dip direction of the face (from field measurements), and the dip direction of each joint set(s), true spacing has been calculated (summarised in Appendix C-3.4).

Master and small joints both occur in the Aglime. One master joint set is identified with orientations of 86/322 and 74/128. Average true joint spacing is 0.31 ± 0.03 m. Master joint persistence is estimated as >20 m and joint aperture from 0-50 mm. All master joint surfaces observed ranged between dry and moist, and contained infills that are slightly moist to moist. Infills varied from light medium brown to cream to orange silt, to rusty orange clay, to limestone fragments (pebble size). Other infills include white brittle material (up to 15 mm thick), re-precipitated calcite (up to 50 mm thick), and palygorskite (clay mineral) occupying up to 30 mm of the width of the filled discontinuity.

One small joint set is identified with orientations of 85/149 and 88/323. Average true joint spacing is 0.30 ± 0.08 m. Small joint persistence was estimated at <1 m terminating against limestone flags, and the joint width from 0-20 mm. All small joints are dry and most contained infills. Infills are typically rusty orange clay (up to 4 mm thick), palygorskite (5-20 mm thick), and re-precipitated calcite (15 mm thick).

Figure 3.7 Thick discrete dissolution seams (white arrows) in the Aglime limestone unit that have preferentially weathered back to produce a flaggy limestone, northern face, on road to drying plant.

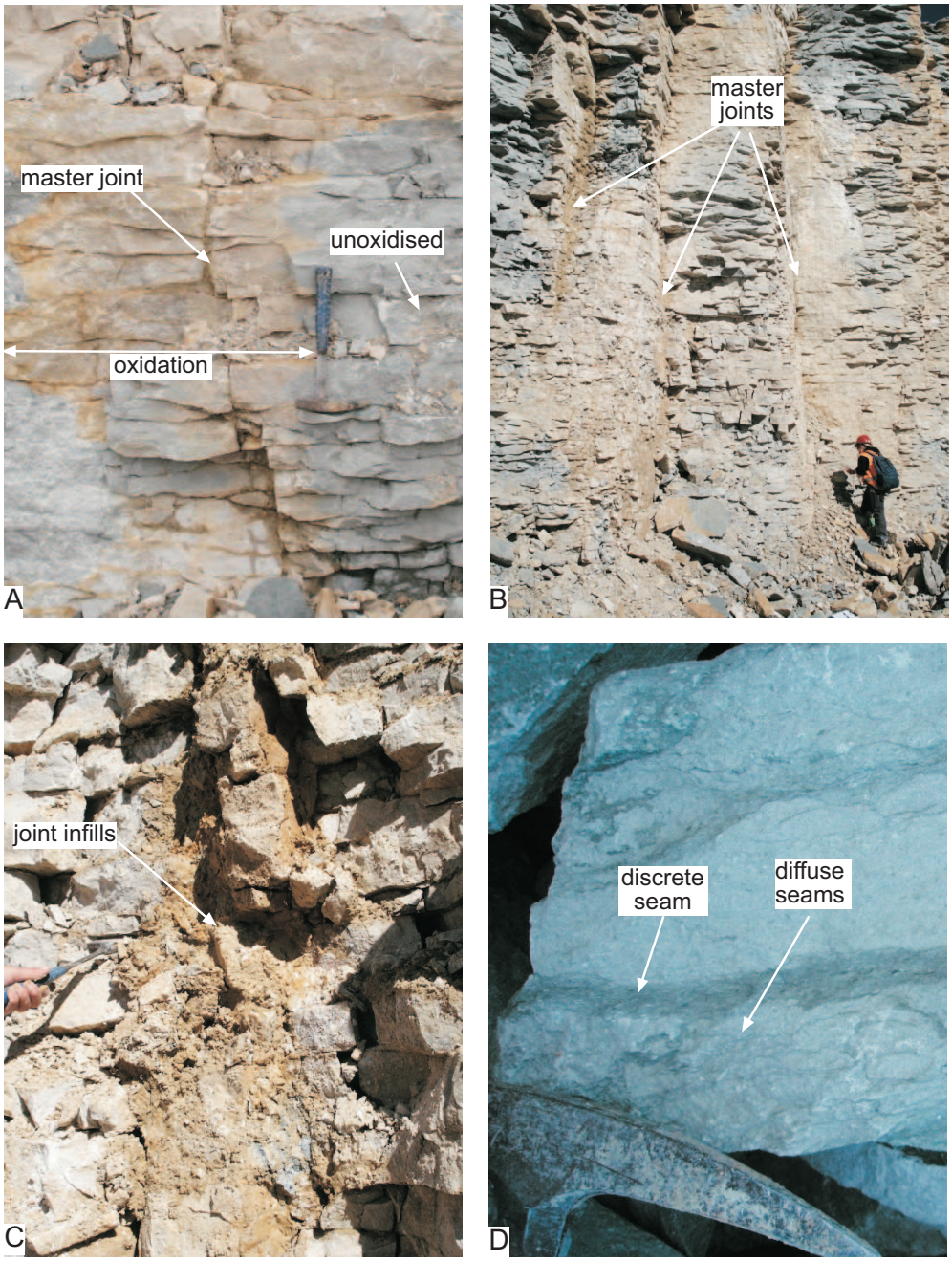

Figure 3.8 Rock mass characteristics (arrowed) in the Aglime limestone unit: (A) Discolouration from the oxidation of rock along a vertical master joint, compared with unoxidised rock either side of this zone of discolouration, southern face. (B) Vertical master joints, southern face. (C) Infill material in a vertical master joint typically consisting of brownish orange clays, white clays such as palygorskite, and limestone fragments, southern face. (D) Diffuse and discrete dissolution seams in a blasted limestone boulder. Note the wispy appearance of the diffuse seams. Western bench.

3.5 High Grade rock mass results

Field data sheets containing rock mass information about the High Grade limestone unit are given in Appendix C-3.1.

Weathering, rock type, and bedding: The High Grade limestone unit is typically an unoxidised, fresh, blue-grey sparry limestone. Oxidised orange to light brown rock is common, particularly along joint surfaces. Discolouration is present either side of many master joints, similarly to the Aglime unit, occurring up to 0.3 m wide either side. The face ranged from dry to moist at time of observation. High Grade limestone unit looks similar to the Aglime unit, and has variable flag characteristics across the quarry. These range from subhorizontal regular thickness flags to wavy lozenge shaped (Figure 3.9D) flags involving thicknesses ranging from 50-220 mm with an average of 120 mm.

Discontinuities: Discontinuities in the High Grade limestone unit include dissolution seams, caves, and joints. Seams are thinner (typically <10 mm thick) than the seams in the Aglime, but thicker than in the Upper Steel (which have seams that are typically <3 mm thick). Seams are discrete and concentrated, dry to moist, dark blue grey or rusty brown silts or clays ranging from 2-4 mm in thickness. One large cave approximately 2.5 m high and 2 m wide was identified (western side, second bench) and is shown in Figure 3.10. Cave infills are moist to wet, medium brown to orange clays. No stylolites were observed in the High Grade.

Joints: Once again to identify joint sets, dip and dip direction data were plotted on stereonets for master and small joints (Appendix C-3.2). Bearing and distance measurements used to calculate dip and dip direction from the stereonets are summarised in Appendix C-3.3. Using apparent spacing, dip direction of the face (from field measurements), and the dip direction of each joint set(s), true spacing has been calculated (summarised in Appendix C-3.4).

Master and small joints both occur in the High Grade limestone unit. One master joint set is identified with orientations of 85/141 and 87/324. Average true joint spacing is 2.45 ± 0.32 m.

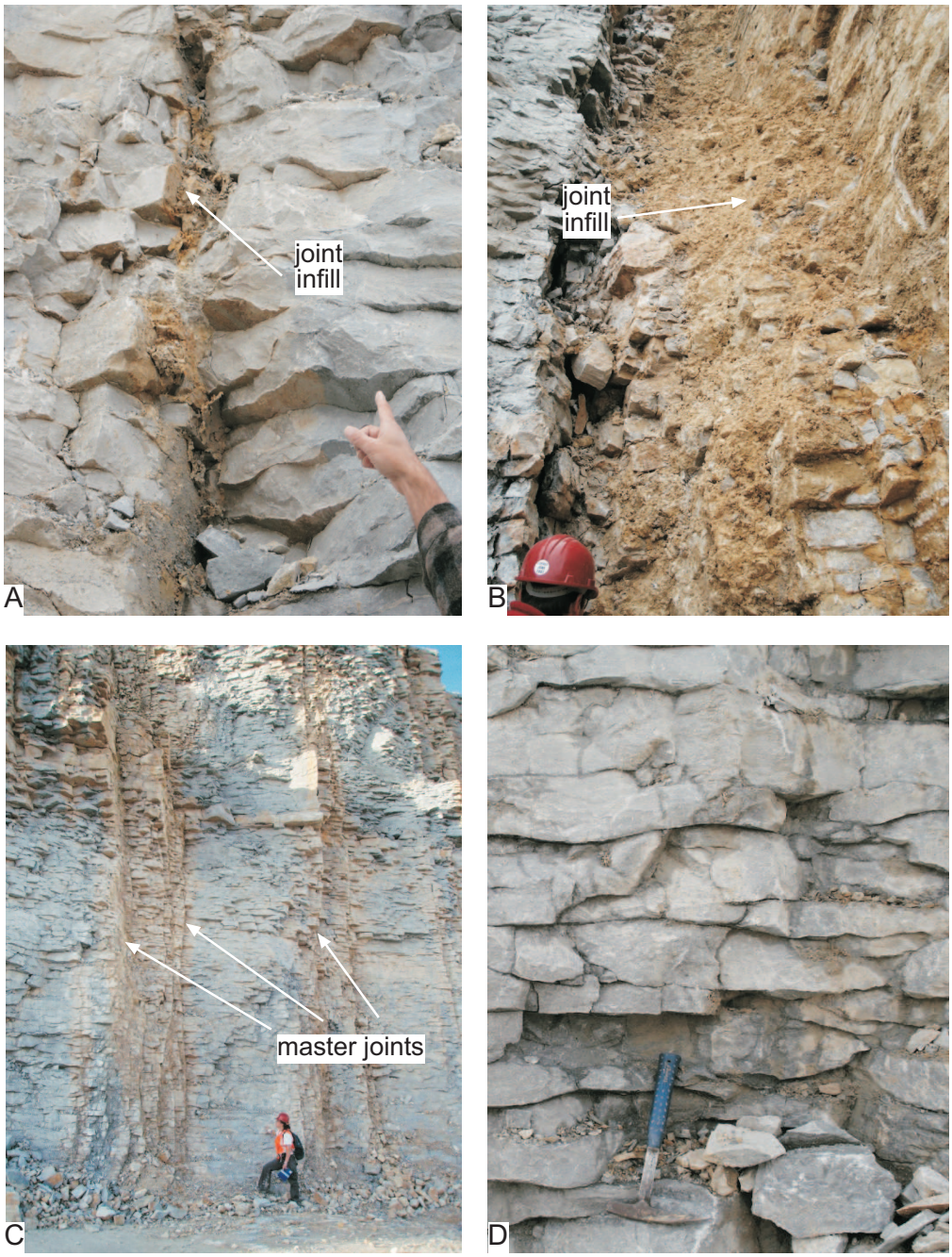

Figure 3.9 Rock mass features in the High Grade limestone unit: (A) A relatively tight or closed vertical master joint containing clay rich infill. (B) A relatively open vertical master joint containing clay rich infill. (C) Vertical master joints showing discolouration due to oxidation (brown to light orange) zones along joint surfaces. (D) Unoxidised rock showing wavy, regular, flaggy bedding. All photos taken of a northern face.

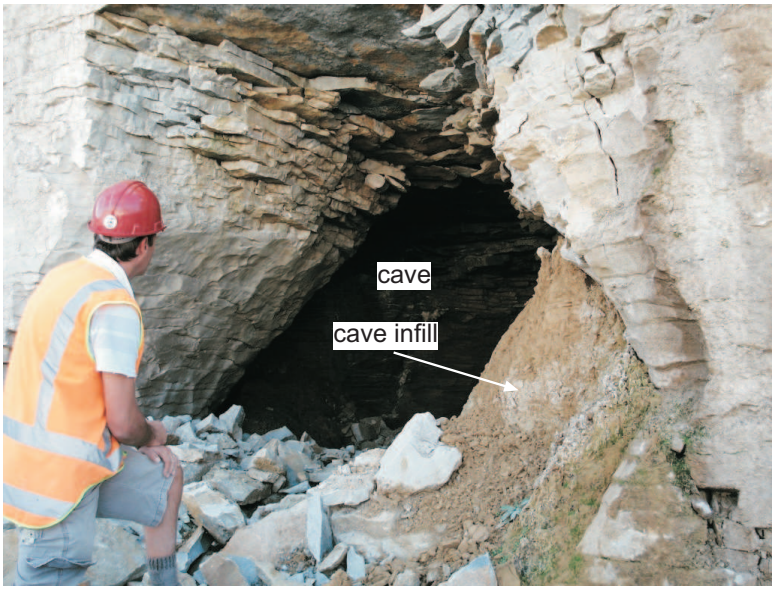

Figure 3.10 A limestone cave in the High Grade unit containing cave infill, typically a brown, moist, clay rich material. The infill is generally accumulated near the sides and at the bottom of the cave, western face.

Figure 3.11 Palygorskite (creamy white clay mineral originally) on an exposed joint surface in the High Grade limestone unit. Palygorskite has leathery, flexible, and sheet like characteristics.

Master joint (Figure 3.9C) persistence is estimated to be >20 m, and joint aperture 0-300 mm (maximum aperture corresponds to a open joint zone). Joints ranged from dry to moist. The majority of the master joints have infills (Figure 3.9A and B). Infills are mainly dry, ranging from light brown to orange or dark grey clays (300 mm thick), limestone fragments (pebble size), palygorskite (3-10 mm thick) (Figure 3.11), and re-precipitated calcite (up to 10 mm thick).

One small joint set is identified with orientations of 81/141 and 81/337. Average true joint spacing is 0.68 ± 0.24 m. Small joint persistence is estimated at <1 m terminating against limestone flags, and joint aperture 0-10 mm. All small joints are dry and half contain infills. Infills are typically dry to moist, white or orange yellow or grey silt (up to 5 mm thick) and palygorskite (up to 2 mm thick).

3.6 Lower Steel rock mass results

Field data sheets containing rock mass information about the Lower Steel limestone unit are given in Appendix C-3.1.

Weathering, rock type, and bedding: The Lower Steel limestone unit is a predominantly moderately weathered, mainly oxidised, creamy white or orange yellow sparry limestone. The upper two or three metres of the unit (Figure 3.12A) are un-oxidised, blue-grey flaggy limestone, where the flags are typically horizontal (0-7° dip). In some locations, below these upper few metres, is a relatively sharp contact between oxidised, light yellow, low angle cross beds (Figure 3.12A) which are also flaggy. In other locations, it is not cross bedded (approximately horizontal bedding). Discolouration occurs either side of master joints (top of Figure 3.12B), approximately 0.3-0.5 m wide either side of the joints if they are in unoxidised rock. Some parts of the face are dry, and others seeping at time of observation. Flag thicknesses range between 30 and 280 mm, and average 120 mm.

Discontinuities: Discontinuities in the Lower Steel unit include dissolution seams, subvertical and subhorizontal stylolites, caves, and joints. Seams are typically discrete and condensed/concentrated in silica minerals, dry to moist, medium brown silt and clay, ranging from <1-3 mm thick. White soft sand was also observed rarely (10 mm thick). Stylolites of both orientations are typically <1 mm thick, and involve rusty orange clays. On the northwestern face of the quarry, another cave is exposed (in the Lower Steel limestone unit) at the time of observation that was approximately 1 m high by 2 m wide. A period of heavy rainfall occurred during description. A few minutes after the rainfall event ended, muddy water flowed out from the cave.

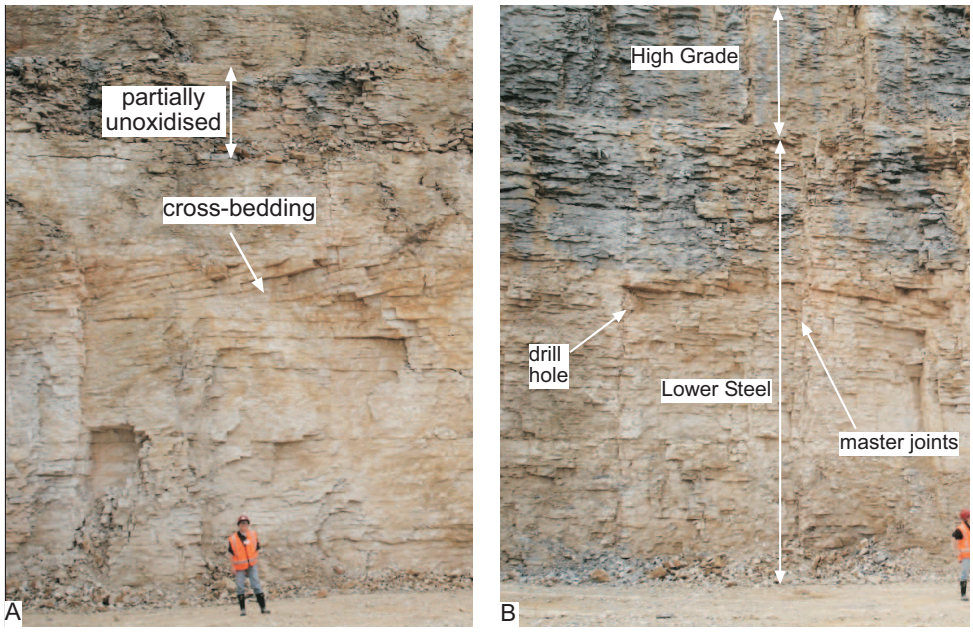

Figure 3.12 Rock mass features in the Lower Steel limestone unit: (A) The top of the unit consists of approximately 2 m of partially unoxidised subhorizontal flaggy limestone, which overlies approximately 1 m of flaggy cross-beds, which then overlies more subhorizontal flaggy limestone (oxidised), eastern face. (B) Tight vertical master joints, northern face. The High Grade unit is shown overlying the Lower Steel unit (top).

Although the flow rate was not measured, the flow was relatively fast and comparable to flow discharge of a storm drainage pipe after heavy rainfall. Karst features such as fissures are also present on the same face and contain infills. The face containing the Lower Steel limestone units cave was blasted the same day. Cave infills were able to be sampled and are moist to wet, medium brown to orange clays.

Joints: To identify joint sets, dip and dip direction data are plotted on stereonets for master and small joints (Appendix C-3.2). Bearing and distance measurements used to calculate dip and dip direction from the stereonets are summarised in Appendix C-3.3. Using apparent spacing, dip direction of the face (from field measurements), and the dip direction of each joint set(s), true spacing has been is calculated (summarised in Appendix C-3.4). Master and small joints both occur in the Lower Steel. One master joint set is identified with orientations of 87/172. Average true joint spacing is 3.70 ± 0.58 m. Master joint persistence is estimated at >20 m, and joint aperture from 2-40 mm. The majority of the master joints have infills. Joints ranged between dry to wet where water was flowing. Infills are dry to moist, comprising brown clays (1-2 mm thick), limestone fragments (pebble size), and palygorskite (up to 3 mm thick).

Three small joint sets were identified with orientations of 84/174, 87/122, and 85/152. Average true joint spacings are 0.37 ± 0.10 m, 0.13 ± 0.05 m, 0.17 ± 0.07 m. Small joint persistence is estimated as <1 m terminating against limestone flags, and joint aperture from 0-8 mm. Small joints ranged from dry to wet (water flowing). The majority of small joints have little (<1 mm thick) or no infills. Infills are dry to moist, and include re-precipitated calcite (up to 5 mm thick), white to fawn clay (up to 2 mm thick), and white brittle material (up to 4 mm thick) later identified as calcite.

3.7 Discussion

Table 3.1 summarises the rock mass characteristics of the four quarry limestone units. The Upper Steel and Lower Steel units are more weathered than the Aglime and High Grade units. The Upper Steel occurs at the top of the stratigraphy and is therefore more exposed to infiltrating water than the other units; in addition, the Upper Steel is locally porous. The level of the water table could have covered most of the Lower Steel unit, and can be offered as a possible explanation as to why it is relatively more weathered, and almost completely oxidised. Discolouration of master joints, particularly in the Aglime and High Grade units, and some small joint surfaces provides evidence that water is percolating down along these discontinuities. Water is proposed as the most likely transport mechanism for carrying joint infills from overlying external sources (e.g. Mahoenui Group mudstones and Kauroa Ash) down vertically into the joints.

All the units are well cemented limestones and are predominantly flaggy limestones, however, the Upper Steel unit does have sections that are knobbly, and porous.

3.7.1 Dissolution seams

All limestone units contain dissolution seams which occur between flags as a variety of thicknesses across the four quarry units. In decreasing order of thickness, Aglime (typically 2-10 mm thick) has the thickest followed by the High Grade (typically 2-4 mm thick), Lower Steel (typically <1-3 mm), and Upper Steel (typically <2-3 mm thick) units. Seam material characteristics are similar for all units (rusty brown or blue grey silts and clays).

Table 3.1 Rock mass characteristics summarised for each quarry unit.

Quarry unit	Rock type	Weathering	Discontinuity types present	Flag thickness range & average (mm)	Flag orientation	Seam moisture, colour, texture, thickness (mm)	Apparent joint spacing (m)	True joint spacing (m)	Joint orientation
Upper Steel	Creamy white/ light yellow, sparry limestone	Moderately weathered	Dissolution seams Subvertical and subhorizontal stylolites Collapsed dolines (karst)	100-560 Av. = 240	Horizontal	Moist-wet rusty brown silt (<2-3 mm)	-	-	-
Aglime	Blue-grey/ orangey yellow, micritic limestone	Fresh	Dissolution seams Master joints Smaller joints between master joints	20-200 Av.=100	Horizontal	Dry-damp,med brown or rusty brown or orange or grey clay, (2-10 mm)	Master = 2.53 Small = 1.23	Master = 0.31 Small = 0.30	Master = 86/322 74/128 Small = 85/149 88/323
High Grade	Blue-grey/ orangey yellow, sparry limestone	Fresh	Dissolution seams Master joints Smaller joints between master joints Caves	50-220 Av. = 120	Horizontal	Dry-moist dark blue/grey-rusty brown silt/ clay (2-4 mm),	Master = 2.66 Small = 0.74	Master = 2.45 Small = 0.68	Master = 85/141 87/324 Small = 81/141 81/337
Lower Steel	Creamy white/ orangey yellow, sparry limestone	Moderately weathered	Dissolution seams Master joints Smaller joints between master joints Subvertical & subhorizontal stylolites Caves	30-280 Av. = 120	Horizontal/ low angle cross-beds	Dry-moist med brown silty clay (<0.1-1 mm), white, soft sand (10 mm),	Master = 7.40 Small = 0.49-0.69	Master = 3.70 Small = 0.13-0.37	Master = 87/172 Small = 84/172 84/174 85/152 87/122

NB: - = not present. Infill thicknesses if measured are quoted in brackets

Table 3.1 continued.

Quarry unit	Joint persistence (m)	Joint aperture (mm)	Joint infill moisture, colour, texture, thickness (width of filled discontinuity (mm)	Stylolites	Cave infill texture, colour, moisture, size	Seepage
Upper Steel	-	-	-	<1 mm thick rusty orange, clay residue	Moist-wet, med brown-orange clay, approx. 1 m high by 1 m wide	Face: Moist-water flowing, surface water Seam: Wet
Aglime	Master = >20 Small = <1 terminate against flags	Master = 0-50 Small = 0-20	**Master:** All joints have infill. Infill slightly moist-moist. Fill material ranges from light-med brown/cream/orange silt, soft white leached limestone?, palygorskite (30 mm), rusty orange clay, brittle white material (15 mm), re-precipitated calcite (50 mm) **Small:** Rusty orange clay (4 mm), palygorskite, (5-20 mm) re-precipitated calcite (15 mm)	-	-	Face : Dry Master joints : Dry-very wet Small joints : Dry Seams: Dry-damp
High Grade	Master = >20 Small = <1 terminate against flags	Master = 0-300 Small = 0-10	**Master:** Majority of joints have infill. Infill dry. Fill material ranges from light brown-orange sticky clay (300 mm),palygorskite (3-10 mm), dark grey clay, re-precipitated calcite crystals (10 mm), **Small:** Half the joints have infill. Infill dry-moist. Fill material ranges from white/orangey yellow coating (5 mm), grey silt, palygorskite	-	Moist-wet, med brown-orange clay, approx. 2.5 m high by 2 m wide	Face: Dry-moist Master joints : Dry-moist Small joints : Dry Seams: Dry-moist
Lower Steel	Master = >20 Small = <1 terminate against flags	Master = 2-40 Small = 0-8	**Master:** Majority of joints have infill. Infill dry-moist. Fill material ranges from light brown clay, (1-2 mm), Palygorskite **Small:** Majority of joints have either a thin coating (<1 mm) to no infill. Re-precipitated calcite (5 mm), white-fawn clay (2 mm), white brittle material (4 mm)	<1 mm thick rusty orange, clay residue	Moist-wet, med brown-orange clay	Face: Dry-water flowing Master joints : Dry-water flowing Small joints : Dry-water flowing Seams: Dry-moist

NB: - = not present. Infill thicknesses if measured are quoted in brackets

Moist seams are common, and are likely the result of lateral water movement along these horizons in the rock mass.

3.7.2 Stylolites

Two units contain subhorizontal and subvertical stylolites (Upper Steel and Lower Steel). Stylolites show similar characteristics for the Upper Steel and Lower Steel units (i.e. thin <1 mm thick residues of clay). Dissolution seams and stylolites are quantified in detail for each quarry unit in Chapter 4, Sections 4.3 and 4.4.

3.7.3 Caves and other karst features

Three units contain caves, collapsed dolines, and/or fissures (Upper Steel, High Grade, and Lower Steel). Since these have been identified in three of the four units it is probably reasonable to presume that the Aglime also has caves and/or other karst features that are not currently exposed. The infills in the caves (all clay rich) are likely to have been sourced from both the overlying Mahoenui Group mudstones and the Kauroa Ash.

3.7.4 Limestone flags

Flag orientation is generally horizontal in all quarry limestone units, and low angle cross-beds are common in the Lower Steel unit. Flag thickness varies across the units. Figure 3.13 shows a box plot of the mean, and variability of the flag thicknesses. Summary statistics of flag thickness are shown in Table 3.2 for all quarry units. Upper Steel has the greatest range of flag thicknesses (100-560 mm), followed by Lower Steel (30-280 mm), High Grade (50-220 mm), and Aglime (20-200 mm). In view of the fact that dissolution seams separate each flag, thickness is important because it gives an indication of the amount of silica (associated with the seams) each unit contains.

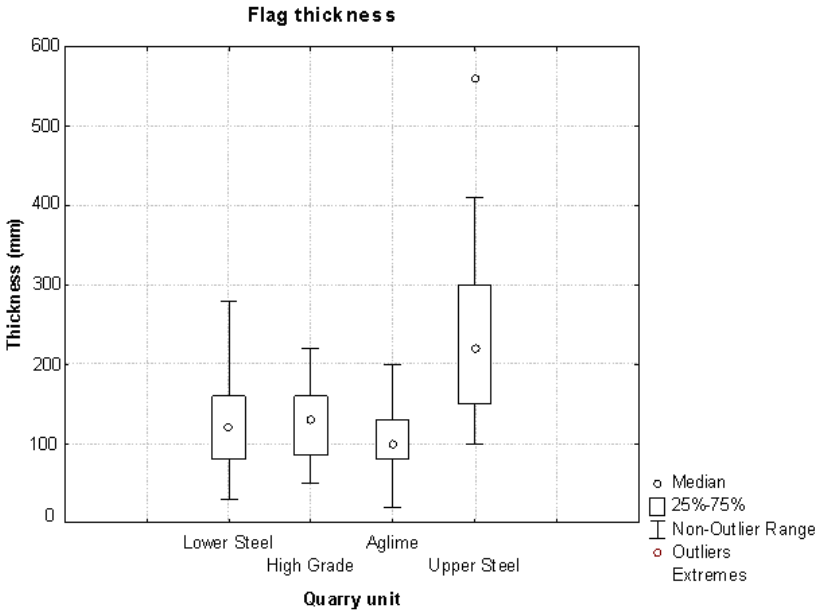

Figure 3.13 Box and whisker plot showing the distribution of flag thicknesses in the quarry limestone units.

Table 3.2 Summary statistics for limestone flag thickness (mm) for Upper Steel, Aglime, High Grade, and Lower Steel limestone units.

Statistics	Upper Steel	Aglime	High Grade	Lower Steel
Mean	237	101	122	123
Std error	15	4	5	6
Median	220	100	130	120
Mode	130	90	70	80
Std dev.	99	38	44	50
Range	460	180	170	250
Minimum	100	20	50	30
Maximum	560	200	220	280
Sum	995	905	869	925
Count	42	90	71	75

For example, if you have a unit with ten flags in a metre, and another unit with three flags in a metre, and assuming that the host rock in both units contains the same silica %, and seam thickness between each flag is the same in both units, you could expect the amount of silica to be more in the unit with ten flags as there is more seam material present.

A t-Test was carried out to compare flag thickness between the quarry units. Full details on the t-Test results are given in Appendix C-3.5. Table 3.3 shows results of t-Test statistics with a null hypothesis stating that each unit has the same average flag thickness. The t-Test showed that the Lower Steel and High Grade have the same average flag thickness (large p value), and that all other units are

from different flag thickness populations (i.e. their flag thicknesses are not the same). The p-values (Table 3.3) derived from the t-Tests were small enough to provide sufficient evidence to conclude that there is a significant statistical difference amongst the other units.

Table 3.3 t-Test results that compare flag thickness between quarry limestone units (Upper Steel, Aglime, High Grade, and Lower Steel). The null hypothesis assumes equal variances across two samples.

Unit comparisons	Lower Steel vs. High Grade	Lower Steel vs. Aglime	Lower Steel vs. Upper Steel	High Grade vs. Aglime	High Grade vs. Upper Steel	Aglime vs. Upper Steel
Confidence interval	95%	95%	95%	95%	95%	95%
p-value	0.9038	0.0010	3.2027×10^{-13}	0.0009	1.3706×10^{-13}	3.2303×10^{-21}
Result	accept null	reject null	reject null	reject null	reject null	reject null
	same thickness	different thickness	different thickness	different thickness	different thickness	different thickness

3.7.5 Joints

Three units contain joint systems (i.e. Aglime, High Grade, and Lower Steel). The average true master and small joint spacings vary across the units (Table 3.4). Raw data for these calculations are given in Appendix C-3.4. The small joints appear to have similar orientations to the master joints and probably belong to the same joint set as the masters, however, this study subdivided joints based on field characteristics, therefore the data set for these two joint types were dealt with separately. Figure 3.14 shows the joint spacings in stratigraphic array for the quarry units. In general, the master joint spacings decrease from the lowest unit (Lower Steel, av. 3.70 ± 0.58 m) to the highest unit (Aglime, av. 0.31 ± 0.03 m) with the High Grade having an intermediate average master joint spacing of 2.45 ± 0.32 m. There is a relatively large standard error associated with the Lower Steel master joint set (± 0.58 m) so more measurements would likely decrease this error.

Table 3.4 Joint spacing for quarry limestone units in outcrop.

Quarry unit	Joint type and set number	Apparent spacing (m)	True spacing (m)	No. joints	Std. error
Aglime	Master set 1	2.53	0.31	13	0.03
	Small set 1	1.23	0.30	7	0.08
High Grade	Master set 1	2.66	2.45	22	0.32
	Small set 1	0.74	0.68	4	0.24
Lower Steel	Master set 1	7.4	3.70	7	0.58
	Small set 1	0.69	0.37	9	0.10
	Small set 2	0.74	0.13	6	0.05
	Small set 3	0.49	0.17	9	0.07

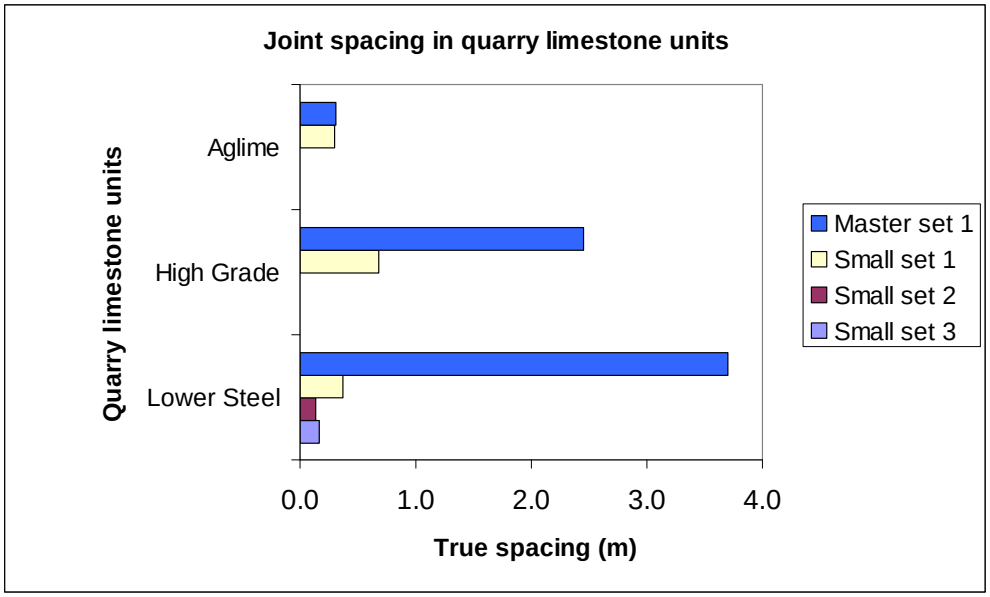

Figure 3.14 Joint spacing in stratigraphic array for quarry units.

The small joints do not show the same pattern as the master joints, for example, the Lower Steel has a range of joint spacings (three small joint sets) ranging from 0.13-0.37 ± 0.05-0.10 m, High Grade 0.68 ± 0.24 m, and Aglime 0.30 ± 0.08 m. The Lower Steel and Aglime show similar small joint spacings whereas the High Grade has quite different spacings. This is probably a result of the lack of small joint measurements in the High Grade unit (relatively high standard errors associated with spacing) as we would expect the small joint spacings to also be similar to the other units. Table 3.4 emphasises the variation of the numbers of joints measured in each unit. It is recommended that extra measurements (of more joints) are taken to create a more robust data set to generate better statistics in the future.

Master and small joint sets in the quarry are tectonic joints with orientations that correspond (parallel) to the main fault in the quarry (Chapter 2, Section 2.6.1), thus they are likely to be part of the same tectonic stress fields. These joints have formed as a result of uplift activity which has caused the limestones to fracture (brittle deformation) as a response to horizontal stresses. As uplift occurred, valleys cut by rivers near the quarry region has probably allowed stress release causing some of the limestone to relax, and opening joints as a consequence. The master and small joints were formed in the same way, except more relaxation has occurred along the master joints giving them different field characteristics, such as

larger aperture, which in turn allows more water and infills to percolate through them, whereas small joints remained tight. The master joints are remarkably regular in their spacing in each limestone unit in each limestone unit.

From the bottom unit (Lower Steel) to the top (Aglime) unit shows a general trend of decreasing joint spacings between the joints. More joints have likely formed in the higher units as overburden pressure (burial stresses) is not as significant compared to lower units where overburden pressure is more significant. The removal or decrease of overburden pressure allows the rock mass to expand and thus more joints form.

Interestingly there are no obvious joint sets in the Upper Steel unit. The Upper Steel is dominated by fissures which have been exploited by the percolation of water. Furthermore, collapse dolines are also common in the Upper Steel unit where the dissolution of limestone has occurred to a greater extent than in the underlying quarry units (based on what was exposed at time of observation). The Upper Steel also possesses rock mass attributes that are different to the other quarry units. For example, the limestones are knobbly, locally porous, and flags are much thicker than the other limestone units. Nelson (1978a) also found marine cements in this unit (equivalent to Waitanguru Limestone Member, Otorohanga Limestone) which are not found in the other limestone units in the quarry. A possible explanation for the lack of jointing could be that the Upper Steel limestones may have responded differently to the uplift and/or deformation processes acting on the limestones. It is the unit which has the least overburden pressure compared to the other quarry units. Jointing is caused by brittle deformation, therefore, it is possible that the Upper Steel did not experience as much brittle deformation as the other units, or maybe it experienced different deformation processes such as plastic deformation instead. It is most likely that there were joints originally and that they have subsequently formed into fissures. It is possible that one or more properties of the rock mass has caused the Upper Steel to respond differently compared to the other units.

Joint infill types are similar for all units that contain vertical joints. These types include calcite that has re-precipitated from the solution of limestone; limestone fragments which have fallen down from above blasted units; clays which have

been washed down from overburden units particularly Mahoenui Group mudstones and possibly Kauroa Ash also; and palygorskite which is a leathery clay mineral which precipitates *in situ* within joints, and is associated with silica and calcite minerals.

3.7.6 Discontinuity classification

As a consequence of this work a discontinuity classification has been devised (Figure 3.15). The classification is based on observations made in the quarry, as well as the use of appropriate references, to help define each discontinuity type. Dissolution seams are subdivided into two types, namely discrete (common) and diffuse (rare) seams. Stylolites are also subdivided into two orientation types, namely subhorizontal and subvertical. Vertical joints are mainly subdivided on the presence or absence of infills. Limestone caves do not have any further subdivisions.

Discontinuity feature	Feature types	Description	Examples
Dissolution seams		Smooth undulating seam of insoluble residue without sutures	 A
	Discrete seams	Condensed seam, insoluble residues concentrated and closely packed, seam continuous at core scale	
	Diffuse seams	Also known as wispy seams, converging and diverging, insoluble residues dispersed and loosely packed, seam discontinuous at core scale	
Stylolites		Produced by burial or tectonic processes, are a stratiform structure that displays a serrated/sutured surface having variable insoluble residue accumulation along these surfaces, amplitudes typically < 10 mm wide, laterally continuous at core scale	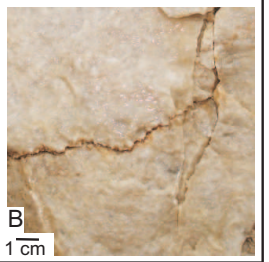 B 1 cm
	Subhorizontal stylolite	Produced by burial	
	Subvertical stylolite	Produced by tectonics	
Joints		Fractures in the rock mass formed as a result of deformation processes such as folding, faulting, and uplift	 C
	Vertical joint	Vertical joint with no infill	
	Vertical joint with infill/ precipitated minerals	Vertical joint with infill e.g. clays	
Caves		Cavities that are formed in the limestones as a result of dissolution processes (weathering), that act as natural sediment traps	 D

Figure 3.15 Discontinuity classification based on features observed in the quarry and references in the literature (i.e. Moore, 2001, Bathurst, 1995; and Williams, 2004b). (A) Discrete dissolution seams in the Aglime unit. (B) Subhorizontal stylolite in the Upper Steel unit. (C) Vertical joint with infill in the High Grade unit. (D) Limestone cave in the High Grade unit.

CHAPTER FOUR

Discontinuities in cores

4.1 Introduction

The 500 drill hole series includes five cores, three of which (BH501, BH502, and BH503) were drilled outside the current extractable boundary of the quarry, and two (BH504 and BH505) which have been drilled within the quarry itself. Figure 4.1 shows the locations and drill depths of these five cores. Details on quarry unit thickness, elevation, and depth are given for each core in Appendix D-4.1. This chapter presents the results of core logging carried out on BH501, BH502, and BH503 that especially focuses on the identification and description of discontinuity features in the cores since they commonly high concentrations of siliceous impurities in the limestones. The discontinuity features are also quantified for each quarry unit in terms of frequency and thickness.

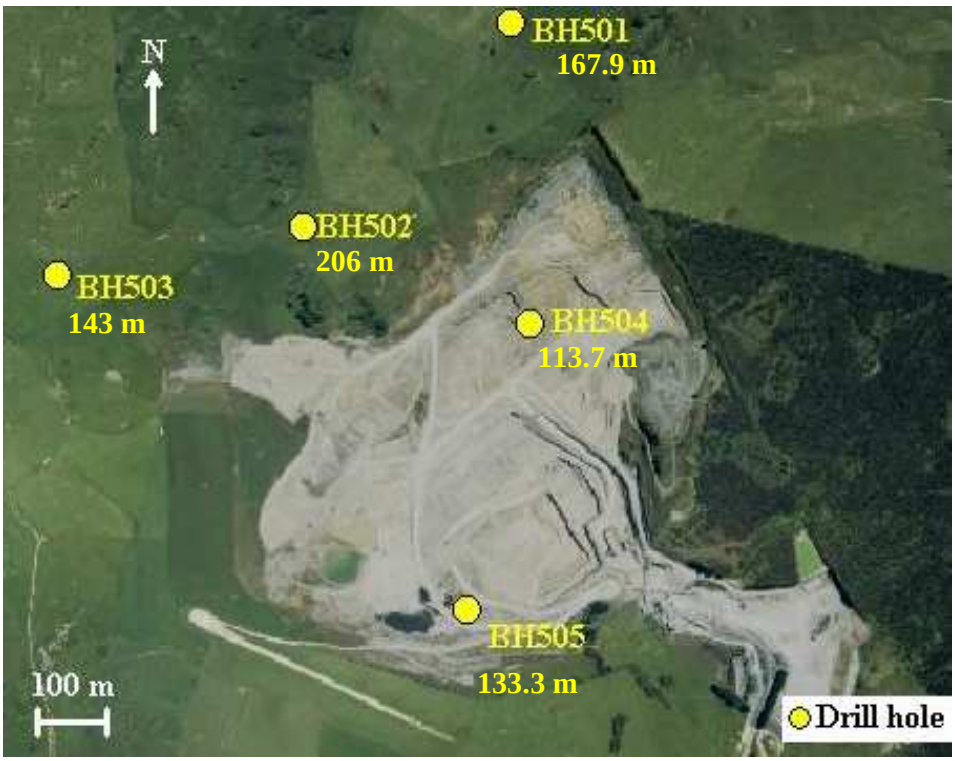

Figure 4.1 Aerial photo of McDonald's Oparure Lime Quarry showing drill hole locations and associated drill depths from the 500 series. Note depths represent the length of core. Aerial courtesy of McDonald's Lime Ltd (2005).

4.1.1 Drill cores

After drilling of the 500 drill hole series was completed in 2005, the core was stored in waterproof boxes in an onsite quarry shed (Figure 4.2). Ormiston Associates Ltd logged the five cores in reasonable detail recording information such as lithology, colour, weathering, and strength. To determine major element chemistry, a half-split of the core was sampled by Ormiston Associates and McDonald's Quarry continuously at 0.3-1 m intervals (or where there was a lithological change) up to the base of the Lower Steel and then at up to 3.0 m intervals down into the Aotea Formation. The samples were powdered and analysed using x-ray fluorescence (XRF) by Spectrachem Ltd in Wellington. A series of multi-page geology and chemistry logs were produced combining the recorded information and XRF results (recorded in an Excel spreadsheet). An example showing a portion of each of these logs is shown in Figures 4.3 and 4.4. The remaining logs are held by Holcim NZ Ltd.

Using the geological and XRF data provided by Ormiston Associates Ltd some new single-page summary logs have been produced in this study for drill holes BH501, BH502, and BH503 (Figures 4.5-4.7).

Figure 4.2 Photo from inside core shed showing boxes of core from drill hole BH502.

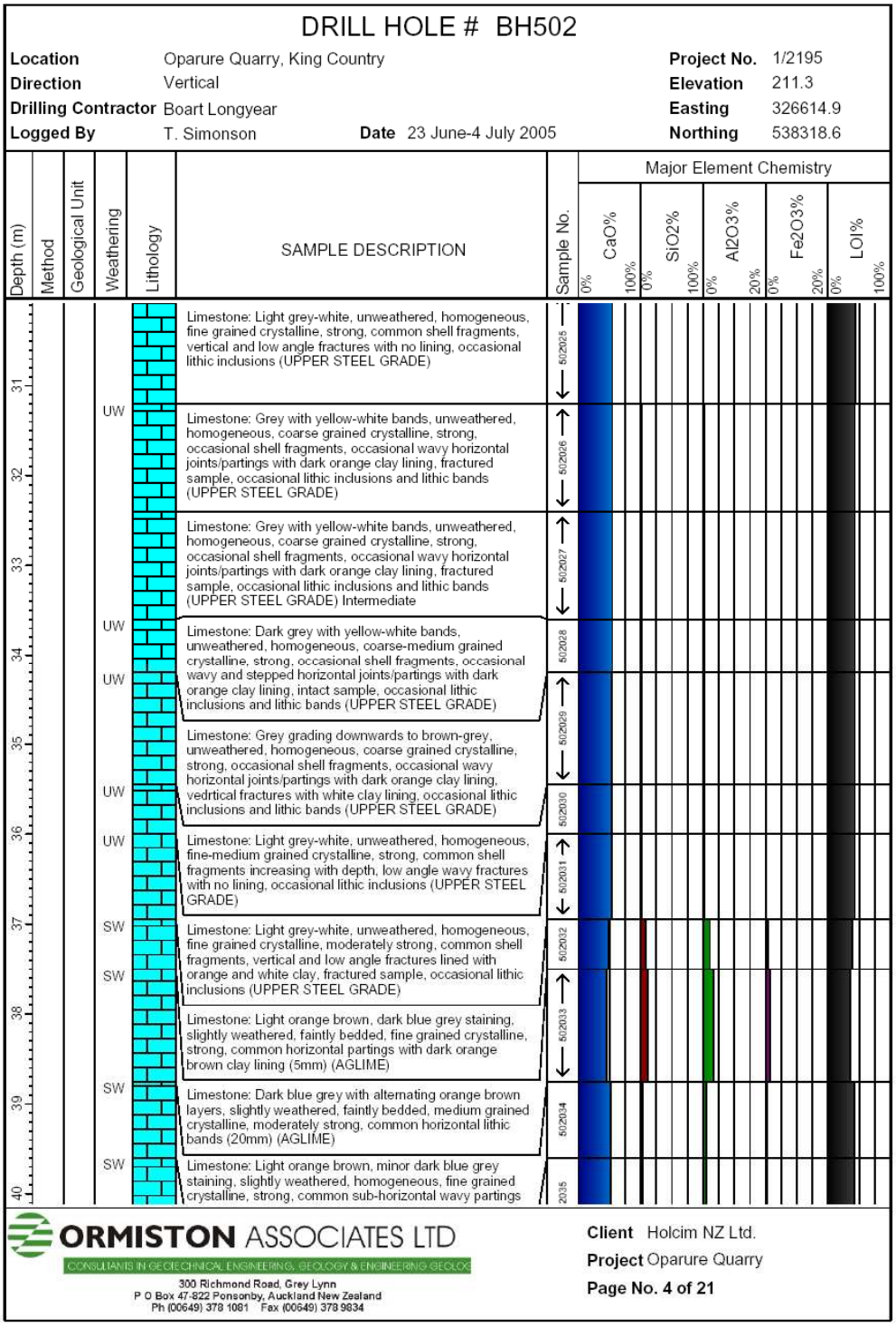

Figure 4.3 Chemistry log data from 30-40 m depth (along hole) for drill hole BH502. Elevation is metres above mean sea level, and the grid coordinate system is Mt Eden Circuit. Log courtesy of Ormiston Associates Ltd (2005).

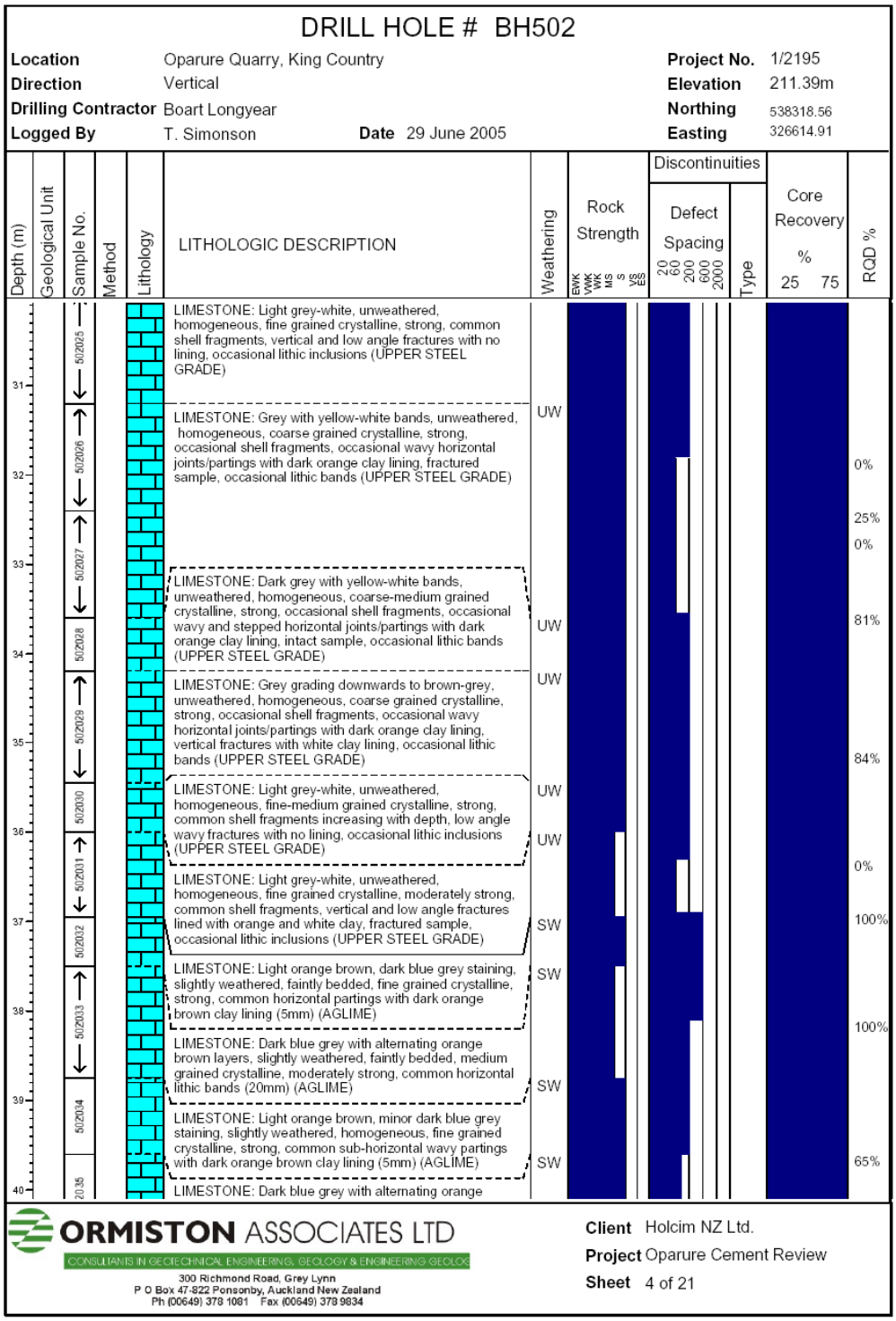

Figure 4.4 Geology log data from 30-40 m depth (along hole) for drill hole BH502. Elevation is metres above mean sea level, and the grid coordinate system is Mt Eden Circuit. Log courtesy of Ormiston Associates Ltd (2005).

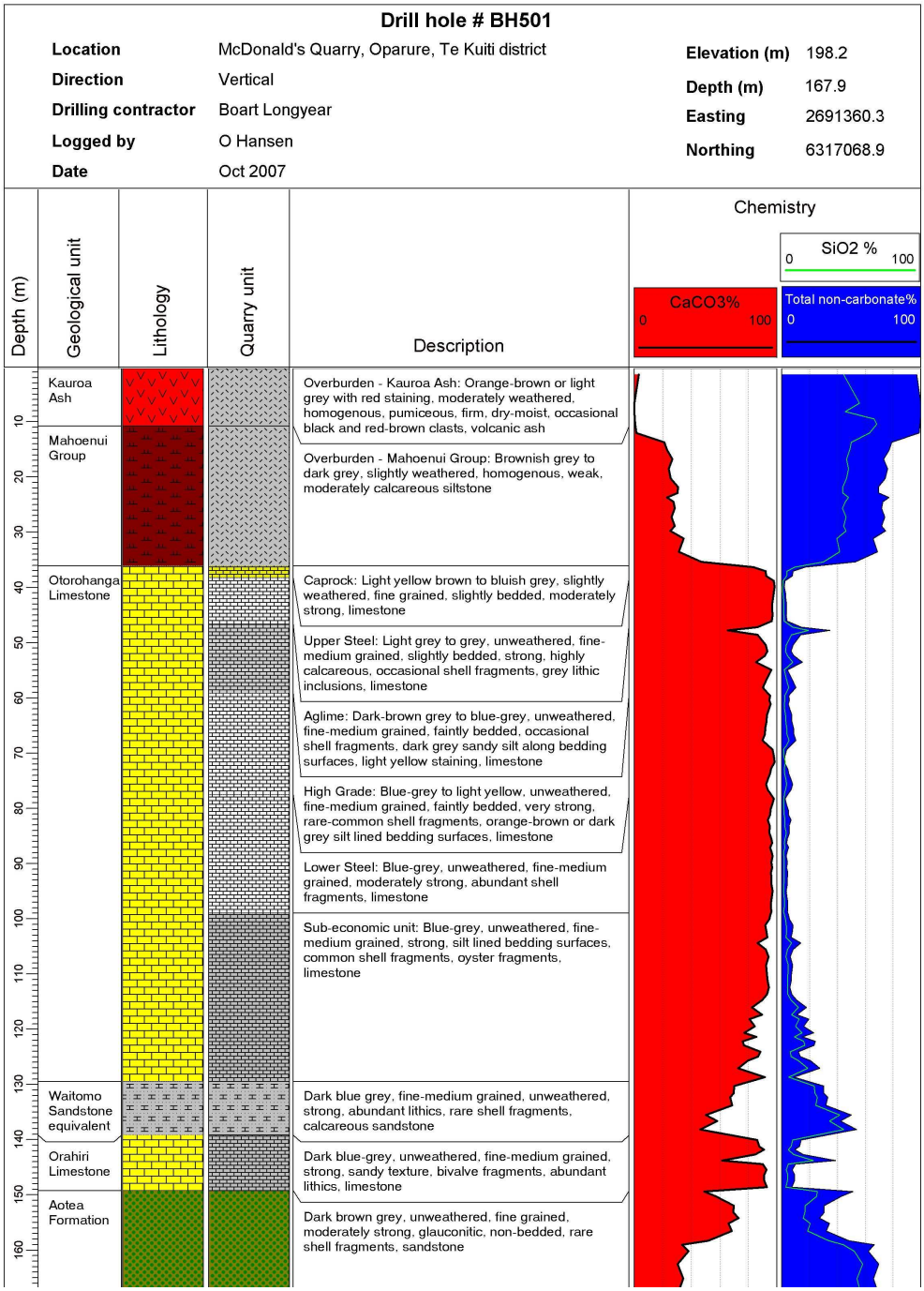

Figure 4.5 Geology log summarising lithologic descriptions, $CaCO_3$ content, non-carbonate content, and SiO_2 content for drill hole BH501. Depth (m) is the total length of core, elevation is metres above mean sea level. Grid coordinate system is NZ Map Grid. Data courtesy of Ormiston Associates Ltd (2005).

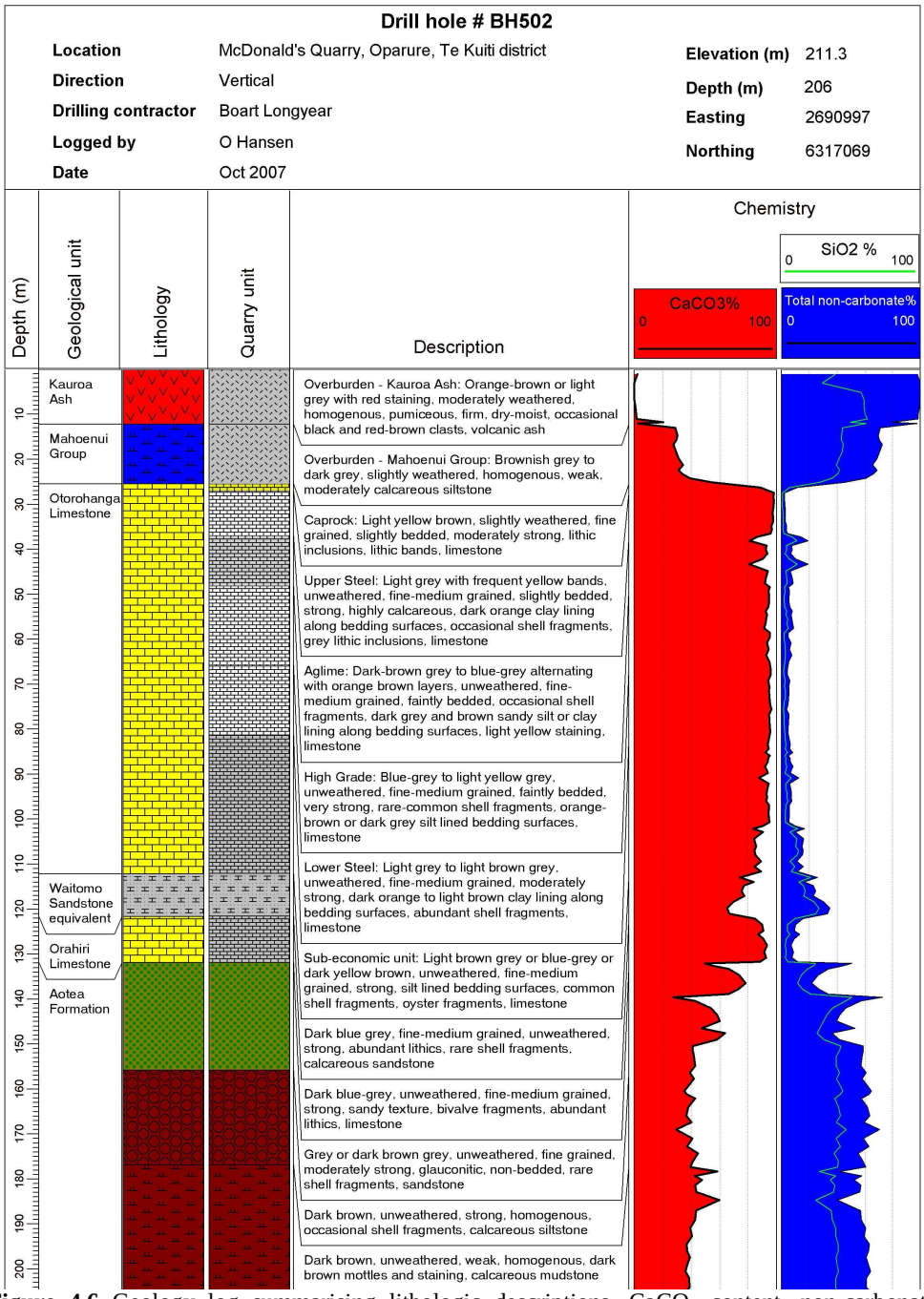

Figure 4.6 Geology log summarising lithologic descriptions, $CaCO_3$ content, non-carbonate content, and SiO_2 content for drill hole BH502. Depth (m) is the total length of core, elevation is metres above mean sea level. Grid coordinate system is NZ Map Grid. Data courtesy of Ormiston Associates Ltd (2005).

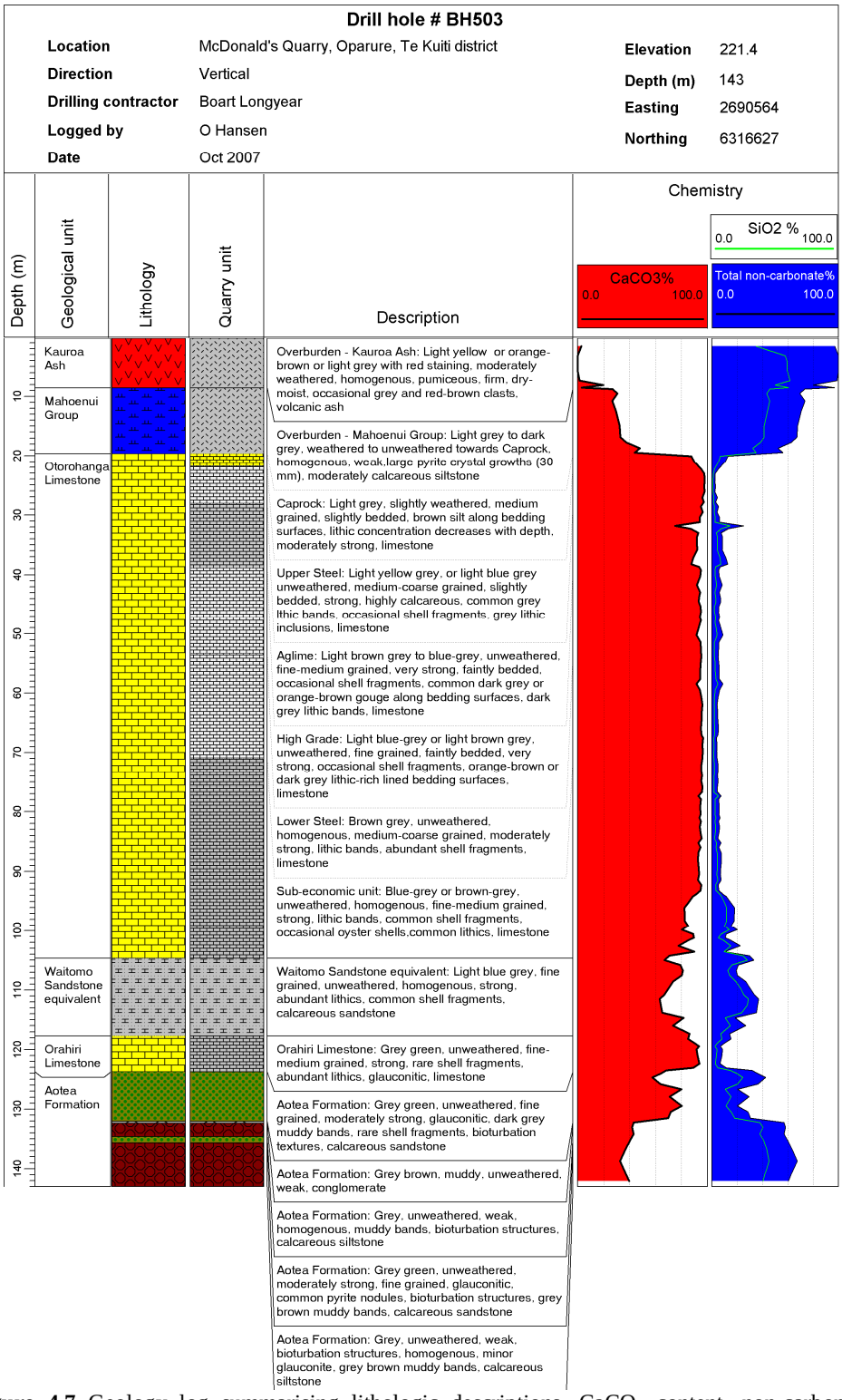

Figure 4.7 Geology log summarising lithologic descriptions, $CaCO_3$ content, non-carbonate content, and SiO_2 content for drill hole BH503. Depth (m) is the total length of core, elevation is metres above mean sea level. Grid coordinate system is NZ Map Grid. Data courtesy of Ormiston Associates Ltd (2005).

These summary logs include the following features plotted according to depth in the cores: graphic logs of the lithology, the geological units, and the quarry units; general lithological information for each quarry unit; and two chemistry graphs showing first the total $CaCO_3$% and second the total non-$CaCO_3$% with total silica% superimposed upon it. Cores BH501, BH502, and BH503 are expectedly relatively similar in terms of stratigraphy and rock unit characteristics. BH502 and BH503, however, have several different lithologies present in the Aotea Formation in the lower part of the two cores (Figures 4.6 and 4.7). Furthermore, there are variations in the $CaCO_3$ and silica contents down the stratigraphy in all three cores.

Following the initial re-logging of cores BH501, BH502, and BH503, they were again re-logged in relationship to their lithological discontinuity features in an attempt to seek evidence that the variation in silica, and hence $CaCO_3$ content in samples, is primarily a function of the frequency and thickness of these discontinuities. The following sections present the information gained from this discontinuity analysis.

4.1.2 Recognising quarry units in the field vs. the core

Contacts are levels or horizons that separate different rock units. These can be sharp, irregular, wavy, or gradational (i.e. changes between two units can be so minor or gradual that an exact contact is difficult to discern). Contacts can also be difficult to recognise due to weathering. For example, at first glance in field outcrops the quarry units are indistinguishable (except for the Upper Steel which is knobbly in the upper parts), partly due to the fact that the exposed units in the quarry have weathered through oxidation to a similar extent to much the same colours (i.e. white, fawn, or orangey yellow). The Aglime and underlying High Grade units are not entirely these colours with parts still remaining unoxidised or reduced; the rock is then medium to dark bluish grey. Areas where the limestone is fawn are typically along master joint surfaces (see Chapter 3, Sections 3.4 and 3.5). Percolation of water down these joints produces an iron staining (weathering) either side of the joint. A similar problem is faced when describing the core. Some portions are more weathered than others due to the percolation of water beneath the subsurface. Because of these weathering colour variations the

chemical composition analyses and other lithological variations (e.g. bedding) are often the best to use to subdivide the limestones.

The overall visual characteristics of the host limestones are reasonably similar down the quarry units except that the Caprock, Aglime, and Sub-economic units contain more non-carbonate material compared to the other limestone units. Using what is known from field observations; below I briefly mention the criteria used to define the contacts between the quarry units.

The following general contact colour and weathering observations were made. In all three cores the contact between the Mahoenui Group and the Otorohanga Limestone Caprock is transitional or gradational, even if relatively rapid (Figure 4.8A and 4.8B). As the contact is approached upwards, the Caprock becomes more argillaceous and finer grained, eventually passing into the true mudstones of the Mahoenui Group. In this case colour can also help locate the contact, the mudstones being dark greyish blue and the Caprock limestone fawny yellow.

The Caprock and underlying Upper Steel (white-fawn) units are oxidised. The contact (Figure 4.8C) between them in outcrop is mainly obvious, both because the Caprock is less pure and the Upper Steel unit has a less evident flaggy nature, tending to a blocky, more irregular weathering appearance that Nelson (1978a) called semi-knobbly and knobbly. This weathering feature can not be seen in the cores, so purity is used to position the contact between the Caprock and Upper Steel units.

The contact (Figure 4.8D) between the Upper Steel and Aglime units is less obvious. The main change involves the limestone purity and colour, from pure and creamy white above (Upper Steel) to less pure and dark grey below (Aglime).

The Aglime and High Grade units appear the most similar. The Aglime and High Grade are dominantly unoxidised (bluish grey) with occasional oxidised horizons. Exact contacts between the Aglime and High Grade units are difficult to define in the cores, and likewise between the High Grade and Lower Steel units. The Aglime, however, is less pure than the High Grade, and the High Grade less pure than the Lower Steel unit.

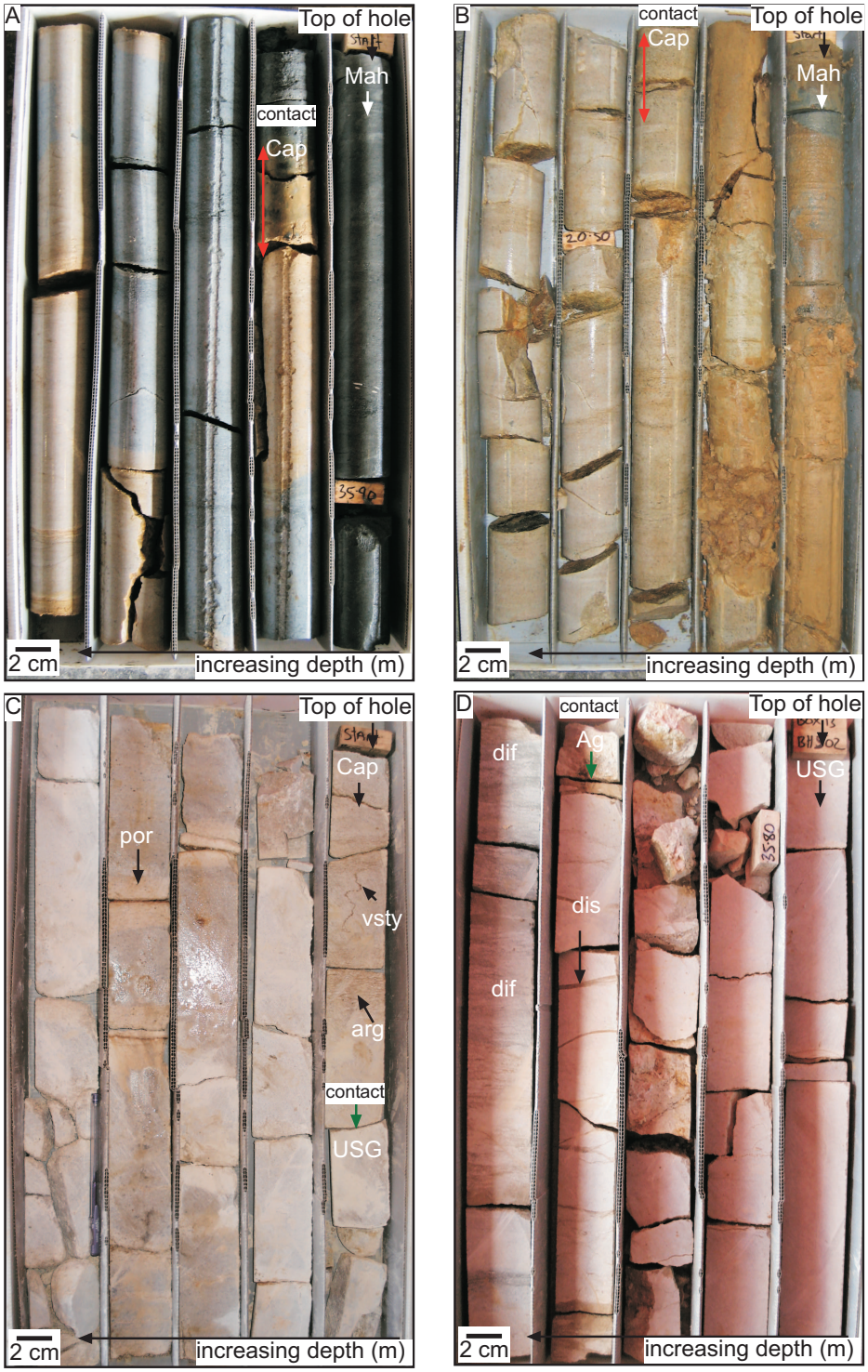

Figure 4.8 Boxes of core showing the nature of various contacts between quarry units. A = Mahoenui Group mudstone (bluish grey) and Otorohanga Limestone Caprock (brownish yellow) gradational contact shown by the red arrow, BH503, box 6, 18.5-21.5 m depth. B = Mahoenui Group mudstone (Mah) (brownish grey) and Otorohanga Limestone Caprock (yellow brown) gradational contact shown by red arrow. The contact is argillaceous and the core becomes progressively less argillaceous with depth, BH501, box 10, 35.5-38.3 m depth. C = Clear contact (green arrow) between the Caprock and Upper Steel limestone. The Upper Steel (USG) is much purer than the overlying argillaceous (arg) Caprock (Cap). Other features present include a vertical stylolite (vsty) in the Caprock and porous zones (por) in the Upper Steel. BH502, box 10, 26.6-29.5 m depth. D = Clear contact (green arrow) between the Upper Steel (USG) and Aglime (Ag). Some other features present include discrete (dis) and diffuse (dif) seams. BH502, box 13, 35.1-38.1 m depth.

The Lower Steel unit is predominantly unoxidised. The contact between the Lower Steel and Sub-economic units is not obvious either, the Sub-economic unit being also predominantly unoxidised, but it is less pure than the Lower Steel unit.

4.1.3 Discontinuity classification

Except for cavities, the same discontinuities that are observed in outcrop are also observed in the cores. Chapter 3 introduced the discontinuity types and discussed their origin, formation, and characteristics. An outcrop-based discontinuity classification was developed in Chapter 3, Figure 3.15. This classification can also be used to describe the discontinuities in the cores (Figure 4.9) except that core examples are used instead of field examples. Additionally, Figure 4.10 shows some non-discontinuity features used to log the cores.

4.1.4 Discontinuity logs

Based on the discontinuity classification (Figure 4.9) the three cores were logged in terms of their discontinuity features. The discontinuities proper include dissolution seams, stylolites, and vertical joints (defined in Figure 4.9). On the basis of visual differences, dissolution seams have been further subdivided into discrete and diffuse wispy seams adapted from Moore (2001). Stylolites have also been subdivided into subhorizontal and subvertical stylolites, likely related to fundamentally different origins. In many cases stylolites depart from being subhorizontal or subvertical, and they meander and cross over each other. Some stylolites outline interesting shapes, including parabolas. These types of stylolites are classified as stylolite networks. And finally vertical joints are subdivided into joints with no infill and joints with infill. Weathering discontinuities (discussed in Chapter 3, Section 3.1.5), such as caves or cavities, are not included in Figure 4.9 due to the absence of these in the three cores that were logged. Non-discontinuity features as defined in Figure 4.10 include porous zones and host limestone.

Discontinuity feature	Feature types	Description	Examples
Dissolution seams		Smooth undulating seam of insoluble residue without sutures	
	Discrete seams	Condensed seam, insoluble residues concentrated and closely packed, seam continuous at core scale	
	Diffuse seams	Also known as wispy seams, converging and diverging, insoluble residues dispersed and loosely packed, seam discontinuous at core scale	
Stylolites		Produced by burial or tectonic processes, are a stratiform structure that displays a serrated/sutured surface having variable insoluble residue accumulation along these surfaces, amplitudes typically < 10 mm wide, laterally continuous at core scale	
	Subhorizontal stylolite	Produced by significant burial	
	Subvertical stylolite	Produced by compressive tectonics	
	Stylolite network	Combination of subhorizontal and subvertical stylolites	
Joints		Fractures in the rock mass formed as a result of deformation processes such as folding, faulting, and uplift	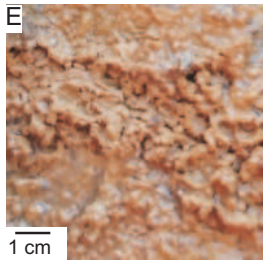
	Vertical joint	Vertical joint with no infill	
	Vertical joint with infill/ precipitated minerals	Vertical joint with infill e.g. clays	

Figure 4.9 Discontinuity classification used to log discontinuities in the BH501, 502, and 503 cores. A = Oxidised, concentrated discrete seam in the Sub-economic BH503, box 30, 88 m depth. A thinner seam can be seen diverging off the main seam (right). B = Oxidised, wispy, diffuse seams in the Aglime BH502, box 15, 41 m depth. C = Subhorizontal, oxidised stylolite in the Lower Steel BH503, box 20, 60 m depth. The amplitude (relief) of the sutures is a few millimetres. D = Subvertical, oxidised stylolite in the Caprock BH502, box 10, 27 m depth. E = Moist, orange-brown clay lining a vertical joint in the Lower Steel BH505, box 15, 42 m depth.

Non-discontinuity features	Description	Examples
Porous zones	Post-depositional feature where water has preferentially and selectively leached out calcium carbonate along localised horizons	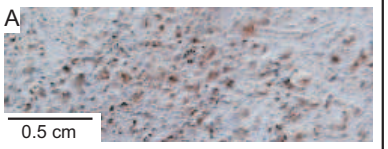
Host limestone	Limestone between discontinuities which has background levels of insoluble residue	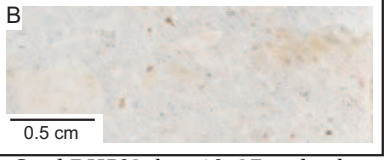

Figure 4.10 Non-discontinuity classification used to log the BH501, 502, and 503 cores. A = Porous limestone in the Upper Steel BH502, box 10, 27 m depth. B = Host rock in the Upper Steel, BH502, box 13, 35 m depth.

4.2 Logging method

As mentioned in earlier chapters (e.g. Chapter 3), discontinuities are generally associated with silica-rich materials; therefore it is relevant to attempt to quantify the discontinuities in each quarry unit. Figure 4.11 shows how the logging was setup. All of the features in the discontinuity classification (Figure 4.9) were described, measured, and recorded in relation to the six quarry units in the cores, and recorded onto data sheets (e.g. Figure 4.12). The data sheets for all cores appear in Appendix D-4.2.A (BH501), 4.2.B (BH502), and 4.2.C (BH503). Figure 4.13 shows a box of core where each box line is labelled with a letter. These letters correspond to rows in the discontinuity log data sheets, where discontinuity information was recorded. The summary raw data used to produce graphs in the following sections are given in Appendix D-4.3.

Only the limestone units (i.e. Caprock, Upper Steel, Aglime, High Grade, Lower Steel and Sub-economic units) have been logged for discontinuity features. The first five limestone units were logged entirely, whereas only a portion of the Sub-economic unit was logged due to the fact that it is currently regarded to be uneconomic to extract. The boxes logged are: boxes 10-38 (BH501), boxes 10-39 (BH502), and boxes 6-32 (BH503), totalling about 253 m. Each box was logged separately.

Figure 4.11 Tables set up outside the core shed for logging discontinuities in cores BH501, 502, and 503.

Discontinuity core log data sheet

Page 32 of 32

Logged by	Orla Hansen											
Location	Mc Donald's Quarry											
Date logged	Apr-07											
Borehole number	501											
Box number	38											
Depth (m)	118-120.9											
Total thickness in box (m)	2.9											
Thickness described (m) if two units in same box												
Geological unit	Otorohanga Limestone											
Quarry unit	Sub-economic unit											
	Discrete seam thickness (mm)							**Thicknesses (mm)**	**Tot. thick. (mm) of**	**Diffuse seam (mm)**	**Subhorizontal stylolite**	**Subvertical stylolite**
Box lines	**1**	**2-4**	**5-7**	**8-10**	**11-13**	**14-16**	**17-19**	**(discrete seams)**	**discrete seams**			
Line A (bottom)		1	2	1	1			2,11,6,10,6	35		6	
Line B	2	1	1	2	1			2,6,10,13,10,1,1	43			
Line C	1		2	2	1	1		10,10,6,15,11,6,1	59			1
Line D	2		1	2	1			8,8,7,11,1,1	36		2	2
Line E (top)	3		1	2			1	10,10,18,5,1,1,1	46		3	2
Total	**8**	**2**	**7**	**9**	**4**	**1**	**1**		**219**		**11**	**5**
Total broken thickness (m)												
No. of metres in box - broken	2.9											
Comments/notes e.g. porosity, stylolite networks	Last box logged - getting too sandy											

Figure 4.12 Example of a core log data sheet used to record discontinuity information observed in the limestone cores. All other data sheets are given in Appendix D, 4.2.

Figure 4.13 Box lines labelled by the letters A-E used in the discontinuity logging exercise for each box of cores, showing the top of the core (top right) and bottom of the core (bottom left).

The areas where core recovery was poor were not logged; however, the length of broken core was recorded. It is evident that the core preferentially breaks or splits along discontinuities such as dissolution seams and stylolites. As a consequence, it is important to appreciate the potential for losses of material from the cores during processing. For example, during continuous drilling the water used to lubricate the drill bit could therefore potentially remove loose material. Furthermore, the subsequent sawing of the core into halves noted in Chapter 1, Section 1.1 could have affected the original condition of the cores and possibly caused some silica-rich materials occurring along discontinuities to be lost.

4.3 Results for dissolution seams

Discrete and diffuse seams were counted to determine their frequency, and their thicknesses measured for each quarry limestone unit.

4.3.1 Discrete seams

Figure 4.14A-D shows some examples of discrete seams in limestone cores. Discrete seams are by far the dominant discontinuity type in the limestones. Figures 4.15, 4.16, and 4.17 show box plots generated from summary statistics noted in Appendix D.4.4.A-C. The box plots show the spread of the discrete seam thickness data in each core. In BH501 the Sub-economic unit has the largest range of seam thicknesses, followed in decreasing order by Aglime, then Caprock, High Grade, Upper Steel, and Lower Steel units. In BH502 the Sub-economic unit again has the largest seam thickness range, followed by Aglime, High Grade, Lower Steel, Caprock, and Upper Steel units. However, in BH503 the Aglime has the largest range followed by Lower Steel, Sub-economic, Caprock, High Grade, and Upper Steel units. All three cores show a modal (most commonly occurring) seam thickness of about 1 mm. There are variations in maximum seam thickness for the quarry units in each of the three cores.

The number of seams per metre was calculated irrespective of their actual thicknesses and is shown in Figure 4.18. All three cores show the same trends; Aglime has the most seams per metre followed in decreasing order by High Grade, Sub-economic, Lower Steel, Caprock and Upper Steel units.

The total thickness of discrete seams per metre was also calculated and the results are shown in Figure 4.19. The general trends of the three cores show that Aglime has the greatest seam thickness per metre followed by decreased thicknesses in the Sub-economic, High Grade, Lower Steel, Caprock and Upper Steel units.

Figure 4.20 shows the percentage of core taken up by discrete seams in the three cores. Discrete seams are most abundant in the Aglime unit, moderately abundant in the Sub-economic and High Grade units, and least abundant in Caprock, Lower Steel, and Upper Steel units.

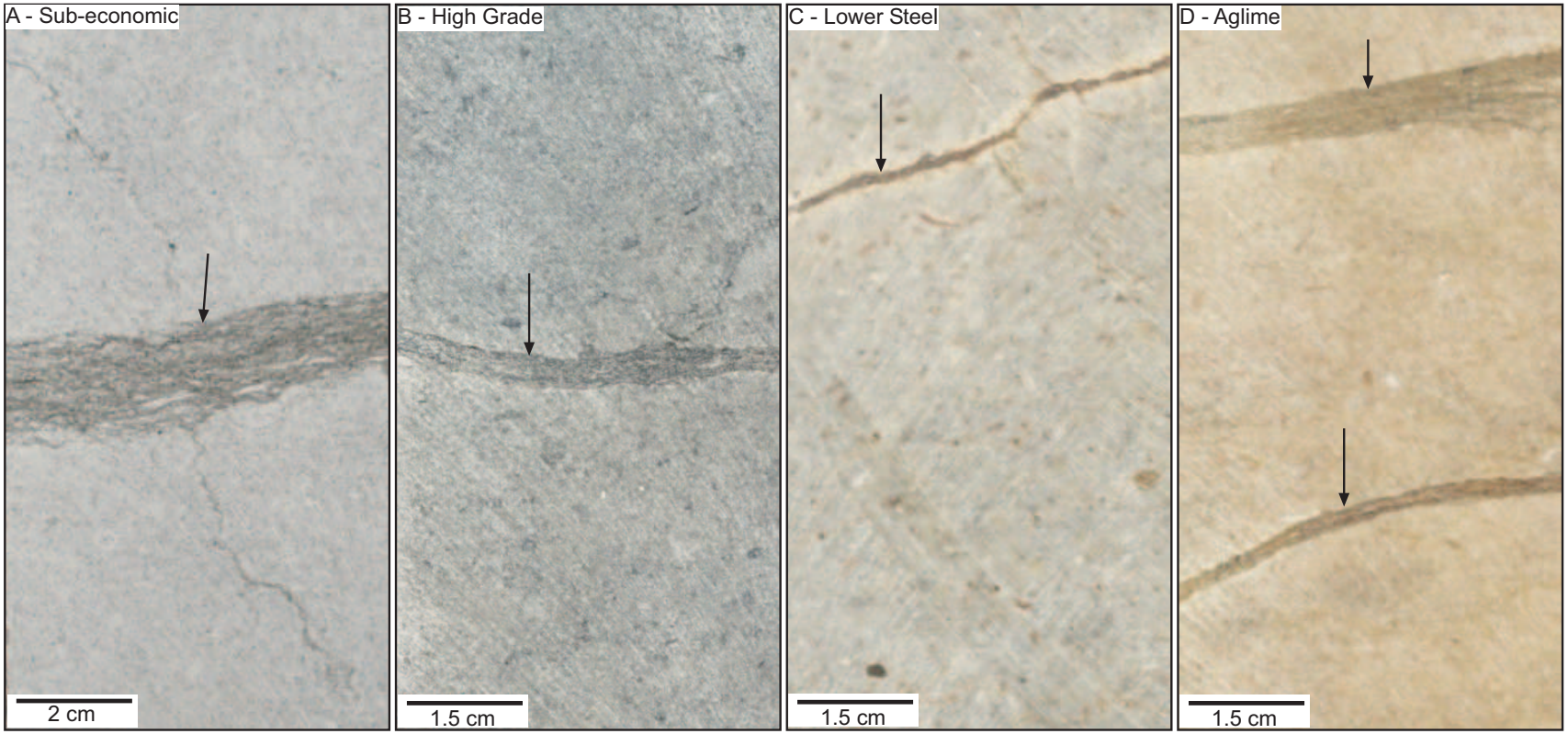

Figure 4.14 Discrete seams arrowed in limestone core. A = A relatively thick, unoxidised discrete seam that is slightly concentrated. Subvertical stylolites can be seen branching off either side of the seam. Sub-economic BH501, box 37, 115 m depth. B = Concentrated, unoxidised discrete seam in the High Grade, BH502, box 19, 53 m depth. C = Thin, oxidised discrete seam in the Lower Steel, BH502, box 37, 105 m depth. D = Two discrete seams of different thicknesses in the Aglime, BH502, box 13, 14 m depth. Photos B-D show sharp boundaries between the seams and adjacent host limestone.

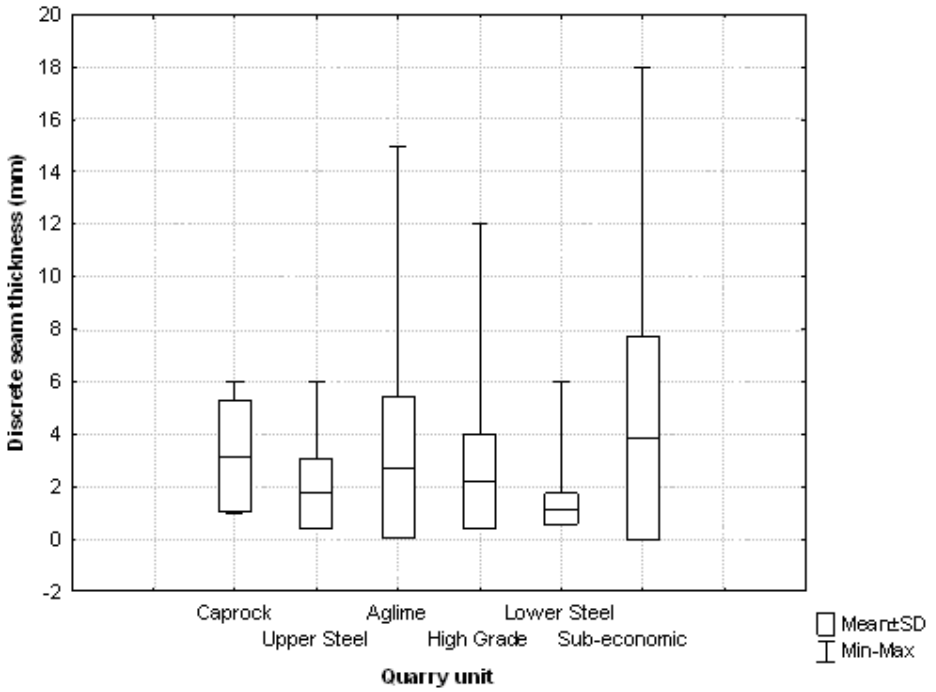

Figure 4.15 Box plots for discrete seam summary statistics data for BH501 (data in Appendix D-4.4.A).

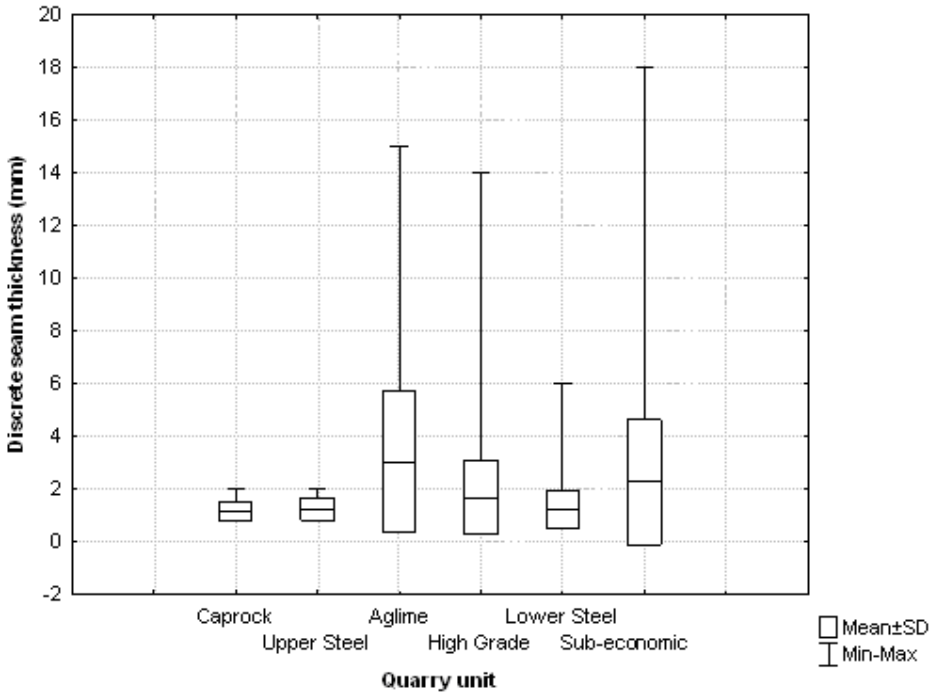

Figure 4.16 Box plots for discrete seam summary statistics data for BH502 (data in Appendix D-4.4.B).

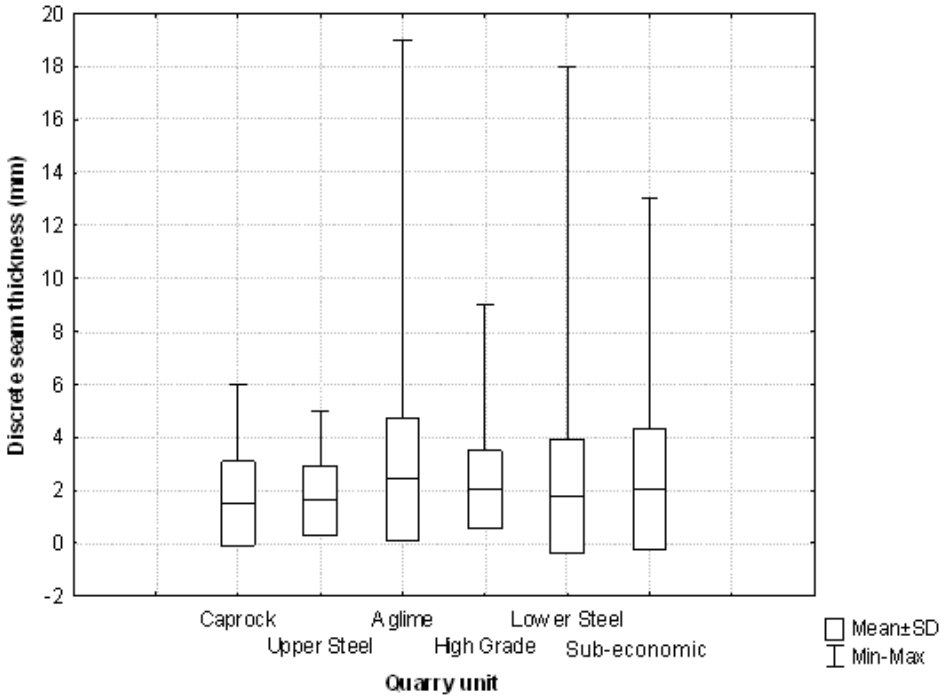

Figure 4.17 Box plots for discrete seam summary statistics data for BH503 (data in Appendix D-4.4.C).

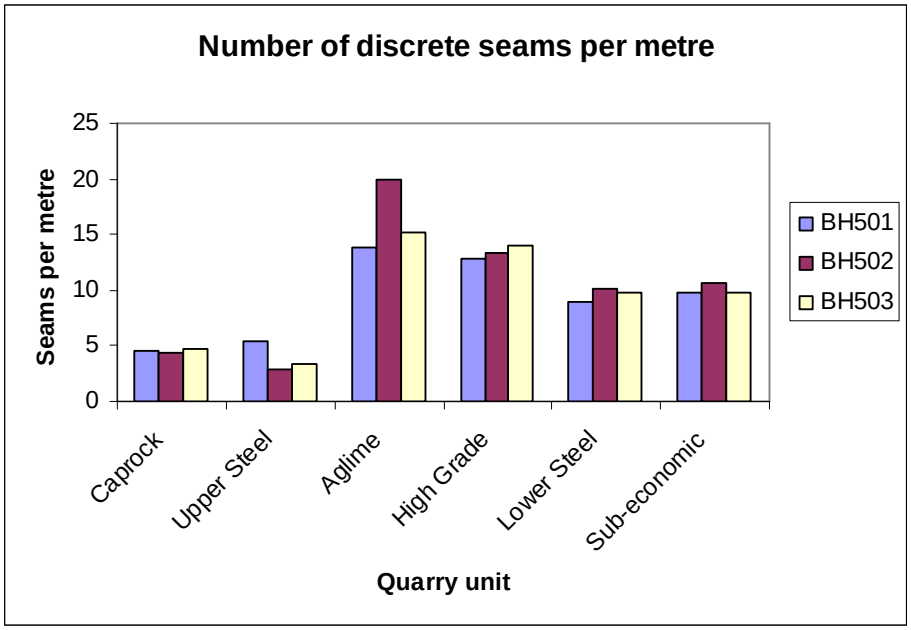

Figure 4.18 Number of discrete seams per metre for limestone quarry units in cores BH501, BH502, and BH503.

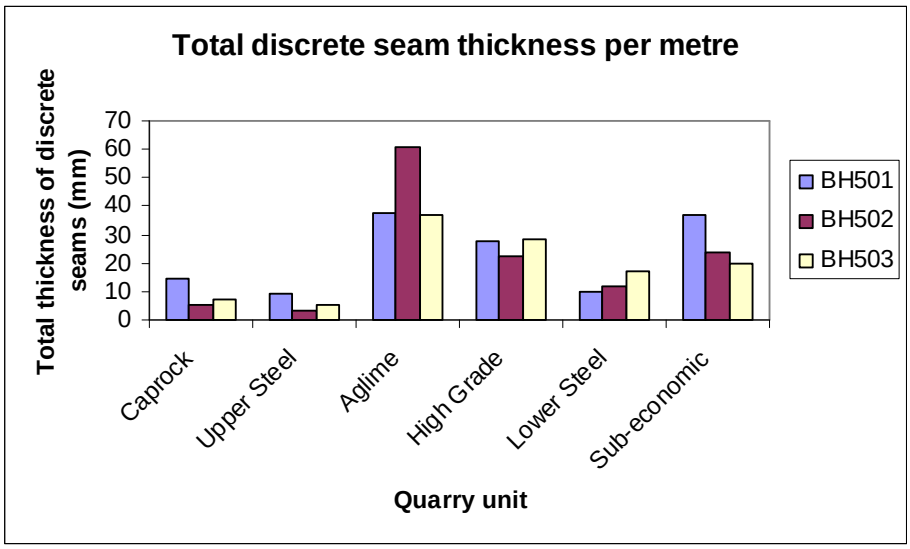

Figure 4.19 Total discrete seam thickness per metre for limestone quarry units in cores BH501, BH502, and BH503.

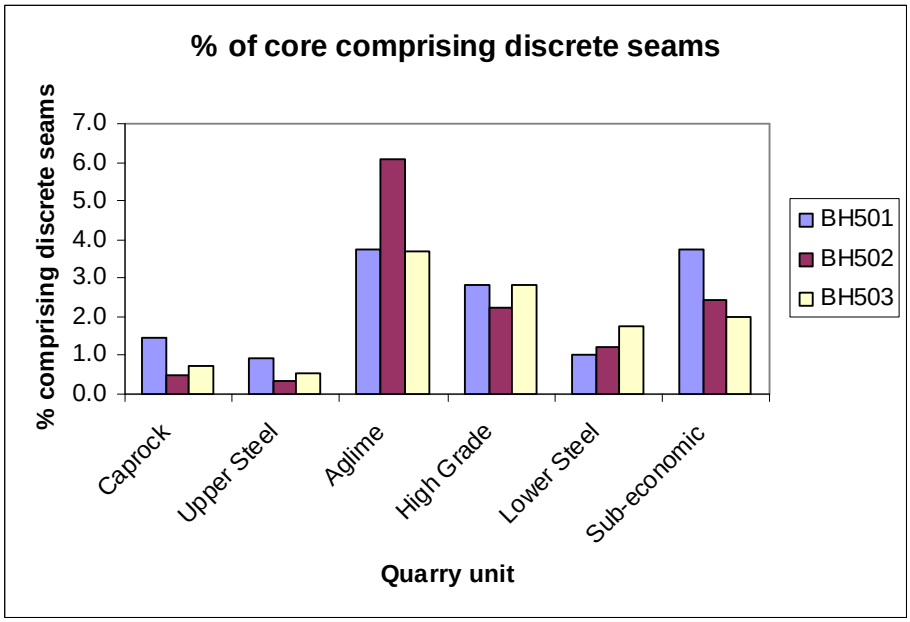

Figure 4.20 Percentage of core comprising discrete seams for limestone quarry units in cores BH501, BH502, and BH503.

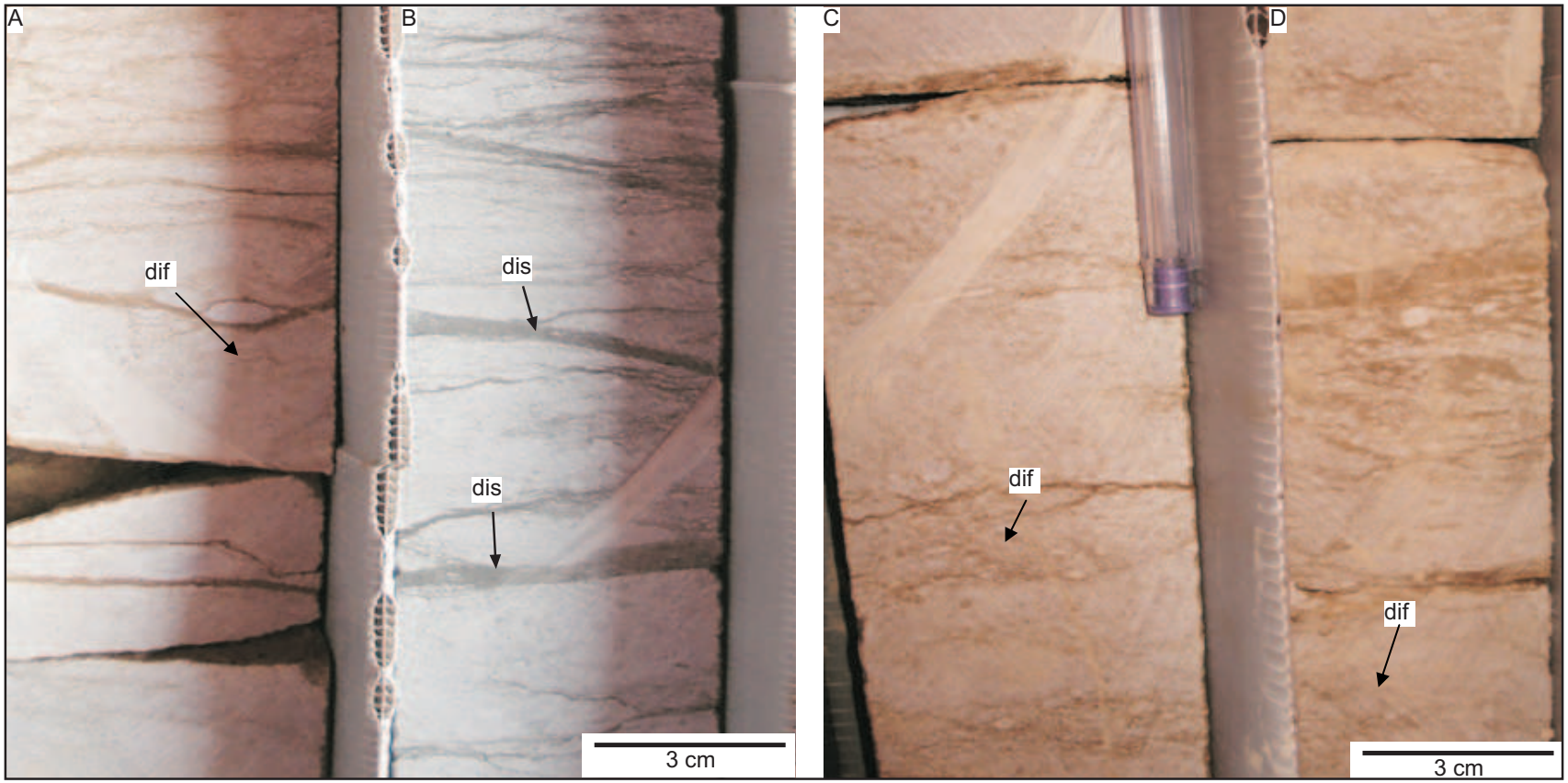

Figure 4.21 Examples of mainly diffuse (dif) and discrete (dis) seams in Aglime core. A = Oxidised diffuse seams with some thinner discrete seams, BH503, box 12, 38 m depth. B = Unoxidised diffuse seams with thicker discrete seams (arrows), BH503, box 12, 38 m depth. C and D = Oxidised, wispy, diffuse seams, BH502, box 15, 43 m depth.

4.3.2 Diffuse seams

Figure 4.21A-D shows some examples of diffuse seams in limestone cores. The total thickness of diffuse seams per metre of core is shown in Figure 4.22. The Aglime unit has the greatest thickness of diffuse seams, followed by moderate thickness in the Caprock and Sub-economic units, relatively small thicknesses for the Upper Steel and Caprock, and rare to absent diffuse seams in the High Grade and Lower Steel units.

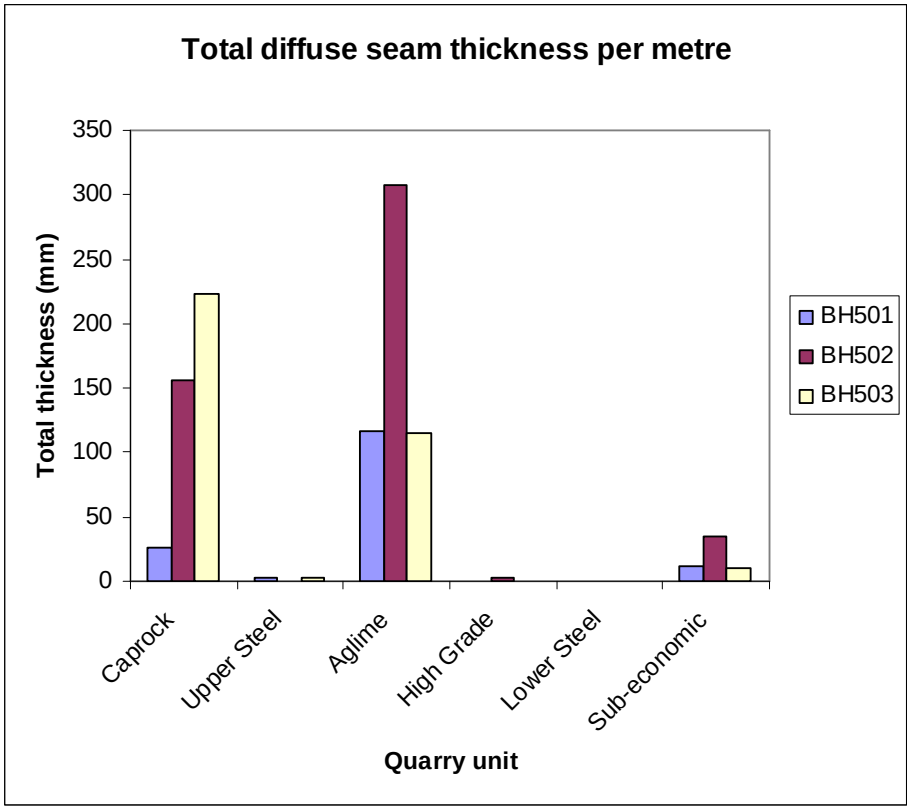

Figure 4.22 Total diffuse seam thickness per metre for limestone quarry units in cores BH501, BH502, and BH503.

Figure 4.23 shows the percentage of core taken up by diffuse seams in the three cores. Diffuse seams are most abundant in the Aglime, less abundant in the Caprock and Sub-economic units, and rare to absent in the Upper Steel, High Grade, and Lower Steel units.

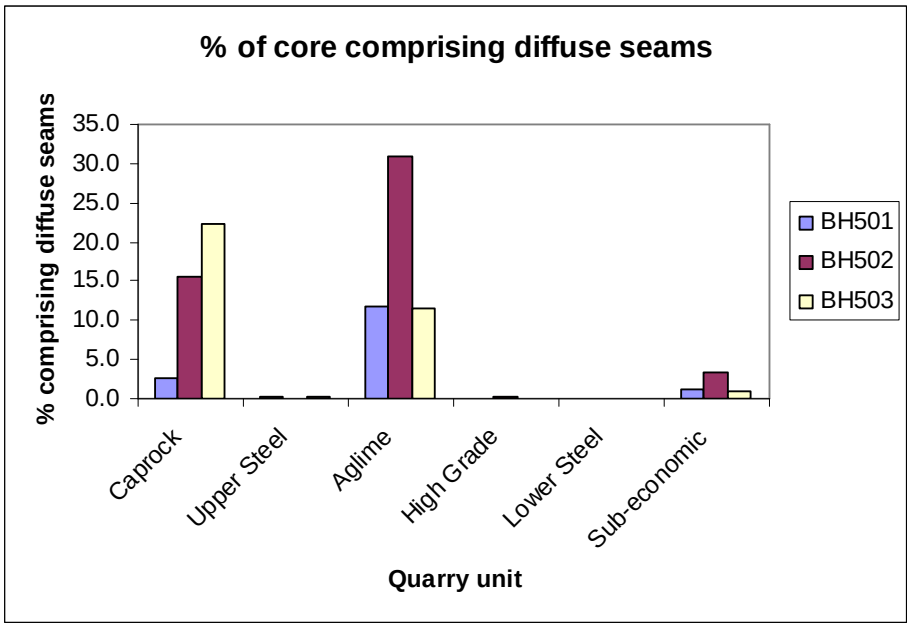

Figure 4.23 Percentage of core comprising diffuse seams for limestone quarry units in cores BH501, BH502, and BH503.

4.4 Results for stylolites

Figures 4.24A-F show some examples of stylolites in limestone cores. **Subhorizontal stylolites:** The number of subhorizontal stylolites per metre for each core is shown in Figure 4.25. All three cores show variations in the number of subhorizontal stylolites across the six quarry units and there are no definite trends, although the Lower Steel and Sub-economic units mainly have the most subhorizontal stylolites.

Subvertical stylolites: Figure 4.26 shows the number of subvertical stylolites per metre found in the three cores. As for the subhorizontal stylolites, there appears to be no major trends and the quarry units in all three cores show variable data, although overall the Caprock appears to contain more subvertical stylolites than the other units.

Stylolite networks: These were recorded when observed, but overall are relatively rare in the three cores.

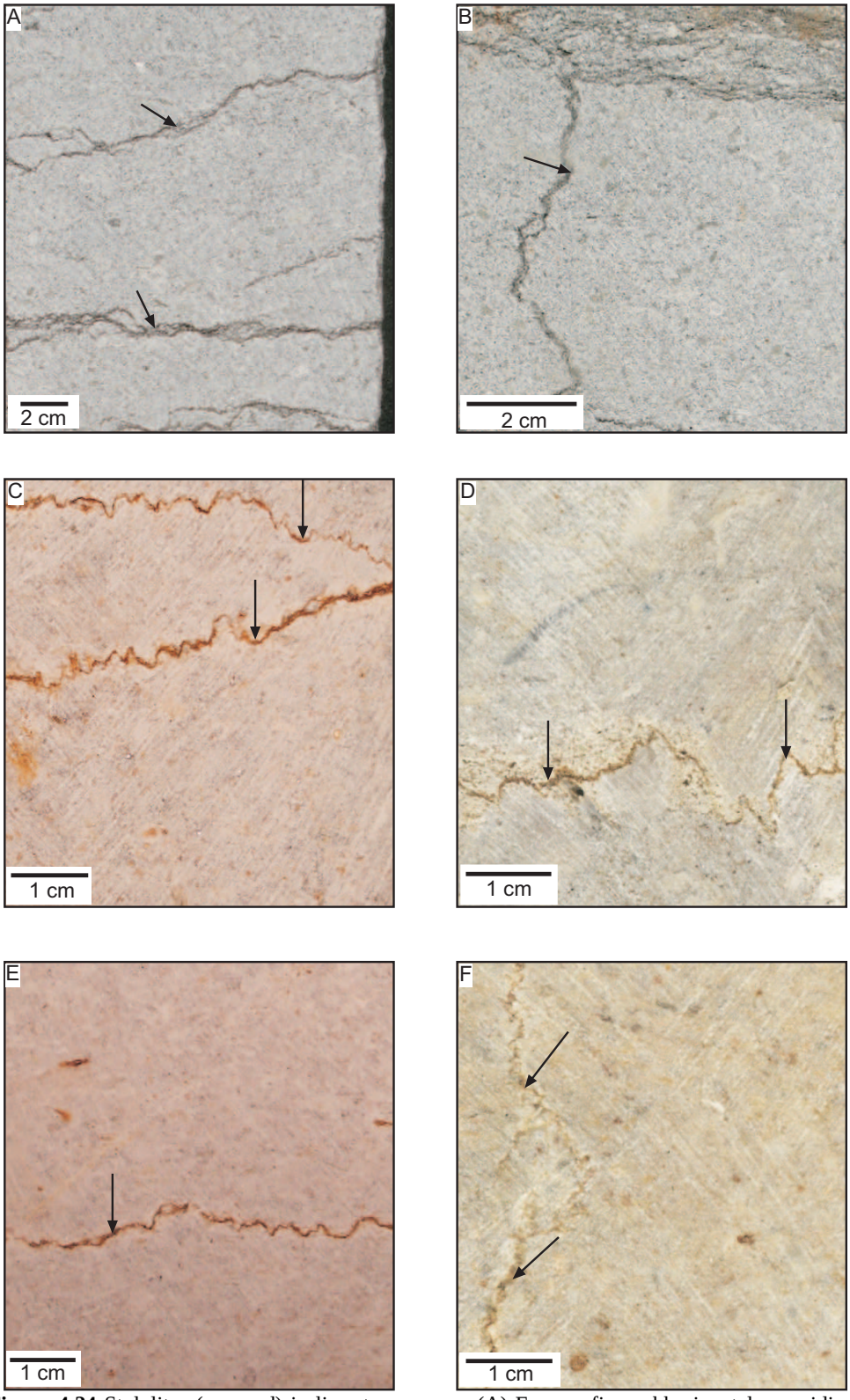

Figure 4.24 Stylolites (arrowed) in limestone cores. (A) Four or five subhorizontal, unoxidised stylolites with relatively low relief in the Sub-economic, BH501, box 37, 115 m depth. (B) Subvertical, unoxidised stylolite branching off from a discrete seam (top) in the Sub-economic, BH501, box 38, 118 m depth. (C) Two merging subhorizontal, oxidised stylolites in the Lower Steel, BH503, box 20, 60 m depth. (D) Subhorizontal, oxidised stylolite with relatively high relief (>1 cm suture amplitude) in the Upper Steel, BH502, box 11, 30 m depth. (E) Subhorizontal, oxidised, low relief stylolite in the Lower Steel, BH503, box 22, 65 m depth. (F) Subvertical, oxidised stylolite in the Lower Steel, BH502, box 24, 67 m depth.

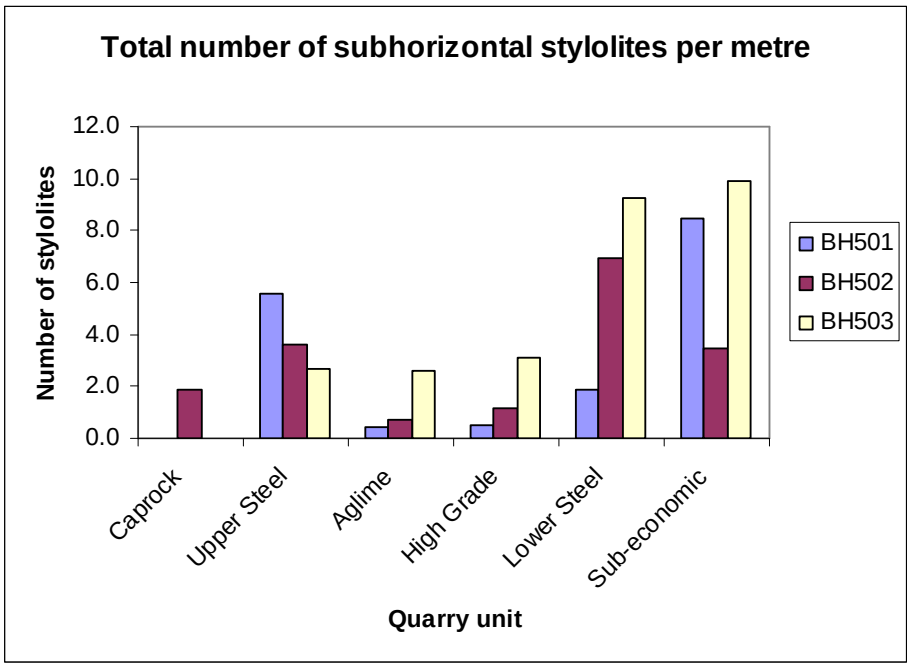

Figure 4.25 Total number of subhorizontal stylolites per metre for limestone quarry units in cores BH501, BH502, and BH503.

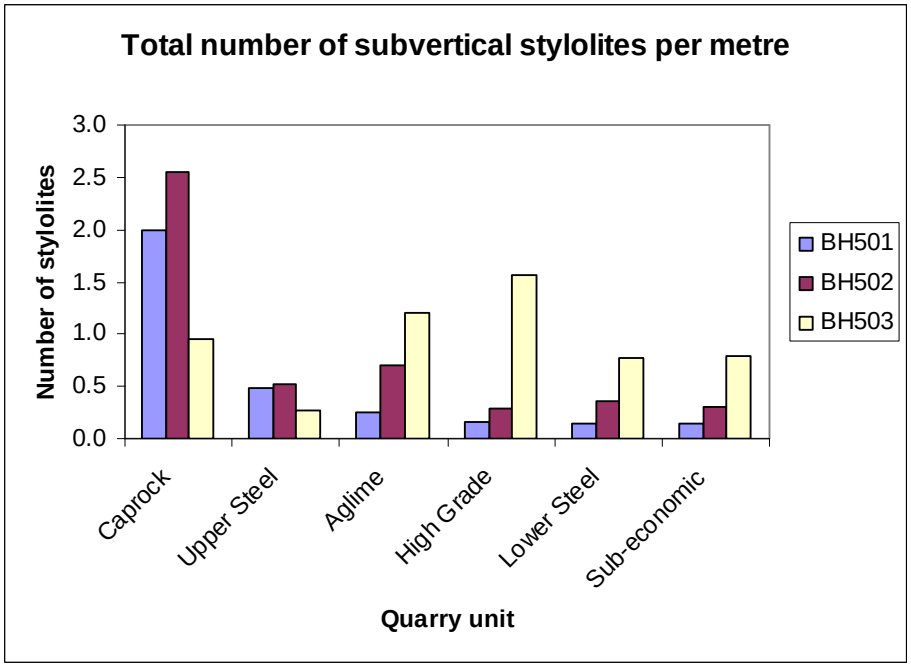

Figure 4.26 Total number of subvertical stylolites per metre for limestone quarry units in cores BH501, BH502, and BH503.

4.5 Results for vertical joints

Two types of joints occur; (1) healed joints (or veins) where calcite precipitates have healed fractures; and (2) unhealed open joints with or without infill. Types 1 and 2 joints are both rare in the cores. Type 2 joints show remnants of infill (i.e.

small amounts present, and not enough to fill the joint completely), with the remaining infill probably lost to drilling or splitting. Figure 4.27A and B shows some examples of joint infills in limestone cores. A papery clay mineral later identified by x-ray diffraction (Chapter 5 Section 5.4.6) as palygorskite (Figure 4.27B) was present on several vertical joint surfaces, as well as an orange brown clay (Figure 4.27A) on other joint surfaces.

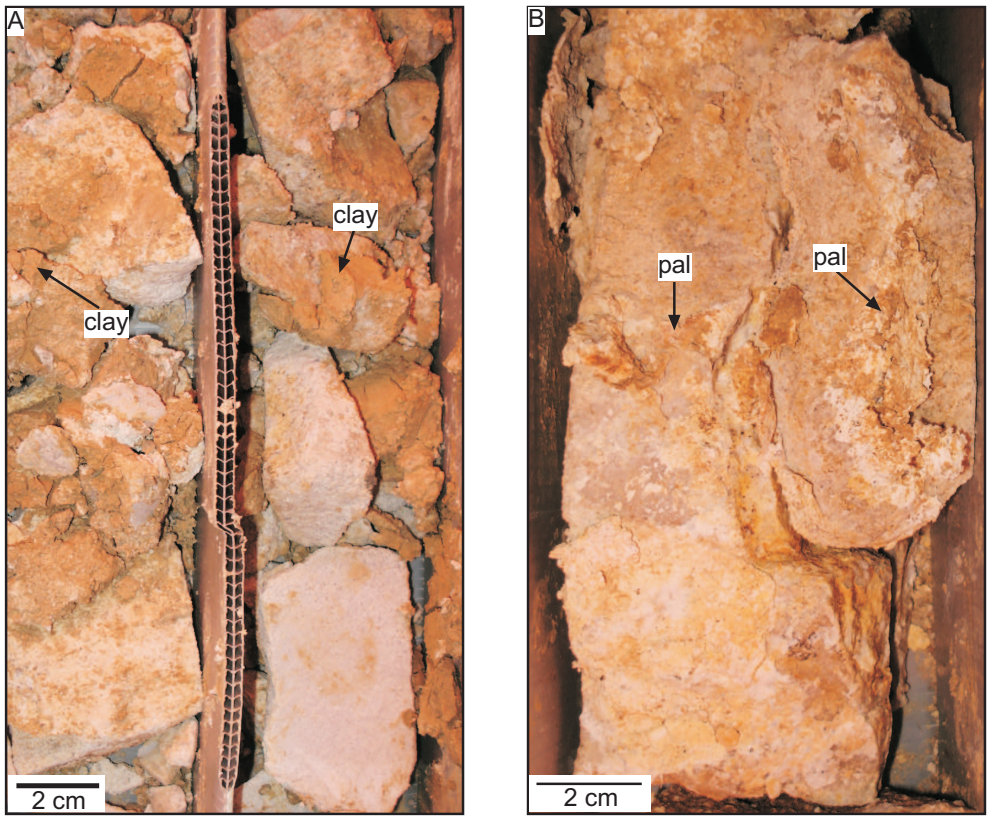

Figure 4.27 Examples of vertical joint infill in limestone core. A = Orange brown clays in a vertical joint in the Upper Steel, BH503, box 8, 24 m depth. B = Palygorskite (pal) (clay mineral) forming on a joint surface in the Lower Steel limestone, BH503, box 21, 64 m depth.

4.6 Results for porous zones and host limestone

In general, the limestone hosting the discontinuities is tight and non-porous (Figure 4.28). However, on occasions, zones of porous limestone (Figure 4.28) are evident, most commonly in the Upper Steel and Lower Steel units, and rarely in the High Grade, Aglime, and Sub-economic units. Porous zones were usually associated with discrete seams and stylolites, the zones occurring over thicknesses up to 30 mm either side of these discontinuities.

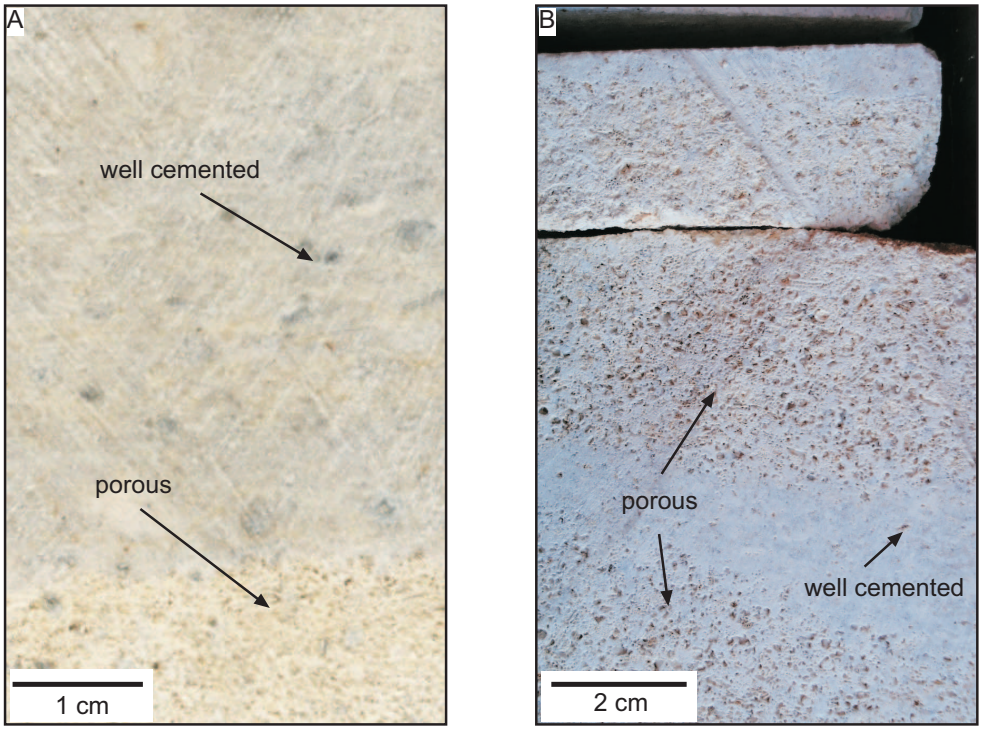

Figure 4.28 Photos of (A) porous and well cemented limestone, and (B) well cemented non-porous limestone core from the Upper Steel unit, BH502, box 10, 27 m depth.

4.7 Discussion

The data for dissolution seams are summarised in Figure 4.29 which shows the seam thickness range, number of seams per metre, total thickness of seam material per metre, and percentage of core taken up by dissolution seams in each of the three cores. A variety of discrete seam thickness ranges occurs across the quarry units. In decreasing order of thickness these are: Aglime (1-19 mm), Lower Steel (1-18 mm), Sub-economic (1-18 mm), High Grade (1-14 mm), Caprock (1-6 mm), and Upper Steel (1-6 mm). The trend is slightly different in terms of the number of discrete seams per metre, namely Aglime (14-20), High Grade (13-14), Sub-economic (10-11), Lower Steel (9-10), Upper Steel (3-5), and (Caprock 4-5). The Aglime has the most variation in number of discrete seams per metre for all three cores. The most important data here are the actual amount or total thickness of discrete seam material present in a given metre.

Categories	Quarry unit	Results			
		BH501	BH502	BH503	All cores
Discrete seam thickness range (mm)	Caprock	1-6	1-2	1-6	1-6
	Upper Steel	1-6	1-2	1-5	1-6
	Aglime	1-15	1-15	1-19	1-19
	High Grade	1-12	1-14	1-9	1-14
	Lower Steel	1-6	1-6	1-18	1-18
	Sub-economic unit	1-18	1-18	1-13	1-18
Number of discrete seams per metre	Caprock	5	4	5	4-5
	Upper Steel	5	3	3	3-5
	Aglime	14	20	15	14-20
	High Grade	13	13	14	13-14
	Lower Steel	9	10	10	9-10
	Sub-economic unit	10	11	10	10-11
Total thickness of discrete seams per metre (mm)	Caprock	15	5	7	5-15
	Upper Steel	9	4	6	4-9
	Aglime	37	61	37	37-61
	High Grade	28	22	28	22-28
	Lower Steel	10	12	17	10-17
	Sub-economic unit	37	24	20	20-37
% of core comprising discrete seams	Caprock	1.5	0.5	0.7	0.5-1.5
	Upper Steel	0.9	0.4	0.6	0.4-0.9
	Aglime	3.7	6.1	3.7	3.7-6.1
	High Grade	2.8	2.2	2.8	2.2-2.8
	Lower Steel	1.0	1.2	1.7	1.0-1.7
	Sub-economic unit	3.7	2.4	2.0	2.0-3.7
Total thickness of diffuse seams per metre (mm)	Caprock	26	155	224	26-224
	Upper Steel	3	0	2	0-3
	Aglime	117	308	115	115-308
	High Grade	0	3	0	0-3
	Lower Steel	0	0	0	0
	Sub-economic unit	12	34	11	11-34
% of core comprising diffuse seams	Caprock	2.6	15.5	22.4	2.6-22.4
	Upper Steel	0.3	0	0.2	0-0.3
	Aglime	11.7	30.8	11.5	11.5-30.8
	High Grade	0	0.3	0	0-0.3
	Lower Steel	0	0	0	0
	Sub-economic unit	1.2	3.4	1.1	1.1-3.4

Figure 4.29 Summary data for discrete and diffuse seams including seam thickness range, total thickness per metre, and % of core comprising seams.

As expected, the lower quality limestones (i.e. Aglime and Sub-economic) have the largest total thickness of discrete material in a given metre. This provides strong evidence that it is the discrete seams that potentially affect the overall amount of silica in the rock (i.e. the amount of seam material in the limestones corresponds to lower quality overall). The total thickness of discrete seams per metre for the remaining limestones is, in decreasing order, High Grade, Lower Steel, Caprock, and Upper Steel. Although the Caprock has relatively low values for discrete seam thicknesses, the fact that it is clay-rich (argillaceous) makes it a low quality unit. The units with the largest percentage of core taken up by discrete seams shows a similar trend: Aglime (3.7-6.1%, highest), Sub-economic (2-3.7%), High Grade (2.2-2.8%), Lower Steel (1-1.7%), Caprock (0.5-1.5%), and Upper Steel (0.4-0.9%).

Diffuse seams are less common in the cores than discrete seams. They are most common in the Aglime (115-308 mm per metre), Caprock (26-224 mm), and Sub-economic (11-34 mm) units. They are rare to absent in the Upper Steel, High Grade, and Lower Steel units. The trend is similar for the percentage of core taken up by diffuse seams. Aglime core can contain as much as 30% of diffuse seams per metre.

Stylolites are also not as common as discrete seams. These are very thin features mostly 1 mm or less in thickness. In terms of the silica issue, they do not contribute as much silica as the discrete and diffuse dissolution seam types. Subhorizontal stylolites are a lot more common than subvertical stylolites. In decreasing order the number of subhorizontal stylolites per metre is as follows: Sub-economic (10), Lower Steel (9), Upper Steel (6), Aglime (4), and High Grade (3) units. In decreasing order, the number of subvertical stylolites per metre is Caprock (3), High Grade (2), Lower Steel (1), Sub-economic (1), Aglime (1), and Upper Steel (less than 1) units. Stylolite networks are rare in all cores.

Due to the fact that drill cores represent a relatively small and narrow window of the subsurface, one would not expect to intercept vertical joints often. However, the cores studied do show joints that have either been healed by secondary precipitation (calcite veins) or infilled with siliceous materials such as clays. The

physical characteristics of these infills are similar to those observed in vertical joints in outcrop (Chapter 3, Table 3.1).

The non-discontinuity (porous zones and host rock) portion of the cores shows that the limestones are generally well cemented. Porous zones are occasionally found in the Upper Steel and Lower Steel units. The host rock is typically purer in the Upper Steel and Lower Steel, and the Aglime, High Grade, and Sub-economic units are visually less pure.

CHAPTER FIVE

Petrographic, mineral, and textural characteristics

5.1 Introduction

The objective of this chapter is to describe the mineralogical and textural composition of the quarry limestone units sampled from core BH502, the overburden units (i.e. Kauroa Ash, Mahoenui Group mudstones), and siliceous materials associated with discontinuities (i.e. discrete seams, diffuse seams, stylolites, joint infills, cave infills) sampled from outcrop in the main quarry. Surface accumulations are also included in the analyses (in discontinuity materials for convenience) which are scrapings sampled from limestone faces that have been coated with quarry dust sourced from vehicle traffic and/or blasting. An introduction to carbonate rock terminology, limestone classification, and the basic descriptions of the techniques used are first given.

The mineralogy of six quarry limestone units (Caprock, Upper Steel, Aglime, High Grade, Lower Steel and Sub-economic) is determined using microscope petrography (both standard and cathodoluminescent) and/or x-ray diffraction (XRD) analysis. Because discrete and diffuse seams, and also stylolites, are inherent parts of the limestone, their mineralogy is also determined using petrography. The $CaCO_3$ content for host rock and seams is also estimated, but includes only the bioclast component and not the much less abundant matrix/cement material (typically 5-25% in Te Kuiti Group limestones; Dodd and Nelson, 1998). Bioclasts and/or cement have been grouped together for petrographic analyses to determine total carbonate content because little would be gained by separating the two from a commercial perspective. It is all carbonate therefore it is not an issue for commercial operation. Porosity, fabrics, modal grain size, grain shape, and sorting, are also determined using petrography.

The mineralogy of discontinuity types (including discrete seam samples from outcrop) is determined by XRD and their texture by wet sieving and laser particle size analysis. Scanning electron microscopy (SEM) was also used to describe the texture of both the limestones and discontinuity types. The chemical elements in some of the samples prepared were also determined using the EDAX (energy dispersive spectroscopy) attachment on the SEM.

5.1.1 Limestone classification and carbonate terminology

In the past, limestones have been subdivided on the basis of the dominant size of their mechanically deposited grains, namely as calcilutite (grains <63 μm), calcarenite (grains >63 μm <2 mm), or calcirudite (grains >2 mm) (Scoffin, 1987). Several other methods have been proposed since the 1950s to classify limestones, mostly based on descriptive properties as seen under a microscope. These include: (1) discrete carbonate grains or clasts; (2) fine grained carbonate matrix (micrite); and (3) carbonate cement (sparry calcite or sparite) which is chemically precipitated from solution into interparticle pore space. Incompletely filled spaces are known as pores, responsible for porosity (Scoffin, 1987). Two microscope-based (petrographic) classifications of limestones have been universally accepted, namely that of Folk (1959) and Dunham (1962). This study uses the scheme devised by Folk (1959).

5.1.2 Folk classification

Folk's (1959) limestone classification is shown in Figure 5.1 and basically considers whether the carbonate particles are held together by carbonate cement (spar) or sit within a carbonate mud (micrite) matrix. The ratio of micrite to spar is deemed to reflect different degrees of hydraulic energy during deposition, the lower the energy the higher micrite content. On this basis Folk (1962) devised a textural maturity classification for limestones (Figure 5.2) which considers not only the micrite:spar ratio but also the degree of sorting and rounding of the carbonate grains. Increasingly higher energy depositional conditions go with decreasing amounts of micrite, increased spar cement, and better sorting and rounding of grains. Note that on Figures 5.1 and 5.2 black boxes highlight the

limestone types that characterise the Te Kuiti Group limestones, where bioclasts are essentially the only carbonate grain type present.

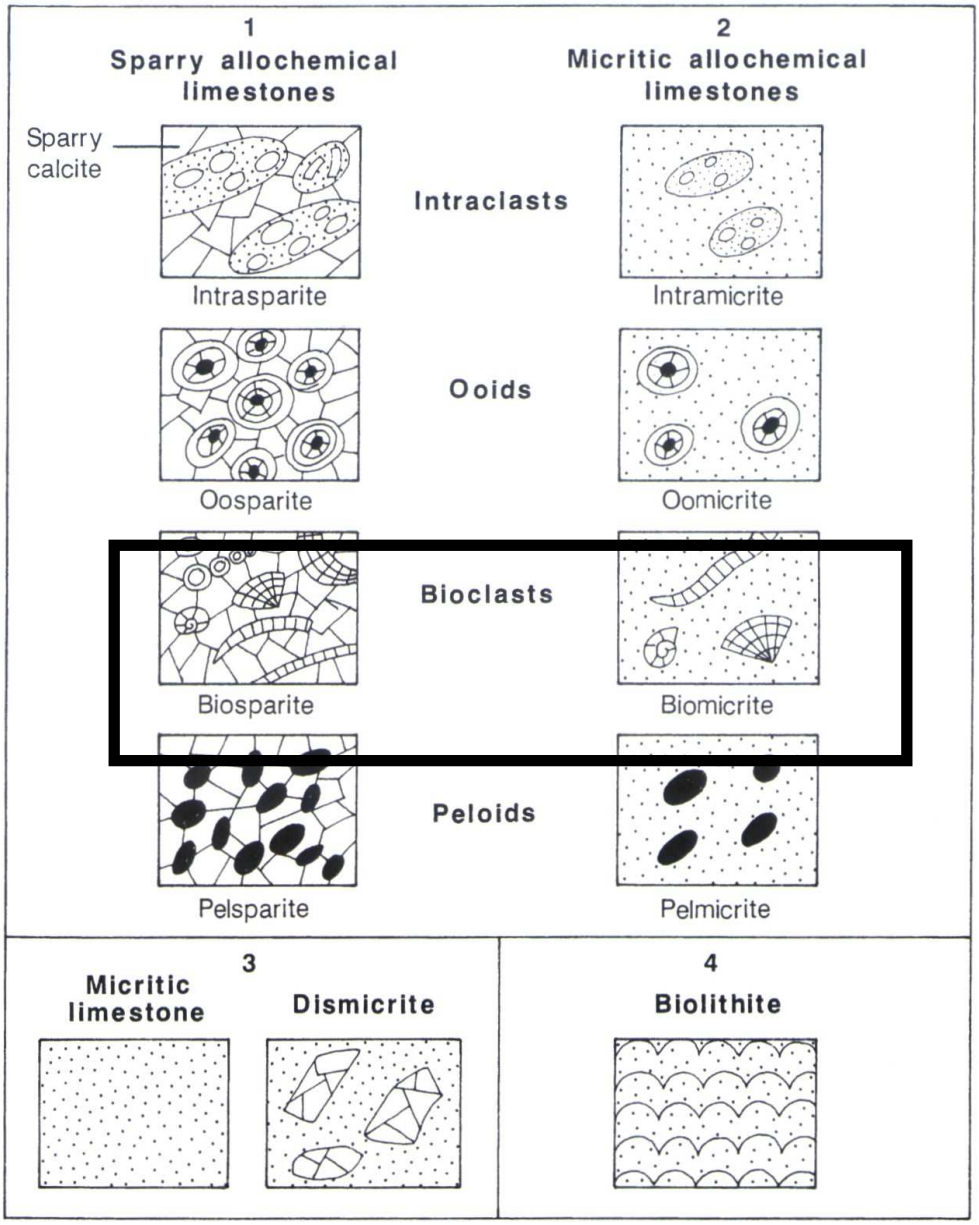

Figure 5.1 Folk's (1959) classification of basic limestone types (from Tucker and Wright, 1990). The nomenclature is based on the nature of the grains (allochems) and the relative abundance of micritic matrix versus open pore space/sparry calcite that may fill such pores. The main grain types are listed down the middle of the figure. Box 3 refers to micritic matrix lacking allochems, the dismicrite variety including blebs of sparry calcite from burrowing. Box 4 is a biolithite which is a biologically bound rock (i.e. a reef). Note the bold box surrounds the only limestone types found at the quarry.

The three main components in Folk's limestone classification are grains, matrix, and cement. There are four main grain types in limestones generally: (1) Skeletal

carbonate grains or fossils (abbreviated as bio), which are the skeletal remains of carbonate secreting organisms, referred to also as bioclasts (used in this study).

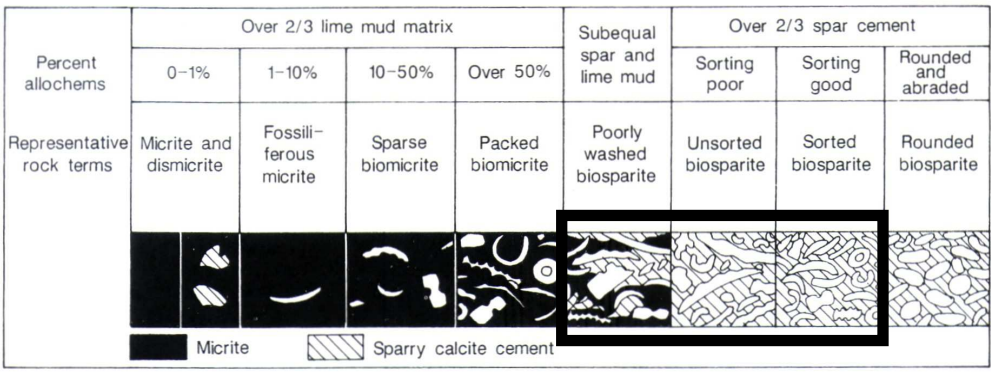

Figure 5.2 Folk's (1962) textural maturity classification of limestones (from Tucker and Wright, 1990) showing 8 classes that generally reflect an increase in environmental energy level from low (left) to very high (right). Note the bold box surrounds the dominant limestones found at the quarry.

These are formed by the biochemical precipitation of $CaCO_3$ by organisms and are the principal/and often only carbonate grain type in New Zealand limestones. (2) Non-skeletal carbonate grains such as ooids (oo) are small round grains with radial or concentric internal structure. They form without organic intervention where chemical precipitation from carbonated saturated seawater occurs. Ooids contain one or more lamellae formed as successive coatings around a nucleus such as a fragment of a skeleton, pellet, another ooid, lithoclast, or siliciclastic grain. Ooids are typically spherical or ovoid and 0.2-1 mm in diameter. They generally do not form in non-tropical latitudes and so are not found in New Zealand Cenozoic limestones. (3) Pellets (pel) form mainly from the ingestion of fine calcareous detritus during grazing on organic rich sediment by marine organisms. $CaCO_3$ is excreted with their waste products as faecal pellets having elliptical, oval, or rod-like shapes which are rich in organic matter when fresh. If the faecal pellets are exposed to supersaturated waters, they may harden with interstitial precipitation of cement (Scoffin, 1987). Pellets are rarely preserved in New Zealand limestones. (4) Intraclasts (intra) are lithoclasts or fragments of limestone that have been derived from within the basin of deposition. They can be well cemented or semi-consolidated (Scoffin, 1987). Again they are absent or rare in most New Zealand limestones.

In the Folk scheme, the petrographic limestone name is constructed from the abbreviations for the various carbonate grain types (i.e. bio, oo, pel, and intra above) followed by the matrix or cement abbreviated name (i.e. mic or spar), and then the –ite rock suffix ending. Thus, bioclasts in a micrite matrix define a biomicrite, while in a spar cement the name would be biosparite. To encompass different sizes of bioclasts (bios), Folk incorporated the names lutite (<0.06 mm), arenite (0.06-2.0 mm), and rudite (>2.00 mm), so giving rock names like biomiclutite, biospararenite, and biosparrudite. Because sand-sized components dominate in most limestones he also suggested the arenite name could be dropped, so that biospararenites would become biosparites and biomicarenites would become biomicrites.

In addition to carbonate material, non-carbonate material can also occur in limestones, including terrigenous or siliciclastic grains (transported ones) such as quartz and clay minerals, and authigenic (chemically precipitated) components like glauconite and pyrite. These non-carbonate components more or less correspond to the silica materials responsible for the so-called silica issue in the quarry limestones.

5.1.3 Bioclast types

At different periods of geological time different types of organisms have been capable of producing calcareous skeletons (Tucker and Wright, 1990). The main factors that contribute to the changes in assemblages of biogenic (bioclastic) grains are time and environment. Skeletal organisms can be planktic (float in the water column) or benthic (bottom dwelling). Identification of bioclasts relies on determining their shape and size. Some common organisms found in Te Kuiti Group limestones include foraminifera (Figure 5.3), which are unicellular chambered skeletons ranging from 1-10 mm in size (Tucker and Wright, 1990). Other bioclasts include the calcareous remains of echinoderms (Figure 5.3), including plates, sclerites and spines, where each part behaves as a single crystal of calcite; using a light microscope such particles display unit extinction under crossed polars led light (Tucker and Wright, 1990). Bryozoans (Figure 5.3) are sessile colonial animals that can occur as encrusting sheets or plant-like tuffs,

fleshy lobes, or erect branching calcareous structures. Body walls and chambers (zooecia, Figure 5.3) occur in a cellular arrangement in thin section, making bryozoans reasonably easy to identify. They are a major grain contributor in the quarry limestones. Useful compendiums including descriptions and images of the many different types of skeletal and non-skeletal carbonate grains are those by Tucker and Wright (1990), Scoffin (1987), and Scholle and Ulmer-Scholle (2003).

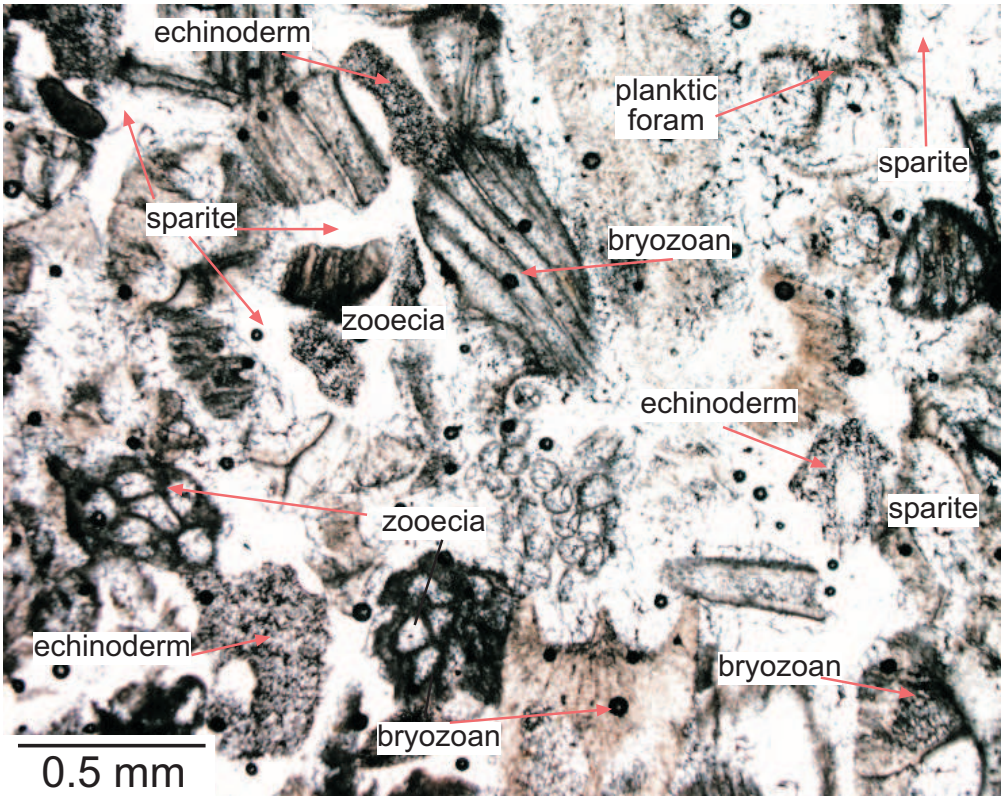

Figure 5.3 Thin section of host rock in the Upper Steel limestone showing bioclasts including bryozoans and their body chambers or zooecia, echinoderms, and planktic forams set in sparite cement. The fabric of the rock is open and the sparite cement occurs both within (intraparticle) and between (interparticle) grains. PPL (= plane polarised light). Field sample no. 24.1, BH502, 28.5 m depth.

5.1.4 Granulometric and morphometric properties

Although carbonate grain types are the most useful in environmental interpretation of limestones, granulometric (i.e. grain size and sorting) and morphometric (i.e. grain shape and roundness) properties are also important (Tucker and Wright, 1990). Grain sizes in a rock are used as a guideline of energy levels in the depositional environment. The grain size scale used in this study is reproduced in Appendix E-5.1. Skeletal grains have unique

hydrodynamic properties. Some are porous or hollow, and they have different architectures and therefore disintegrate in different ways. For example, codiacean algae like *Halimeda* decay to sand and mud sized carbonate, whereas the coral *Acropora* forms gravel and sand sized fragments (Tucker and Wright, 1990). Sorting characteristics can help determine environmental energy levels and are dependent on the transportation and depositional regime, and the nature of the source material. A comparison chart can be used to describe sorting.

Grain shape and roundness are a function of the amount of transportation and abrasion a grain has experienced. One must be careful when describing this property as grains such as ooids and pellets are already well rounded and in the case of bioclasts some, like many foraminifera, are originally round in shape (Tucker and Wright, 1990).

5.1.5 Matrix

Matrix (Figure 5.4A) in carbonate rocks consists of dense, fine grained calcite crystals referred to as microcrystalline calcite, carbonate mud, or micrite (used in this study) where the carbonate crystals are <5 μm in size (Adams and MacKenzie, 1998). Micrite appears dark coloured (grey to dark brown) under the microscope (e.g. Figure 5.4A). Micrite can be precipitated directly from sea water (in which case it is strictly a cement) or can result from the disintegration and erosion of skeletal grains (Adams and MacKenzie, 1998). Many matrices are originally made of the carbonate crystals aragonite and high-Mg calcite which are later replaced by low-Mg calcite during diagenesis (all processes which affect sediments after deposition until early metamorphism). The origin of micrite is often difficult to determine and a number of scenarios are recognised (Tucker and Wright, 1990): (1) Inorganic precipitation associated with high temperatures and salinities or a change in partial pressure of CO_2; (2) Disintegration of calcareous green algae; (3) Direct biogenic formation of micrite occurs with accumulation of shell fragments of calcareous plants like coccolithophorids; (4) Breakdown of skeletal organisms other than plants, bioerosion by organisms (rasp, crunch, or borings) into carbonate substrates to form carbonate mud; and (5) Marginal marine and freshwater algal marshes produced by precipitation by cyanobacteria.

5.1.6 Cement

Burial cements, which are common in Te Kuiti Group limestones (Nelson et al., 1988b), are cements that have been precipitated in a burial environment. These cements are mostly clear, coarse, calcite spar cements (Tucker and Wright, 1990). Sparry calcite or sparite (Figure 5.4B) comprises crystals >5 μm in size and often much larger (Tucker and Wright, 1990), and are typically the pore-filling cement responsible for the lithification (hardening) of a skeletal sediment into limestone. Two common cement mosaic types occur, namely drusy and syntaxial. (1) Drusy equant calcite is a pore filling cement that usually increases in crystal size towards the cavity centre. Drusy mosaic occurs as a result of this growth competition having a preferred orientation of optic axes normal to the substrate (Tucker and Wright, 1990). (2) Syntaxial calcite spar occurs as overgrowths about echinoderm fragments (Figure 5.4B and C), and can be zoned like drusy calcite spar. It forms in optical continuity with its host substrate (Scholle and Ulmer-Scholle, 2003), in this case single crystal echinoderm grains.

5.1.7 Porosity

Other features that limestones may possess include porosity. Modern carbonate sediments in general have porosities of 40% or more, however, during burial of the sediment, mechanical and chemical compaction can reduce the porosity close to zero (Dodd and Nelson, 1998). Porosity is the ratio of total pore space to the total volume of rock and is expressed as a percentage. In limestones it is mostly of diagenetic origin.

Figure 5.4 (Facing page) These photomicrographs show examples of the matrix and cement types, and some bioclast types in the quarry limestones. (A) Thin section under PPL of the Aglime (field sample no. 12.3, BH502, 41.3 m depth) host rock. It is dominated by micrite which appears as a dark grey, fine-grained intraparticle and interparticle material, especially evident in the bryozoan zooecia (chambers). The fabric of this rock is tight, and bioclasts are dominated by fragments of bryozoans. Microspar (within bryozoan) is recrystallised micrite, which generally ranges from 5-30μm crystal size (Folk, 1965). (B) Thin section under PPL of the Sub-economic host rock (field sample no. 19.1, BH502, 87.6 m depth). It is dominated by interparticle sparite cement. This sample is also bryozoan dominated, and the fabric is slightly open. In the lower centre of the photomicrograph, syntaxial rim cement has formed around an echinoderm fragment. (C) A porous sample under PPL from the Upper Steel (field sample no. 24.2, BH502, 28.55 m depth) host rock. It is cement poor and has interparticle and intraparticle porosity, and is dominated by bryozoan and some echinoderm fragments. The rock fabric is open.

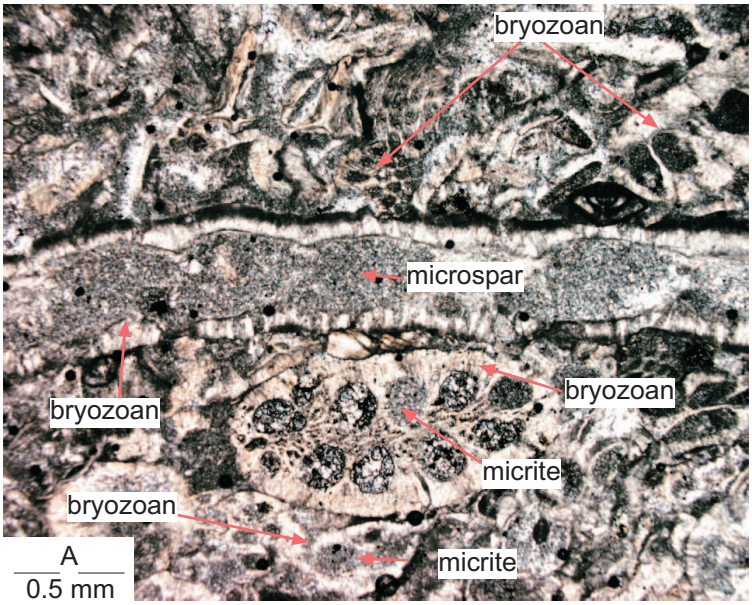
bryozoan
microspar
bryozoan
bryozoan
micrite
bryozoan
micrite
A
0.5 mm

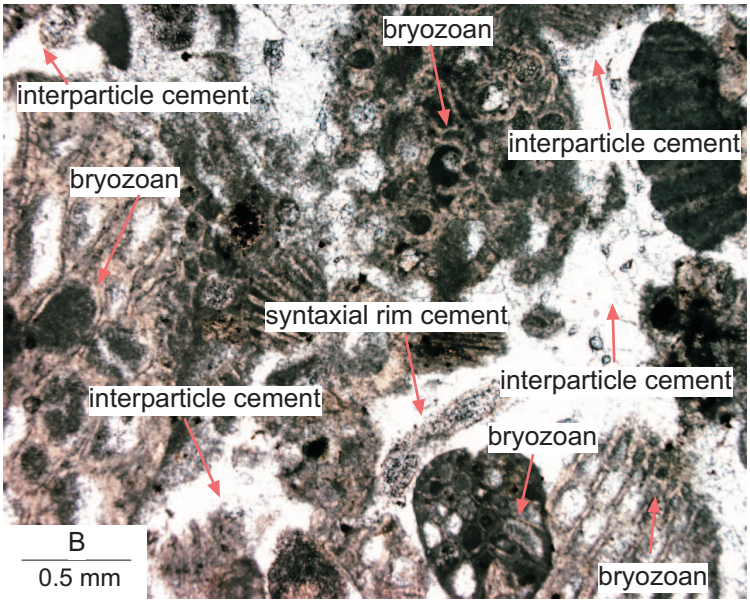
bryozoan
interparticle cement
interparticle cement
bryozoan
syntaxial rim cement
interparticle cement
interparticle cement
bryozoan
bryozoan
B
0.5 mm

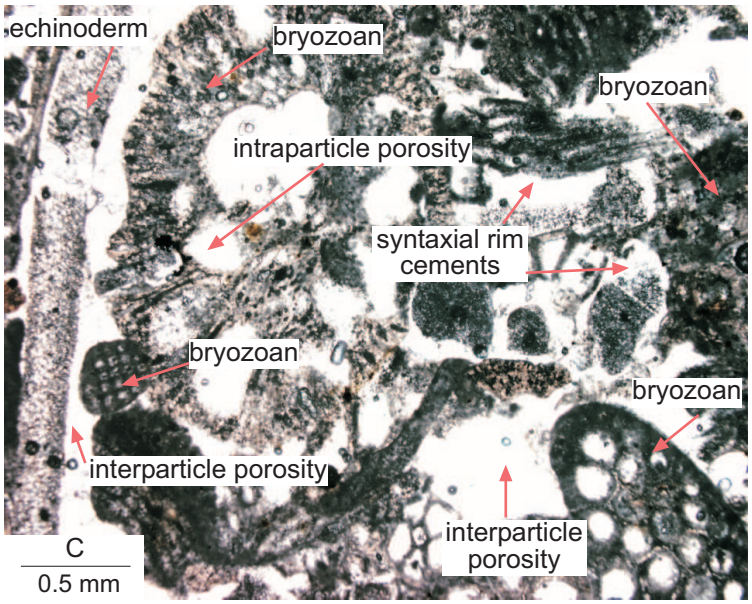
echinoderm
bryozoan
bryozoan
intraparticle porosity
syntaxial rim cements
bryozoan
bryozoan
interparticle porosity
interparticle porosity
C
0.5 mm

Porosity types range from fabric selective where pores are defined by fabric elements of the rock (e.g. grains or crystals), to non-fabric selective (Figure 5.5) where porosity cross cuts the actual fabric of the rock (e.g. fracture porosity), and fabric controlled or not (Figure 5.5). Some of the main fabric selective porosities include interparticle porosity resulting from the original, primary depositional fabric of a sediment (Figure 5.4C). Types of packing fabric are important in controlling the shape of the pore space formed. Another fabric selective porosity is intraparticle porosity (Figure 5.4C). This porosity occurs within grains, particularly in shell material. It is localised and dependent on the skeletal grain type (i.e. bryozoans have pores whereas bivalves do not) and the overall fabric of the rock. Intercrystalline porosity occurs between crystals, and commonly occurs in the replacement of dolomite (another $Ca(MgCO_3)_2$ carbonate mineral), and represents secondary porosity. Mouldic porosity (Figure 5.5) occurs when shallow water carbonate grains such as aragonite and high Mg calcite (i.e. skeletal types such as gastropods and infaunal bivalves) are prone to dissolution in undersaturated water. Dissolution of bioclasts and ooids leaves behind biomoulds and oomoulds, respectively.

An example of a not-fabric selective porosity is fracture porosity which cuts across fabric elements of the rock (Figure 5.5). This can result from tectonic deformation, slumping or solution collapse associated with limestone dissolution, and commonly greatly increases the permeability of a limestone.

5.1.8 Burial features

Once carbonate sediments are deposited they eventually undergo burial where a number of processes can occur that begin to convert the loose sediment into a hardened or lithified limestone. The physical and chemical processes involved usually reduce porosity and permeability but sometimes can increase them (Scholle and Ulmer-Scholle, 2003). In general, loss of porosity and permeability occurs with increased time and depth of burial. Physical processes include mechanical compaction (dewatering and deformation, or reorientation of grains), as well as fracturing (Figure 5.6A) and shattering (Figure 5.6B) of grains. The rearrangement of particles and grains aids in packing and marks the early stages of

compaction (Tucker and Wright, 1990). Compaction due to overburden stresses accounts for the thickness reduction in carbonate sequences (Tucker and Wright, 1990).

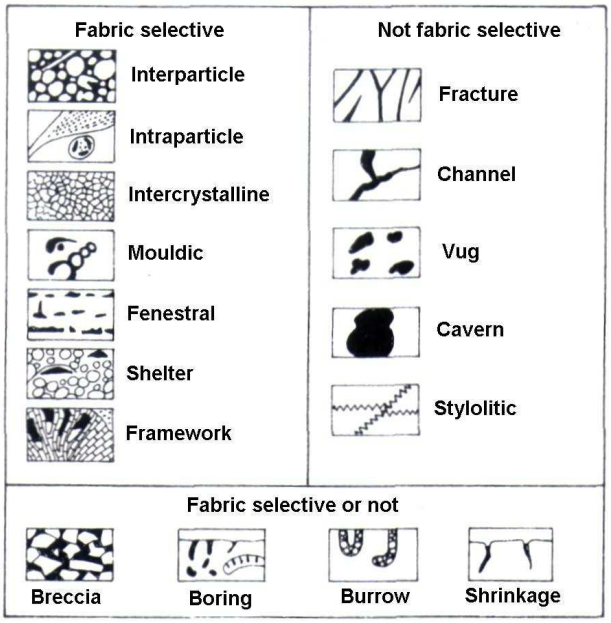

Figure 5.5 Porosity types which are either fabric selective or not fabric selective, based on Choquette and Pray (1970) modified from Tucker and Wright (1990). Fabric selective porosity is controlled by the grains, crystals or other physical structures where the pores do not cross these boundaries. Not fabric selective porosity can cross cut grains.

Chemical compaction follows after physical compaction generally and leads to local rock compaction and puts $CaCO_3$ into solution for precipitation as cements at other available pore space sites (Scholle and Ulmer-Schoelle, 2003). Chemical processes include cementation (filling of pore space of either a primary or secondary origin with newly precipitated materials), which involves the local dissolution of skeletal grains mainly along surfaces such as dissolution seams or stylolites. Microstylolites (Figures 5.7A and B), sometimes referred to as fitted fabrics, also occur. These are formed by the interpenetration of grains where grain surfaces can be sutured, curved, or planar (Figure 5.8). They differ from typical stylolites because they do not extend beyond the two grains in contact (Tucker and Wright, 1990). Dissolution can also lead to the leaching of unstable minerals (e.g. aragonite, high-Mg calcite) to form secondary porosity (Scholle and Ulmer-Scholle, 2003). In addition, these unstable minerals may become replaced and re-precipitated as low-Mg calcite, which is relatively stable. Fractures formed during burial stresses can also be healed by the precipitation of calcite cement as calcite veins (Figure 5.9).

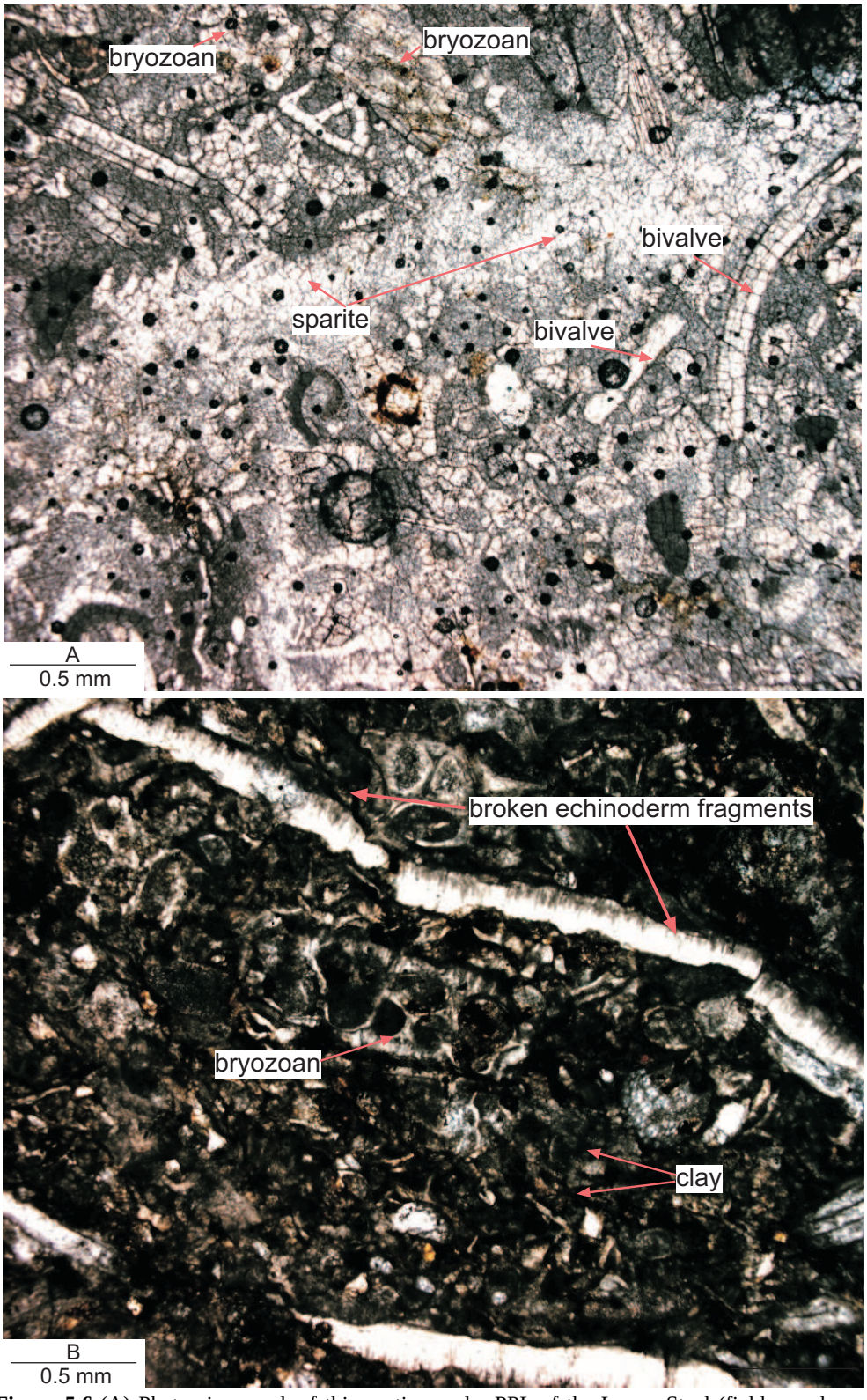

Figure 5.6 (A) Photomicrograph of thin section under PPL of the Lower Steel (field sample no. 49.1, BH502, 70.7 m depth) host rock. The dominant cement is sparite, but note the fracturing that has occurred throughout the rock. Although fracturing (a burial feature) can make grain identification difficult, bryozoans and bivalves remain evident. (B) Photomicrograph of thin section under PPL of a clay rich sample in the Aglime unit (field sample no. 13.3, BH502, 42.9 m depth). A few bryozoans can be identified. The main feature is the large broken skeletons (echinoderms) in the image. It has been broken as a result of burial stresses on the rock. The fabric of the rock is tight and the bioclasts are fragmented.

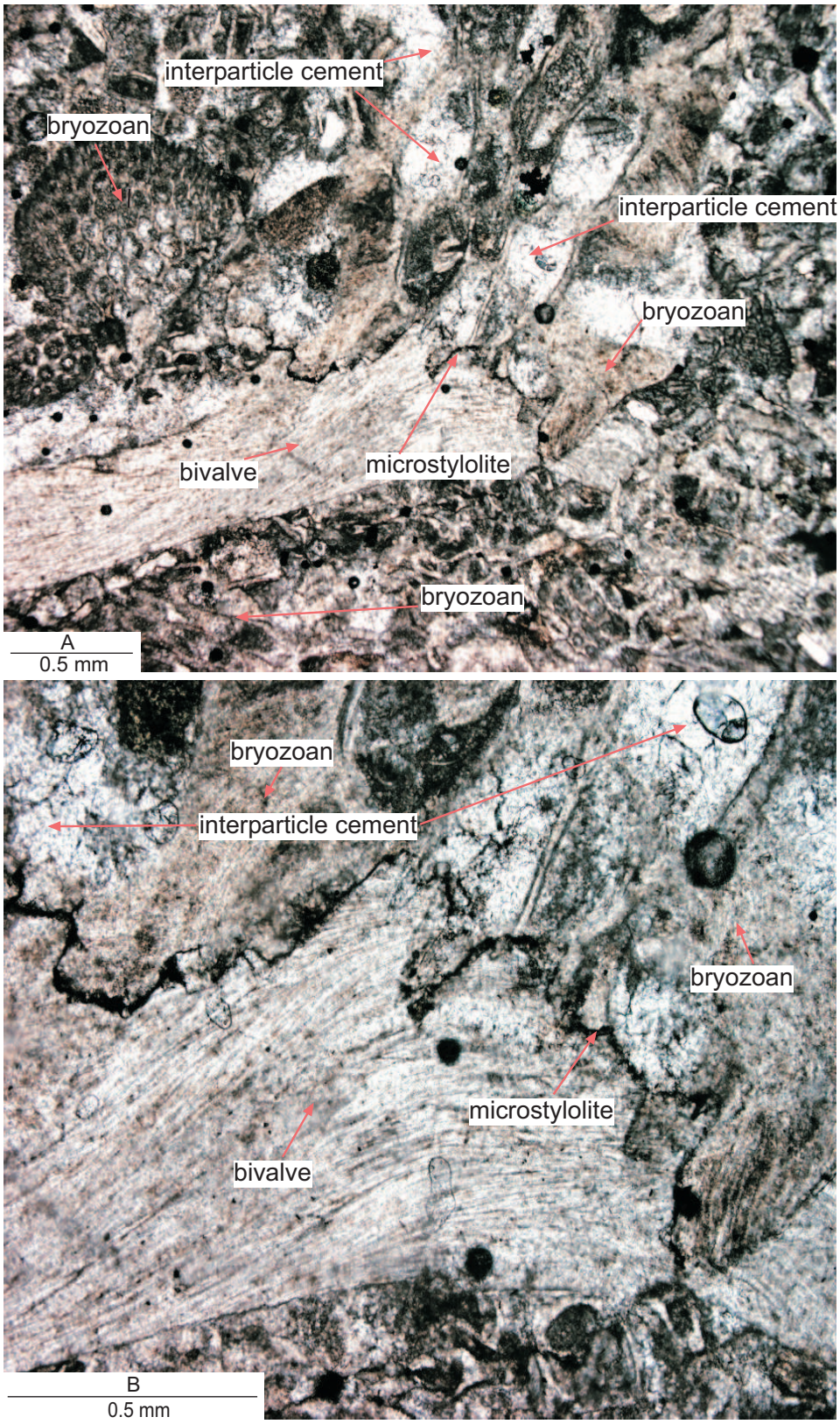

Figure 5.7 (A) Photomicrograph of thin section under PPL of the High Grade (field sample no. 15.1, BH502, 56.65 m depth) host rock. The rock has a tight fabric and is dominated by bryozoans and interparticle sparite cement. At the centre of the image is a microstylolite, a typical burial feature produced by pressure dissolution at grain to grain contacts. Like stylolites, the feature is sutured, but the term 'micro' implies that the feature does not extend beyond the two grains in contact (Tucker and Wright, 1990). The two fragments involved are a bivalve (left) and bryozoan (right). (B) Photomicrograph of the same microstylolite in (A) but at a higher magnification.

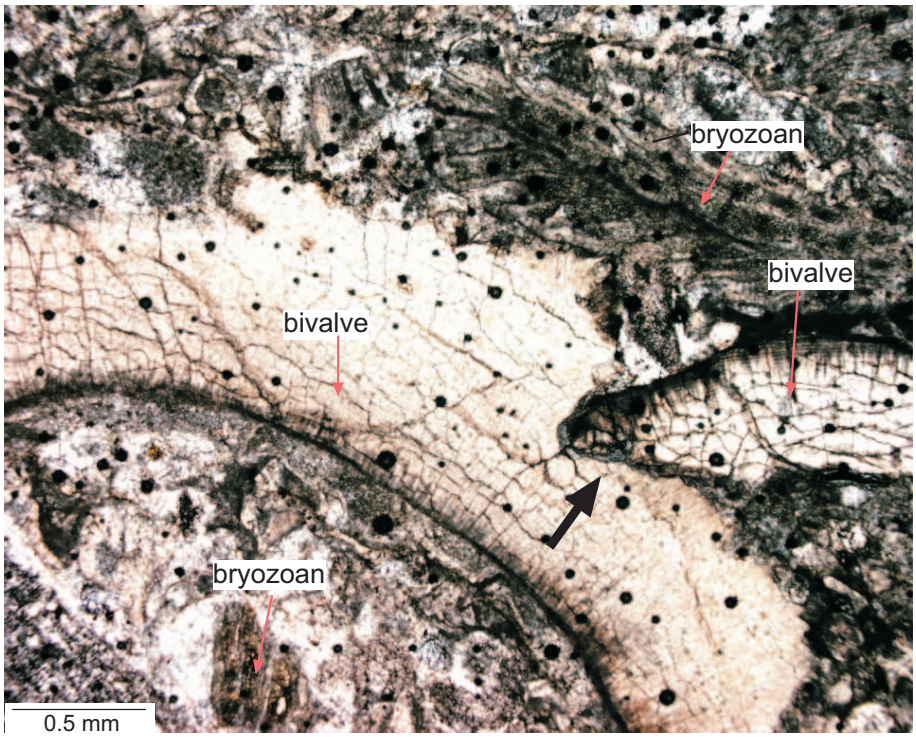

Figure 5.8 This photomicrograph, under PPL from the Aglime (field sample no. 11, BH502, 40.2 m depth) host rock, shows another burial feature commonly observed in the quarry limestones. Burial stress has caused pressure dissolution to occur at the contact (black arrow) of two interpenetrating bivalve fragments, where the bivalve on the right, has preferentially dissolved into the bivalve on the left. Bryozoans and sparite cement are also present, and the rock fabric is tight.

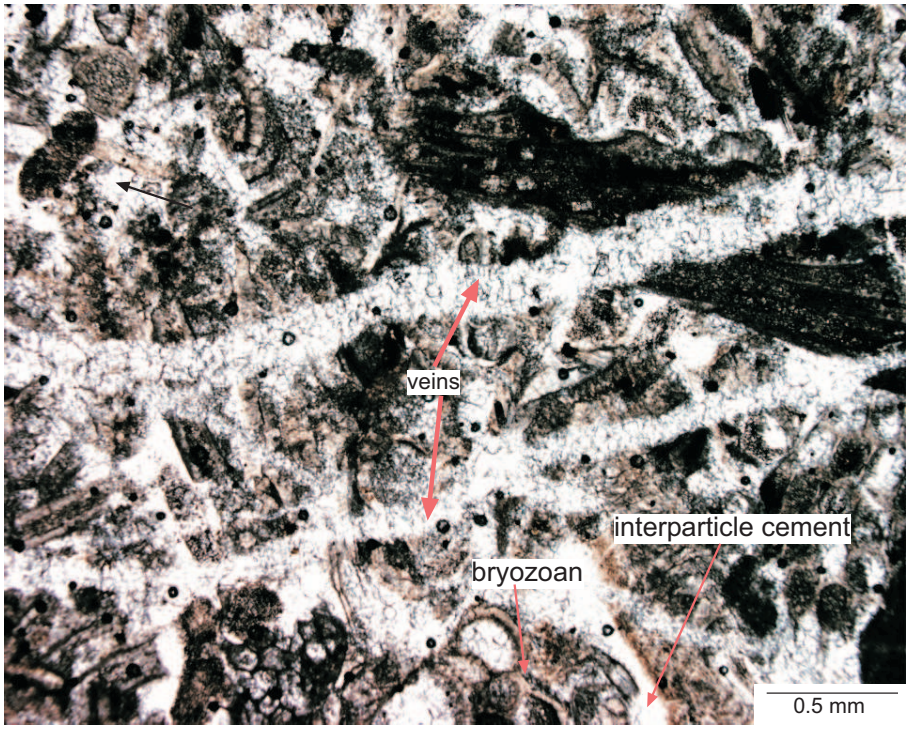

Figure 5.9 Photomicrograph of thin section under PPL of the High Grade (field sample no. 38, BH502, 50.1 m depth) host rock. The dominant cement type is interparticle sparite. Two calcite veins are the dominant feature in the centre of the image, where fractures have been healed by secondary calcite precipitation. Bryozoan bioclasts are also common.

5.2 Analytical methods

5.2.1 Petrography

Petrography is the study of limestones, dolomites, and associated deposits under the electron or optical microscope (Scholle and Ulmer-Scholle, 2003). Cathodoluminescence (CL) is also petrography using a different light source. In CL, natural materials under an optical microscope are bombarded with an electron beam that emits visible light (Adams and MacKenzie, 1998). These CL characteristics can provide information on the identification and spatial distribution of minerals for example carbonate versus silica minerals (Scholle and Ulmer-Scholle, 2003). To determine the distribution of carbonate and non-carbonate minerals, CL is an excellent technique to use. Calcite luminesces bright orange or yellow, whereas silica minerals such as quartz and feldspar, which are often difficult to distinguish under only plane polarised light (PPL), luminesce to brown (quartz), bright blue to green (feldspar). The way these minerals emit light differently therefore makes them much easier to distinguish. Pyrite and clay do not luminesce and show up black under CL light. Further information on the CL method is noted in Appendix E-5.2.

For this study, one core (BH502) from the 500 drill hole series was chosen as a reference core to carry out sampling of host rocks and discontinuity features for thin section study. The selection basis for sampling was that the rock needed to be intact to assist with mounting the samples onto glass slides for thin sectioning, especially in the case of discontinuity features such as dissolution seams and stylolites that otherwise are difficult to produce fully representative slices. Approximately 60 thin sections were prepared using more or less standard procedures that are outlined in Appendix E-5.3. Polished thin sections provide a better result for CL petrography, so that a selection of thin sections was polished. Using an optical microscope (4x objective), petrographic descriptions for each thin section were recorded onto petrographic data sheets, as shown in Figure 5.10. Light sources used include plane polarised light (PPL), cross polarised light (XPL), and cathodoluminescent light (CL). Photomicrographs taken during the course of petrography work are given in Appendix H-5.19 on CD.

Petrographic data sheet - McDonald's Lime Quarry 2007			
Sample number		18.4	
Quarry unit		Lower Steel	
Analyst		Orla Hansen	
Photomicrographs			
BIOCLASTS	**Total bioclast %**	97	
		%	**Abundance limit**
	Bryozoans	94	very abundant
	Echinoderms	2	some
	Benthic foraminifera	<1	rare
	Planktic foraminifera	-	absent
	Bivalves	<1	rare
	Pteropods	-	absent
	Gastropods	-	absent
	Calcareous red algae	-	absent
	Barnacles	-	absent
	Porifera	-	absent
	Brachiopods	-	absent
	Corals	-	absent
	Annelids	-	absent
	Other	-	absent
	Modal size 1 (mm)	2.16	
	Modal size 2 (mm)	0.97	
	Grain shape/abrasion	slightly abraded	
	Sorting	poorly	
SILICICLASTS	**Total siliciclast grain %**	3	
		%	**Abundance limit**
	Quartz	-	absent
	Feldspar	-	absent
	Igneous rock fragments	-	absent
	Sedimentary rock fragments	-	absent
	Micas	-	absent
	Pyrite grains	<1	rare
	Pyrite infills	<1	rare
	Glauconite pellets	<1	rare
	Glauconite infills	<1	rare
	Clays	-	absent
	Modal size 1 (mm)	0.36	
	Modal size 2 (mm)	0.24	
	Grain shape/abrasion	subrounded	
	Sorting	poorly	
FEATURES	Cements/porosity/fabric	sparite, no porosity	
	Distribution of siliciclastics	scattered or along stylolite	
	Oxidation characteristics	oxidised	
	Discrete seams - Orientation, thickness (mm), mineralogy, oxidation state	-	
	Diffuse seams - Orientation, pattern, oxidiation state, mineralogy, thickness (mm)	-	
	Stylolites - Orientation, suture amplitude (mm), mineralogy, oxidation state	hori. Amp = 0.5 mm, clay, big round quartz & feldspar dominant crystals = .48 mm long, glauconite	
	Microstylolites	-	

Figure 5.10 Example of a petrographic data sheet used to record thin section information.

Bioclast and siliciclast composition and other characteristics (e.g. grain size, sorting, cements, and porosity) were recorded. The abundance limits used are as follows: 0% = absent, <1% = rare, 1-5% = some, 5-15% = many, 15-25% = common, 25-50% = very common, 50-75% = abundant, and >75% = very abundant. Three main sections make up the data sheets; a section for bioclasts (the main carbonate component), a section for siliciclasts (non-carbonate component), and a third section covering discontinuity features such as dissolution seams and stylolites.

5.2.2 Scanning electron microscopy (SEM)

Scanning electron microscopy (SEM) uses an electron beam to form magnified images of specimens where special instruments can resolve detail to approximately 3 nm (Fleger et al., 1993). The SEM produces images in 3D showing texture and morphology of the specimen of interest. The SEM used was equipped with an energy dispersive analyser (EDAX) which can provide semi-quantitative chemical analysis (Fleger et al., 1993) and thereby assist with mineral identification.

SEM was used to analyse a selection of limestones and discontinuity materials for their micro-texture using 3D imaging. Sample preparation for SEM is noted in Appendix E-5.4. The scale of the samples in the images taken ranges from 6-100 μm.

5.2.3 X-ray diffraction (XRD)

X-ray diffraction (XRD) analysis determines bulk mineralogy, characterises the spectrum of minerals present, and provides information on crystal structure. Crystalline materials possess characteristic lattice structures where atoms, molecules, and ions are ordered in a 3D array. In the crystal lattice, the ordering is expressed as layers at different orientations. XRD measures the d-spacing (Å) which is the atomic spacing of a layer (Bertin, 1975).

The purpose of using XRD in this study is to identify the bulk mineral content present in a range of samples, including quarry limestones and discontinuity

material like Kauroa Ash, Mahoenui Group mudstone, discrete seams, cave infills, surface accumulations, and joint infills. XRD is a good tool to use when one wishes to confirm a mineral that is suspected to be present. Each sample (dried powder) was analysed in the XRD, and diffractograms were generated by the XRD software which recorded the mineral peaks to be interpreted.

An example of a diffractogram is show in Figure 5.11. Each peak on a diffractogram is associated with a d-spacing or angstrom (symbol Å) value, position 2θ, and a corresponding mineral. Using a list of minerals expected to be in each sample, angstrom values from the main peaks were recorded and looked up in angstrom (d-spacing) mineral charts using those listed in Hume and Nelson (1982) and JCPDS International Centre for Diffraction Data (1980). As the peak position indicates crystal structure, peak intensity refers to the intensity of the reflection from the total scattering from each plane in the crystal structure. This is dependent on the distribution of atoms in the structure (Connolly, 2003). The intensity gives a first order approximation of mineral abundance in a sample (i.e. the larger the intensity the greater the mineral content). The intensity of each mineral was also recorded.

5.2.4 Wet sieving

Wet sieving was used to determine the grain sizes for samples comprising grains greater than 2 mm. The majority of discontinuity type samples were not wet sieved because their grain sizes were less than 2 mm; however, 7 samples contained limestone fragments which were larger than 2 mm. These samples were those taken exclusively from vertical joints where the limestone fragments are likely to have been sourced from the surrounding rock mass (possibly as a result of shearing along joint zones, or blasting of overlying limestone into fragments which has subsequently fallen into the joints). The mineral palygorskite (identified from XRD, discussed in Section 5.4.6 in this Chapter) was found in some of the joint infills. It was taken out of the samples before the sieving (does not sieve effectively).

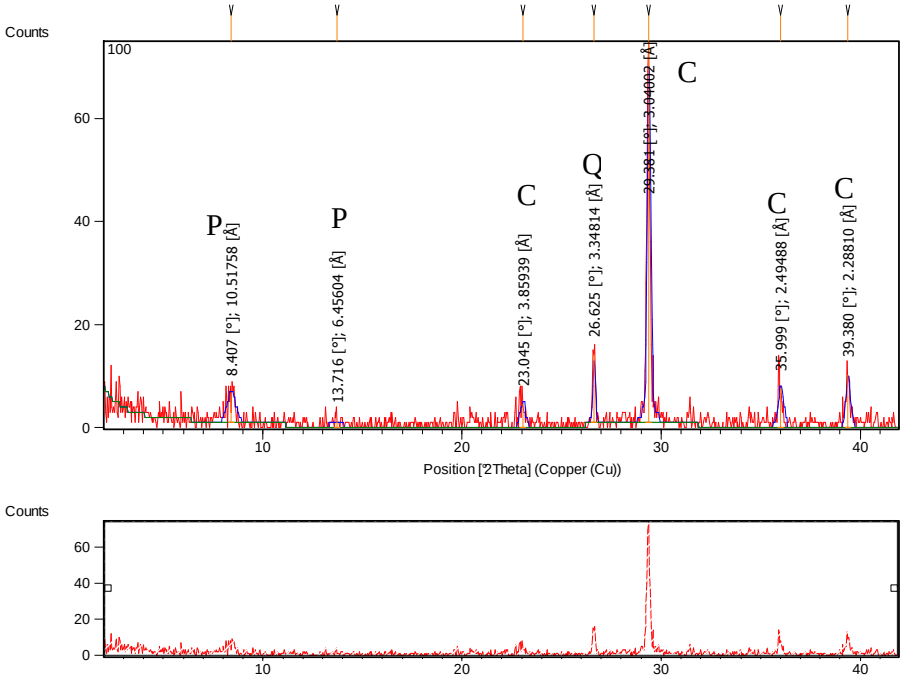

Figure 5.11 Diffractogram (top) showing x-ray diffraction results of a sample taken from an exposed joint surface in the Lower Steel, eastern face (field sample no. 100). It shows peaks of the minerals palygorskite (P), calcite (C), and quartz (Q). The lower chart shows the number of counts for each peak corresponding to the above diffractogram.

This was dried then weighed and the values converted into a percentage of the total sample. Each sample was shaken down a series of sieves with different phi sizes (that had water running through). The amount of sample caught in each sieve size was dried then weighed to determine the weight percent of sample in each grain size class (or sieve size). Further information about the wet sieve method is contained in Appendix E-5.5. Grain size classes were determined using Wentworth (Appendix E-5.1) size classes, found in Berkman (2001). Moisture content was also calculated for these 7 samples.

5.2.5 Laser particle size analysis

To determine the size fraction below 2 mm, laser particle size analysis was carried out on 28 samples. This included the less than 2 mm fraction retained from the 7 joint infill samples analysed in the wet sieving, plus samples of the Kauroa Ash, Mahoenui Group mudstones, discrete seams, and cave infill. A Malvern Mastersizer-S instrument was used for analysis. Sample preparations involved the removal of organic and carbonate content. Further analytical details are noted in Appendix E- 5.6. Grain size classes were also determined using the Wentworth

(Appendix E-5.1) grain size classes and, together with the sieve data, the two data sets were combined in a texture spreadsheet, kindly made available by Dr Willem de Lange (pers. comm., 2007), that calculates textural statistics such as mean grain size and sorting.

5.3 Results for host rock in quarry limestones

5.3.1 Caprock

The XRD data for Caprock samples are given in Appendix E-5.7 and the petrography information in Appendix E-5.8. XRD shows that the dominant mineral in the Caprock is calcite. The Caprock is the topmost limestone unit at the quarry and becomes progressively finer grained toward the contact with the overlying Mahoenui Group mudstones. This is clearly evident in the cores (see Chapter 4 Section 4.1.2) where the limestone becomes more argillaceous (clayey) towards the top. In thin section the uppermost levels of the Caprock become planktic foram and clay rich (Figure 5.12A), reflecting the rapid transition from shallow marine deposition to deep marine deposition characterising the overlying Mahoenui Group mudstone. Figure 5.13A shows the average composition of bioclasts (70-95%) found in the Caprock. The bioclast (70-75%) component of the samples near the contact is characterised by a concentration of planktic forams (Figure 5.12B) (abundant). The remaining bioclasts found near this contact include echinoderms (some), benthic forams (some), and bryozoans (some). In contrast, samples taken beneath this transition comprise bioclasts (80-95%) that are dominated by bryozoans (very abundant), echinoderms (many), planktic forams (some), benthic forams (some), and bivalves (rare). Figure 5.13C shows the modal grain size distribution for the bioclasts and siliciclasts across all the Caprock samples. Bioclasts for both sample types share the same textural characteristics. They are poorly-well sorted, moderately abraded, and have modal grain sizes of medium sand, coarse sand, and very coarse sand (0.29-1.3 mm). Both sparite and micrite are present, although generally micrite predominates.

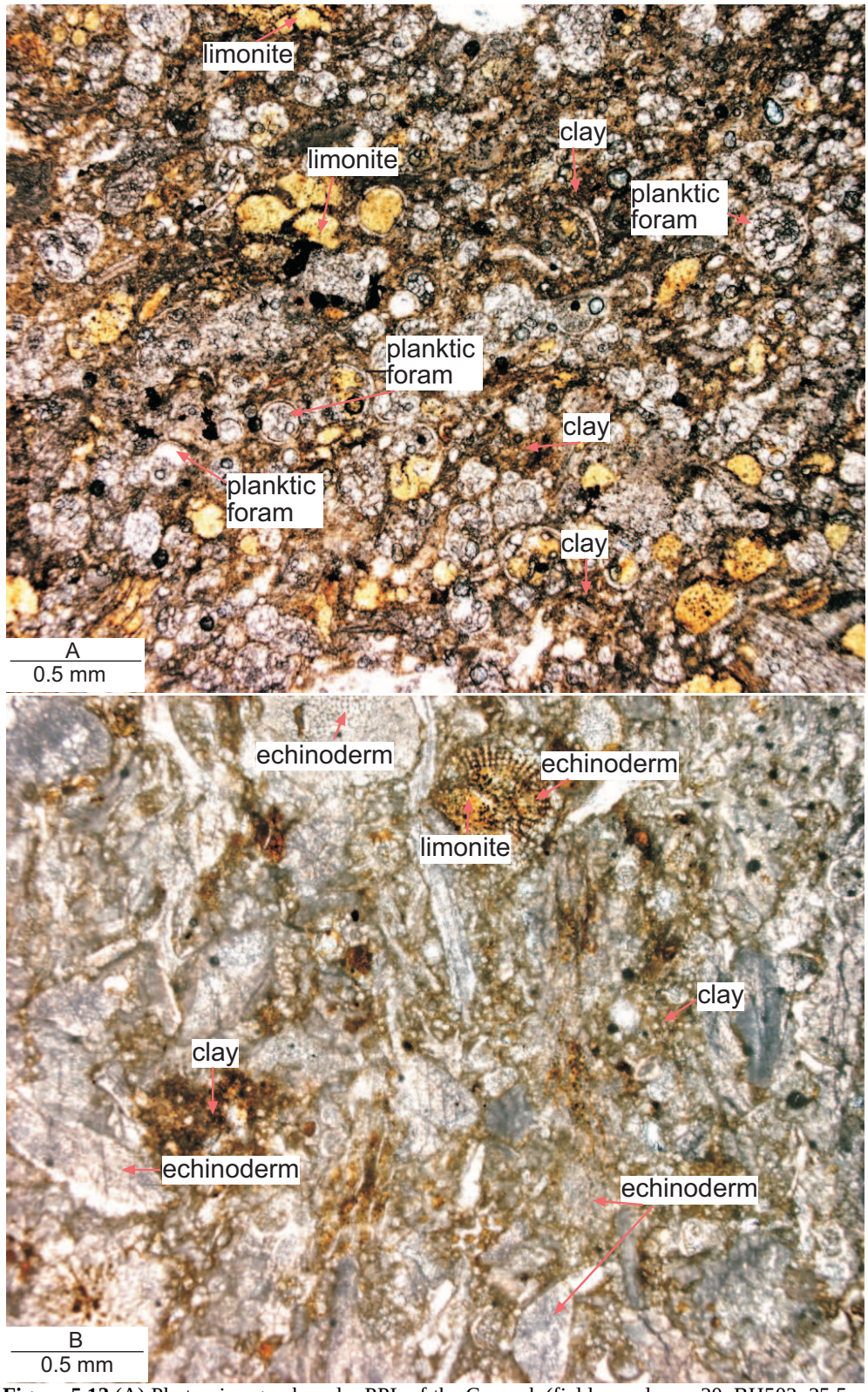

Figure 5.12 (A) Photomicrograph under PPL of the Caprock (field sample no. 20, BH502, 25.5 m depth) host rock taken near the contact with the overlying Mahoenui Group mudstones. The sample is very fine-grained, and dominated by clay, limonite and planktic forams. The fabric of the rock is tight. (B) Photomicrograph under PPL of the Caprock (field sample no. 9.2, BH502, 26.25 m depth) host rock contains echinoderms and is dominated by clays. The rock also has a tight fabric.

(A)

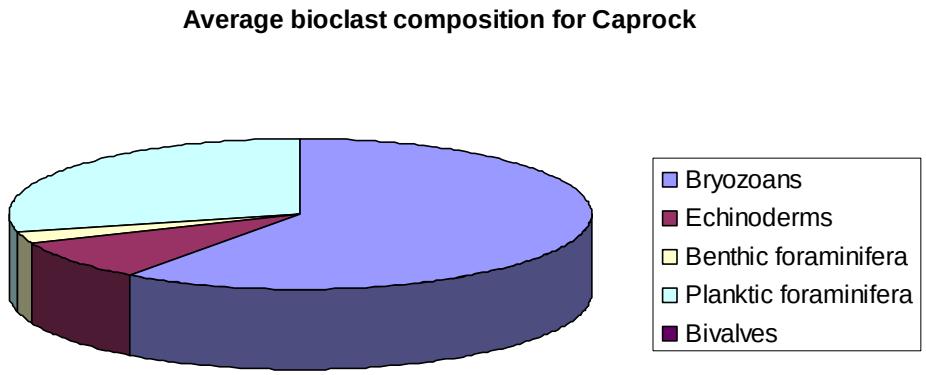

(B)

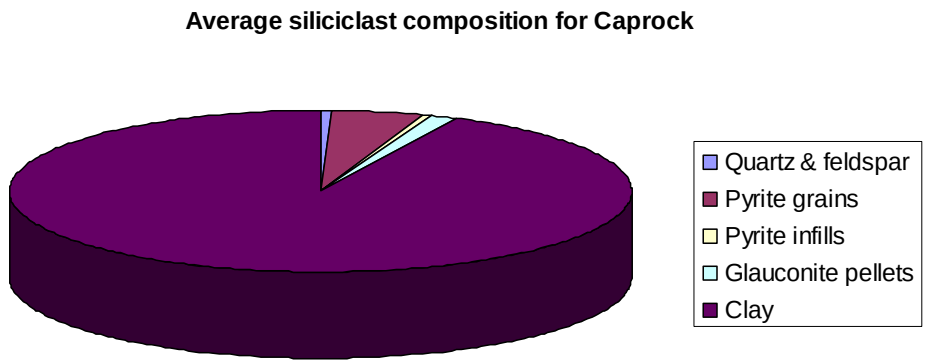

(C)

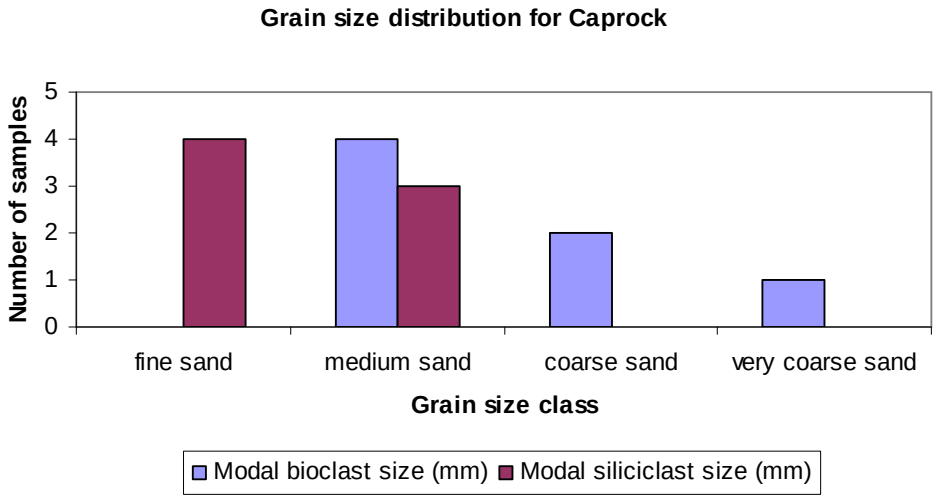

Figure 5.13 (A) Average bioclast composition given as a percentage from petrographic descriptions for Caprock host rock. (B) Average representative percentages from petrographic descriptions, of the different siliciclast types found in Caprock host rock. (C) Grain size distribution from petrographic descriptions including modal bioclast and siliciclast size for Caprock host rock.

No porosity was observed in the samples, fabric is open or tight, and bioclasts are generally packed and fragmented (except for forams which are not fragmented). Fractures are common and have been healed by secondary calcite precipitation.

Average siliciclast composition is shown in Figure 5.13B. The siliciclast (5-30%) component consists of clays (very common), pyrite grains (some), pyrite infills (rare), and glauconite pellets (rare). Clay, pyrite, and glauconite commonly occur within zooecia of bryozoans (intraparticle), and are limonitised. These grains are scattered throughout the host rock, poorly-well sorted, subrounded, with modal grain sizes of fine sand and medium sand (Figure 5.13C) (0.07-0.29 mm). Using Folk's (1959) classification, the Caprock limestone is a packed biomicrite.

5.3.2 Upper Steel

The XRD data for the Upper Steel are given in Appendix E-5.7 and the petrography information in Appendix E-5.8. XRD shows that calcite is also the dominant mineral in the Upper Steel unit. Figure 5.14A shows the average bioclast composition for the Upper Steel limestone. Bioclasts comprise 98-99% of the Upper Steel unit and are dominated by bryozoans (Figure 5.15A) (very abundant), echinoderms (common), benthic forams (some), planktic forams (some), and bivalves (rare). Figure 5.14C shows the modal grain size distribution of bioclasts and siliciclasts. Bioclasts are typically moderately sorted, moderately abraded and fragmented, fine sand to granule modal size (0.12-2.52 mm). The dominant cement type is sparite (Figure 5.15A), with one thin section showing minor micrite. Some samples showed interparticle porosity as for example seen in Figure 5.15B. The energy dispersive analyser showed the presence of calcium, minor iron, magnesium, and silica (see inset of Figure 5.15B). Other samples were not porous. The Upper Steel unit shows a range of fabrics, from tight where the bioclasts are packed, squashed, and elongated, to more open fabrics where the bioclasts are only slightly packed or just only in point contact.

(A)

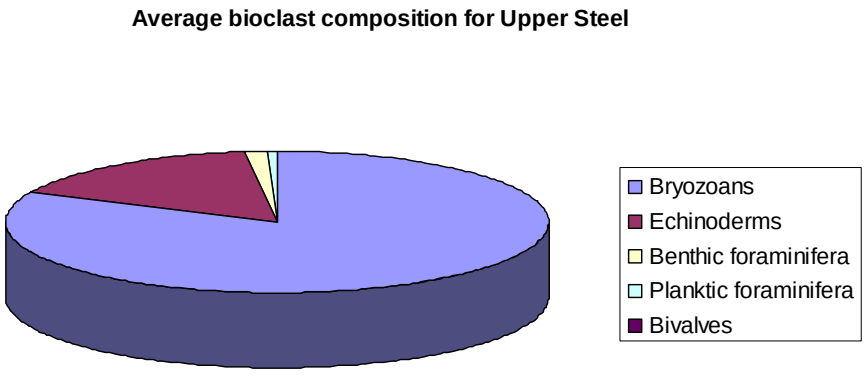

(B)

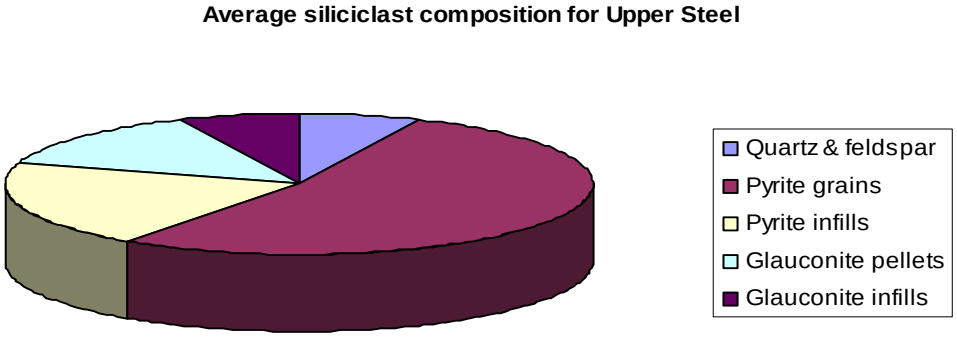

(C)

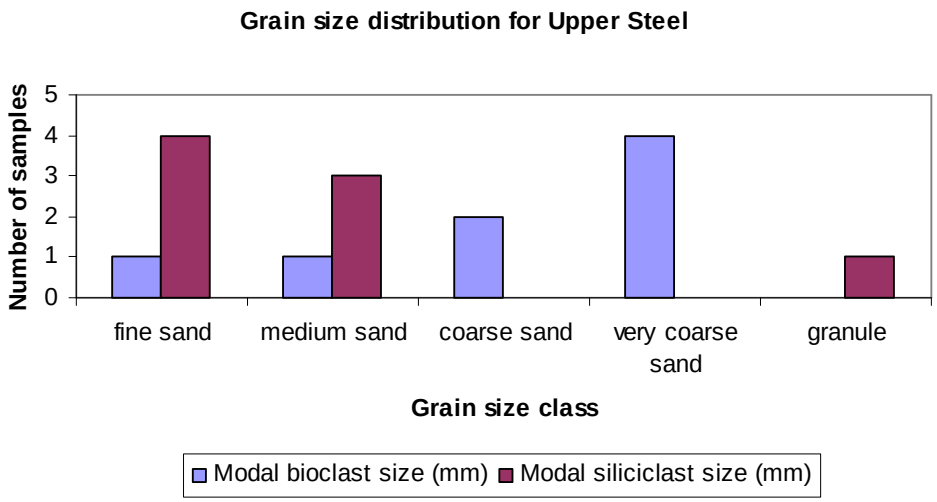

Figure 5.14 (A) Average bioclast composition given as a percentage from petrographic descriptions for Upper Steel host rock. (B) Average representative percentages from petrographic descriptions, of the different siliciclast types found in Upper Steel host rock. (C) Grain size distribution from petrographic descriptions including modal bioclast and siliciclast size for Upper Steel host rock.

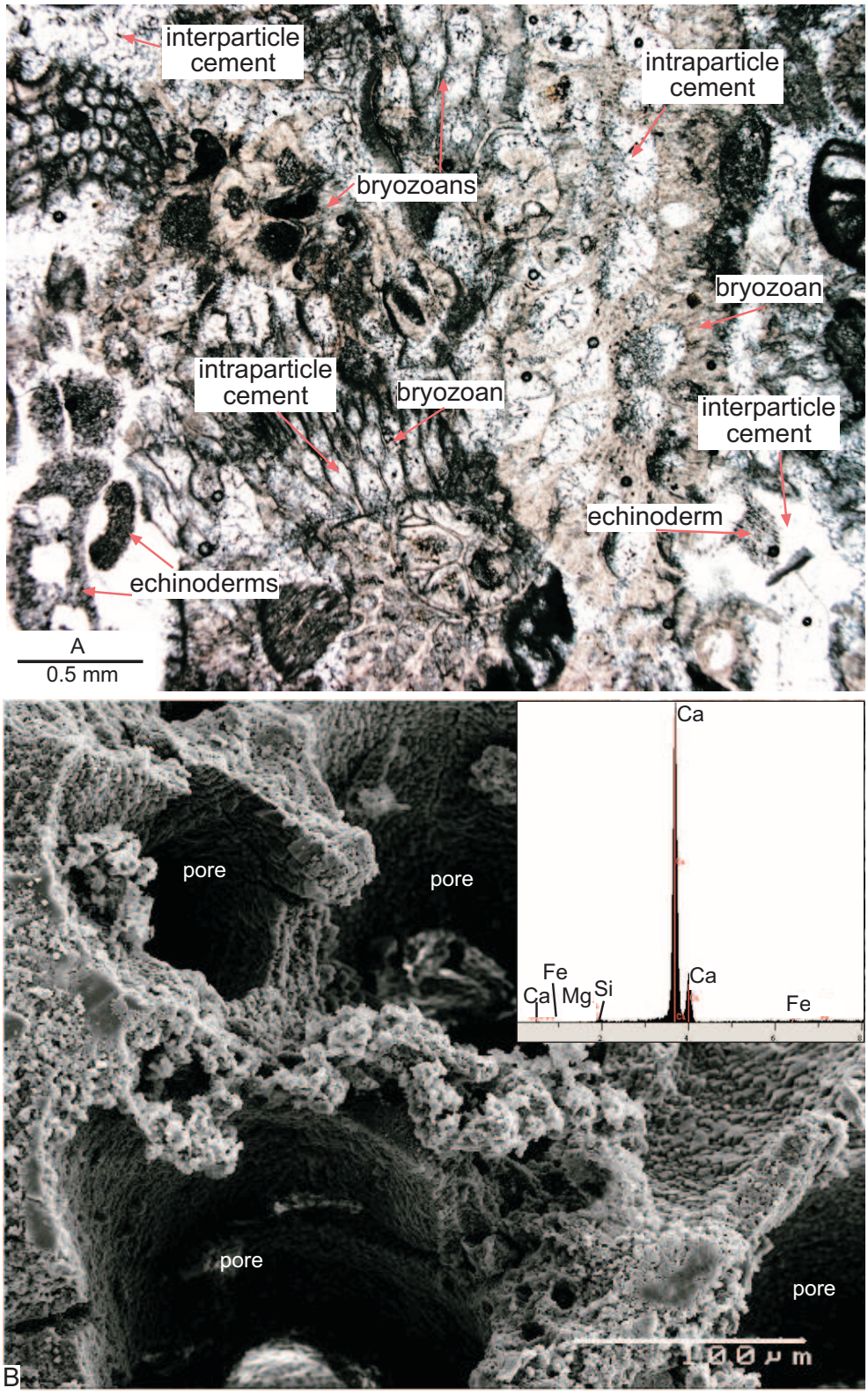

Figure 5.15 (A) Thin section under PPL of host rock in the Upper Steel limestone showing bioclasts including bryozoans, which are very abundant, and echinoderms. Sparite cement occurs both within (intraparticle) and between (interparticle) grains (field sample no. 24.1, BH502, 28.5 m depth). (B) SEM image of a porous limestone sampled from the Upper Steel unit. There is no cement in the pore spaces (labelled). The inset is a spectra showing results from the energy dispersive analyser, which shows elements detected in the cemented portion of the sample. The sample is dominated by calcium (Ca) (large peak on graph), and contains minor silica (Si), magnesium (Mg), and iron (Fe) (field sample no. 24.1, BH502, 28.5 m depth).

Figure 5.14B shows the average siliciclast composition. Siliciclasts (1-2%) comprise pyrite grains (rare), pyrite infills (rare), glauconite pellets (rare), and quartz and feldspar (rare). Siliciclasts are scattered throughout the host rock, are poorly sorted, subrounded to angular, and have fine sand to granule modal sizes (0.12-2.4 mm) (Figure 5.14C). Under Folk's (1959) classification, Upper Steel limestones are unsorted biosparites or unsorted biosparrudites.

5.3.3 Aglime

The XRD data for Aglime samples are given in Appendix E-5.7 and the petrography information in Appendix E-5.8. XRD shows that calcite is the dominant mineral in the Aglime unit. Figure 5.16A shows the average bioclast composition. The bioclast (92-98%) component comprises bryozoans (very abundant), echinoderms (rare), benthic forams (rare), planktic forams (rare), and bivalves (some). Figure 5.17 shows one of the Aglime samples that had high $\%CaCO_3$ (bioclasts and cement) content, supporting evidence that the main concentration of silica minerals is in the discontinuities. Grain size distribution of bioclasts and siliciclasts are shown in Figure 5.16C. Bioclasts are poorly sorted, slightly abraded and fragmented, and have fine sand to very coarse sand size modes (0.05-1.68 mm). Micrite is the dominant interparticle fill and often occurs as intraparticle fill as well, particularly in bryozoan zooecia. Minor sparite cement also occurs. No porosity was observed in the samples. Fabrics are tight and bioclasts are packed against each other. Fracturing is also common.

Average siliciclast composition is shown in Figure 5.16B. The siliciclasts (2-8%) are composed of pyrite grains (some), glauconite pellets (some), pyrite infills (rare), and glauconite infills (rare). These are poorly sorted, subrounded or angular have mainly coarse silt to fine sand size modes (Figure 5.16C) (0.05-0.24 mm), and are scattered throughout the host rock. Under Folk's (1959) classification, Aglime limestones are unsorted biosparites to unsorted biosparrudites.

(A)

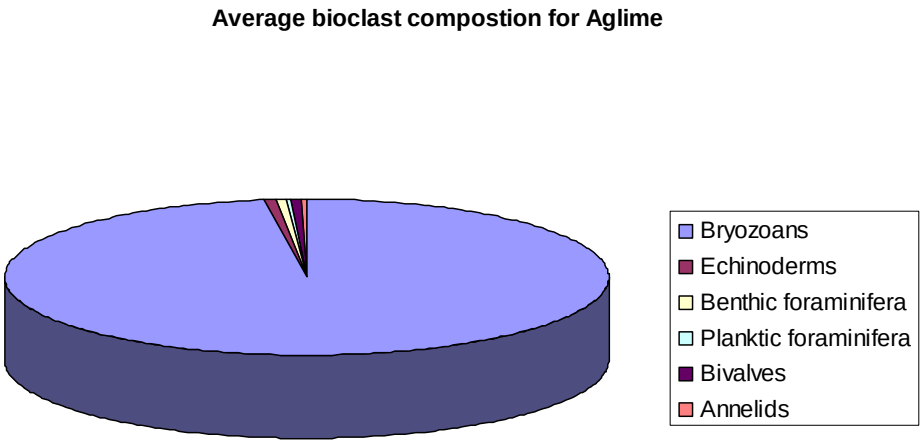

(B)

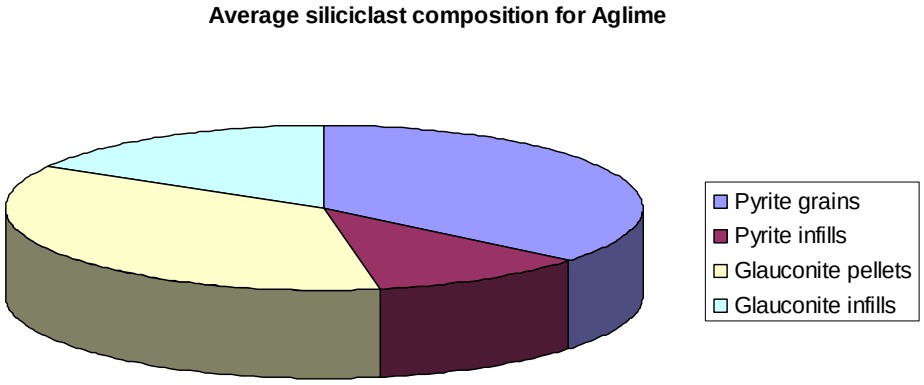

(C)

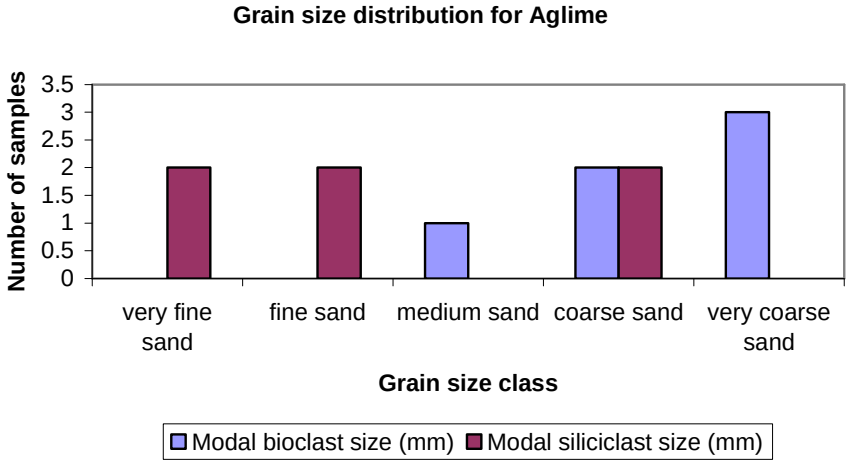

Figure 5.16 (A) Average bioclast composition given as a percentage from petrographic descriptions for Aglime host rock. (B) Average representative percentages from petrographic descriptions, of the different siliciclast types found in Aglime host rock. (C) Grain size distribution from petrographic descriptions including modal bioclast and siliciclast size for Aglime host rock.

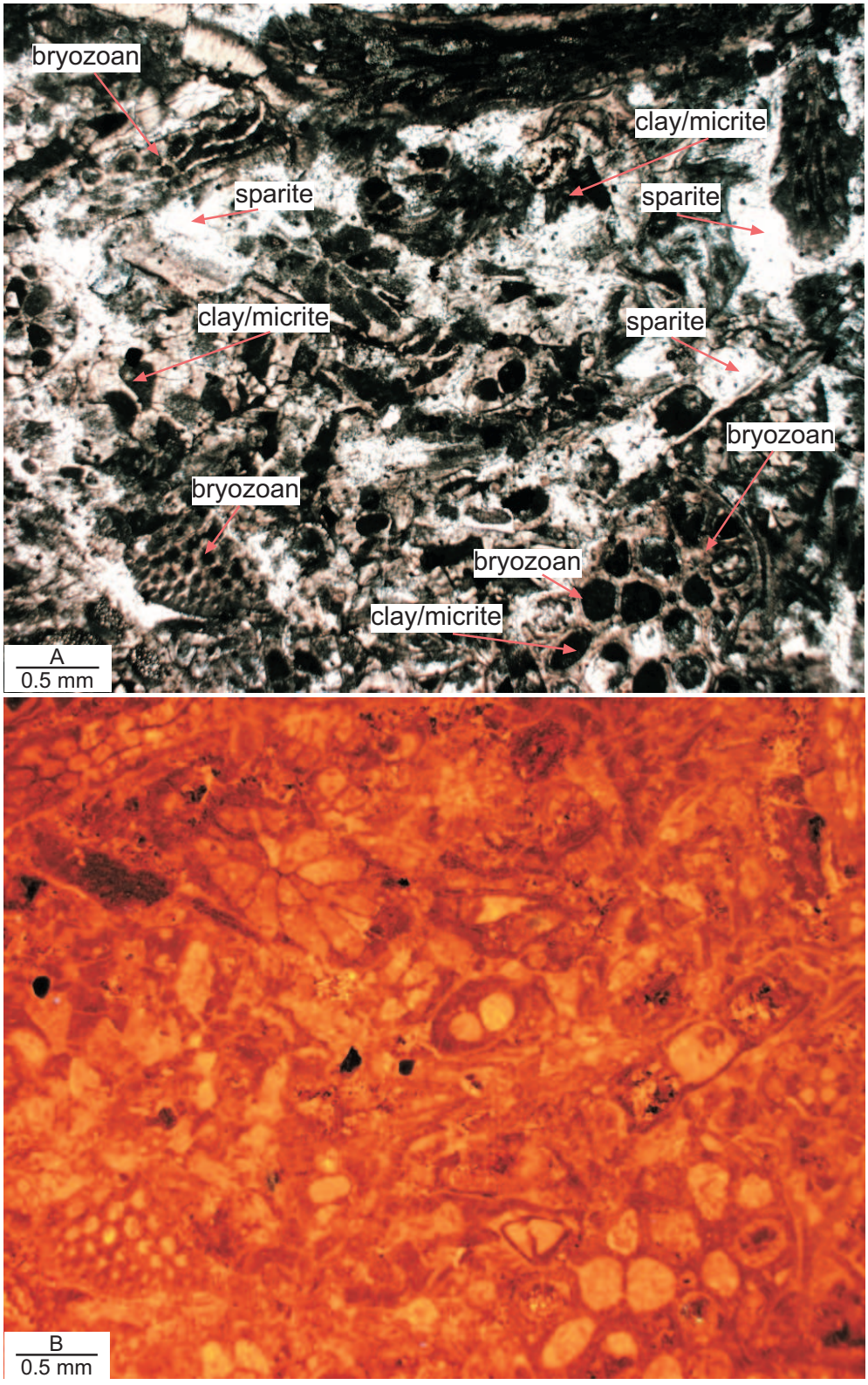

Figure 5.17 (A) Photomicrograph under PPL of the Aglime (field sample no. 11.2, BH502, 40.2 m depth) host rock. The sample is mostly composed of bryozoans and sparite cement. The dark black areas are either clays or micrite. The rock fabric is tight. (B) Photomicrograph of the same sample in (A) under CL. The calcite luminesces pale to bright orange, and indicates that the sample is predominantly calcite.

5.3.4 High Grade

The XRD data for High Grade are given in Appendix E-5.7 and the petrography information in Appendix E-5.8. XRD results show that calcite is the dominant mineral in the High Grade limestone. Average bioclast composition is shown in Figure 5.18A. Bioclasts (94-98%) comprise bryozoans (Figure 5.19B) (very abundant), echinoderms (some), benthic forams (some), planktic forams, and bivalves (rare). Grain size distribution of modal bioclast and siliciclast sizes are shown in Figure 5.18C. Bioclasts are poorly sorted, moderately abraded, are of coarse sand to granule modal size (0.6-2.16 mm). The dominant cement is sparite; micrite is minor and is found commonly as intraparticle fill in bioclast chambers (e.g. Figure 5.19A). Porosity is absent in all the samples, and fabrics range from tight (bioclasts packed) to open (bioclasts touching). Bioclasts are generally highly fragmented. Fractures are common and are typically healed by secondary calcite precipitation.

Average siliciclast composition is shown in Figure 5.18B. Siliciclasts (2-6%) comprise pyrite grains (some-many), quartz and feldspar (some), pyrite infills, glauconite pellets, and glauconite infills (rare). Pyrite (Figure 5.19A) is more abundant in the High Grade samples compared to the other quarry limestones. Bioclasts are poorly sorted, angular or subrounded, and have of very fine to fine sand size (Figure 5.18C) (0.07-0.24 mm). Siliciclasts are generally scattered throughout the host rock and sometimes occur in clusters. Under Folk's (1959) classification, High Grade limestones are unsorted biosparites to unsorted biosparrudites.

(A)

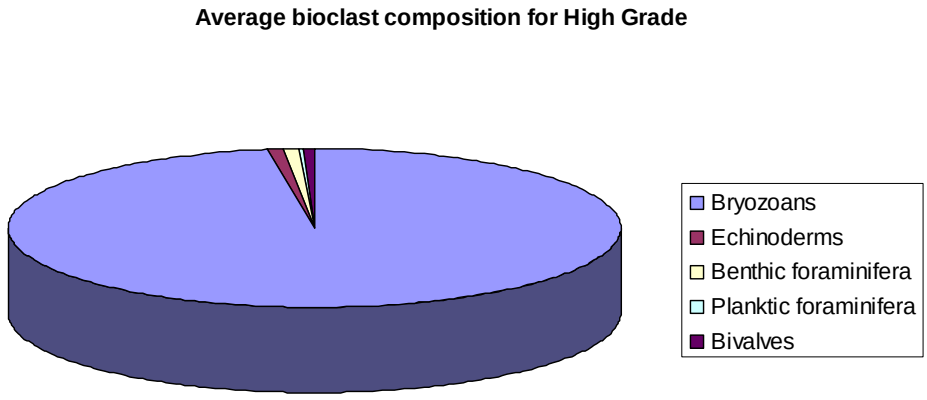

(B)

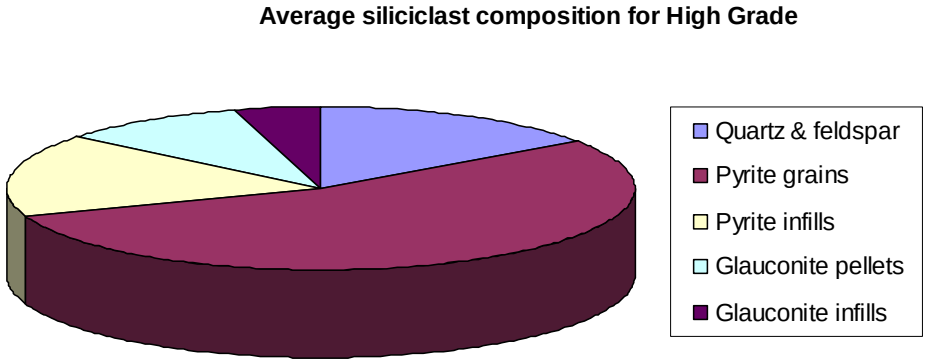

(C)

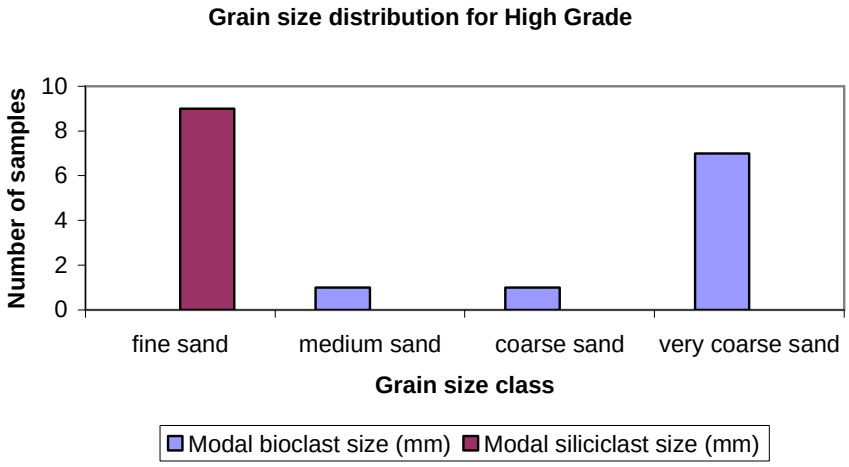

Figure 5.18 (A) Average bioclast composition given as a percentage from petrographic descriptions for High Grade host rock. (B) Average representative percentages from petrographic descriptions, of the different siliciclast types found in High Grade host rock. (C) Grain size distribution from petrographic descriptions including modal bioclast and siliciclast size for High Grade host rock.

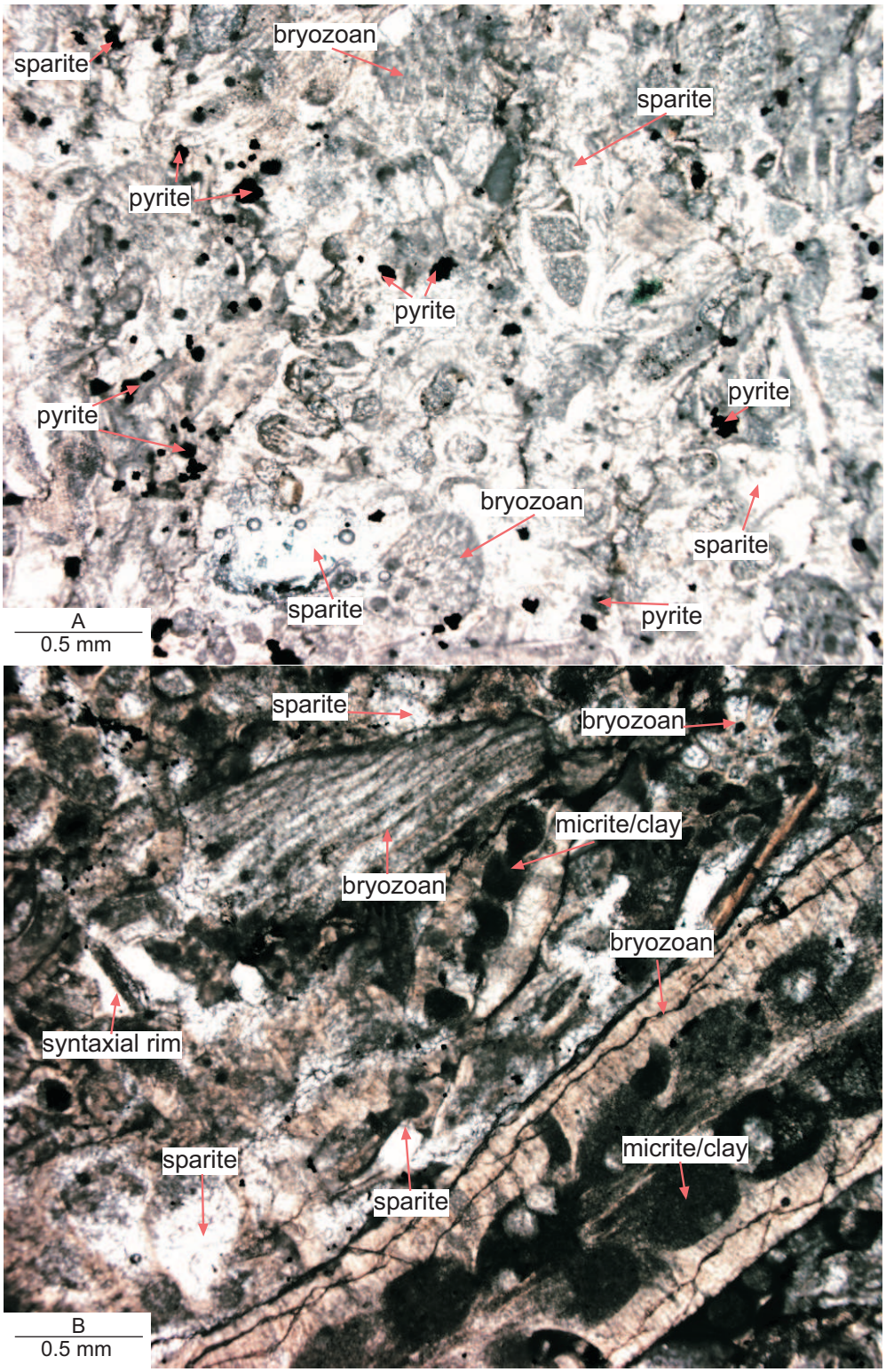

Figure 5.19 (A) Photomicrograph under PPL of the High Grade (field sample no. 15.2, BH502, 56.7 m depth) host rock. The image is purposely overexposed to emphasise the presence of pyrite. Pyrite is particularly common in the High Grade and is shown as opaque (black) minerals in thin section. (B) Photomicrograph under PPL of the High Grade (field sample no. 14.4, BH502, 52.6 m depth) host rock. The sample shows sparite, and micrite or clay, where the latter occurs within zooecia of bryozoan fragments, which are the dominant bioclast type. The rock has a tight fabric.

5.3.5 Lower Steel

The XRD data for Lower Steel are given in Appendix E-5.7 and the petrography information in Appendix E-5.8. XRD results show that calcite is the dominant mineral in the Lower Steel unit. Average bioclast composition is shown in Figure 5.20A. The bioclast (96-98%) component consists of bryozoans (very abundant), echinoderms (some), benthic forams (rare), bivalves (some), annelids (rare) and planktic forams (rare). An example of a host rock sample under PPL and CL is shown in Figure 5.21. Grain size distribution for bioclasts and siliciclasts is shown in Figure 5.20C. Bioclasts are poorly to moderately sorted, moderately abraded and fragmented, and have grain sizes in the medium sand to granule range (0.43-2.88 mm). Sparite is generally the dominant cement, although a few samples are dominated by micrite. No porosity was observed in the samples. In general, fabrics were open where bioclasts were slightly packed or just touching.

Figure 5.20B shows the average siliciclast composition. Siliciclasts (2-4%) comprise quartz and feldspar (some), pyrite grains, pyrite infills, glauconite pellets, glauconite infills, and sedimentary rock fragments (rare). These are poorly sorted, subrounded, and have modal sizes in the very fine to coarse sand range (Figure 5.20C) (0.1-0.72 mm), and are scattered or clustered throughout the host rock. Clustered siliciclast grains were typically limonitised. Under Folk's (1959) classification, Lower Steel limestones are unsorted biosparites to unsorted biosparrudites.

(A)

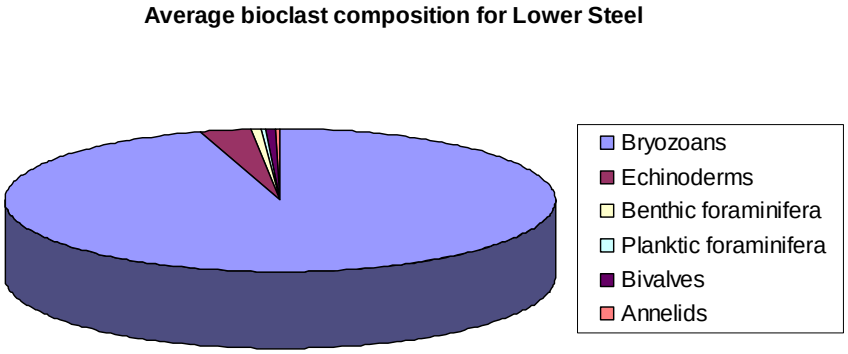

(B)

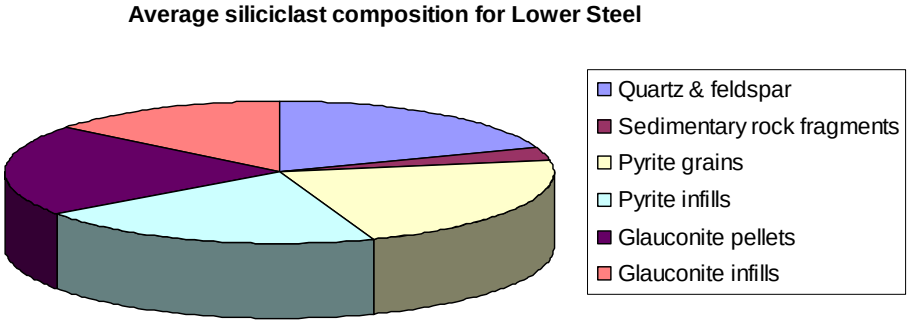

(C)

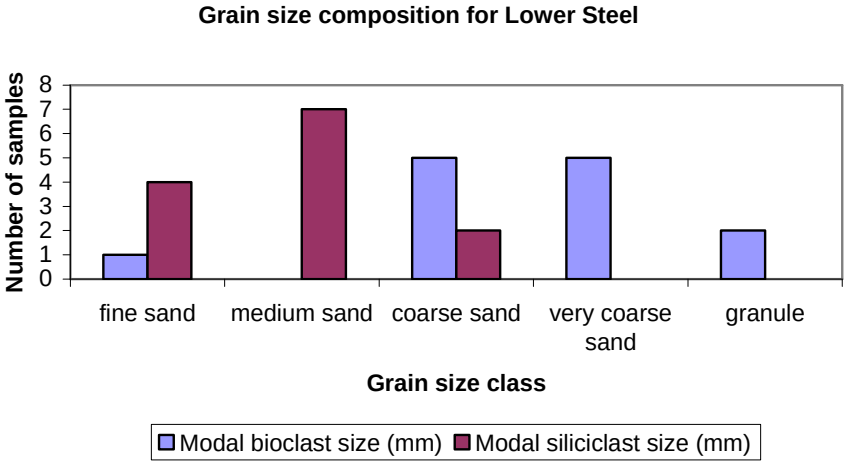

Figure 5.20 (A) Average bioclast composition given as a percentage from petrographic descriptions for Lower Steel host rock. (B) Average representative percentages from petrographic descriptions, of the different siliciclast types found in Lower Steel host rock. (C) Grain size distribution from petrographic descriptions including modal bioclast and siliciclast size for Lower Steel host rock.

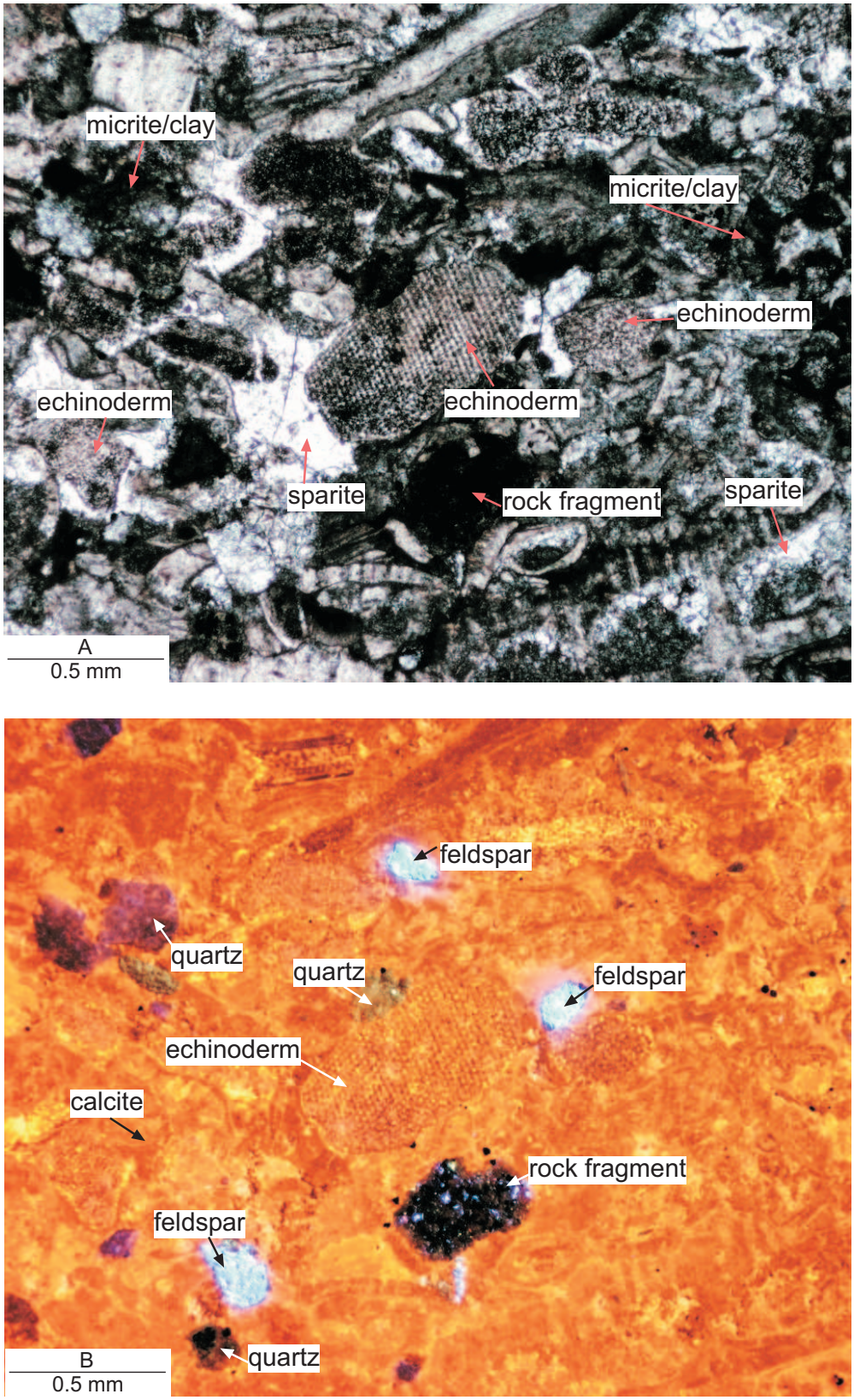

Figure 5.21 (A) Photomicrograph of a thin section under PPL of the Lower Steel (field sample no. 16.1, BH502, 74.1 m depth) host rock. Some sparite cement occurs, as well as some echinoderm fragments in the centre of the image. Under PPL it is difficult to pick out quartz and feldspar grains as they are commonly white, like calcite crystals. (B) Photomicrograph of (A) under CL. The CL reveals quartz as greeny brown grains, and feldspar that is blue and purple in colour. The remaining and surrounding host rock is calcite which luminesces bright orange.

5.3.6 Sub-economic

The XRD data for Sub-economic are given in Appendix E-5.7 and the petrography information in Appendix E-5.8. Once again XRD results showed that calcite is the dominant mineral in the Sub-economic unit. Average bioclast composition is shown in Figure 5.22A. The bioclast (90-96%) component comprises bryozoans (Figure 5.23B) (very abundant), echinoderms (some), bivalves (some), annelids (some), benthic forams (rare), planktic forams (rare), and calcareous red algae (rare). Annelids (worm tubes) are shown in Figure 5.23A and are more common in the Sub-economic unit compared to the other limestones. Modal grain sizes for bioclasts and siliciclasts are shown in Figure 5.22C. Bioclasts are poorly sorted, coarse sand to granule sizes (0.72-2.64 mm). Sparite is the dominant cement present, with minor micrite in several samples. Porosity is absent. Fabrics range from slightly open to tightly packed. Bioclasts are slightly abraded and fragmented.

Average siliciclast composition is shown in Figure 5.22B. The siliciclasts (4-10%) comprise quartz and feldspar (some), pyrite grains, pyrite infills (some), glauconite pellets, glauconite infills, and sedimentary rock fragments (rare). These are poorly sorted, subangular or subrounded, have modal grain sizes in the very fine to coarse sand range (Figure 5.22C) (0.1-0.53 mm), and are mainly scattered throughout the host rock or sometimes clustered. Under Folk's (1959) classification, Sub-economic limestones are unsorted biosparites to unsorted biosparrudites.

5.3.7 Petrographic overview

Actual percentages for bioclasts and siliciclasts for each thin section are summarised into Tables (Appendix E-5.9 and E-5.10). Details on thin section number, approximate depth of sample, total % $CaCO_3$, and total % silica are also included in these Tables. Grain size and shape data are given in Appendix E-5.11.

(A)

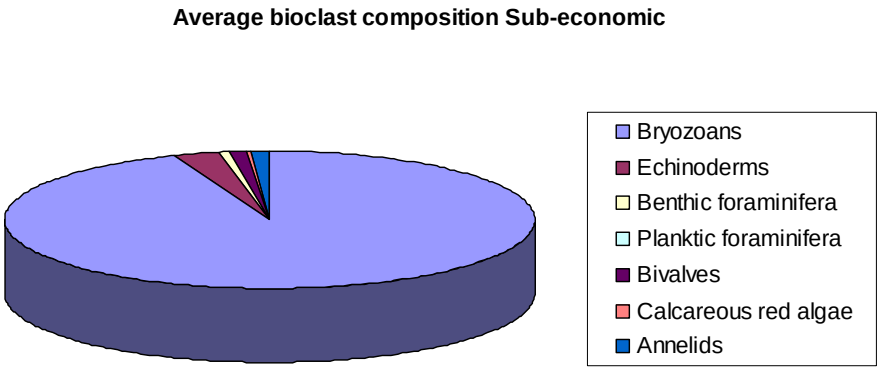

(B)

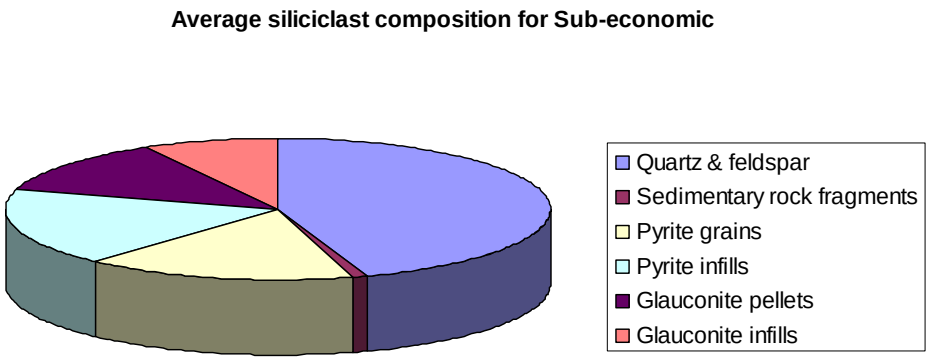

(C)

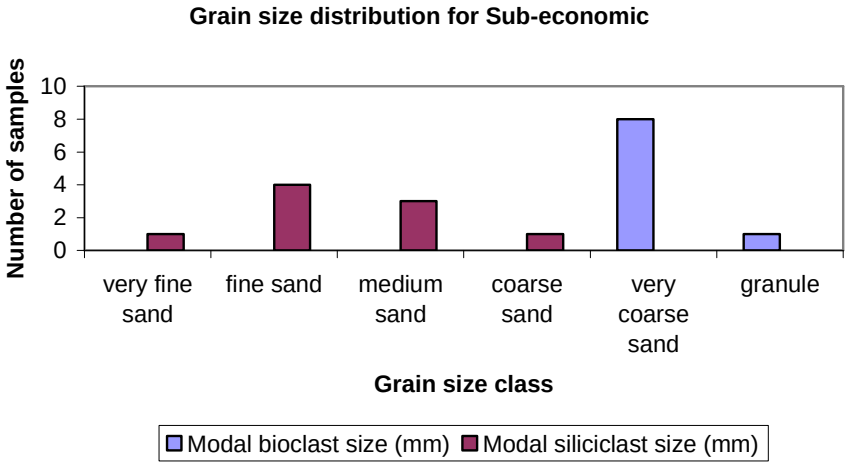

Figure 5.22 (A) Average bioclast composition given as a percentage from petrographic descriptions for Sub-economic host rock. (B) Average representative percentages from petrographic descriptions, of the different siliciclast types found in Sub-economic host rock. (C) Grain size distribution from petrographic descriptions including modal bioclast and siliciclast size for Sub-economic host rock.

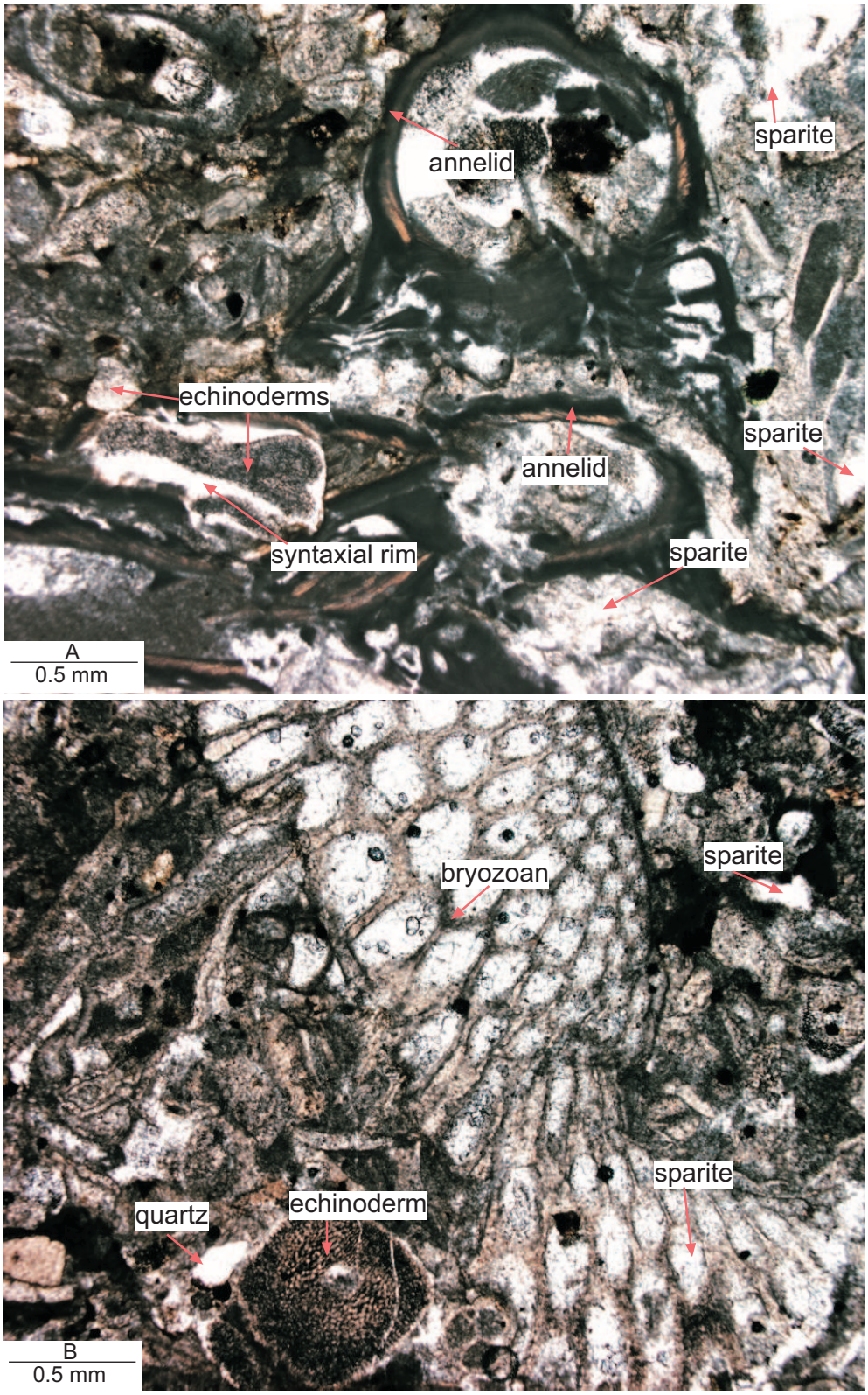

Figure 5.23 (A) Photomicrograph shows a thin section under PPL of the Sub-economic (field sample no. 57.2A, BH502, 86.9 m depth) host rock. Annelids or worm tubes are common in this limestone, as evident in this image. (B) Photomicrograph shows a thin section under PPL of the Sub-economic (field sample no. 19.1, BH502, 87.6 m depth) host rock. The image is dominated by a large bryozoan fragment. Echinoderm fragments occur to the bottom left. The fabric of the rock is tight, and the main cement type is sparite (white areas).

5.4 Results for overburden units and discontinuity materials

Of the different discontinuity types, only the diffuse and discrete dissolution seams were able to be thin sectioned as part of their host limestone. Consequently, the petrographic approach for mineral information could be used for these seams, but for the overburden units and other discontinuity materials (e.g. joint and cave infills) only XRD and grain texture features are used to characterise their mineral make up.

The laser particle size data set for the discontinuity type samples is summarised into tables located in Appendix E-5.12. The individual analysis reports (PDF format) can be found on Appendix H-5.17 on CD. The spreadsheets for combined texture including grain size statistics for each sample are given Appendix H-5.18 on CD.

5.4.1 Kauroa Ash

The XRD data for Kauroa Ash are given in Appendix E-5.7. XRD suggests the minerals vermiculite, halloysite, gibbsite, and cristobalite are present in varying amounts, as well as unspecified iron oxide materials. Further analyses are warranted to better identify the mineral components in these tephras. Grain size and sorting characteristics of the Kauroa Ash samples are summarised in Table 5.1. These show it to be a poorly to moderately sorted, medium silt sized with a unimodal size distribution.

Table 5.1 Results from textural analyses of Kauroa Ash samples. The table includes mean grain size, grain size class, size distribution, and sorting characteristics of each sample.

Kauroa Ash					
Sample number	Mean size (mm)	Sorting (phi)	Wentworth size class	Sorting class	Size distribution
72	0.01	0.82	medium silt	moderately sorted	unimodal
71	0.02	1.23	medium silt	poorly sorted	unimodal
167	0.01	0.81	medium silt	moderately sorted	unimodal

5.4.2 Mahoenui Group mudstones

XRD shows the main minerals present are clays (smectite montmorillonite and

illite), calcite, quartz, feldspar, and locally gypsum (Appendix E, 5.7). Large crystals of gypsum are commonly found near the boundary with the underlying Caprock limestone. Grain size and sorting characteristics of Mahoenui Group mudstone samples are summarised in Table 5.2. These show it to be a poorly to moderately sorted, fine sand with a unimodal size distribution.

Table 5.2 Results from textural analyses of Mahoenui Group mudstone samples. The table includes mean grain size, grain size class, size distribution, and sorting characteristics of each sample.

Mahoenui Group mudstones					
Sample number	Mean size (mm)	Sorting (phi)	Wentworth size class	Sorting class	Size distribution
22	0.194	0.93	fine sand	moderately sorted	unimodal
126	0.157	1.25	fine sand	poorly sorted	unimodal
127	0.201	0.91	fine sand	moderately sorted	unimodal

5.4.3 Discrete seams

Examples of photomicrographs of discrete seams are shown in Figures 5.24 and 5.25A-24G. XRD suggests the minerals present in decreasing order of abundance are quartz, oligoclase (feldspar), calcite, clays (e.g. smectite and illite), and rarely the Ca-Mg carbonate mineral dolomite (Appendix E-5.7). The principal peak for dolomite was observed in one of the dissolution seam samples (Appendix E-5.7). Furthermore, dolomite rhombs associated with clay minerals were identified in CL petrography (Figure 5.24). This finding is interesting because dolomite has previously not been identified in the Otorohanga Limestone, probably because earlier studies analysed only the host rock and not the dissolution seams (e.g. Nelson 1978; White and Waterhouse 1991).

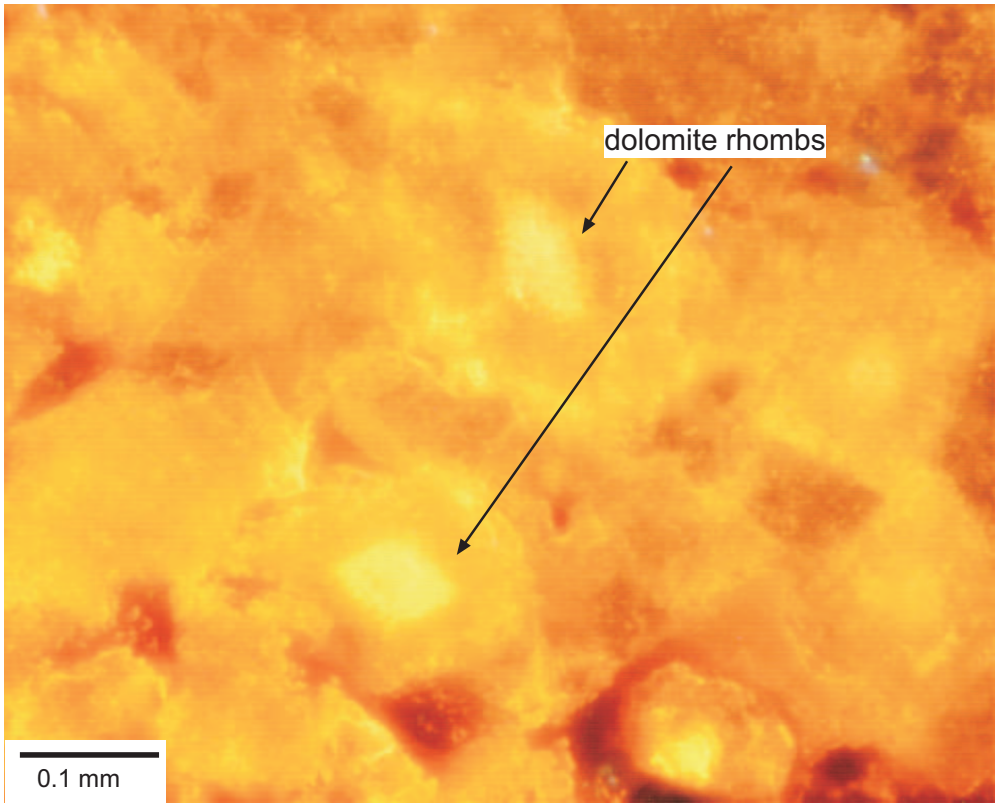

Figure 5.24 Photomicrograph of thin section under CL of the Sub-economic unit (field sample no. 59.4, BH502, 88.9 m depth) containing a discrete seam comprising crystals of dolomite rhombs.

Thin sections show that the total silica component within the seams ranges from 9-90% (av. 56%), and the $CaCO_3$ component range from for 10-91% (av. 44%). Figure 5.25 shows the average mineral composition within 23 discrete seams. The petrography reflects the XRD results, with quartz and feldspar (2-69%), clay (5-64%), and calcite (10-91%) being identified. However, the authigenic minerals glauconite (0-5%) and pyrite (0-25%) have also been identified in thin section but are not detected by XRD. Calcite occurs as any of fragmented bioclasts, micrite, or sparite cement. Grain size and sorting characteristics are summarised in Table 5.3. The data for texture results can be found in Appendix E-5.13. Textural data shows that discrete seams are poorly to moderately sorted, and have medium silt sized grains with a unimodal distribution. Siliciclasts range from angular to rounded in grain shape.

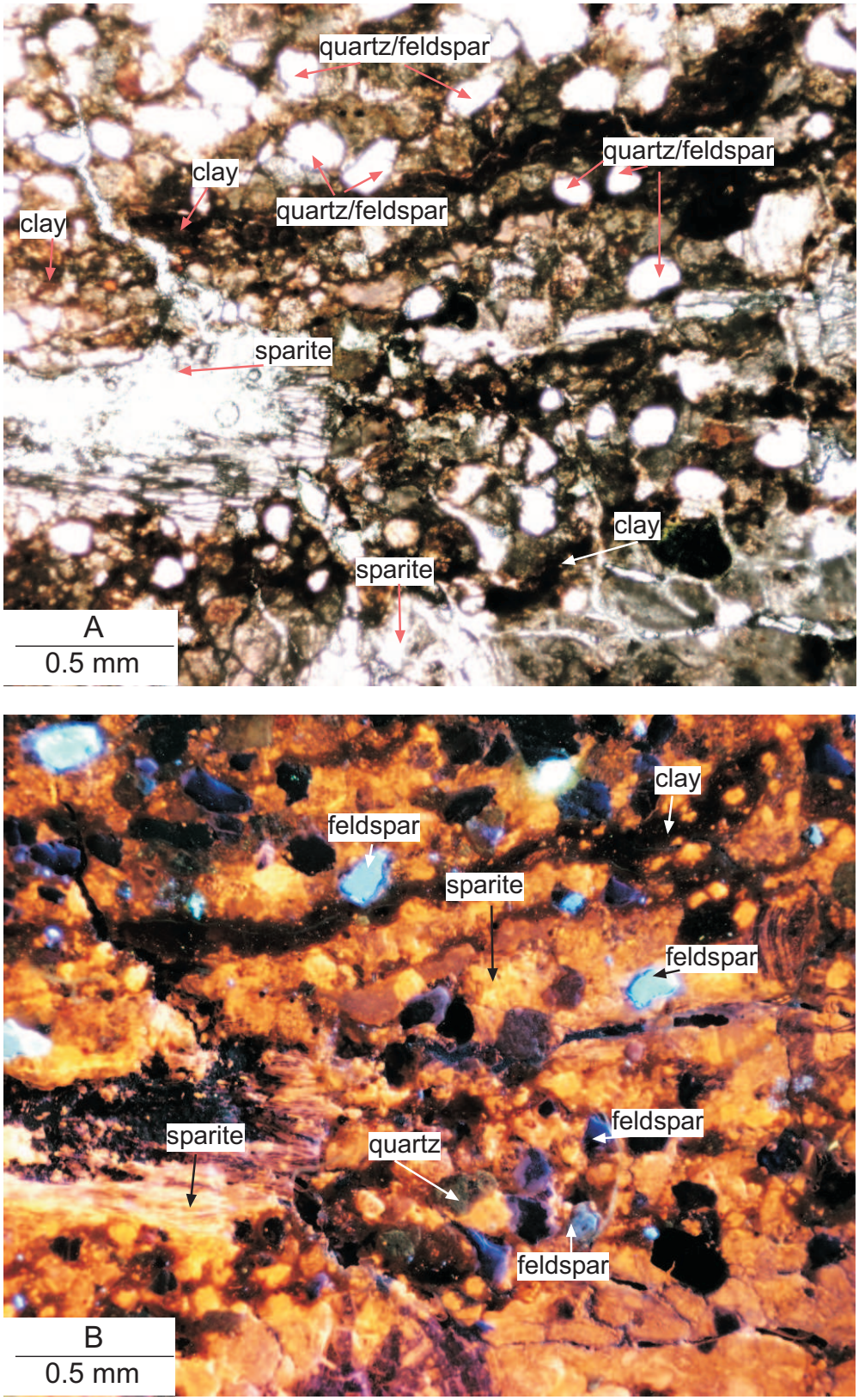

Figure 5.25 (A) Photomicrograph of a thin section under PPL of the High Grade (field sample no. 43, BH502, 62.1 m depth) containing a discrete seam showing quartz and feldspar, sparite, and clay. Host rock is shown in the lower right corner and is slightly fractured. (B) Photomicrograph of the same thin section under CL. The discrete seam under CL light reveals quartz luminescing to greenish brown, and feldspar luminescing to blue and purple.

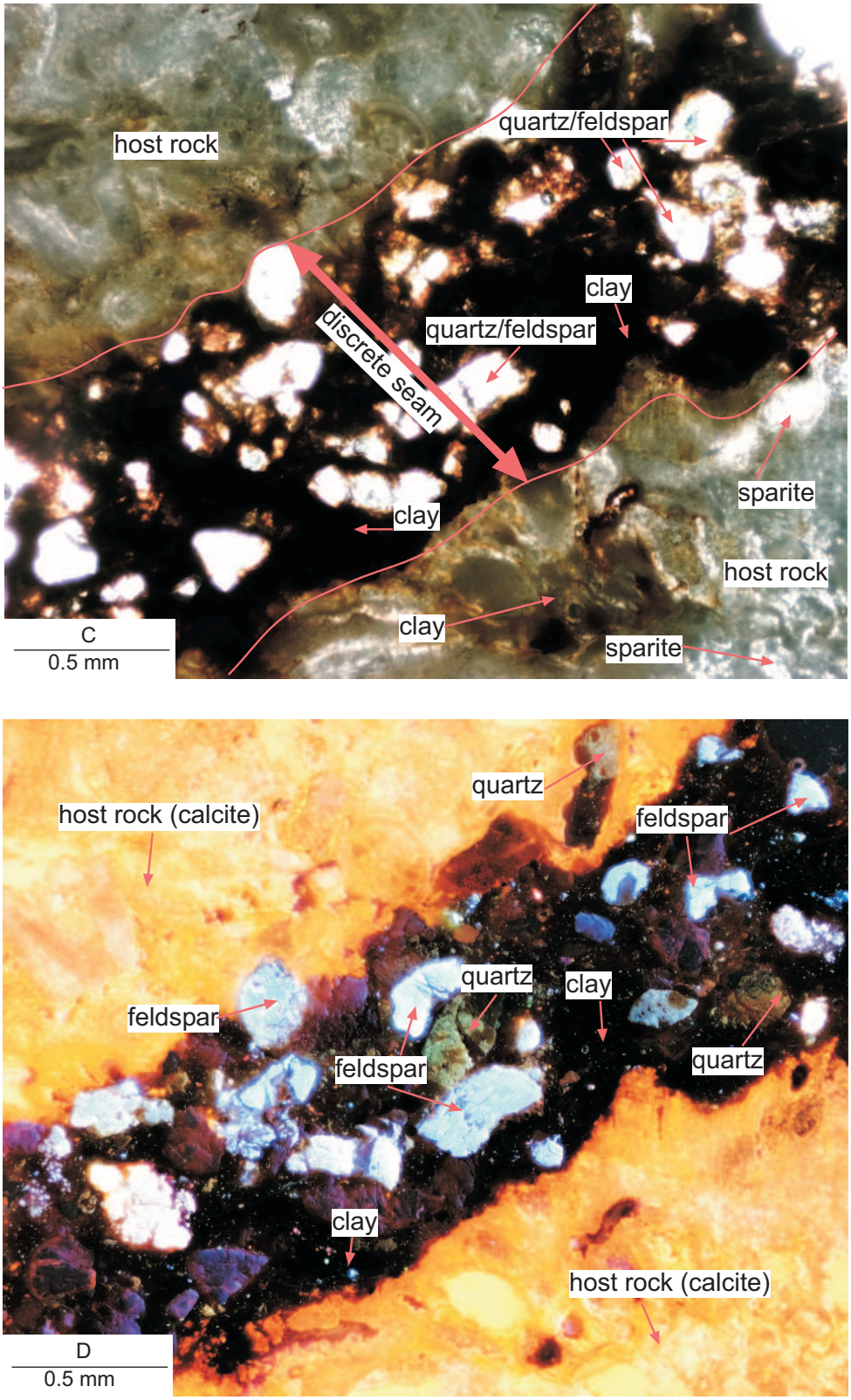

Figure 5.25 (C) Photomicrograph of thin section under PPL of the Lower Steel (field sample no. 16, BH502, 74.1 m depth) containing a discrete seam. The seam is surrounded by host limestone (predominantly calcite) either side. The seam itself is concentrated in clays, and quartz or feldspar. (B) Photomicrograph of the same thin section under CL light. Quartz and feldspar can now be distinguished as they luminesce to different colours (i.e. quartz = greenish brown; feldspar = blues and purples). Iron-stained clay does not luminesce and remains opaque. The calcite luminesces bright yellow orange.

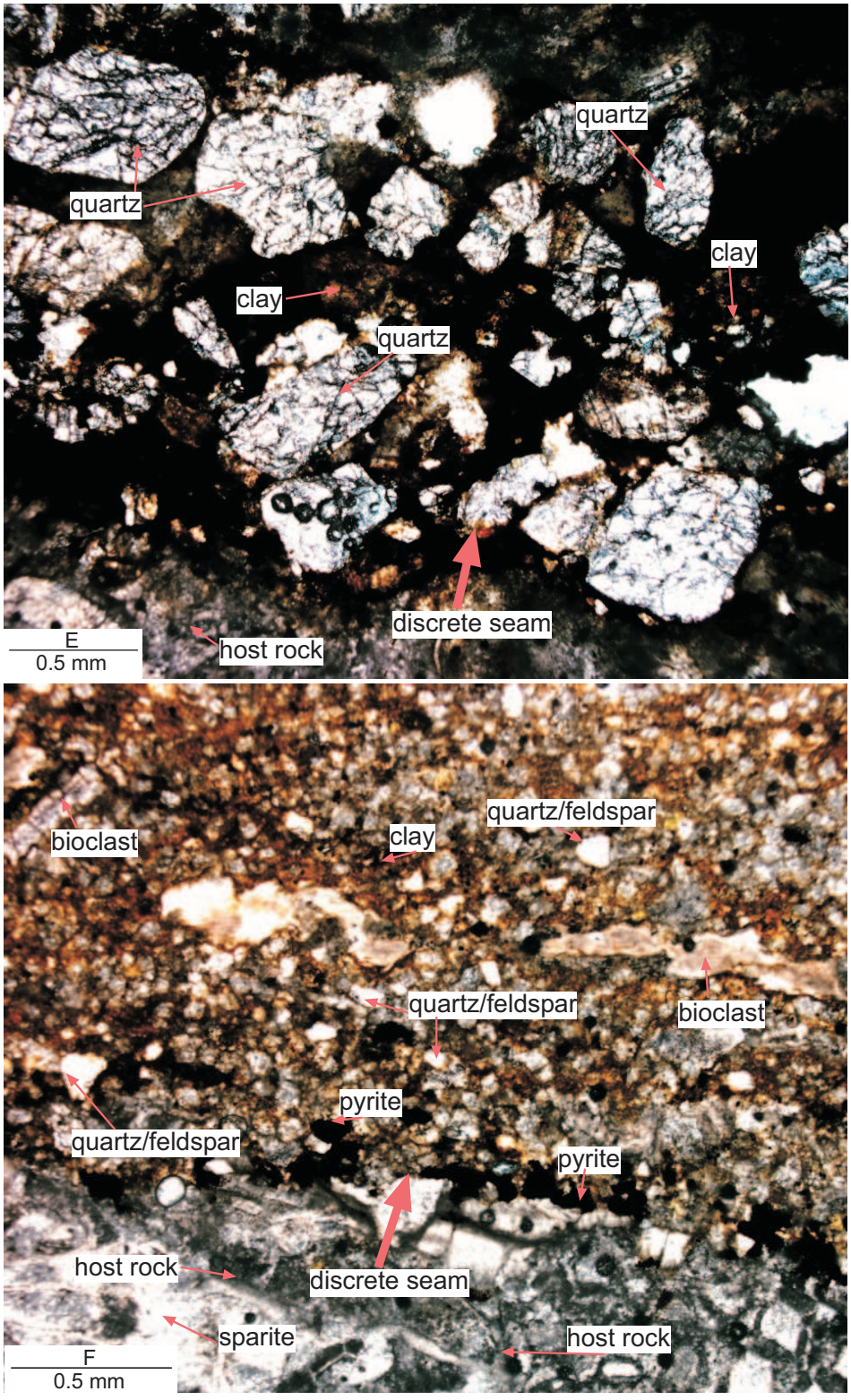

Figure 5.25 (E) Photomicrograph of thin section under PPL of the Lower Steel limestone (field sample no. 51, BH502, 72.6 m depth) containing a discrete seam. The seam is full of large quartz grains that appear fractured. The remaining seam material is predominantly iron-stained clay. A small part of the image shows the surrounding host rock. The seam is well sorted. (F) Photomicrograph of thin section under PPL of the Aglime limestone (field sample no. 35, BH502, 39.45 m depth) containing a discrete seam. The main minerals shown are quartz or feldspar, clay, pyrite, calcite (as bioclasts and/or sparite cement). Host rock is shown on the bottom of the image and strongly contrasts to the seam.

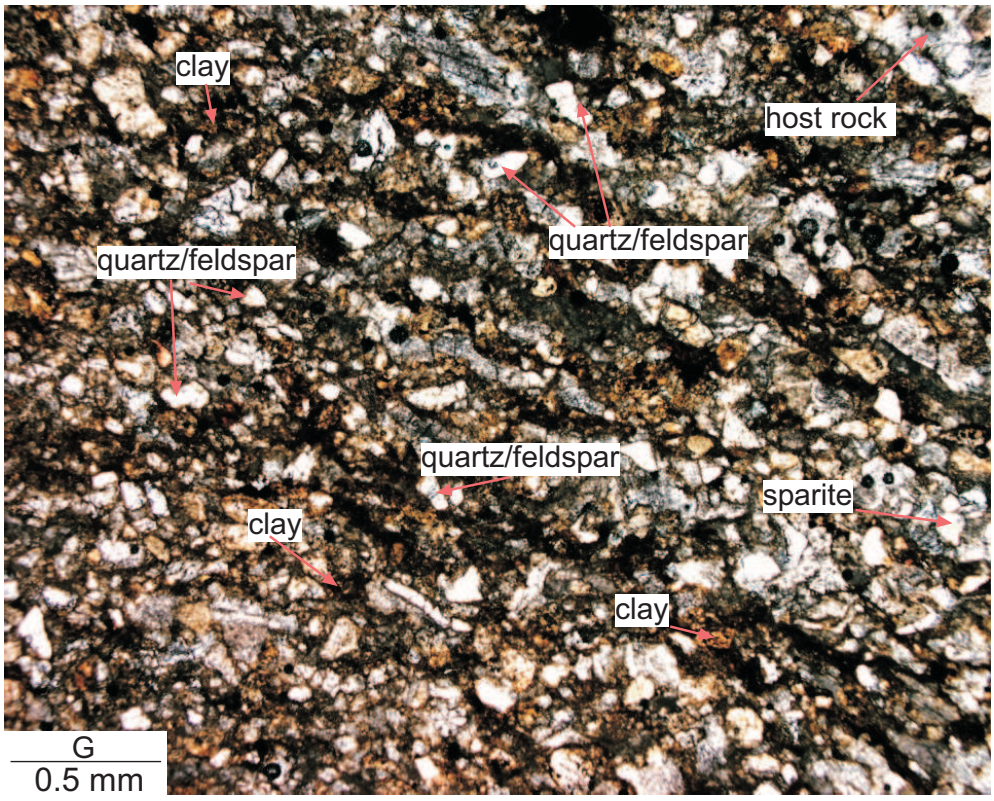

Figure 5.25 (G) Photomicrograph of thin section under PPL of the Aglime limestone (field sample no. 32, BH502, 37 m depth) containing a discrete seam (seam occupies entire image). The dominant minerals present are quartz or feldspar, pyrite (opaque minerals), and iron-stained clay. The seam also contains calcite (either sparite cement or bioclast fragments).

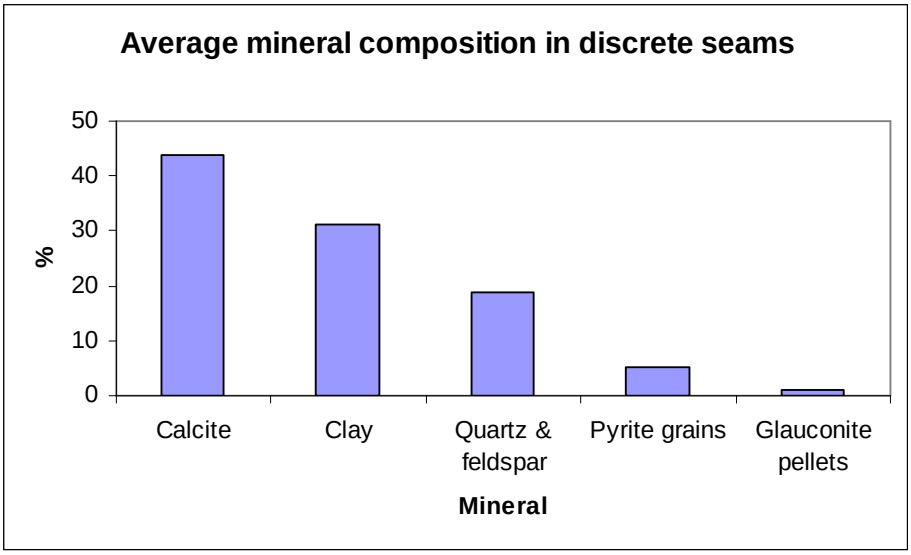

Figure 5.26 Average mineral composition of discrete seams determined from thin section study. See Appendix E-5.13 for data.

Table 5.3 Results from textural analyses of discrete seam samples. The table includes mean grain size, grain size class, and sorting characteristics of each sample. Size distribution of the grain size data are generally unimodal.

Discrete seam					
Sample number	Mean size (mm)	Sorting (phi)	Wentworth size class	Sorting class	Size distribution
171	0.01	1.39	medium silt	poorly sorted	bimodal
117	0.01	0.38	medium silt	well sorted	unimodal
141	0.01	1.11	medium silt	poorly sorted	unimodal
138	0.01	0.49	medium silt	moderately well sorted	unimodal
108	0.01	0.39	medium silt	well sorted	unimodal
118	0.01	0.83	medium silt	moderately sorted	unimodal
139	0.01	1.58	medium silt	poorly sorted	unimodal
163	0.02	1.49	medium silt	poorly sorted	unimodal
152	0.01	1.2	medium silt	poorly sorted	unimodal
172	0.02	1.33	medium silt	poorly sorted	unimodal
162	0.02	1.42	medium silt	poorly sorted	unimodal

5.4.4 Diffuse seams

Examples of some photomicrographs of diffuse seams are shown in Figures 5.27A-C. The minerals identified and their grain size and sorting were all determined by petrography (Appendix E-5.13). The total silica component in the seams ranged from 30-60%, and the $CaCO_3$ from 40-70%. In decreasing order of abundance the minerals present include calcite (40-70%), clay (0-60%), quartz and feldspar (5-10%), pyrite (0-5%), and glauconite (0-1%).

Calcite is in the form of either fragmented bioclasts, micrite, or sparite cement. Textural data can be found in Appendix E-5.13. These show that diffuse seams are generally well sorted, have angular to subangular grain shapes, and grain sizes ranged from very fine sand to fine sand having a unimodal distribution.

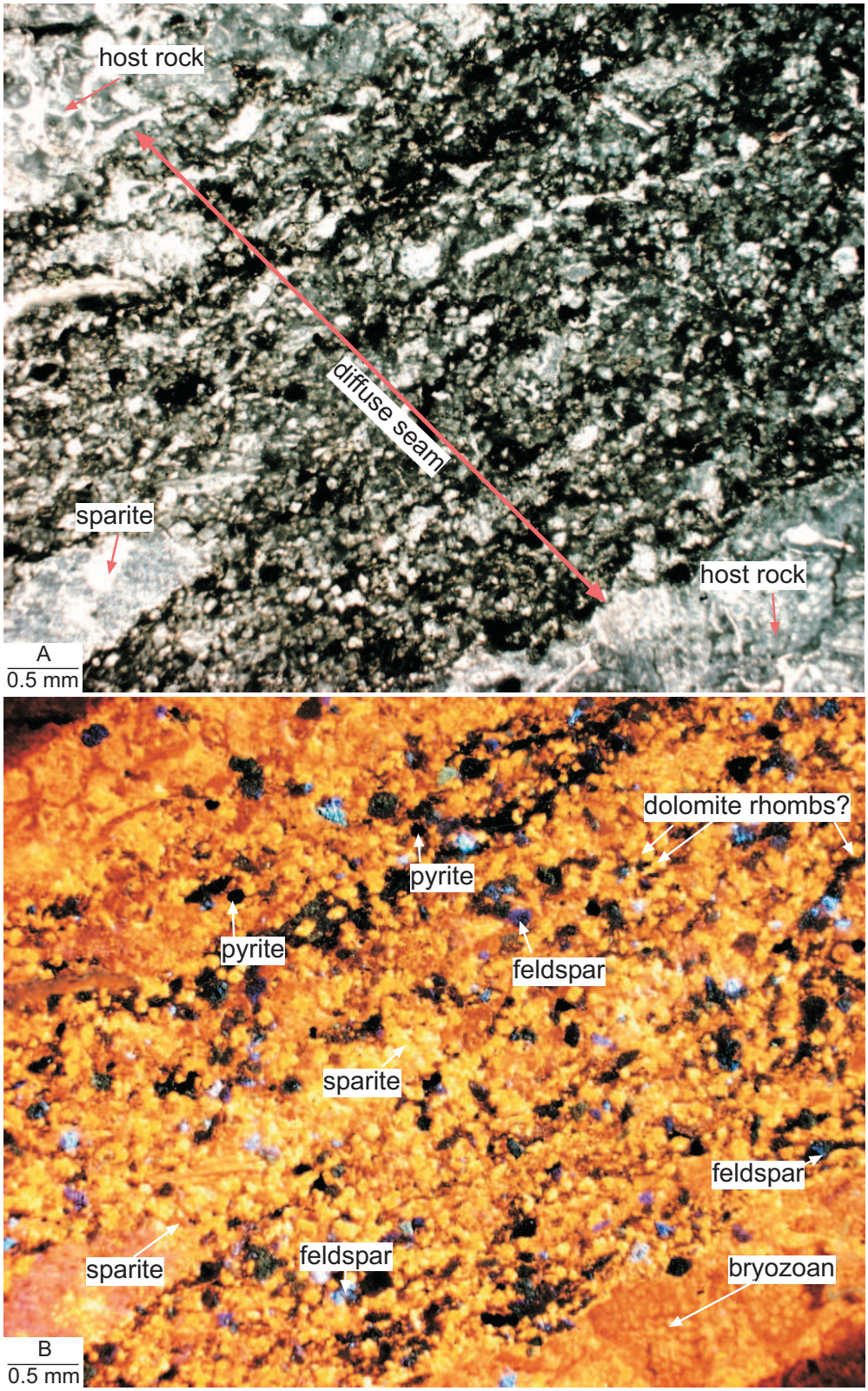

Figure 5.27 (A) Photomicrograph of thin section under PPL of the Aglime limestone (field sample no. 12.2, 41.25 m depth) containing a diffuse seam (entire image). It shows pyrite (opaque), quartz or feldspar, calcite, and bioclasts. (B) Photomicrograph of same thin section under CL light where the pyrite remains opaque, and the calcite has luminesced to bright orange. Here, feldspar can be distinguished from quartz. The sample is dominated by feldspar which luminesces blue and purple. Quartz is probably present but does not emit light as obviously and the sample is quite fine-grained.

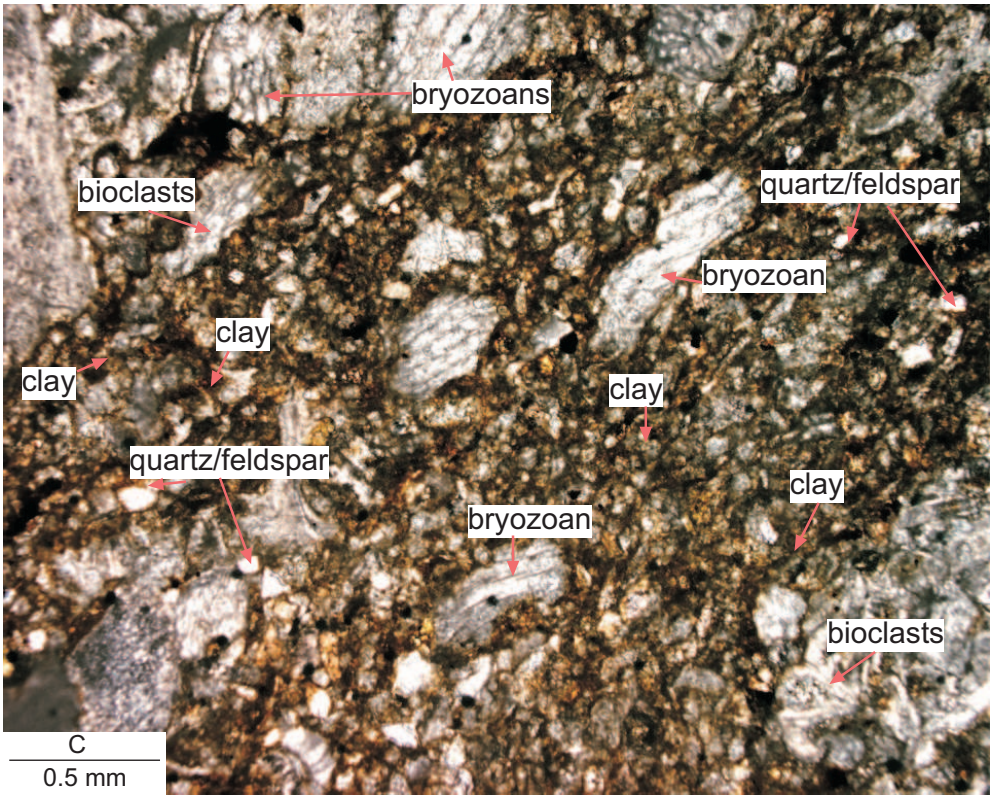

Figure 5.27 (C) Photomicrograph of thin section under PPL of the Aglime limestone (field sample no. 13.2, 42.85 m depth) containing a diffuse seam (occupies entire image). The seam shows bryozoans surrounded by smaller quartz or feldspar grains and clay. Calcite is also common in the seam and is either sparite cement or fragmented bioclasts.

5.4.5 Stylolites (subhorizontal and subvertical)

Photomicrographs of stylolites (defined in Chapter 3, Section 3.1.3) are shown in Figures 5.28A-F. Due to their typical thinness (<1 mm) the mineralogy of the stylolites was determined by petrography. The main minerals found, in decreasing order of abundance, are clay, quartz, feldspar, pyrite, glauconite, and calcite (as fragments of bioclasts). However, subvertical stylolites mostly contain clays.

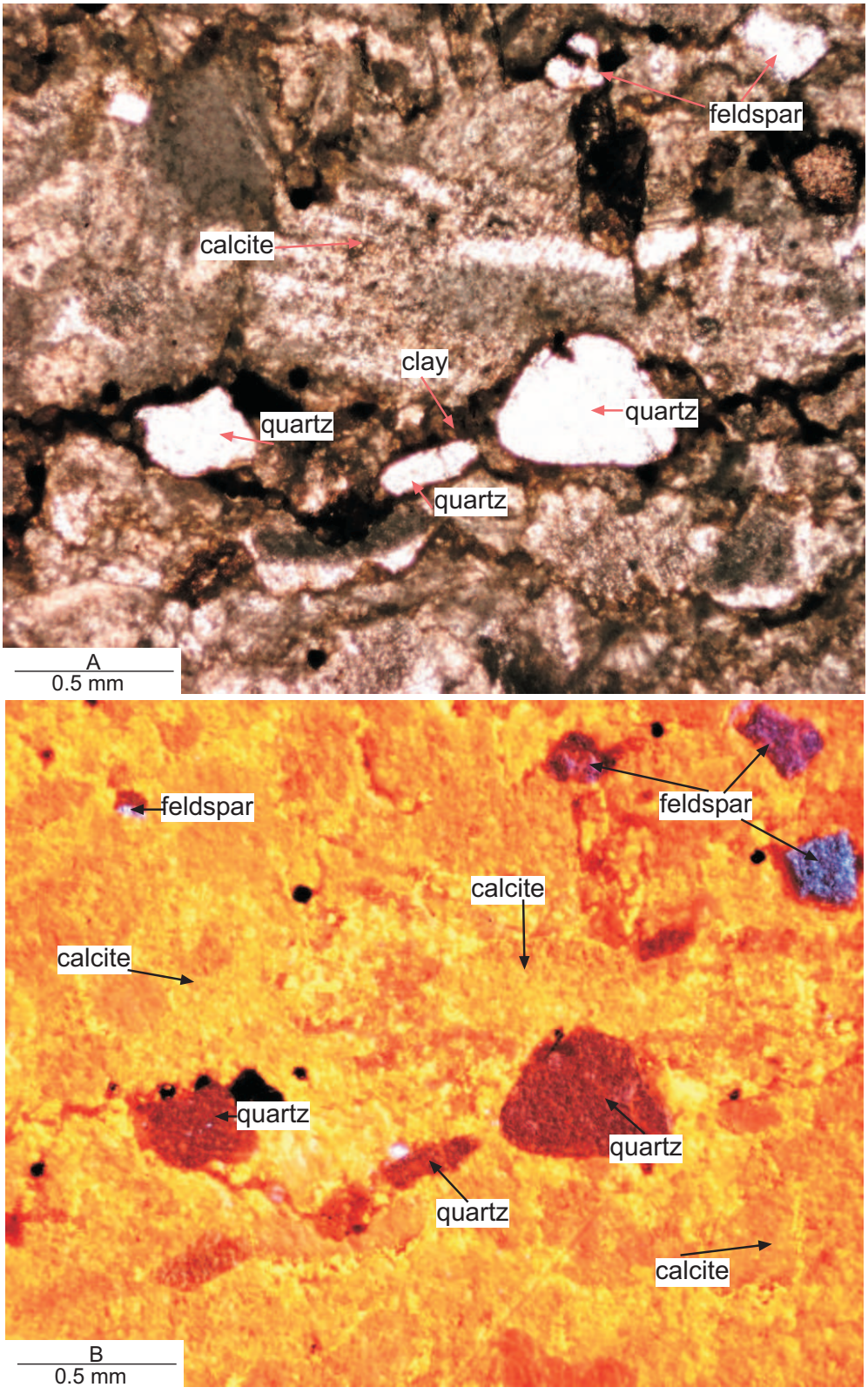

Figure 5.28 (A) Photomicrograph of thin section under PPL of the Lower Steel limestone (field sample no. 18.4, 78 m depth) containing a subhorizontal stylolite. The stylolite contains rounded and subangular quartz grains and clay. A few quartz or feldspar grains occur in the top right corner. The majority of the image shows calcite. (B) Photomicrograph of same thin section under CL light. The quartz grains are brown, and the grains in the top right corner are identified as feldspar which have luminesced purple. The clay does not show as clearly as it did under PPL.

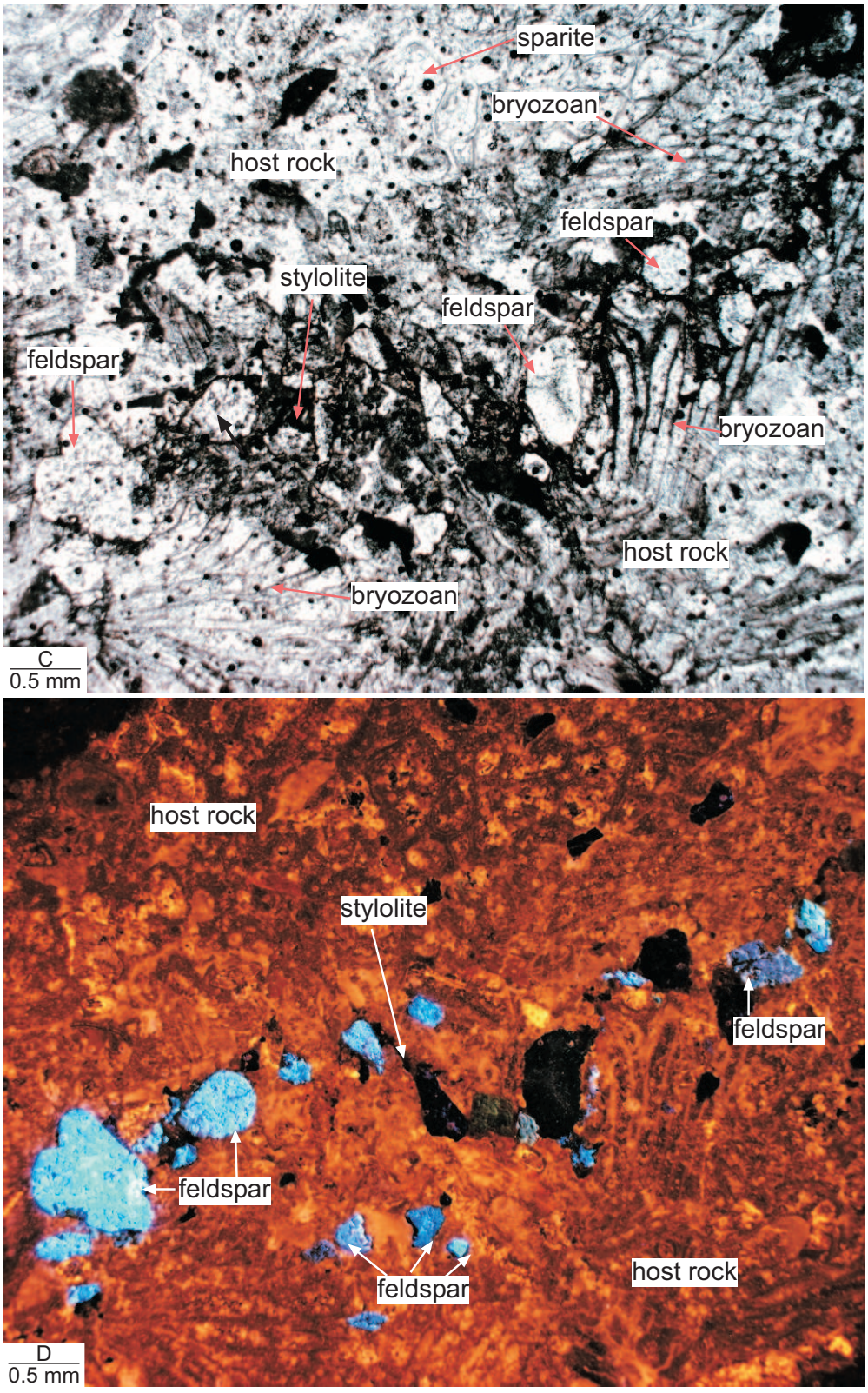

Figure 5.28 (C) Photomicrograph of thin section under PPL of a subhorizontal stylolite in the Lower Steel limestone (field sample no. 17.3, BH502, 74.7 m depth). The stylolite is difficult to see but it is marked by a concentration of quartz or feldspar. The stylolite is surrounded by host rock (calcite dominated), mainly as bioclasts. (D) Photomicrograph of same thin section but under CL light. The stylolite is clearly dominated by feldspar shown as the blue and dark purple minerals. Calcite luminesces to reddish orange.

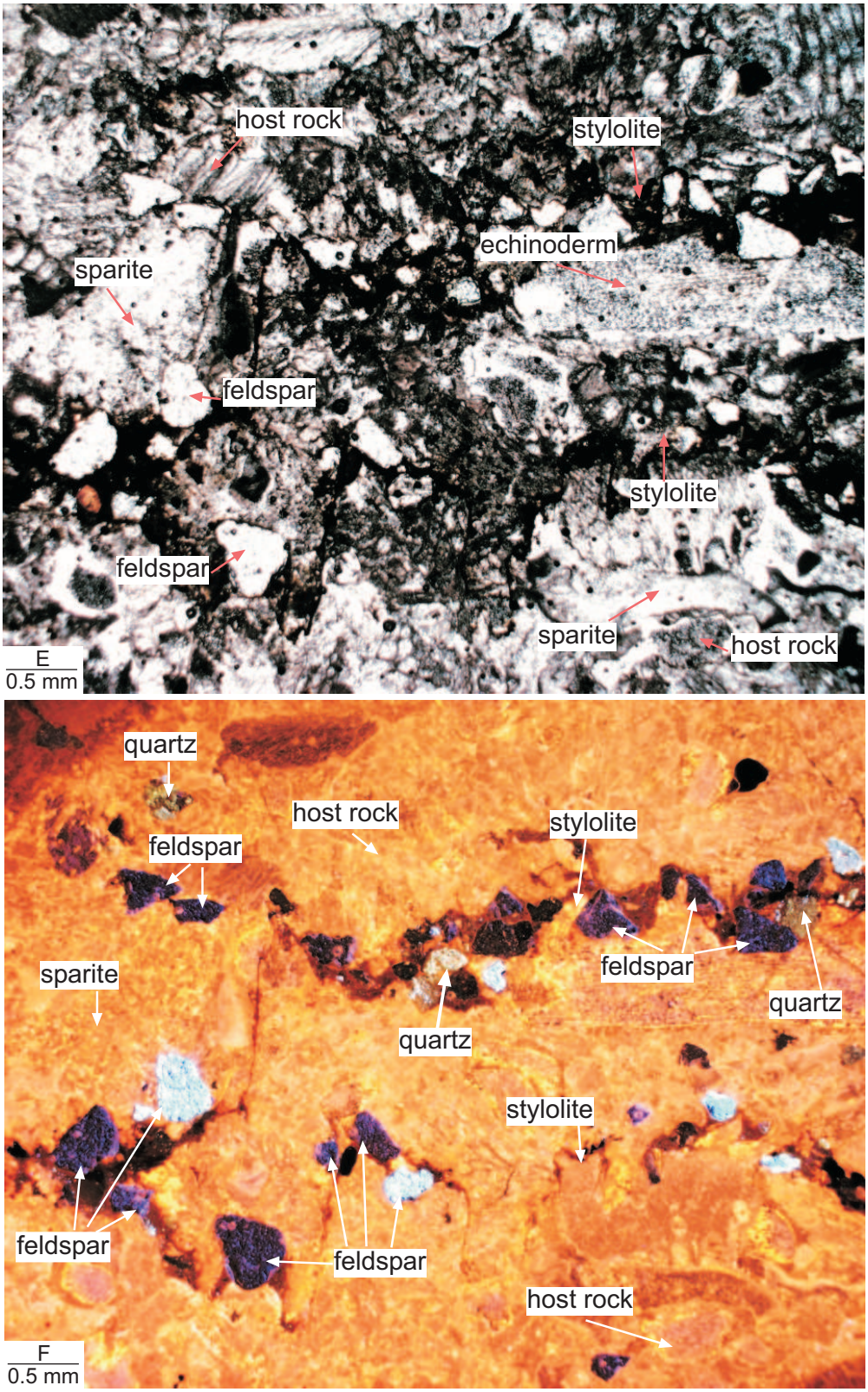

Figure 5.28 (E) Photomicrograph of thin section under PPL of the Lower Steel limestone (field sample no. 17.3, BH502, 73.7 m depth) showing two subhorizontal stylolites. Most of the section contains calcite. The stylolites contain quartz or feldspar. (F) Photomicrograph of same thin section under CL light. Calcite luminesces bright orange and the minerals in the stylolites are identified as mainly feldspar and some quartz.

5.4.6 Joint infills

Two joint infill types occur in the quarry limestones. The first type is typically clay rich and contains limestone fragments. The second type, however, is a rubbery, flexible sheet-like mineral identified by XRD as the clay mineral palygorskite, $(Mg, Al)_2S_{14}O_{10}(OH)$. The two infill types are described separately below.

Type 1: The main minerals identified by XRD in the joint infill samples are clays (smectite, palygorskite), quartz, calcite, and oligoclase (feldspar) (Appendix E-5.7). Comparing the mineralogy of the Mahoenui Group mudstones and Kauroa Ash to the joint infills, the mineral suites are reasonably similar. Combining the wet sieving and laser particle size analysis data shows that the joint infills have a bimodal grain size distribution (Table 5.4; which, however, only shows the mean grain size which ranges from fine silt to granule). Wet sieve data (weight %) are summarised in Table 5.5 and show that grain sizes in the joint infills are as large as pebble grade (4-32 mm). The remaining data can be found in Appendix E-5.14. As a result of this bimodality the joint infills are typically extremely poorly sorted.

Type 2: XRD shows that calcite and quartz minerals are associated with the dominant clay mineral palygorskite (Appendix E-5.7). Figures 5.29A and B show palygorskite that has been dried after sampling, and under the SEM, respectively. The SEM image shows that palygorskite is very fibrous, characterised by a chaotic ordering of interlaced fibres. In addition to taking SEM images, an energy dispersive analyser was used to identify the chemical elements present. Investigating different surfaces of the palygorskite confirmed the presence of silica and calcium (Appendix E-5.15). Table 5.6 shows the weight percent (0-41%) of palygorskite that occurred in the joint infills prior to the wet sieving of those infills. Texture can be described as papery, leathery, rubbery, and extremely fibrous, analogous to a woven cloth.

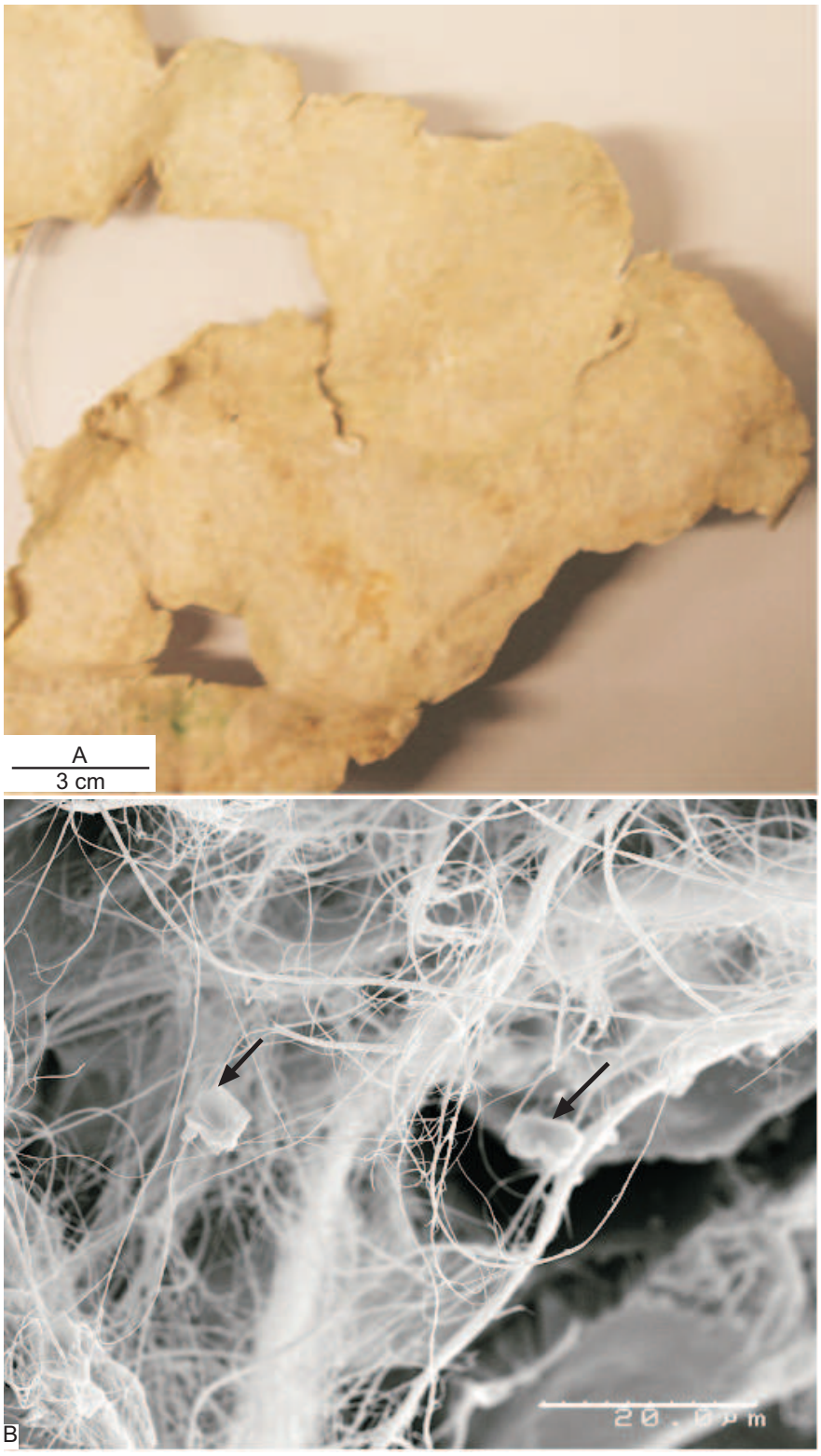

Figure 5.29 (A) Joint infill type 2 palygorskite (clay mineral) found along joint surfaces in the quarry limestones. The mineral looks and feels like paper when dry (field sample no. 105), northern face, Lower Steel. (B) SEM image of palygorskite showing a chaotic tangle of fibres. Small crystals of calcite can be seen hanging amongst the fibres (black arrows) (field sample no. 105), northern face, Lower Steel.

Table 5.4 Results from textural analyses of joint infill (type 1) samples, including mean grain size, grain size class, size distribution, moisture content (some samples) and sorting characteristics of each sample.

	Joint infill					
Sample number	Mean size (mm)	Sorting (phi)	Wentworth size class	Sorting class	Moisture content (%)	Size distribution
164	1.18	4.77	very coarse sand	extremely poorly sorted	25%	bimodal
168	1.19	4.36	very coarse sand	extremely poorly sorted	18%	bimodal
107	0.24	4.86	fine sand	extremely poorly sorted	26%	bimodal
169	1.21	4.28	very coarse sand	extremely poorly sorted	37%	bimodal
154	0.15	4.75	fine sand	extremely poorly sorted	46%	bimodal
165	2.38	4.78	granule	extremely poorly sorted	29%	bimodal
109	0.18	4.33	fine sand	extremely poorly sorted	-	bimodal
114	0.009	0.5	fine silt	moderately well sorted	-	unimodal
144	0.02	1.5	medium silt	poorly sorted	-	unimodal
160	0.01	0.8	medium silt	moderately sorted		unimodal

Table 5.5 Results from wet sieving joint infills. Note that these data only include the weight percent of sample >2 mm in diameter.

	Wentworth size class	
Sample number	Weight % In Granule (2-4 mm)	Weight % In Pebble (4-32 mm)
164	6	57
168	11	56
107	4	44
169	11	45
154	2	38
165	0	31
109	7	38

Table 5.6 Results of weight % for palygorskite from joint infills.

	Samples						
	164	168	107	169	154	165	109
Weight %	2	4	0	17	7	41	3

5.4.7 Surface accumulations

Surface accumulations are surface coatings sampled from quarry faces which have accumulated quarry dust including material from quarry roads which have washed down over the face. XRD shows the minerals present to be palygorskite, quartz, and calcite (Appendix E- 5.7). Grain size and sorting properties were not determined as sampling involved taking a scraping (scraped to a fine powder) from the quarry face surface, so altering the original texture of the material.

5.4.8 Cave infills

The main minerals present determined by XRD are clays (smectite or chlorite, vermiculite, palygorskite), quartz, and calcite (Appendix E-5.7). Grain size and sorting characteristics are summarised in Table 5.7. The textural analyses show

that cave infills are moderately well sorted, medium silts with a unimodal distribution.

Table 5.7 Results from textural analyses of cave infill samples, including mean grain size, grain size class, size distribution, and sorting characteristics of each sample.

		Cave infill			
Sample number	Mean size (mm)	Sorting (phi)	Wentworth size class	Sorting class	Size distribution
166	0.01	0.61	medium silt	moderately well	unimodal
146	0.01	0.69	medium silt	moderately	unimodal
143	0.01	0.47	medium silt	well	unimodal
161	0.01	0.59	medium silt	moderately well	unimodal

5.5 Discussion

5.5.1 Quarry limestone mineralogy

Figure 5.30 presents a stratigraphic summary of the bioclast and siliciclast mineral composition of the limestones at the quarry. The limestones are dominated by the carbonate mineral calcite and contain small (typically <10%) concentrations of siliciclasts such as quartz, feldspar, glauconite, pyrite, and clay. Evidence of the dominance of calcite is shown in XRD results (Table 5.8). In the host rock the total $CaCO_3$ component (i.e. bioclasts, micrite, sparry calcite) of the limestones ranges from approximately 70-99% and the total % siliciclast material (silica grains and infills) from about 1-30%. Figure 5.30 shows that the limestone that has the lowest % $CaCO_3$ (determined by petrography) is the Caprock (70-95%), followed by the Sub-economic (90-96%), Aglime (90-98%), High Grade (93-98%), Lower Steel (96-98%), and Upper Steel (98-99%). The trend is the opposite for the siliciclast content i.e. Upper Steel (1-2%) (lowest), High Grade (2-7%), Sub-economic (4-10%), Aglime (2-10%), and Caprock (5-30%) (highest).

Petrographic data: Drill hole #BH502

THE UNIVERSITY OF WAIKATO
Te Whare Wānanga o Waikato

Location	McDonald's Quarry, Oparure, Te Kuiti district	Elevation	211.3
Direction	Vertical	Depth (m)	206
Drilling contractor	Boart Longyear	Easting	2690996.9
Petrography by	O Hansen	Northing	6316710.15
Date	Oct 2007		

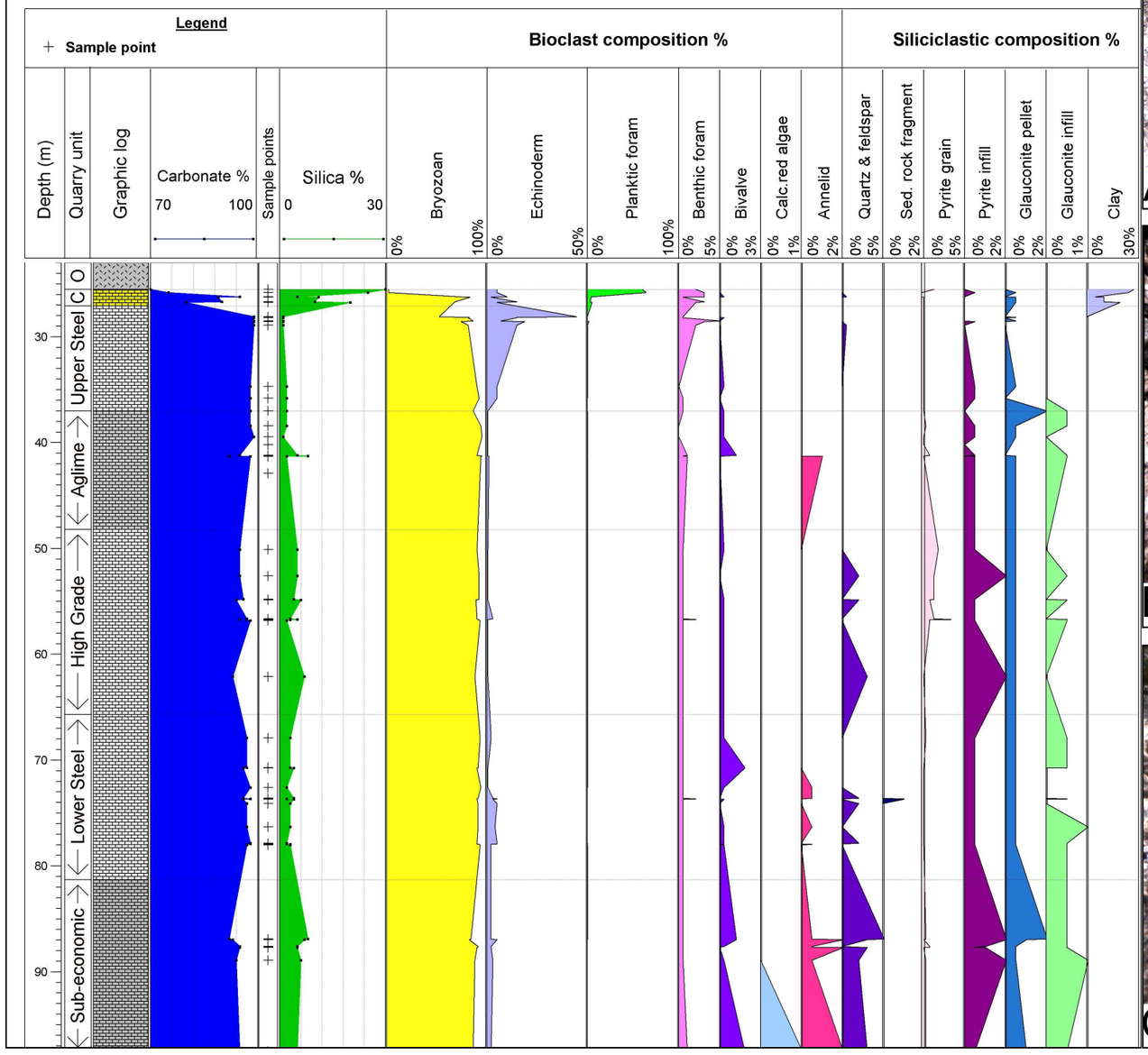

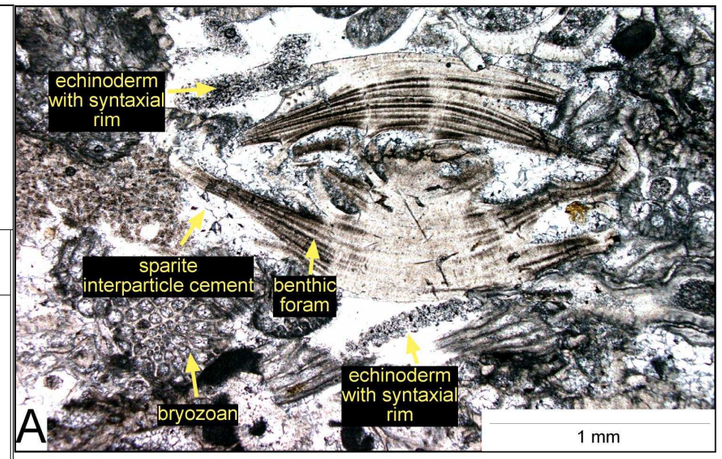

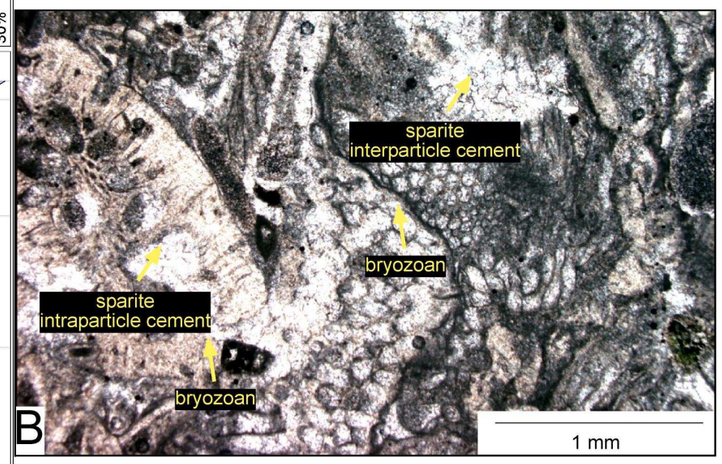

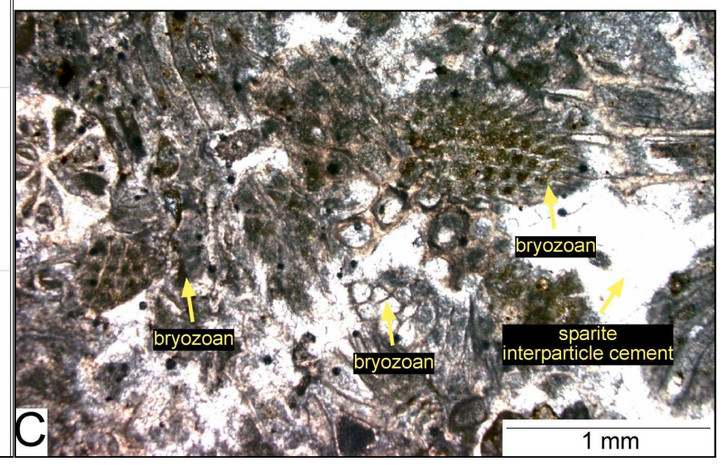

Figure 5.30 This figure summarises the petrographic data collected from thin section study of host rock (i.e. no discontinuities) from the quarry limestones. The data are presented in relationship to depth (m) from top of drill hole, and the graphic log shows variations of the colour grey which corresponds to the variable silica across each quarry unit (darker grey = higher silica content). The estimated percentage of $CaCO_3$ and silica is shown as the blue and green graphs on the left. The bioclast and siliciclast composition is also shown as curves. The photomicrographs to the far right of the figure show examples of host rock: (A) Upper Steel (field sample no. 24.1, BH502, 28.5 m depth) host rock showing interparticle (between) sparite cement, echinoderms with syntaxial rims formed round them, a large benthic foram in the centre, and common bryozoans; (B) Lower Steel (field sample no. 16, BH502, 74.1 m depth) host rock showing inter and intra-particle sparite cement and bryozoans (dominant bioclasts); (C) Aglime (field sample no. 35, BH502, 39.45 m depth) host rock containing interparticle sparite cement between dominant bryozoans. Grid coordinate system is NZ map grid and elevation = metres above mean sea level. O = Overburden, C = Caprock.

Table 5.8 Minerals present in each quarry limestone determined by XRD, the position 2θ for the main peaks and their intensities. Due to the fact that calcite is the dominant mineral in these limestones, other minerals that occur in small concentrations are often not detected by XRD due to the overwhelming amount of calcite present.

Quarry limestone unit	Minerals present	Position [°2θ]	Main peak intensities
Caprock	calcite	29.38	100
		39.40	18
		35.93	14
Upper Steel	calcite	29.60	100
		39.37	18
		35.92	14
Aglime	calcite	29.34	100
		39.45	18
		35.92	14
High Grade	calcite	29.36	100
		39.39	18
		35.94	14
Lower Steel	calcite	39.37	3.04
		39.37	18
		35.95	14
Sub-economic	calcite	29.37	100
		39.33	18
		35.95	14

5.5.2 Quarry limestone bioclast composition

Figure 5.30 shows in order of decreasing overall abundance that the bioclast composition of the host rock comprises bryozoans, echinoderms, benthic forams, bivalves, annelids, planktic forams, and calcareous red algae. Bryozoan fragments are the most abundant faunal type in all quarry limestones units with the exception of a few samples taken near the contact of the Caprock with the overlying mudstones of the Mahoenui Group where planktic forams predominate. Echinoderm fragments show higher percentages in the Upper and Lower Steel compared to the other units. Benthic forams show similar abundances in all quarry limestones, however, they are slightly more common in the Upper Steel limestone. Bivalves are variable across the units. Annelids are mainly present in the Aglime, Lower Steel, and particularly in the Sub-economic unit. Calcareous red algae are mainly absent in the quarry limestones, but rare occurrences were noted in a few samples from the Sub-economic unit.

Figure 5.31 summarises the grain size distribution of bioclasts in the host rock. The distribution in grain sizes ranges between very fine sand to granule, however, most grain sizes occur within the medium to coarse sand size class. In general, bioclasts are fragmented and rarely whole. Abrasion characteristics of bioclasts are similar for all quarry limestones, ranging from slightly abraded to moderately abraded.

5.5.3 Quarry limestone siliciclast composition

Siliciclast composition is shown in Figure 5.30. The siliciclast components identified in the host rock in decreasing order of abundance include pyrite grains, pyrite infills, glauconite pellets, glauconite infills, quartz, feldspar, clays, and sedimentary rock fragments. Figure 5.30 shows that pyrite grains and pyrite infills have highest values in the High Grade, Aglime, and Sub-economic units. Glauconite pellets increase in the Aglime, High Grade, and Sub-economic units. Glauconite infill percentages are generally similar (rare) for all of the quarry limestones, however, infills are absent in the Caprock and Upper Steel. Quartz and feldspar increase above a few percent in the High Grade and the Lower Steel, as well as across most of the Sub-economic unit, otherwise they are generally rare or absent. Clay material appears to be absent in all quarry limestones except for the Caprock limestone, although clear distinction is difficult to make because of fineness of grain size. Sedimentary rock fragments are generally absent except for a few samples in the Lower Steel where they are rare.

Figure 5.32 summarises the grain size of siliciclasts in the host rock. Similar to the grain size distribution of the bioclasts, the siliciclast grain sizes range from very fine sand to granule. However, the most common grain size is in the fine sand size class. There are generally no trends shown for siliciclast shape when comparing all the limestones (e.g. shape ranges from angular to subrounded for all), however, subrounded grains are most common. Siliciclasts are almost exclusively scattered within the host rock and rarely occur in clusters of several associated grains.

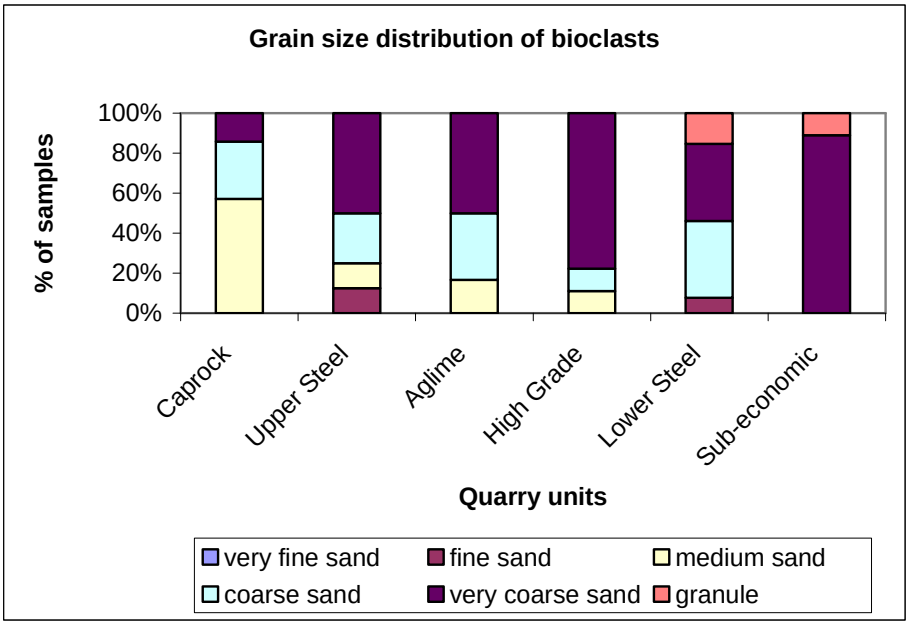

Figure 5.31 Grain size distribution results from thin section study of bioclasts in the quarry limestone units.

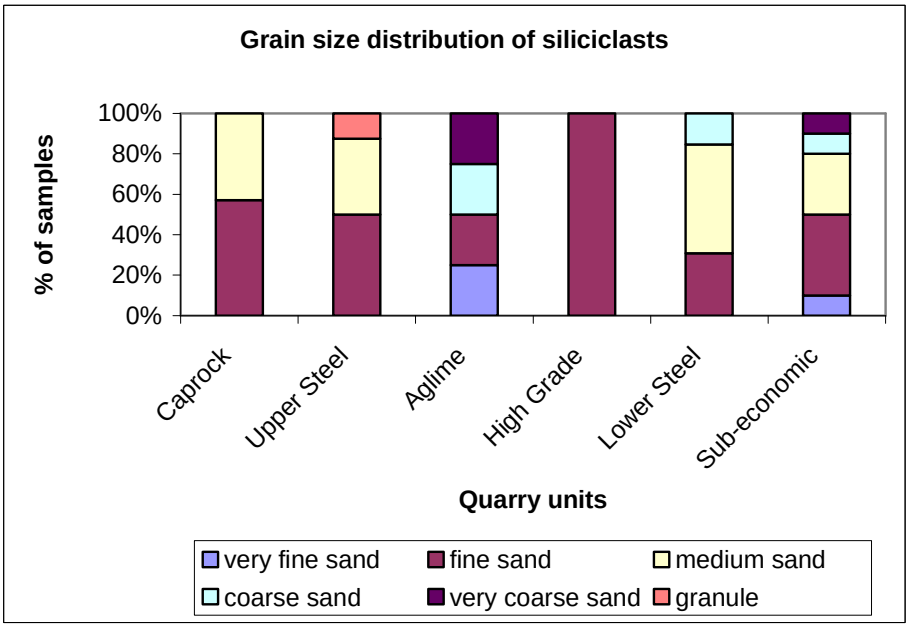

Figure 5.32 Grain size distribution results from thin section study of siliciclasts in the quarry limestones.

5.5.4 Cements

Micrite is the dominant cement type in the Caprock and Aglime units (typically biomicrites). The major cement type in the other four quarry units (Upper Steel, High Grade, Lower Steel, and Sub-economic) is clear sparite (i.e. they are biosparites), which occurs between and within the skeletal grains (interparticle

and intraparticle cement, respectively). As well as interparticle and intraparticle cement, sparite also occurs in veins where it typically heals fractures in the limestones. Calcite veins sealing fractures are common in all the limestones.

5.5.5 Porosity and burial features

The majority of the host limestone samples across the six quarry units lack porosity. However, interparticle porosity is evident in some thin sections from the Upper Steel unit. Fracture and stylolitic porosity is not uncommon in the Aglime, High Grade, Lower Steel, and Sub-economic units.

The quarry limestones are dominated by tight fabrics with occasional slightly open fabrics (e.g. Upper Steel). The limestones show a combination of mechanical compaction features (e.g. fragmented bioclasts, shattered grains), and chemical compaction features (e.g. dissolution features including dissolution seams, subhorizontal and subvertical stylolites, and microstylolites or fitted fabrics, which have led to effective porosity destruction.

5.5.6 Mineralogy of overburden units and discontinuity materials

Table 5.9 shows a summary of XRD results of the minerals present in the overburden units and discontinuity materials. In contrast to the limestone units, minerals in the overburden units and discontinuity materials are typically dominated by non-carbonate minerals including clays (smectite, illite, palygorskite), quartz, and feldspar (probably oligoclase). Calcite is found in most (e.g. Mahoenui Group mudstones, discrete seams, diffuses seams, stylolites, joint infill, surface accumulation, and cave infill), but in much lower concentrations than in the limestones.

The joint infills and cave infills share similar mineral characteristics to the Mahoenui Group mudstones and Kauroa Ash (overburden). This is significant because it is highly likely that the joint infills are sourced from the overlying overburden (i.e. ash and mudstones).

Table 5.9 Minerals present and the position 2θ of the main peaks and their intensities in overburden units and discontinuity materials determined by XRD.

Quarry unit/discontinuity material		Minerals present	Position [°2θ]	Main peak intensities
Kauroa Ash (overburden)		quartz	26.62	100
			20.82	35
			36.55	12
		vermiculite (clay)	6.27	100
			31.67	40
		halloysite (clay)	8.74	100
		gibbsite (clay)	18.29	100
		cristobalite (quartz)	20.27	100
			36.55	90
		oligoclase (feldspar)	28.04	100
			21.95	80
			27.75	80
Mahoenui Group mudstones (overburden)		gypsum	11.70	100
			20.77	50
		calcite	29.39	100
			39.42	18
		quartz	26.58	100
		smectite (clay)	5.55	100
		illite (clay)	20.08	100
		oligoclase (feldspar)	28.49	100
			22.05	80
Discrete seams		quartz	26.66	100
			20.87	35
			39.45	12
		calcite	29.44	100
			39.44	18
		smectite (clay)	6.00	100
			5.89	90
		illite (clay)	9.94	100
			19.75	90
		dolomite (carbonate)	30.78	100
		oligoclase (feldspar)	22.05	80
			23.57	70
			27.94	100
Diffuse seams		calcite	29.40	100
			39.41	18
		quartz	26.60	100
			20.99	35
		oligoclase (feldspar)	27.97	100
			27.84	80
Vertical joints				
	Type 1	smectite (clay)	6.04	100
			19.77	80
		palygorskite (clay)	19.68	80
		quartz	26.62	100
			20.82	35
		calcite	29.43	100
			39.43	18
		oligoclase (feldspar)	21.98	80
	Type 2	palygorskite (clay)	8.40	100
			13.71	60
		calcite	29.38	100
			39.38	18
		quartz	26.62	100
Cave infills		smectite/chlorite	19.68	100
			19.86	18
			29.76	60
		vermiculite (clay)	19.20	50
		quartz	26.59	100
			20.77	35
		palygorskite (clay)	8.50	100
		calcite	29.40	100
Surface accumulations		palygorskite (clay)	8.37	100
			27.93	18
		smectite (clay)	19.77	18
		calcite	29.41	100
			39.40	18
		quartz	26.61	100
			20.82	35

Vertical joints and cave infills contain palygorskite, which is not found in the other discontinuities. Palygorskite is formed *in situ* (i.e. not washed in like the other joint infills), and is commonly found in carbonate environments (Post and Crawford, 2007). The following section offers some information about palygorskite, such as its physical and chemical characteristics, and occurrences in New Zealand.

5.5.7 Palygorskite

Palygorskite was first found in 1860 near a place called Palygorsk in the Perm District in Russia. Palygorskite occurs as sheets in tension fracture zones, fault zones, caves in rock strata (commonly hanging from cave roofs and sides in soft dangling masses), and forming strata in alluvial terraces (Post and Crawford, 2007). Palygorskite has also been found in metal mines in western United States (e.g. Cosumnes Mine copper gold mine). These fibrous clays that occur in these geologic host rock systems range from Paleozoic to Quaternary ages (Post and Crawford, 2007).

Chemical composition: Chemically, palygorskite is an hydrated magnesium aluminium silicate $(Mg, Al)_2S_{14}O_{10}(OH)$. The elemental composition of some New Zealand samples shows that palygorskite contains Fe, Si, Mg, Ca, Na, K, and Ti (Soong, 1992). It belongs to the group of clays, is classed as a silicate, subclass phyllosilicate (Post and Crawford, 2007). Physically it forms a fibrous matted felted mass, commonly named 'mountain leather'. It varies from white to pale grey to lavender in colour, has a silky to dull lustre, and has perfect cleavage in one direction forming thin sheets or flakes. The matted masses are often interwoven with attached calcite crystals and embedded with isolated quartz crystals. Associated minerals include calcite, clays, and serpentine (Soong, 1992).

Formation: The formation and persistence of palygorskite requires certain conditions, and they are alkaline pH, high Mg and Si, and low Al activities. Constituents necessary for formation of palygorskite include the percolation of subsurface water charged with soluble constituents sourced from the breakdown of minerals (Soong, 1992).

Occurrence and geochemistry: Interestingly, large deposits (e.g. Georgia, and Florida, United States) of palygorskite are used as industrial minerals as a substitute for asbestos. In New Zealand, palygorskite was first reported in 1961 by the New Zealand Speleological Society as a result of the exploration of caves in the Te Kuiti district (i.e. Oyster Cave and Lucky Strike) (Lowry, 1964). The mineral was described as white absorbent sheets about 5 mm thick, occurring as fine matted fibres filling vertical joint openings in limestones of the Te Kuiti Group (as seen in McDonald's Quarry). Partial analysis showed that the palygorskite samples contained 14.5% alumina, 8.9% magnesia, and low lime (Lowry, 1964). At one location, palygorskite was found forming as a median filling of a vertical joint where coarse calcite crystals lined the joint; this has also been observed at McDonald's Quarry (see Chapter 3, Section 3.5). Other records of occurrences include Mahoenui, Taranaki, Piopio, King Country, Karori, Wellington City, Cromwell Gorge, and Central Otago (Soong, 1992). These occurrences were mostly associated with limestone, and more recent occurrences have been noted in fault gouges in greywacke and schists.

Although palygorskite at McDonald's Quarry can occur in significant amounts (up to 41 weight % in joint infills), it is unlikely to have a major effect on the silica issue. The properties of the mineral would allow easy removal during the crushing and screening process.

5.5.8 Dissolution seams – discrete and diffuse

Since petrographic information was collected in detail for dissolution seams (both discrete and diffuse seams), Figure 5.33 was produced to summarise the mineral composition of these seams. This figure shows the relative abundance of minerals in each seam described, as well as thickness and % carbonate for each seam. In contrast to the quarry limestone host rock, the % carbonate in the discrete and diffuse seams ranges from 10-93% (70-99% in host rock) and the total % siliciclasts from 7-90% (recall 1-30% in host rock). This is significant and shows how compositionally different the host rock is compared to the discrete seams in terms of carbonate and mineral content. Diffuse seams have a higher carbonate content (40-70%) than discrete seams (Figure 5.33). Clay material is the

dominant siliciclast in both discrete and diffuse seams. Quartz and feldspar are far more common in the seams (7-70%) compared to their relatively low abundances in the host rock for all the quarry limestones (0-5%) (Figure 5.30). Quartz and feldspar occur in lower abundances in the diffuse seams compared to the discrete seams. Pyrite is common and glauconite rare within both seam types.

For discrete seams, Figure 5.33 shows that grain shapes range from angular to rounded, and that grain sizes range from very fine sand to coarse sand. For diffuse seams, grain shape ranges from angular to subangular, and grain sizes from very fine sand to fine sand.

5.5.9 Texture summary

Sorting characteristics of the main discontinuity materials and overburden units are shown in Figure 5.34. Discrete seams show variable sorting (well to extremely poorly sorted), cave infills and Kauroa Ash are generally moderately to well sorted, and joint infills (moderately well to extremely poorly sorted) show the greatest variation due to the presence of limestone fragments in these samples, as well as clays.

Figure 5.35 shows a summary of the grain size distribution for representative samples from the Kauroa Ash, Mahoenui Group mudstones, discrete seams, joint infills, and cave infills (all samples were plotted initially and can be found in Appendix E-5.16). In general, the Kauroa Ash, Mahoenui Group mudstones, cave infills, and discrete seams show a unimodal distribution. The joint infills show a bimodal distribution. In terms of the silica issue, the grain sizes across the discontinuities with the exception of the joint infills are fine enough to pass through the scalper that is currently used onsite at the crushing plant. The scalper comprises a series of vibrating beds that have gaps between them that can be adjusted. The main role of the scalper is to reduce the amount of silica-rich material that passes through and into the crusher, screens, and finally the stock piles that are ready for pick up. The joint infills have larger limestone fragments (pebble size) which may or may not pass through the scalper.

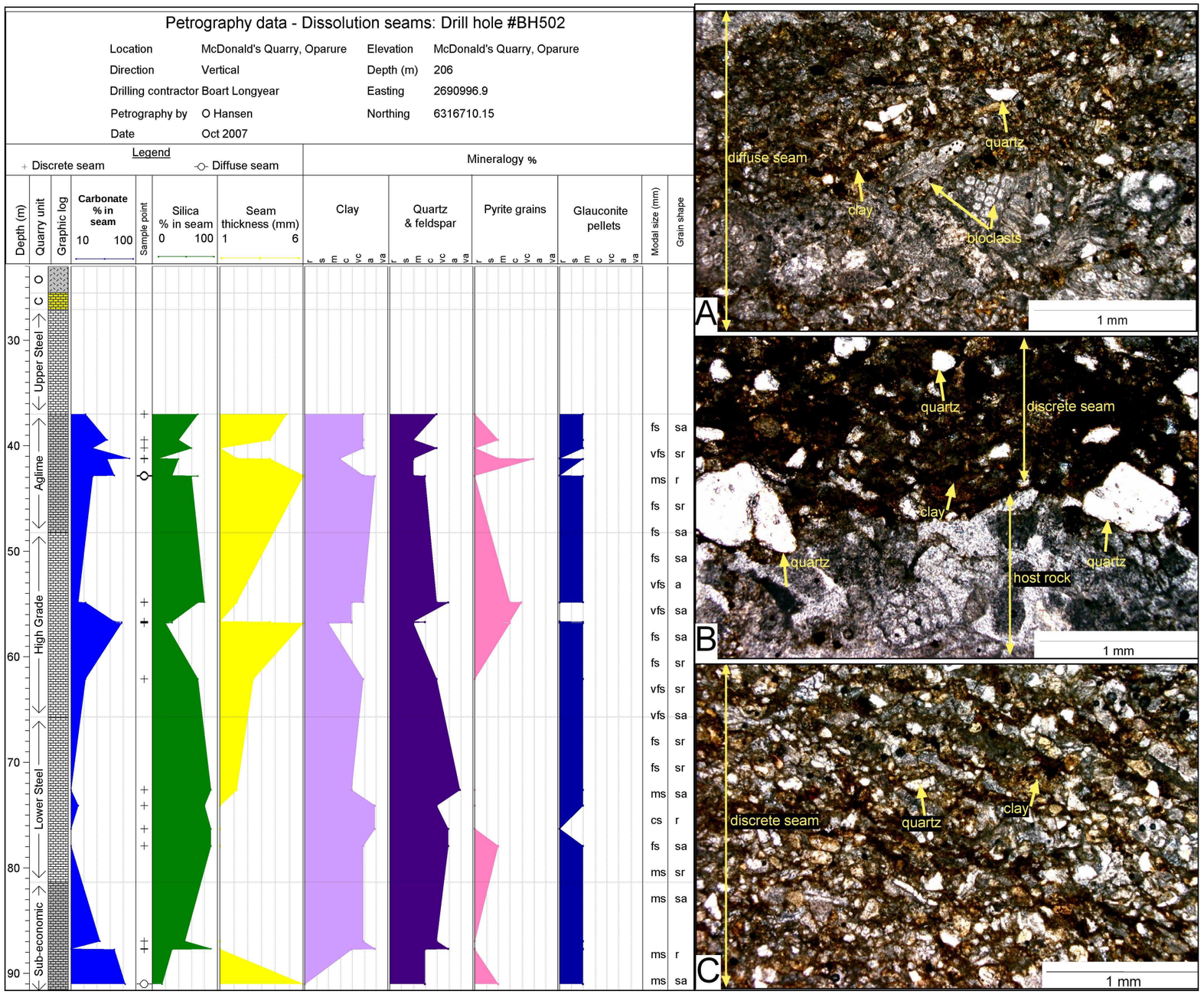

Figure 5.33 This figure summarises the petrographic data collected from thin section study of dissolution seams (i.e. discrete and diffuse seams) from the quarry limestones. The data are plotted against depth from top of drillhole. The graphic log shows the units in different shades of grey where units with higher silica are shown in a darker shade. The carbonate and silica percent are estimated and shown as the blue and green graphs on the left of the figure. Other information shown includes seam thickness: note that diffuse seams are much thicker than the discrete seams (thicker than thin section glass) so their thicknesses are not plotted. The other curves show the relative abundance of the main minerals identified in the seams. The following abbreviations are: r = rare (<1%), s = some (1-5%), m= many (5-15%), c = common (15-25%), vc = very common (25-50%), a = abundant (50-75%), and va = very abundant (>75%). The most common grain size that occurs in each seam is also noted (modal size column). The abbreviations are: vfs = very fine sand, fs = fine sand, ms = medium sand, and cs = coarse sand. Grain shape is also plotted next to this where the abbreviations are: a = angular, sa = subangular, sr = subrounded, and r = rounded. The photomicrographs on the far right of the figure show examples of seams: (A) An Aglime (field sample no. 13.2, BH502, 42.85 m depth) diffuse seam which contains clays, quartz, and bioclasts; (B) A Lower Steel (field sample no. 18,2, BH502, 77.9 m depth) discrete seam which contains large quartz grains and abundant clays. The surrounding host rock is shown at the bottom of the image; (C) An Aglime (field sample no. 32, BH502, 37 m depth) discrete seam containing abundant clay, quartz or feldspar, and calcite. The seam occupies the entire image. Grid coordinate system used is NZ map grid, and elevation is in metres above mean sea level.

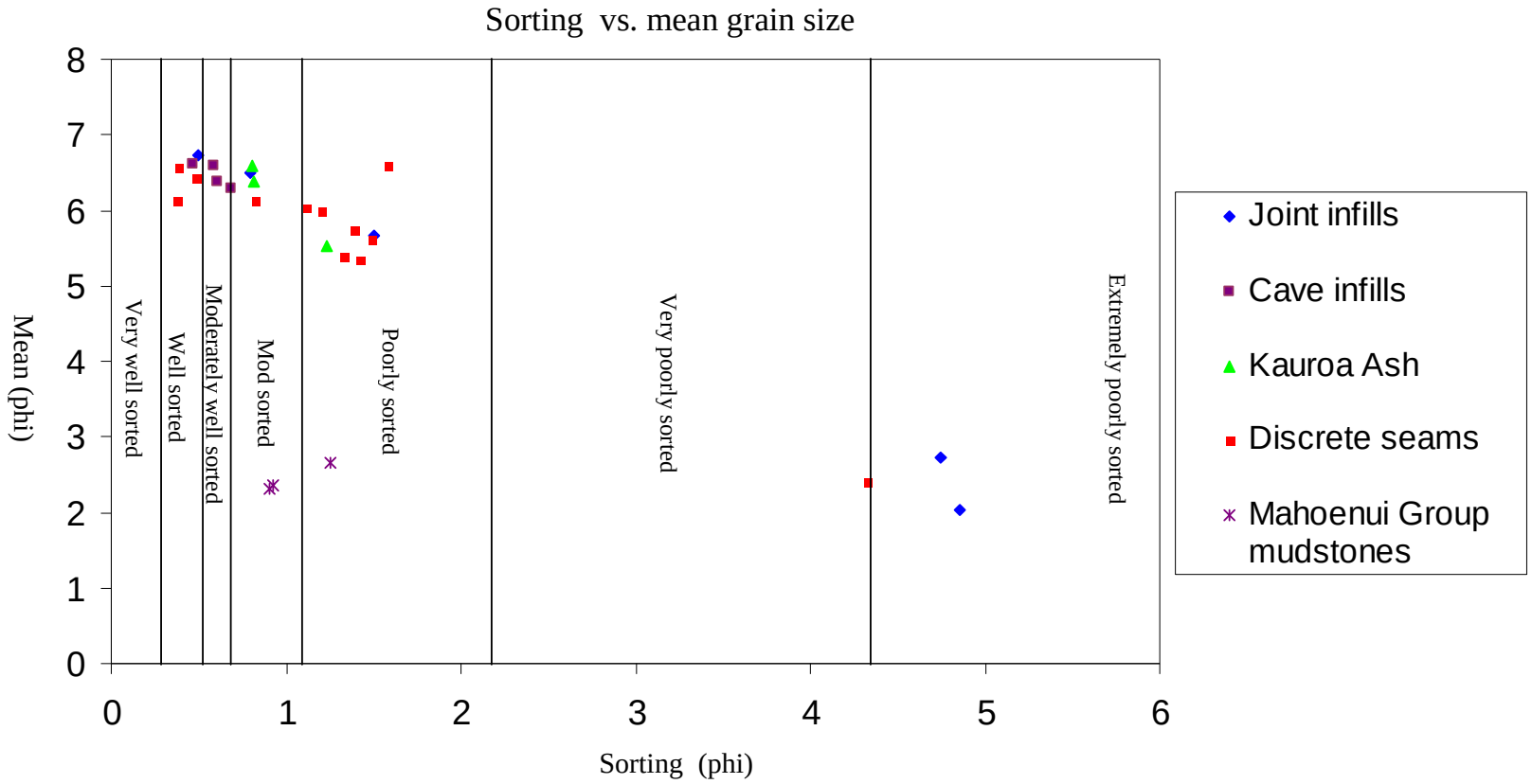

Figure 5.34 This chart shows mean grain size versus sorting characteristics for samples from discontinuity types including joint infills, cave infills, and discrete seams, and overburden units Kauroa Ash, and Mahoenui Group mudstones. Sorting classes have been subdivided according to phi values (based on Wentworth scale).

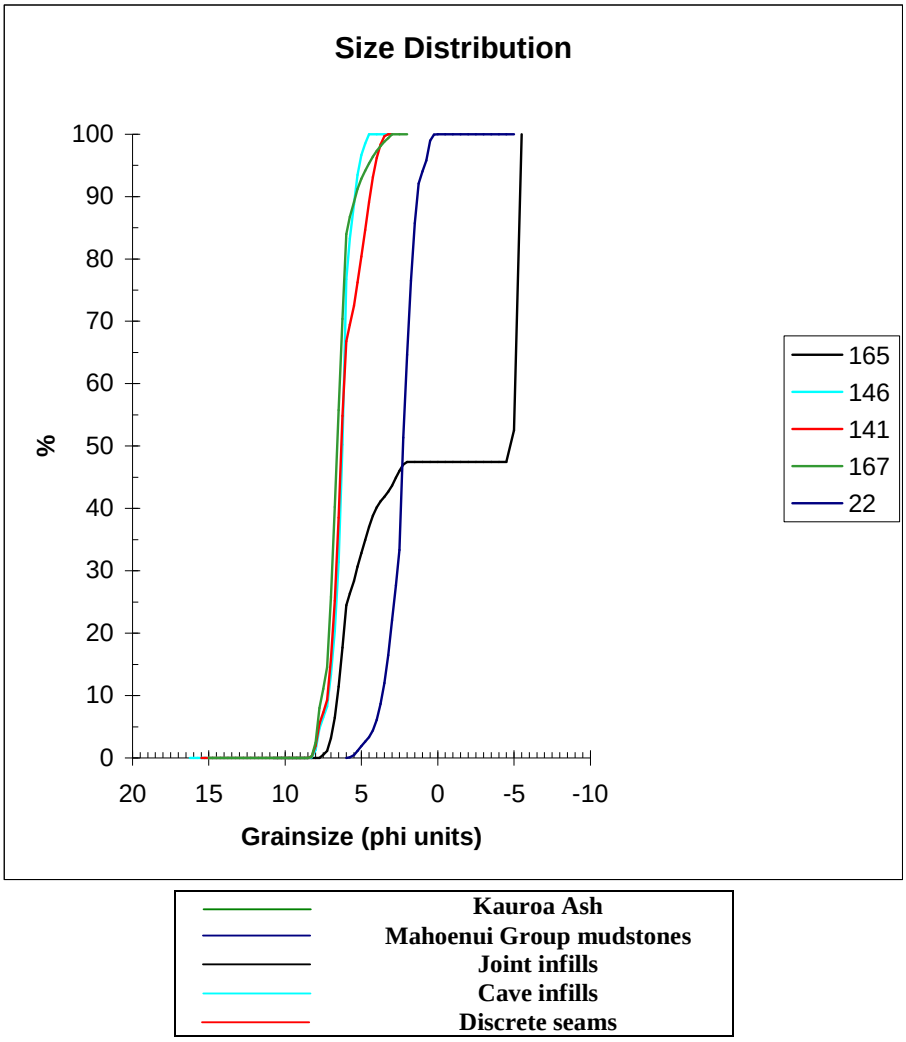

Figure 5.35 Cumulative graph showing combined texture (sieve and laser particle size) data including the grain size distribution of a representative sample from the Kauroa Ash, Mahoenui Group mudstone, a cave infill, joint infill, and discrete seam. The coloured lines next to the sample numbers shown on the right of the figure correspond to the sample type in the legend below. The Kauroa Ash shows a distribution of very fine sand (3 phi) through to fine silt (7 phi) grain sizes, cave infills: fine silt (7 phi) to medium silt (6 phi), and discrete seams: fine silt (7 phi) to coarse silt (4 phi). These all show a unimodal distribution, whereas the joint infills show bimodality and are characterised by clay (10 phi) through to pebble (-5 phi) sized grains.

It is unlikely that the composition of the fragments (e.g. Aglime versus Upper Steel limestone) will affect the overall bulk quality of the unit being processed as the contribution of these fragments to the underlying unit would be minor.

It is important to note that discrete seams are partially cemented to the limestones. Consequently, although crushing will increase the chance of 'shaking' off the seams, some silica may be left behind and remain cemented to the limestones.

CHAPTER SIX

Chemical composition

6.1 Introduction

On completion of the 500 drill hole series in 2005, each core was cut longitudinally in half and one half was sampled continuously over about 0.3-1.0 m intervals from the Kauroa Ash to the base of the Lower Steel limestone, and at 2.0 m intervals below this into the Aotea Formation or where there was a lithological change. These bulk samples were crushed to a powder and then analysed by SpectraChem Analytical for major and minor oxides using x-ray fluorescence (XRF). The complete data set are held by Holcim NZ Ltd.

Since the quarry limestones involve both host limestone rock plus any discontinuities (e.g. dissolution seams and joints; Chapter 3, Sections 3.1.2, and 3.1.4) as shown in this study, it is highly relevant to distinguish between the chemical compositions of the limestones versus the materials found in the discontinuities, compositions otherwise masked by the continuous bulk sample analyses. Such an approach can highlight any differences in chemical composition between the limestones constructing the different quarry units as well as between the various siliceous materials found in the discontinuities that also characterise these units.

This chapter initially presents the results of carbonate content analyses from acid titration of a range of sample types, including overburden at the quarry (i.e. Kauroa Ash, Mahoenui Group mudstones), the quarry limestones themselves, and the associated discontinuity materials. A representative selection of these samples (60 in total) was then sent to SpectraChem Analytical to determine their major (CaO, loss on ignition (LOI), SiO_2, Al_2O_3, Fe_2O_3) and minor oxide (MgO, Na_2O, MnO, TiO_2, K_2O, SO_3, P_2O_5) composition using the same XRF procedure originally employed for the continuous core analyses. LOI is the measure of moisture or impurities lost when a sample is ignited. Carbonate samples are

heated to 1000°C to expel volatiles such as H_2O and CO_2, the weight% of the sample before and after ignition being determined.

6.2 Acid titration determination of carbonate content

Results from an earlier chapter (e.g. Chapter 3, Section 3.1) show that silica is concentrated in discontinuities. Since the mineralogy and nature of the discontinuity materials have been described (Chapter 5, Section 5.4), it is important to determine their chemical composition so as to ascertain if any carbonate ($CaCO_3$) is present in the discontinuities and to compare this $CaCO_3$ value with that of the host limestone. Macroscopic observations show that carbonate is certainly associated with some of these discontinuity features, such as dissolution seams which are mainly diagenetically inherited from the limestone.

Acid titration was carried out to determine the carbonate content of 64 samples (Table 6.1). Samples were oven dried at 110°C over night and ground to a fine powder using a tungsten carbide ringmill. The powders were then back titrated using an autotitrater using the procedures outlined in Appendix F-6.1. The treatment of errors is outlined in Appendix F-6.2. The total percentage error was calculated for each sample and ranged from 2.86-2.95% across the 74 samples titrated.

6.3 Results of carbonate analyses

6.3.1 Quarry limestone units

The raw analytical data for each sample (from outcrop and/or drill core) that was titrated and its associated $CaCO_3$ content are given in Appendix Table F-6.3. These data are summarised in Table 6.1. Samples analysed include the six quarry limestone units (i.e. Caprock, Upper Steel, Aglime, High Grade, Lower Steel, Sub-economic), two overburden units (i.e. Kauroa Ash and Mahoenui Group mudstones), and six materials associated with their corresponding discontinuity types (i.e. joint infills, palygorskite, cave infills, discrete seams, and diffuse seams).

Table 6.1 Results from acid titration carbonate content analyses. This table shows the sample numbers and corresponding units, %$CaCO_3$, and an average %$CaCO_3$ calculated from all samples in each unit. * = discrete seam that contains $CaCO_3$ leached sandy material.

Field numbers and standards	Quarry unit/sample type	%$CaCO_3$	Average $CaCO_3$
126	Mahoenui Group	35.6	
127	Mahoenui Group	34.7	35.1
9	Caprock	92.2	
27B	Caprock	93.1	
21	Caprock	86.9	
27	Caprock	83.4	
136	Caprock	96.8	
26	Caprock	93.3	
hq3a	Caprock	74.1	
hq3b	Caprock	96.2	89.5
121	Upper Steel	97.3	
123	Upper Steel	98.0	
135	Upper Steel	98.3	
31A	Upper Steel	98.8	
29	Upper Steel	98.9	
28	Upper Steel	98.0	98.2
36	Aglime	95.4	
37	Aglime	94.6	
35	Aglime	94.8	
124	Aglime	94.5	
151	Aglime	94.7	
125	Aglime	93.0	94.5
13	Diffuse seam	84.1	
34	Diffuse seam	87.4	
61	Diffuse seam	84.6	85.4
42	High Grade	97.9	
39	High Grade	99.5	
41	High Grade	95.6	
111	High Grade	95.3	
156	High Grade	96.1	
128	High Grade	98.7	97.2
112	Lower Steel	98.7	
153	Lower Steel	97.1	
46	Lower Steel	97.6	
52	Lower Steel	96.9	
48	Lower Steel	96.3	97.3
58	Sub-economic	94.9	
56	Sub-economic	94.5	
60	Sub-economic	95.6	95.0
40% calcite run A	Standard	37.0	
60% calcite run A	Standard	54.7	
80% calcite run A	Standard	79.8	
100% calcite run A	Standard	97.0	
100% quartz run A	Standard	-2.2	
147	Discrete seam	20.8	
159	Discrete seam	30.1	
138	Discrete seam	26.8	
130	Discrete seam	24.2	
110	Discrete seam	43.9	
145	Discrete seam	47.1	
117	Discrete seam	27.6	
141	Discrete seam	56.7	
148	Discrete seam	62.1	37.7
155	Surface accumulation	73.3	
150	Surface accumulation	68.7	71.0
107	Joint infill (type 1)	7.3	
116	Joint infill (type 1)	94.6	
119	Joint infill (type 1)	84.3	
114	Joint infill (type 1)	5.8	

Table 6.1 continued.

Field numbers and standards	Quarry unit/sample type	%$CaCO_3$	Average $CaCO_3$
144	Joint infill (type 1)	78.5	
102	Joint infill (type 1)	72.7	
105	Joint infill (type 1)	95.9	62.7
143	Cave infill	0.3	
154	Cave infill	10.7	
146	Cave infill	-2.7	2.7
140	Palygorskite (type 2)	68.8	
100/101	Palygorskite (type 2)	65.1	67.0
100% calcite run B	Standard	98.7	
60% calcite run B	Standard	59.1	
80% calcite run B	Standard	78.8	
100% quartz A	Standard	-9.1	
100% calcite B	Standard	81.5	
80% calcite C	Standard	76.6	
167	Kauroa Ash	-5.0	
71	Kauroa Ash	-2.9	
72	Kauroa Ash	-3.3	0.0

Surface accumulations are also analysed that are sample scrapings sampled from quarry faces that include accumulated quarry dust and material washed down from the above roads in the quarry. For convenience, these are graphed together with discontinuity types. Standards were also run to compare results.

Table 6.2 shows the range and average content of $CaCO_3$ for the different quarry limestone units.

Table 6.2 Acid titration carbonate analyses summary results for quarry limestones showing range and mean %$CaCO_3$.

Quarry limestone units	Number of samples	%$CaCO_3$ range	%$CaCO_3$ mean
Caprock	8	74.1-96.8	89.5
Upper Steel	6	97.3-98.9	98.2
Aglime	6	90.5-95.4	94.5
High Grade	6	95.3-99.5	97.2
Lower Steel	5	96.3-98.7	97.3
Sub-economic	3	94.5-95.6	95

Additionally, in Figure 6.1 the average values for $CaCO_3$ in the six limestone units are portrayed alongside one another using bar plots. The Upper Steel limestone has the highest $CaCO_3$ content (av. 98.2%) followed by the Lower Steel and High Grade units which have similar values (av. 97.3% and 97.2%, respectively). The Sub-economic limestone unit (av. 95%) has a similar $CaCO_3$

content to the Aglime unit (av. 94.5%), and the Caprock (av. 89.5%) has the lowest carbonate content of all the quarry limestone units.

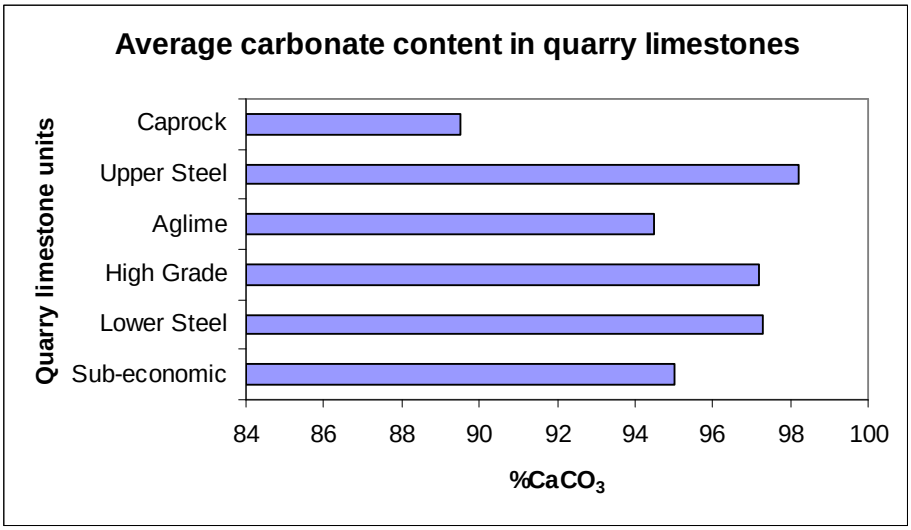

Figure 6.1 Bar plot showing acid titration results for the average $CaCO_3$ content of the host rock from the quarry limestones.

6.3.2 Contrasting host limestone and discrete seams

As a short experiment, a slab of core sampled from the Aglime with three discrete seams was divided into 1 cm blocks and, together with each seam, these were analysed for $CaCO_3$ content (total of 15 samples) (Figure 6.2). The host limestone blocks gave $CaCO_3$ contents from 91-93%, while the discrete seams yielded values from 16-29% (Table 6.3). These results are also presented as bar plots (Figure 6.2). The results emphasise the potential carbonate disparity between host limestones and their contained discontinuity features.

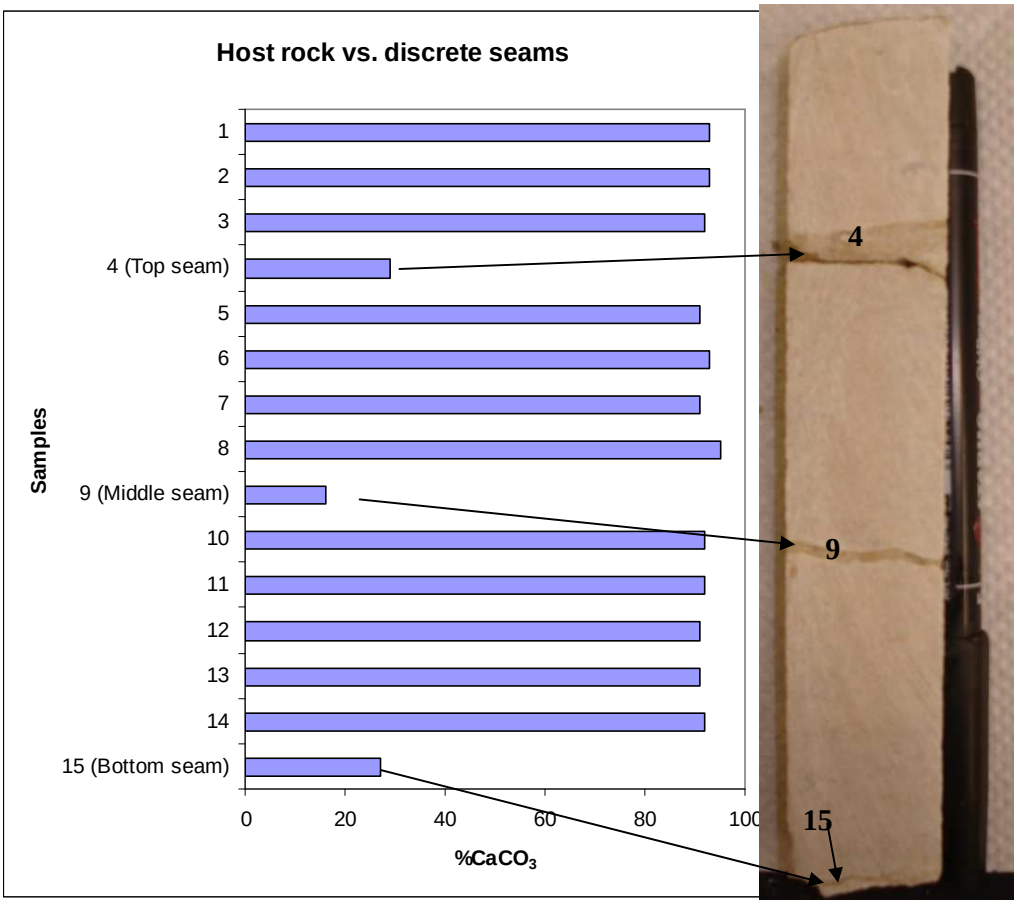

Figure 6.2 Bar plot (left) showing acid titration results for the $CaCO_3$ content of 15 samples consisting of 12 x 1 cm blocks of host rock and 3 discrete seams sampled from a slab of core taken from the Aglime, sample 35, BH502, 39 m depth. The photo on the right is the slab of core and shows the discrete seams labeled with their recorded sample numbers.

Table 6.3 Results from acid titration analyses from samples taken from a core slab of Aglime that included three discrete seams and surrounding host rock divided into 1 cm blocks (see Figure 6.2). % $CaCO_3$ (right side) shows that the discrete seams have a much lower content than the host rock samples.

Sample number	Sample type	% $CaCO_3$
1	Host	93
2	Host	93
3	Host	92
4 (Top seam)	Discrete seam	29
5	Host	91
6	Host	93
7	Host	91
8	Host	95
9 (Middle seam)	Discrete seam	16
10	Host	92
11	Host	92
12	Host	91
13	Host	91
14	Host	92
15 (Bottom seam)	Discrete seam	27

6.3.3 Overburden units and discontinuity materials

Table 6.4 shows results from $CaCO_3$ analyses for the overburden units and discontinuity materials. Note that there are two joint infill types namely type (1): joint infills, that are clay rich and contain limestone fragments typically washed down into the joint; and type (2): palygorskite, also clay but forms as a precipitate on the joint surface. The $CaCO_3$ content of the overburden units and discontinuity materials is much lower than the quarry limestones. From highest to lowest av. $CaCO_3$ content the order is: diffuse seams 85.4%, joint infill (type 1) 62.7%, surface accumulation 71%, palygorskite (type 2) 67%, discrete seams 37.78%, Mahoenui Group mudstones 35.1%, cave infill 2.7%, and Kauroa Ash 0% (Figure 6.3).

Table 6.4 Acid titration carbonate analyses summary results for overburden units and discontinuity types showing range and mean %$CaCO_3$.

Discontinuity types and overburden units	Number of samples	%$CaCO_3$ range	%$CaCO_3$ mean
Kauroa Ash	3	0	0
Mahoenui Group	2	34.7-35.6	35.1
Discrete seams	9	16-62.1	37.7
Diffuse seams	3	84.1-87.4	85.4
Joint infills (type 1)	7	5.8-95.9	62.7
Palygorskite (type 2)	2	65.1-68.8	67
Cave infills	3	0-10.7	2.7
Surface accumulations	2	68.7-73.3	71

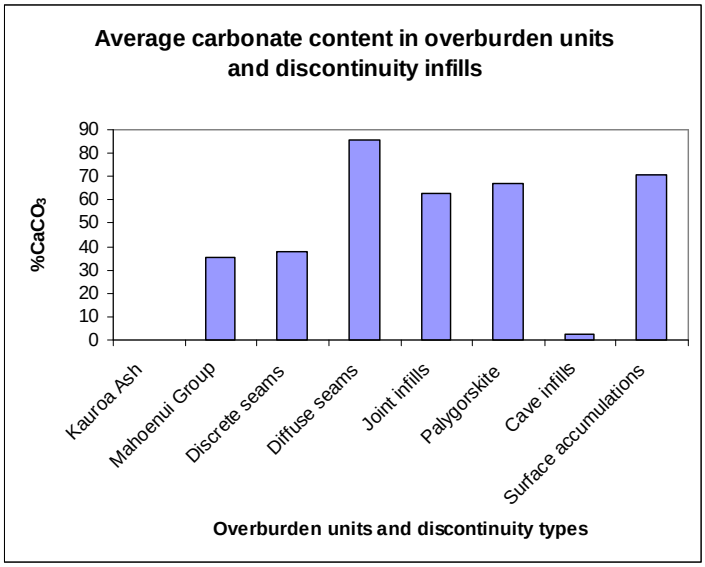

Figure 6.3 Bar plot showing acid titration results for the average $CaCO_3$ content of the host rock from the quarry limestones.

6.4 XRF determination of elemental composition

McDonald's Lime have their limestone samples analysed for major oxides by SpectraChem using specialised software calibrated specifically for the quarry limestone units at McDonald's Oparure Lime Quarry. For this thesis study 60 samples carefully chosen to represent the various lithologies at the quarry, were also analysed by SpectraChem using the same XRF method. In addition to these 60, 3 Kauroa Ash samples were chosen from McDonald's XRF data set from BH502 to include in the results. Samples were oven dried (at approximately 70°C), crushed, and powdered using a tungsten carbide ring mill, and sent to the SpectraChem laboratory in Wellington. Here, the samples were further prepared for XRF by heating to 110°C prior to analysis. The analytical procedures are documented in Appendix F-6.4, and a report (produced by SpectraChem) on the raw elemental data presented in Appendix F-6.5.

After reviewing the XRF report the samples were grouped into the different quarry limestone units, overburden units, and discontinuity infill types (Appendix Table F-6.6). Due to the nature of the data, oxides were divided into major (e.g. Fe_2O_3, CaO, SiO_2, Al_2O_3) and minor (e.g. MgO, Na_2O, MnO, TiO_2, K_20, SO_3, P_2O_5) oxides. Since McDonald's Lime lists loss on ignition (LOI) together with major oxides, LOI has been graphed together with major oxides for this study. For presentation, the oxide values have been averaged for each quarry limestone unit, overburden unit, and discontinuity type, as shown Appendix Table F-6.7.

6.5 Major and minor oxide results for quarry limestone units

6.5.1 Caprock (Figures 6.4A and B)

Relatively high values of CaO (43.53-53.97%) and LOI occur in the Caprock (Figure 6.4A). A range of SiO_2 (1.73-12.09%) values occurs, the higher values being associated with samples taken near the contact with the overlying Mahoenui Group mudstones. Likewise, despite small amounts, the Fe_2O_3 and Al_2O_3 contents increase towards this contact.

In terms of the minor oxides, MgO is relatively high (0.5-1.24%), SO_3 is abnormally high in one sample taken from the upper contact with the overlying Mahoenui Group mudstones (possibly due to the presence of the mineral gypsum [$CaSO_4 2H_2O$), and the other elements remain consistently low in abundance (Figure 6.4B).

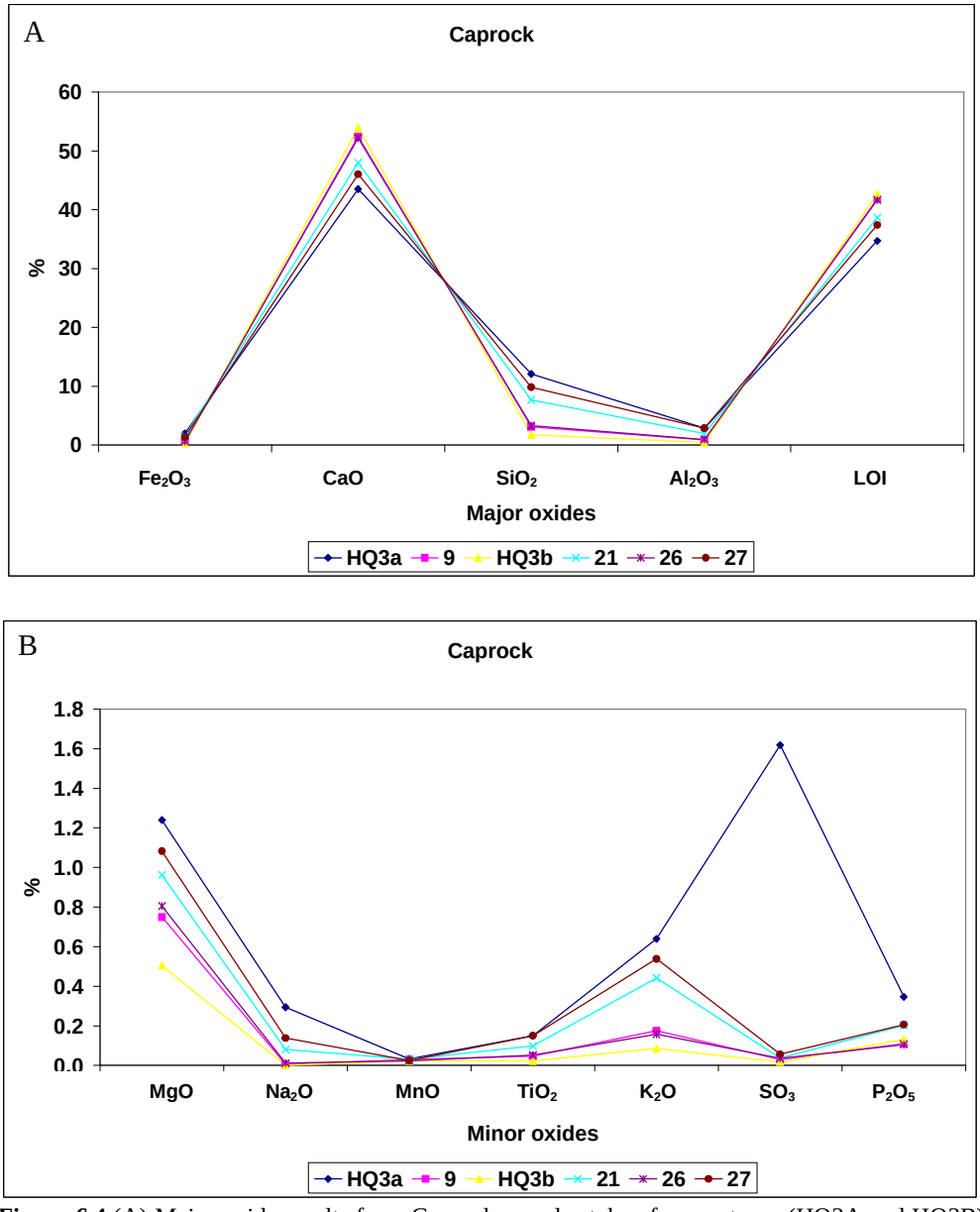

Figure 6.4 (A) Major oxide results from Caprock samples taken from outcrop (HQ3A and HQ3B) and drill hole BH502 (21, 26, and 27). (B) Minor oxide results from Caprock of the same samples in (A).

6.5.2 Upper Steel (Figures 6.5A and B)

Samples from the Upper Steel are dominated by high CaO (54.6-55.55%) and very low Fe_2O_3, SiO_2 (0.23-1.19 %), and Al_2O_3 content (Figure 6.5A).

MgO is variable across the Upper Steel samples (up to 0.4%), while the remaining minor oxides occur in low concentrations (<0.1%) (Figure 6.5B).

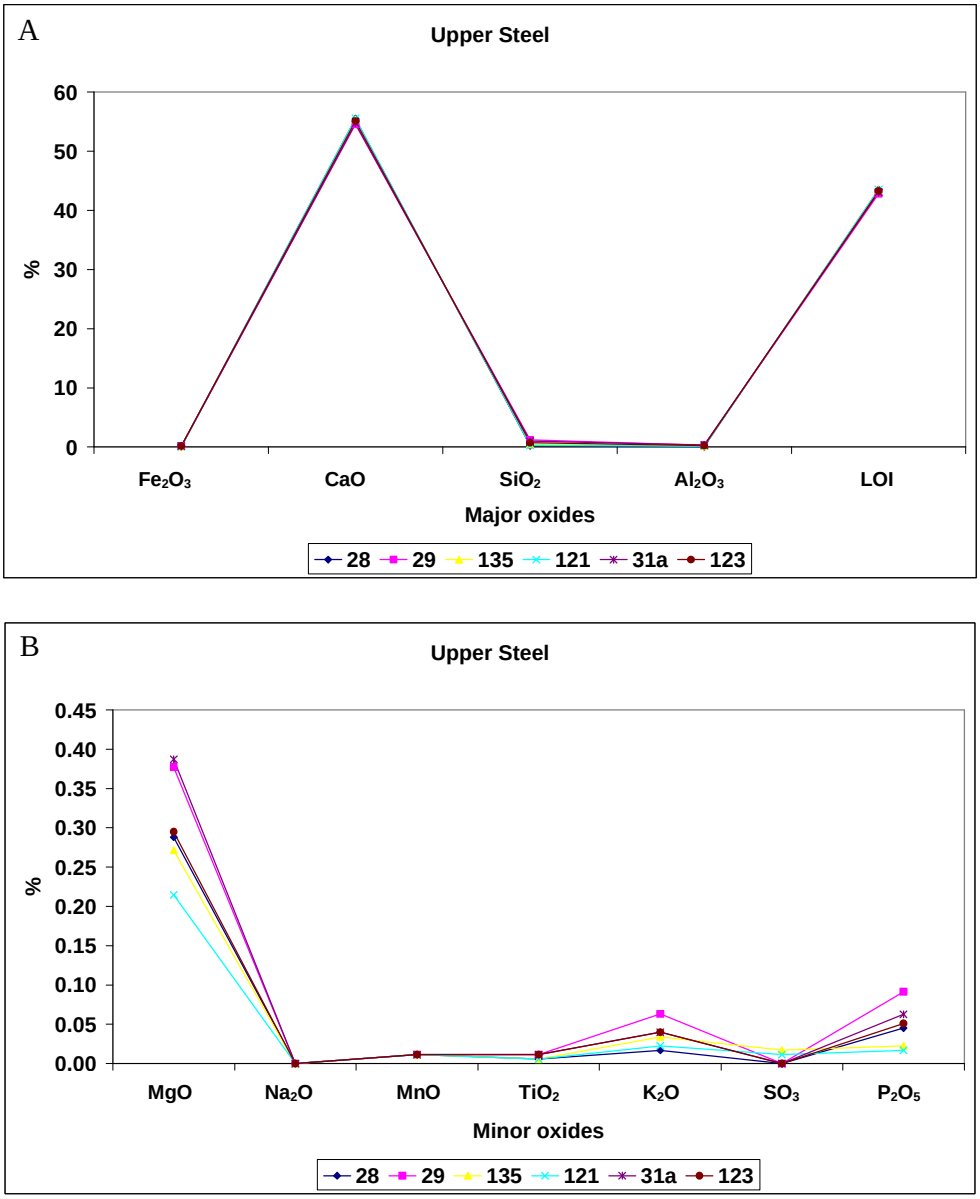

Figure 6.5 (A) Major oxide results from Upper Steel samples taken from outcrop (121, 123, and 135) and drill hole BH502 (28, 29, and 31a). (B) Minor oxide results from Upper Steel of the same samples in (A).

6.5.3 Aglime (Figures 6.6A and B)

CaO (51.57-53.44%) occurs in high concentrations whereas the other major oxides have low concentrations (<2%). The SiO_2 range is 2-3.51% (Figure 6.6A).

MgO (up to 1.1%) and SO_3 (up to 0.4%) are variable whereas the other minor oxides occur in lower, more similar concentrations (<0.2%) (Figure 6.6B).

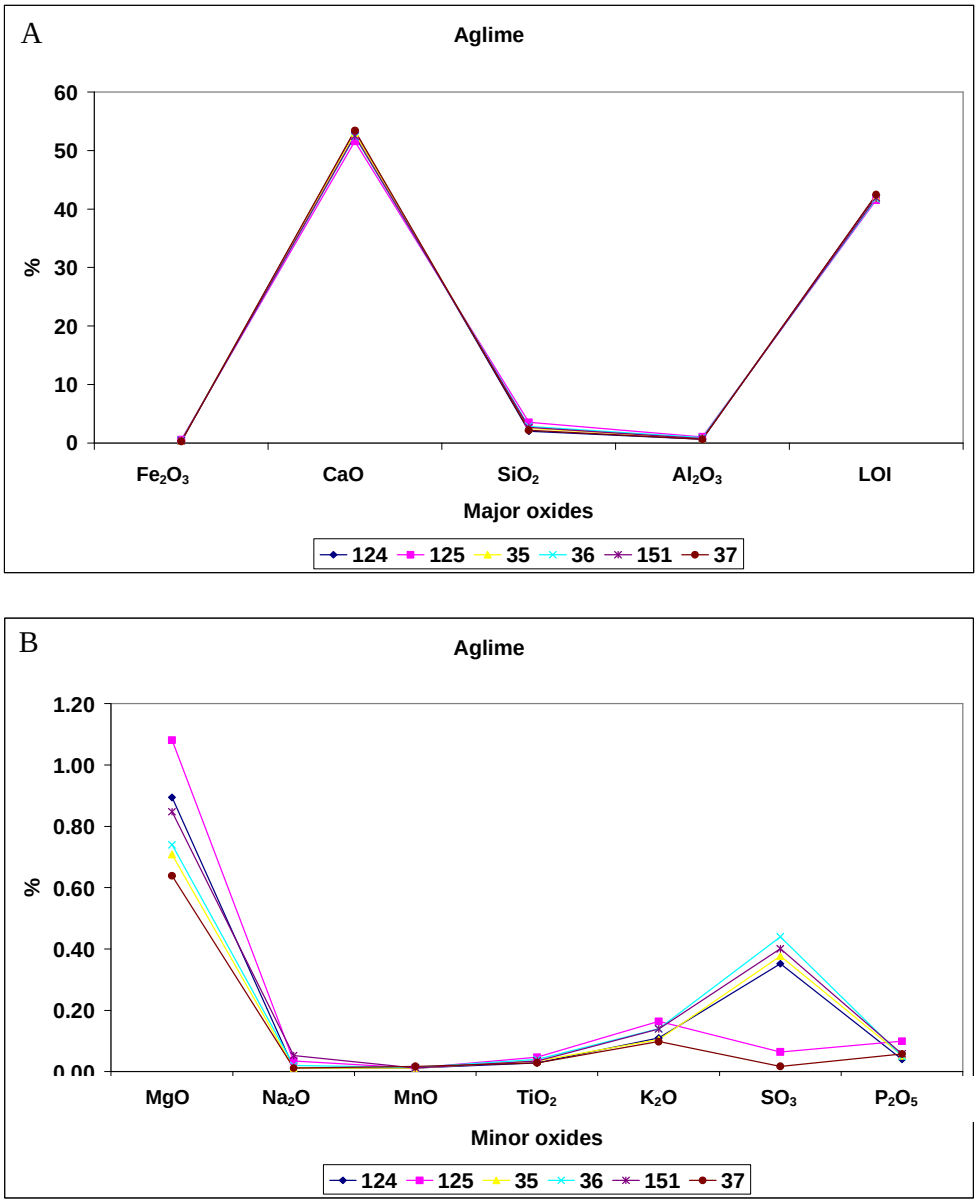

Figure 6.6 (A) Major oxide results from Aglime samples taken from outcrop (124, 125, and 151) and drill hole BH502 (35, 36, and 37). (B) Minor oxide results from Aglime of the same samples in (A).

6.5.4 High Grade (Figures 6.7A and B)

The major oxide content is dominated by CaO (53.37-54.78%) with low occurrences of Fe_2O_3, Al_2O_3, and SiO_2 (0.76-1.95%) (Figure 6.7A).

MgO (up to 0.9%) and SO_3 (up to 0.4%) contents are small but variable, while the other minor oxides occur in low, similar concentrations across the samples (<0.1%) (Figure 6.7B).

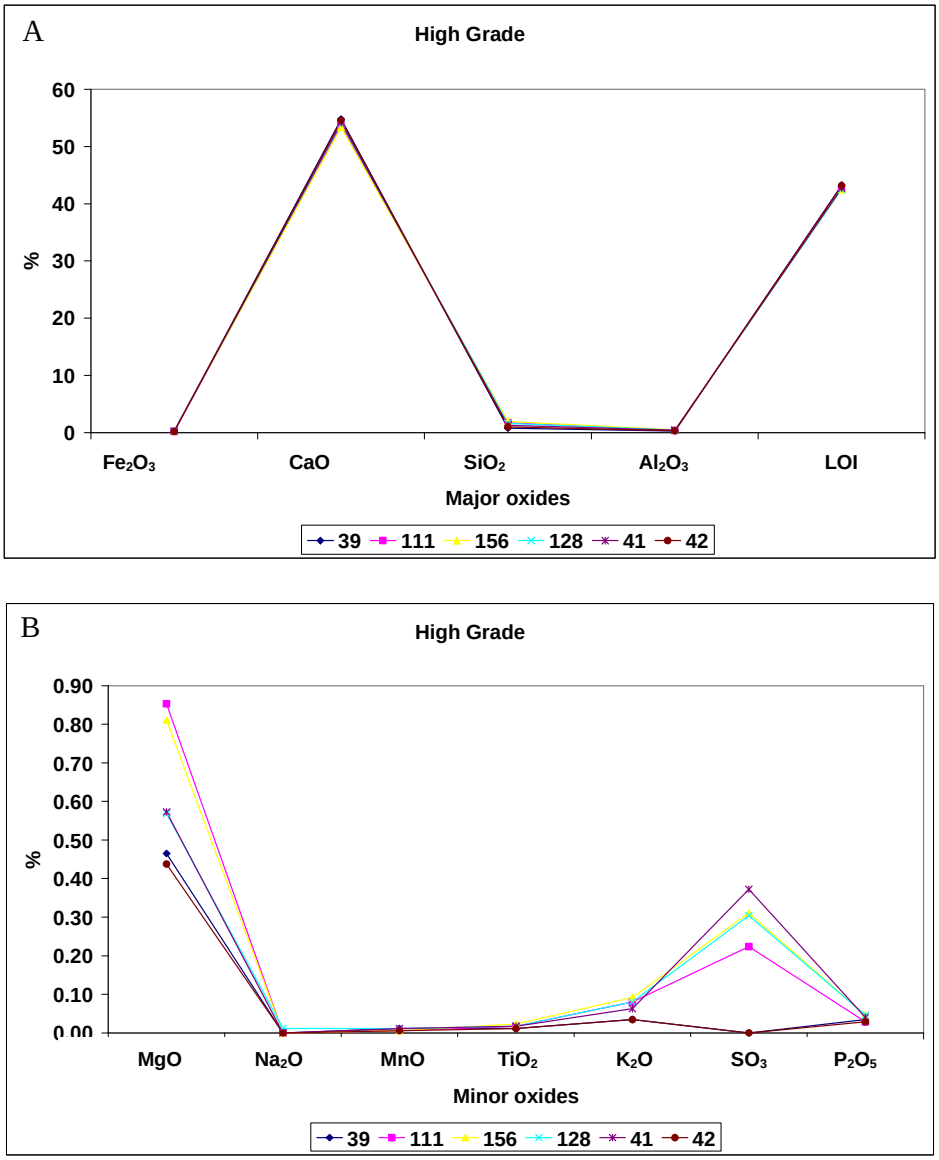

Figure 6.7 (A) Major oxide results from High Grade samples taken from outcrop (111, 128, and 156) and drill hole BH502 (39, 41, and 42). (B) Minor oxide results from High Grade of the same samples in (A).

6.5.5 Lower Steel (Figures 6.8A and B)

Samples from the Lower Steel are dominated by high CaO (54-55.12%) and very low Fe_2O_3, SiO_2 (0.71-1.59%), and Al_2O_3 content (Figure 6.8A).

MgO (up to 0.6%) is variable across the Lower Steel samples and the remaining minor oxides occur in low concentrations (0.15%) (Figure 6.8B).

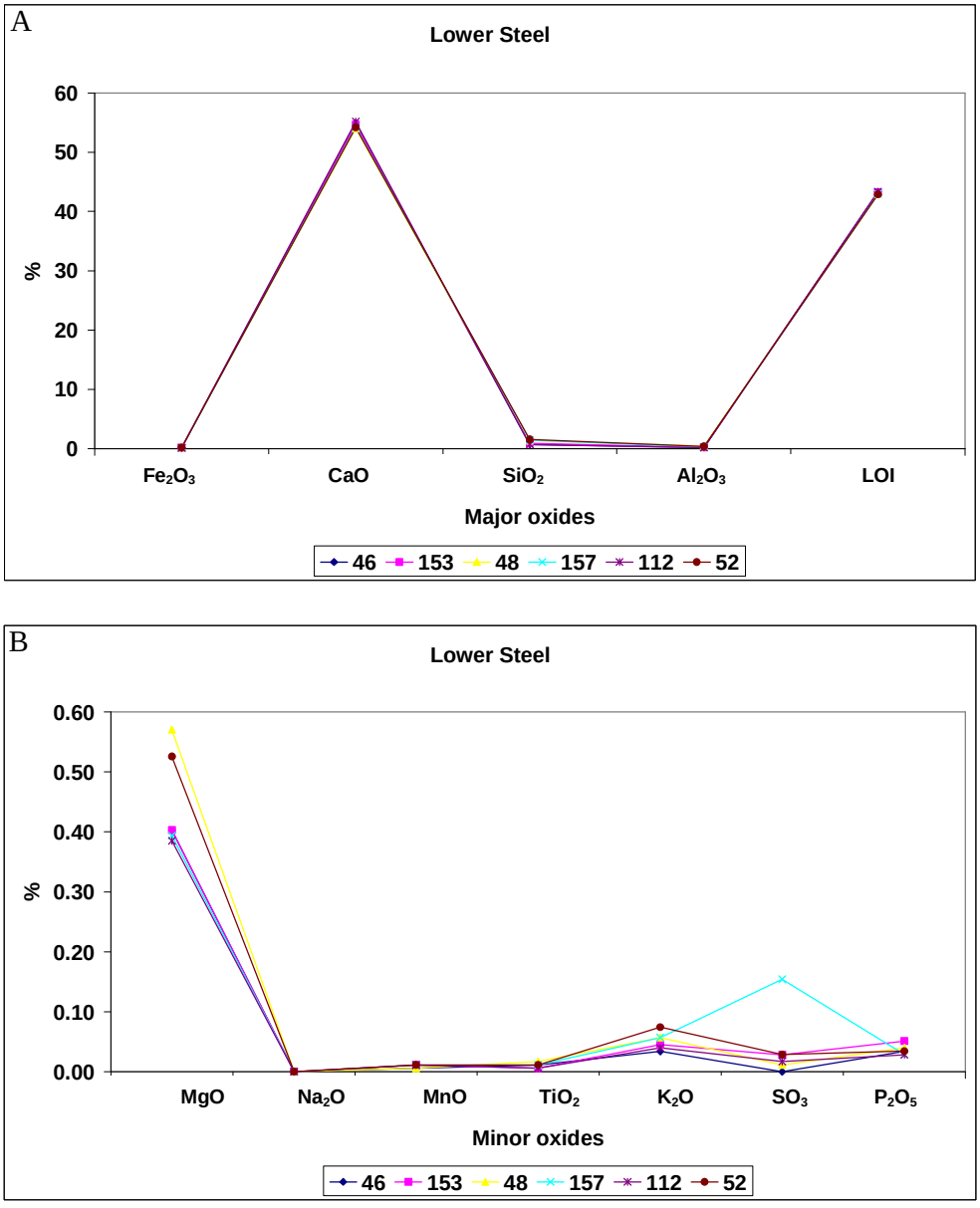

Figure 6.8 (A) Major oxide results from Lower Steel samples taken from outcrop (112, 153, and 157) and drill hole BH502 (46, 48, and 52). (B) Minor oxide results from Lower Steel of the same samples in (A).

6.5.6 Sub-economic (Figures 6.9A and B)

CaO (53.91-53.96%) is dominant in the Sub-economic limestones, while SiO_2 (1.45-2.23%) occurs in slightly lower concentrations than in the Aglime unit. The other major oxides occur in low concentrations (<2%) (Figure 6.9A).

MgO (up to 0.55%) is relatively high and K_2O and P_2O_5 slightly increased compared to the other minor oxides, which are relatively low (<0.01%) (Figure 6.9B).

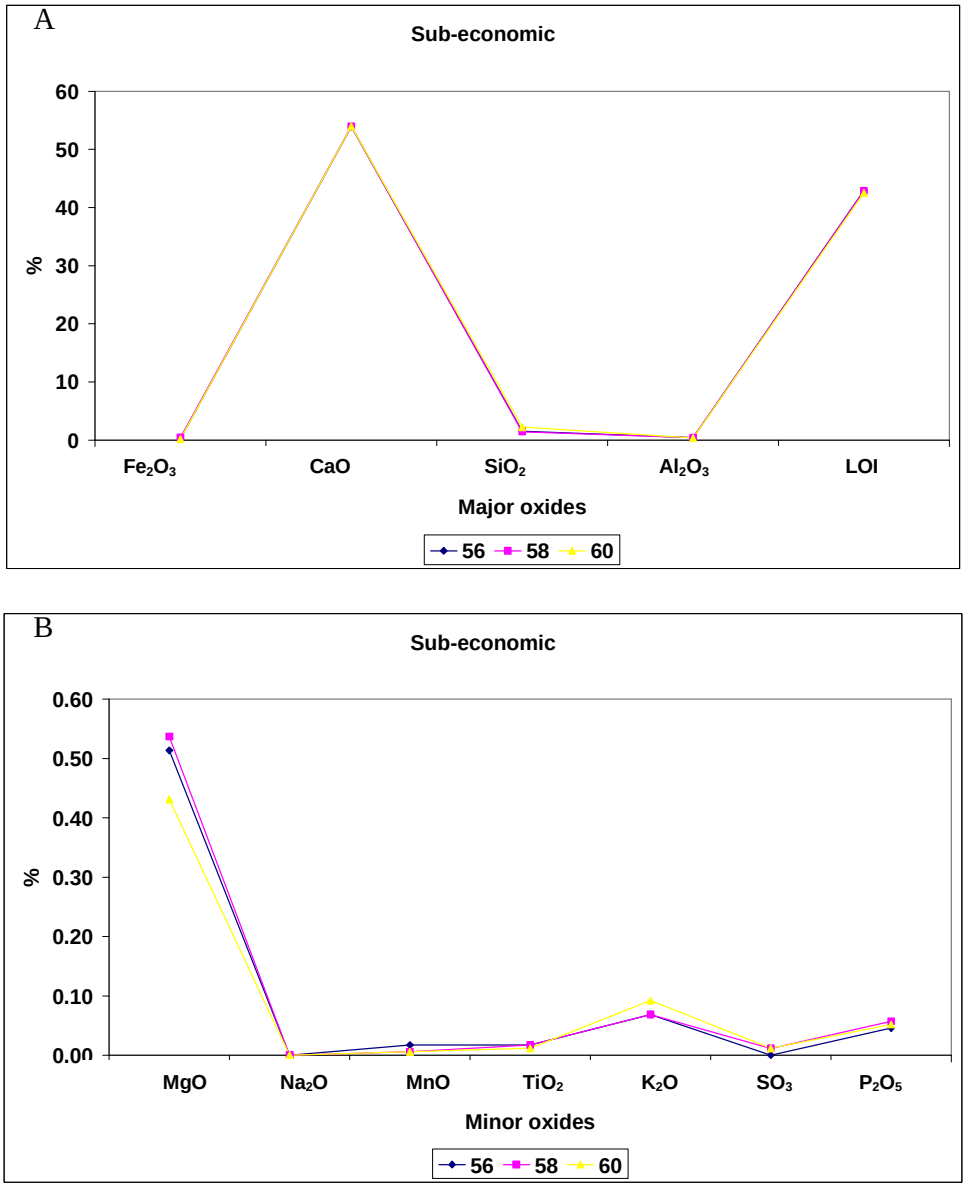

Figure 6.9 (A) Major oxide results from Sub-economic samples taken from drill hole BH502 (56, 58, and 60). (B) Minor oxide results from Sub-economic of the same samples in (A).

6.5.7 Contrasting bulk samples and host limestone

The following account compares major and minor oxide results for (1) bulk samples (includes discontinuities); (2) host limestone samples; and (3) discrete samples. Diffuse seams are not included in the comparison as they are generally rare in the quarry limestone units except the Aglime, and there were only several samples taken. The bulk analyses are taken from McDonald's Quarry XRF data set (2005) held by Holcim. An average value (for each oxide) has been calculated for each unit from a number of samples (i.e. 1 from Caprock sample, 10 from Upper Steel, 10 from Aglime, 18 from High Grade, 16 from Lower Steel, and 29 from Sub-economic). These bulk samples include a mixture of the limestone host rock and discrete and diffuse seams (discontinuities). The host rock and discrete seam analyses are taken from this study (given in Appendix F-6.7). The discrete seams (9 samples in total) are further divided into the units they were sampled from and an average (from ~2 discrete seams for each unit) has been calculated. The raw data are given in Appendix Tables F-6.8. Figures 6.10-6.12 show a series of bar plots for the three sample types side by side against each major oxide. Note that discrete seam samples were not collected in the Caprock because the unit was dangerous to access, and the Sub-economic unit because it is not exposed in the quarry at present.

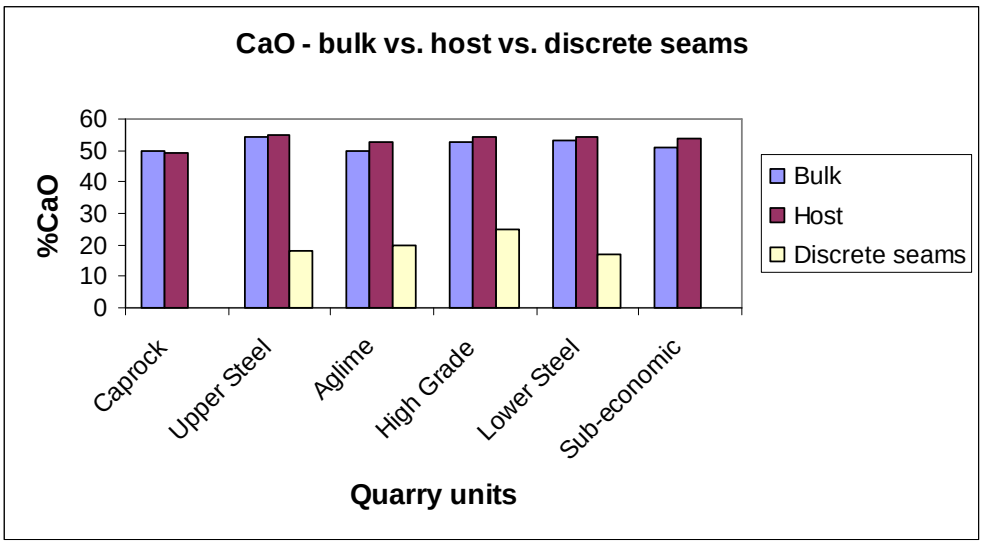

Figure 6.10 XRF results comparing the average CaO content from bulk analyses used from McDonald's Quarry drill hole BH502 data set, host limestone, and discrete seam analyses from this study.

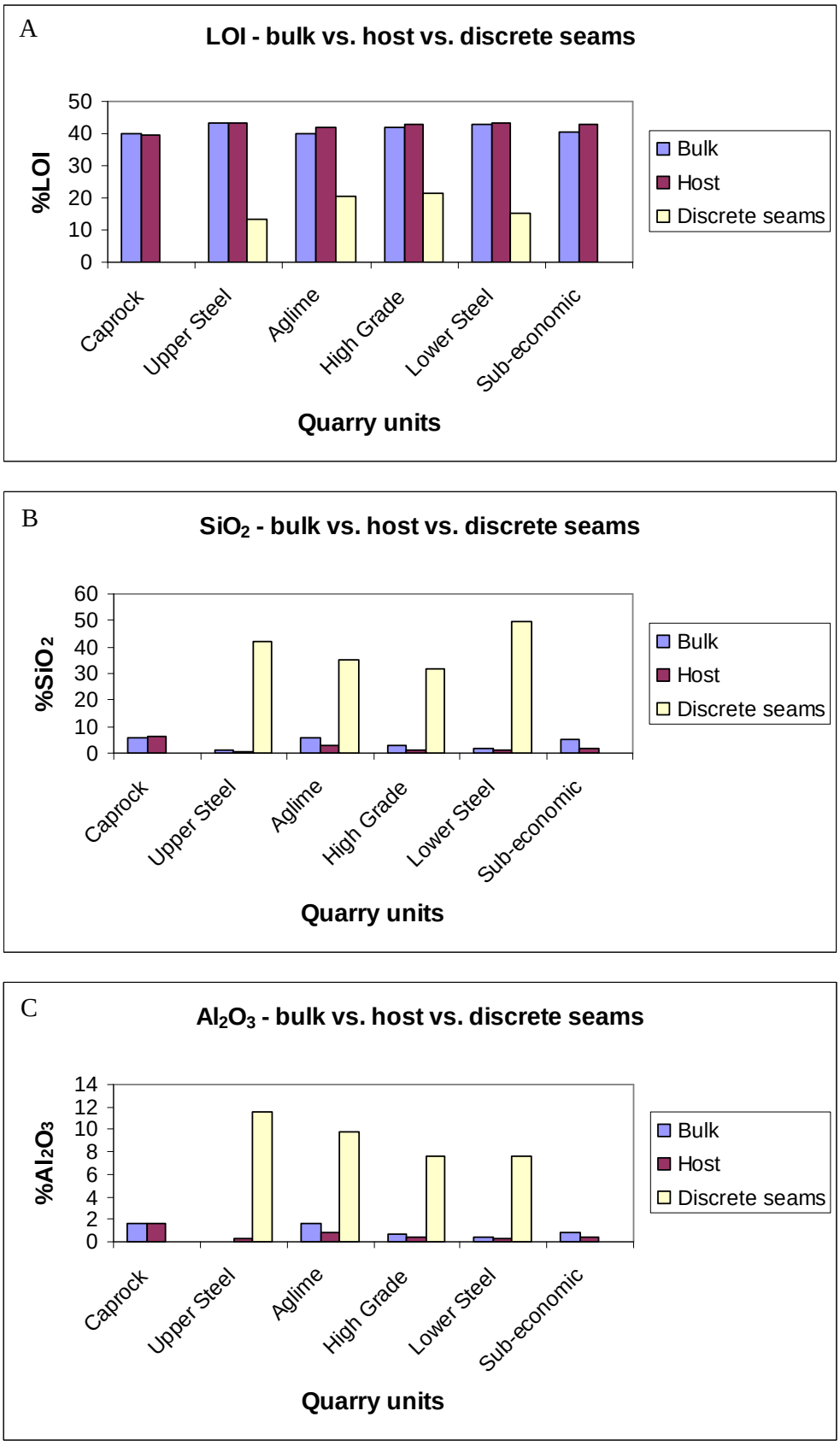

Figure 6.11 XRF results comparing the average (A) LOI, (B) SiO_2, and (C) Al_2O_3 content from bulk analyses used from McDonald's Quarry drill hole BH502 data set, host limestone, and discrete seam analyses from this study.

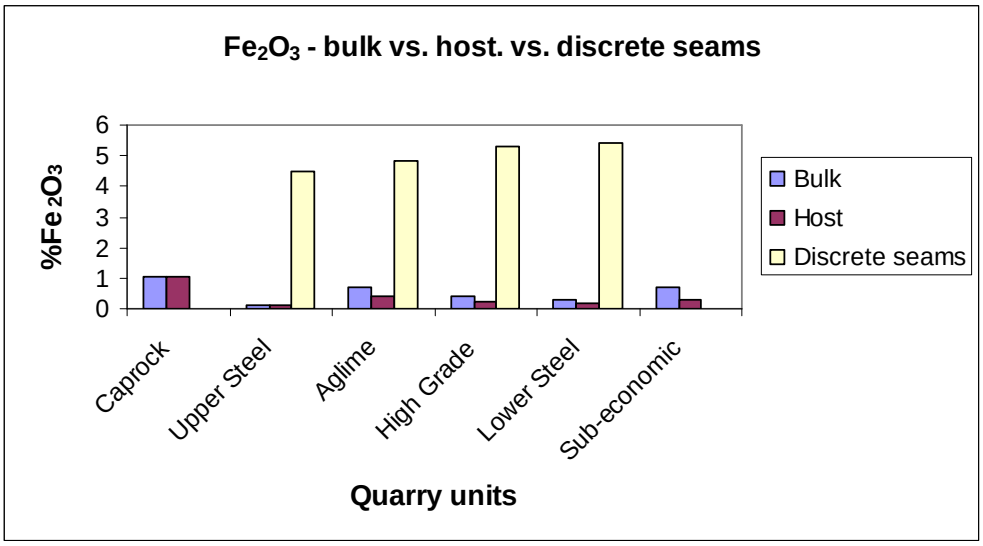

Figure 6.12 XRF results comparing the average Fe_2O_3 content from bulk analyses used from McDonald's Quarry drill hole BH502 data set, host limestone, and discrete seam analyses from this study.

CaO is higher in the host rock samples compared to the bulk samples for all the limestones except the Caprock (because it is argillaceous), and it is also considerably lower in the discrete seams (Figure 6.10). LOI mirrors the trends seen in CaO (Figure 6.11A). SiO_2, Al_2O_3, and Fe_2O_3 show similar trends where content is higher in bulk samples compared to host limestone samples. SiO_2 in discrete seams is extremely high (up to 50%) compared to the other oxides (typically <15%). The content in discrete seams for these oxides is significantly higher (Figures 6.11B and C, and 6.12). Figures 6.13-6.15 show a series of bar plots showing the three sample types side by side against each minor oxide.

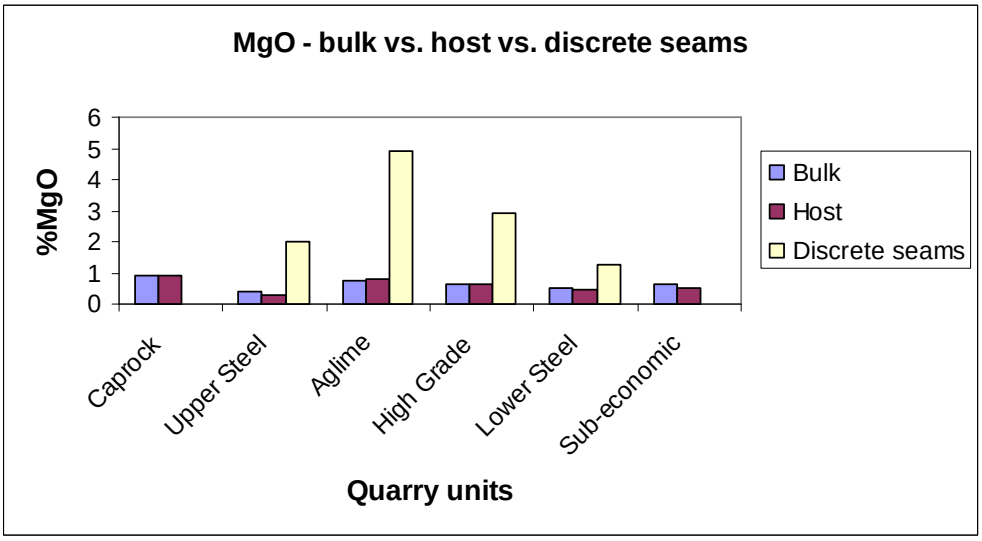

Figure 6.13 XRF results comparing the average MgO content from bulk analyses used from McDonald's Quarry drill hole BH502 data set, host limestone, and discrete seam analyses from this study.

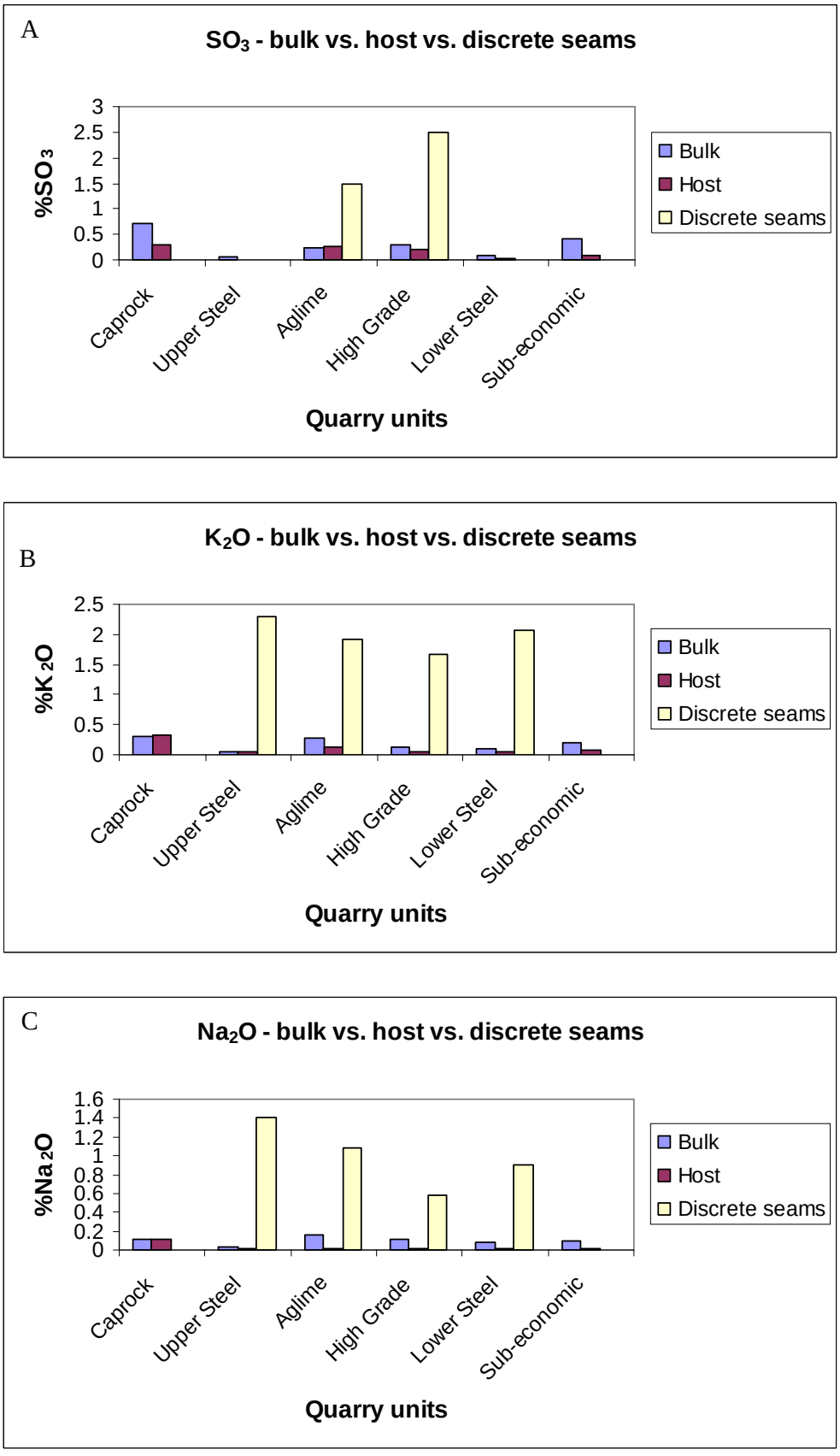

Figure 6.14 XRF results comparing the average (A) SO_3, (B) K_2O, and (C) Na_2O content from bulk analyses used from McDonald's Quarry drill hole BH502 data set, host limestone, and discrete seam analyses from this study.

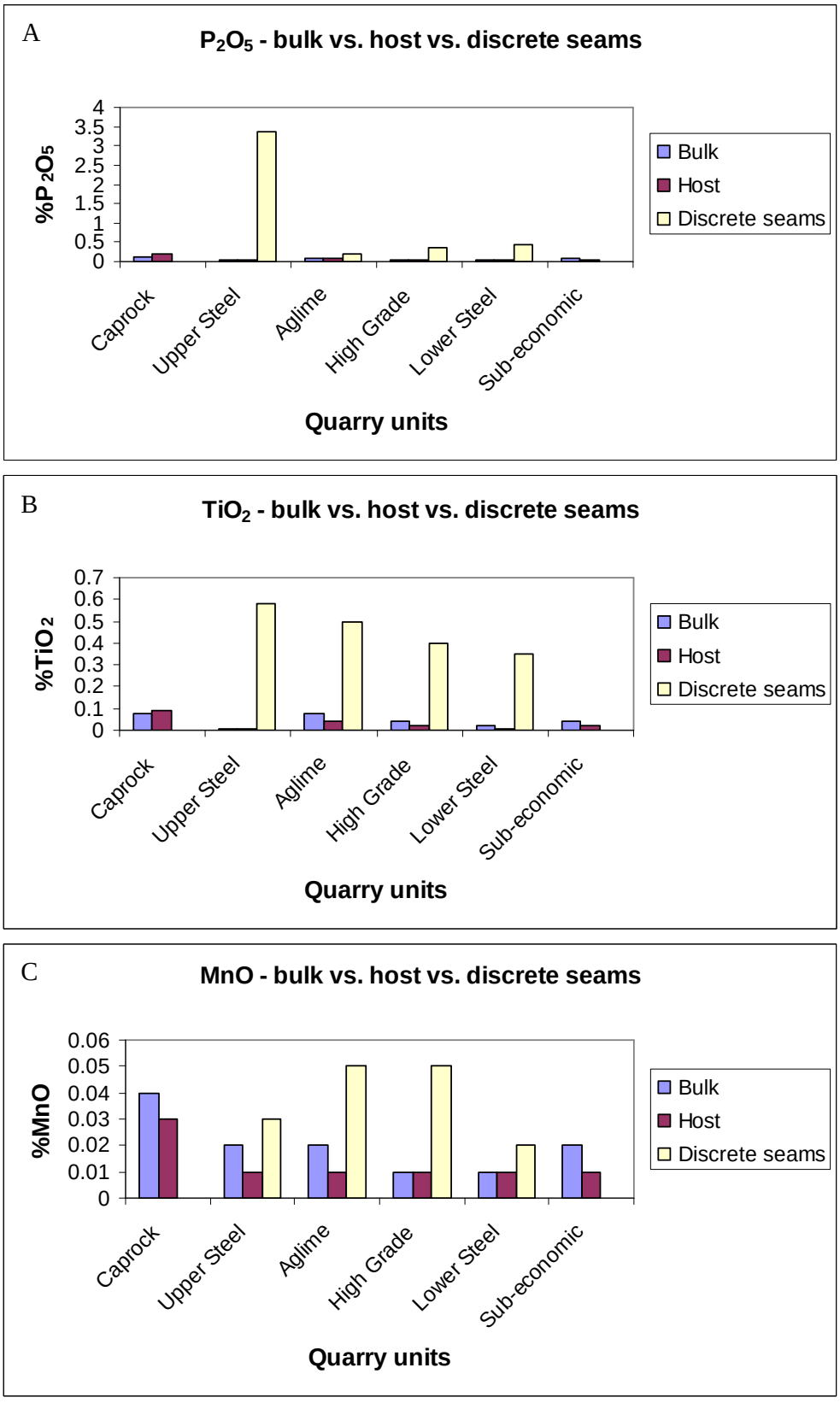

Figure 6.15 XRF results comparing the average (A) P_2O_5, (B) TiO_2, and (C) MnO content from bulk analyses used from McDonald's Quarry drill hole BH502 data set, host limestone, and discrete seam analyses from this study.

MgO shows different trends amongst the limestones; for example Caprock, Upper Steel, Lower Steel, and Sub-economic bulk samples have higher values than the host rock samples, whereas Aglime host rock is higher than the bulk samples. High Grade shows similar values for bulk and host limestone samples. Discrete seams show a significantly higher content than the bulk and host limestone samples (Figure 6.13). SO_3 shows that the host rock has higher values than bulk samples for Caprock and Aglime. Bulk samples have higher values than bulk samples for Upper Steel, High Grade, Lower Steel, and Sub-economic. Values for discrete seams are variable, with some units having seams with close to 0.01% SO_3 and others (e.g. High Grade and Aglime) up to 2.5% SO_3 (Figure 6.14A). K_2O, Na_2O, P_2O_5, TiO_2, and MnO are all higher in bulk samples for all limestones except the Caprock. This is probably due to the host limestone samples being taken close to the upper contact with the overlying Mahoenui Group mudstones. The discrete seams show significantly higher content than the bulk and host rock samples in these oxides (Figures 6.14B and C, and 6.15A-C).

6.6 Major and minor oxide results for overburden units and discontinuity materials

6.6.1 Kauroa Ash (Figures 6.16A and B)

SiO_2 (29.32-57.1%) is the dominant major oxide in the ash samples, followed by high concentrations of Al_2O_3 (up to 35%) and lesser Fe_2O_3 (up to 10%) (Figure 6.16A). One sample showed a relatively high CaO value (~58%).

MgO, (up to 2%) TiO_2 (up to 1%), and K_2O (up to 2%) occur in much higher levels than in any of the quarry limestone units (Figure 6.16B). Na_2O is variable (up to 1%), while MnO, SO_3, and P_2O_5 show similar values in samples and occur in low concentrations (all <0.25%).

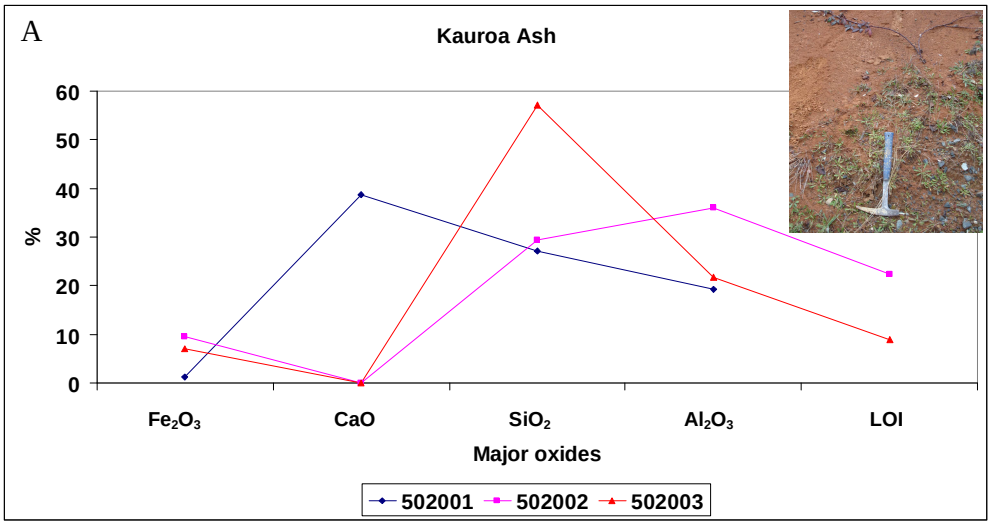

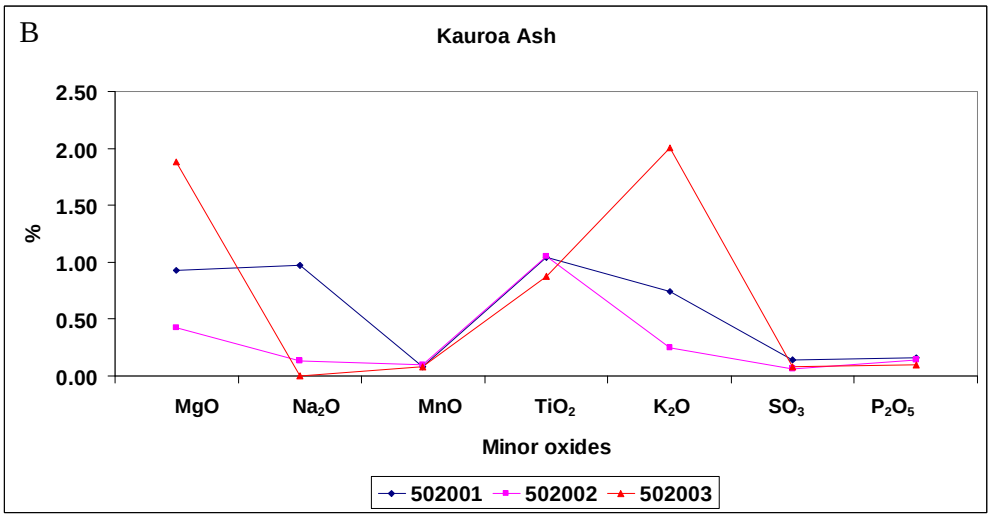

Figure 6.16 (A) Major oxide results from Kauroa Ash samples taken from drill hole BH502 (502001, 502002, and 502003). The inset shows a roadside exposure of the Kauroa Ash near the quarry, Troopers Rd, Oparure. The ash is typically a reddish brown weathered tephra that is a likely source of cave infill and/or joint infill. (B) Minor oxide results from Kauroa Ash of the same samples in (A).

6.6.2 Mahoenui Group mudstones (Figures 6.17A and B)

SiO_2 (37.02-38.66%) is the most abundant major oxide in the Mahoenui Group mudstones, followed by lesser amounts of CaO (<25%), Al_2O_3, (<15%) and Fe_2O_3 (<5%) (Figure 6.17A).

MgO and K_2O (both up to 2%) show relatively high values, compared to the other minor oxides which occur in much lower concentrations (<1%) except for SO3 which has one sample showing a high value (~3%) (Figure 6.17B).

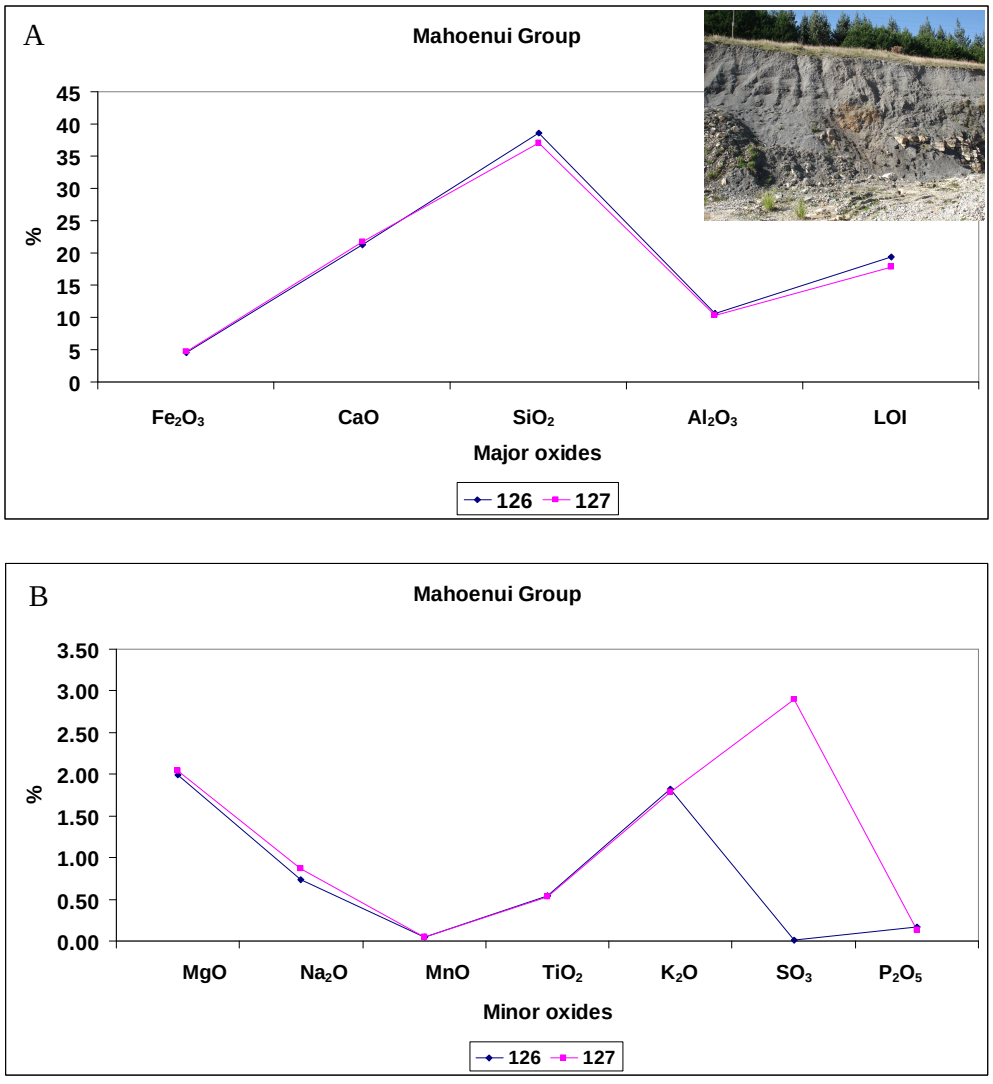

Figure 6.17 (A) Major oxide results from Mahoenui Group mudstone samples taken from outcrop (126, and 127). The inset shows Mahoenui Group mudstone in the quarry, northern side, close to current boundary. It is typically a grey or brown highly weathered frittery mudstone that is likely a source for cave and/or joint infill found washed into the underlying limestones. (B) Minor oxide results from Mahoenui Group mudstones of the same samples in (A).

6.6.3 Diffuse seams (Figures 6.18A and B)

CaO (47-49.51%) is moderately high in the diffuse seams, but still lower in concentration compared to all host limestones. Fe_2O_3, (<1%) Al_2O_3 (<3%), and SiO_2 (7.4-9.21%) are overall relatively low, but occur in higher levels compared to the quarry limestones (Figure 6.18A).

MgO concentrations are approximately twice the concentration of some quarry limestones (i.e. Upper Steel, High Grade, Lower Steel, Sub-economic). Na_2O (<0.2%), TiO_2 (<0.2%), K_2O (<0.5%), SO_3 (<1%), and P_2O_5 (<0.2%) also occur in much higher concentrations compared to the limestones, but MnO and P_2O_5 remain low (both <0.05%) (Figure 6.18B).

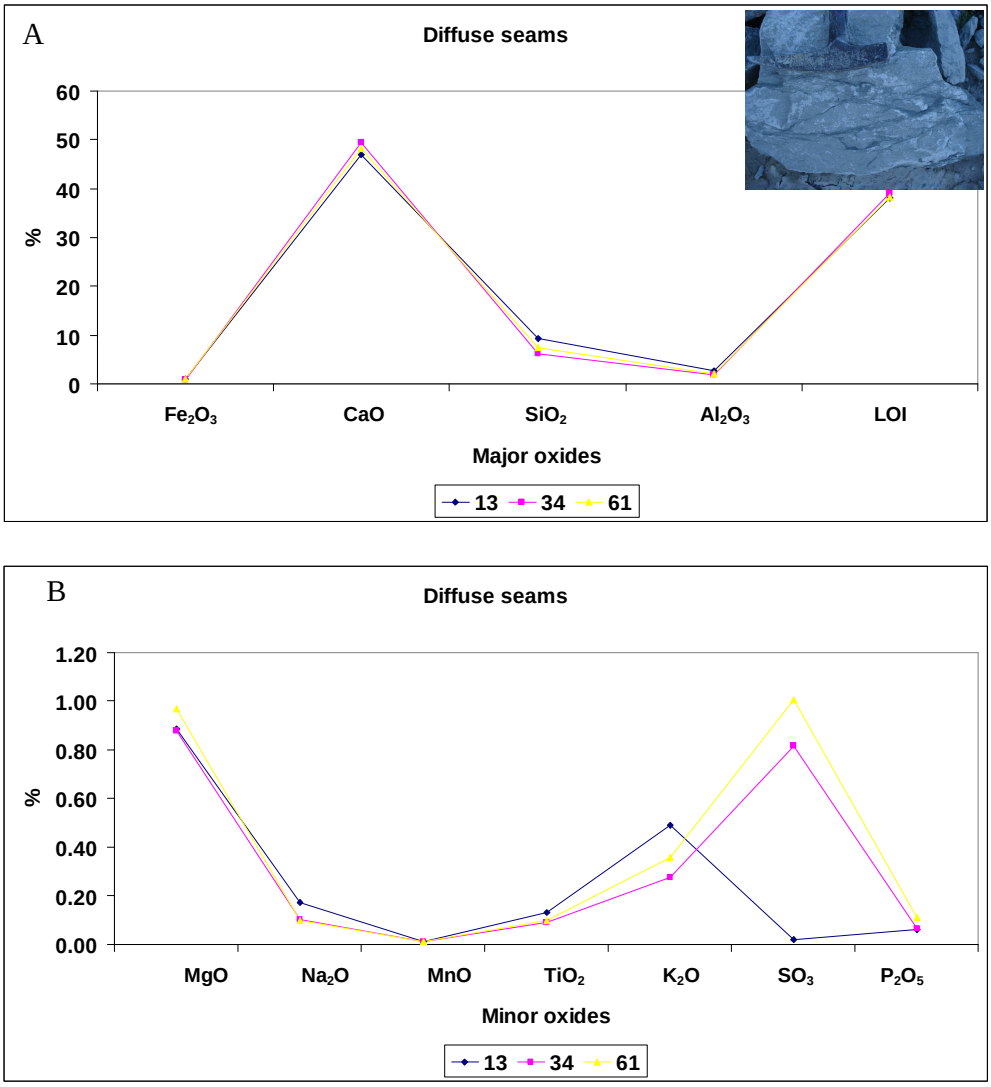

Figure 6.18 (A) Major oxide results from diffuse seam samples taken from drill hole BH502 (13, 34, and 61). Inset shows a blasted block of Aglime in the quarry showing diffuse seams (darkish grey streaky bands). (B) Minor oxide results from diffuse seams of the same samples in (A).

6.6.4 Discrete seams (Figures 6.19A and B)

SiO_2 (26.73-56.67%) occurs over a wide range of values in discrete seams. CaO (<30%), Al_2O_3 (<15%), and Fe_2O_3 (<8%) occur in relatively lower concentrations but still at much higher levels than in the limestones and diffuse seams (Figure 6.19A).

A range of MgO (up to 7%) and Na_2O (<2%) concentrations occur in discrete seams (Figure 6.19B). One sample showed a relatively high value for SO_3 (~5%) and for P_2O_5 (~6%). The remaining minor oxides occur at higher concentrations compared to the limestones and diffuse seams (with values typically up to 3%) (Figure 6.19B).

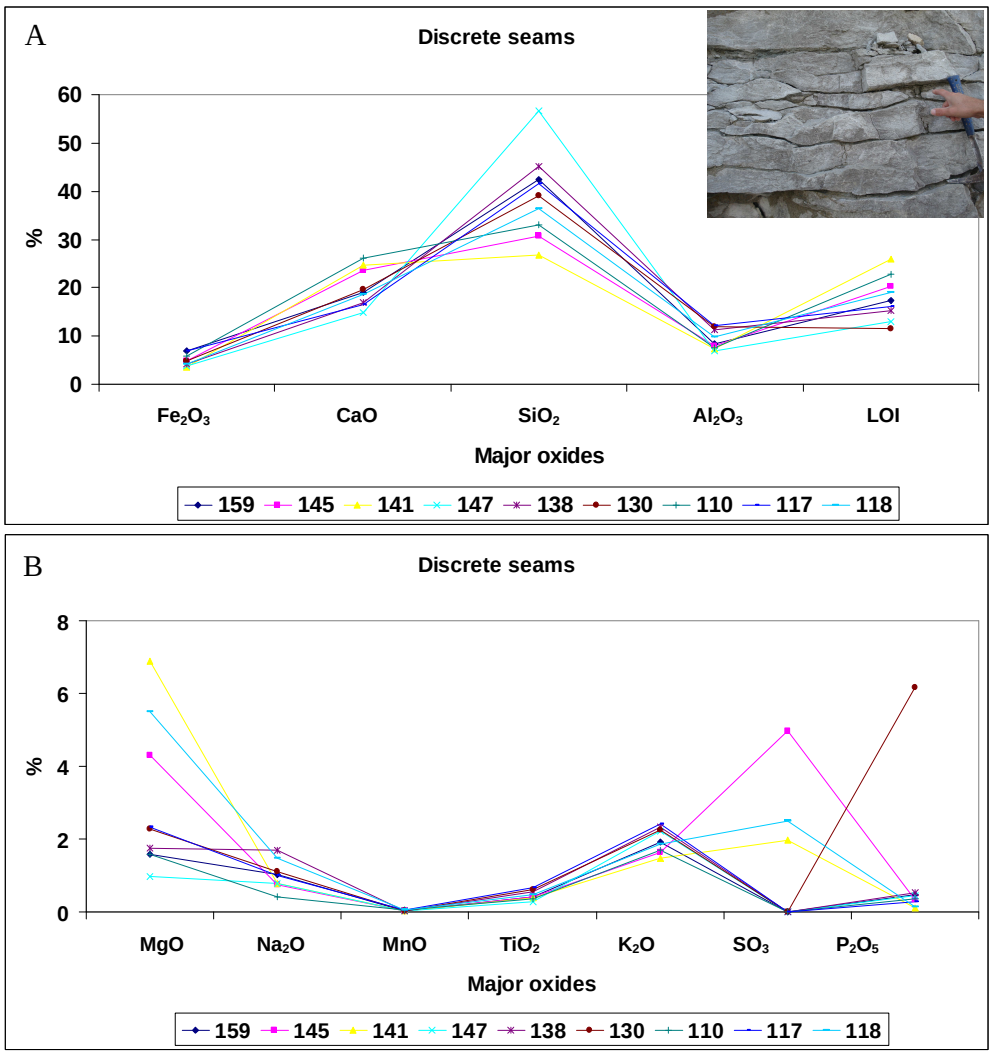

Figure 6.19 (A) Major oxide results from discrete seam samples taken from outcrop (110, 117, 118, 130, 138, 141, 145, 147, and 159). Inset shows discrete dissolution seams (dark grey bands) separating the intact host rock or limestone flags in the Aglime unit in the quarry, northern face along road to drying plant. (B) Minor oxide results from discrete seams of the same samples in (A).

6.6.5 Joint infills

Type 1 (Figures 6.20A and B): SiO_2 is variable, ranging from 7.23-59.46%. CaO is also variable ranging from 1.43-49.07% (Figure 6.20A).

MgO (up to 3%) and K_2O (<2.5%) occur in relatively high concentrations, although there is much variability across the samples. MnO and P_2O_5 occur in low concentrations (<0.5%) (Figure 6.20B).

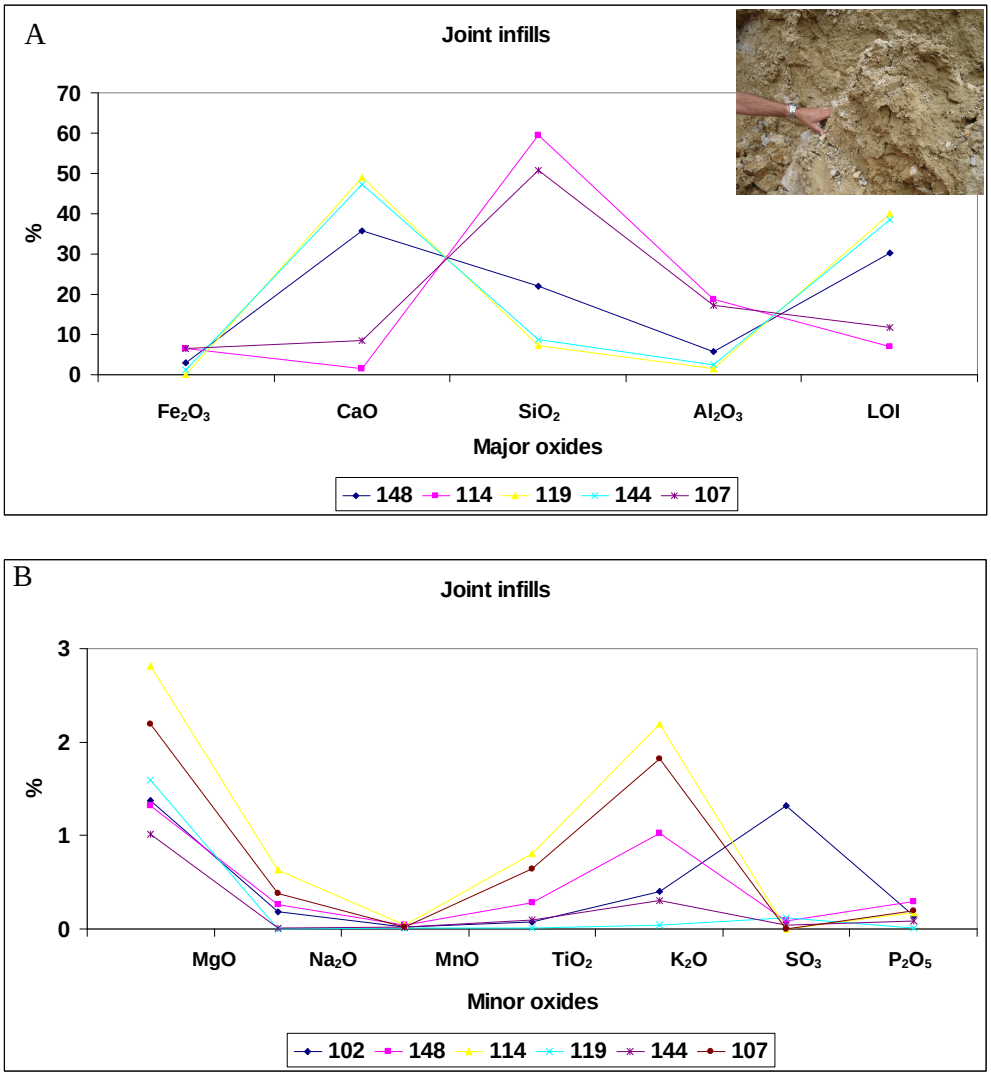

Figure 6.20 (A) Major oxide results from joint infill samples taken from outcrop (102, 107, 114, 119, 144, and 148). Inset shows joint infill in the High Grade unit in the quarry, northern side, eastern face which typically consists of a sticky brown clay rich material that commonly contains fragments of blasted limestone. (B) Minor oxide results from joint infills of the same samples in (A).

Type 2 (Figures 6.21A and B): CaO (36.94-38.02%) occurs in high concentrations in palygorskite compared to most discontinuity materials, followed in abundance by SiO_2 (18.86-20.52%). Fe_2O_3 (<0.1%) and Al_2O_3 (<0.5%) are relatively low (Figure 6.21A). Palygorskite, earlier identified by XRD (Chapter 5, Section 5.1.5), is associated with calcite and quartz, as reflected in these analyses.

MgO concentrations are particularly high in palygorskite compared to the other minor oxides (up to 3.8%) (Figure 6.21B). The other oxides occur in low concentrations (<0.5%).

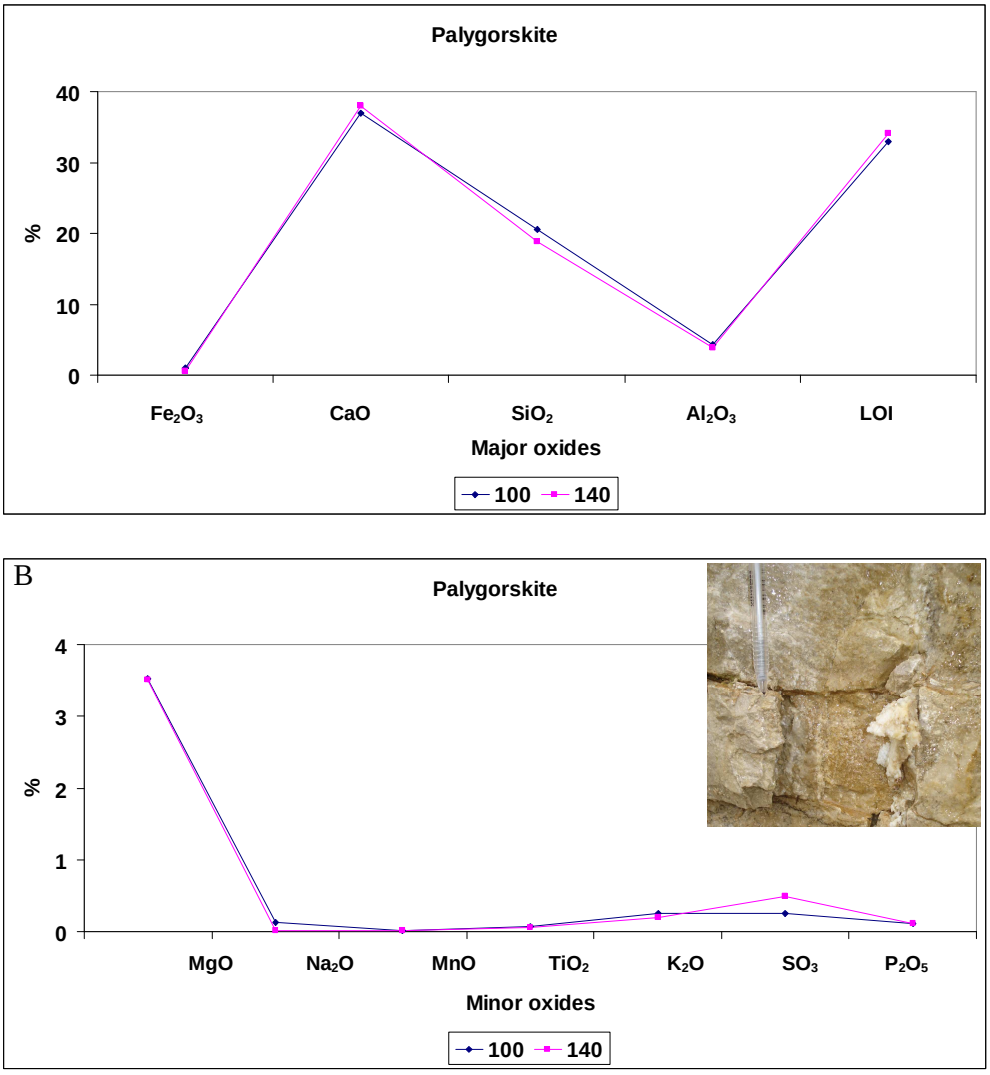

Figure 6.21 (A) Major oxide results from palygorskite (joint infill type 2) samples taken from outcrop (100, and 140). (B) Minor oxide results from palygorskite of the same samples in (A). Inset shows palygorskite within a joint in the Upper Steel unit, northern face that has had water seeping through it. In the quarry, it is a white, flexible, leathery clay mineral.

6.6.6 Surface accumulations (Figures 6.22A and B)

CaO (40.67-41.18%) occurs at the highest concentration in these samples. SiO_2 (12.91-15.08%) is also an important major oxide, present in relatively high concentrations compared to the quarry limestone units (Figure 6.22A).

The minor oxide content of surface accumulations shows high levels of MgO (<2.25%) in particular, as well as K_2O (<0.75%) and SO_3 (<0.8%) relative to the other oxides (<0.25%) (Figure 6.22B).

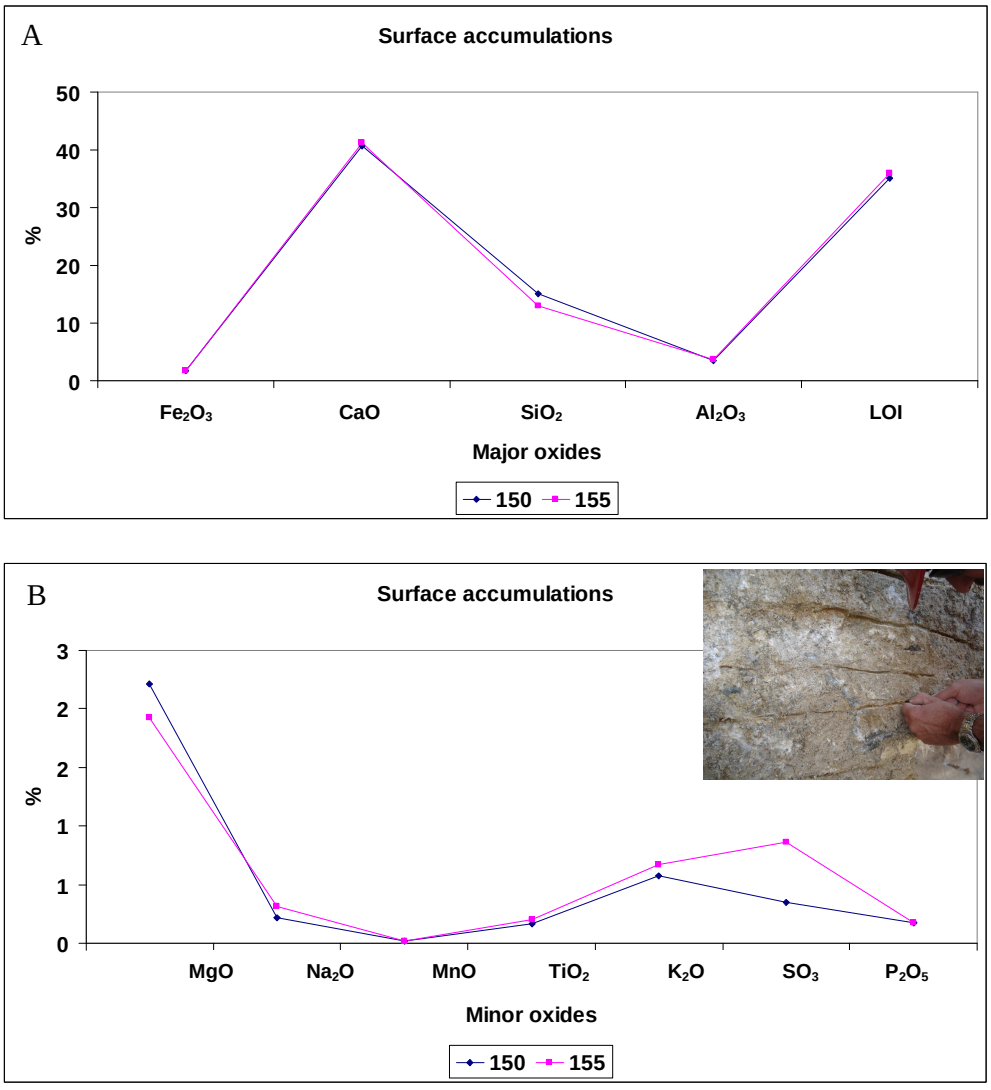

Figure 6.22 (A) Major oxide results from surface accumulation samples taken from outcrop (150, and 155). Inset shows a quarry face in the Aglime, southern side, western face showing material that has accumulated on the surface over time. The material is possibly sourced from joint infill including any combination of clay, ash, or mudstone. Another source could be quarry dust from quarry operations such as blasting, or vehicular traffic. (B) Minor oxide results from surface accumulations of the same samples in (A).

6.6.7 Cave infills (Figures 6.23A and B)

SiO_2 (49.71-61.49%) is the dominant major oxide in cave infills, along with high concentrations of Al_2O_3 and Fe_2O_3 (Figure 6.23A). CaO (1.04-8.91%) occurs in low concentrations.

MgO (up to 2.7%) and K_2O (~2%) have lower concentrations in cave infills than in discrete and diffuse seams. Other minor oxides occur at relatively low concentrations, particularly SO_3 (<1%) (Figure 6.23B).

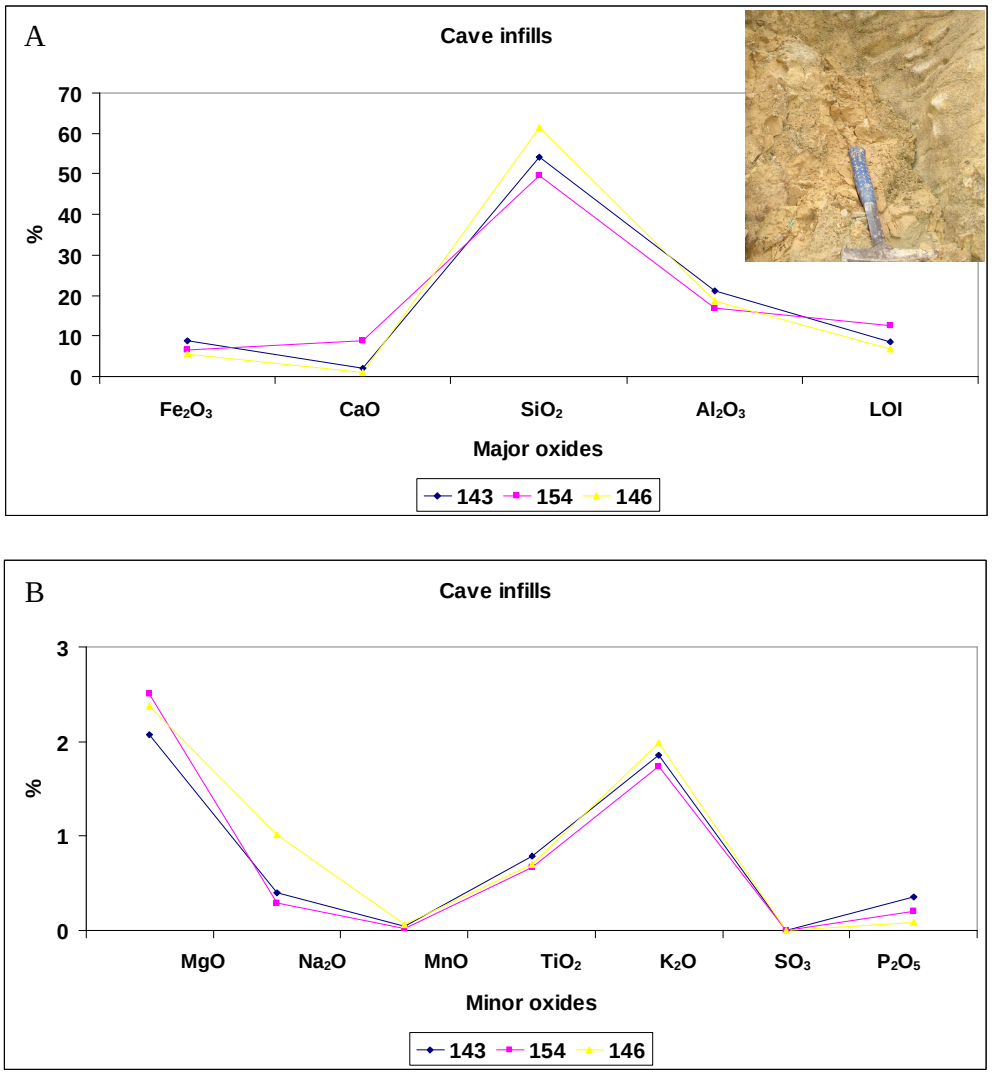

Figure 6.23 (A) Major oxide results from cave infill samples taken from outcrop (143, 146, and 154). Inset shows cave infill in the Upper Steel unit, northern side which is a typically orange brown sticky clay rich material, sitting in a remnant cave which has been exposed from blasting. (B) Minor oxide results from cave infills of the same samples in (A).

6.7 Discussion

6.7.1 Quarry limestone units – major elements

The major element composition of the quarry limestone units is summarised in stratigraphic array for all samples analysed (Figure 6.24). Additionally, in Figure 6.25, the average values for each major element in the six limestone units are portrayed alongside one another using bar plots. These diagrams emphasise the following major element properties for the quarry limestones:

1. CaO shows reasonably similar values throughout all the limestone units, but is highest in the Upper Steel, variable in the Caprock, similar in the Lower Steel and Sub-economic units, and lowest in the Aglime. CaO is associated with the mineral calcite, which is the dominant mineral in the limestone units (Chapter 5, Section 5.5.1).

2. LOI values parallel the CaO trends because it mainly reflects the CO_2 content in $CaCO_3$. Upper Steel has the highest average value followed by Caprock, Lower Steel, and Sub-economic units with similar values, and Aglime the lowest value.

3. SiO_2 shows higher values in the Caprock and Aglime units compared with lower values in the Upper Steel, Lower Steel, High Grade, and Sub-economic. SiO_2 is associated with the minerals quartz, feldspar, glauconite, and clay minerals, all identified in the quarry limestone units in Chapter 5, Section 5.5.3.

4. Al_2O_3 is highest in the Caprock. Lower values occur in the Aglime and similar much lower values occur in the other limestones. Al_2O_3 is less than, but mirrors, the SiO_2 content because it largely resides in alumino-silicate minerals such as feldspars, glauconite, and clays. Caprock contains the highest content of these minerals compared to the other limestone units, recognised in Chapter 5, Section 5.5.3.

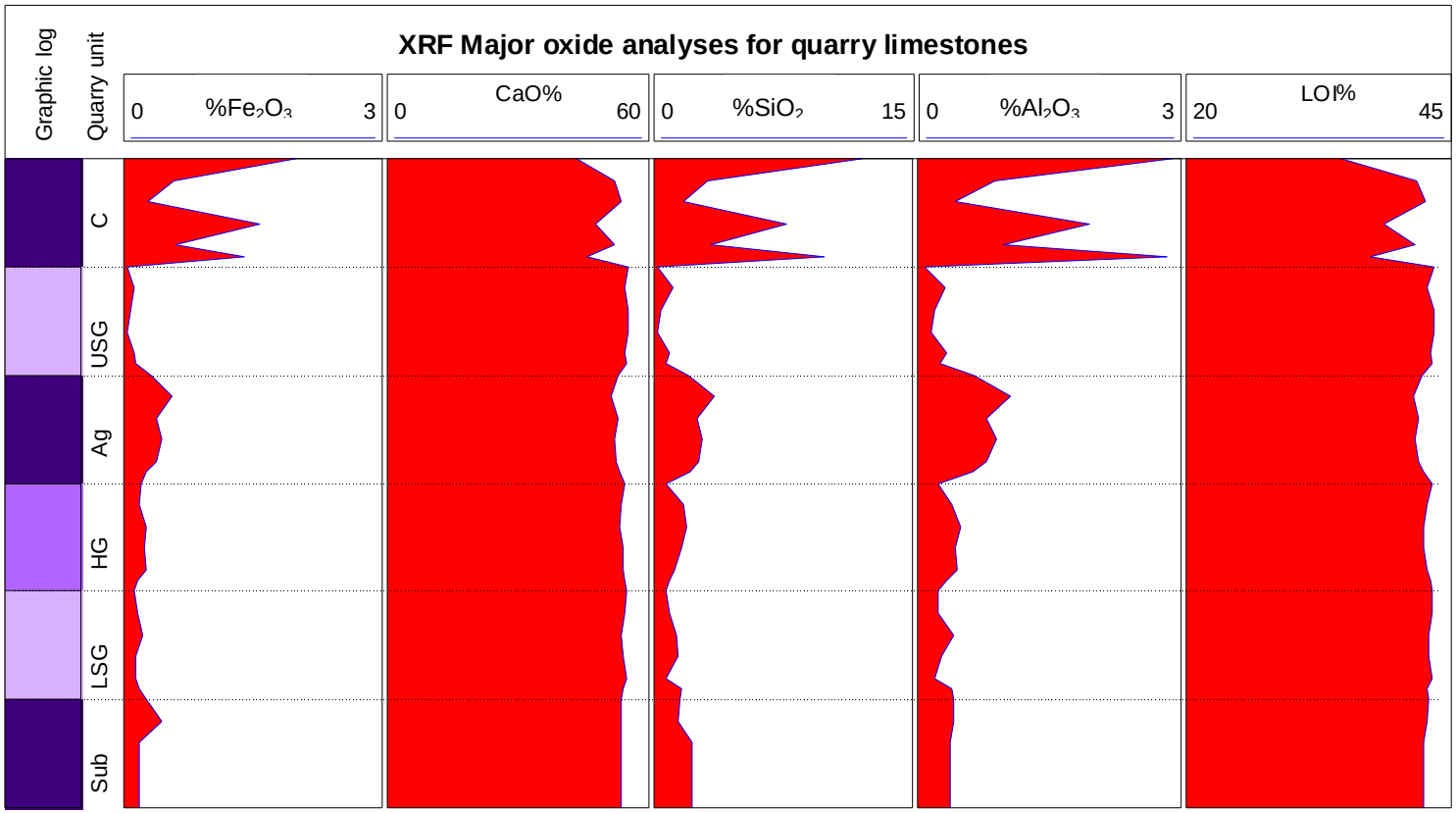

Figure 6.24 Major oxide trends in stratigraphic array showing the changes between each limestone unit. C = Caprock, USG = Upper Steel, Ag = Aglime, HG = High Grade, LSG = Lower Steel, and Sub = Sub-economic. Caprock is particularly variable for most major oxides. Aglime and Sub-economic units show clear increases in Fe_2O_3, SiO_2, and Al_2O_3. The various shades of purple (graphic log) correspond to varying amounts of silica in the units where the lighter the colour, the purer the unit (in terms of $CaCO_3$ content).

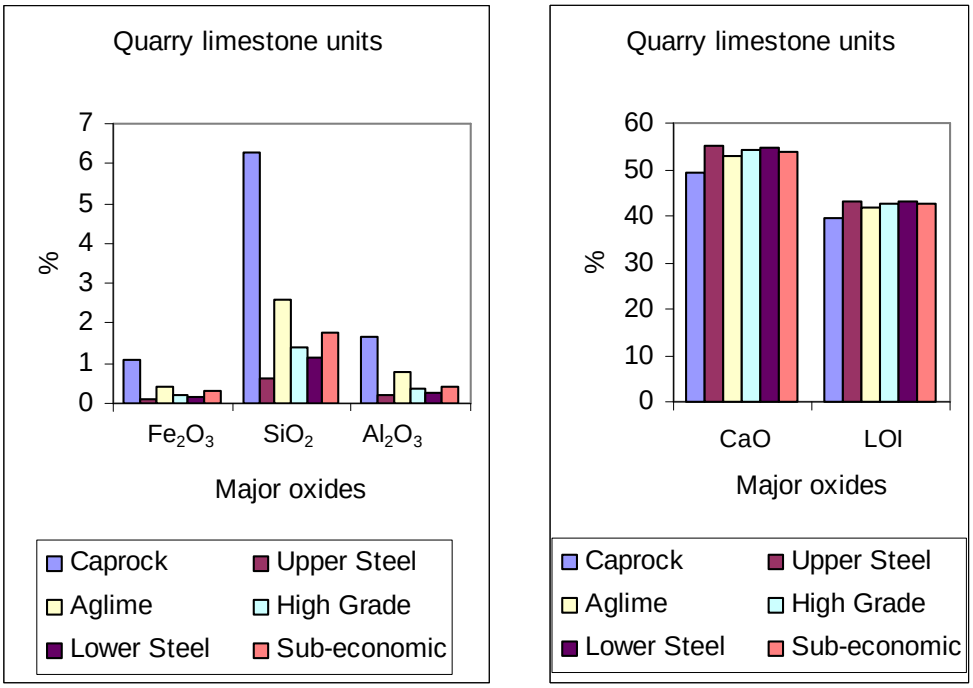

Figure 6.25 Summary of the average major oxide content found in each of the six quarry limestone units. CaO dominates across all units, whereas Fe_2O_3, Al_2O_3, and SiO_2 occur in relatively low concentrations. SiO_2 is variable across the different units.

5. In general, Fe_2O_3 shows higher values in the lower quality (lower $CaCO_3$ content) units (i.e. Caprock, Aglime, and Sub-economic). The Fe_2O_3 is associated with glauconite and clay minerals, both highest in the Caprock unit which underlies the Mahoenui Group mudstone and is commonly distinctly argillaceous. Also being the topmost unit, tends to collect weathering residues leaching down from above. Much lower values occur in the Upper Steel, High Grade, and Lower Steel units. Furthermore, Fe_2O_3 is associated with ferroan calcite cements common in Te Kuiti Group limestones (ref).

A CaO vs. SiO_2 cross-plot is presented delineating the different limestone units (Figure 6.26A and B). The Caprock is variable and covers a large area of the plot (i.e. the Caprock samples show a variety of values for CaO and SiO_2). The trend shows that as CaO decreases, SiO_2 increases, with the higher quality limestone units (Upper Steel, High Grade, and Lower Steel) occurring towards the left of the plot, and the lower quality limestone units (Caprock, Aglime, and Sub-economic) towards the right side of the cross plot (increasing SiO_2).

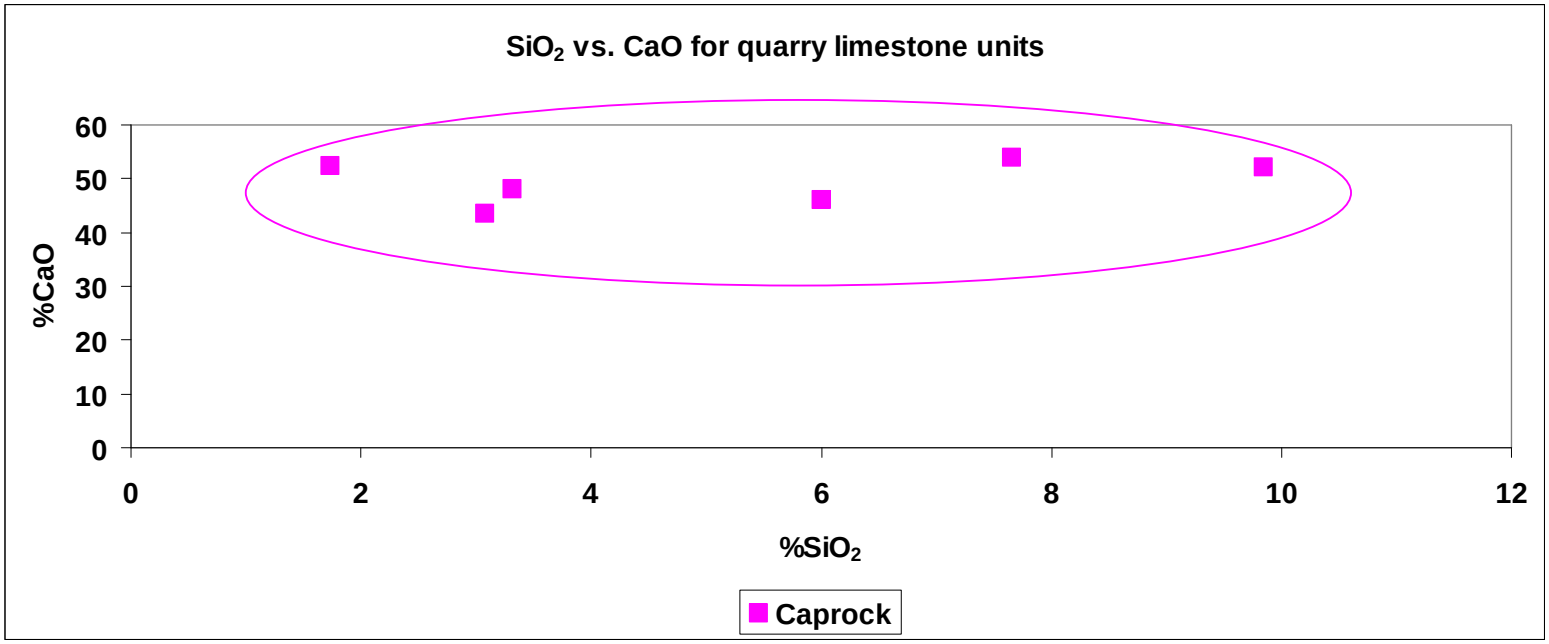

Figure 6.26 (A) Cross plot delineating limestone fields. The Caprock occurs over a wide range of values compared to the other limestone units (Figure 6.26B). In general, as CaO increases, SiO_2 decreases. A field is drawn around sample points for the Caprock unit.

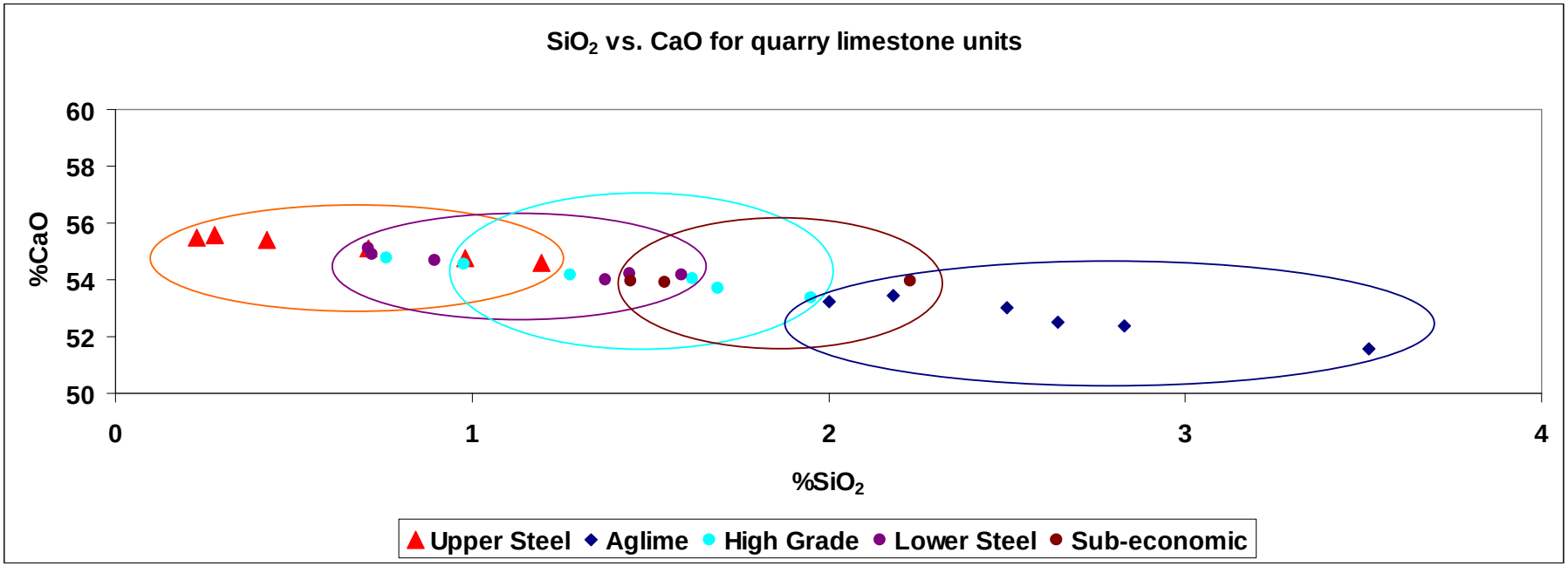

Figure 6.26 (B) Cross plot delineating limestone fields. The Aglime occurs over a wide range of values compared to the other limestone units. In general, as CaO increases, SiO_2 decreases. Fields are delineated by circles for each unit (i.e. Upper Steel = orange, Aglime = blue, High Grade = cyan, Lower Steel = purple, and Sub-economic = brown).

6.7.2 Quarry limestone units – minor oxides

The minor element composition of the quarry limestone units is summarised in stratigraphic array for all samples analysed in each unit in Figure 6.27. Additionally, in Figure 6.28, the average values for each major element in the six limestone units are portrayed alongside one another using bar plots. These diagrams emphasise the following minor element properties for the quarry limestone units:

1. MnO is highest in the Caprock and shows lower but similar values in the Upper Steel, High Grade, and Lower Steel units. The Aglime and Sub-economic units have slightly higher values than the Upper Steel, High Grade, and Lower Steel. MnO is a typical oxide found in carbonates or associated with weathering with weathering products.

2. TiO_2 shows variable values across the Caprock unit, and low but similar values in the Upper Steel, High Grade, Lower Steel, and Sub-economic units. The Aglime shows a slight increase compared to these units, but values are not as high as in the Caprock.

3. K_2O shows similar trends to TiO_2. It is variable across the Caprock and occurs as low similar values for the Upper Steel, High Grade, Lower Steel, and Sub-economic units. There is a slight increase in the Aglime (higher values compared to the Upper Steel, High Grade, Lower Steel, Sub-economic). K_2O is associated with clays and feldspars.

4. SO_3 shows the highest average value in the Caprock. SO_3 is associated with the minerals pyrite (iron sulphide) and gypsum (calcium sulphate) which are locally common in the Mahoenui Group mudstones which overlie the Caprock. There is a substantial increase of SO_3 in the Aglime, High Grade, and Sub-economic units corresponding to the relatively high abundance of pyrite in these units (Chapter 5, Section 5.5.3). Lower values occur in the Upper Steel, Lower Steel, and Sub-economic units.

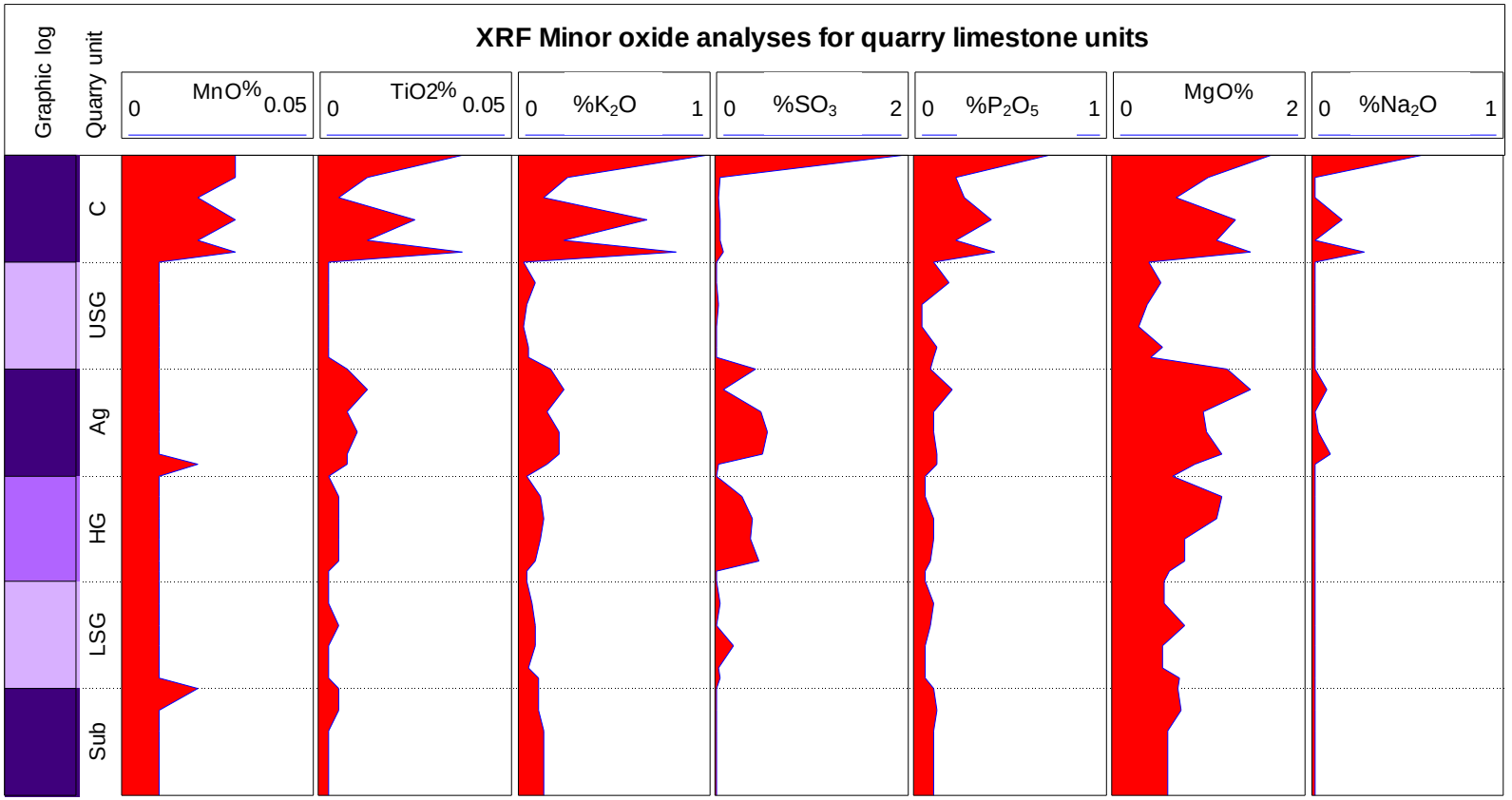

Figure 6.27 Minor oxide trends in stratigraphic array showing the changes between each limestone unit. C = Caprock, USG = Upper Steel, Ag = Aglime, HG = High Grade, LSG = Lower Steel, and Sub = Sub-economic. Caprock is particularly variable for most minor oxides. The other limestones have similar lower values. Aglime and High Grade show some increases relative to the other units for TiO_2, K_2O, SO_3, and MgO. The various shades of purple (graphic log) correspond to varying amounts of silica in the units where the lighter the colour, the purer the unit (in terms of $CaCO_3$ content).

5. P_2O_5 shows the highest values in the Caprock and varies in the Upper Steel and Aglime. P_2O_5 occurs in relatively low similar amounts in the High Grade, Lower Steel, and Sub-economic units.

6. MgO shows the highest average values in the Caprock, Aglime, and High Grade units. Lower values occur in the other limestones and in decreasing content are Sub-economic, Lower Steel, and Upper Steel (lowest). These low values (i.e. <1% MgO) reflect the low-Mg calcite (<4 wt% $MgCO_3$) mineralogy of the limestone units (Nelson, 1978a).

7. Na_2O shows highest values in the Caprock and Aglime units. Na_2O occurs as relatively lower values in the other limestones (typically <0.01%). Na_2O resides in the mineral feldspar that has been identified in the limestone units (Chapter 5, Section 5.5.3).

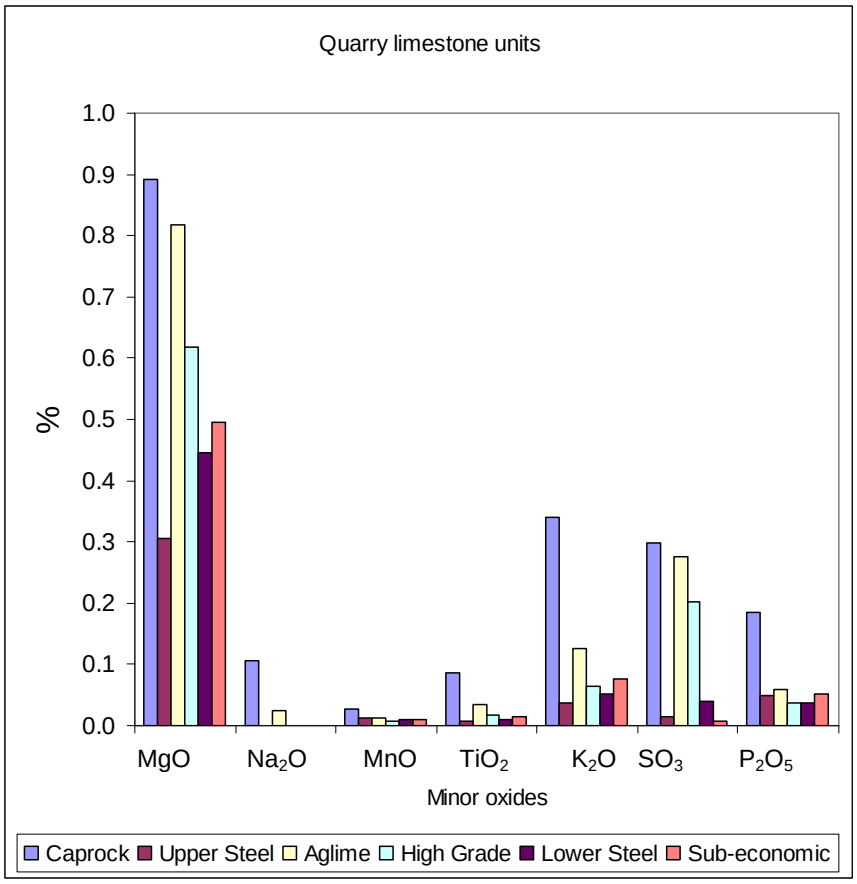

Figure 6.28 Summary of the average minor oxide content found each of the six quarry limestone units. MgO occurs in much higher content relative to the other oxides such as Na_2O, MnO, and TiO_2.

6.7.3 Overburden units and discontinuity materials – major elements

The trends for the average major oxide content in the discontinuity types are shown in Figure 6.29.

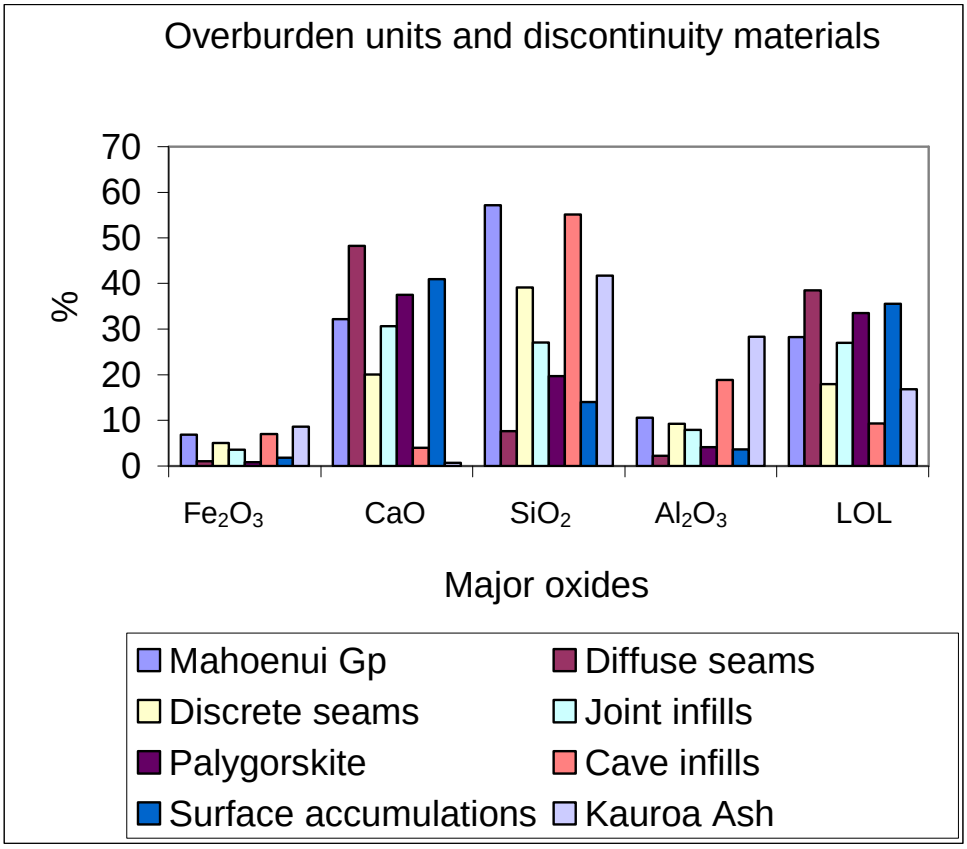

Figure 6.29 Summary of the average major oxide content found in the eight discontinuity types. Fe_2O_3 is relatively low and shows similar values for all the discontinuities. CaO, SiO_2, Al_2O_3, and LOI are variable across the units.

Figure 6.29 emphasises the following major element properties for the discontinuity types:

1. CaO is variable across the overburden units and discontinuity types. Diffuse seams show the highest values followed by surface accumulations, palygorskite, Mahoenui Group mudstones, joint infills, discrete seams, cave infills, and Kauroa Ash (lowest). CaO resides in the mineral calcite and has been identified (Chapter 5, Table 5.9) as a common mineral in the diffuse and discrete seams (inherited from the limestones), palygorskite (associated with formation), Mahoenui Group mudstones (calcareous mudstone), joint infills (contain limestone fragments), and cave infills (in

contact with the limestones). Surface accumulations are also directly associated with the limestones (scrapings from limestone surfaces).

2. LOI is variable across the discontinuity types. The trend is similar as for CaO and relates to the associated CO_2 content in $CaCO_3$. Diffuse seams show the highest values followed by surface accumulations, palygorskite, Mahoenui Group mudstones, joint infills, discrete seams, cave infills, and Kauroa Ash (lowest).

3. SiO_2 is highly variable across the overburden units and discontinuity types. Mahoenui Group mudstones show the highest values followed by cave infills, Kauroa Ash, discrete seams, joint infills, palygorskite, surface accumulations, and diffuse seams (lowest). SiO_2 largely resides in quartz, feldspar, a number of clays (i.e. smectite, palygorskite, halloysite, vermiculite), and in minor cristobalite. The minerals that have been identified (e.g. Chapter 5, Table 5.9) in the overburden units and discontinuity types that contain SiO_2 are as follows: quartz and clays in the Mahoenui Group mudstones; smectite, quartz, palygorskite in cave infills; quartz, vermiculite, halloysite, and cristobalite in the Kauroa Ash; quartz, smectite, and oligoclase (feldspar) in discrete seams; clays, quartz, and feldspar in joint infill type 1; palygorskite and quartz in joint infill; type 2 palygorskite and quartz in surface accumulations; and quartz, feldspars, and glauconite in diffuse seams.

4. Al_2O_3 is variable across the overburden units and discontinuity types. Kauroa Ash shows the highest values followed by cave infills, Mahoenui Group mudstones, discrete seams, joint infills, palygorskite, surface accumulations, and diffuse seams (lowest). Al_2O_3 largely resides in aluminosilicates (clay minerals) and feldspars (e.g. oligoclase). The Kauroa Ash contains clay minerals that include Al_2O_3 (i.e. vermiculite, halloysite), as well as gibbsite and oligoclase. Cave infills also contain many clay minerals (i.e. smectite, vermiculite, palygorskite) (Chapter 5, Table 5.9). Clays also occur in the other discontinuities, but the, Al_2O_3 is in much lower concentrations.

5. All the discontinuity types have similar Fe_2O_3 values. The Fe_2O_3 is associated with the following minerals: clays (vermiculite, illite), glauconite, pyrite (iron sulphide), and Fe_2O_3 in calcite cement.

6.7.4 Overburden units and discontinuity materials – minor elements

The trends for the average minor oxide content in the overburden units and discontinuity materials are shown in Figure 6.30.

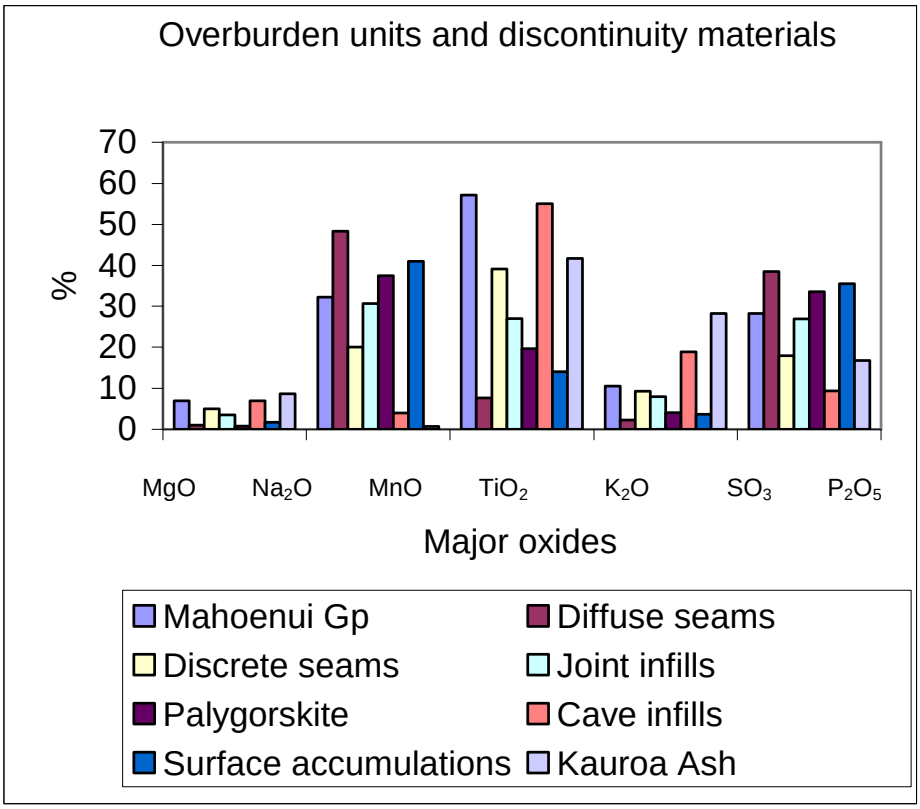

Figure 6.30 Summary of the average minor oxide content found in the eight sample types including overburden units and materials associated with discontinuity types. MgO and K_2O occur in larger concentrations than the other minor oxides. The remaining oxides occur in relatively low concentrations and are variable across the discontinuity types.

Figure 6.30 emphasises the following minor element properties for the discontinuity types:

1. MgO is variable across the overburden units and discontinuity types. Palygorskite shows the highest values followed by discrete seams,

Mahoenui Group mudstones, cave infills, surface accumulations, joints infills, Kauroa Ash, and diffuse seams (lowest).

2. Na_2O is variable across the overburden units and discontinuity types. Mahoenui Group mudstones show the highest values followed by discrete seams, cave infills, Kauroa Ash, surface accumulations, joint infills, diffuse seams, and palygorskite.

3. MnO values are similar for all overburden units and discontinuity types, occurring in low concentrations.

4. P_2O_5 shows generally low values across the overburden units and discontinuity types; however, discrete seams show the highest value which is greater than twice the content found in the other discontinuity types. In decreasing order the Mahoenui Group mudstones show the second highest values, followed by surface accumulations, Kauroa Ash, joint infills, palygorskite, and diffuse seams.

5. TiO_2 is variable across the overburden units and discontinuity types. The highest values occur in the Kauroa Ash, followed by cave infills, Mahoenui Group mudstones, discrete seams, joint infills, surface accumulations, diffuse seams, and palygorskite.

6. K_2O is variable across the overburden units and discontinuity types. Mahoenui Group mudstones show the highest values followed by discrete seams, cave infills, joint infills, surface accumulations, diffuse seams, and palygorskite. As mentioned above, K_2O is mainly associated with clays.

7. SO_3 is variable across the overburden units and discontinuity types. Mahoenui Group mudstones show the highest values followed by discrete seams, diffuse seams, surface accumulations, palygorskite, joint infills, Kauroa Ash, and cave infills.

The variation in the chemical composition of the overburden units and fills in the discontinuity types are a result of their different sources and origins. For example,

discrete and diffuse seams are diagenetic in origin, Kauroa Ash has a volcanic origin, Mahoenui Group mudstones have a deep marine origin, and palygorskite (joint infill type 2) is a secondary clay mineral precipitate.

Figure 6.31 shows a cross-plot (CaO vs. SiO_2) of the overburden units and discontinuity infills delineated into their different fields. The cross-plot shows that as CaO decreases, SiO_2 increases, and the overburden units and discontinuity types are reasonably different from each other.

6.7.5 Contrasting bulk, host, and discrete seam samples

A comparison of bulk, host rock, and discrete seam samples was made to show that host rock samples are purer in terms of $CaCO_3$ than bulk samples, which contain discontinuities (i.e. a mixture of host limestone, discrete and diffuse seams, and joint infills). Additionally, bulk samples were expected to have higher $CaCO_3$ contents than the discrete seams, and therefore an intermediate composition between the host rock and discrete seams.

Major elements: CaO (associated with the mineral calcite) is higher in host rock samples for the majority of the limestone units except for the Caprock, whereas discrete seams have much lower CaO content. These trends have also been observed in thin section study (see Chapter 5, Section 5.5.1). Although Caprock CaO values are an exception, probably due to the location the samples were taken for this study (i.e. mainly very close to the contact with the overlying Mahoenui Group mudstones). LOI results mirror trends observed in CaO. SiO_2, Al_2O_3, and Fe_2O_3 are generally higher in bulk samples compared to host rock samples, and much higher in the discrete seams overall. These oxides are associated with minerals such as clays, quartz, glauconite, and feldspar. The relatively high content of these minerals within discrete seams has been observed in thin section study as well (Chapter 5, Section 5.5.8).

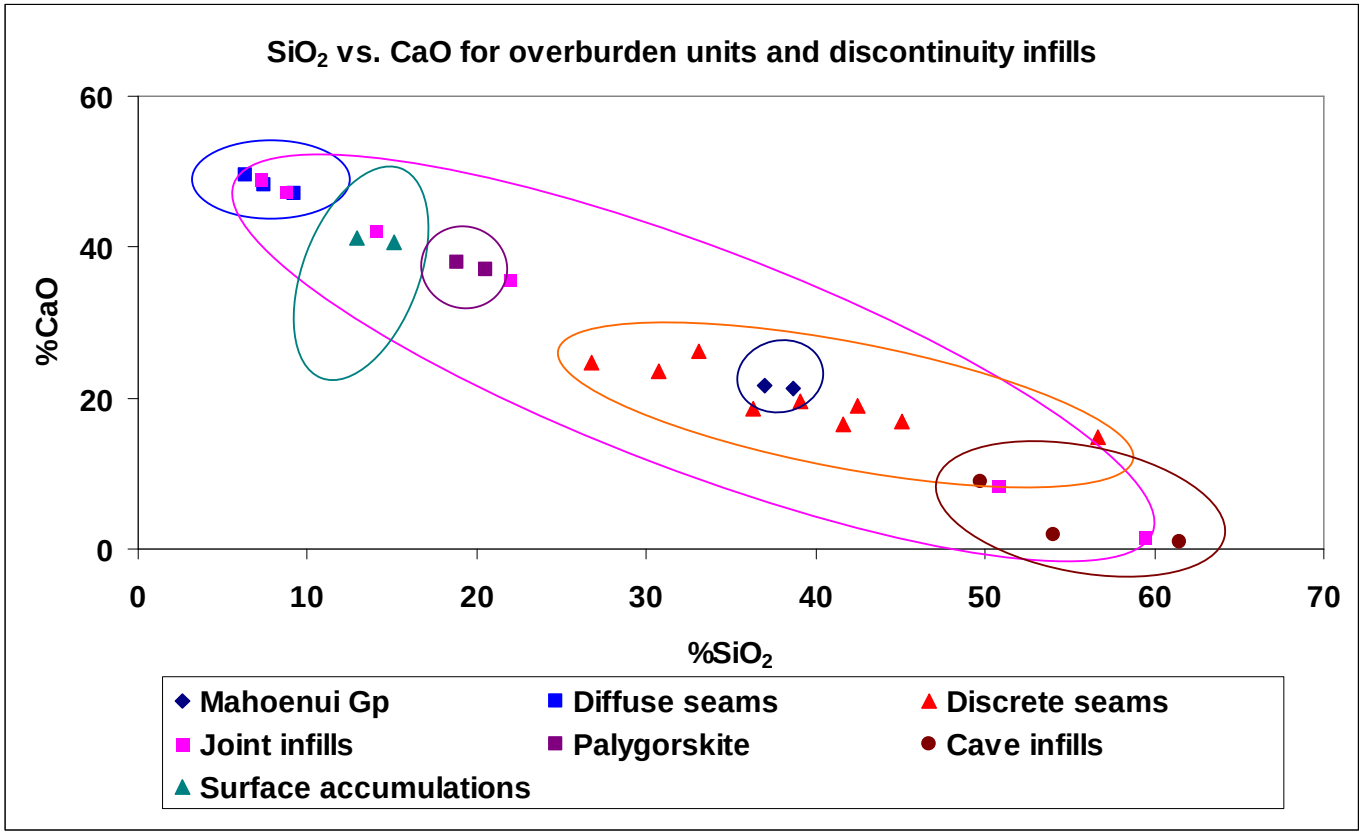

Figure 6.31 Cross-plot delineating discontinuity fields. Collectively, the overburden units and discontinuity infills cover a range of values. Joint infills show the greatest variability. In general, as CaO decreases, SiO_2 increases. Fields are delineated by circles (i.e. diffuse seams = medium blue, surface accumulations = green, palygorskite = purple, Mahoenui Group mudstones = dark blue, cave infills = brown, joint infills = magenta, and discrete seams = orange.

Minor elements: In general, there appears to be no significant difference in MgO content between the bulk and host rock samples. Discrete seams, however, have much higher MgO contents in comparison. Results are varied for SO_3 values for bulk and host rock samples, although contents are low in both. The Caprock and Aglime units show larger values in the host rock samples, whereas the Upper Steel, High Grade, Lower Steel, and Sub-economic units show larger values in the bulk samples. SO_3 is significantly higher in the discrete seams compared to bulk and host rock samples, but only in the Aglime and High Grade units; the discrete seams in the others units show relatively low SO_3 content in comparison. K_2O, Na_2O, P_2O5, TiO_2, and MnO generally show higher values in the bulk samples compared to the host rock samples, and discrete seams show significantly higher contents to the bulk and host rock samples. Na_2O is associated with feldspars which are common in discrete seams (up to 2% e.g. Figure 6.19B), whereas Na_2O content in the limestone units rarely exceeds 0.15%.

It is significant that we see differences between the averages in the bulk and host limestone samples. There is strong evidence that shows calcite or CaO dominates in host limestone samples, and is much less abundant in discrete seams. Discrete seams are dominated by siliceous minerals and therefore, by SiO_2. Bulk samples show higher SiO_2 contents than host rock, and less content than discrete seams. The bulk composition is closer to the host rock composition as opposed to the discrete seam composition due to the overwhelming CaO content that predominates in the limestone units. Additionally, the total thickness of limestone is much greater than the total thickness of discrete seams, which allows the contribution of siliceous discrete seams to be partially masked by the abundance of CaO.

CHAPTER SEVEN

Ground penetrating radar

7.1 Introduction

Ground penetrating radar (GPR) is a geophysical technique commonly used to study the shallow subsurface. Limestone caves (a discontinuity feature, Chapter 3, Section 3.1.5) are present in the McDonald's Oparure Quarry and are associated with silica-rich infill (i.e. material accumulating within the caves that is likely to have been washed in from an external source). In July 2007 GPR was trialled to investigate whether it is a good tool to use for locating caves in the limestone deposit. If GPR can accurately predict areas of the McDonald's resource that contain caves or voids, quarry operators can make predictions of their locations in confidence, and therefore make better decisions for future plans thus: (1) ensuring improved safety of their team; and (2) identifying silica rich areas. This chapter describes the basic concept of how GPR works, the method used in the trial, and results.

7.2 How GPR operates

This study used a RAMAC GPR (manufactured by MalÅ Geoscience) that was unshielded. Figure 7.1 shows the basic setup of the GPR system. Two antennae are used to generate pulses of radar waves via a control signal sent from a transmitter that is attached to one antenna. The receiver is attached to the other antenna which measures the incoming radar waves. The transmitter and receiver are linked via fibre optic cables to a control and recorder unit (CRU) (usually mounted onto a back pack worn by the operator). The CRU sends the signal to the transmitter to generate radar pulses, and also collects the data from the receiver. The CRU is linked to a portable PC loaded with GPR software, by a communication cable, where the data can be viewed (Milsom, 1996).

The antennae are spaced at an equal distance apart by a fixed bar on a wooden frame (attached to the transmitter and receiver, Figure 7.1). The entire setup is dragged or moved along the ground surface during data collection. When collecting a sample the control unit sends a signal to the transmitter, the transmitter generates pulses (through the antenna) of radar waves at a determined frequency, and a wave train of radar waves then propagate away (large beam) (Reynolds, 1997). The pulse reflects on any object, layer or structure beneath the ground surface which alters the speed of transmission of the radar signal and is echoed back to the receiver (Chamberlain et al., 2000). The moment the receiver detects a signal, it collects a sample and passes the information to the control unit. This is repeated at controlled intervals (fixed distance) where the operator hits the enter button on the PC at the end of each interval. To help determine the end of each interval, the operator walks along a measuring tape. The control unit collects samples that make up a trace (along a transect that is walked during collection).

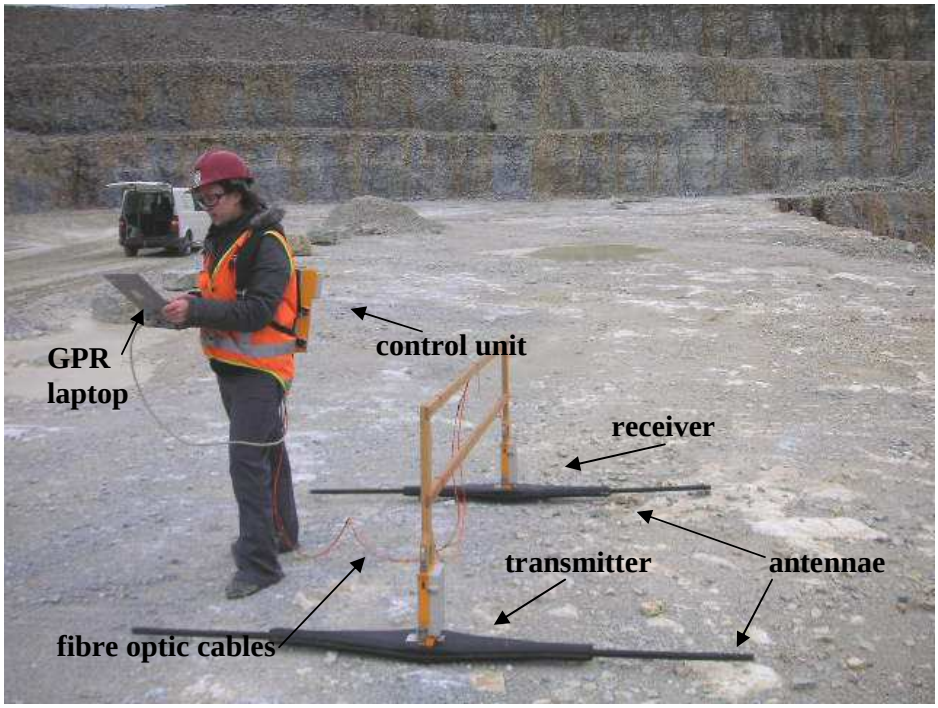

Figure 7.1 RAMAC GPR setup showing the control unit mounted onto a backpack carried by the operator. Attached to the control unit are fibre optic cables (orange) connected to a transmitter and receiver each mounted onto antennae of 50 MHz frequency spaced 2 m apart. The control unit is also connected via a communication cable to a portable laptop which is being held by the operator in the photo. This photo was taken on top of the Lower Steel limestone on the western side of the quarry (coordinates E2691273 N6316310 elev. 150 m).

The travel time (i.e. the time taken from instant of transmission to time of detection by receiver) is in the order of tens to thousands of nanoseconds (Reynolds, 1997). Two way time is converted to depth by the software which

includes assumed travel velocities. However, conversion is not always successful. For example the interpreted GPR thickness can sometimes be distorted if there are changes in conditions or calibration of velocities. The total two-way travel time range (scan) is displayed on the PC screen in the form of a radar gram, so as the antennae are moved over the ground the radar obtains a reflection profile (Reynolds, 1997). Profiles (section created by plotting traces side by side) are generated by the GPR software where the horizontal axis equals distance (across transect), and the vertical scale equals two-way reflection time which is converted into depth in metres for convenience by the GPR software. Further details on the RAMAC GPR can be found in the MalÅ Geoscience software manual version 2.28.

7.3 Application of GPR in carbonate environments

GPR is widely used to study the shallow subsurface at construction, archaeological, and landfill sites (Milsom, 1996). Carbonate environments have also been studied where good images of cave structures have been obtained using GPR, indicating effective applicability of the method. Pre-published field work trials suggest that GPR can effectively detect <10 m diameter caves and fissures in karstic terranes (Chamberlain et al., 2000). Such detections of caves produce prominent reflections on profiles (images) (Moldoveanu et al., 2002). GPR has lead to the success in interpreting the location of caves for example in the Corozal Basin in Belize (Moldoveanu et al. 2002). The detection of caves is of interest because they are natural sediment traps where certain deposits contain archaeological remains and Pleistocene fauna which may be preserved (Chamberlain et al., 2000). However, for this study cave detection is necessary due to the association of silica with the caves, and perhaps is more important for safety reasons. Ground failure and flooding can be difficult to manage if extensive karst occurs within quarry deposits. The manoeuvring of heavy machinery on top of voids can be potentially dangerous if the roof of the void was to collapse.

GPR is commonly used in quarries and mine excavation environments for detection of bedrock fractures, karst features, and geological discontinuities (Tillard and Dubois, 1995; Grasmueck, 1996; Botelho and Mufti, 1998; Dērobert

and Abraham, 2000; Beres et al., 2001; Orlando, 2003; Grégorie et al., 2006). Most GPR trials in limestone quarries focus on investigating different stratigraphic layers. For example, Schack von Brockdorff et al. (2003) determined the location of high $CaCO_3$ bryozoan (skeletal faunal species) mounds and relatively silica rich flint beds, in a limestone quarry in Southwest Sweden. GPR has also been successful in detecting caves and karst features in limestone quarries such as Kitley Caves within a Devonian limestone, Yealmpton, South Devon, U.K that intersect a disused lime quarry (Chamberlain et al., 2000). A good example of the use of GPR in a limestone quarry is the trial by Henson et al., (1997). A limestone quarry near Anna, Illinois contains clay and air filled karst that disrupted quarry operations. GPR (using 50 and 100 MHz antenna frequency) successfully imaged the fine grained limestone and chert quarry deposit, providing information regarding fractures to quarry operators. Reflections of caves on the profile images appeared as (half) hyperbolas (Henson et al., 1997).

7.4 Method

Site selection: For this study, two areas of interest were targeted for the GPR trial. These were confirmed locations of caves: (1) the observed cave in the upper bench of the High Grade unit (western face); and (2) the cave structures above the Upper Steel (north western face). Other sites were chosen at random, and included a transect over at least one site in each limestone quarry unit.

Transects: A transect is a line running across an area (e.g. over a cave). An example of a transect used in this study is shown in Figure 7.2. Walking alongside a transect, the GPR setup is carried by an assistant, side by side with the operator (carrying the control unit and PC). The trend of each transect was chosen at random, and in a few cases, a number of trends (e.g. north-south versus east-west) at the same site were measured. Transects are mainly across quarry benches, however, one was also carried out near the airstrip southwest of the quarry pit. Locations of all transect sites are shown on Figure 7.3. Table 7.1 shows the location and number of each of the 13 transects or profiles, and any additional comments.

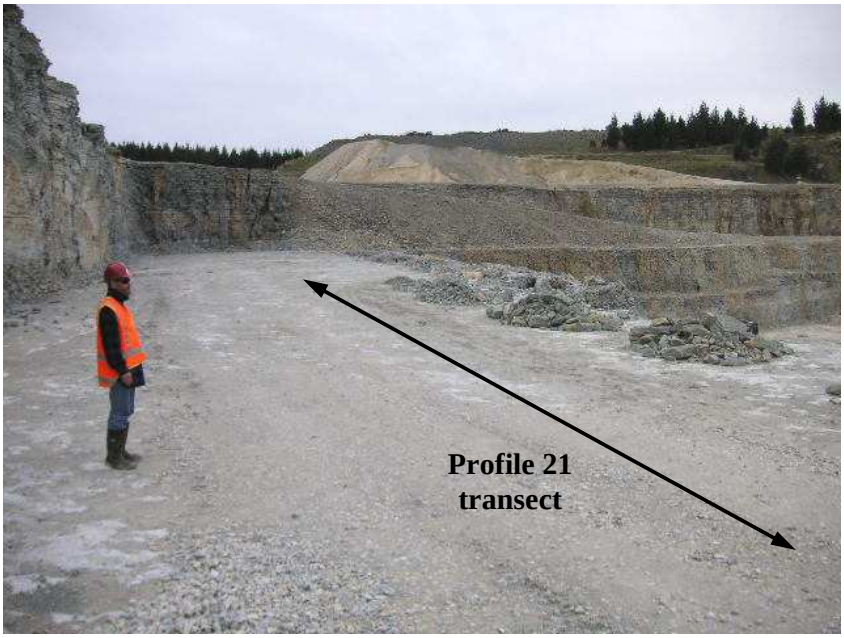

Figure 7.2 Photo taken of the transect walked (arrow) for profile 21. The transect is located on the top of the second High Grade bench below which a limestone cave is exposed, western side.

Settings: The GPR survey type used is fixed-offset profiling where a constant antenna spacing is maintained. Antennae frequency, sample distance, and the antennae spacing was based on recommendations from the MalÅ Geoscience software manual version 2.28, and settings used in some trials from previous workers, for example Henson et al. (1997); Sigurdsson and Overgaard (1998); Elfouly (2000). Two antennae with a frequency of 50 MHz were linked by a wooden bar at a fixed distance apart of 2 m. A frequency of 50 MHz is suitable for a target size ≥5 m, has an effective penetration depth range of 5-20 m, and a maximum penetration depth of 20-30 m. A recommended sampling interval is 0.20-0.50 m. Consequently, samples were collected by the GPR every 0.2 m, and set as a sample collection interval on the PC.

Figure 7.3 Transect location map for all profiles measured using ground penetrating radar in McDonald's Oparure Lime Quarry. The cluster of points (centre, top), are located on top of the upper High Grade bench below which a limestone cave is exposed. Aerial photo taken Feb 2007, sourced from McDonald's Lime Ltd..

Table 7.1 Transect information including profile number, location, length, and comments for all measured profiles.

Transect and profile No.	Site location	Transect description	Transect length approx. (m)	Radar gram comments
19	On second High Grade bench, western side	2 m from bench edge, 3 m above existing cave, trending from south-north	30	Clear parabolic reflections, cave exposed and detected
20	On second High Grade bench, western side	4 m from bench edge, 3 m above existing cave, trending from south-north	30	Clear parabolic reflections, cave exposed and detected
21	On second High Grade bench, western side	6 m from bench edge, 3 m above existing cave, trending from south-north	25	Clear parabolic reflections, cave exposed and detected
22	On second High Grade bench, western side	14 m from bench edge, 3 m above existing cave, trending from south-north	25	Clear parabolic reflections, cave exposed and detected
23	On second High Grade bench, western side	2 m from bench edge, 3 m above existing cave, trending from east-west	12	Slightly angled reflections, cave exposed, and not detected
24	On second High Grade bench, western side	5 m (north) from start point of transect 19, 3 m above existing cave, trending from east-west	10	Subhorizontal reflections displaced by sharp vertical contact, possible master joint structure
25	On second High Grade bench, western side	30 m (north) from start point of transect 19, 3 m above existing cave, trending from south-north	28	No reflections of structures, no caves or voids exposed, or detected
26	On Aglime, east of road, western side	Approx. 5 m from bench edge, approx. 18 m above existing cave in upper bench of the High Grade, trending from south-north	90	Weak reflections convex in shape, cave indicated by 1) drill hole information near location and 2) observed cave in the upper bench of the High Grade
27	On Aglime, on western road, western side	Unknown ground (no exposed cave structures evident), trending from south-north	62	No reflections of structures, no caves or voids exposed, or detected
28	South of western end of airstrip, near farm fence	Unknown ground, above soil profile, Kauroa Ashes, Mahoenui Group mudstones, and Otorohanga Limestone, trending from east-west, and north-south	47	No reflections of structures, no caves or voids observed, or detected
29	On floor of quarry, above Sub-economic	Unknown ground, trending from south-north	42	Very weak reflections of a concave shape, no caves observed, possible structure, cave or other discontinuity
30	On Lower Steel close to northern face	Unknown ground, approaching steel pipe near end of transect, trending from south-north	74	Steeply angled reflections, close to quarry face, and steel pipe, also slightly concave reflections of an unknown structure
31	On second High Grade bench, south side	Unknown ground, trending from east-west	44	No reflections of structures, no caves or voids exposed, or detected

7.5 Results

Some filtering of the data was conducted to attempt to remove noise, focus the images, and optimise data quality. However, the available filters did not seem to improve the radar grams, so only the raw profiles are presented.

All radar gram profiles corresponding to each transect are located in Appendix G-7.1. All profiles that indicate main structures (e.g. caves) show prominent reflections corresponding to an effective penetration depth of between 6-10 m. Features below the penetration thickness cannot be detected by the GPR system, therefore, anything shown on the profile below the effective penetration depth are multiples and are ignored.

At the time of the trial only one cave was exposed within the quarry walls. This cave (Figure 7.4) was located within the second bench of the High Grade unit on the western side of the quarry and provided a good location to test whether the GPR could detect caves. Initially, the cave was closely inspected to estimate the approximate depth from the top of the bench to the top of the cave structure (approx 3 m). The trend of this cave is approximately east-west.

Transect numbers 19-24 (Table 7.1) are located on top of this cave. Transects 19-22 were parallel, and orientated north-south, perpendicular to the assumed cave trend. The profile generated from transect 21 is shown in Figure 7.5. The reflections shown in the profile reveal a hyperbolic shape, and indicate the presence of a cave structure. The cave is not originally shaped like a hyperbola (more cylindrical), this is because the GPR receives signal from objects that are not only directly beneath it, but objects that are at a close distance. The time required for the signal to travel from an object and back will vary depending on the distance between the object and antenna. The shortest time is received is when the antenna is directly above the object (shown as highest point on hyperbola), therefore the cave cross section is read by the GPR as a hyperbola. Profiles 19, 20, and 22 show similar patterns.

Figure 7.4 (A) Photo of the western side of the quarry (looking west) showing the location of the main limestone cave exposed within the second (upper) bench of the High Grade unit. (B) Photo showing entrance to limestone cave within the second bench of the High Grade unit. Previous blasting (indicated by rubble surrounding entrance) has exposed the cave.

The depth to the cave structure only matched field observations for one profile, that is profile 19 (Figure 7.6). The top of the structure occurs at approximately 3 m on the y axis, which was observed in the field. However, the other profiles for the same cave do not match these observations, with apparent depths of ~1-2 m. This could be because the cave may be getting closer to the surface at these profile locations.

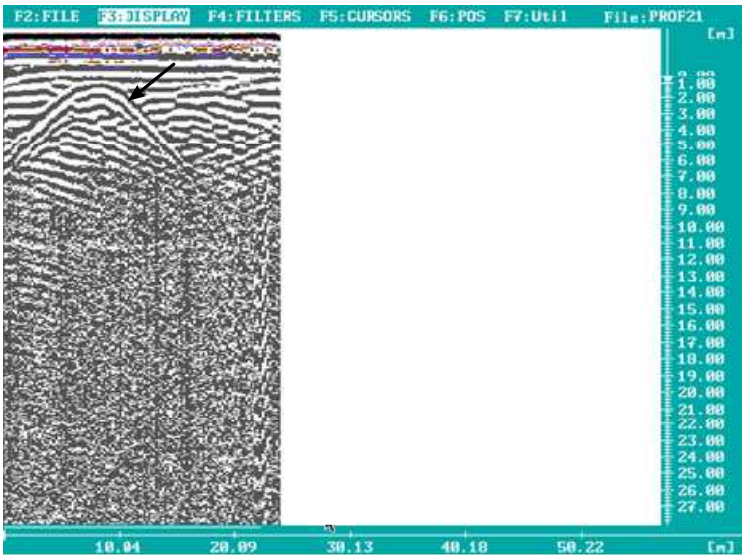

Figure 7.5 Radar gram of profile 21 trending N-S measured over an observed limestone cave within the second bench of the High Grade unit, western side of McDonald's Oparure Quarry. A clear reflection of a cave structure is shown by the arrow.

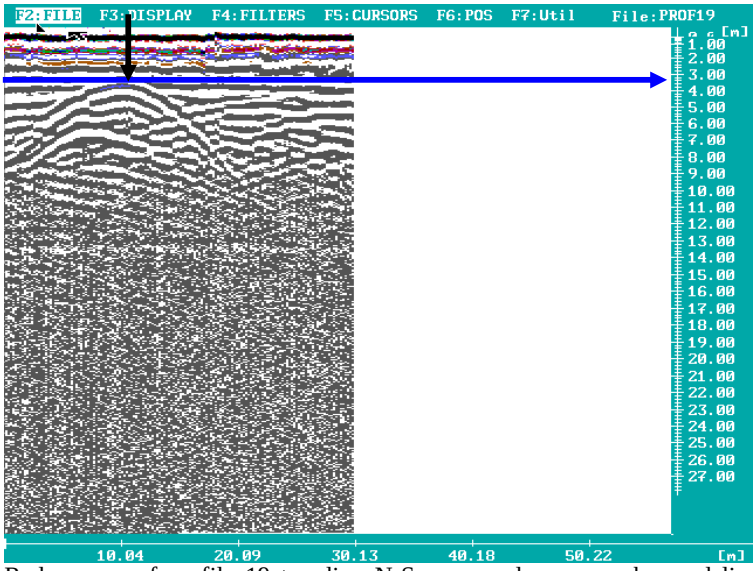

Figure 7.6 Radar gram of profile 19 trending N-S measured over an observed limestone cave within the second bench of the High Grade unit, western side McDonald's Oparure Quarry (2007). A clear reflection of the top of a cave structure is shown by the black arrow. The blue line indicates the depth to the top of this structure.

Transects 23 and 24 were at different orientations (e.g. along the trend of the cave east-west). Profiles from these transects (Appendix G-7.1) do not show the same reflections as the profiles measured perpendicular to the cave trend. Any reflections that would indicate a structure are absent. However, there is a sharp vertical line on profile 24 displacing the reflections; it could represent a master joint set. Nevertheless, the GPR does not detect the cave if the transect is trending parallel to the cave. Running multiple transects at different orientations across the same area is therefore crucial to the detection of caves.

On top of the Aglime unit on the western side of the quarry previous drilling has intercepted a cavity not yet exposed at time of the trial located approximately 18 m from the top of the bench to the top of the cavity. A profile (transect 26) was measured across this area (Figure 7.7). Again, there is a clear cave structure detected as indicated by the convex hyperbolic reflections. The question then becomes is this the same cave detected in the underlying second High Grade bench?

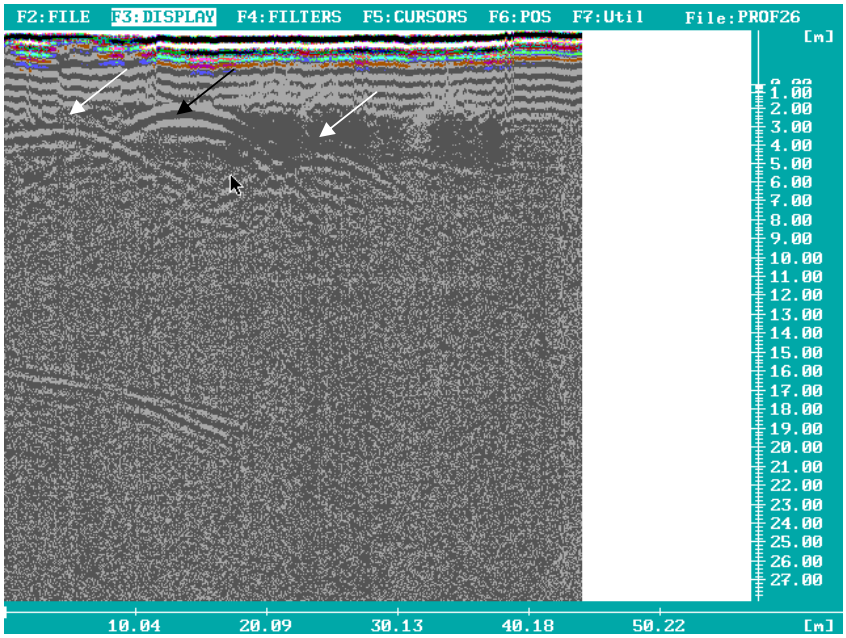

Figure 7.7 Radar gram of profile 26 trending N-S measured east of the road on top of Aglime unit where a drill hole has intercepted a cavity, western side. The cave observed in the upper bench of the High Grade is approximately 18 m below the transect. The black arrow points to a clear reflection indicating a cave structure is present, and the white arrows represent multiples of cave walls.

It is likely that the GPR cannot effectively penetrate this far, and reflections suggest 2-3 m depth so the structure may be another separate cave, or a different cave within the same cave system that the High Grade cave belongs to.

Transects 25 (above upper High Grade bench past the cave below), 27 (above Aglime on western road), 28 (near airstrip), 29 (above Sub-economic on floor of quarry), 30 (above Lower Steel), and 31 (above upper High Grade bench, southern) (Appendix 7.1) are all areas where caves are not detected. Lack of major hyperbolic structures in the reflection profiles are evidence of this. However, other orientations were not investigated, so it is recommended that transect grids are setup to measure a range of orientations for future studies. The profiles typically show a series of horizontal reflections (Figure 7.8). Transect 28 near the airstrip probably required changing the GPR settings to obtain effective penetration for a different medium (i.e. soils, ashes, and mudstones). Nevertheless, the depth of the limestone at greater than 10 m (which essentially contains the caves) probably exceeded effective penetration.

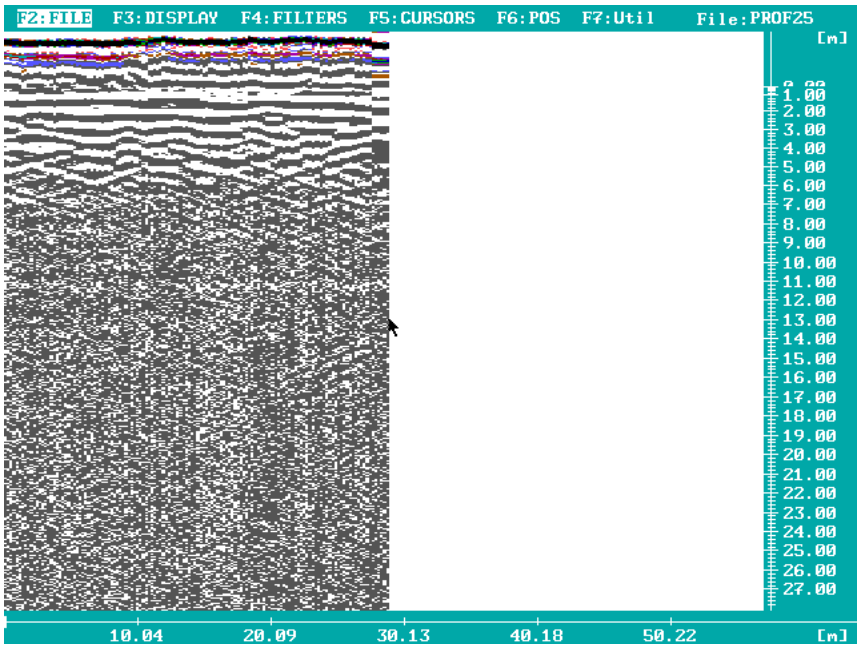

Figure 7.8 Radar gram of profile 25 trending N-S measured over the second bench of High Grade, western side. No obvious structure appears to be present.

Since the GPR used was unshielded there is potential for interference to occur, particularly the interference of high quarry walls close to the locations measured. At transect 30 (above the Lower Steel), as a quarry wall was approached with the GPR some reflections displayed on the profile became progressively steeper as the wall was approached closer and closer. Figure 7.9 shows the profile from transect 30 showing these steeply dipping reflectors on the right side of the profile. A steel pipe was also lying on the ground near the quarry wall and could have also caused some interference.

Figure 7.9 Radar gram of profile 30 trending N-S measured on top of the Lower Steel. To the right of the profile steeply dipping reflectors (white arrow) represent interference caused by a quarry wall and possibly a steel pipe lying on the ground near the end of the transect. Slightly curved reflections in the circle might represent multiples of the interfering quarry wall. The black arrow is a mouse pointer.

7.6 Discussion

Results from this trial show that GPR is a good tool for identifying caves in the shallow subsurface at McDonald's Oparure Quarry. Direct comparison of profile 21 (Figure 7.5) and others was able to be made with outcrop (below the profile) containing a cave, verifying the integrity of the GPR data. Due to the radar waves moving at a higher velocity in air compared to a solid medium, caves are

relatively easy to detect using GPR and therefore can be identified prior to blasting and drilling. The detailed interpretation of the size and shape of caves detected is beyond the scope of this study. The GPR software available for this study is not capable of interpreting the data. It is uncertain whether cave size, continuity, and extent can be assessed from these profiles. Caves and karst landscapes are complex 3D features. Previous studies recommend that data integration combining other geophysical methods (e.g. microgravimetric) is important in achieving accurate interpretations of cave shapes and sizes (Beres et al. 2000). Microgravimetric surveying measures minute variations in the gravitational pull of the Earth, caused by differences in the density of rocks in the subsurface. Voids and cavities can be interpreted from these readings and reveal information on depth and shape (Reynolds, 1998). This method is sometimes used in combination with GPR (Beres et al., 2000).

Furthermore, this GPR method is not a method for quantifying cave infill. However, cave infill can be studied once caves have become exposed in the quarry, where access into the caves is possible. Quantification could prove to be difficult because one would need to enter the caves to measure infill thickness.

Another important aspect is the fact that the GPR only detects caves when the profiles are measured perpendicular to the trend of the caves. It is recommended that transects are oriented across a number of different trends to ensure caves are definitely detected. This is recommended for all the locations that are measured.

Interference is a common problem with GPR. Metal objects and radio transmitters can often saturate receiver electronics (Milsom, 1996). However, the problem identified at the quarry is the interference caused by the quarry faces in the vicinity of the GPR equipment. It is recommended that a shielded GPR is used in the future to avoid this. Another aspect to take into consideration is that the RAMAC GPR only has an effective depth penetration of approximately 6-10 m; therefore any features below this penetration thickness are not detected with the GPR system.

CHAPTER EIGHT

Summary, conclusions, and recommendations

8.1 Introduction

McDonald's Lime Ltd operates an industrial quarry at Oparure near Te Kuiti, in the King Country region of North Island, New Zealand. This quarry extracts high quality limestone (>90% $CaCO_3$) from the latest Oligocene-earliest Miocene aged Otorohanga Limestone, the topmost formation in the Te Kuiti Group. The geology at the quarry comprises two overburden units, namely Quaternary Kauroa Ash overlying Early Miocene Mahoenui Group mudstone, above the main Otorohanga Limestone which has been subdivided into six quarry units. The topmost of these (Caprock) is thin (2-5 m) and is treated as overburden. The remaining five units are Upper Steel, Aglime, High Grade, Lower Steel, and Sub-economic, each of which has a particular product end use, such as for the agricultural industry (Aglime), road construction industry (High Grade), or iron and steel industry (Upper and Lower Steel). The Sub-economic unit represents the limestone that is presently beneath the quarry pit and is currently uneconomic to extract. The chemical composition of the different limestone grades must follow strict quality guidelines imposed by the different industries. For example, the iron and steel industry imposes a strict requirement of <1.7% silica and <0.09% sulphur in the burnt lime product derived from the steel grade limestone. Silica and sulphur have a negative effect on some stages of the steel manufacturing process as they are impurities which affect the overall quality of steel; furthermore, silica can act as an abrasive (under high pressure) and cause mechanical wear of equipment. The mechanical wear is of greatest concern to New Zealand Steel who use lime as a flux in the steel manufacturing process.

Throughout this study the use of the word silica is more or less synonymous with silica-bearing minerals, siliceous materials, insoluble residue, and siliciclasts (non-carbonate grains that have been eroded and transported to a depositional environment), and includes minerals such as quartz, feldspar, glauconite, and clay minerals. Other non-carbonate components can be non-siliceous minerals, such as

pyrite (iron sulphide) and gypsum (calcium sulphate). Collectively, these non-carbonate impurities constitute what is referred to as the 'silica issue' in this study.

McDonald's Lime are aware that silica levels vary across their Oparure limestone resource, and so hold some concerns about their ability to maintain quality guidelines on their limestone products. Consequently, it is relevant that knowledge be gained about the nature, distribution, and origin of silica-rich zones within the limestone resource so as to allow for greater certainty in quarry planning and operations.

To achieve this aim a combination of field and core logging work was undertaken. Rock mass characteristics were described and measured in the field including the description of physical properties of the intact rock and discontinuities such as joint spacing, aperture, and infill. Rock mass was also described in three limestone drill cores. Additionally, the textural, mineral, and chemical composition was determined for the six quarry limestone units. This work shows that silica-rich materials are mainly associated with the discontinuities in the limestone units.

8.2 Discontinuity types

Discontinuities are naturally occurring features such as joints and bedding that separate the intact rock blocks (host limestone) within a rock mass. This study has identified that silica is mainly associated with six discontinuity types in the resource at McDonald's Oparure Lime Quarry. Silica is also associated with coatings of dust on rock surfaces, here referred to as surface accumulations, sourced from quarry operations such as blasting and vehicle traffic, but this source is minor compared to the siliceous materials within the six main discontinuity types. A classification scheme has been devised for the six discontinuity types (Chapter 3, Figure 3.15). These are:

(1) **Discrete seams** - Dissolution seams characterised by smoothly undulating, non-sutured, thin zones of insoluble residue/non-carbonate materials. The

insoluble residues are concentrated and closely packed, and are continuous at core scale. In outcrop they range from rusty brown to blue-grey silts and clays.

(2) **Diffuse seams** – Dissolution seams characterised by their wispy nature that converge and diverge within the host limestone. The non-carbonate materials are dispersed within the limestone, are loosely packed, and are continuous at a core scale.

(3) **Subhorizontal stylolites** – Features produced by pressure dissolution during burial that are stratiform and laterally continuous at core scale. Stylolites display a prominently sutured surface that concentrates variable amounts of insoluble residue such as clays, quartz, and feldspar. Their amplitudes are typically <10 mm high, and the stylolites themselves are generally <1 mm thick.

(4) **Subvertical stylolites** – Features produced by pressure dissolution due to tectonic processes such as compressive stresses rather than simple burial forces. Their characteristics are similar to these of subhorizontal stylolites except for their typically near-vertical (to bedding) orientation.

(5) **Joints** – Near-vertical fractures in the rock mass formed as a result of deformation processes such as folding, faulting, and uplift. Joints may have two types of infill, including clays washed in from an external source and/or clays such as palygorskite which have chemically precipitated *in situ* within joints. Two joint types have been identified in the quarry based on their different field characteristics: (1) master joints which are more open, more persistent, and commonly contain more joint infills than small joints; and (2) small joints which are mainly tight, persistent over shorter distances compared to master joints, and rarely contain infill.

(6) **Caves and other karst features** – Caves, dolines, and fissures that have formed in the limestones as a result of dissolution by percolating fresh water during weathering. These act as natural sediment traps for siliceous materials, the infills being enriched in clay minerals, including palygorskite as identified in joint infills.

8.3 Rock mass characteristics of quarry limestones

The rock mass characteristics of the quarry limestone units are summarised in Figure 8.1. The Upper Steel, Aglime, High Grade, and Lower Steel units possess different characteristics, the Upper Steel being the most distinctive of the quarry limestone units. The Upper Steel comprises both blocky bedding (upper section) and flaggy bedding (lower section), while the other units are predominantly flaggy. All the limestones are well cemented; however, the Upper Steel is locally porous. The flaggy appearance is a result of the sedimentary layering of two characteristic beds types modified by pressure dissolution during burial, namely thicker limestone beds relatively poor in silica materials (flags) and thinner beds (dissolution seams) relatively enriched in silica materials such as quartz, feldspar, clay, and glauconite minerals. The location of dissolution zones relates closely to a primary sedimentary control involving the alternation of carbonate-rich sediments, possibly mainly storm emplaced, and more siliceous enriched sediments associated with finer background sedimentation between carbonate deposition.

The average thickness of the dissolution seams between the limestone flags varies across the four quarry limestones, decreasing from Aglime, to High Grade, to Lower Steel, to Upper Steel (Chapter 4, Section 4.3.1 Figures 4.15-4.17). The limestone flags (referred to as host rock in this study) bounding the dissolution seams show similar thicknesses for the Lower Steel and High Grade units, while Aglime has the thinnest flags, and Upper Steel the thickest (Figure 8.1).

Figure 8.1 (Facing page) Rock mass characteristics of quarry limestone units at McDonald's Oparure Lime Quarry including rock material, flag thickness, joint spacing and joint aperture. Sparry limestone = sparite cement dominant, micritic limestone = micrite cement dominant. Percentage of core comprising stylolites, and discrete and diffuse seams are based on averages calculated from drill core information in cores BH501, BH502, and BH503. Joint spacing has been converted to true spacing. Master joints are characteristically longer (extend beyond the height of a quarry bench), more open, and commonly contain joint infills, whereas small joints are shorter (terminate across the distance of several limestone flags), are tighter, and rarely contain joint infill. Image (A) shows an example of dolines (karst features) in the Upper Steel unit, western face. (B) Shows an example of a radar gram containing recorded reflections (from transmission of radar waves below the subsurface), showing a clear structure (likely a void or cave) detected using ground penetrating radar in the Aglime unit. (C) A limestone cave exposed in the High Grade unit containing limestone rubble, lower bench, western face. (D) A relatively small void exposed in the Lower Steel unit, western face. Subhori. = Subhorizontal, Subvert. = Subvertical.

Figure 8.1 Rock mass characteristics of McDonald's Oparure Lime Quarry limestone units

Quarry limestone unit	Rock material	Flag thickness (0–250)	% of core comprising discrete seams (0–5)	% of core comprising diffuse seams (0–20)	% of core comprising stylolites: Subhorizontal	% of core comprising stylolites: Subvertical	Joint spacing	Joint aperture	Caves and other karst features
Upper Steel	Creamy white/light yellow sparry limestone Moderately weathered Locally porous Upper section knobbly Lower section flaggy Contains the thickest flags of all the limestone units	Av. = 240 mm	0.6%	0.2%		Subhori. = 0.004% Subvert. = <0.001%	No joint system		A: dolines; silica-rich infill; Collapsed dolines and fissures
Aglime	Blue-grey/orangey yellow micritic limestone Fresh Flaggy Contains thinnest flags of all limestone units	Av. = 100 mm	4.5%	18%		Subhori. = 0.001% Subvert. = <0.001%	Master = 0.31 m Small = 0.30 m	Master = 6.7 mm Small = 1.2 mm	B: convex reflections of a structure; 10 m; Cave/void detected (arrow) by GPR
High Grade	Blue-grey/orangey yellow sparry limestone Moderately weathered Flaggy Contains similar flag thicknesses to Lower Steel limestone unit	Av. = 120 mm	2.6%	0.1%		Subhori. = 0.002% Subvert. = <0.001%	Master = 2.45 m Small = 0.68 m	Master = 4.1 mm Small = 2 mm	C: cave; 0.5 m; Cave detected by GPR
Lower Steel	Creamy white/orangey yellow Sparry limestone Moderately weathered Flaggy Local cross-bedding Contains similar flag thicknesses to Aglime limestone unit	Av. = 120 mm	1.3%	0%		Subhori. = 0.006% Subvert. = <0.001%	Master = 3.70 m Small = 0.49-0.69 m	Master = 14.4 mm Small = 1.6 mm	D: 0.5 m; Void (arrow)
Sub-economic	Not exposed in outcrop		2.7%	1.9%		Subhori. = 0.007 % Subvert. = <0.001%	Not exposed in outcrop		Caves/voids not detected

Outcrop observations show that subhorizontal and subvertical stylolites occur especially in the Upper and Lower Steel units, but core studies indicate that they occur in all the limestone units.

Vertical joints generally become more closely spaced from the bottom unit (Lower Steel) to the top unit (Aglime) (Figure 8.1), and contain silica-rich infills likely sourced from the overlying Mahoenui Group mudstones, and clay minerals (palygorskite) that formed *in situ.* There appears to be no trend in average joint aperture width.

Caves, collapsed dolines, and/or fissures occur in all limestone units. These karst features have clay-rich infills, most likely washed in from the overlying Mahoenui Group mudstones.

8.4 Discontinuities in cores

The following results include information gained from the detailed logging of discontinuity types in three drill hole cores from the 500 series (BH501, BH502, and BH503).

A variety of seam thicknesses occurs in the cores through the different quarry limestone units. In decreasing order of thickness these are: Aglime (1-19 mm), Lower Steel (1-18 mm), Sub-economic (1-18 mm), High Grade (1-14 mm), Caprock (1-6 mm), and Upper Steel (1-6 mm). The modal seam thickness is 1 mm for all limestone units. In terms of the number of seams per metre, the Aglime unit has the most (14-20), then High Grade (13-14), Sub-economic (10-11), Lower Steel (9-10), Upper Steel (3-5), and Caprock (4-5). The most important data here relate to the total seam thickness of discrete seam material in a given metre of limestone. The lowest quality limestones (i.e. Aglime and Sub-economic) have the largest total thickness of discrete seam material per metre, followed by High Grade, Lower Steel, Caprock, and Upper Steel. This trend provides strong evidence that it is the discrete seams that potentially affect the overall amount of silica in the rock (bulk composition), and so to a decrease in overall carbonate quality. Regardless of the relatively small amount of seam material in the Caprock, it is still low quality because the host limestone itself is

very argillaceous or clay rich. Discrete seams comprise up to 6% of the Aglime unit, up to 4% in the Sub-economic unit, up to 3% in the High Grade, up to 2% in the Lower Steel, up to 1.5% in the Caprock, and <1% in the Upper Steel unit. The average (from the three cores) percent of limestone comprising discrete seams is shown in Figure 8.1.

Diffuse seams are less common than discrete seams. They mainly occur within the Aglime unit (up to 308 mm per metre), Caprock (up to 224 mm per metre), and Sub-economic (up to 34 mm per metre) units. Diffuse seams are rare in the remaining limestone units (Upper Steel, High Grade, and Lower Steel). The average percentage of limestone occupied by diffuse seams for each limestone unit is shown in Figure 8.1.

Subvertical and subhorizontal stylolites are also not as common as discrete seams. Subhorizontal stylolites are much more common than subvertical stylolites. In decreasing order the maximum number of subhorizontal stylolites per metre is as follows: Sub-economic (10), Lower Steel (9), Upper Steel (6), Aglime (4), and High Grade (3) units. In decreasing order, the number of subvertical stylolites per metre is Caprock (3), High Grade (2), Lower Steel (1), Sub-economic (1), Aglime (1), and Upper Steel (less than 1) unit. The average percentage of stylolites (from the three cores) comprising the quarry limestone units is shown in Figure 8.1.

Joint infills are rare in the cores, but include calcite veins (partially healing some joints by secondary precipitation), and siliceous materials such as clay minerals (e.g. palygorskite).

Core logging has shown that all the limestone units are well cemented, and only occasionally porous. Porous zones occur sporadically in the Upper Steel and Lower Steel units. The host limestone is typically purer in the Upper Steel and Lower Steel, and the Aglime, High Grade, and Sub-economic units are visually less pure.

8.5 Rock mass composition

Based on field and core measurements the percentage of carbonate and non-carbonate material in the intact limestone (host limestone) has been calculated. In addition, the percentage of non-carbonate material from discrete and diffuse seams and joint infills has been calculated. This was determined for all the exposed limestone units in the quarry in an attempt to show the relative contribution of silica (non-carbonate material) from discontinuities and the intact rock, to the rock mass as a whole (Figure 8.2). There is some error involved in the discrete and diffuse seam percentages as the seam spacings were not able to be converted to true spacings because their orientation is unknown. Furthermore, some error was involved in the joint spacings, especially for the High Grade unit due to the paucity of the number of joints measured. To determine the joint infill percentage the number of joints per metre was calculated together with the average aperture width per metre. The joint infill is assumed to fill in the full width of the aperture. Figure 8.2 shows that the majority of the rock mass in each unit comprises carbonate material, followed next by non-carbonate material in the intact limestone except for the Aglime, then non-carbonate material in the discrete and diffuse seams, and finally non-carbonate material in the joint infills.

8.6 Mineral and textural composition of quarry limestone units

A summary of the mineral and textural composition of the quarry limestone units is contained in Table 8.1. Low-Mg calcite is the dominant mineral in all the quarry limestone units. The carbonate content of the quarry limestone units derives from the bioclasts or skeletons that construct the limestones, and the micrite and calcite spar cement that occurs within and between these skeletal grains, cementing them together. Carbonate content was determined by petrography and ranged from 70-99% (estimate), with the lower values in the Caprock (av. 83%) and the highest values from the High Grade (av. 96%), Upper Steel (av. 99%), and Lower Steel (av. 97%). Aglime (av. 91%) and Sub-economic (av. 94%) show intermediate values.

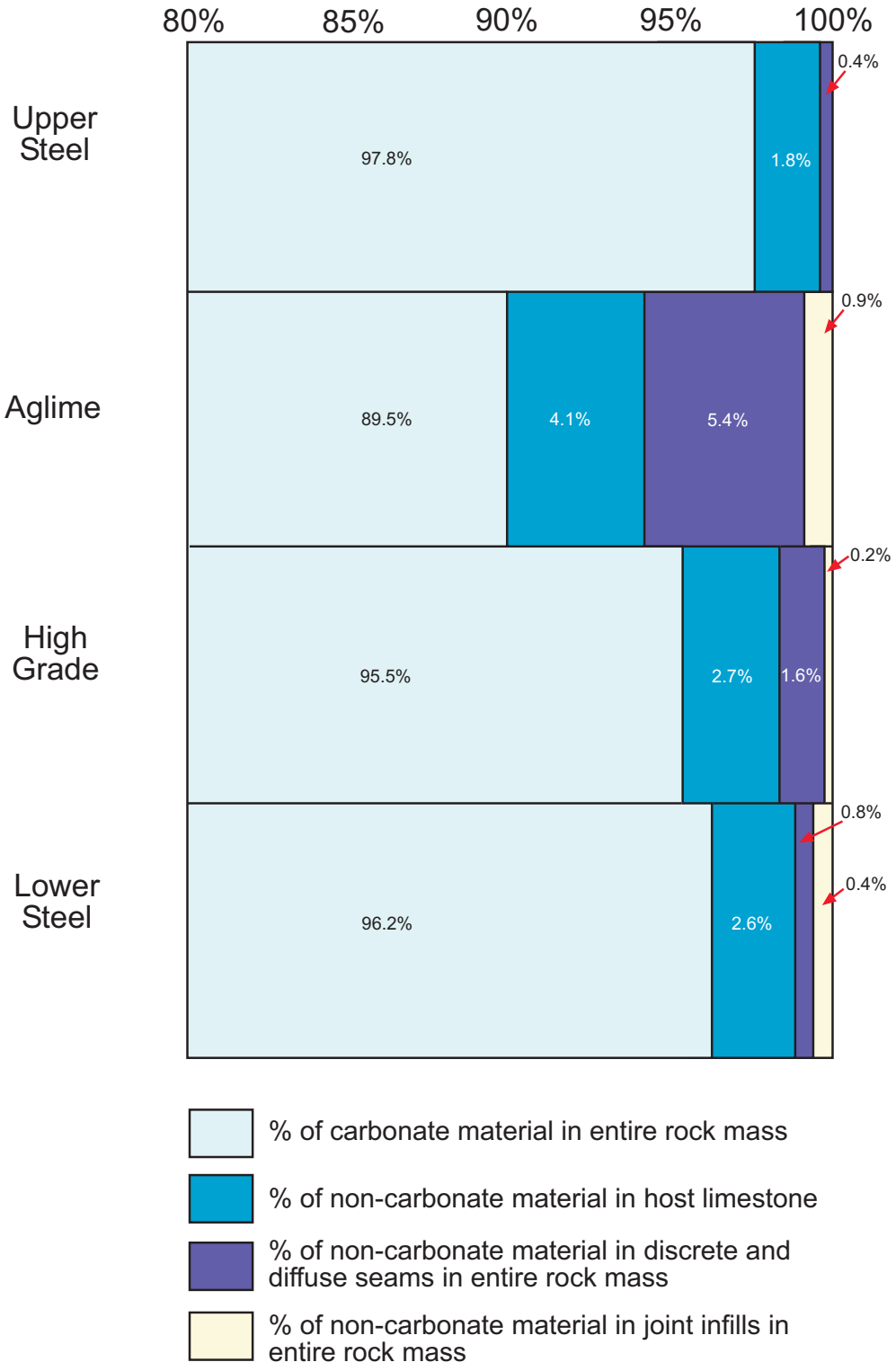

Figure 8.2 The contribution of carbonate and non-carbonate materials as a percentage of the entire rock mass from host limestone, discrete and diffuse seams, and joint infills, for each of the exposed quarry limestone units at McDonald's Oparure Lime Quarry.

The dominant bioclast in all the quarry limestones is bryozoan skeletal fragments, with the exception of some Caprock samples taken near the upper contact with the overlying deeper water Mahoenui Group mudstones which contain abundant planktic foraminifera. Other skeletal types, in decreasing order of abundance, include benthic foraminifera, echinoderms, bivalves, worm tubes (annelids), planktic foraminifera, and calcareous red algae, collectively typical of non-tropical carbonates. Bioclasts are rarely whole, fragmented, slightly to moderately abraded, and typically of medium to coarse sand size. Sparite cement occurs in interparticle and intraparticle pore space, and dominates in the Upper Steel, High Grade, Lower Steel, and Sub-economic units (biosparites). However, micrite dominates over sparite in the Caprock and Aglime units (biomicrites). Calcite also occurs in veins in thin section (common in all limestones except Caprock), where it typically partially heals fractures in the limestone units. Interparticle porosity is also common in the Upper Steel unit in thin section, and is observed locally in outcrop.

The remaining portion of the quarry limestone units comprises siliciclasts (non-carbonate fraction) ranging from 1-30%. These include the following siliceous minerals, in decreasing order of abundance: pyrite grains, pyrite infills, glauconite pellets, glauconite infills, quartz, feldspar, clays, and sedimentary rock fragments. Siliciclasts are predominantly evenly dispersed throughout the host limestone, and range in their shape from angular to subrounded (subrounded most common), and occur in a range of grains sizes from very fine sand to granule, but typically fine sand size.

8.7 Mineral and textural composition of overburden units and discontinuity materials

The mineral and textural composition of overburden units and discontinuity materials is also summarised inside Table 8.1. In contrast to the limestones, the overburden units and discontinuity materials are dominated by siliceous minerals. Kauroa Ash (overburden unit) comprises clays (vermiculite, halloysite, gibbsite) and quartz (minor cristobalite, a polymorph of quartz); and Mahoenui Group mudstones comprise clays (smectite, illite), calcite, quartz, feldspar, and locally gypsum.

Joint and cave infill material shows similar compositional characteristics to the overburden units (Kauroa Ash and Mahoenui Group mudstones). Type 1 joint infills comprise clays (smectite, palygorskite), quartz, calcite, and oligoclase feldspar, and type 2 joint infills comprise palygorskite, quartz, and calcite. Palygorskite [Mg, $Al)_2S_{14}O_{10}(OH)$] is an unusual clay mineral precipitated *in situ* as a joint infill and is also found in cave systems. It is characterised by a leathery texture, is extremely fibrous, and commonly forms as discrete sheets. Cave infills have clays (smectite/chlorite, palygorskite), quartz, and calcite.

The mineral types in discrete and diffuse seams largely reflect the minerals occurring in the host limestones. Mineral estimates were obtained from petrography and show that calcite (as micrite, sparite cement, or bioclast fragments) ranges from 10-93% (av. 44%) within discrete seams. In thin section, diffuse seams show a carbonate content of about 40-70% (av. 60%). Clays (identified as smectite and illite from XRD) are the dominant siliceous mineral in both seam types, followed by quartz and feldspar 7-70% (av. 19%). Pyrite and glauconite are also present in both seams types, but in much lower concentrations, similar to that in the host limestone units (typically <2%). Discrete and diffuse seam siliciclasts range from very fine sand to coarse sand in size, and are angular to rounded in grain shape. The carbonate component is dominated by sparite cement and less common bioclast fragments in the discrete seams; and micrite is common together with common bioclast fragments in diffuse seams generally. An interesting finding was the identification of dolomite in some seams, a carbonate mineral not previously identified in the Otorohanga Limestone, probably because earlier studies analysed only the host limestone and not the dissolution seams.

Stylolites are very thin discontinuity features that collectively contribute very small concentrations of silica to the overall composition of the limestones compared to the seams (Figure 8.1). Clay is the dominant silica-bearing mineral found in these features, and quartz, feldspar, and glauconite in minor amounts occur as individual siliciclasts within the clay residue.

Table 8.1 Mineral, chemical, and textural information for overburden quarry units, quarry limestone units, discontinuity materials, and operation induced materials. %$CaCO_3$ was determined by acid titration, the values on the top line are a range, and the value on the second line is an average. Oxides were determined by x-ray fluorescence where the top values are also a range and the second line is an average. Black dots indicate if a mineral is present determined by petrography and/or x-ray diffraction. Grain size and sorting information was determined by petrography or laser particle size analysis. Oper. Ind. = Operation Induced.

Chemical composition of quarry units and discontinuity materials at McDonald's Oparure Lime Quarry

	Quarry unit or discontinuity material	No. of samples	% $CaCO_3$ range & average	No. of samples	Oxide range and average (%)										
					CaO	SiO_2	SO_3	Al_2O_3	Fe_2O_3	MgO	Na_2O	MnO	TiO_2	K_2O	P_2O_5
Overburden	Kauroa Ash	3	0 0	3	<0.01-1.23 0.65	29.32-57.10 41.70	0.06-0.14 0.09	21.82-36.01 28.32	7.03-9.59 8.65	0.42-1.88 1.08	<0.01-0.97 0.55	0.08-0.10 0.09	0.88-1.05 0.99	0.25-2.01 1.00	0.10-0.16 0.13
	Mahoenui Group mudstones	2	34.7-35.6 35.1	2	21.32-21.72 32.18	37.02-38.66 37.84	0.01-2.89 1.46	10.36-10.67 10.52	4.56-4.65 6.89	2.00-2.04 3.02	0.74-0.87 0.81	0.05 0.07	0.53-0.54 0.80	1.78-1.83 2.72	0.13-0.17 0.23
Limestone	Caprock	8	74.1-96.8 89.5	6	43.53-53.97 49.35	1.73-12.09 6.29	0.02-1.62 0.30	0.42-2.91 1.66	0.29-2.00 1.07	0.50-1.24 0.89	<0.01-0.29 0.11	0.02-0.03 0.03	0.02-0.15 0.09	0.09-0.64 0.34	0.11-0.35 0.18
	Upper Steel	6	97.3-98.9 98.2	6	54.60-55.55 55.15	0.23-1.19 0.64	<0.01-0.02 0.01	0.06-0.32 0.21	0.05-0.15 0.10	0.29-0.39 0.31	<0.01 <0.01	0.01 0.01	0.01 0.01	0.02-0.06 0.04	0.02-0.09 0.05
	Aglime	6	90.5-95.4 94.5	6	51.57-53.44 52.69	2.00-3.51 2.61	0.02-0.44 0.28	0.62-1.05 0.79	0.27-0.57 0.40	0.64-1.08 0.82	0.01-0.05 0.02	0.01-0.02 0.01	0.03-0.05 0.04	0.10-0.16 0.13	0.04-0.10 0.06
	High Grade	6	95.3-99.5 97.2	6	53.37-54.78 54.10	0.76-1.95 1.38	<0.01-0.37 0.20	0.23-0.48 0.38	0.17-0.27 0.22	0.44-0.85 0.62	<0.01-0.01 <0.01	0.01 0.01	0.01-0.02 0.02	0.03-0.09 0.06	0.03-0.05 0.04
	Lower Steel	5	96.3-98.7 97.3	6	54.00-55.12 54.51	0.71-1.59 1.12	<0.01-0.15 0.04	0.18-0.41 0.28	0.12-0.22 0.16	0.39-0.57 0.45	<0.01 <0.01	0.01 0.01	0.01-0.02 0.01	0.03-0.07 0.05	0.03-0.05 0.04
	Sub-economic	3	94.5-95.6 95	3	53.91-53.96 53.94	1.45-2.23 1.74	<0.01-0.01 0.01	0.36-0.41 0.39	0.18-0.44 0.29	0.43-0.54 0.49	<0.01 <0.01	0.01-0.02 0.01	0.01-0.02 0.02	0.07-0.09 0.08	0.05-0.06 0.05
Discontinuity materials	Diffuse seams	3	84.1-87.4 85.4	3	47.00-49.51 48.27	6.31-9.21 7.64	0.02-1.01 0.61	1.88-2.74 2.23	0.90-1.04 0.99	0.89-0.97 0.91	0.10-0.17 0.13	0.01 0.01	0.09-0.13 0.11	0.27-0.49 0.37	0.076-0.11 0.08
	Discrete seams	9	16-62.1 37.7	9	14.86-26.18 20.01	26.73-56.67 39.10	<0.01-4.97 1.05	6.98-12.03 9.22	3.48-6.99 4.99	0.97-6.90 3.02	0.42-1.70 1.00	0.02-0.06 0.04	0.28-0.65 0.46	1.48-2.34 1.98	0.12-6.16 0.98
	Joint infills (type 1)	7	5.8-95.9 62.7	6	1.43-49.07 30.67	7.23-59.46 27.02	<0.01-1.32 0.26	1.48-18.84 7.93	0.11-6.54 3.54	1.02-2.81 1.72	<0.01-0.63 0.29	0.01-0.05 0.03	0.01-0.81 0.32	0.05-2.19 0.97	0.01-0.30 0.15
	Palygorskite (type 2)	2	65.1-68.8 67	2	36.94-38.02 37.48	18.86-20.52 19.69	0.26-0.49 0.37	3.86-4.33 4.09	0.64-0.94 0.79	3.51-3.52 3.51	0.02-0.12 0.07	0.02 0.02	0.05-0.07 0.06	0.20-0.26 0.23	0.11 0.11
	Cave infills	3	0-10.7 2.7	3	1.04-8.91 3.96	49.71-61.49 55.09	<0.01 <0.01	16.87-21.06 18.86	5.57-8.86 6.96	2.07-2.50 2.31	0.29-1.02 0.57	0.03-0.06 0.05	0.67-0.78 0.72	1.74-1.98 1.86	0.08-0.36 0.22
Oper. Ind.	Surface accumulations	2	68.7-73.3 71	23	40.67-41.18 40.93	12.91-15.08 13.99	0.34-0.86 0.60	3.57-3.72 3.65	1.76-1.78 1.77	1.93-2.22 2.07	0.21-0.31 0.26	0.02 0.02	0.16-0.20 0.18	0.57-0.67 0.62	0.34-0.86 0.17

Table 8.1 continued. Note abbreviations: Dolo. = Dolomite, Cristo. = Cristobalite, Feld. = Feldspar, Glauc. = Glauconite, Smec. = Smectite, Vermic. = Vermiculite, Halloy. = Halloysite, Paly. = Palygorskite, Gibb. = Gibbsite, mod. = moderately, and ext. = extremely.

Mineral composition and textural characterisitics of quarry units and discontinuity materials

	Quarry unit or discontinuity material	Calcite	Dolo.	Quartz	Cristo.	Feld.	Pyrite	Glauc.	Gypsum	Smec.	Clay minerals: Vermic.	Clay minerals: Halloy.	Clay minerals: Illite	Clay minerals: Paly.	Clay minerals: Gibb.	Range & average grain size of siliciclasts (mm)	Sorting
Overburden	Kauroa Ash			•	•	•					•	•			•	0.002-0.18 av. 0.01	poorly to mod.
Overburden	Mahoenui Group mudstones	•		•		•			•	•			•			0.01-0.84 av. = 0.01	sorted poorly to mod.
Limestone	Caprock	•		•		•	•	•								0.07-0.29	sorted mod. sorted
Limestone	Upper Steel	•		•		•	•	•								0.12-2.4	mod. sorted
Limestone	Aglime	•		•		•	•	•								0.05-0.24	mod. sorted
Limestone	High Grade	•		•		•	•	•								0.07-0.24	mod. sorted
Limestone	Lower Steel	•		•		•	•	•								0.1-0.72	mod. sorted
Limestone	Sub-economic	•		•		•	•	•								0.1-0.53	mod. sorted
Discontinuity materials	Diffuse seams	•		•		•	•	•								0.08-0.2	well sorted
Discontinuity materials	Discrete seams	•	•	•		•	•	•		•			•			0.001-0.18 av. = 0.01	poorly to well sorted
Discontinuity materials	Joint infills (type 1)	•		•		•				•				•		0.002-32 av. = 0.66	mod. well to ext. poorly sorted
Discontinuity materials	Palygorskite (type 2)	•		•										•		-	-
Discontinuity materials	Cave infills	•		•						•	•			•		0.002-0.04 av. = 0.01	mod. to well sorted
Oper. Ind.	Surface accumulations	•		•						•						-	-

8.8 Chemical composition of quarry limestone units

The range and average chemical composition of the quarry limestone units is included in Table 8.1. The chemical composition of all sample types largely reflects their mineral composition.

In general, CaO associated with the mineral calcite is abundant in all quarry limestone units where concentrations are similar, but is highest in the Upper Steel unit, variable in the Caprock, similar in the Lower Steel and High Grade, and lowest in the Aglime and Sub-economic units. SiO_2, Al_2O_3, and Fe_2O_3 are associated with the minerals quartz, feldspar, glauconite, and clays and are most common in the lower quality quarry limestones such as the Caprock, Aglime, and Sub-economic units compared to the High Grade, Lower Steel, and Upper Steel units. Minor oxides, including MnO, TiO_2, K_2O, SO_3, P_2O_5, MgO, and Na_2O, occur in very low concentrations in all quarry limestones (<2%). SO_3 is associated with the minerals pyrite and/or gypsum which are locally common in the Mahoenui Group mudstones which overlie the Caprock. SO_3 is highest in some Caprock samples (likely sourced from pyrite in this unit), followed by Aglime and High Grade where SO_3 probably resides in pyrite grains or infills. SO_3 occurs in much lower concentrations in the Upper Steel, Lower Steel, and Sub-economic units where pyrite occurs in relatively lower abundance (determined from petrography) compared to the other quarry limestone units.

8.9 Chemical composition of overburden units and discontinuity materials

The chemical composition of overburden units and discontinuity materials is summarised in Table 8.1. The chemical data are highly variable between these deposits as a result of their different sources and origins. The chemical composition of the overburden units and mineral material occurring in the discontinuities is very different to that in the quarry limestone units.

The highest CaO values occur in the Mahoenui Group mudstones because they are calcareous (i.e. rich in calcareous fossils such as planktic foraminifera). The concentration of CaO is very low in the Kauroa Ash (<1.3%).

CaO concentrations are also relatively high in discontinuity materials which have been inherited from the limestone, such as diffuse and discrete seams. Joint type 1 (smectite-rich) infills show a variation of CaO values reflected in the relative contribution of blasted limestone fragments in these samples. Joint type 2 infill (palygorskite-rich) has relatively high CaO (av. 38%) as formation of this clay mineral is associated with limestone. Surface accumulations also show relatively high CaO values because they are a dust coating from blasting and vehicle traffic on roads.

SiO_2 and Al_2O_3 are also highly variable across the overburden units and discontinuity materials. SiO_2 largely resides in the minerals quartz (and minor cristobalite), feldspar, and a number of clays such as smectite, palygorskite, halloysite, gibbsite, and vermiculite (proven using XRD).

Al_2O_3 largely resides in aluminosilicate clay minerals and feldspars so, as expected, clay rich overburden units and discontinuity materials show high Al_2O_3 concentrations, including the Kauroa Ash, cave infills, and Mahoenui Group mudstones.

Fe_2O_3 shows a range of concentrations for overburden units, discontinuity materials, and surface accumulations, and is associated with clay minerals such as vermiculite and illite, and authigenic minerals such as glauconite and pyrite.

Minor oxides including MnO (<0.1%), TiO_2 (up to 1.1%), P_2O_5, (up to 6.2%), and Na_2O (up to 1.7%) all occur at relatively low concentrations. MgO occurs up to 7%, K_2O associated with clay minerals up to 2.4%, and SO_3 associated with pyrite and gypsum (up to 5%) is more variable across the overburden units, discontinuity materials, and surface accumulations (Table 8.1).

8.10 Ground penetrating radar (GPR)

GPR was trialled in July 2007 as a geophysical technique for detecting subsurface caves within the quarry. A cave exposed in the lower bench of the High Grade on the western side of the quarry was detected by GPR. Transects trending north-south (perpendicular to trend of cave) and east-west (parallel to trend of cave)

were completed, and showed that the cave was best detected when the transects were perpendicular to the trend of the cave. Another cave in the Aglime unit above was also detected.

However, some limitations in the trial were also identified, including: (1) cave infills cannot be quantified as they are not imaged using the GPR technique; (2) caves cannot be detected beyond an effective penetration depth of about 10 m with the system used; (3) quarry walls interfere with received reflections; (4) caves are not detected if the GPR transects are trending parallel to the cave structure; and (5) shape, size, and continuity of caves cannot be determined using this system.

8.11 Conclusions

Sources of silica in McDonald's Oparure Lime Quarry are mainly associated with discontinuities which can be grouped into primary sources (discrete and diffuse seams, and stylolites) and secondary sources (joint infills, cave infills). Surface accumulations are also a source of silica but are operation induced, and arise from blast and road dust coating rock surfaces. Figure 8.3 summarises the main geological events that have introduced silica into the limestone resource over time. This study has demonstrated the following conclusions:

- Significant quantities of silica are mostly associated with discrete and diffuse seams in the limestone units which effectively control the bulk composition, including the $CaCO_3$ content, of each quarry limestone unit.

- Silica levels inside the host rock limestone to some extent control their chemical quality, particularly in the Aglime and Sub-economic units, but values are much lower (typically less than 10%) compared to materials within the discontinuities.

- High contents of silica are also associated with the overburden units at the quarry, including the Kauroa Ash and Mahoenui Group mudstones.

- Discontinuities containing silica-rich materials have been introduced during different stages of limestone evolution through time (Figure 8.3), Three broad types of discontinuities are identified: (1) diagenetic discontinuities involve discrete (concentrated) and diffuse (more dispersed throughout the limestone) dissolution seams, and subhorizontal stylolites; (2) tectonic discontinuities (vertical joints) and subvertical stylolites; and (3) weathering discontinuities (caves and other karst features).

- Discrete and diffuse seams and stylolites are intimately associated with the limestones and are cemented in the rock. The siliceous minerals in the seams and stylolites were sourced during deposition intermittently or simultaneously with the associated skeletal carbonate sediments, and have become concentrated as a result of pressure dissolution during burial and cementation of the limestones.

- Vertical joints have silica-rich infills that have been washed in and are mainly sourced externally from the overlying Mahoenui Group mudstones and Kauroa Ash (overburden units). Palygorskite (clay mineral) also forms *in situ* within joints as a chemical precipitate, acting as another infill.

- Caves have silica-rich infills that have mainly been washed in and sourced externally from the overlying Mahoenui Group mudstones and Kauroa Ash. Palygorskite has also been identified in cave infills, but is generally less common than in joint infills.

- Ground penetrating radar (GPR) has been successful in detecting caves in the McDonald's Oparure Lime Quarry resource, and is deserving of further more detailed assessment as an exploration tool.

- The thickness relationships of the limestone flags (host limestone) and their contained seams are critical when quantifying the total amount of silica present in the rock mass.

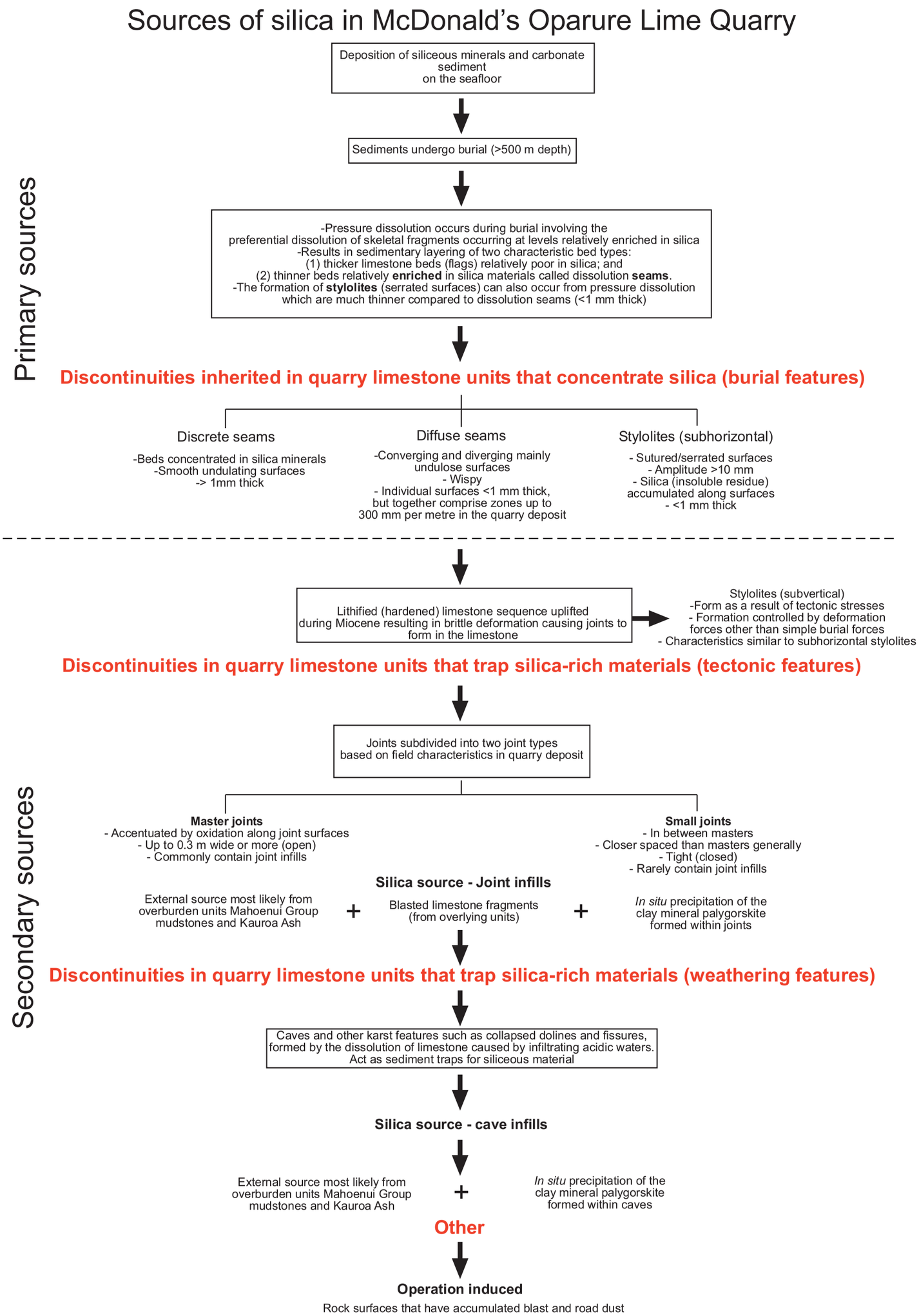

Figure 8.3 Sources of silica introduced into McDonald's Oparure Lime resource during different geological events. Each event corresponds to the formation of a discontinuity that is associated with silica-rich materials. Primary sources include burial features (discrete and diffuse seams, and subhorizontal stylolites), and are inherited from within the limestone units. In contrast, secondary sources have been introduced as infills into joints (tectonic discontinuities), and caves (weathering discontinuities). Subvertical stylolites are also tectonic discontinuities. There are two main infill types, including those washed in from external sources (most likely overlying Mahoenui Group mudstones, Kauroa Ash, and blasted limestone fragments) and/or infills that have precipitated *in situ* such as palygorskite (clay mineral). Minor contributions of silica come from operation induced sources such as blasting and traffic on quarry roads (other).

8.12 Recommendations

The joint and cave discontinuity infill materials are unconsolidated and so should easily be shaken off the limestone during stone processing (e.g. blasting, crushing), before ultimately reaching the stockpiles. Both these infills share some characteristics with overburden units, such as fine grain size and similar mineral and oxide content. The infills cannot be easily fingerprinted to see if they match the compositions of the overburden units. This is because the materials washing down into the caves and joints are likely to be mixed in origin and to have been substantially altered by weathering and during transport in acidic waters.

Discrete and diffuse seams are inherited from within the limestone, so any method to attempt to remove these discontinuities requires a different approach. They are cemented in the limestones by varying amounts of low-Mg calcite cement. After initial blasting, any discrete seam material left behind has important implications for limestone processing. Any discrete seam material on the host limestone block surfaces would tend to drop off during crushing and screening of the limestone. However, some significant residual seam material could be anticipated to remain on the limestone block surfaces, and would require a degree of encouragement to maximise removal of remaining discrete seam material. Personal observations, noted when cutting samples using a saw that is lubricated by water, show that water effectively loosens discrete seam material from the host limestone surfaces.

Diffuse seams are much less common than discrete seams across the quarry limestone units. From outcrop and core observations, it appears that diffuse seams occur mainly in the Aglime where they comprise up to 30% (and typically 12%) of the limestone, but they do also occur rarely in the other limestone units. Because silica in diffuse seams is disseminated throughout the limestone, it is not readily removed during current processing procedures.

In regards to any further GPR work, it is imperative that multiple transects at different orientations are made in order to detect any caves that may be present. The use of a shielded GPR is also advised, to avoid interferences from features such as quarry walls. This trial has confirmed that GPR is a valid tool to use to help detect caves beneath the quarry floor, which has three important

implications: (1) the location of caves can be predicted prior to quarry blasting; (2) knowing cave locations can potentially improve the safety of quarry staff, as they can anticipate any problems that are associated with caves in quarry operations; and finally (3) because caves have been identified as traps for siliceous materials, quarry operators can anticipate the interception of silica rich zones prior to blasting and proceed more cautiously.

REFERENCES

Aali, J., Rahimpour-Bonab, H., Kamali, R.M. 2006: Geochemistry and origin of the world's largest gas field from Persian Gulf, Iran. Journal of Petroleum Science and Engineering 50: 161-175.

Adams, A.E., MacKenzie, W.S. 1998: A colour atlas of carbonate sediments and rocks under the microscope. Manson Publishing, London. 180p.

Arlegui, L., Simon, J.L. 2001: Geometry and depth of regional joint sets in a non-homogenous stress field: case study in Ebro basin (Spain). Journal of Structural Geology 23: 297-313.

Barrett, P.J. 1964: Residual seams and cementation in Oligocene shell calcarenites, Te Kuiti Group. Journal of Sedimentary Petrology 34: 524-531.

Barrett, P.J. 1967: Te Kuiti Group in the Waitomo – Te Anga area. New Zealand Journal of Geology and Geophysics 10: 1009-1026.

Bathurst, R. 1971: Carbonate sediments and their Diagenesis. Elsevier Science, New York. 658p.

Bathurst, R.G.C. 1995: Burial diagenesis of limestones under simple overburden. Stylolites, cementation and feedback. Bulletin de la Société Géologique de France: 166, 181-192.

Becker, A., Gross, M.R. 1996: Mechanisms for joint saturation in mechanically layered rocks: an example from southern Israel. Tectonophysics 257: 223-237.

Beddows, P.A., Smart, P.L., Whitaker, F.F., Smith, S.L. 2007: Decoupled fresh-saline groundwater circulation of a coastal carbonate aquifer. Spatial patterns of temperature and specific electrical conductivity. Journal of Hydrology 346: 18-32.

Ben-Itzhak, L.L., Gvirtzman, H. 2005: Groundwater flow along and across structural folding: an example from the Judean Desert, Israel. Journal of Hydrology 312: 51-69.

Beres, M., Luestscherm M., Olivier, R. 2001: Integration of ground-penetrating radar and microgravimetric methods to map shallow caves. Journal of Applied Geophysics 46: 249-262.

Berkman, D.A. 2001: Field Geologists' Manual. Fourth Edition. The Australasian Institute of Mining and Metallury Level 3, 15-31 Pelham Street, Carlton, Victoria, Australia 3005. 395p.

Bertin, E.P.P. 1975: Principles and practice of x-ray spectrometric analysis. 2nd Ed. Plenum Press, London. 1079p.

Botelho, M.A.B., Mufti, I.R. 1998: Exploitation of limestone quarries in Brazil with depth migrated ground penetrating radar data. Proceedings of the 68th Annual International Meeting, Society of Exploration Geophysicists, Expanded Abstracts 2: 898–903.

Buxton, T.M., Sibley, D.F. 1981: Pressure solution features in a shallow buried limestone. Journal of Sedimentary Petrology 51: 19-26.

Chave, K.E. 1967: Recent carbonate sediments: an unconventional view. Journal of Geological Education 15: 200-204.

Chamberlain, A.T., Sellers, W., Proctor, C., Coard, R. 2000: Cave detection in Limestone using Ground Penetrating Radar. Journal of Archaeological Science 27: 957-964.

Choquette, P.W., Pray, L.C. 1970: Geologic nomenclature and classification of porosity in sedimentary carbonates. American Association of Petroleum Geologists Bulletin 54: 207-250.

Christie, A.B., Brathwaite, R.L. 1999: The mineral potential of New Zealand. Institute of Geological and Nuclear Sciences, Science Report 99/4. 84p.

Christie, A.B., Barker, R.G. 2007: Mineral resource assessment of the Northland Region, New Zealand. Institute of Geological and Nuclear Sciences, Science Report. 2007/06. 179p.

Christie, T., Thompson, B., Brathwaite, B. 2001: Mineral Commodity Report 21 – Limestone, marble and dolomite. New Zealand Mining, vol. 29. August 2001.

Connolly, J.R. 2003: Introduction quantitative x-ray diffraction methods. Earth and Planetary Sciences. 400: 002 1-14.

Cooper, R.A. (Compiler). 2004: New Zealand geological timescale 2004/2 wallchart. Institute of Geological and Nuclear Sciences. Information series 64.

Crowns Minerals. 2001: Explore New Zealand minerals. Crowns Minerals, Ministry of Economic Development, Wellington, New Zealand.

Crowns Minerals. 2005: Minerals production rises over 8% to NZ$1.1 billion in 2004. Crowns Minerals website.
http://www.crownminerals.govt.nz/cms/news/2005/news. Cited 10.08.2007.

Crowns Minerals. 2007a: Overview. Crowns Minerals website.
http://www.crownminerals.govt.nz/cms/minerals/overview. Cited 10.08.2007.

Crowns Minerals. 2007b: Crowns Minerals annual report 2005/2006. Crowns Minerals website. http://www.crownminerals.govt.nz. Cited 15.01.2008.

De´robert, X., Abraham, O. 2000: GPR and seismic imaging in a gypsum quarry. Journal of Applied Geophysics 45: 157– 169.

Dodd, J.R., Nelson, C.S. 1998: Diagenetic comparisons between non-tropical Cenozoic limestones of New Zealand and tropical Mississippian limestones from

Indiana, USA: Is the non-tropical model better than the tropical model? Sedimentary Geology 121: 1-21.

Dunham, R.J. 1962: Classification of carbonate rocks according to their depositional texture. *In:* Ham, W.E. *ed*. Classification of carbonate rocks. Tulsa, OK, American Association of Petroleum Geologists Memoir 1: 108-121.

Edbrooke, S.W. (compiler). 2005: Geology of the Waikato area. Institute of Geological & Nuclear Sciences 1:250 000 geological map 4. 1 sheet +68p. Lower Hutt, New Zealand. Institute of Geological & Nuclear Sciences Limited.

Elfouly, A. 2000: Voids investigation at Gabbari Tombs, Alexandria, Egypt using ground penetrating radar techniques. Cairo University, Egypt. 84-90p.

Evans, M.A., Elmore, D.R. 2006: Fluid control of localized mineral domains in limestone pressure solution structures. Journal of Structural Geology 28: 284-301.

Folk, R.L. 1959: Practical petrographic classification of limestones. American Association of Petroleum Geologists Bulletin 43: 1-38.

Folk, R.L. 1962: Spectral subdivision of limestone types. *In* Ham, W.E. *ed*. Classification of Carbonate rocks. Tulsa, OK. American Association of Petroleum Geologists Memoir 1: 62-84.

Fleger, S.L., Heckman, J.W., Klomparens, K.L. 1993: Scanning and transmission electron microscopy an introduction. Oxford University Press, New York. 1-173p.

Gehle, C., Kutter, H.K. 2003: Breakage and shear behaviour of intermittent rock joints. International Journal of Rock Mechanics and Mining Sciences 40: 687-700.

Gillespie, P.A., Walsh, J.J., Watterson, J., Bonson, C.G., Manzocchi, T. 2001: Scaling relationships of joint and vein arrays from the Burren, Co. clare, Ireland. Journal of Structural Geology 23: 183-201.

Grasmueck, M. 1996: 3-D ground-penetrating radar applied to fracture imaging in gneiss. Geophysics 61: 1050–1064.

Grégoire, C., Joesten, P.K., Lane, J.W. (Jr). 2006: Use of borehole radar reflection logging to monitor steam-enhanced remediation in fractured limestone – results of numerical modelling and a field experiment. Journal of Applied Geophysics 60: 41-54.

Han, R., Liu, C., Huang, Z., Chen, J., Ma, D., Lei, L., Ma, G. 2007: Geological features and origin of the Kuize carbonate-hosted Zn-Pb-(Ag) District, Yunnan, South China. Ore Geology Reviews 31: 360-383.

Hayton, S., Nelson, C.S., Hood, S.D. 1995: A skeletal assemblage classification system for non-tropical carbonate deposits based on New Zealand Cenozoic limestones. Sedimentary Geology 100: 123-141.

Heckel, P.H. 1972: Recognition of ancient shallow marine environments. *In*: Rigby, J.K; Hamblin, W.K. *ed*. Recognition of ancient sedimentary environments. Society of Economic Paleontologists and Mineralologists. Special Publication 16: 226-286.

Henson, H. (Jr)., Sexton, J.L., Henson, M.A., Jones, P. 1997: Georadar investigation of karst in a limestone quarry near Anna, Illinois. Department of Geology, Southern Illinois University, Carbondale, IL 62901-43224.

Höll, R., Kling, M., Schroll, E. 2007: Metallogenesis of Germanium-A review. Ore Geology Reviews 30: 145-180.

Hood, S.D., Nelson, C.S. 1996: Cementation scenarios for New Zealand Cenozoic nontropical limestones. New Zealand Journal of Geology and Geophysics 39: 109-122.

Hood, S.D., Nelson, C.S., Kamp, P.J.J. 2003: Modification of fracture porosity by multiphase vein mineralisation in an Oligocene nontropical carbonate reservoir, Taranaki Basin, New Zealand. American Association of Petroleum Geologists Bulletin 87: 1575-1597.

Hood, S.D., Nelson, C.S., Kamp, P.J.J. 2004: Discriminating cool-water carbonates from warm-water carbonates and their diagenetic environments using element geochemistry: the Oligocene Tikorangi Formation (Taranaki Basin) and the dolomite effect. New Zealand Journal of Geology and Geophysics 47: 857-869.

Hume, T.M., Nelson, C.S. 1982: X-ray diffraction analytical procedures and some mineralogical characteristics for South Auckland region sediments and sedimentary rocks, with special reference to their clay fraction. Occasional report No. 10, University of Waikato. Dept. of Earth Sciences.

JCPDS International Centre for Diffraction Data. Bayliss, P., Berry, L.G., Mrose, M.E., Smith, D.K. *ed.* 1980: Mineral powder diffraction file data book. Swarthmore, Pennsylvania, U.S.A.

Irwin, M.L. 1965: General theory of epeiric clear water sedimentation. American Association of Petroleum Geologists Bulletin 49: 445-459.

James, N.P. 1997: The cool-water carbonate depositional realm. *In*: James, N.P.; Clarke, J.A.D. *ed.* Cool-water carbonates. SEPM Special Publication 56: 1-20.

Kamp, P.J.J., Nelson, C.S. 1988: Nature and occurrence of modern and Neogene active margin limestones in New Zealand. New Zealand Journal of Geology and Geophysics 31: 1-20.

Kaufmann, G., Romanov, D. 2008: Cave development in the Swabian Alb, South-west Germany: A numerical perspective. Journal of Hydrology 349: 302-317.

Kear, D., Schofield, J.C. 1959: Te Kuiti Group. New Zealand Journal of Geology and Geophysics 2: 685-717.

King, P.R., Thrasher, G.P. 1996: Cretaceous-Cenozoic geology and petroleum systems of the Taranaki Basin, New Zealand. Institute of Geological & Nuclear Sciences monograph 13. Institute of Geological & Nuclear Sciences Limited. Lower Hutt, New Zealand.

Lees, A., Buller, A.T. 1972: Modern temperate-warm and warm-water shelf carbonate sediments contrasted. Marine Geology 13: M67-M73.

Lowry, D.C. 1964: Palygorskite in cave in New Zealand. New Zealand Journal of Geology and Geophysics 7: 917.

Mattavelli, L., Pieri, M., Groppi, G. 1992: Petroleum exploration in Italy: a review. Marine and Petroleum Geology 10: 410-425.

Milsom, J. 1996: Field Geophysics, 2nd Ed. John Wiley & Sons, England. 198p.

Misi, A., Kaufman, A.J., Veizer, J., Powis, K., Azmy, K., Boggiani, P., Gaucher, C., Batisa, J., Texieira, G., Sanches, A.L., Iyer, S.S.S. 2007: Chemostratigraphic correlation of Neoproterozoic successions in North America. Chemical Geology 237: 143-167.

Moldoveanu, M., Stewart, R.R., Aitken, J.A. 2002: Shallow imaging using ground-penetrating radar (GPR) data in a carbonate environment: Belize, Central America. Crewes Research Report: 14.

Moore, C.H. 2001: Carbonate reservoirs porosity evolution and diagenesis in a sequence stratigraphic framework. Developments in Sedimentology 55: 297-307.

National Geophysical Data Center, NOAA Satellite and Information Service. http://www.ngdc.noaa.gov/seg/geomag/jsp/struts/calcDeclination 2007. Cited on 12.08.07.

Naydowski, C., Hess, P., Strauch, D., Kuhlmann, R., Rohleder, J. 2001: Calcium carbonate and its industrial application. *In*: Tegethoff, F.W.; Rohleder, J.; Kroker, E. *ed.* Calcium carbonate from the Cretaceous period into the 21st century. Birkhauser Verlag, Basel – Boston - Berlin. 197-301p.

Nelson, C.S. 1973: Stratigraphy and sedimentology of the Te Kuiti Group, Waitomo County, South Auckland. Unpublished Ph.D thesis, lodged in the library, University of Auckland, Auckland.

Nelson, C.S. 1978a: Stratigraphy and paleontology of the Oligocene Te Kuiti Group, Waitomo County, South Auckland, New Zealand. New Zealand Journal of Geology and Geophysics 21: 553-594.

Nelson, C.S. 1978b: Temperate shelf carbonate sediments in the Cenozoic of New Zealand. Sedimentology 25: 737-771.

Nelson, C.S. 1982: Compendium of sample data for temperate carbonate sediments, Three Kings Plateau, northern New Zealand. University of Waikato, Department of Earth Sciences occasional report 7. 95p.

Nelson, C.S. 1988: An introductory perspective on non-tropical shelf limestones. Sedimentary Geology 60: 3-12.

Nelson, C.S. 1993: A synopsis of the geological history of the King Country. Proceedings of the New Zealand Farm Forestry Association Annual Conference, King Country. 8-12p.

Nelson, C.S., Hancock, G.E. 1984: Composition and origin of temperate skeletal carbonate sediments on South Maria Ridge, northern New Zealand. New Zealand Journal of Marine and Freshwater Research 18: 221-239.

Nelson, C.S., Hancock, G.E., Kamp, P.J.J. 1982: Shelf to basin, temperate skeletal carbonate sediments, Three Kings Plateau, New Zealand. New Zealand Journal of Sedimentary Petrology 52: 717-732.

Nelson, C.S., Keane, S.L., Head, P.S. 1988a: Non-tropical carbonate deposits on the modern New Zealand shelf. Sedimentary Geology 60: 71-94.

Nelson, C.S., Harris, G.J., Young, H.R. 1988b: Burial-dominated cementation in non-tropical carbonates of the Oligocene Te Kuiti Group, New Zealand. Sedimentary Geology 60: 233-250.

Nelson, C.S., Winefield, P.R., Hood, S.D., Caron, V., Pallentin, A., Kamp, P.J.J. 2003: Pliocene Te Aute limestones, New Zealand: expanding concepts for cool-water shelf carbonates. New Zealand Journal of Geology and Geophysics 46: 363-386.

Nicolaides, S., Wallace, M.W. 1997: Pressure-dissolution and cementation in an Oligo-Miocene non-tropical limestone (Clifton Formation), Otway Basin, Australia. *In*: James, N.P., Clark, A.D. (Ed., Cool-water carbonates. Society for Sedimentary Geology Special Publication 56: 249-262.

Odonne, F., Lẻzin, C., Massonnat, G., Escadillas, G. 2007: The relationship between joint aperture, spacing distribution, vertical dimensions and carbonate stratification: An example from the Kimmeridgian limestones of Pointe-du-Chay (France). Journal of Structural Geology 29: 746-758.

Orlando, L. 2003: Semiquantitative evaluation of massive rock quality using ground penetrating radar. Journal of Applied Geophysics 52: 1-9.

Post, J.L. Crawford, S. 2007: Varied forms of palygorskite and sepiolite from different geologic systems. Applied Clay Science 36: 237-244.

Reynolds, J.M. 1997: An introduction to applied and environmental geophysics. John Wiley and Sons Ltd, England. 681-749p.

Rohleder, J., Huwald, E. 2001: Calcium carbonate – a modern resource. *In*: Tegethoff, F.W.; Rohleder, J.; Kroker, E. *ed.* Calcium carbonate from the Cretaceous period into the 21st century. Birkhauser Verlag, Basel – Boston - Berlin. 137-193p.

Schack von Brockdorff, A., Nielsen, L., Boldreef, L.O., Overgaard, T. 2003: 2D and 3D imaging of mound structures from GPR measurements in Danish and Swedish limestone quarries. Geophysical Research. Abstracts 5: 08244. European Geophysical Society.

Scholle, P.A., Ulmer-Scholle, D.S. 2003: A color guide to the petrography of carbonate rocks: Grains, textures, porosity, diagenesis, AAPG Memoir 77. The American Association of Petroleum Geologists Tulsa, Oklahoma, U.S.A.

Scoffin, T.P. 1987: An introduction to carbonate sediments and rocks. Chapman and Hall, New York. 274p.

Siegel, F.R. 1967: Physical and chemical aspects. *In*: Chilingar, G.V.; Bissell, H.J.; Fairbridge, R.W. *ed.* Carbonate rocks. Developments in Sedimentology 9b: 343-394. Elsevier Publishing Co., Amsterdam.

Sigurdsson, T., Overgaard, T. 1998: Application of GPR for 3-D visualization of geological and structural variation in a limestone formation. Journal of Applied Geophysics 40: 29-36.

Simonson, T.L. 2005: Summary report on the 2005 drilling programmes undertaken at Oparure Quarry, Te Kuiti for McDonald's Lime Ltd. Ormiston Associates Ltd. Auckland, New Zealand. 28p.

Soong, R. 1992: Palygorskite occurrence in northwest Nelson, South Island, New Zealand. New Zealand Journal of Geology and Geophysics 35: 325-330.

Tada, R., Siever, R. 1989: Pressure solution during diagenesis. Annual reviews Earth Planetary Sciences 17: 89-118.

Thompson, B.N., Brathwaite, R.L., Christie, A.B. 1995: Mineral wealth of New Zealand. Lower Hutt. Institute of Geological and Nuclear Sciences, information series 33. 180p.

Tillard, S., Dubois, J. 1995: Analysis of GPR data: wave propagation velocity determination. Journal of Applied Geophysics 33: 77-91.

Tripathi, A. PhD thesis in prep. Sequence stratigraphic analyses of the early Tertiary Te Kuiti Group, western North Island. University of Waikato, Hamilton, New Zealand.

Tucker M.E., Wright, P. 1990: Carbonate Sedimentology. Blackwell Scientific Publications, London. 482p.

Waltham, T., Bell, F., Culshaw, M. 2005: Sinkholes and subsidence karst and cavernous rocks in engineering and construction. Praxis Publishing Ltd, Chichester. 382p.

Wanless, H.R. 1981: Burial diagenesis in limestones. *In*: Parker, A.; Sellwood, B.W. *ed*. Sediment diagenesis. D. Reidel Publishing Company: 379-417.

White, P.J., Waterhouse, B.C. 1993: Lithostratigraphy of the Te Kuiti Group: a revision. New Zealand Journal of Geology and Geophysics 36: 255-266.

Willett, J.C. 2007: U.S. Geological Survey, Mineral Commodity Summaries, January 2007. http://minerals.usg.gov/minerals/pubs/commodity/lime/index.html. Cited on 04/01/08.

Williams, G. 2004a: An introduction to the layout and a basic description of operations of the slabmaking plant. New Zealand Steel Ltd. 27p.

Williams, P.W. 2004b: Polygonal karst and paleokarst of the King Country, North Island, New Zealand. Zeitschrift fur Geomorphologie 136: 45-67.

Wyllie, D.C., Mah, C.W. 2004: Rock slope engineering civil and mining 4th Ed. Spon Press, London. 431p.

APPENDICES

Appendix A-1.1: Sourced from Simonson (2005): Summary report on the 2005 drilling programme undertaken at Oparure Quarry, Te Kuiti for McDonald's Lime Ltd. Ormiston Associates Ltd. October 2005.

1.4 Silica Concentration Limit

Recent experimental work on the silica concentration limit in the raw materials has been carried out by McDonald's Lime. Cuttings from four blast drillholes within the lower steel grade and one blast hole within the high grade limestone were compiled into composite samples, within one sample representing the entire shot. These samples were analysed by XRF.

Once blasted the rock was crushed and samples collected of the screened product for use in the Otorohanga plant. The full quantities of rock produced by the sampled blast was used in the trial. The samples taken were riffled into a composite sample which was also XRF-analysed by Spectrachem Ltd. The results of the analyses are included in Table 2 below:

Table 2: Silica Concentrations, Raw Material VS Kiln Feed

PARAMETER	252C			257 C			259 C			264 C			Average Change	
	Shot	Kiln Feed	Change	Shot	Kiln Feed	Change	Shot	Kiln Feed	Change	Shot	Kiln Feed	Change		
Fe_2O_3	0.31	0.23	0.08	0.29	0.24	0.05	0.29	0.23	0.06	0.29	0.21	0.08	0.07	reduction
MnO	0.01	0.01	0.00	0.01	0.01	0.00	0.01	0.01	0.00	0.01	0.01	0.00	0.00	reduction
TiO_2	0.02	0.02	0.01	0.02	0.02	0.00	0.02	0.01	0.01	0.02	0.01	0.01	0.01	reduction
CaO	54.92	54.35	0.57	53.5	54.35	-0.85	53.26	54.41	-1.15	53.72	54.31	-0.58	-0.50	increase
K_2O	0.09	0.06	0.03	0.08	0.07	0.01	0.09	0.07	0.02	0.08	0.06	0.02	0.02	reduction
SO_3	0.06	0.03	0.03	0.03	0.05	-0.02	0.05	0.06	-0.01	0.04	0.04	0.00	0.00	reduction
P_2O_5	0.05	0.06	0.00	0.06	0.05	0.01	0.06	0.05	0.01	0.06	0.04	0.02	0.01	reduction
SiO_2	2.01	1.51	0.50	1.70	1.44	0.26	2.00	1.44	0.56	2.04	1.33	0.71	0.51	reduction
Al_2O_3	0.48	0.29	0.20	0.42	0.28	0.14	0.47	0.25	0.22	0.35	0.26	0.09	0.16	reduction
MgO	0.43	0.40	0.03	0.44	0.50	-0.06	0.45	0.45	0.00	0.48	0.46	0.02	0.00	reduction
Na_2O	0.02	0.02	0.00	0.04	0.02	0.02	0.02	0.03	-0.01	0.04	0.02	0.02	0.01	reduction
LOI	41.55	42.91	-1.36	42.85	42.93	-0.08	42.74	42.95	-0.21	42.62	43.06	-0.44	-0.52	increase
SUM	99.96	99.88	0.08	99.45	99.96	-0.51	99.45	99.84	-0.49	99.76	99.81	-0.05	-0.24	increase

The results confirm the supposition previously observed that that silica concentrations are reduced by the processes of blasting, extracting and crushing the limestone. An average reduction of 0.51% was observed as above therefore the SiO_2 limit was raised from the previous 1.7% to 2.2% in the drill hole data for the purposes of this report. While the results of the trial show a definite decrease in silica levels from drill hole data to kiln feed, it should be noted that the quantitative value of 0.5% is based on only four tests, within which the decrease observed varied from 0.26% to 0.71%. In order to more rigorously define the silica limit, we recommend more testing should be undertaken.

The remainder of the results above indicate that most oxides remain unchanged through the process, with the exception of a reductions in Fe_2O_3 (0.07%) and Al_2O_3 (0.16%). Given the low concentrations of these elements the reductions shown equate to approximately one third of both the iron oxide and the alumina.

As both of these oxides can be considered related to weathering processes their losses may be linked to fine grained clays and joint-lining material being lost from the raw material by the moving and crushing processes.

1.5 Calcium Oxide Concentration Limit

The CaO content in most of the test samples above increased by an average of 0.5%, which is considered to be a proportionate reflection of the loss of silica. Therefore there may be scope to decrease the CaO limits in the raw material. However, the CaO results from the trial were variable, with Shot 252C decreasing by 0.57%, and the CaO content of the remaining three samples increasing by 0.58 to 1.15%. The standard deviation of the results is 0.75, therefore we recommend further work is undertaken prior to applying any change to the CaO raw material limits at this stage. This work is certainly significant, as a decrease in required CaO content in the order of 0.5% could potentially greatly increase the raw material volumes designated as steel grade quality.

Appendix A-1.2 Sample catalogue. Grid coordinates (NZ Map Grid) for McDonald's Quarry are N6316539.8, E2691394.5 and for drill hole BH502 N63167105, E2690996.9. Abbreviations: Argill. lst = Argillaceous limestone, Sparry lst. = Sparry limestone, Micritic lst. = Micritic limestone, T-sect = Thin section, A-titration = Acid titration, XRF = X-ray fluorescence, XRD = X-ray diffraction, Las-siz = Laser particle size analysis, SEM = Scanning electron microscopy, Surf. accum = Surface accumulation, Handspec = Hand specimen, Ot = Otorohanga Limestone, Calc. mudstone = Calcareous mudstone. * = core sample.

Running number	E Sc. Store No.	Field number	Lithological	Quarry unit	Location	Sample type(s)	Lab methods
1	W20080001	*9	Argill. lst.	Caprock, Ot	BH502, box 9, 26 m depth	Powder	XRF, A-titration
2	W20080002	*9.1	Argill. lst.	Caprock, Ot	BH502, box 9, 26 m depth	T-sect	Petro
3	W20080003	*9.2	Argill. lst.	Caprock, Ot	BH502, box 9, 26 m depth	T-sect	Petro
4	W20080004	*10.1	Sparry lst.	Upper Steel, Ot	BH502, box 10, 28 m depth	T-sect	Petro
5	W20080005	*10.2	Sparry lst.	Upper Steel, Ot	BH502, box 10, 28 m depth	T-sect	Petro
6	W20080006	*10.3	Sparry lst.	Upper Steel, Ot	BH502, box 10, 28 m depth	T-sect	Petro
7	W20080007	*11	Micritic lst.	Aglime, Ot	BH502, box 14, 40 m depth	T-sect	Petro
8	W20080008	*12.1	Micritic lst.	Aglime, Ot	BH502, box 15, 41 m depth	T-sect	Petro
9	W20080009	*12.2	Micritic lst.	Aglime, Ot	BH502, box 15, 41 m depth	T-sect	Petro
10	W20080010	*12.3	Micritic lst.	Aglime, Ot	BH502, box 15, 41 m depth	T-sect	Petro
11	W20080011	*13	Diffuse seam	Aglime, Ot	BH502, box 15, 43 m depth	Powder	XRF, A-titration
12	W20080012	*13.1	Micritic lst.	Aglime, Ot	BH502, box 15, 43 m depth	T-sect	Petro
13	W20080013	*13.2	Micritic lst.	Aglime, Ot	BH502, box 15, 43 m depth	T-sect	Petro
14	W20080014	*13.3	Micritic lst.	Aglime, Ot	BH502, box 15, 43 m depth	T-sect	Petro
15	W20080015	*14	Sparry lst.	High Grade, Ot	BH502, box 19, 53 m depth	T-sect	Petro
16	W20080016	*15.1	Sparry lst.	High Grade, Ot	BH502, box 20, 57 m depth	T-sect	Petro
17	W20080017	*15.2	Sparry lst.	High Grade, Ot	BH502, box 20, 57 m depth	T-sect	Petro
18	W20080018	*15.3	Sparry lst.	High Grade, Ot	BH502, box 20, 57 m depth	T-sect	Petro
19	W20080019	*15.4	Sparry lst.	High Grade, Ot	BH502, box 20, 57 m depth	T-sect	Petro
20	W20080020	*16	Sparry lst.	Lower Steel, Ot	BH502, box 26, 74 m depth	T-sect	Petro
21	W20080021	*17.1	Sparry lst.	Lower Steel, Ot	BH502, box 26, 74.6 m depth	T-sect	Petro
22	W20080022	*17.2	Sparry lst.	Lower Steel, Ot	BH502, box 26, 74.6 m depth	T-sect	Petro
23	W20080023	*17.3	Sparry lst.	Lower Steel, Ot	BH502, box 26, 74.6 m depth	T-sect	Petro
24	W20080024	*18.1	Sparry lst.	Lower Steel, Ot	BH502, box 27, 78 m depth	T-sect	Petro
25	W20080025	*18.2	Sparry lst.	Lower Steel, Ot	BH502, box 27, 78 m depth	T-sect	Petro
26	W20080026	*18.3	Sparry lst.	Lower Steel, Ot	BH502, box 27, 78 m depth	T-sect	Petro
27	W20080027	*18.4	Sparry lst.	Lower Steel, Ot	BH502, box 27, 78 m depth	T-sect	Petro
28	W20080028	*19.1	Sparry lst.	Sub-economic, Ot	BH502, box 31, 88 m depth	T-sect	Petro
29	W20080029	*19.2	Sparry lst.	Sub-economic, Ot	BH502, box 31, 88 m depth	T-sect	Petro
30	W20080030	*19.3	Sparry lst.	Sub-economic, Ot	BH502, box 31, 88 m depth	T-sect	Petro
31	W20080031	*20	Argill. lst.	Caprock, Ot	BH502, box 9, 25.5 m depth	T-sect	Petro
32	W20080032	*21	Diffuse seam	Caprock, Ot	BH502, box 9, 26 m depth	T-sect/powder	Petro, XRF, A-titration
33	W20080033	*22	Calc. mudstone	Mahoenui Group	BH502, box 9, 25 m depth	Handspec	Las-siz
34	W20080034	*23.2	Argill. lst.	Caprock, Ot	BH502, box 10, 27 m depth	T-sect	Petro
35	W20080035	*24.1	Sparry lst.	Upper Steel, Ot	BH502, box 10, 28 m depth	T-sect	Petro
36	W20080036	*24.2	Sparry lst.	Upper Steel, Ot	BH502, box 10, 28 m depth	T-sect	Petro
37	W20080037	*24.3	Sparry lst.	Upper Steel, Ot	BH502, box 10, 28 m depth	T-sect	Petro
38	W20080038	*25	Sparry lst.	Upper Steel, Ot	BH502, box 12, 35 m depth	T-sect	Petro

Appendix A-1.2 continued.

Running number	E Sc. Store No.	Field number	Lithological	Quarry unit	Location	Sample type(s)	Lab methods
39	W20080039	*26	Argill. lst.	Caprock, Ot	BH502, box 9, 25 m depth	Powder	XRF, XRD, A-titration
40	W20080040	*27	Diffuse seam	Caprock, Ot	BH502, box 10, 27 m depth	T-sect/powder	Petro, XRF, A-titration
41	W20080041	27B	Argill. lst.	Caprock, Ot	BH502, box 10, 27 m depth	Powder	A-titration
42	W20080042	*28	Sparry lst.	Upper Steel, Ot	BH502, box 10, 28 m depth	Powder	XRF, A-titration
43	W20080043	*29	Sparry lst.	Upper Steel, Ot	BH502, box 11, 36.5 m depth	Powder	XRF, XRD, A-titration
44	W20080044	*30	Sparry lst.	Upper Steel, Ot	BH502, box 13, 36 m depth	T-sect	Petro
45	W20080045	*31a	Sparry lst.	Upper Steel, Ot	BH502, box 13, 36 m depth	Powder	XRF, A-titration
46	W20080046	*32	Micritic lst.	Aglime, Ot	BH502, box 13, 36 m depth	T-sect	Petro
47	W20080047	*34	Diffuse seam	Aglime, Ot	BH502, box 14, 38 m depth	T-sect/powder	Petro, XRF, XRD, A-titration
48	W20080048	*35	Micritic lst.	Aglime, Ot	BH502, box 14, 38 m depth	T-sect/powder	Petro, XRF, A-titration
49	W20080049	*36	Micritic lst.	Aglime, Ot	BH502, box 15, 41 m depth	Powder	XRF, A-titration
50	W20080050	*37	Micritic lst.	Aglime, Ot	BH502, box 16, 44 m depth	Powder	XRF, XRD, A-titration
51	W20080051	*38	Sparry lst.	High Grade, Ot	BH502, box 18, 50 m depth	T-sect	Petro
52	W20080052	*39	Sparry lst.	High Grade, Ot	BH502, box 18, 50 m depth	Powder	XRF, XRD, A-titration
53	W20080053	*40	Sparry lst.	High Grade, Ot	BH502, box 19, 55 m depth	T-sect	Petro
54	W20080054	*40.2	Sparry lst.	High Grade, Ot	BH502, box 19, 55 m depth	T-sect	Petro
55	W20080055	*41	Sparry lst.	High Grade, Ot	BH502, box 19, 55 m depth	Powder	XRF, A-titration
56	W20080056	*42	Sparry lst.	High Grade, Ot	BH502, box 21, 56 m depth	Powder	XRF, A-titration
57	W20080057	*43	Sparry lst.	High Grade, Ot	BH502, box 22, 61.5 m depth	T-sect	Petro
58	W20080058	*46	Sparry lst.	Lower Steel, Ot	BH502, box 24, 67 m depth	Powder	XRF, A-titration
59	W20080059	*47	Sparry lst.	Lower Steel, Ot	BH502, box 24, 67 m depth	T-sect	Petro
60	W20080060	*48	Sparry lst.	Lower Steel, Ot	BH502, box 24, 67 m depth	Powder	XRF, A-titration
61	W20080061	*49.1	Sparry lst.	Lower Steel, Ot	BH502, box 25, 70 m depth	T-sect	Petro
62	W20080062	*49.2	Sparry lst.	Lower Steel, Ot	BH502, box 25, 70 m depth	T-sect	Petro
63	W20080063	*51	Sparry lst.	Lower Steel, Ot	BH502, box 26, 73 m depth	T-sect	Petro
64	W20080064	*52	Sparry lst.	Lower Steel, Ot	BH502, box 26, 73 m depth	Powder	XRF, XRD, A-titration
65	W20080065	*55	Sparry lst.	Lower Steel, Ot	BH502, box 27, 76 m depth	T-sect	Petro
66	W20080066	*56	Sparry lst.	Sub-economic, Ot	BH502, box 30, 85 m depth	Powder	XRF, XRD, A-titration
67	W20080067	*57.2A	Sparry lst.	Sub-economic, Ot	BH502, box 30, 85 m depth	T-sect	Petro
68	W20080068	*57.1B	Sparry lst.	Sub-economic, Ot	BH502, box 30, 85 m depth	T-sect	Petro
69	W20080069	*58	Sparry lst.	Sub-economic, Ot	BH502, box 31, 87.3 m	Powder	XRF, A-titration
70	W20080070	*59.4	Sparry lst.	Sub-economic, Ot	BH502, box 31, 88 m depth	T-sect	Petro
71	W20080071	*60	Sparry lst.	Sub-economic, Ot	BH502, box 32, 90.5 m depth	Powder	XRF, A-titration
72	W20080072	*61	Diffuse seam	Sub-economic, Ot	BH502, box 32, 91 m depth	T-sect/powder	Petro, XRF, A-titration
73	W20080073	*66.1	Sparry lst.	Sub-economic, Ot	BH502, box 34, 97.5 m depth	T-sect	Petro
74	W20080074	*66.3	Sparry lst.	Sub-economic, Ot	BH502, box 34, 97.5 m depth	T-sect	Petro
75	W20080075	*66.4	Sparry lst.	Sub-economic, Ot	BH502, box 34, 97.5 m depth	T-sect	Petro
76	W20080076	*71	Volc. ash	Kauroa Ash	BH502, box 1, 2 m depth	Handspec/powder	Las-siz, XRD, A-titration

Appendix A-1.2 continued.

Running number	E Sc. Store No.	Field number	Lithological	Quarry unit	Location	Sample type(s)	Lab methods
77	W20080077	*72	Volc. ash	Kauroa Ash	BH502, box 2, 5 m depth	Handspec/powder	Las-siz, XRD, A-titration
78	W20080078	100	Joint infill	Lower Steel, Ot	Lower Steel, eastern face, McD's Q	Handspec/powder	XRF, XRD, A-titration
79	W20080079	102	Joint infill	Lower Steel, Ot	Lower Steel, eastern face, McD's Q	Powder	XRF, XRD, A-titration
80	W20080080	105	Joint infill	High Grade, Ot	High Grade northern face, McD's Q	Handspec/powder	SEM, A-titration
81	W20080081	107	Joint infill	High Grade, Ot	High Grade, eastern face, McD's Q	Handspec/powder	Sieving, Las-siz, XRF, XRD, A-titration
82	W20080082	108	Discrete seam	High Grade, Ot	High Grade, northern face, McD's Q	Handspec	Las-siz
83	W20080083	109	Joint infill	High Grade, Ot	High Grade northern face, McD's Q	Handspec	Sieving, Las-siz
84	W20080084	110	Discrete seam	High Grade, Ot	High Grade northern face, McD's Q	Powder	XRF, A-titration
85	W20080085	111	Sparry lst.	High Grade, Ot	High Grade northern face, McD's Q	Powder/handspec	XRF, A-titration
86	W20080086	112	Sparry lst.	Lower Steel, Ot	Lower Steel, northern face, McD's Q	Powder/handspec	XRF, A-titration
87	W20080087	114	Joint infill	Aglime, Ot	Aglime, southern face, McD's Q	Handspec/powder	Las-siz, XRF, XRD, A-titration
88	W20080088	116	Joint infill	Aglime, Ot	Aglime, southern face, McD's Q	Powder	A-titration
89	W20080089	117	Discrete seam	Aglime, Ot	Aglime, southern face, McD's Q	Handspec, powder	Las-siz, XRF, XRD, A-titration
90	W20080090	118	Discrete seam	Aglime, Ot	Aglime, southern face, McD's Q	Handspec, powder	Las-siz, XRF
91	W20080091	119	Joint infill	Aglime, Ot	Aglime, southern face, McD's Q	Powder	XRF, XRD, A-titration
92	W20080092	121	Sparry lst.	Upper Steel, Ot	Upper Steel, northern face, McD's Q	Powder/handspec/T-sect	XRF, A-titration
93	W20080093	123	Sparry lst.	Upper Steel, Ot	Upper Steel, northern face, McD's Q	Powder/handspec	XRF, A-titration
94	W20080094	124	Sparry lst.	Aglime, Ot	Aglime, southern face, McD's Q	Powder/handspec	XRF, A-titration
95	W20080095	125	Sparry lst.	Aglime, Ot	Aglime, southern face, McD's Q	Powder/handspec/T-sect	XRF, A-titration
96	W20080096	126	Calc. mudstone	Mahoenui Group	Mahoenui Gp, northern face, McD's Q	Handspec/powder	XRF, XRD, A-titration
97	W20080097	127	Calc. mudstone	Mahoenui Group	Mahoenui Gp, northern face, McD's Q	Handspec/powder	XRF, XRD, A-titration
98	W20080098	128	Sparry lst.	High Grade, Ot	High Grade, northern face, McD's Q	Powder	XRF, A-titration
99	W20080099	130	Discrete seam	Upper Steel, Ot	Upper Steel, northern face, McD's Q	Powder	XRF, XRD, A-titration
100	W20080100	135	Sparry lst.	Upper Steel, Ot	Upper Steel, northern face, McD's Q	Powder/T-sect	XRF, A-titration
101	W20080101	136	Argill. lst.	Caprock, Ot	Caprock, northern face, McD's Q	Powder	A-titration
102	W20080102	138	Discrete seam	Upper Steel, Ot	Upper Steel, northern face, McD's Q	Powder	Las-siz, XRF, A-titration
103	W20080103	139	Discrete seam	Upper Steel, Ot	Upper Steel, northern face, McD's Q	Handspec/powder	Las-siz, A-titration
104	W20080104	140	Joint infill	Upper Steel, Ot	Upper Steel, northern face, McD's Q	Powder	XRF, A-titration
105	W20080105	141	Discrete seam	Aglime, Ot	Aglime, northern face, McD's Q	Handspec, powder	Las-siz, XRF, A-titration
106	W20080106	143	Cave infill	Upper Steel, Ot	Upper Steel, western face, McD's Q	Powder	Las-siz, XRF, XRD, A-titration
107	W20080107	144	Joint infill	High Grade, Ot	High Grade, northern face, McD's Q	Handspec, powder	Las-siz, XRF, A-titration
108	W20080108	145	Discrete seam	High Grade, Ot	High Grade, northern face, McD's Q	Powder	XRF, XRD, A-titration
109	W20080109	146	Cave infill	High Grade, Ot	High Grade, western face, McD's Q	Powder/handspec	Las-siz, XRF, XRD, A-titration
110	W20080110	147	Discrete seam	Lower Steel, Ot	Lower Steel, western face, McD's Q	Powder	XRF, XRD, A-titration
111	W20080111	148	Joint infill	Lower Steel, Ot	Lower Steel, western face, McD's Q	Powder	XRF, A-titration
112	W20080112	150	Surf. accum.	Aglime, Ot	Aglime, northern face, McD's Q	Powder	XRF, XRD, A-titration
113	W20080113	151	Sparry lst.	Aglime, Ot	Aglime, southern face, McD's Q	Handspec, powder	XRF, A-titration
114	W20080114	152	Discrete seam	Aglime, Ot	Aglime, eastern face, McD's Q	Handspec	Las-siz

Appendix A-1.2 continued.

Running number	E Sc. Store No.	Field number	Lithological	Quarry unit	Location	Sample type(s)	Lab methods
115	W20080115	153	Sparry lst.	Lower Steel, Ot	Lower Steel, northern face, McD's Q	Powder/handspec/T-sect	XRF, A-titration
116	W20080116	154	Cave infill	Lower Steel, Ot	Lower Steel, western face, McD's Q	Powder	Sieving, Las-siz, XRF, XRD, A-titration
117	W20080117	155	Surf. accum.	Aglime, Ot	Aglime, northern face, McD's Q	Powder	XRF, A-titration
118	W20080118	156	Sparry lst.	High Grade, Ot	High Grade, western face, McD's Q	Powder/T-sect	XRF, A-titration
119	W20080119	157	Sparry lst.	Lower Steel, Ot	Lower Steel, northern face, McD's Q	Powder/handspec	XRF
120	W20080120	159	Discrete	Lower Steel, Ot	Lower Steel, northern face, McD's Q	Powder	XRF, A-titration
121	W20080121	160	Cave infill	Upper Steel, Ot	Upper Steel, northern face, McD's Q	Handspec	Las-siz
122	W20080122	161	Cave infill	Upper Steel, Ot	Upper Steel, western face, McD's Q	Handspec	Las-siz
123	W20080123	162	Discrete seam	Upper Steel, Ot	Upper Steel, northern face, McD's Q	Handspec	Las-siz
124	W20080124	163	Discrete seam	Upper Steel, Ot	Upper Steel, northern face, McD's Q	Handspec	Las-siz
125	W20080125	164	Joint infill	Aglime, Ot	Aglime, southern face, McD's Q	Handspec	Sieving, Las-siz
126	W20080126	165	Joint infill	Aglime, Ot	Aglime, southern face, McD's Q	Handspec	Sieving, Las-siz
127	W20080127	166	Joint infill	Upper Steel, Ot	Upper Steel, western face, McD's Q	Handspec	Las-siz
128	W20080128	167	Volc. ash	Kauroa Ash	Roadside outcrop, Trooper's Rd	Handspec/powder	Las-siz, XRD, A-titration
129	W20080129	168	Joint infill	High Grade, Ot	High Grade, western face, McD's Q	Handspec	Sieving, Las-siz
130	W20080130	169	Joint infill	High Grade, Ot	High Grade, western face, McD's Q	Handspec	Sieving, Las-siz
131	W20080131	171	Discrete seam	Lower Steel, Ot	Lower Steel, northern face, McD's Q	Handspec	Las-siz
132	W20080132	172	Discrete seam	High Grade, Ot	High Grade, northern face, McD's Q	Handspec	Las-siz
133	W20080133	HQ3a	Argill. lst.	Caprock, Ot	Caprock, northern face, McD's Q	Powder	XRF, A-titration
134	W20080134	HQ3b	Argill. lst.	Caprock, Ot	Caprock, northern face, McD's Q	Powder	XRF, A-titration

Appendix B-2.1 Comparison of some properties typical of the traditional tropical shelf carbonate model (A) with those for nontropical limestones as exemplified by modern (B) and Cenozoic (C) carbonate deposits of New Zealand. Modified from Nelson et al., (1988a), Hayton et al., (1995), and Hood and Nelson (1996). LMC = Low Mg calcite (<4 mol% $MgCO_3$), IMC = intermediate Mg calcite (4-10 mol% $MgCO_3$), HMC = high Mg calcite (>10 mol% $MgCO_3$).

Environmental or facies parameter	**A.** Tropical shelf carbonates	**B.** New Zealand modern shelf carbonates	**C.** New Zealand Cenozoic shelf limestones
Latitude	From 30°S to 30°N	From 49°S to 33°S	From 60°S to 35°S
Depositional setting	Shallow rimmed shelves and platforms	Deeper open shelves, ramps and platforms	Open shelves, platforms and seaways
Marine climate zone	Tropical-warm subtropical	Warm-cool temperate	Warm-cool temperate
Sea-water temp. (mean)	Above 23°C	13-19°C	Below 20°C
Sea-water temp. (min.)	About 14°C	9-12°C	About 5°C
Sea-water salinity	Normal-hypersaline	Normal	Normal
$CaCO_3$ saturation at/in sea bed	Highly supersaturated	Mildly supersaturated to ?locally undersaturated	Infer mild supersaturation to local undersaturation
Water circulation	Restricted-open	Open, strongly storm- and tide-dominated	Open, storm- and tide- dominated shelves/seaways
Tectonic regime	Stable, slow subsidence	Stable-unstable	Stable-unstable
Shelf gradient	<0.5 m/km	0.25-2 m/km	>0.5 m/km
Reef structures	Common (especially coral/coralgal)	None (some oyster banks)	Rare (oyster banks; bryozoan mounds)
Sedimentation rates	10-100+ cm/ky	1-15 cm/ky, often relict	<5 cm/ky, many diastems
$CaCO_3$ content	>90%	50-100%	50-100%
Siliciclastic grains	Rare	Rare-abundant	Rare-abundant
Glauconite	Rare	Common, especially in skeletal chambers	Common, pelletal and in skeletal chambers
Dolomite and evaporite minerals	Common-rare	Absent	Absent (locally rare late diagenetic dolomite)
Non-skeletal carbonate grains (e.g. ooids, pellets)	Common-abundant	Absent	Absent

Appendix B-2.1 continued.

Environmental or facies parameter	**A.** Tropical shelf carbonate model	**B.** New Zealand modern shelf carbonates	**C.** New Zealand Cenozoic shelf limestones
Main skeletal assemblages (Hayton et al. 1995)	Chlorozoan Chloralgal	Bryomol Bimol (Nannofor)	Bryomol, Echinofor Barnamol, Rhodechfor Bimol (Nannofor)
Algal mats/stromatolites	Common	Absent (or not preserved)	Absent
Overall diagenetic regime	Constructive	Destructive	Destructive
Carbonate mud	Common-abundant	Absent-rare, flushed and by-passed offshore	Absent-rare, locally as matrix, increases offshore
Main origins of carbonate mud	Disintegration calc. green algae and inorganic pptn.	Physical abrasion, bioeros. & maceration of skeletons	Skeletal abrasion and bioerosion; nannofossils
Primary sediment mineralogy	Aragonite > HMC > IMC > LMC	LMC+IMC > HMC ≥ aragonite	LMC+IMC > HMC ≥ aragonite
Main environs. of alteration of metastable carb. grains	Subaerial/meteoric	Beginning submarine	Submarine to shallow burial, rarely subaerial
Environment of major lithification	Submarine and subaerial/ meteoric	Unlithified	Subsurface burial, rarely subaerial/meteoric
Timing of cementation	Mainly early diagenetic	-	Rarely early, mainly later diagenetic
Major carbonate cements	Aragonite and HMC	-	Rare IMC, mainly LMC (often ferroan)
Major sources of cements	Sea water and dissolution of aragonite grains	-	Pressure-dissolution of calcitic skeletons
Carbonate petrography	Mud-, wacke-, pack-, rud-, grain- and boundstones	Grain- and rudstones	Grain-, pack- and rudstones

Appendix C-3.1 Rock mass data sheets

Date	28.6.07
Location:	McDonald's Quarry, Upper Steel, northern face
Joint type:	Horizontal flags
Northing	N6316540
Easting	E2691661
Elevation (m)	177
Orient. of face	88/010
Line No.	1

	Flag thick.		Distance	App. joint				Aperture		
Flag No.	(mm)	Joint No.	(mm)	spac. (m)	No. of joints	Dip	Dip direction	Width (mm)	Infill*	Moisture
1	250		250					0	yes	wet
2	190		440					0	yes	wet
3	410		850					0	yes	wet
4	130		980			1	159	0	yes	wet
5	560		1540			0	160	0	yes	wet
6	100		1640			1	148	0	yes	wet
7	170		1810					0	yes	wet
8	130		1940					0	yes	wet

Comments e.g. colour, infill material, weathering, discolouration

up to 1 inch leached seam above/below dissolution seam
same seam material as others (rusty brown silt) up to 4 mm thick
stylotised
photo 16 leached seam
infill* = infill type is a dissolution seam
All upper steel scanlines - wet/seepage from top rain few days earlier
NB: Orients. Don't match flags i.e. 3 randomly measured orients. along scanline

Date	28.6.07
Location:	McDonald's Quarry, Upper Steel, northern face
Joint type:	Horizontal flags
Northing	N6316540
Easting	E2691661
Elevation (m)	177
Orient. of face	88/010
Line No.	2

	Flag thick.		Distance	App. joint				Aperture		
Flag No.	(mm)	Joint No.	(mm)	spac. (m)	No. of joints	Dip	Dip direction	Width (mm)	Infill*	Moisture
1	290		290					0	yes	moist
2	290		580					0	yes	moist
3	300		880			1	258	0	yes	moist
4	160		1040			1	182	0	yes	moist
5	230		1270			1	178	0	yes	moist
6	120		1390					0	yes	moist
7	320		1710					0	yes	moist
8	220		1930					0	yes	moist
9	220		2150					0	yes	moist

Comments e.g. colour, infill material, weathering, discolouration

leached seam thick up to one inch
Rusty brown silt inside seams, max seam thickness is 3 mm
stylotised
infill* = infill type is a dissolution seam
NB: Orients. Don't match flags i.e. 3 randomly measured orients. along scanline

Date	28.6.07
Location:	McDonald's Quarry, Upper Steel, northern face midway
Joint type:	Horizontal flags
Northing	N6316540
Easting	E2691661
Elevation (m)	177
Orient. of face	88/010
Line No.	3

	Flag thick.		Distance	App. joint				Aperture		
Flag No.	(mm)	Joint No.	(mm)	spac. (m)	No. of joints	Dip	Dip direction	Width (mm)	Infill*	Moisture
1	200		200					0	yes	moist
2	220		420					0	yes	moist
3	370		790					0	yes	moist
4	150		940			0.5	182	0	yes	moist
5	410		1350			1	162	0	yes	moist
6	280		1630			0	150	0	yes	moist
7	170		1800					0	yes	moist
8	260		2060					0	yes	moist

Comments e.g. colour, infill material, weathering, discolouration

up to 1 cm thick leached seams
up to 3 mm thick seams
<2 mm thick rusty brown seams - silty
infill* = infill type is a dissolution seam
stylotised
NB: Orients. Don't match flags i.e. 3 randomly measured orients. along scanline

Date	28.6.07
Location:	McDonald's Quarry, Upper Steel, northern face east corner
Joint type:	Horizontal flags
Northing	N6316540
Easting	E2691661
Elevation (m)	177
Orient. of face	88/010
Line No.	4

Flag No.	Flag thick. (mm)	Joint No.	Distance (mm)	App. joint spac. (m)	No. of joints	Dip	Dip direction	Aperture Width (mm)	Infill*	Moisture
1	210		210					0	yes	moist
2	150		360					0	yes	moist
3	350		710			0	197	0	yes	moist
4	370		1080			1	194	0	yes	moist
5	380		1460			1	124	0	yes	moist
6	210		1670					0	yes	moist
7	260		1930					0	yes	moist

Comments e.g. colour, infill material, weathering, discolouration

Up to 2 cm thick leached seams
NB: Orients. Don't match flags i.e. 3 randomly measured orients. along scanline
infill* = infill type is a dissolution seam
<2 mm thick rusty brown seams - silty
stylotised

Date	28.6.07
Location:	McDonald's Quarry, Upper Steel, northern face east corner
Joint type:	Horizontal flags
Northing	N6316540
Easting	E2691661
Elevation (m)	177
Orient. of face	88/010
Line No.	5

Flag No.	Flag thick. (mm)	Joint No.	Distance (mm)	App. joint spac. (m)	No. of joints	Dip	Dip direction	Aperture Width (mm)	Infill*	Moisture
1	200		200					0	yes	moist
2	320		520					0	yes	moist
3	140		660					0	yes	moist
4	140		800			0.5	154	0	yes	moist
5	250		1050			0.5	153	0	yes	moist
6	150		1200			0	192	0	yes	moist
7	170		1370					0	yes	moist
8	130		1500					0	yes	moist
9	130		1630					0	yes	moist
10	240		1870					0	yes	moist

Comments e.g. colour, infill material, weathering, discolouration

NB: Orients. Don't match flags i.e. 3 randomly measured orients. along scanline
<2 mm thick rusty brown seams - silty
infill* = infill type is a dissolution seam
stylotised

Date	19.4.07
Location:	McDonald's Quarry, Aglime, south western
Joint type:	Master joint
Northing	N6316013
Easting	E2691289
Elevation (m)	167
Orient. of face	88/295
Line No.	1

Flag No.	Flag thick. (mm)	Joint No.	Distance (m)	App. joint spac. (m)	No. of joints	Dip	Dip direction	Aperture Width (mm)	Infill	Moisture
		1	0	0	1-dogleg	90	314	0-2	yes	dry-damp
		2	2.3	2.3	1	85	303	tight	yes	sl.moist
		3	5.4	3.1	1	90	308	tight	yes	infill moist
		4	9.5	4.1	1	82	312	0-10	yes	dry+dry infill
		5	11	1.5	1	80	324	tight-relaxed	yes	dry+moist infill
		6	0	0		86	296	v.relaxed	yes	dry
		7	2.5	2.5	4	85	302	0	yes	wet
		8	6.6	4.1		87	302	0	yes	dry, moist infill
		9	6.9	2.8	2	-	-	relaxed	yes	dry, moist infill
		10	9.1	2.2		81	303/124	0-5	yes	dry, infill wet
		11	11.3	2.2	8	87	298	0-10	yes	v.wet
		12	12.4	1.1	1	86	296	tight	yes	wet seepage
		13	15.4	3	1	74	108	tight	yes	dry,infill moist
		14	19.7	4.3	4	89	309	tight	yes	dry,damp infill

Comments e.g. colour, infill material, weathering, discolouration

Joint infill med brown/cream/orange and soft white, infill moist, face dry, wetter higher up and paly
Light brown rock, soft white paly? Up to 3 cm of paly - v. moist-wet. Lots of infill
Light pink/brown coating on rock, and dry paly - relaxed probably blast induced
Cavern 30 cm wide, note extensive brown infill material, shattered hard brittle white material?unusual. Meanders, curvaceous,
Oxidised 30 cm each side of joint, 1-2 mm aperture at bottom
Paly infill, curvy joint, soft and wet near top, shear zone? Cavity? 1.5 m wide zone
Joint 7 is a joint zone
Another joint grey rock, discoloured 20 cm wide either side of joint, thin papery paly, white brittle infill material
Paly, orange stained, thick in places, rock lightish orange/whitish, shattered. Joints closely spaced, relaxed 30 mm at bottom
Paly thick up to 2 cm, brittle white crystals, light grey/brown infill, rusty orange clay
300-400 mm spacing, paly, mix of light brown yellow infill and joint surfaces dripping water off face, joints curve with some masters
Mostly semi-continuous. 0.5 cm calcite lining, 2.9 m joint zone
Apparent spacing measured from end of zone. Rock oxidised 30 cm either side of joint. Straight joint. Major paly up to
2.5 cm thick. Light brown/orangey clay, joint relaxed at bottom
Paly, calcite lining
Paly few cm thick, semi-continuous joints, some straight some curved, orange brown clay, joints 30-40 cm spaced, 2 continuous,
2 semi-continous. 4 joints in 1 metre zone.
- difficult surface to measure

Date	19.4.07
Location:	McDonald's Quarry, Aglime, south western
Joint type:	Small joints between master J3 and J4
Northing	N6316013
Easting	E2691289
Elevation (m)	167
Orient. of face	88/295
Line No.	2

Flag No.	Flag thick. (mm)	Joint No.	Distance (m)	App. joint spac. (m)	No. of joints	Dip	Dip direction	Aperture Width (mm)	Infill	Moisture
		1	1.77	1.77		80	131	0-2	yes	dry
		2	2.3	0.53		86	314	0-2	yes	dry
		3	2.8	2.27		87	142	3	yes	dry
		4	3.2	0.93		84	294	3	yes	dry

Comments e.g. colour, infill material, weathering, discolouration

Gen tight, thin paly. Up to 4 mm rusty orange infill - damp
Paly 4 mm thick
Orange rusty clay infill, paly up to 0.5 thick
Orient not confident, paly up to 5 mm thick, jt relaxed

Date	19.4.07
Location:	McDonald's Quarry, Aglime, south western
Joint type:	Small joints between master J13 and J14
Northing	N6316013
Easting	E2691289
Elevation (m)	167
Orient. of face	86/296
Line No.	3

Flag No.	Flag thick. (mm)	Joint No.	Distance (m)	App. joint spac. (m)	No. of joints	Dip	Dip direction	Aperture Width (mm)	Infill	Moisture
		1	0.25	0.25		87	127	0-3	yes	dry
		2	0.62	0.37		86	294	0	yes	dry
		3	1	0.63				0	yes	dry
			1-2.7	BLAST EFFECTED						
		4	3.1	2.47		87	305	0	yes	dry

Comments e.g. colour, infill material, weathering, discolouration

Paly on calcite infill
Paly , calcite 1.5 cm thick + 2 cm paly, infill damp
Calcite + paly 0.5 cm thick

white calcite?, paly up to 2 cm thick

Date	19.4.07
Location:	McDonald's Quarry, Aglime, south western
Joint type:	Horizontal flags between master J13 and J14
Northing	N6316013
Easting	E2691289
Elevation (m)	167
Orient. of face	86/296
Line No.	4

Flag No.	Flag thick. (mm)	Joint No.	Distance (mm)	App. joint spac. (m)	No. of joints	Dip	Dip direction	Aperture Width (mm)	Infill*	Moisture
1	140		140					0	yes	dry-damp
2	150		290					0	yes	dry-damp
3	40		330					0	yes	dry-damp
4	20		350					0	yes	dry-damp
5	90		440					0	yes	dry-damp
6	180		620					0	yes	dry-damp
7	70		690			<1	294	0	yes	dry-damp
8	130		820					0	yes	dry-damp
9	90		910					0	yes	dry-damp
10	120		1030					0	yes	dry-damp
11	80		1110					0	yes	dry-damp
12	130		1240					0	yes	dry-damp
13	50		1290					0	yes	dry-damp
14	80		1370					0	yes	dry-damp
15	80		1450					0	yes	dry-damp
16	120		1570					0	yes	dry-damp
17	90		1660					0	yes	dry-damp
18	60		1720					0	yes	dry-damp
19	100		1820					0	yes	dry-damp
20	140		1960					0	yes	dry-damp
21	90		2050					0	yes	dry-damp

Comments e.g. colour, infill material, weathering, discolouration

Interflag/seam infill med bwn clay material
Seam infill typically 3-4 mm thick
Seam material dry to damp
Tight apertures
infill* = infill type is a dissolution seam
Fault identified - flag offset 4 cm
NB: Orients. Don't match flags i.e. 3 randomly measured orients. along scanline

Date	19.4.07
Location:	McDonald's Quarry, Aglime, south western
Joint type:	J3 and J4
Northing	N6316013
Easting	E2691289
Elevation (m)	167
Orient. of face	88/295
Line No.	5

Flag No.	Flag thick. (mm)	Joint No.	Distance (mm)	App. joint spac. (m)	No. of joints	Dip	Dip direction	Aperture Width (mm)	Infill*	Moisture
1	120		120					0	yes	dry
2	90		210					0	yes	dry
3	110		320					0	yes	dry
4	100		420					0	yes	dry
5	70		490					0	yes	dry
6	80		570					0	yes	dry
7	150		720			10	294	0	yes	dry
8	50		770					0	yes	dry
9	40		810					0	yes	dry
10	160		970					0	yes	dry
11	60		1030					0	yes	dry
12	50		1080					0	yes	dry
13	110		1190					0	yes	dry
14	80		1270					0	yes	dry
15	70		1340					0	yes	dry
16	150		1490					0	yes	dry
17	90		1580					0	yes	dry
18	90		1670					0	yes	dry
19	110		1780					0	yes	dry
20	30		1810					0	yes	dry

Comments e.g. colour, infill material, weathering, discolouration

Tight apertures
Orient. - 10/294
Rusty bwn orange clay seam material
Grey unoxidised and orange oxidised zones
Up to 5 mm seam thickness typical
infills are dry, infill* = infill type is a dissolution seam
NB: Orients. Don't match flags i.e. 3 randomly measured orients. along scanline

Date	28.6.07
Location:	McDonald's Quarry, Aglime, southern face
Joint type:	Horizontal flags
Northing	N6316036
Easting	E2691251
Elevation (m)	143
Orient. of face	south
Line No.	6

Flag No.	Flag thick. (mm)	Joint No.	Distance (mm)	App. joint spac. (m)	No. of joints	Dip	Dip direction	Aperture Width (mm)	Infill*	Moisture
1	150		150					0	yes	dry
2	90		240					0	yes	dry
3	150		390					0	yes	dry
4	140		530			1	82	0	yes	dry
5	40		570			1	322	0	yes	dry
6	80		650			1	28	0	yes	dry
7	180		830					0	yes	dry
8	100		930					0	yes	dry
9	110		1040					0	yes	dry
10	100		1140					0	yes	dry
11	110		1250					0	yes	dry
12	160		1410					0	yes	dry
13	90		1500					0	yes	dry
14	50		1550					0	yes	dry
15	130		1680					0	yes	dry
16	150		1830					0	yes	dry
17	90		1920					0	yes	dry

Comments e.g. colour, infill material, weathering, discolouration

dry
unoxidised seams
infill* = infill type is a dissolution seam
most typically 2-3 mm thick
NB: Orients. Don't match flags i.e. 3 randomly measured orients. along scanline

Date	28.6.07
Location:	McDonald's Quarry, Aglime, southern face
Joint type:	Horizontal flags
Northing	N6316036
Easting	E2691251
Elevation (m)	143
Orient. of face	south
Line No.	7

Flag No.	Flag thick. (mm)	Joint No.	Distance (mm)	App. joint spac. (m)	No. of joints	Dip	Dip direction	Aperture Width (mm)	Infill*	Moisture
1	140		140					0	yes	dry
2	100		240					0	yes	dry
3	100		340					0	yes	dry
4	130		470					0	yes	dry
5	90		560					0	yes	dry
6	50		610			1	284	0	yes	dry
7	120		730			0	348	0	yes	dry
8	110		840			0	349	0	yes	dry
9	110		950					0	yes	dry
10	40		990					0	yes	dry
11	130		1120					0	yes	dry
12	200		1320					0	yes	dry
13	100		1420					0	yes	dry
14	130		1550					0	yes	dry
15	80		1630					0	yes	dry
16	120		1750					0	yes	dry

Comments e.g. colour, infill material, weathering, discolouration

dry
oxidised seams
2 mm - 1 cm thick seams
wavy flag surfaces
infill* = infill type is a dissolution seam
tight apertures
2 mm aperture - rock affected by quarrying
photo 28 - wavy lower 2 m
29 subhorizontal - hori bedded flags
30 paly on joint
NB: Orients. Don't match flags i.e. 3 randomly measured orients. along scanline

Date	28.6.07
Location:	McDonald's Quarry, Aglime, southern face
Joint type:	Horizontal flags
Northing	N6316036
Easting	E2691251
Elevation (m)	143
Orient. of face	south
Line No.	8

Flag No.	Flag thick. (mm)	Joint No.	Distance (mm)	App. joint spac. (m)	No. of joints	Dip	Dip direction	Aperture Width (mm)	Infill*	Moisture
1	150		150					0	yes	dry
2	120		270					0	yes	dry
3	140		410					0	yes	dry
4	110		520					0	yes	dry
5	50		570					0	yes	dry
6	50		620			1	150	0	yes	dry
7	90		710			1	148	0	yes	dry
8	80		790			1	170	0	yes	dry
9	110		900					0	yes	dry
10	100		1000					0	yes	dry
11	50		1050					0	yes	dry
12	120		1170					0	yes	dry
13	130		1300					0	yes	dry
14	130		1430					0	yes	dry
15	70		1500					0	yes	dry
16	20		1520					0	yes	dry

Comments e.g. colour, infill material, weathering, discolouration

up to 4 mm thick seams
rusty brown and blue grey
infill* = infill type is a dissolution seam
dry
NB: Orients. Don't match flags i.e. 3 randomly measured orients. along scanline

Date	11.4.07
Location:	McDonald's Quarry, High Grade, northern face
Joint type:	Master joint
Northing	N6316308
Easting	E2691520
Elevation (m)	137
Orient. of face	75/028
Line No.	1

Flag No.	Flag thick. (mm)	Joint No.	Distance (m)	App. joint spac. (m)	No. of joints	Dip	Dip direction	Aperture Width (mm)	Infill	Moisture
		1	0	0	4	80	142	open zone	yes	dry
		2	3.3	3.3	1	85	142	0-4	yes	dry
		3	8.7	5.4	2	81	120	?	yes	dry
		4	9.9	2.2	1	fallen	n/a	0	yes	dry
		5	10.7	0.8	1			0	yes	dry
		6	15.2	4.5	1	84	124	0	yes	moist
		7	16.4	1.2	1	78	118	0	yes	dry
		8	19.4	3	1	89	141	0	yes	dry
		9	20.7	1.3	1	90	136	0	yes	moist
		10	23.3	2.6	1	80	128	0	yes	moist
		11	25.8	2.5	1	85	349	3/blast	no	dry
		11a	25.9	2.6					no	dry
		12	30.1	4.3	6-7	90	296	0-4	zone	
		13	34.8	4.8		90	310	0		dry
		14	40.5	5.7	2 ma jts	74	123	0		dry
		15	42.6	2.1	1	83	294	0	yes	moist
		16	44.3	1.78	1	85	121	0	can't see	dry
		17	48.9	4.6	1	89	154	relaxed?	no	dry
		18a	52.6	3.7	1	84	132	0	yes	dry
		18b	56.4	0.5	1	90	132	open-15	yes	moist
		18c	56.8	0.4	1	83	114	0	no	dry
		19	57.2	3.9	1	90	115	0	yes	moist
		20	61.1	1.5	1	85	115	0-3	yes	moist
		20a	62.6	2.7						
		21	65.3	3.65	1	90	122	v.relaxed	yes	dry
		22	68.9	0.75	1	89	304	0-10	yes	moist

Comments e.g. colour, infill material, weathering, discolouration

Joint descriptions begin on the right (east) of the face moving left. Joint zone 30+ cm clay and paly - sampled
Orange clay, sticky
30 cm wide joint zone, orange clay, light brown. Joint meanders
Paly. infill dark grey lining, relaxed and collapsed
paly, orange/brown
paly, brown/grey surface infill
orange/yellow infill. Joint meanders, not good surface for measuring
1 cm thick paly.
light yellow-brown infill, fallen material, possible. Blast -pink coating
Light grey, dog legged joint, orange stained - thin coat
very tight, no discolouration, grey unoxidised rock
Shear zone? Some margin discolouration and paly in other grit
paly, light orange/yellow and brown/grey. Calcite crystals ininfilling - 1 cm thick
grey/brown clay infill and paly, generally blue unoxidised rock
little discolouration (3 cm) joint meanders around
Blue/grey clay infill, white powders, poss shear zone-crushed rock
joint zone. Paly brown/grey and light yellow/orange infill. Rock generally blue/grey, unoxidised. Blast? Relaxed at base-orange stained. Paly and thin calcite, light brown/yellow infill
3-4 mm thick paly. Joint 20a semi-continuous
Med-brown infill. White powder on surfaces-associated with blast hole
very thick moist paly on calcite and more brittle material-paly?

Date	11.4.07
Location:	McDonald's Quarry, High Grade, northern
Joint type:	Small joints between master J11 and J12
Northing	N6316308
Easting	E2691520
Elevation (m)	137
Orient. of face	75/028
Line No.	2

Flag No.	Flag thick. (mm)	Joint No.	Distance (m)	App. joint spac. (m)	No. of joints	Dip	Dip direction	Aperture Width (mm)	Infill	Moisture
		1	0.4	0.4			319	0-10	yes	dry
		2	1.5	1.5			313	0	coating	dry

Comments e.g. colour, infill material, weathering, discolouration

white, orangey pale yel thin coat-0.5 cm thick, little bit of paly. infill is moist
light grey powdery coating - above eye level darker grey coating and paly

Date	11.4.07
Location:	McDonald's Quarry, High Grade, northern face
Joint type:	Small joints bewteen master J17 and J18
Northing	N6316308
Easting	E2691520
Elevation (m)	137
Orient. of face	75/028
Line No.	4

Flag No.	Flag thick. (mm)	Joint No.	Distance (m)	App. joint spac. (m)	No. of joints	Dip	Dip direction	Aperture Width (mm)	Infill	Moisture
		1	0.45	0.45		75	126	0-4	yes	dry
		2	1.05	0.6		85	116	0-2	no	dry

Comments e.g. colour, infill material, weathering, discolouration

Paly infill + light bwn/grey infill
Paly at top of scanline

NB: J18 is on left and 0 m on tape measure
Photo 62-64 of hori scanline
single flag fractures not counted in field

Date	11.4.07
Location:	McDonald's Quarry, High Grade, northern face
Joint type:	Horizontal flags between master J1 and J2
Northing	N6316308
Easting	E2691520
Elevation (m)	137
Orient. of face	75/028
Line No.	3

Flag No.	Flag thick. (mm)	Joint No.	Distance (mm)	App. joint spac. (m)	No. of joints	Dip	Dip direction	Aperture Width (mm)	Infill*	Moisture
1	100		100					0	yes	moist
2	60		160					0	yes	moist
3	60		220					0	yes	moist
4	90		310					0	yes	moist
5	70		380					0	yes	moist
6	100		480			1	348	0	yes	moist
7	180		660					0	yes	moist
8	170		830					0	yes	moist
9	200		1030					0	yes	moist
10	170		1200					0	yes	moist
11	70		1270					0	yes	moist
12	60		1330					0	yes	moist
13	90		1420					0	yes	moist
14	130		1550					0	yes	moist
15	130		1680					0	yes	moist
16	70		1750					0	yes	moist
17	100		1850					0	yes	moist

Comments e.g. colour, infill material, weathering, discolouration

Moist dk blue-grey infill, silty slightly gritty, unoxidised infill typically 0-4 mm thick
infill* = infill type is a dissolution seam
Rock is grey unoxidised, fresh
Photos 28-31
NB: Orients. Don't match flags i.e. 3 randomly measured orients. along scanline

Date	11.4.07
Location:	McDonald's Quarry, High Grade, northern face
Joint type:	Horizontal flags between master J17and J18
Northing	N6316308
Easting	E2691520
Elevation (m)	137
Orient. of face	75/028
Line No.	5

Flag No.	Flag thick. (mm)	Joint No.	Distance (mm)	App. joint spac. (m)	No. of joints	Dip	Dip direction	Aperture Width (mm)	Infill*	Moisture
1	150		150					0	yes	dry
2	70		220					0	yes	dry
3	70		290					0	yes	dry
4	120		410					0	yes	dry
5	70		480			2	122	0	yes	dry
6	140		620			1	111	0	yes	dry
7	80		700					0	yes	dry
8	130		830					0	yes	dry
9	220		1050					0	yes	dry
10	180		1230					0	yes	dry
11	60		1290					0	yes	dry
12	90		1380					0	yes	dry
13	50		1430					0	yes	dry
14	90		1520					0	yes	dry
15	70		1590					0	yes	dry
16	60		1650					0	yes	dry

Comments e.g. colour, infill material, weathering, discolouration

tight apertures
dk grey infill up to 3 mm thick, silty slightly gritty
Dissolution seam dry, infill* = infill type is a dissolution seam
infill slightly moist
2/122, 1/111? Orient. No good surfaces to measure
big variation in flag thickness, wavy
NB: Compared to Lower Steel, High Grade difficult to measure orient on flat avail. surfaces
Rock sample taken from bet J17 and J18 code B
NB: Orients. Don't match flags i.e. 3 randomly measured orients. along scanline

Date	28.6.07
Location:	McDonald's Quarry, High Grade, northern face
Joint type:	Horizontal flags
Northing	N6316306
Easting	E2691383
Elevation (m)	121
Orient. of face	75/028
Line No.	6

Flag No.	Flag thick. (mm)	Joint No.	Distance (mm)	App. joint spac. (m)	No. of joints	Dip	Dip direction	Aperture Width (mm)	Infill*	Moisture
1	130		130					0	yes	dry
2	180		310					0	yes	dry
3	120		430					0	yes	dry
4	120		550					0	yes	dry
5	170		720			0	200	0	yes	dry
6	170		890			1	189	0	yes	dry
7	130		1020			1	186	0	yes	dry
8	150		1170					0	yes	dry
9	200		1370					0	yes	dry
10	190		1560					0	yes	dry

Comments e.g. colour, infill material, weathering, discolouration

rusty brown and blue grey
2-3 mm thick
infill* = infill type is a dissolution seam
dry
tight apertures
wavy flag surfaces
NB: Orients. Don't match flags i.e. 3 randomly measured orients. along scanline

Date	28.6.07
Location:	McDonald's Quarry, High Grade, northern face
Joint type:	Horizontal flags
Northing	N6316306
Easting	E2691383
Elevation (m)	121
Orient. of face	75/028
Line No.	7

Flag No.	Flag thick. (mm)	Joint No.	Distance (mm)	App. joint spac. (m)	No. of joints	Dip	Dip direction	Aperture Width (mm)	Infill*	Moisture
1	140		140					0	yes	dry
2	100		240					0	yes	dry
3	160		400					0	yes	dry
4	170		570			1	200	0	yes	dry
5	160		730			1	210	0	yes	dry
6	180		910			1	206	0	yes	dry
7	150		1060					0	yes	dry
8	140		1200					0	yes	dry
9	90		1290					0	yes	dry
10	60		1350					0	yes	dry
11	140		1490					0	yes	dry
12	70		1560					0	yes	dry
13	130		1690					0	yes	dry
14	160		1850					0	yes	dry

Comments e.g. colour, infill material, weathering, discolouration

dry
unoxidised blue grey seams
infill* = infill type is a dissolution seam
Seam thickness 3-10 mm
NB: Orients. Don't match flags i.e. 3 randomly measured orients. along scanline

Date	28.6.07
Location:	McDonald's Quarry, High Grade, northern face
Joint type:	Horizontal flags
Northing	N6316306
Easting	E2691383
Elevation (m)	121
Orient. of face	75/028
Line No.	8

Flag No.	Flag thick. (mm)	Joint No.	Distance (mm)	App. joint spac. (m)	No. of joints	Dip	Dip direction	Aperture Width (mm)	Infill*	Moisture
1	120		120					0	yes	dry
2	100		220					0	yes	dry
3	130		350					0	yes	dry
4	120		470			2	202	0	yes	dry
5	150		620			2	208	0	yes	dry
6	80		700			1.5	210	0	yes	dry
7	170		870					0	yes	dry
8	130		1000					0	yes	dry
9	80		1080					0	yes	dry
10	140		1220					0	yes	dry
11	200		1420					0	yes	dry
12	120		1540					0	yes	dry
13	100		1640					0	yes	dry
14	40		1680					0	yes	dry

Comments e.g. colour, infill material, weathering, discolouration

dry
tight aperture
infill* = infill type is a dissolution seam
all oxidised blue grey
wavy flag surfaces
1-4 mm thick seams
\silty- clay
NB: Orients. Don't match flags i.e. 3 randomly measured orients. along scanline

Date	30.03.07
Location:	McDonald's Quarry, Lower Steel Grade, northern
Joint type:	Master joint
Northing	N6316251
Easting	E2691507
Elevation (m)	118
Orient. of face	85/302
Line No.	1

	Flag thick.		Distance	App. joint				Aperture		
Flag No.	(mm)	Joint No.	(m)	spac. (m)	No. of joints	Dip	Dip direction	Width (mm)	Infill	Moisture
		1	0	0	3-4	75	184	40	yes	moist
		2	11.7	11.7	5	85	152	2-5	yes	seepage
		3	22.3	10.5	1	85	332	5-10	none	dry
		4	26.75	4.45	1-2	86	164	3-6	none	wet
		5	31.15	4.4	3-4	90	148	3-5	none	dry-sl. Moist
		6	40.15	9	3-6	86	133	20	yes	dry
		7	47.05	6.9	1-4	86	136	10-30	none	dry
		8	51.9	4.85	3	85	334	10-20	none	dry

Comments e.g. colour, infill material, weathering, discolouration

black discolouration near bottom, infill light brown clay
joints closely spaced, clay infill
aperture tight higher up
raining on the day
thin brown lining on joint surface

Date	30.3.07
Location:	McDonald's Quarry, Lower Steel Grade, northern face
Joint type:	Master joint
Northing	N6316251
Easting	E2691507
Elevation (m)	118
Orient. of face	86/132
Line No.	1b

	Flag thick.		Distance	App. joint				Aperture		
Flag No.	(mm)	Joint No.	(m)	spac. (m)	No. of joints	Dip	Dip direction	Width (mm)	Infill	Moisture
		9	n/a	n/a	1	86	132	blast effected	yes	dry

Comments e.g. colour, infill material, weathering, discolouration

exposed joint surf. Perpend. To main joint sets, light brown/white coating on surf. Med sand granules, 1-2 mm thick dry lining on surf. Extensive up to 1 m sq patches of ropey clay but not continuous (blobs on face) ubitquitous along joint surf. Rock face colour varies to pale yel, yel orange, med brown. Many vert. joints terminate at disconformity (boundary bet. subhori. bedding and x-bedding 2/3 way up face. oxidised rock beneath disconfomrity and approx. 1 m thick strip of unoxidised rock above. Sample OH100 taken on surface

Date	30.3.07
Location:	McDonald's Quarry, Lower Steel Grade, northern face
Joint type:	Small joints between masters J1 and J2
Northing	N6316251
Easting	E2691507
Elevation (m)	118
Orient. of face	85/302
Line No.	2

	Flag thick.		Distance	App. joint				Aperture		
Flag No.	(mm)	Joint No.	(m)	spac. (m)	No. of joints	Dip	Dip direction	Width (mm)	Infill	Moisture
		1	2.53	2.53 [2]		80	128	0	none	wet
		2	3.4	0.87 [1]		85	152	0	none	wet
		3	3.75	0.35 [2]		75	138	3	none	wet
		4	3.8	0.05 [3]		85	96	3	none	
		5	4.15	0.35 [2]		88	140	0	none	wet
		6	4.38	0.23 [1]		85	152	0-3	none	wet
		7	4.73	0.35 [2]		82	130	0-2	none	seepage
		8	4.87	0.14 [3]		87	280	0	none	wet
		9	4.94	0.07 [3]		80	103	0-1	none	wet
		10	5.59	0.64 [2]		85	302	0	hard lining	
			5.59-7					2-3	none	
		11	7.23	1.64 [3]		89	282	0-2	hard lining	wet
		12	7.75	0.52 [3]		75	112	0-1	none	wet
		13	7.81	0.06 [2]		79	135	0-3	none	wet
		14	7.97	0.16 [2]		74	135	0-6	none	wet
		15	8.25	0.28 [1]		87	153	0-3	none	wet
		16	8.75	0.5 [3]		89	106	?	?	wet
		17	9.31	0.56 [1]		89	339	0	hard lining	wet
		18	9.72	0.41 [1]		90	150	≤3	hard lining	wet
		19	10.3	0.58 [1]		75	158	0-8	none	wet
		20	11.28	0.98 [2]		79	132	0-3	none	wet

Comments e.g. colour, infill material, weathering, discolouration

many not well exposed, some have calcite lining (secondary precipitate) about 1-5 mm thick. Gap between joint 10 and 11 has 9 vertical joints persistent through more than a single flag. All flags have similar pattern but no linking of joints. Day is wet, light showers. Joints are leading into a joint zone of master joint 2.
Superscripts indicate joint set number for small joints in the Lower Steel unit

Date	30.3.07
Location:	McDonald's Quarry, Lower Steel Grade, northern face
Joint type:	Small joints between masters J7 and J8
Northing	N6316251
Easting	E2691507
Elevation (m)	118
Orient. of face	85/302
Line No.	3

Flag No.	Flag thick. (mm)	Joint No.	Distance (m)	App. joint spac. (m)	No. of joints	Dip	Dip direction	Aperture Width (mm)	Infill	Moisture
		1	0.17	0.17 [1]		85	332	3	none	dry
		2	1.7	1.53 [1]		80	162	tight-no side	hard white lin	
		3	1.7-3						none	dry
		4	3.25	1.55 [1]		80	154	3	none	dry
		5	4.44	1.19 [2]		90	132	2-3	none	dry

Comments e.g. colour, infill material, weathering, discolouration

ininfill fawn to white, clay up to 2 mm thick. 6 vertical joints only occur through a single flag. White brittle lining 4 mm thick.
Superscripts indicate joint set number for small joints in the Lower Steel unit

Date	30.3.07
Location:	McDonald's Quarry, Lower Steel Grade, northern face
Joint type:	Horizontal flags between masters J1 and J8
Northing	N6316251
Easting	E2691507
Elevation (m)	118
Orient. of face	85/302
Line No.	4

Flag No.	Flag thick. (mm)	Joint No.	Distance (mm)	App. joint spac. (m)	No. of joints	Dip	Dip direction	Aperture Width (mm)	Infill*	Moisture
1	80		80					0	yes	dry
2	90		170					0	yes	dry
3	60		230					0	yes	dry
4	100		330					0	yes	dry
5	80		410			3	238	0	yes	dry
6	120		530					0	yes	dry
7	30		560			7	220	0	yes	dry
8	90		650					0	yes	dry
9	90		740					0	yes	dry
10	70		810					0	yes	dry
11	170		980			0.5	236	0	yes	dry
12	120		1100					0	yes	dry
13	60		1160					0	yes	dry
14	90		1250					0	yes	dry
15	120		1370					0	yes	dry
16	110		1480					0	yes	dry
17	80		1560					0	yes	dry
18	80		1640					0	yes	dry
19	80		1720					0	yes	dry
20	140		1860					0	yes	dry

Comments e.g. colour, infill material, weathering, discolouration

All apertures tight, occassionally <1 mm wide
Brown oxidised material along every interflag surface v. thin 1 mm max.
infill* = infill type is a dissolution seam
Seam material contains trace clay (discolours hand) with some coarse grit
Rough coating on bedding surfs. Dry? But hard to tell today - rainfall on the day
NB: Orients. Don't match flags i.e. 3 randomly measured orients. along scanline

Date	30.3.07	Sheet 1 of 1
Location:	McDonald's Quarry, Lower Steel Grade, northern	
Joint type:	Horizontal flags between masters J7 and J8	
Northing	N6316251	
Easting	E2691507	
Elevation (m)	118	
Orient. of face	85/302	
Line No.	5	

Flag No.	Flag thick. (mm)	Joint No.	Distance (mm)	App. joint spac. (m)	No. of joints	Dip	Dip direction	Aperture Width (mm)	Infill*	Moisture
1	100		100					0	yes	moist
2	60		160					0	yes	moist
3	130		290					0	yes	moist
4	100		390					0	yes	moist
5	160		550					0	yes	moist
6	70		620					0	yes	moist
7	240		860			0	223	0	yes	moist
8	140		1000					0	yes	moist
9	100		1100					0	yes	moist
10	160		1260					0	yes	moist
11	170		1430					0	yes	moist
12	200		1630					0	yes	moist

Comments e.g. colour, infill material, weathering, discolouration

Apertures all tight
Med. Bwn, soft sand, up to 1 mm thick seam material
White, soft, sand with trace clay up to 10 mm thick to v. pale bwn seam material
infill* = infill type is a dissolution seam
bwn infill finer than sample from jt. 9?
All seams moist
Avg flag thickness = 13.5 cm
NB: Orients. Don't match flags i.e. 3 randomly measured orients. along scanline
NB: Orients difficult to measure

Date	28.6.07
Location:	McDonald's Quarry, Lower Steel Grade, northern face
Joint type:	Horizontal flags
Northing	N6316251
Easting	E2691507
Elevation (m)	118
Orient. of face	85/302
Line No.	6

	Flag thick.		Distance	App. joint				Aperture		
Flag No.	(mm)	Joint No.	(mm)	spac. (m)	No. of joints	Dip	Dip direction	Width (mm)	Infill*	Moisture
1	150		150					0	yes	dry
2	140		290					0	yes	dry
3	140		430					0	yes	dry
4	50		480					0	yes	dry
5	80		560			0.5	183	0	yes	dry
6	160		720			1	183	0	yes	dry
7	50		770			0.5	181	0	yes	dry
8	160		930					0	yes	dry
9	80		1010					0	yes	dry
10	60		1070					0	yes	dry
11	120		1190					0	yes	dry
12	130		1320					0	yes	dry
13	170		1490					0	yes	dry
14	90		1580					0	yes	dry
15	130		1710					0	yes	dry
16	110		1820					0	yes	dry
17	160		1980					0	yes	dry
18	100		2080					0	yes	dry
19	140		2220					0	yes	dry

Comments e.g. colour, infill material, weathering, discolouration

<1 mm thick seams - silt rusty brown
all oxidised
stylotised
subhorizontal flag surfaces
infill* = infill type is a dissolution seam
tight apertures
dry
up to inch leached seam on some flags
NB: Orients. Don't match flags i.e. 3 randomly measured orients. along scanline

Date	28.6.07
Location:	McDonald's Quarry, Lower Steel Grade, northern face
Joint type:	Horizontal flags
Northing	N6316251
Easting	E2691507
Elevation (m)	118
Orient. of face	85/302
Line No.	7

	Flag thick.		Distance	App. joint				Aperture		
Flag No.	(mm)	Joint No.	(mm)	spac. (m)	No. of joints	Dip	Dip direction	Width (mm)	Infill*	Moisture
1	280		280					0	yes	dry
2	130		410					0	yes	dry
3	150		560					0	yes	dry
4	100		660			1	200	0	yes	dry
5	140		800			1	194	0	yes	dry
6	100		900			0.5	168	0	yes	dry
7	110		1010					0	yes	dry
8	100		1110					0	yes	dry
9	80		1190					0	yes	dry
10	180		1370					0	yes	dry
11	200		1570					0	yes	dry
12	170		1740					0	yes	dry

Comments e.g. colour, infill material, weathering, discolouration

dry
tight aperture
infill* = infill type is a dissolution seam
rusty brown seam
<1 mm typical seam thickness
stylotised
NB: Orients. Don't match flags i.e. 3 randomly measured orients. along scanline

Date	28.6.07
Location:	McDonald's Quarry, Lower Steel Grade, northern
Joint type:	Horizontal flags
Northing	N6316251
Easting	E2691507
Elevation (m)	118
Orient. of face	85/302
Line No.	8

Flag No.	Flag thick. (mm)	Joint No.	Distance (mm)	App. joint spac. (m)	No. of joints	Dip	Dip direction	Aperture Width (mm)	Infill*	Moisture
1	80		80					0	yes	dry
2	150		230					0	yes	dry
3	100		330					0	yes	dry
4	210		540					0	yes	dry
5	80		620			1	228	0	yes	dry
6	80		700			1	218	0	yes	dry
7	220		920			1	210	0	yes	dry
8	130		1050					0	yes	dry
9	140		1190					0	yes	dry
10	200		1390					0	yes	dry
11	180		1570					0	yes	dry
12	230		1800					0	yes	dry

Comments e.g. colour, infill material, weathering, discolouration

all tight apertures
dry
infill* = infill type is a dissolution seam
rusty brown seam <1 mm thick
stylotised
leached seam up to 1.5 cm
NB: Orients. Don't match flags i.e. 3 randomly measured orients. along scanline

Appendix C-3.2 Stereonets

Upper Steel

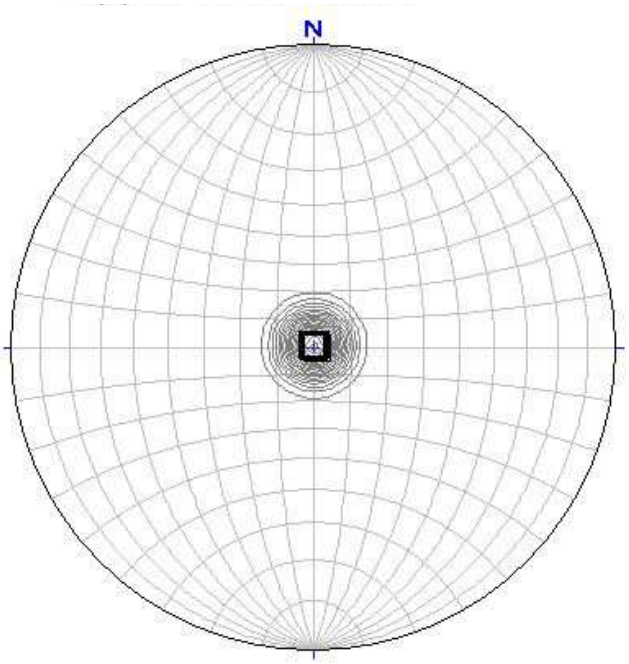

Stereonet showing orientations of limestone flags in the Upper Steel unit, northern face, McDonald's Quarry (2007). Bearing 0, distance = 0. The beds are therefore horizontal.

Aglime

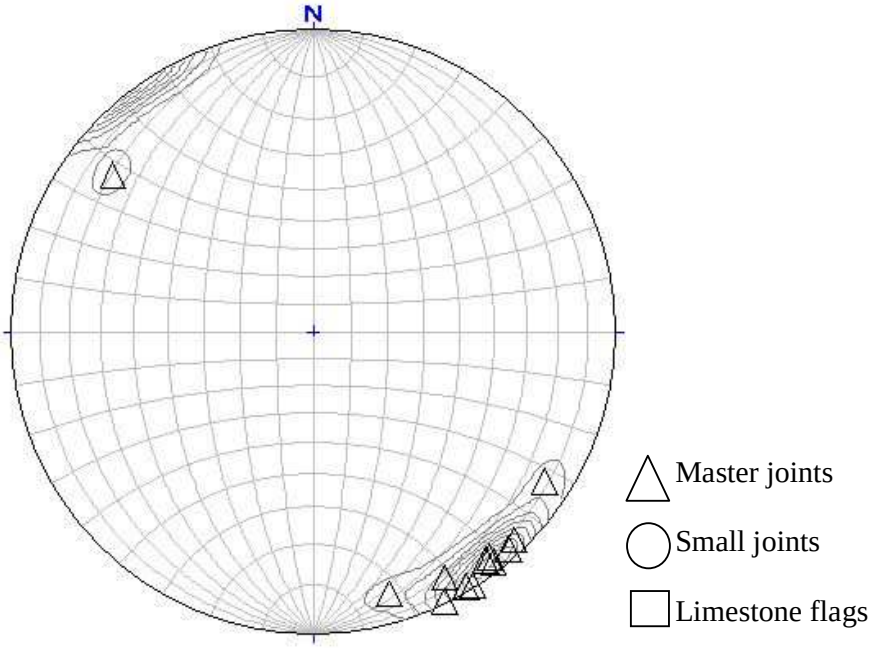

Stereonet showing orientations of master joints in the Aglime unit. There is one master joint set indicated by the bottom right cluster with a dip/dip direction of 86/322. The master joint to the top left is an outlier.

Aglime

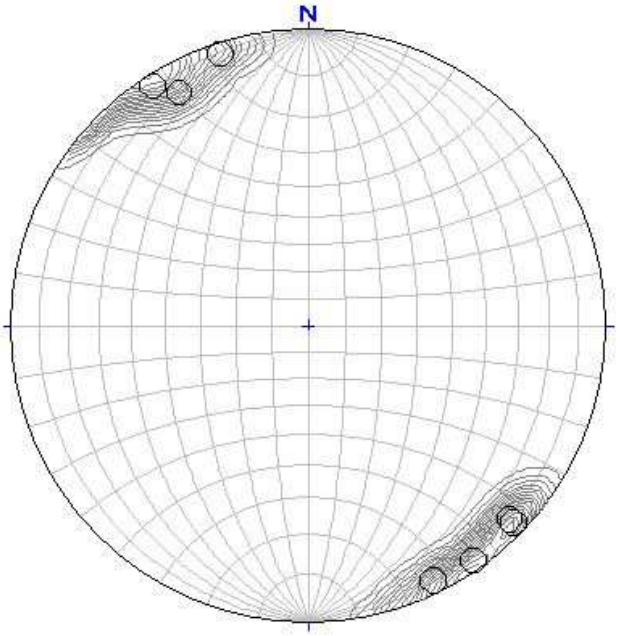

Stereonet showing orientations of small joints in the Aglime unit. There is one cluster of small joints which falls across the circumference of the stereonet. They have a dip/dip direction of 85/149.

Aglime

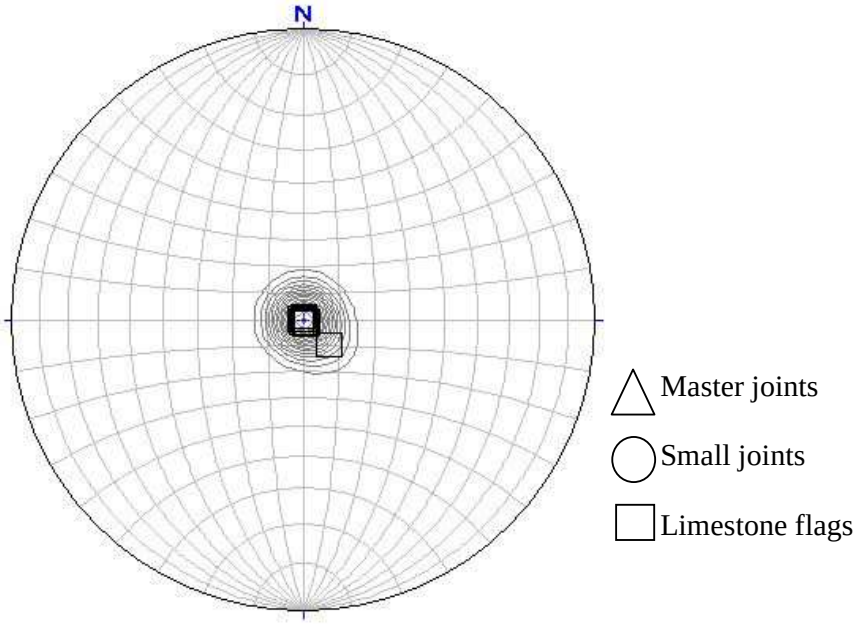

Stereonet showing orientations of horizontal joints for the Aglime unit. One joint deviates from the main central cluster and is considered an outlier. The main cluster has a bearing of 0 and a distance of 0. The joints are therefore horizontal.

High Grade

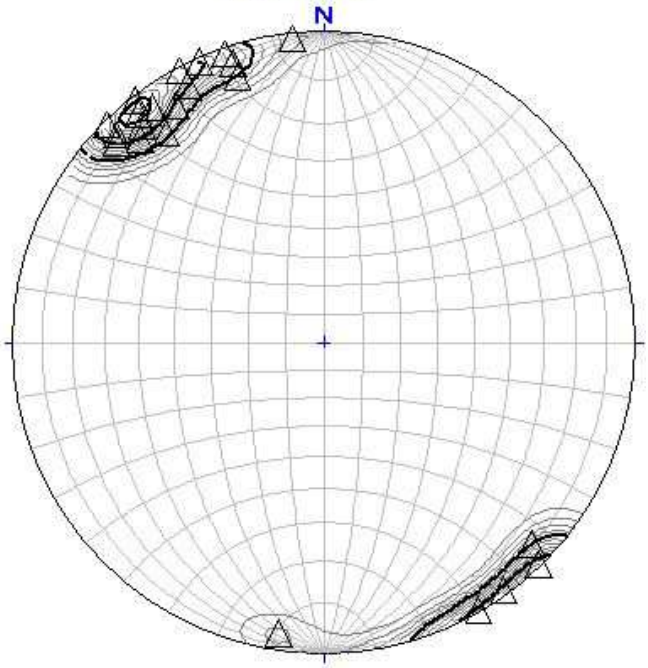

Stereonet showing master joints in the High Grade showing one master joint cluster belonging to the same joint set. The dip/dip direction is 85/141.

High Grade

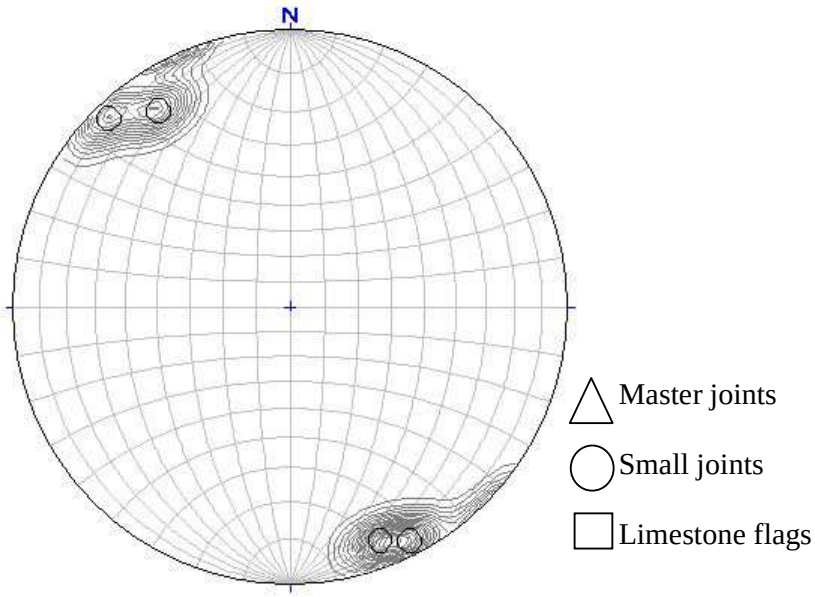

Stereonet showing small joints in the High Grade unit showing one cluster that belongs to the same joint set which has a dip/dip direction of 81/141.

High Grade

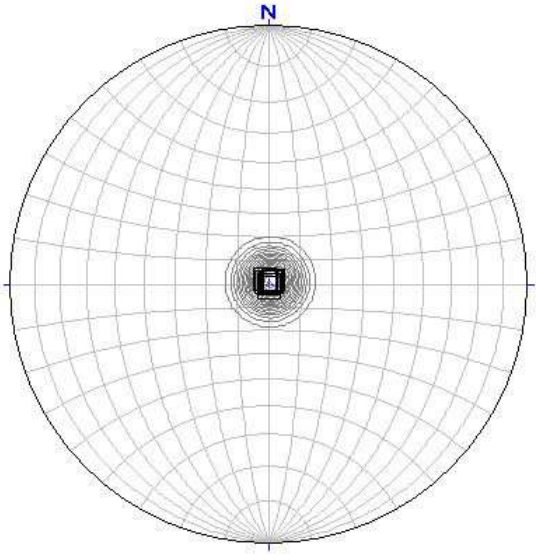

Stereonet showing orientations of horizontal joints in the High Grade unit. The central cluster of joints have a bearing of 0 and a distance of 0. These joints are therefore horizontal.

Lower Steel

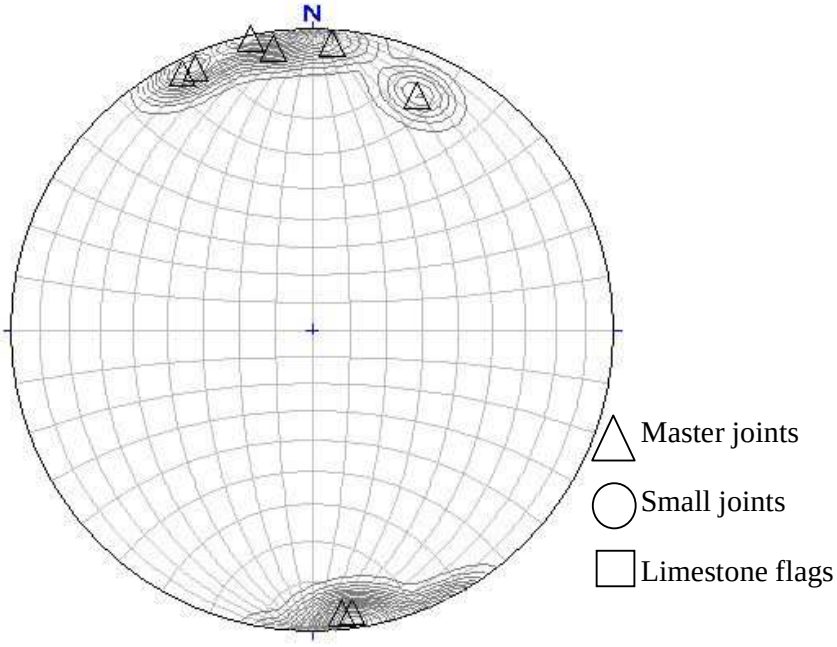

Stereonet showing master joints in the Lower Steel unit. Three master joint clusters occur in the top left and one in the bottom right. These clusters belong to the same joint set and have a dip/dip direction of 87/172. Spread of dip is ± 1° and dip direction is ± 16°.

Lower Steel

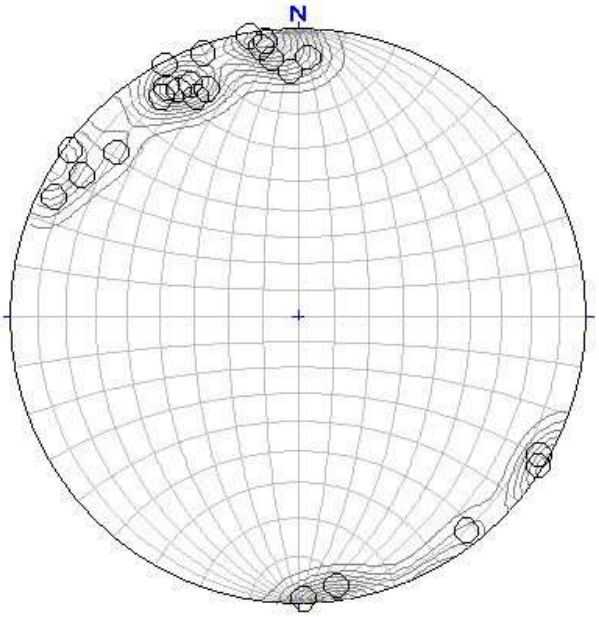

Stereonet showing small joints in the Lower Steel unit. There are five clusters in the small joints, and an outlier. These are part of the same joint set also and have dip/dip directions of 84/172, 85/122, and 87/322.

Lower Steel

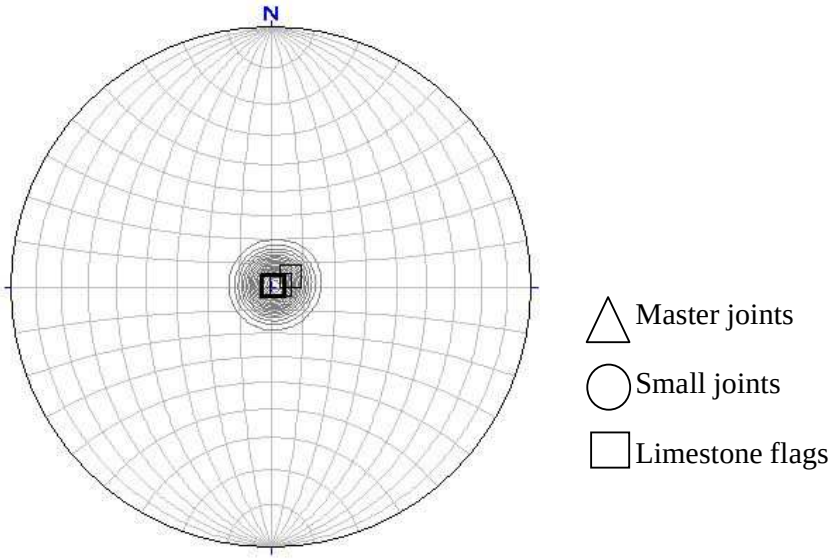

Stereonet showing orientations of horizontal joints in the Lower Steel unit. The central cluster has a bearing of 0 and a distance of 0. Therefore, these joints are horizontal.

Appendix C-3.3 Dip and dip direction measurements

Stereonet measurement results (bearing and distance), showing calculated dip and dip direction for each joint set identified in each quarry limestone unit. The orientation (corrected for magnetic declination) of each face of the units is on the left, followed by the joint type, joint set number, and orientation data.

Quarry unit and orient. of face	Joint type	Set No.	Bearing	Distance	Orient.
Upper Steel 88/030	Flag	1	0	0	0/0
Aglime 88/315	Master	1	142	482	86/322
	Small	1	329	479	85/149
	Flag	1	0	0	0/0
High Grade 75/028	Master	1	321	478	85/141
	Small	1	321	461	81/141
	Flag	1	0	0	0/0
Lower Steel 85/322	Master	1	352	488	87/172
	Small	1	354	472	84/174
	Small	2	332	447	85/152
	Small	3	302	478	87/122
	Flag	1	0	0	0/0

Appendix C-3.4 True joint spacing calculations. Sapp = apparent spacing.

Quarry unit	Joint type and set number	Apparent spacing (Sapp) (m)	Apparent std. deviation	No. joints	Dip dire. of face (A)	Dip dire. of joint (B)	θ (A-B)	True spacing (S = Sappsinθ) (m)	True std. error
Aglime	Master set 1	2.53	1.01	13	315	322	7	0.31	0.03
	Small set 1	1.23	0.93	7	315	149	166	0.30	0.08
High Grade	Master set 1	2.66	1.64	22	28	141	113	2.45	0.32
	Small set 1	0.74	0.52	4	28	141	113	0.68	0.24
Lower Steel	Master set 1	7.40	3.03	7	322	172	150	3.70	0.58
	Small set 1	0.69	0.53	9	322	174	148	0.37	0.10
	Small set 2	0.74	0.77	6	322	152	170	0.13	0.05
	Small set 3	0.49	0.60	9	322	122	20	0.17	0.07

Appendix C-3.5

t-Test data results comparing Lower Steel and High Grade flag thickness.

t-Test: Two-Sample Assuming Equal Variances

	Lower Steel	*High Grade*
Mean	12.33	12.24
Variance	24.74	18.98
Observations	75	71
Pooled Variance	21.94	
Hypothesized Mean Difference	0	
df	144	
t Stat	0.1211	
P(T<=t) one-tail	0.4519	
t Critical one-tail	1.6555	
P(T<=t) two-tail	0.9038	
t Critical two-tail	1.9766	

t-Test data results for comparing Lower Steel and Aglime flag thickness.

t-Test: Two-Sample Assuming Equal Variances

	Lower Steel	*Aglime*
Mean	12.33	10.06
Variance	24.74	14.57
Observations	75	90
Pooled Variance	19.19	
Hypothesized Mean Difference	0	
df	163	
t Stat	3.3260	
P(T<=t) one-tail	0.0005	
t Critical one-tail	1.6543	
P(T<=t) two-tail	0.0011	
t Critical two-tail	1.9746	

t-Test data results for comparing Lower Steel and Upper Steel flag thickness.

t-Test: Two-Sample Assuming Equal Variances

	Lower Steel	*Upper Steel*
Mean	12.33	23.69
Variance	24.74	99.00
Observations	75	42
Pooled Variance	51.21	
Hypothesized Mean Difference	0	
df	115	
t Stat	-8.2345	
P(T<=t) one-tail	0.0000	
t Critical one-tail	1.6582	
P(T<=t) two-tail	0.0000	
t Critical two-tail	1.9808	

t-Test data results for comparing High Grade and Aglime flag thickness.

t-Test: Two-Sample Assuming Equal Variances

	High Grade	*Aglime*
Mean	12.24	10.06
Variance	18.98	14.57
Observations	71	90
Pooled Variance	16.51	
Hypothesized Mean Difference	0	
df	159	
t Stat	3.3857	
P(T<=t) one-tail	0.0004	
t Critical one-tail	1.6545	
P(T<=t) two-tail	0.0009	
t Critical two-tail	1.9750	

t-Test data results for comparing High Grade and Upper Steel flag thickness.

t-Test: Two-Sample Assuming Equal Variances

	High Grade	*Upper Steel*
Mean	12.24	23.69
Variance	18.98	99.00
Observations	71	42
Pooled Variance	48.54	
Hypothesized Mean Difference	0	
df	111	
t Stat	-8.4433	
P(T<=t) one-tail	0.0000	
t Critical one-tail	1.6587	
P(T<=t) two-tail	0.0000	
t Critical two-tail	1.9816	

t-Test data results for comparing Aglime and Upper Steel flag thickness.

t-Test: Two-Sample Assuming Equal Variances

	Aglime	*Upper Steel*
Mean	10.06	23.69
Variance	14.57	99.00
Observations	90	42
Pooled Variance	41.20	
Hypothesized Mean Difference	0	
df	130	
t Stat	-11.3678	
P(T<=t) one-tail	0.0000	
t Critical one-tail	1.6567	
P(T<=t) two-tail	0.0000	
t Critical two-tail	1.9784	

Appendix D-4.1 Depth, thickness, and elevation data for the 500 drill hole series. Adapted from Ormiston Associates Ltd (2005).

	Hole No.	Coordinates N (NZ Map Grid)	E (NZ Map Grid)	Coordinates N (Mt Eden Circuit)	E (Mt Eden Circuit)	Collar R.L. (m)	Total depth (m)	Hole Type	Geology: Depth to Top of Unit (m) Overburden: Kauroa Ash	Overburden: Taumatamaire Formation	Otorohanga Limestone: Cap Rock	Otorohanga Limestone: Upper Steel grade
mAH Depth	BH501	6317068.9	2691360.3	538684.4	326970.9	198.4	167.9	Core	0.0	10.8	36.1	38.3
	BH502	6316710.5	2690996.9	538318.6	326614.9	211.3	206.0	Core	0.0	12.2	25.5	27.1
	BH503	6316627.3	2690563.9	538226.7	326183.7	221.4	143.0	Core	0.0	8.6	19.7	21.8
	BH504	6316539.8	2691394.7	538156.0	327016.1	159.1	113.7	Core				
	BH505	6316036.6	2691284.3	537650.6	326915.9	162.2	133.3	Core				
mAH Thickness	BH501	6317068.9	2691360.3	538684.4	326970.9	198.4	167.9	Core	6.4	28.8	2.4	-37.6
	BH502	6316710.5	2690996.9	538318.6	326614.9	211.3	206.0	Core	3.0	18.1	1.8	10.0
	BH503	6316627.3	2690563.9	538226.7	326183.7	221.4	143.0	Core	4.6	17.9	1.9	8.6
	BH504	6316539.8	2691394.7	538156.0	327016.1	159.1	113.7	Core				
	BH505	6316036.6	2691284.3	537650.6	326915.9	162.2	133.3	Core				
masl Elevation	BH501	6317068.9	2691360.3	538684.4	326970.9	198.4	167.9	Core	198.4	187.6	162.3	160.1
	BH502	6316710.5	2690996.9	538318.6	326614.9	211.3	206.0	Core	211.3	199.1	185.8	184.2
	BH503	6316627.3	2690563.9	538226.7	326183.7	221.4	143.0	Core	221.4	212.8	201.8	199.6
	BH504	6316539.8	2691394.7	538156.0	327016.1	159.1	113.7	Core				
	BH505	6316036.6	2691284.3	537650.6	326915.9	162.2	133.3	Core				

masl = metres above sea level
mAH = metres along hole

Appendix D-4.1 continued.

	Hole No.	Geology: Depth to Top of Unit (m)						
		Otorohanga Limestone						
		AgLime	High Grade	Lower Steel Grade	Sub-economic	Waitomo Sandstone Eq.	Orahiri Limestone	Aotea Formation
mAH Depth	BH501	46.5	59.2	77.5	79.0	129.5	139.2	149.2
	BH502	37.0	48.2	65.8	68.5	112.2	121.7	132.0
	BH503	31.6	42.4	60.2	77.1	103.8	117.0	123.2
	BH504	0.0	18.0	30.9	43.3	74.4	79.7	92.3
	BH505	0.0	20.7	28.2	46.0	78.9	83.3	92.8
mAH Thickness	BH501	0.0	0.0	0.0	0.0	0.0	0.0	38.6
	BH502	-32.9	0.0	0.0	0.0	0.0	0.0	34.0
	BH503	-33.0	0.0	0.0	0.0	0.0	0.0	33.9
	BH504	0.0	0.0	0.0	0.0	0.0	0.0	37.9
	BH505	-26.8	0.0	0.0	0.0	0.0	0.0	33.6
masl Elevation	BH501	151.9	139.2	120.9	119.5	68.9	59.3	49.2
	BH502	174.3	163.1	145.5	142.8	99.1	89.6	79.3
	BH503	189.9	179.1	161.3	144.3	117.6	104.4	98.2
	BH504	159.1	141.1	128.2	115.8	84.7	79.4	66.8
	BH505	162.2	141.6	134.1	116.2	83.3	78.9	69.4

masl = metres above sea level
mAH = metres along hole

Appendix D-4.2.A Discontinuity data sheets for drill hole BH501

Discontinuity core log data sheet

Page 1 of 32

Logged by	Orla Hansen											
Location	Mc Donald's Quarry											
Date logged	Mar-07											
Borehole number	501											
Box number	10											
Depth (m)	35.5-38.3											
Total thickness in box (m)	2.8											
Thickness described (m) if two units in same box	2.2											
Geological unit	Otorohanga Limestone											
Quarry unit	Caprock											
	Discrete seam thickness (mm)							**Thicknesses (mm)**	**Tot. thick. (mm) of**	**Diffuse seam (mm)**	**Subhorizontal stylolite**	**Subvertical stylolite**
Box lines	**1**	**2-4**	**5-7**	**8-10**	**11-13**	**14-16**	**17-19**	**(discrete seams)**	**discrete seams**			
Line A (bottom)	1		1					1, 6	7	40		1
Line B	1	2	1					1, 3, 3, 6	13			
Line C		1						2	2			1
Line D												1
Line E (top)	Mahoenui Group											
Total	**2**	**3**	**2**	**0**	**0**	**0**	**0**		**22**	**40**	**0**	**3**
Total broken thickness (m)	0.69											
No. of metres in box - broken	1.51											
Comments/notes e.g. porosity, stylolite networks	Other 0.6 m = Mahoenui Group. Vertical joint 18 cm long lined with orange clay											

Discontinuity core log data sheet

Page 2 of 32

Logged by	Orla Hansen											
Location	Mc Donald's Quarry											
Date logged	Mar-07											
Borehole number	501											
Box number	11											
Depth (m)	38.3-41.5											
Total thickness in box (m)	3.2											
Thickness described (m) if two units in same box												
Geological unit	Otorohanga Limestone											
Quarry unit	Upper Steel											
	Discrete seam thickness (mm)							**Thicknesses (mm)**	**Tot. thick. (mm) of**	**Diffuse seam (mm)**	**Subhorizontal stylolite**	**Subvertical stylolite**
Box lines	**1**	**2-4**	**5-7**	**8-10**	**11-13**	**14-16**	**17-19**	**(discrete seams)**	**discrete seams**			
Line A (bottom)	Broken											
Line B	1							1	1			
Line C	1	1						1, 2	3			
Line D											1	
Line E (top)	2							1, 1	2		7	
Total	**4**								**6**		**8**	
Total broken thickness (m)	1.42											
No. of metres in box - broken	1.78											
Comments/notes e.g. porosity, stylolite networks	Porous zones of limestone (30-50%), med brown seam material											

Discontinuity core log data sheet

Page 3 of 32

Logged by	Orla Hansen											
Location	Mc Donald's Quarry											
Date logged	Mar-07											
Borehole number	501											
Box number	12											
Depth (m)	41.5-44.6											
Total thickness in box (m)	3.1											
Thickness described (m) if two units in same box												
Geological unit	Otorohanga Limestone											
Quarry unit	Upper Steel											
	Discrete seam thickness (mm)							**Thicknesses (mm)**	**Tot. thick. (mm) of**	**Diffuse seam (mm)**	**Subhorizontal stylolite**	**Subvertical stylolite**
Box lines	**1**	**2-4**	**5-7**	**8-10**	**11-13**	**14-16**	**17-19**	**(discrete seams)**	**discrete seams**			
Line A (bottom)	1	1	1					6, 1, 2	9		6	
Line B		2	1					5, 2, 2	9		4	
Line C	1	1	1					5, 2, 1	8		3	
Line D	2	2						2, 1, 3, 1	7	10		
Line E (top)												
Total	4	6	3									
Total broken thickness (m)	0.58								33	10	13	
No. of metres in box - broken	2.52											
Comments/notes e.g. porosity, stylolite networks	Porous zones (7-10%)											

Discontinuity core log data sheet

Page 4 of 32

Logged by	Orla Hansen
Location	Mc Donald's Quarry
Date logged	Mar-07
Borehole number	501
Box number	13
Depth (m)	44.6-47.6
Total thickness in box (m)	3
Thickness described (m) if two units in same box	2.1
Geological unit	Otorohanga Limestone
Quarry unit	Upper Steel

	Discrete seam thickness (mm)									Diffuse seam (mm)	Subhorizontal stylolite	Subvertical stylolite
Box lines	**1**	**2-4**	**5-7**	**8-10**	**11-13**	**14-16**	**17-19**	**Thicknesses (mm) (discrete seams)**	**Tot. thick. (mm) of discrete seams**			
Line A (bottom)	Aglime											
Line B	2	1						1, 4, 1	6	6	1	
Line C	5							1, 1, 1, 1, 1	5		6	1
Line D	4	1						1, 1, 1, 1, 2	6		2	1
Line E (top)	3							1, 1, 1	3		5	
Total	**14**	**2**							**20**	**6**	**14**	**2**
Total broken thickness (m)	0.13											
No. of metres in box - broken	1.97											
Comments/notes e.g. porosity, stylolite networks	Line B is a transition zoen. Porous zones (1-5%)											

Discontinuity core log data sheet

Page 5 of 32

Logged by	Orla Hansen
Location	Mc Donald's Quarry
Date logged	Mar-07
Borehole number	501
Box number	13
Depth (m)	44.6-47.6
Total thickness in box (m)	3
Thickness described (m) if two units in same box	0.9
Geological unit	Otorohanga Limestone
Quarry unit	Aglime

	Discrete seam thickness (mm)									Diffuse seam (mm)	Subhorizontal stylolite	Subvertical stylolite
Box lines	**1**	**2-4**	**5-7**	**8-10**	**11-13**	**14-16**	**17-19**	**Thicknesses (mm) (discrete seams)**	**Tot. thick. (mm) of discrete seams**			
Line A (bottom)		2						2, 2	4	390		1
Line B	2	1	1	1				1, 10, 4, 5, 1	21		1	1
Line C	Upper Steel											
Line D	Upper Steel											
Line E (top)	Upper Steel											
Total	**2**	**3**	**1**	**1**					**25**	**390**	**1**	**2**
Total broken thickness (m)												
No. of metres in box - broken	0.9											
Comments/notes e.g. porosity, stylolite networks	Grey seams, difficult to distinguish diffuse seams from discrete seams											

Discontinuity core log data sheet

Page 6 of 32

Logged by	Orla Hansen
Location	Mc Donald's Quarry
Date logged	Mar-07
Borehole number	501
Box number	14
Depth (m)	47.6-50.5
Total thickness in box (m)	2.9
Thickness described (m) if two units in same box	
Geological unit	Otorohanga Limestone
Quarry unit	Aglime

	Discrete seam thickness (mm)									Diffuse seam (mm)	Subhorizontal stylolite	Subvertical stylolite
Box lines	**1**	**2-4**	**5-7**	**8-10**	**11-13**	**14-16**	**17-19**	**Thicknesses (mm) (discrete seams)**	**Tot. thick. (mm) of discrete seams**			
Line A (bottom)	2	3	1					2, 2, 1, 5, 2, 1	13			
Line B	3		2	1				1, 1, 7, 8, 7, 1	25		1	1
Line C		2	3	1		1		2, 7, 10, 5, 7, 2, 15	48			2
Line D	1	1		1				1, 10, 2	13	50		1
Line E (top)				1				10	10	460		1
Total	6	6	6	4		1			109	510	1	5
Total broken thickness (m)												
No. of metres in box - broken	2.9											
Comments/notes e.g. porosity, stylolite networks	All grey seams											

Discontinuity core log data sheet

Page 7 of 32

Logged by	Orla Hansen
Location	Mc Donald's Quarry
Date logged	Mar-07
Borehole number	501
Box number	15
Depth (m)	50.5-53.5
Total thickness in box (m)	3
Thickness described (m) if two units in same box	
Geological unit	Otorohanga Limestone
Quarry unit	Aglime

	Discrete seam thickness (mm)								
Box lines	**1**	**2-4**	**5-7**	**8-10**	**11-13**	**14-16**	**17-19**	**Thicknesses (mm) (discrete seams)**	**Tot. thick. (mm) of discrete seams**
Line A (bottom)		2						2, 2	4
Line B	5	6	1					2, 6, 1, 3, 2, 1, 2, 1, 2,1,2,1	24
Line C	5	5	3					2,7,5,7,1,4,3,1,1,3,2,1,1	38
Line D	9	1	1					1,6,1,1,1,1,1,1,3,1,1	18
Line E (top)	8		2					1,1,7,1,1,1,1,1,5,1	20
Total	**27**	**14**	**7**						**104**
Total broken thickness (m)									
No. of metres in box - broken	3								

Diffuse seam (mm)	**Subhorizontal stylolite**	**Subvertical stylolite**
490		
		3
490		**3**

Comments/notes e.g. porosity, stylolite networks	Small orange patches, orange and grey areas together with orange and grey seams

Figure * Example of a core log data sheet used to record discontinuity information observed in the limestone cores.

Discontinuity core log data sheet

Page 8 of 32

Logged by	Orla Hansen
Location	Mc Donald's Quarry
Date logged	Mar-07
Borehole number	501
Box number	16
Depth (m)	53.5-56.4
Total thickness in box (m)	2.9
Thickness described (m) if two units in same box	
Geological unit	Otorohanga Limestone
Quarry unit	Aglime

	Discrete seam thickness (mm)								
Box lines	**1**	**2-4**	**5-7**	**8-10**	**11-13**	**14-16**	**17-19**	**Thicknesses (mm) (discrete seams)**	**Tot. thick. (mm) of discrete seams**
Line A (bottom)	5	2						2,2,1,1,1,1,1	9
Line B	5	1						2,1,1,1,1,1	7
Line C	9	1						1,1,1,2,1,1,1,1,1,1	11
Line D	4	4	1	1				10,3,2,1,5,2,4,1,1,1	30
Line E (top)	2	5	1			1		15,2,4,5,4,1,3,2,1	37
Total	**25**	**13**	**2**	**1**					**94**
Total broken thickness (m)									
No. of metres in box - broken	2.9								

Diffuse seam (mm)	**Subhorizontal stylolite**	**Subvertical stylolite**
	2	
	1	
		2
60	**3**	**2**

Comments/notes e.g. porosity, stylolite networks	Porous zones (1%), orange and grey areas of limestone

Discontinuity core log data sheet

Page 9 of 32

Logged by	Orla Hansen
Location	Mc Donald's Quarry
Date logged	Mar-07
Borehole number	501
Box number	17
Depth (m)	56.4-59.3
Total thickness in box (m)	2.9
Thickness described (m) if two units in same box	2.77
Geological unit	Otorohanga Limestone
Quarry unit	Aglime

	Discrete seam thickness (mm)								
Box lines	**1**	**2-4**	**5-7**	**8-10**	**11-13**	**14-16**	**17-19**	**Thicknesses (mm) (discrete seams)**	**Tot. thick. (mm) of discrete seams**
Line A (bottom)	3	2	1			1		5,14,3,3,1,1,1	28
Line B	4	9	1					4,5,4,2,3,3,4,2,3,2,1,1,1,1	36
Line C	3	5	2					7,3,4,4,4,4,6,1,1,1	35
Line D	6	3	1					5,3,3,3,1,1,1,1,1,1	20
Line E (top)	6	3						2,2,2,1,1,1,1,1,1	12
Total	22	22	5						131
Total broken thickness (m)	0.1								
No. of metres in box - broken	2.67								

Diffuse seam (mm)	**Subhorizontal stylolite**	**Subvertical stylolite**
		1
		1
		1
		3

Comments/notes e.g. porosity, stylolite networks	Last 13.5 cm of line A = High Grade & transition. NB: Ormiston logs show last 10 cm is High Grade (artificial cut), grey seams

Discontinuity core log data sheet

Page 10 of 32

Logged by	Orla Hansen
Location	Mc Donald's Quarry
Date logged	Mar-07
Borehole number	501
Box number	17
Depth (m)	56.4-59.3
Total thickness in box (m)	0.13
Thickness described (m) if two units in same box	
Geological unit	Otorohanga Limestone
Quarry unit	High Grade

	Discrete seam thickness (mm)									Diffuse seam (mm)	Subhorizontal stylolite	Subvertical stylolite
Box lines	**1**	**2-4**	**5-7**	**8-10**	**11-13**	**14-16**	**17-19**	**Thicknesses (mm) (discrete seams)**	**Tot. thick. (mm) of discrete seams**			
Line A (bottom)	1	1						4,1	5			
Line B												
Line C												
Line D												
Line E (top)												
Total	**1**	**1**							**5**			
Total broken thickness (m)												
No. of metres in box - broken	0.13											
Comments/notes e.g. porosity, stylolite networks	Porous zones (1%), orange seams											

Discontinuity core log data sheet

Page 11 of 32

Logged by	Orla Hansen
Location	Mc Donald's Quarry
Date logged	Mar-07
Borehole number	501
Box number	18
Depth (m)	59.3-62.2
Total thickness in box (m)	2.9
Thickness described (m) if two units in same box	
Geological unit	Otorohanga Limestone
Quarry unit	High Grade

	Discrete seam thickness (mm)									Diffuse seam (mm)	Subhorizontal stylolite	Subvertical stylolite
Box lines	**1**	**2-4**	**5-7**	**8-10**	**11-13**	**14-16**	**17-19**	**Thicknesses (mm) (discrete seams)**	**Tot. thick. (mm) of discrete seams**			
Line A (bottom)	8	1						4,1,1,1,1,1,1,1,1	12		2	
Line B	5	2						3,2,1,1,1,1,1	10		1	
Line C	4	3						3,3,4,1,1,1,1	14			
Line D	6	1						3,1,1,1,1,1,1	9			
Line E (top)	2	3						2,2,4,1,1	10		2	
Total	**25**								**55**		**5**	
Total broken thickness (m)	0.04											
No. of metres in box - broken	2.86											
Comments/notes e.g. porosity, stylolite networks	grey and orange seams											

Discontinuity core log data sheet

Page 12 of 32

Logged by	Orla Hansen
Location	Mc Donald's Quarry
Date logged	Mar-07
Borehole number	501
Box number	19
Depth (m)	62.2-65.2
Total thickness in box (m)	3
Thickness described (m) if two units in same box	
Geological unit	Otorohanga Limestone
Quarry unit	High Grade

	Discrete seam thickness (mm)									Diffuse seam (mm)	Subhorizontal stylolite	Subvertical stylolite
Box lines	**1**	**2-4**	**5-7**	**8-10**	**11-13**	**14-16**	**17-19**	**Thicknesses (mm) (discrete seams)**	**Tot. thick. (mm) of discrete seams**			
Line A (bottom)	5	5						2,2,2,2,2,1,1,1,1,1	15			
Line B	5	4						2,2,3,2,1,1,1,1,1	14			
Line C	4	7	1					3,3,2,4,3,3,5,2,1,1,1,1	29			
Line D	4	5						4,4,3,2,2,1,1,1,1	19			
Line E (top)	6	1						4,1,1,1,1,1,1	10		1	3
Total	**24**	**22**	**1**						**87**		**1**	**3**
Total broken thickness (m)												
No. of metres in box - broken	3											
Comments/notes e.g. porosity, stylolite networks												

Discontinuity core log data sheet

Page 13 of 32

Logged by	Orla Hansen
Location	Mc Donald's Quarry
Date logged	Mar-07
Borehole number	501
Box number	20
Depth (m)	65.2-68.2
Total thickness in box (m)	3
Thickness described (m) if two units in same box	
Geological unit	Otorohanga Limestone
Quarry unit	High Grade

	Discrete seam thickness (mm)										
Box lines	**1**	**2-4**	**5-7**	**8-10**	**11-13**	**14-16**	**17-19**	**Thicknesses (mm) (discrete seams)**	**Tot. thick. (mm) of discrete seams**	**Diffuse seam (mm)**	**Subhorizontal stylolite**	**Subvertical stylolite**
Line A (bottom)	3	5	1	1				3,10,4,2,3,3,7,1,1,1	35			
Line B	4	5	2					4,4,3,3,6,6,2,1,1,1,1	32			
Line C	4	4	2					2,4,3,3,5,6,1,1,1,1	27			
Line D	4	2	3					4,6,6,2,6,1,1,1,1	28			
Line E (top)	3	4	1					4,3,2,3,5,1,1,1	20			
Total	**18**	**20**	**9**	**1**					**142**			**2**
Total broken thickness (m)												
No. of metres in box - broken	3											
Comments/notes e.g. porosity, stylolite networks	All grey seams											

Discontinuity core log data sheet

Page 14 of 32

Logged by	Orla Hansen
Location	Mc Donald's Quarry
Date logged	Mar-07
Borehole number	501
Box number	21
Depth (m)	68.2-71.1
Total thickness in box (m)	2.9
Thickness described (m) if two units in same box	
Geological unit	Otorohanga Limestone
Quarry unit	High Grade

	Discrete seam thickness (mm)										
Box lines	**1**	**2-4**	**5-7**	**8-10**	**11-13**	**14-16**	**17-19**	**Thicknesses (mm) (discrete seams)**	**Tot. thick. (mm) of discrete seams**	**Diffuse seam (mm)**	**Subhorizontal stylolite**	**Subvertical stylolite**
Line A (bottom)	5		1					6,1,1,1,1,1	11		1	
Line B	5	3						3,3,3,1,1,1,1,1	14			
Line C	4	1	1					5,3,1,1,1,1	12			
Line D	4	1						4,1,1,1,1	8			1
Line E (top)	3	2	2	1	1			12,9,5,6,2,2,1,1,1	39			1
Total	21	7	4	1					84		1	2
Total broken thickness (m)	0.1											
No. of metres in box - broken	2.8											
Comments/notes e.g. porosity, stylolite networks												

Discontinuity core log data sheet

Page 15 of 32

Logged by	Orla Hansen
Location	Mc Donald's Quarry
Date logged	Mar-07
Borehole number	501
Box number	22
Depth (m)	71.1-74.1
Total thickness in box (m)	3
Thickness described (m) if two units in same box	
Geological unit	Otorohanga Limestone
Quarry unit	High Grade

	Discrete seam thickness (mm)										
Box lines	**1**	**2-4**	**5-7**	**8-10**	**11-13**	**14-16**	**17-19**	**Thicknesses (mm) (discrete seams)**	**Tot. thick. (mm) of discrete seams**	**Diffuse seam (mm)**	**Subhorizontal stylolite**	**Subvertical stylolite**
Line A (bottom)	3	4						2,3,2,4,1,1,1	14			
Line B	5	3						3,2,3,1,1,1,1,1	13		1	
Line C	6	1						3,1,1,1,1,1,1	9			
Line D	3	3	1					6,4,4,3,1,1,1	20			
Line E (top)	4	4	1					5,2,2,3,4,1,1,1,1	20			
Total	**21**	**15**	**2**						**76**		**1**	
Total broken thickness (m)												
No. of metres in box - broken	3											
Comments/notes e.g. porosity, stylolite networks	All grey seams											

Discontinuity core log data sheet

Page 16 of 32

Logged by	Orla Hansen											
Location	Mc Donald's Quarry											
Date logged	Mar-07											
Borehole number	501											
Box number	23											
Depth (m)	74.1-77.1											
Total thickness in box (m)	3											
Thickness described (m) if two units in same box												
Geological unit	Otorohanga Limestone											
Quarry unit	High Grade											
	Discrete seam thickness (mm)							**Thicknesses (mm)**	**Tot. thick. (mm) of**	**Diffuse seam (mm)**	**Subhorizontal stylolite**	**Subvertical stylolite**
Box lines	**1**	**2-4**	**5-7**	**8-10**	**11-13**	**14-16**	**17-19**	**(discrete seams)**	**discrete seams**			
Line A (bottom)	4	3						2,2,2,1,1,1,1	10			
Line B	3	1	2					6,5,2,1,1,1	16			2
Line C	3	1	1					3,7,1,1,1	13		1	
Line D	5	1						4,1,1,1,1,1	9			2
Line E (top)	2	3						4,3,2,1,1	11			
Total	**17**	**9**	**3**						**59**		**1**	**4**
Total broken thickness (m)												
No. of metres in box - broken	3											
Comments/notes e.g. porosity, stylolite networks												

Discontinuity core log data sheet

Page 17 of 32

Logged by	Orla Hansen											
Location	Mc Donald's Quarry											
Date logged	Mar-07											
Borehole number	501											
Box number	24											
Depth (m)	77.1-80											
Total thickness in box (m)	2.9											
Thickness described (m) if two units in same box	0.4											
Geological unit	Otorohanga Limestone											
Quarry unit	High Grade											
	Discrete seam thickness (mm)							**Thicknesses (mm)**	**Tot. thick. (mm) of**	**Diffuse seam (mm)**	**Subhorizontal stylolite**	**Subvertical stylolite**
Box lines	**1**	**2-4**	**5-7**	**8-10**	**11-13**	**14-16**	**17-19**	**(discrete seams)**	**discrete seams**			
Line A (bottom)	wer Steel											
Line B	wer Steel											
Line C	wer Steel											
Line D	wer Steel											
Line E (top)	2	2						2,2,1,1	6			1
Total	**2**	**2**							**6**			**1**
Total broken thickness (m)												
No. of metres in box - broken	0.4											
Comments/notes e.g. porosity, stylolite networks	First 40 cm of line E is High Grade											

Discontinuity core log data sheet

Page 18 of 32

Logged by	Orla Hansen											
Location	Mc Donald's Quarry											
Date logged	Mar-07											
Borehole number	501											
Box number	24											
Depth (m)	77.1-80											
Total thickness in box (m)	2.9											
Thickness described (m) if two units in same box	2.5											
Geological unit	Otorohanga Limestone											
Quarry unit	Lower Steel											
	Discrete seam thickness (mm)							**Thicknesses (mm)**	**Tot. thick. (mm) of**	**Diffuse seam (mm)**	**Subhorizontal stylolite**	**Subvertical stylolite**
Box lines	**1**	**2-4**	**5-7**	**8-10**	**11-13**	**14-16**	**17-19**	**(discrete seams)**	**discrete seams**			
Line A (bottom)	6							1,1,1,1,1,1	6		2	1
Line B	7	2						3,3,1,1,1,1,1,1,1	13		2	
Line C	6	1						2,1,1,1,1,1,1,1	8		3	
Line D	3							1,1,1	3			
Line E (top)	1							1	1			
Total	**24**	**3**							**31**		**7**	**1**
Total broken thickness (m)	0.06											
No. of metres in box - broken	2.44											
Comments/notes e.g. porosity, stylolite networks	First 40 cm of line E = High Grade. Seams med brown or grey. Porous zones (10-15%)											

Discontinuity core log data sheet

Page 19 of 32

Logged by	Orla Hansen
Location	Mc Donald's Quarry
Date logged	Mar-07
Borehole number	501
Box number	25
Depth (m)	80-82.9
Total thickness in box (m)	2.9
Thickness described (m) if two units in same box	
Geological unit	Otorohanga Limestone
Quarry unit	Lower Steel

	Discrete seam thickness (mm)										
Box lines	**1**	**2-4**	**5-7**	**8-10**	**11-13**	**14-16**	**17-19**	**Thicknesses (mm) (discrete seams)**	**Tot. thick. (mm) of discrete seams**	**Diffuse seam (mm)**	**Subhorizontal stylolite**	**Subvertical stylolite**
Line A (bottom)	5	1						2,1,1,1,1,1	7			
Line B	5	1						4,1,1,1,1,1	9			3
Line C	6							1,1,1,1,1,1	6			
Line D	4	2						2,2,1,1,1,1	8			1
Line E (top)	6	1						3,1,1,1,1,1,1	9		3	2
Total	**26**	**5**							**39**		**3**	**6**
Total broken thickness (m)												
No. of metres in box - broken	2.9											
Comments/notes e.g. porosity, stylolite networks	All seams grey, some seams stringy (<1 mm)											

Discontinuity core log data sheet

Page 20 of 32

Logged by	Orla Hansen
Location	Mc Donald's Quarry
Date logged	Mar-07
Borehole number	501
Box number	26
Depth (m)	82.9-85.7
Total thickness in box (m)	2.8
Thickness described (m) if two units in same box	
Geological unit	Otorohanga Limestone
Quarry unit	Lower Steel

	Discrete seam thickness (mm)										
Box lines	**1**	**2-4**	**5-7**	**8-10**	**11-13**	**14-16**	**17-19**	**Thicknesses (mm) (discrete seams)**	**Tot. thick. (mm) of discrete seams**	**Diffuse seam (mm)**	**Subhorizontal stylolite**	**Subvertical stylolite**
Line A (bottom)	6	1						3,1,1,1,1,1,1	9			
Line B	4		1					5,1,1,1,1	9		1	
Line C	2	3						2,2,2,1,1	8		1	
Line D	4		1					6,1,1,1,1	10			
Line E (top)	5	1						2,1,1,1,1,1	7			
Total	**21**	**5**	**2**						**43**		**2**	
Total broken thickness (m)												
No. of metres in box - broken	2.8											
Comments/notes e.g. porosity, stylolite networks	Dark grey seams, and orange brown seams, stringy seams (couple). Porous zones (5-30%), highly porous box, speckly											

Discontinuity core log data sheet

Page 21 of 32

Logged by	Orla Hansen
Location	Mc Donald's Quarry
Date logged	Mar-07
Borehole number	501
Box number	27
Depth (m)	85.7-88.7
Total thickness in box (m)	3.7
Thickness described (m) if two units in same box	
Geological unit	Otorohanga Limestone
Quarry unit	Lower Steel

	Discrete seam thickness (mm)										
Box lines	**1**	**2-4**	**5-7**	**8-10**	**11-13**	**14-16**	**17-19**	**Thicknesses (mm) (discrete seams)**	**Tot. thick. (mm) of discrete seams**	**Diffuse seam (mm)**	**Subhorizontal stylolite**	**Subvertical stylolite**
Line A (bottom)	2							1,1	2		3	
Line B	4							1,1,1,1	4		2	
Line C	4							1,1,1,1	4			
Line D	2							1,1	2			
Line E (top)	5							1,1,1,1,1	5		3	
Total	**17**								**17**		**8**	
Total broken thickness (m)	0.63											
No. of metres in box - broken	3.07											
Comments/notes e.g. porosity, stylolite networks	Porous zones (5-20%), seams all grey, seam material coarse dark grey sand											

Discontinuity core log data sheet

Page 22 of 32

Logged by	Orla Hansen
Location	Mc Donald's Quarry
Date logged	Mar-07
Borehole number	501
Box number	28
Depth (m)	88.7-91.7
Total thickness in box (m)	3
Thickness described (m) if two units in same box	
Geological unit	Otorohanga Limestone
Quarry unit	Lower Steel

	Discrete seam thickness (mm)								
Box lines	**1**	**2-4**	**5-7**	**8-10**	**11-13**	**14-16**	**17-19**	**Thicknesses (mm) (discrete seams)**	**Tot. thick. (mm) of discrete seams**
Line A (bottom)	7							1,1,1,1,1,1,1	7
Line B	7							1,1,1,1,1,1,1	7
Line C	8							1,1,1,1,1,1,1,1	8
Line D	7							1,1,1,1,1,1,1	7
Line E (top)	4							1,1,1,1	4
Total	**33**								**33**
Total broken thickness (m)									
No. of metres in box - broken	3								
Comments/notes e.g. porosity, stylolite networks	Seams in line E <1 mm thick, granular, coarse dark grey. Vertical joint 51 cm long lined with whitish brown clay and palygorskite, porous zones along seams (2%), seams all grey								

Diffuse seam (mm)	**Subhorizontal stylolite**	**Subvertical stylolite**
	1	
	1	

Discontinuity core log data sheet

Page 23 of 32

Logged by	Orla Hansen
Location	Mc Donald's Quarry
Date logged	Mar-07
Borehole number	501
Box number	29
Depth (m)	91.7-94.6
Total thickness in box (m)	2.9
Thickness described (m) if two units in same box	
Geological unit	Otorohanga Limestone
Quarry unit	Lower Steel

	Discrete seam thickness (mm)								
Box lines	**1**	**2-4**	**5-7**	**8-10**	**11-13**	**14-16**	**17-19**	**Thicknesses (mm) (discrete seams)**	**Tot. thick. (mm) of discrete seams**
Line A (bottom)	4							1,1,1,1	4
Line B	3							1,1,1	3
Line C	2							1,1	2
Line D	4							1,1,1,1	4
Line E (top)	All broken, not logged								
Total	**13**								**13**
Total broken thickness (m)	1.12								
No. of metres in box - broken	1.78								
Comments/notes e.g. porosity, stylolite networks	All seams grey, stylolites 2 mm thick, dark green infill, box quite broken, porous zones (20%)								

Diffuse seam (mm)	**Subhorizontal stylolite**	**Subvertical stylolite**
	4	
	4	
	2	
	4	
	11	

Discontinuity core log data sheet

Page 24 of 32

Logged by	Orla Hansen
Location	Mc Donald's Quarry
Date logged	Mar-07
Borehole number	501
Box number	30
Depth (m)	94.6-97.4
Total thickness in box (m)	2.8
Thickness described (m) if two units in same box	
Geological unit	Otorohanga Limestone
Quarry unit	Lower Steel

	Discrete seam thickness (mm)								
Box lines	**1**	**2-4**	**5-7**	**8-10**	**11-13**	**14-16**	**17-19**	**Thicknesses (mm) (discrete seams)**	**Tot. thick. (mm) of discrete seams**
Line A (bottom)	3							1,1,1	3
Line B	4							1,1,1,1	4
Line C	3							1,1,1	3
Line D	4							1,1,1,1	4
Line E (top)	6							1,1,1,1,1,1	6
Total	**20**								**20**
Total broken thickness (m)									
No. of metres in box - broken	2.8								
Comments/notes e.g. porosity, stylolite networks	Porous zones (50%), all seams counted <1 mm, most of box porous and broken								

Diffuse seam (mm)	**Subhorizontal stylolite**	**Subvertical stylolite**
	1	
	1	
	2	

Discontinuity core log data sheet

Page 25 of 32

Logged by	Orla Hansen
Location	Mc Donald's Quarry
Date logged	Mar-07
Borehole number	501
Box number	31
Depth (m)	97.4-100.4
Total thickness in box (m)	3
Thickness described (m) if two units in same box	
Geological unit	Otorohanga Limestone
Quarry unit	Lower Steel

	Discrete seam thickness (mm)										
Box lines	**1**	**2-4**	**5-7**	**8-10**	**11-13**	**14-16**	**17-19**	**Thicknesses (mm) (discrete seams)**	**Tot. thick. (mm) of discrete seams**	**Diffuse seam (mm)**	**Subhorizontal stylolite**	**Subvertical stylolite**
Line A (bottom)	6							1,1,1,1,1,1	6		1	
Line B	4							1,1,1,1	4			
Line C	3							1,1,1	3			
Line D	5							1,1,1,1,1	5		4	
Line E (top)	4							1,1,1,1	4		1	1
Total	**22**								**22**		**6**	**1**
Total broken thickness (m)	0.3											
No. of metres in box - broken	2.7											
Comments/notes e.g. porosity, stylolite networks	Seams in line C & E white/grey lining <1 mm thick. Dark grey seam material. Vertical cracks in limestone, porous zones (10%)											

Discontinuity core log data sheet

Page 26 of 32

Logged by	Orla Hansen
Location	Mc Donald's Quarry
Date logged	Mar-07
Borehole number	501
Box number	32
Depth (m)	100.4-103.3
Total thickness in box (m)	2.9
Thickness described (m) if two units in same box	
Geological unit	Otorohanga Limestone
Quarry unit	Sub-economic unit

	Discrete seam thickness (mm)										
Box lines	**1**	**2-4**	**5-7**	**8-10**	**11-13**	**14-16**	**17-19**	**Thicknesses (mm) (discrete seams)**	**Tot. thick. (mm) of discrete seams**	**Diffuse seam (mm)**	**Subhorizontal stylolite**	**Subvertical stylolite**
Line A (bottom)	9							1,1,1,1,1,1,1,1,1	9		3	1
Line B	1	4	1					4,2,4,6,3,1	20			1
Line C	1	4						4,4,4,4,1	17			
Line D	9							1,1,1,1,1,1,1,1,1	9			
Line E (top)	7							1,1,1,1,1,1,1,	7			
Total	**27**	**8**	**1**						**62**		**3**	**2**
Total broken thickness (m)												
No. of metres in box - broken	2.9											
Comments/notes e.g. porosity, stylolite networks	All dark grey seams											

Discontinuity core log data sheet

Page 27 of 32

Logged by	Orla Hansen
Location	Mc Donald's Quarry
Date logged	Mar-07
Borehole number	501
Box number	33
Depth (m)	103.3-106.2
Total thickness in box (m)	2.9
Thickness described (m) if two units in same box	
Geological unit	Otorohanga Limestone
Quarry unit	Sub-economic unit

	Discrete seam thickness (mm)										
Box lines	**1**	**2-4**	**5-7**	**8-10**	**11-13**	**14-16**	**17-19**	**Thicknesses (mm) (discrete seams)**	**Tot. thick. (mm) of discrete seams**	**Diffuse seam (mm)**	**Subhorizontal stylolite**	**Subvertical stylolite**
Line A (bottom)	3	1	1	1				6,3,10,1,1,1	22		3	
Line B	5							1,1,1,1,1	5	220		
Line C	2	3		2				3,10,3,2,9,1,1	29			
Line D	1		2	2				1,8,8,7,5	29			2
Line E (top)	3	2						3,2,1,1,1	8			
Total	**14**	**6**	**3**	**5**					**93**	**220**	**3**	**2**
Total broken thickness (m)												
No. of metres in box - broken	2.9											
Comments/notes e.g. porosity, stylolite networks	Stringy seams, all grey											

Discontinuity core log data sheet

Page 28 of 32

Logged by	Orla Hansen
Location	Mc Donald's Quarry
Date logged	Apr-07
Borehole number	501
Box number	34
Depth (m)	106.2-109.10
Total thickness in box (m)	2.9
Thickness described (m) if two units in same box	
Geological unit	Otorohanga Limestone
Quarry unit	Sub-economic unit

	Discrete seam thickness (mm)										
Box lines	**1**	**2-4**	**5-7**	**8-10**	**11-13**	**14-16**	**17-19**	**Thicknesses (mm) (discrete seams)**	**Tot. thick. (mm) of discrete seams**	**Diffuse seam (mm)**	**Subhorizontal stylolite**	**Subvertical stylolite**
Line A (bottom)	2	3	1					3,5,3,4,1,1	17		4	1
Line B		2	2					4,3,5,5	17		8	1
Line C		3	1					6,4,4,2	16		5	3
Line D	1	4						2,4,4,3,1	14		3	2
Line E (top)	4		1					1,1,1,1,5	9		10	1
Total	**7**	**12**	**5**						**73**		**30**	**8**
Total broken thickness (m)												
No. of metres in box - broken	2.9											
Comments/notes e.g. porosity, stylolite networks	Whole box unoxidised, stylolites wispy, big shells											

Discontinuity core log data sheet

Page 29 of 32

Logged by	Orla Hansen
Location	Mc Donald's Quarry
Date logged	Apr-07
Borehole number	501
Box number	35
Depth (m)	109.1-112.1
Total thickness in box (m)	3
Thickness described (m) if two units in same box	
Geological unit	Otorohanga Limestone
Quarry unit	Sub-economic unit

	Discrete seam thickness (mm)										
Box lines	**1**	**2-4**	**5-7**	**8-10**	**11-13**	**14-16**	**17-19**	**Thicknesses (mm) (discrete seams)**	**Tot. thick. (mm) of discrete seams**	**Diffuse seam (mm)**	**Subhorizontal stylolite**	**Subvertical stylolite**
Line A (bottom)	4	2	1					3,6,4,1,1,1,1	17		5	1
Line B	4	1						4,1,1,1,1	8		11	
Line C		3	1					2,2,2,7	13		7	
Line D	2	1	3					7,5,5,3,1,1	22		10	
Line E (top)		2						3,4	7		14	
Total	**10**	**9**	**5**						**67**		**47**	**1**
Total broken thickness (m)												
No. of metres in box - broken	3											
Comments/notes e.g. porosity, stylolite networks	Stringy wispy seams, thick shell material up to 2 cm thick											

Discontinuity core log data sheet

Page 30 of 32

Logged by	Orla Hansen
Location	Mc Donald's Quarry
Date logged	Apr-07
Borehole number	501
Box number	36
Depth (m)	112.1-115.1
Total thickness in box (m)	3
Thickness described (m) if two units in same box	
Geological unit	Otorohanga Limestone
Quarry unit	Sub-economic unit

	Discrete seam thickness (mm)										
Box lines	**1**	**2-4**	**5-7**	**8-10**	**11-13**	**14-16**	**17-19**	**Thicknesses (mm) (discrete seams)**	**Tot. thick. (mm) of discrete seams**	**Diffuse seam (mm)**	**Subhorizontal stylolite**	**Subvertical stylolite**
Line A (bottom)	1	2	1					2,7,4,1	14		7	
Line B	5	2			1			2,2,11,1,1,1,1,1	20		11	
Line C	4	1						3,1,1,1,1	7		12	
Line D	8	1	1					2,5,1,1,1,1,1,1,1,1	15		7	
Line E (top)	6							1,1,1,1,1,1	6		8	
Total	**24**	**6**	**2**		**1**				**62**		**45**	
Total broken thickness (m)												
No. of metres in box - broken	3											
Comments/notes e.g. porosity, stylolite networks	Stylolite thickness about 2 mm thick. Porous zones up to 5 mm either side of stylolites and seams											

Discontinuity core log data sheet

Page 31 of 32

Logged by	Orla Hansen
Location	Mc Donald's Quarry
Date logged	Apr-07
Borehole number	501
Box number	37
Depth (m)	115.1-118
Total thickness in box (m)	2.9
Thickness described (m) if two units in same box	
Geological unit	Otorohanga Limestone
Quarry unit	Sub-economic unit

	Discrete seam thickness (mm)									Diffuse seam (mm)	Subhorizontal stylolite	Subvertical stylolite
Box lines	**1**	**2-4**	**5-7**	**8-10**	**11-13**	**14-16**	**17-19**	**Thicknesses (mm) (discrete seams)**	**Tot. thick. (mm) of discrete seams**			
Line A (bottom)	2	1			1			12,4,1,1	18	20	10	2
Line B	1	1	1					4,5,1	10		13	1
Line C				2	2	1		10,12,10,16,12	59		3	3
Line D	1		1	1	1	1	1	17,15,10,12,6,1	61		6	1
Line E (top)	2		1	2		1		15,10,5,8,1,1	40		2	2
Total	**6**	**2**	**3**	**5**	**4**	**3**	**1**		**188**	**20**	**34**	**9**
Total broken thickness (m)												
No. of metres in box - broken												
Comments/notes e.g. porosity, stylolite networks	Shell material, stylolite bold than boxes 36 and 35											

Discontinuity core log data sheet

Page 32 of 32

Logged by	Orla Hansen
Location	Mc Donald's Quarry
Date logged	Apr-07
Borehole number	501
Box number	38
Depth (m)	118-120.9
Total thickness in box (m)	2.9
Thickness described (m) if two units in same box	
Geological unit	Otorohanga Limestone
Quarry unit	Sub-economic unit

	Discrete seam thickness (mm)									Diffuse seam (mm)	Subhorizontal stylolite	Subvertical stylolite
Box lines	**1**	**2-4**	**5-7**	**8-10**	**11-13**	**14-16**	**17-19**	**Thicknesses (mm) (discrete seams)**	**Tot. thick. (mm) of discrete seams**			
Line A (bottom)		1	2	1	1			2,11,6,10,6	35		6	
Line B	2	1	1	2	1			2,6,10,13,10,1,1	43			
Line C	1		2	2	1	1		10,10,6,15,11,6,1	59			1
Line D	2		1	2	1			8,8,7,11,1,1	36		2	2
Line E (top)	3		1	2			1	10,10,18,5,1,1,1	46		3	2
Total	**8**	**2**	**7**	**9**	**4**	**1**	**1**		**219**		**11**	**5**
Total broken thickness (m)												
No. of metres in box - broken	2.9											
Comments/notes e.g. porosity, stylolite networks	Last box logged - getting too sandy											

Appendix D-4.2.B Discontinuity data sheets for drill hole BH502

Discontinuity core log data sheet

Page 1 of 35

Logged by	Orla Hansen
Location	McDonald's Quarry
Date logged	Nov-06
Borehole number	502
Box number	9
Depth (m)	23.7-26.6
Total thickness in box (m)	2.9
Thickness described (m) if two units in same box	1.1
Geological unit	Otorohanga Limestone
Quarry unit	Caprock

	Discrete seam thickness (mm)							Thicknesses (mm)	Tot. thick. (mm) of	Diffuse seam (mm)	Subhorizontal stylolite	Subvertical stylolite
Box lines	1	2-4	5-7	8-10	11-13	14-16	17-19	(discrete seams)	discrete seams			
Line A (bottom)										131		
Line B	5	1						2,1,1,1,1,1	7			
Line C	Mahoenui Group											
Line D	Mahoenui Group											
Line E (top)	Mahoenui Group											
Total	5	1							7	131	2	3
Total broken thickness (m)												
No. of metres in box - broken	1.1											
Comments/notes e.g. porosity, stylolite networks	Seam not distiguishable from host rock colour, stylolitic network											

Discontinuity core log data sheet

Page 2 of 35

Logged by	Orla Hansen
Location	McDonald's Quarry
Date logged	Nov-06
Borehole number	502
Box number	10
Depth (m)	26.6-29.5
Total thickness in box (m)	2.98
Thickness described (m) if two units in same box	0.47
Geological unit	Otorohanga Limestone
Quarry unit	Caprock

	Discrete seam thickness (mm)							Thicknesses (mm)	Tot. thick. (mm) of	Diffuse seam (mm)	Subhorizontal stylolite	Subvertical stylolite
Box lines	1	2-4	5-7	8-10	11-13	14-16	17-19	(discrete seams)	discrete seams			
Line A (bottom)												
Line B												
Line C												
Line D												
Line E (top)												
Total	1								1	113	1	1
Total broken thickness (m)												
No. of metres in box - broken	0.47											
Comments/notes e.g. porosity, stylolite networks												

Discontinuity core log data sheet

Page 3 of 35

Logged by	Orla Hansen
Location	McDonald's Quarry
Date logged	Nov-06
Borehole number	502
Box number	10
Depth (m)	26.6-29.5
Total thickness in box (m)	2.98
Thickness described (m) if two units in same box	2.51
Geological unit	Otorohanga Limestone
Quarry unit	Upper Steel

	Discrete seam thickness (mm)							Thicknesses (mm)	Tot. thick. (mm) of	Diffuse seam (mm)	Subhorizontal stylolite	Subvertical stylolite
Box lines	1	2-4	5-7	8-10	11-13	14-16	17-19	(discrete seams)	discrete seams			
Line A (bottom)												
Line B												
Line C												
Line D												
Line E (top)												
Total	4	2						2,2,1,1,1,1	8		13	
Total broken thickness (m)	0.35											
No. of metres in box - broken	2.16											
Comments/notes e.g. porosity, stylolite networks	Highly porous - (25% of limestone), stylolite amplitude = 2 mm, one stylolitic network											

Discontinuity core log data sheet

Page 4 of 35

Logged by	Orla Hansen
Location	McDonald's Quarry
Date logged	Nov-06
Borehole number	502
Box number	11
Depth (m)	29.5-32.4
Total thickness in box (m)	2.9
Thickness described (m) if two units in same box	
Geological unit	Otorohanga Limestone
Quarry unit	Upper Steel

	Discrete seam thickness (mm)									Diffuse seam (mm)	Subhorizontal stylolite	Subvertical stylolite
Box lines	**1**	**2-4**	**5-7**	**8-10**	**11-13**	**14-16**	**17-19**	**Thicknesses (mm) (discrete seams)**	**Tot. thick. (mm) of discrete seams**			
Line A (bottom)												
Line B												
Line C												
Line D												
Line E (top)												
Total		**1**						2	**2**		**1**	**2**
Total broken thickness (m)	2.33											
No. of metres in box - broken	0.57											
Comments/notes e.g. porosity, stylolite networks	Porous zones (40%), subhorizontal stylolites <2 mm amplitude, subvertical stylolite amplitude = >10 mm and associated with porosity											

Discontinuity core log data sheet

Page 5 of 35

Logged by	Orla Hansen
Location	McDonald's Quarry
Date logged	Nov-06
Borehole number	502
Box number	12
Depth (m)	32.4-35.1
Total thickness in box (m)	2.7
Thickness described (m) if two units in same box	
Geological unit	Otorohanga Limestone
Quarry unit	Upper Steel

	Discrete seam thickness (mm)									Diffuse seam (mm)	Subhorizontal stylolite	Subvertical stylolite
Box lines	**1**	**2-4**	**5-7**	**8-10**	**11-13**	**14-16**	**17-19**	**Thicknesses (mm) (discrete seams)**	**Tot. thick. (mm) of discrete seams**			
Line A (bottom)												
Line B												
Line C												
Line D												
Line E (top)												
Total	**4**							1,1,1,1	**4**		**5**	**1**
Total broken thickness (m)	1.1											
No. of metres in box - broken	1.6											
Comments/notes e.g. porosity, stylolite networks	Two vertical joints with clay infill, porous zones (15%). 2-3 mm amplitude on stylolites											

Discontinuity core log data sheet

Page 6 of 35

Logged by	Orla Hansen
Location	McDonald's Quarry
Date logged	Nov-06
Borehole number	502
Box number	13
Depth (m)	35.1-38.1
Total thickness in box (m)	3
Thickness described (m) if two units in same box	1.9
Geological unit	Otorohanga Limestone
Quarry unit	Upper Steel

	Discrete seam thickness (mm)									Diffuse seam (mm)	Subhorizontal stylolite	Subvertical stylolite
Box lines	**1**	**2-4**	**5-7**	**8-10**	**11-13**	**14-16**	**17-19**	**Thicknesses (mm) (discrete seams)**	**Tot. thick. (mm) of discrete seams**			
Line A (bottom)												
Line B												
Line C												
Line D												
Line E (top)												
Total	**5**	**1**						2	**7**		**2**	
Total broken thickness (m)	0.43											
No. of metres in box - broken	1.47											
Comments/notes e.g. porosity, stylolite networks	Porous zones (5%), stylolites 2-3 mm amplitudes, stylolitic network											

Discontinuity core log data sheet

Page 7 of 35

Logged by	Orla Hansen
Location	McDonald's Quarry
Date logged	Nov-06
Borehole number	502
Box number	13
Depth (m)	35.1-38.1
Total thickness in box (m)	3
Thickness described (m) if two units in same box	1.1
Geological unit	Otorohanga Limestone
Quarry unit	Aglime

	Discrete seam thickness (mm)											
Box lines	**1**	**2-4**	**5-7**	**8-10**	**11-13**	**14-16**	**17-19**	**Thicknesses (mm) (discrete seams)**	**Tot. thick. (mm) of discrete seams**	**Diffuse seam (mm)**	**Subhorizontal stylolite**	**Subvertical stylolite**
Line A (bottom)												
Line B												
Line C												
Line D												
Line E (top)												
Total	**4**	**4**	**2**	**2**		**2**		4,3,3,5,5,2,10,10,15,15,1,1,1,1	**76**	**1110**		**1**
Total broken thickness (m)												
No. of metres in box - broken	1.1											
Comments/notes e.g. porosity, stylolite networks												

Discontinuity core log data sheet

Page 8 of 35

Logged by	Orla Hansen
Location	McDonald's Quarry
Date logged	Nov-06
Borehole number	502
Box number	14
Depth (m)	38.1-40.9
Total thickness in box (m)	2.88
Thickness described (m) if two units in same box	
Geological unit	Otorohanga Limestone
Quarry unit	Aglime

	Discrete seam thickness (mm)											
Box lines	**1**	**2-4**	**5-7**	**8-10**	**11-13**	**14-16**	**17-19**	**Thicknesses (mm) (discrete seams)**	**Tot. thick. (mm) of discrete seams**	**Diffuse seam (mm)**	**Subhorizontal stylolite**	**Subvertical stylolite**
Line A (bottom)												
Line B												
Line C												
Line D												
Line E (top)												
								3,3,3,3,3,3,5,5,5,5,5,5,5,				
Total	**12**	**15**	**10**	**2**				2,2,2,2,2,2,8,4,4,4,6,7,10	**125**	**637**	**3**	**4**
Total broken thickness (m)												
No. of metres in box - broken	2.88											
Comments/notes e.g. porosity, stylolite networks	Vertical joint with infill, stylolitic network, subvertical stylolites = 2 mm amp, subhorizontal stylolites = <10 mm amp											

Discontinuity core log data sheet

Page 9 of 35

Logged by	Orla Hansen
Location	McDonald's Quarry
Date logged	Nov-06
Borehole number	502
Box number	15
Depth (m)	40.9-43.8
Total thickness in box (m)	3.18
Thickness described (m) if two units in same box	
Geological unit	Otorohanga Limestone
Quarry unit	Aglime

	Discrete seam thickness (mm)											
Box lines	**1**	**2-4**	**5-7**	**8-10**	**11-13**	**14-16**	**17-19**	**Thicknesses (mm) (discrete seams)**	**Tot. thick. (mm) of discrete seams**	**Diffuse seam (mm)**	**Subhorizontal stylolite**	**Subvertical stylolite**
Line A (bottom)												
Line B												
Line C												
Line D												
Line E (top)												
								7,7,4,4,4,4,4,4,4,4,4,4,4,2,2				
Total	**14**	**39**	**14**	**1**	**1**			,2,2,2,2,2,2,2,2,2,12,12,5,5	**230**	**830**	**2**	**1**
								,5,5,5,5,5,5,3,3,3,3,3,3,3,3				
Total broken thickness (m)								3,3,3,3,3,3,3,3,6,6,6,6,10,12				
No. of metres in box - broken												
Comments/notes e.g. porosity, stylolite networks	Stylolitic networks ranging <2-4 mm amp.											

Logged by	Orla Hansen											
Location	McDonald's Quarry											
Date logged	Nov-06											
Borehole number	502											
Box number	16											
Depth (m)	43.8-46.8											
Total thickness in box (m)	2.95											
Thickness described (m) if two units in same box												
Geological unit	Otorohanga Limestone											
Quarry unit	Aglime											
	Discrete seam thickness (mm)							**Thicknesses (mm) (discrete seams)**	**Tot. thick. (mm) of discrete seams**	**Diffuse seam (mm)**	**Subhorizontal stylolite**	**Subvertical stylolite**
Box lines	**1**	**2-4**	**5-7**	**8-10**	**11-13**	**14-16**	**17-19**					
Line A (bottom)												
Line B												
Line C												
Line D												
Line E (top)												
Total	**16**	**4**						4,2,2,2	**26**		**1**	
Total broken thickness (m)	2.07											
No. of metres in box - broken	0.88											
Comments/notes e.g. porosity, stylolite networks	One stylolitic network, one vertical joint no infill											

Discontinuity core log data sheet

Logged by	Orla Hansen											
Location	McDonald's Quarry											
Date logged	Nov-06											
Borehole number	502											
Box number	17											
Depth (m)	46.8-49.5											
Total thickness in box (m)	2.96											
Thickness described (m) if two units in same box	1.53											
Geological unit	Otorohanga Limestone											
Quarry unit	Aglime											
	Discrete seam thickness (mm)							**Thicknesses (mm) (discrete seams)**	**Tot. thick. (mm) of discrete seams**	**Diffuse seam (mm)**	**Subhorizontal stylolite**	**Subvertical stylolite**
Box lines	**1**	**2-4**	**5-7**	**8-10**	**11-13**	**14-16**	**17-19**					
Line A (bottom)												
Line B												
Line C												
Line D												
Line E (top)												
Total	**21**	**5**						**2,2,3,3,4**	**35**	**35**		
Total broken thickness (m)												
No. of metres in box - broken	1.53											
Comments/notes e.g. porosity, stylolite networks	One vertical joint no infill, one vertical joint infill											

Discontinuity core log data sheet

Logged by	Orla Hansen											
Location	McDonald's Quarry											
Date logged	Nov-06											
Borehole number	502											
Box number	17											
Depth (m)	46.8-49.5											
Total thickness in box (m)	2.96											
Thickness described (m) if two units in same box	1.43											
Geological unit	Otorohanga Limestone											
Quarry unit	High Grade											
	Discrete seam thickness (mm)							**Thicknesses (mm) (discrete seams)**	**Tot. thick. (mm) of discrete seams**	**Diffuse seam (mm)**	**Subhorizontal stylolite**	**Subvertical stylolite**
Box lines	**1**	**2-4**	**5-7**	**8-10**	**11-13**	**14-16**	**17-19**					
Line A (bottom)												
Line B												
Line C												
Line D												
Line E (top)												
Total	**9**	**7**	**2**					**2,2,2,6,3,3,3,5,4**	**39**		**4**	
Total broken thickness (m)												
No. of metres in box - broken	1.43											
Comments/notes e.g. porosity, stylolite networks	Porous zones (3%), 2 vertical joints with infill											

Discontinuity core log data sheet

Page 13 of 35

Logged by	Orla Hansen												
Location	McDonald's Quarry												
Date logged	Nov-06												
Borehole number	502												
Box number	18												
Depth (m)	49.5-52.3												
Total thickness in box (m)	2.88												
Thickness described (m) if two units in same box													
Geological unit	Otorohanga Limestone												
Quarry unit	High Grade												
	Discrete seam thickness (mm)							**Thicknesses (mm)**	**Tot. thick. (mm) of**	**Diffuse seam (mm)**	**Subhorizontal stylolite**	**Subvertical stylolite**	
Box lines	**1**	**2-4**	**5-7**	**8-10**	**11-13**	**14-16**	**17-19**	**(discrete seams)**	**discrete seams**				
Line A (bottom)													
Line B													
Line C													
Line D													
Line E (top)													
Total	**32**	**5**	**1**					**3,7,2,2,2,2**	**50**		**5**	**1**	
Total broken thickness (m)	0.3												
No. of metres in box - broken	2.58												
Comments/notes e.g. porosity, stylolite networks	Stylolites 2 mm amp, 3 stylolitic networks, porous zones (<1%)												

Discontinuity core log data sheet

Page 14 of 35

Logged by	Orla Hansen												
Location	McDonald's Quarry												
Date logged	Nov-06												
Borehole number	502												
Box number	19												
Depth (m)	52.3-55.3												
Total thickness in box (m)	3.04												
Thickness described (m) if two units in same box													
Geological unit	Otorohanga Limestone												
Quarry unit	High Grade												
	Discrete seam thickness (mm)							**Thicknesses (mm)**	**Tot. thick. (mm) of**	**Diffuse seam (mm)**	**Subhorizontal stylolite**	**Subvertical stylolite**	
Box lines	**1**	**2-4**	**5-7**	**8-10**	**11-13**	**14-16**	**17-19**	**(discrete seams)**	**discrete seams**				
Line A (bottom)													
Line B													
Line C													
Line D													
Line E (top)													
Total	**29**	**17**						**3,3,3,4,4,4,2,2,2,2,2,2,2,2,**	**72**	**8**		**1**	
								2,2,2					
Total broken thickness (m)													
No. of metres in box - broken	3.04												
Comments/notes e.g. porosity, stylolite networks	Two stylolitic networks												

Discontinuity core log data sheet

Page 15 of 35

Logged by	Orla Hansen												
Location	McDonald's Quarry												
Date logged	Nov-06												
Borehole number	502												
Box number	20												
Depth (m)	55.3-58.2												
Total thickness in box (m)	2.88												
Thickness described (m) if two units in same box													
Geological unit	Otorohanga Limestone												
Quarry unit	High Grade												
	Discrete seam thickness (mm)							**Thicknesses (mm)**	**Tot. thick. (mm) of**	**Diffuse seam (mm)**	**Subhorizontal stylolite**	**Subvertical stylolite**	
Box lines	**1**	**2-4**	**5-7**	**8-10**	**11-13**	**14-16**	**17-19**	**(discrete seams)**	**discrete seams**				
Line A (bottom)													
Line B													
Line C													
Line D													
Line E (top)													
Total	**24**	**5**	**1**			**1**		7,2,4,4,14,3,3	**61**	**20**	**4**	**2**	
Total broken thickness (m)	0.04												
No. of metres in box - broken	2.84												
Comments/notes e.g. porosity, stylolite networks	Two stylolitic networks												

Discontinuity core log data sheet

Page 16 of 35

Logged by	Orla Hansen												
Location	McDonald's Quarry												
Date logged	Nov-06												
Borehole number	502												
Box number	21												
Depth (m)	58.2-61.1												
Total thickness in box (m)	2.95												
Thickness described (m) if two units in same box													
Geological unit	Otorohanga Limestone												
Quarry unit	High Grade												
	Discrete seam thickness (mm)								**Thicknesses (mm) (discrete seams)**	**Tot. thick. (mm) of discrete seams**	**Diffuse seam (mm)**	**Subhorizontal stylolite**	**Subvertical stylolite**
Box lines	**1**	**2-4**	**5-7**	**8-10**	**11-13**	**14-16**	**17-19**						
Line A (bottom)													
Line B													
Line C													
Line D													
Line E (top)													
Total	**21**	**19**							4,4,4,4,2,2,2,2,2,2,2,2,2 ,2,3,3,3,3,3	**72**	**8**	**2**	**1**
Total broken thickness (m)	0.03												
No. of metres in box - broken	2.92												
Comments/notes e.g. porosity, stylolite networks	Two stylolitic networks												

Discontinuity core log data sheet

Page 17 of 35

Logged by	Orla Hansen												
Location	McDonald's Quarry												
Date logged	Nov-06												
Borehole number	502												
Box number	22												
Depth (m)	61.1-63.9												
Total thickness in box (m)	2.85												
Thickness described (m) if two units in same box													
Geological unit	Otorohanga Limestone												
Quarry unit	High Grade												
	Discrete seam thickness (mm)								**Thicknesses (mm) (discrete seams)**	**Tot. thick. (mm) of discrete seams**	**Diffuse seam (mm)**	**Subhorizontal stylolite**	**Subvertical stylolite**
Box lines	**1**	**2-4**	**5-7**	**8-10**	**11-13**	**14-16**	**17-19**						
Line A (bottom)													
Line B													
Line C													
Line D													
Line E (top)													
Total	**28**	**8**	**2**						2,2,2,2,5,6,4,4,4,3	**59**		**3**	
Total broken thickness (m)	0.2												
No. of metres in box - broken	2.64												
Comments/notes e.g. porosity, stylolite networks	Three stylolitic networks, 6 vertical joints												

Discontinuity core log data sheet

Page 18 of 35

Logged by	Orla Hansen												
Location	McDonald's Quarry												
Date logged	Nov-06												
Borehole number	502												
Box number	23												
Depth (m)	63.9-66.8												
Total thickness in box (m)	2.87												
Thickness described (m) if two units in same box	1.82												
Geological unit	Otorohanga Limestone												
Quarry unit	High Grade												
	Discrete seam thickness (mm)								**Thicknesses (mm) (discrete seams)**	**Tot. thick. (mm) of discrete seams**	**Diffuse seam (mm)**	**Subhorizontal stylolite**	**Subvertical stylolite**
Box lines	**1**	**2-4**	**5-7**	**8-10**	**11-13**	**14-16**	**17-19**						
Line A (bottom)													
Line B													
Line C													
Line D													
Line E (top)													
Total	14	5	1						2,2,2,2,2,5	29	20	2	
Total broken thickness (m)	0.07												
No. of metres in box - broken	1.75												
Comments/notes e.g. porosity, stylolite networks	3 stylolitic networks												

Discontinuity core log data sheet

Page 19 of 35

Logged by	Orla Hansen												
Location	McDonald's Quarry												
Date logged	Nov-06												
Borehole number	502												
Box number	23												
Depth (m)	63.9-66.8												
Total thickness in box (m)	2.87												
Thickness described (m) if two units in same box	1.05												
Geological unit	Otorohanga Limestone												
Quarry unit	Lower Steel												
	Discrete seam thickness (mm)							**Thicknesses (mm)**	**Tot. thick. (mm) of**	**Diffuse seam (mm)**	**Subhorizontal stylolite**	**Subvertical stylolite**	
Box lines	**1**	**2-4**	**5-7**	**8-10**	**11-13**	**14-16**	**17-19**	**(discrete seams)**	**discrete seams**				
Line A (bottom)													
Line B													
Line C													
Line D													
Line E (top)													
Total	**7**							1,1,1,1,1,1,1	**7**				
Total broken thickness (m)	0.42												
No. of metres in box - broken	0.63												
Comments/notes e.g. porosity, stylolite networks	1 stylolitic network, 1 vertical joint with infill												

Discontinuity core log data sheet

Page 20 of 35

Logged by	Orla Hansen												
Location	McDonald's Quarry												
Date logged	Nov-06												
Borehole number	502												
Box number	24												
Depth (m)	66.8-69.7												
Total thickness in box (m)	2.86												
Thickness described (m) if two units in same box													
Geological unit	Otorohanga Limestone												
Quarry unit	Lower Steel												
	Discrete seam thickness (mm)							**Thicknesses (mm)**	**Tot. thick. (mm) of**	**Diffuse seam (mm)**	**Subhorizontal stylolite**	**Subvertical stylolite**	
Box lines	**1**	**2-4**	**5-7**	**8-10**	**11-13**	**14-16**	**17-19**	**(discrete seams)**	**discrete seams**				
Line A (bottom)													
Line B													
Line C													
Line D													
Line E (top)													
Total	**31**	**3**						2,2,3	**38**		**15**	**2**	
Total broken thickness (m)	0.09												
No. of metres in box - broken	2.77												
Comments/notes e.g. porosity, stylolite networks	1 vertical joint with infill												

Discontinuity core log data sheet

Page 21 of 35

Logged by	Orla Hansen												
Location	McDonald's Quarry												
Date logged	Nov-06												
Borehole number	502												
Box number	25												
Depth (m)	69.7-72.6												
Total thickness in box (m)	2.97												
Thickness described (m) if two units in same box													
Geological unit	Otorohanga Limestone												
Quarry unit	Lower Steel												
	Discrete seam thickness (mm)							**Thicknesses (mm)**	**Tot. thick. (mm) of**	**Diffuse seam (mm)**	**Subhorizontal stylolite**	**Subvertical stylolite**	
Box lines	**1**	**2-4**	**5-7**	**8-10**	**11-13**	**14-16**	**17-19**	**(discrete seams)**	**discrete seams**				
Line A (bottom)													
Line B													
Line C													
Line D													
Line E (top)													
Total	**16**	**5**	**2**					2,2,2,2,5,6,3	**38**		**20**		
Total broken thickness (m)	0.46												
No. of metres in box - broken	2.44												
Comments/notes e.g. porosity, stylolite networks	3 stylolitic networks												

Discontinuity core log data sheet

Page 22 of 35

Logged by	Orla Hansen
Location	McDonald's Quarry
Date logged	Nov-06
Borehole number	502
Box number	26
Depth (m)	72.6-75.5
Total thickness in box (m)	2.94
Thickness described (m) if two units in same box	
Geological unit	Otorohanga Limestone
Quarry unit	Lower Steel

	Discrete seam thickness (mm)									Diffuse seam (mm)	Subhorizontal stylolite	Subvertical stylolite
Box lines	**1**	**2-4**	**5-7**	**8-10**	**11-13**	**14-16**	**17-19**	**Thicknesses (mm) (discrete seams)**	**Tot. thick. (mm) of discrete seams**			
Line A (bottom)												
Line B												
Line C												
Line D												
Line E (top)												
Total	**24**	**3**						2,2,3	**31**		**28**	**1**
Total broken thickness (m)	0.14											
No. of metres in box - broken	2.76											
Comments/notes e.g. porosity, stylolite networks	1 vertical joint no infill											

Discontinuity core log data sheet

Page 23 of 35

Logged by	Orla Hansen
Location	McDonald's Quarry
Date logged	Nov-06
Borehole number	502
Box number	27
Depth (m)	75.5-78.6
Total thickness in box (m)	3
Thickness described (m) if two units in same box	
Geological unit	Otorohanga Limestone
Quarry unit	Lower Steel

	Discrete seam thickness (mm)									Diffuse seam (mm)	Subhorizontal stylolite	Subvertical stylolite
Box lines	**1**	**2-4**	**5-7**	**8-10**	**11-13**	**14-16**	**17-19**	**Thicknesses (mm) (discrete seams)**	**Tot. thick. (mm) of discrete seams**			
Line A (bottom)												
Line B												
Line C												
Line D												
Line E (top)												
Total	**22**	**2**						2,2	**24**		**24**	**2**
Total broken thickness (m)	0.35											
No. of metres in box - broken	2.65											
Comments/notes e.g. porosity, stylolite networks	2 stylolitic networks											

Discontinuity core log data sheet

Page 24 of 35

Logged by	Orla Hansen
Location	McDonald's Quarry
Date logged	Nov-06
Borehole number	502
Box number	28
Depth (m)	78.4-81.3
Total thickness in box (m)	2.94
Thickness described (m) if two units in same box	
Geological unit	Otorohanga Limestone
Quarry unit	Lower Steel

	Discrete seam thickness (mm)									Diffuse seam (mm)	Subhorizontal stylolite	Subvertical stylolite
Box lines	**1**	**2-4**	**5-7**	**8-10**	**11-13**	**14-16**	**17-19**	**Thicknesses (mm) (discrete seams)**	**Tot. thick. (mm) of discrete seams**			
Line A (bottom)												
Line B												
Line C												
Line D												
Line E (top)												
Total	**23**	**2**						4,2	**29**		**10**	
Total broken thickness (m)	0.27											
No. of metres in box - broken	2.67											
Comments/notes e.g. porosity, stylolite networks	1 stylolitic network											

Discontinuity core log data sheet

Page 25 of 35

Logged by	Orla Hansen
Location	McDonald's Quarry
Date logged	Nov-06
Borehole number	502
Box number	29
Depth (m)	81.3-84.4
Total thickness in box (m)	2.98
Thickness described (m) if two units in same box	
Geological unit	Otorohanga Limestone
Quarry unit	Sub-economic unit

	Discrete seam thickness (mm)									Diffuse seam (mm)	Subhorizontal stylolite	Subvertical stylolite
Box lines	1	2-4	5-7	8-10	11-13	14-16	17-19	Thicknesses (mm) (discrete seams)	Tot. thick. (mm) of discrete seams			
Line A (bottom)												
Line B												
Line C												
Line D												
Line E (top)												
Total	20	9	3					2,2,2,2,2,3,3,3,5,4,7,6	61		13	6
Total broken thickness (m)												
No. of metres in box - broken	2.98											
Comments/notes e.g. porosity, stylolite networks	1 vertical joint with infill, 3 stylolitic networks											

Discontinuity core log data sheet

Page 26 of 35

Logged by	Orla Hansen
Location	McDonald's Quarry
Date logged	Nov-06
Borehole number	502
Box number	30
Depth (m)	84.4-87.3
Total thickness in box (m)	2.92
Thickness described (m) if two units in same box	
Geological unit	Otorohanga Limestone
Quarry unit	Sub-economic unit

	Discrete seam thickness (mm)									Diffuse seam (mm)	Subhorizontal stylolite	Subvertical stylolite
Box lines	1	2-4	5-7	8-10	11-13	14-16	17-19	Thicknesses (mm) (discrete seams)	Tot. thick. (mm) of discrete seams			
Line A (bottom)												
Line B												
Line C												
Line D												
Line E (top)												
Total	27	11						4,4,4,4,3,2,2,2,2,2,2	46	100	8	1
Total broken thickness (m)												
No. of metres in box - broken	2.92											
Comments/notes e.g. porosity, stylolite networks	1 stylolitic network											

Discontinuity core log data sheet

Page 27 of 35

Logged by	Orla Hansen
Location	McDonald's Quarry
Date logged	Nov-06
Borehole number	502
Box number	31
Depth (m)	87.1-90.1
Total thickness in box (m)	2.81
Thickness described (m) if two units in same box	
Geological unit	Otorohanga Limestone
Quarry unit	Sub-economic unit

	Discrete seam thickness (mm)									Diffuse seam (mm)	Subhorizontal stylolite	Subvertical stylolite
Box lines	1	2-4	5-7	8-10	11-13	14-16	17-19	Thicknesses (mm) (discrete seams)	Tot. thick. (mm) of discrete seams			
Line A (bottom)												
Line B												
Line C												
Line D												
Line E (top)												
Total	23	19	1					3,3,3,3,3,3,2,2,2,2,2,2, 2,2,2,2,2,2,6,4	75	30	9	
Total broken thickness (m)	0.23											
No. of metres in box - broken	2.58											
Comments/notes e.g. porosity, stylolite networks	3 stylolitic networks											

Discontinuity core log data sheet

Page 28 of 35

Logged by	Orla Hansen										**Diffuse seam (mm)**	**Subhorizontal stylolite**	**Subvertical stylolite**
Location	McDonald's Quarry												
Date logged	Nov-06												
Borehole number	502												
Box number	32												
Depth (m)	90.1-92.9												
Total thickness in box (m)	2.86												
Thickness described (m) if two units in same box													
Geological unit	Otorohanga Limestone												
Quarry unit	Sub-economic unit												
	Discrete seam thickness (mm)							**Thicknesses (mm) (discrete seams)**	**Tot. thick. (mm) of discrete seams**				
Box lines	**1**	**2-4**	**5-7**	**8-10**	**11-13**	**14-16**	**17-19**						
Line A (bottom)													
Line B													
Line C													
Line D													
Line E (top)													
Total	**13**	**16**	**3**					6,6,6,2,2,2,2,2,2,2,2	**72**		**483**	**3**	**1**
								,2,2,3,4,4,4,4					
Total broken thickness (m)	0.15												
No. of metres in box - broken	2.71												
Comments/notes e.g. porosity, stylolite networks	2 stylolitic networks												

Discontinuity core log data sheet

Page 29 of 35

Logged by	Orla Hansen										**Diffuse seam (mm)**	**Subhorizontal stylolite**	**Subvertical stylolite**
Location	McDonald's Quarry												
Date logged	Nov-06												
Borehole number	502												
Box number	33												
Depth (m)	92.9-95.8												
Total thickness in box (m)	2.95												
Thickness described (m) if two units in same box													
Geological unit	Otorohanga Limestone												
Quarry unit	Sub-economic unit												
	Discrete seam thickness (mm)							**Thicknesses (mm) (discrete seams)**	**Tot. thick. (mm) of discrete seams**				
Box lines	**1**	**2-4**	**5-7**	**8-10**	**11-13**	**14-16**	**17-19**						
Line A (bottom)													
Line B													
Line C													
Line D													
Line E (top)													
Total	**19**	**16**	**3**					4,5,5,5,3,2,2,2,2,2,2,2	**69**			**9**	**1**
								,2,2,2,2,2,2,2					
Total broken thickness (m)	0.2												
No. of metres in box - broken	2.75												
Comments/notes e.g. porosity, stylolite networks	2 stylolitic networks, vertical joint no infill												

Discontinuity core log data sheet

Page 30 of 35

Logged by	Orla Hansen										**Diffuse seam (mm)**	**Subhorizontal stylolite**	**Subvertical stylolite**
Location	McDonald's Quarry												
Date logged	Nov-06												
Borehole number	502												
Box number	34												
Depth (m)	95.8-98.6												
Total thickness in box (m)	2.8												
Thickness described (m) if two units in same box													
Geological unit	Otorohanga Limestone												
Quarry unit	Sub-economic unit												
	Discrete seam thickness (mm)							**Thicknesses (mm) (discrete seams)**	**Tot. thick. (mm) of discrete seams**				
Box lines	**1**	**2-4**	**5-7**	**8-10**	**11-13**	**14-16**	**17-19**						
Line A (bottom)													
Line B													
Line C													
Line D													
Line E (top)													
Total	**26**	**7**	**3**					2,2,2,2,3,3,3,5,5,7	**60**			**22**	
Total broken thickness (m)													
No. of metres in box - broken	2.8												
Comments/notes e.g. porosity, stylolite networks	2 stylolitic networks												

Discontinuity core log data sheet

Page 31 of 35

Logged by	Orla Hansen												
Location	McDonald's Quarry												
Date logged	Nov-06												
Borehole number	502												
Box number	35												
Depth (m)	98.6-101.5												
Total thickness in box (m)	2.9												
Thickness described (m) if two units in same box													
Geological unit	Otorohanga Limestone												
Quarry unit	Sub-economic unit												
	Discrete seam thickness (mm)							**Thicknesses (mm)**	**Tot. thick. (mm) of**	**Diffuse seam (mm)**	**Subhorizontal stylolite**	**Subvertical stylolite**	
Box lines	**1**	**2-4**	**5-7**	**8-10**	**11-13**	**14-16**	**17-19**	**(discrete seams)**	**discrete seams**				
Line A (bottom)													
Line B													
Line C													
Line D													
Line E (top)													
Total	**15**	**1**	**10**				**1**	7,7,6,6,6,6,6,2,5,5,5,17	**93**	**28**	**31**		
Total broken thickness (m)													
No. of metres in box - broken	2.9												
Comments/notes e.g. porosity, stylolite networks	1 stylolitic network												

Discontinuity core log data sheet

Page 32 of 35

Logged by	Orla Hansen												
Location	McDonald's Quarry												
Date logged	Nov-06												
Borehole number	502												
Box number	36												
Depth (m)	101.5-104.4												
Total thickness in box (m)	2.73												
Thickness described (m) if two units in same box													
Geological unit	Otorohanga Limestone												
Quarry unit	Sub-economic unit												
	Discrete seam thickness (mm)							**Thicknesses (mm)**	**Tot. thick. (mm) of**	**Diffuse seam (mm)**	**Subhorizontal stylolite**	**Subvertical stylolite**	
Box lines	**1**	**2-4**	**5-7**	**8-10**	**11-13**	**14-16**	**17-19**	**(discrete seams)**	**discrete seams**				
Line A (bottom)													
Line B													
Line C													
Line D													
Line E (top)													
Total	**9**	**9**	**4**	**3**				4,4,4,6,6,2,2,2,2,2,7,3, 10,10,10,5	**88**	**70**	**3**		
Total broken thickness (m)													
No. of metres in box - broken	2.73												
Comments/notes e.g. porosity, stylolite networks	3 stylolitic networks												

Discontinuity core log data sheet

Page 33 of 35

Logged by	Orla Hansen												
Location	McDonald's Quarry												
Date logged	Nov-06												
Borehole number	502												
Box number	37												
Depth (m)	104.4-107.2												
Total thickness in box (m)	2.8												
Thickness described (m) if two units in same box													
Geological unit	Otorohanga Limestone												
Quarry unit	Sub-economic unit												
	Discrete seam thickness (mm)							**Thicknesses (mm)**	**Tot. thick. (mm) of**	**Diffuse seam (mm)**	**Subhorizontal stylolite**	**Subvertical stylolite**	
Box lines	**1**	**2-4**	**5-7**	**8-10**	**11-13**	**14-16**	**17-19**	**(discrete seams)**	**discrete seams**				
Line A (bottom)													
Line B													
Line C													
Line D													
Line E (top)													
Total	**4**	**6**				**1**		2,2,2,2,4,15,3	**34**				
Total broken thickness (m)	1.72												
No. of metres in box - broken	1.08												
Comments/notes e.g. porosity, stylolite networks	1 stylolitic network												

Discontinuity core log data sheet

Page 34 of 35

Logged by	Orla Hansen												
Location	McDonald's Quarry												
Date logged	Nov-06												
Borehole number	502												
Box number	38												
Depth (m)	107.2-110												
Total thickness in box (m)	2.87												
Thickness described (m) if two units in same box													
Geological unit	Otorohanga Limestone												
Quarry unit	Sub-economic unit												
	Discrete seam thickness (mm)							**Thicknesses (mm) (discrete seams)**	**Tot. thick. (mm) of discrete seams**	**Diffuse seam (mm)**	**Subhorizontal stylolite**	**Subvertical stylolite**	
Box lines	**1**	**2-4**	**5-7**	**8-10**	**11-13**	**14-16**	**17-19**						
Line A (bottom)													
Line B													
Line C													
Line D													
Line E (top)													
Total	**7**	**4**	**1**	**2**	**1**			13,2,2,2,2,8,8,5	**49**	**196**			
Total broken thickness (m)													
No. of metres in box - broken	2.87												
Comments/notes e.g. porosity, stylolite networks													

Discontinuity core log data sheet

Page 35 of 35

Logged by	Orla Hansen												
Location	McDonald's Quarry												
Date logged	Nov-06												
Borehole number	502												
Box number	39												
Depth (m)	110-112.9												
Total thickness in box (m)	2.9												
Thickness described (m) if two units in same box													
Geological unit	Otorohanga Limestone												
Quarry unit	Sub-economic unit												
	Discrete seam thickness (mm)							**Thicknesses (mm) (discrete seams)**	**Tot. thick. (mm) of discrete seams**	**Diffuse seam (mm)**	**Subhorizontal stylolite**	**Subvertical stylolite**	
Box lines	**1**	**2-4**	**5-7**	**8-10**	**11-13**	**14-16**	**17-19**						
Line A (bottom)													
Line B													
Line C													
Line D													
Line E (top)													
Total	**17**	**3**	**1**	**1**			**1**	3,18,7,10,2,2	**59**	**91**	**3**		
Total broken thickness (m)	0.22												
No. of metres in box - broken	2.68												
Comments/notes e.g. porosity, stylolite networks	1 stylolitic network												

Appendix D-4.2.C Discontinuity data sheets for drill hole BH503

Discontinuity core log data sheet

Page 1 of 32

Logged by	Orla Hansen
Location	McDonald's Quarry
Date logged	May-07
Borehole number	503
Box number	6
Depth (m)	18.5-21.5
Total thickness in box (m)	3
Thickness described (m) if two units in same box	1.8
Geological unit	Otorohanga Limestone
Quarry unit	Caprock

	Discrete seam thickness (mm)							Thicknesses (mm)	Tot. thick. (mm) of	Diffuse seam (mm)	Subhorizontal stylolite	Subvertical stylolite
Box lines	**1**	**2-4**	**5-7**	**8-10**	**11-13**	**14-16**	**17-19**	**(discrete seams)**	**discrete seams**			
Line A (bottom)										10		2
Line B	4		1					6,1,1,1,1	10	5		
Line C	2							1,1	2	30		
Line D	1							1.00	1			
Line E (top)	Mahoenui Group											
Total	7		1						13	450		2
Total broken thickness (m)												
No. of metres in box - broken	1.8											
Comments/notes e.g. porosity, stylolite networks	Sandy											

Discontinuity core log data sheet

Page 2 of 32

Logged by	Orla Hansen
Location	McDonald's Quarry
Date logged	May-07
Borehole number	503
Box number	7
Depth (m)	21.5-24.4
Total thickness in box (m)	2.9
Thickness described (m) if two units in same box	0.3
Geological unit	Otorohanga Limestone
Quarry unit	Caprock

	Discrete seam thickness (mm)							Thicknesses (mm)	Tot. thick. (mm) of	Diffuse seam (mm)	Subhorizontal stylolite	Subvertical stylolite
Box lines	**1**	**2-4**	**5-7**	**8-10**	**11-13**	**14-16**	**17-19**	**(discrete seams)**	**discrete seams**			
Line A (bottom)	Upper Steel											
Line B	Upper Steel											
Line C	Upper Steel											
Line D	Upper Steel											
Line E (top)	2							1,1	2	20		
Total	2								2	20		
Total broken thickness (m)												
No. of metres in box - broken	0.3											
Comments/notes e.g. porosity, stylolite networks	Sandy											

Discontinuity core log data sheet

Page 3 of 32

Logged by	Orla Hansen
Location	McDonald's Quarry
Date logged	May-07
Borehole number	503
Box number	7
Depth (m)	21.5-24.4
Total thickness in box (m)	2.9
Thickness described (m) if two units in same box	2.6
Geological unit	Otorohanga Limestone
Quarry unit	Upper Steel

	Discrete seam thickness (mm)							Thicknesses (mm)	Tot. thick. (mm) of	Diffuse seam (mm)	Subhorizontal stylolite	Subvertical stylolite
Box lines	**1**	**2-4**	**5-7**	**8-10**	**11-13**	**14-16**	**17-19**	**(discrete seams)**	**discrete seams**			
Line A (bottom)	2	1						4,1,1	6		1	
Line B									3			
Line C	3							1,1,1	8		3	
Line D	1	1	1					5,2,1				
Line E (top)	Caprock											
Total	**6**	**1**	**1**						**17**		**4**	
Total broken thickness (m)	0.74											
No. of metres in box - broken	1.86											
Comments/notes e.g. porosity, stylolite networks	Porous zones (1%), limestone pure white, whole box oxidised, light brown clay lining (possible joint zone?)											

Discontinuity core log data sheet

Page 4 of 32

Logged by	Orla Hansen
Location	McDonald's Quarry
Date logged	May-07
Borehole number	503
Box number	8
Depth (m)	24.4-27.3
Total thickness in box (m)	2.9
Thickness described (m) if two units in same box	
Geological unit	Otorohanga Limestone
Quarry unit	Upper Steel

	Discrete seam thickness (mm)										
Box lines	**1**	**2-4**	**5-7**	**8-10**	**11-13**	**14-16**	**17-19**	**Thicknesses (mm) (discrete seams)**	**Tot. thick. (mm) of discrete seams**	**Diffuse seam (mm)**	**Subhorizontal stylolite**	**Subvertical stylolite**
Line A (bottom)	3							1,1,1	3		2	1
Line B												
Line C	broken											
Line D	broken											
Line E (top)											1	
Total	**3**								**3**		**3**	**1**
Total broken thickness (m)	1.78											
No. of metres in box - broken	1.12											
Comments/notes e.g. porosity, stylolite networks	Porous zones - 10 cm thick, porosity associated with stylolites											

Discontinuity core log data sheet

Page 5 of 32

Logged by	Orla Hansen
Location	McDonald's Quarry
Date logged	May-07
Borehole number	503
Box number	9
Depth (m)	27.3-30.2
Total thickness in box (m)	2.9
Thickness described (m) if two units in same box	0.8
Geological unit	Otorohanga Limestone
Quarry unit	Upper Steel

	Discrete seam thickness (mm)										
Box lines	**1**	**2-4**	**5-7**	**8-10**	**11-13**	**14-16**	**17-19**	**Thicknesses (mm) (discrete seams)**	**Tot. thick. (mm) of discrete seams**	**Diffuse seam (mm)**	**Subhorizontal stylolite**	**Subvertical stylolite**
Line A (bottom)	Aglime											
Line B	Aglime											
Line C	Aglime											
Line D	Aglime											
Line E (top)	1								1		3	
Total	1								1		3	
Total broken thickness (m)												
No. of metres in box - broken	0.8											
Comments/notes e.g. porosity, stylolite networks												

Discontinuity core log data sheet

Page 6 of 32

Logged by	Orla Hansen
Location	McDonald's Quarry
Date logged	May-07
Borehole number	503
Box number	9
Depth (m)	27.3-30.2
Total thickness in box (m)	2.9
Thickness described (m) if two units in same box	2.1
Geological unit	Otorohanga Limestone
Quarry unit	Aglime

	Discrete seam thickness (mm)										
Box lines	**1**	**2-4**	**5-7**	**8-10**	**11-13**	**14-16**	**17-19**	**Thicknesses (mm) (discrete seams)**	**Tot. thick. (mm) of discrete seams**	**Diffuse seam (mm)**	**Subhorizontal stylolite**	**Subvertical stylolite**
Line A (bottom)	6								6			
Line B	7	1						3	10		3	
Line C	4	1						3	7	5	2	
Line D	1								1	10	1	
Line E (top)	Upper Steel											
Total	**18**								**24**	**15**	**6**	
Total broken thickness (m)	0.39											
No. of metres in box - broken	1.71											
Comments/notes e.g. porosity, stylolite networks	32 cm vertical joint with orange/brown clay lining. Discrete seams very wispy											

Discontinuity core log data sheet

Page 7 of 32

Logged by	Orla Hansen
Location	McDonald's Quarry
Date logged	May-07
Borehole number	503
Box number	10
Depth (m)	30.2-33.1
Total thickness in box (m)	2.9
Thickness described (m) if two units in same box	
Geological unit	Otorohanga Limestone
Quarry unit	Aglime

	Discrete seam thickness (mm)									Diffuse seam (mm)	Subhorizontal stylolite	Subvertical stylolite
Box lines	**1**	**2-4**	**5-7**	**8-10**	**11-13**	**14-16**	**17-19**	**Thicknesses (mm) (discrete seams)**	**Tot. thick. (mm) of discrete seams**			
Line A (bottom)	2	6						2,2,2,4,4,2,1,1,	18		2	2
Line B	2		1	2			1	10,19,10,7,1,1	49	80	1	1
Line C	2							1,1,	2	470	1	
Line D	6	1	1					4,6,1,1,1,1,1,1	16		5	1
Line E (top)	2	3						3,3,3,1,1	11		2	
Total	**14**	**10**	**2**	**2**			**1**		**96**	**550**	**11**	**4**
Total broken thickness (m)	0.27											
No. of metres in box - broken	2.63											
Comments/notes e.g. porosity, stylolite networks												

Discontinuity core log data sheet

Page 8 of 32

Logged by	Orla Hansen
Location	McDonald's Quarry
Date logged	May-07
Borehole number	503
Box number	11
Depth (m)	33.1-36.1
Total thickness in box (m)	3
Thickness described (m) if two units in same box	
Geological unit	Otorohanga Limestone
Quarry unit	Aglime

	Discrete seam thickness (mm)									Diffuse seam (mm)	Subhorizontal stylolite	Subvertical stylolite
Box lines	**1**	**2-4**	**5-7**	**8-10**	**11-13**	**14-16**	**17-19**	**Thicknesses (mm) (discrete seams)**	**Tot. thick. (mm) of discrete seams**			
Line A (bottom)	5	5	1					2,3,2,6,2,4,1,1,1,1,1	24			
Line B	8	3						3,2,3,1,1,1,1,1,1,1,1	16		3	1
Line C	1	5	1					4,2,2,6,2,2,1	19		1	1
Line D	1	7	1	1				6,3,2,4,3,2,3,3,10,1	37	130	3	3
Line E (top)		1	4					4,6,5,5,5	25		2	2
Total	**15**	**21**	**7**	**1**					**121**	**130**	**9**	**7**
Total broken thickness (m)												
No. of metres in box - broken	3											
Comments/notes e.g. porosity, stylolite networks	stylolitic networks											

Discontinuity core log data sheet

Page 9 of 32

Logged by	Orla Hansen
Location	McDonald's Quarry
Date logged	May-07
Borehole number	503
Box number	12
Depth (m)	36.1-39
Total thickness in box (m)	2.9
Thickness described (m) if two units in same box	
Geological unit	Otorohanga Limestone
Quarry unit	Aglime

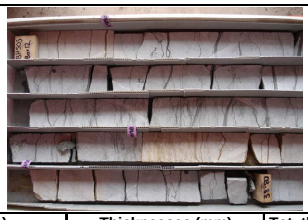

	Discrete seam thickness (mm)									Diffuse seam (mm)	Subhorizontal stylolite	Subvertical stylolite
Box lines	**1**	**2-4**	**5-7**	**8-10**	**11-13**	**14-16**	**17-19**	**Thicknesses (mm) (discrete seams)**	**Tot. thick. (mm) of discrete seams**			
Line A (bottom)	6	6						3,2,4,3,2,3,1,1,1,1,1,1	23			
Line B	6	4	1					2,2,6,2,3,1,1,1,1,1,1	21			
Line C	6	3	1	1				4,3,4,5,9,1,1,1,1,1,1	31			
Line D	7	4	1					4,3,4,6,4,1,1,1,1,1,1	28			
Line E (top)	5	6	3					2,2,4,2,3,6,3,6,5,1,1,1,1,1	38			
Total	**30**	**24**	**6**	**1**					**141**	**550**	**1**	**1**
Total broken thickness (m)												
No. of metres in box - broken	2.9											
Comments/notes e.g. porosity, stylolite networks	NB: seams included inside diffuse portions recorded											

Discontinuity core log data sheet

Page 10 of 32

Logged by	Orla Hansen
Location	McDonald's Quarry
Date logged	May-07
Borehole number	503
Box number	13
Depth (m)	39-42
Total thickness in box (m)	3
Thickness described (m) if two units in same box	0.6
Geological unit	Otorohanga Limestone
Quarry unit	Aglime

	Discrete seam thickness (mm)									Diffuse seam (mm)	Subhorizontal stylolite	Subvertical stylolite
Box lines	**1**	**2-4**	**5-7**	**8-10**	**11-13**	**14-16**	**17-19**	**Thicknesses (mm) (discrete seams)**	**Tot. thick. (mm) of discrete seams**			
Line A (bottom)	gh Grade											
Line B	gh Grade											
Line C	gh Grade											
Line D	gh Grade											
Line E (top)	4	7						2,2,2,2,2,2,3,1,1,1,1	19		1	1
Total	4	7							19		1	1
Total broken thickness (m)												
No. of metres in box - broken	0.6											
Comments/notes e.g. porosity, stylolite networks												

Discontinuity core log data sheet

Page 11 of 32

Logged by	Orla Hansen
Location	McDonald's Quarry
Date logged	May-07
Borehole number	503
Box number	13
Depth (m)	39-42
Total thickness in box (m)	3
Thickness described (m) if two units in same box	2.4
Geological unit	Otorohanga Limestone
Quarry unit	High Grade

	Discrete seam thickness (mm)									Diffuse seam (mm)	Subhorizontal stylolite	Subvertical stylolite
Box lines	**1**	**2-4**	**5-7**	**8-10**	**11-13**	**14-16**	**17-19**	**Thicknesses (mm) (discrete seams)**	**Tot. thick. (mm) of discrete seams**			
Line A (bottom)	3	4	2					4,5,5,5,2,3,1,1,1	25			
Line B	6	4	1					3,2,2,2,6,1,1,1,1,1,1	21		1	1
Line C	2	4						2,3,3,2,1,1,	12		1	1
Line D	6	2						2,3,1,1,1,1,1,1	11		4	
Line E (top)	Aglime											
Total	**17**	**14**	**3**						**69**		**6**	**2**
Total broken thickness (m)	0.12											
No. of metres in box - broken	2.28											
Comments/notes e.g. porosity, stylolite networks	Wispy stylolites											

Discontinuity core log data sheet

Page 12 of 32

Logged by	Orla Hansen
Location	McDonald's Quarry
Date logged	May-07
Borehole number	503
Box number	14
Depth (m)	42-44.8
Total thickness in box (m)	2.8
Thickness described (m) if two units in same box	
Geological unit	Otorohanga Limestone
Quarry unit	High Grade

	Discrete seam thickness (mm)									Diffuse seam (mm)	Subhorizontal stylolite	Subvertical stylolite
Box lines	**1**	**2-4**	**5-7**	**8-10**	**11-13**	**14-16**	**17-19**	**Thicknesses (mm) (discrete seams)**	**Tot. thick. (mm) of discrete seams**			
Line A (bottom)	3	7						3,3,4,2,4,4,3,1,1,1	26		4	1
Line B	4	5						2,2,2,4,4,1,1,1,1	18		2	1
Line C	4	3						3,3,4,1,1,1,1	14		2	
Line D	2	4						2,2,4,2,1,1	12			
Line E (top)	3	2	2					6,6,2,2,1,1,1	19			1
Total	**16**	**21**	**2**						**89**		**8**	**3**
Total broken thickness (m)	0.07											
No. of metres in box - broken	2.73											
Comments/notes e.g. porosity, stylolite networks	wispy sandy seams											

Discontinuity core log data sheet

Page 13 of 32

Logged by	Orla Hansen
Location	McDonald's Quarry
Date logged	May-07
Borehole number	503
Box number	15
Depth (m)	44.8-47.7
Total thickness in box (m)	2.9
Thickness described (m) if two units in same box	
Geological unit	Otorohanga Limestone
Quarry unit	High Grade

	Discrete seam thickness (mm)									Diffuse seam (mm)	Subhorizontal stylolite	Subvertical stylolite
Box lines	**1**	**2-4**	**5-7**	**8-10**	**11-13**	**14-16**	**17-19**	**Thicknesses (mm) (discrete seams)**	**Tot. thick. (mm) of discrete seams**			
Line A (bottom)	7	4						2,2,3,2,1,1,1,1,1,1,1	16		1	2
Line B	4	4	1					6,2,3,3,2,1,1,1,1	20		1	2
Line C	5	5						2,2,2,2,3,1,1,1,1,1	16			1
Line D	4	3						2,2,3,1,1,1,1	11			1
Line E (top)	4	3						2,2,1,1,1,1	8		3	
Total	**24**								**71**		**5**	**6**
Total broken thickness (m)												
No. of metres in box - broken	2.9											
Comments/notes e.g. porosity, stylolite networks	wispy seams very thin <1 mm thick											

Discontinuity core log data sheet

Page 14 of 32

Logged by	Orla Hansen
Location	McDonald's Quarry
Date logged	May-07
Borehole number	503
Box number	16
Depth (m)	47.7-50.6
Total thickness in box (m)	2.9
Thickness described (m) if two units in same box	
Geological unit	Otorohanga Limestone
Quarry unit	High Grade

	Discrete seam thickness (mm)									Diffuse seam (mm)	Subhorizontal stylolite	Subvertical stylolite
Box lines	**1**	**2-4**	**5-7**	**8-10**	**11-13**	**14-16**	**17-19**	**Thicknesses (mm) (discrete seams)**	**Tot. thick. (mm) of discrete seams**			
Line A (bottom)	2	3	3	1				6,5,9,4,5,3,3,1,1	37		4	2
Line B	3	4	2					2,2,6,6,2,2,1,1,1	23			
Line C	2	1	2					5,3,6,1,1	16		6	2
Line D	5	2	1					2,5,2,1,1,1,1,1	14		2	1
Line E (top)	2	5						3,2,2,2,4,1,1	15			1
Total	**14**	**15**	**8**	**1**					**105**		**12**	**6**
Total broken thickness (m)	0.08											
No. of metres in box - broken	2.82											
Comments/notes e.g. porosity, stylolite networks	wispy seam <1 mm thick											

Discontinuity core log data sheet

Page 15 of 32

Logged by	Orla Hansen
Location	McDonald's Quarry
Date logged	May-07
Borehole number	503
Box number	17
Depth (m)	50.6-53.6
Total thickness in box (m)	3
Thickness described (m) if two units in same box	2.8
Geological unit	Otorohanga Limestone
Quarry unit	High Grade

	Discrete seam thickness (mm)									Diffuse seam (mm)	Subhorizontal stylolite	Subvertical stylolite
Box lines	**1**	**2-4**	**5-7**	**8-10**	**11-13**	**14-16**	**17-19**	**Thicknesses (mm) (discrete seams)**	**Tot. thick. (mm) of discrete seams**			
Line A (bottom)	4	3						2,2,3,1,1,1,1,1,1	13		5	
Line B	6	2						2,2,1,1,1,1,1,1	10		4	1
Line C	6							1,1,1,1,1,1	6			2
Line D	6							1,1,1,1,1,1	6		2	
Line E (top)	3	4						3,2,4,2,1,1,1	14			1
Total	**25**	**9**							**49**		**11**	**4**
Total broken thickness (m)	0.06											
No. of metres in box - broken	2.74											
Comments/notes e.g. porosity, stylolite networks												

Discontinuity core log data sheet

Page 16 of 32

Logged by	Orla Hansen
Location	McDonald's Quarry
Date logged	May-07
Borehole number	503
Box number	17
Depth (m)	50.6-53.5
Total thickness in box (m)	3
Thickness described (m) if two units in same box	0.2
Geological unit	Otorohanga Limestone
Quarry unit	Lower Steel

	Discrete seam thickness (mm)									Diffuse seam (mm)	Subhorizontal stylolite	Subvertical stylolite
Box lines	**1**	**2-4**	**5-7**	**8-10**	**11-13**	**14-16**	**17-19**	**Thicknesses (mm) (discrete seams)**	**Tot. thick. (mm) of discrete seams**			
Line A (bottom)	2							1,1	2		3	
Line B	gh Grade											
Line C	gh Grade											
Line D	gh Grade											
Line E (top)	gh Grade											
Total	**2**								**2**		**3**	
Total broken thickness (m)												
No. of metres in box - broken	0.2											
Comments/notes e.g. porosity, stylolite networks												

Discontinuity core log data sheet

Page 17 of 32

Logged by	Orla Hansen
Location	McDonald's Quarry
Date logged	May-07
Borehole number	503
Box number	18
Depth (m)	53.5-56.4
Total thickness in box (m)	2.9
Thickness described (m) if two units in same box	
Geological unit	Otorohanga Limestone
Quarry unit	Lower Steel

	Discrete seam thickness (mm)									Diffuse seam (mm)	Subhorizontal stylolite	Subvertical stylolite
Box lines	**1**	**2-4**	**5-7**	**8-10**	**11-13**	**14-16**	**17-19**	**Thicknesses (mm) (discrete seams)**	**Tot. thick. (mm) of discrete seams**			
Line A (bottom)	6	3						2,2,2,1,1,1,1,1,1	12		8	
Line B	8	3						2,3,2,1,1,1,1,1,1,1,1	15		2	
Line C	2	3	2					7,4,4,6,4,1,1	27		4	
Line D	2	4	1					3,5,2,4,4,1,1	20		4	
Line E (top)	7	2						2,2,1,1,1,1,1,1,1	11		4	
Total	**25**	**15**	**3**						**85**		**22**	
Total broken thickness (m)												
No. of metres in box - broken	2.9											
Comments/notes e.g. porosity, stylolite networks	difficult to discern seams from stylolitic networks											

Discontinuity core log data sheet

Page 18 of 32

Logged by	Orla Hansen
Location	McDonald's Quarry
Date logged	May-07
Borehole number	503
Box number	19
Depth (m)	56.4-59.3
Total thickness in box (m)	2.9
Thickness described (m) if two units in same box	
Geological unit	Otorohanga Limestone
Quarry unit	Lower Steel

	Discrete seam thickness (mm)									Diffuse seam (mm)	Subhorizontal stylolite	Subvertical stylolite
Box lines	**1**	**2-4**	**5-7**	**8-10**	**11-13**	**14-16**	**17-19**	**Thicknesses (mm) (discrete seams)**	**Tot. thick. (mm) of discrete seams**			
Line A (bottom)	3	4	1					6,2,2,4,4,1,1,1	21		1	2
Line B	2	2		1		1	1	4,3,18,16,8,1,1,	51		3	2
Line C	4	2						3,2,1,1,1,1	9			1
Line D	4							1,1,1,1	4		4	2
Line E (top)	5	5						4,2,2,2,3,1,1,1,1,1	18		1	
Total	**18**	**13**	**1**	**1**		**1**	**1**		**103**		**9**	**7**
Total broken thickness (m)	0.07											
No. of metres in box - broken	2.83											
Comments/notes e.g. porosity, stylolite networks												

Discontinuity core log data sheet

Page 19 of 32

Logged by	Orla Hansen
Location	McDonald's Quarry
Date logged	May-07
Borehole number	503
Box number	20
Depth (m)	59.3-62.2
Total thickness in box (m)	2.9
Thickness described (m) if two units in same box	
Geological unit	Otorohanga Limestone
Quarry unit	Lower Steel

	Discrete seam thickness (mm)										
Box lines	**1**	**2-4**	**5-7**	**8-10**	**11-13**	**14-16**	**17-19**	**Thicknesses (mm) (discrete seams)**	**Tot. thick. (mm) of discrete seams**	**Diffuse seam (mm)**	**Subhorizontal stylolite**	**Subvertical stylolite**
Line A (bottom)	6							1,1,1,1,1,1	6		6	
Line B	5							1,1,1,1,1	5		2	
Line C	3							2,1,1,1	5		7	
Line D	7							1,1,1,1,1,1,1	7			
Line E (top)	4	1						4,1,1,1,1	8		1	1
Total	**25**	**1**							**31**		**16**	**1**
Total broken thickness (m)	0.3											
No. of metres in box - broken	2.6											
Comments/notes e.g. porosity, stylolite networks	NB: limestone preferentially breaks along stylolites. 30 cm long vertical joint lined with clay, porous zones up to 5 mm thick either side of stylolites, coarse grains											

Discontinuity core log data sheet

Page 20 of 32

Logged by	Orla Hansen
Location	McDonald's Quarry
Date logged	May-07
Borehole number	503
Box number	21
Depth (m)	62.2-65.1
Total thickness in box (m)	2.9
Thickness described (m) if two units in same box	
Geological unit	Otorohanga Limestone
Quarry unit	Lower Steel

	Discrete seam thickness (mm)										
Box lines	**1**	**2-4**	**5-7**	**8-10**	**11-13**	**14-16**	**17-19**	**Thicknesses (mm) (discrete seams)**	**Tot. thick. (mm) of discrete seams**	**Diffuse seam (mm)**	**Subhorizontal stylolite**	**Subvertical stylolite**
Line A (bottom)	7	1						4,1,1,1,1,1,1,1	11		6	
Line B	4							1,1,1,1	4		2	1
Line C	7							1,1,1,1,1,1,1	7		4	2
Line D	1							1	1		4	
Line E (top)	4							1,1,1,1	4		4	
Total	**23**	**1**							**27**		**20**	**3**
Total broken thickness (m)	0.96											
No. of metres in box - broken	1.94											
Comments/notes e.g. porosity, stylolite networks	brown clay and palygorskite lining on broken limestone, probably a joint zone											

Discontinuity core log data sheet

Page 21 of 32

Logged by	Orla Hansen
Location	McDonald's Quarry
Date logged	May-07
Borehole number	503
Box number	22
Depth (m)	65.1-68
Total thickness in box (m)	2.9
Thickness described (m) if two units in same box	
Geological unit	Otorohanga Limestone
Quarry unit	Lower Steel

	Discrete seam thickness (mm)										
Box lines	**1**	**2-4**	**5-7**	**8-10**	**11-13**	**14-16**	**17-19**	**Thicknesses (mm) (discrete seams)**	**Tot. thick. (mm) of discrete seams**	**Diffuse seam (mm)**	**Subhorizontal stylolite**	**Subvertical stylolite**
Line A (bottom)											9	
Line B											13	
Line C	1							1	1		8	
Line D	6							1,1,1,1,1,1	6		7	
Line E (top)	8							1,1,1,1,1,1,1,1	8		2	1
Total	**15**								**15**		**39**	**1**
Total broken thickness (m)	0.07											
No. of metres in box - broken	2.83											
Comments/notes e.g. porosity, stylolite networks												

Discontinuity core log data sheet

Page 22 of 32

Logged by	Orla Hansen											
Location	McDonald's Quarry											
Date logged	May-07											
Borehole number	503											
Box number	23											
Depth (m)	68-70.9											
Total thickness in box (m)	2.9											
Thickness described (m) if two units in same box	2.3											
Geological unit	Otorohanga Limestone											
Quarry unit	Lower Steel											
	Discrete seam thickness (mm)							**Thicknesses (mm) (discrete seams)**	**Tot. thick. (mm) of discrete seams**	**Diffuse seam (mm)**	**Subhorizontal stylolite**	**Subvertical stylolite**
Box lines	**1**	**2-4**	**5-7**	**8-10**	**11-13**	**14-16**	**17-19**					
Line A (bottom)	conomic unit											
Line B	1							1	1		11	
Line C											12	
Line D	3							1,1,1	3		5	
Line E (top)	2							1,1	2		6	
Total	**5**								**6**		**34**	
Total broken thickness (m)	0.17											
No. of metres in box - broken	2.13											
Comments/notes e.g. porosity, stylolite networks	Broken limestone lined with clay											

Discontinuity core log data sheet

Page 23 of 32

Logged by	Orla Hansen											
Location	McDonald's Quarry											
Date logged	May-07											
Borehole number	503											
Box number	23											
Depth (m)	68-70.9											
Total thickness in box (m)	2.9											
Thickness described (m) if two units in same box	0.6											
Geological unit	Otorohanga Limestone											
Quarry unit	Sub-economic unit											
	Discrete seam thickness (mm)							**Thicknesses (mm) (discrete seams)**	**Tot. thick. (mm) of discrete seams**	**Diffuse seam (mm)**	**Subhorizontal stylolite**	**Subvertical stylolite**
Box lines	**1**	**2-4**	**5-7**	**8-10**	**11-13**	**14-16**	**17-19**					
Line A (bottom)											11	
Line B	Lower Steel											
Line C	Lower Steel											
Line D	Lower Steel											
Line E (top)	Lower Steel											
Total											**11**	
Total broken thickness (m)												
No. of metres in box - broken	0.6											
Comments/notes e.g. porosity, stylolite networks												

Discontinuity core log data sheet

Page 24 of 32

Logged by	Orla Hansen											
Location	McDonald's Quarry											
Date logged	May-07											
Borehole number	503											
Box number	24											
Depth (m)	70.9-73.8											
Total thickness in box (m)	2.9											
Thickness described (m) if two units in same box												
Geological unit	Otorohanga Limestone											
Quarry unit	Sub-economic unit											
	Discrete seam thickness (mm)							**Thicknesses (mm) (discrete seams)**	**Tot. thick. (mm) of discrete seams**	**Diffuse seam (mm)**	**Subhorizontal stylolite**	**Subvertical stylolite**
Box lines	**1**	**2-4**	**5-7**	**8-10**	**11-13**	**14-16**	**17-19**					
Line A (bottom)	broken											
Line B	3							1,1,1	3		8	
Line C	6							1,1,1,1,1,1	6		7	
Line D	4							1,1,1,1	4		5	
Line E (top)	6							1,1,1,1,1,1	6		1	
Total	**19**								**19**		**21**	
Total broken thickness (m)	0.81											
No. of metres in box - broken	2.09											
Comments/notes e.g. porosity, stylolite networks												

Discontinuity core log data sheet

Page 25 of 32

Logged by	Orla Hansen
Location	McDonald's Quarry
Date logged	May-07
Borehole number	503
Box number	25
Depth (m)	73.8-76.7
Total thickness in box (m)	2.9
Thickness described (m) if two units in same box	
Geological unit	Otorohanga Limestone
Quarry unit	Sub-economic unit

	Discrete seam thickness (mm)									Diffuse seam (mm)	Subhorizontal stylolite	Subvertical stylolite
Box lines	**1**	**2-4**	**5-7**	**8-10**	**11-13**	**14-16**	**17-19**	**Thicknesses (mm) (discrete seams)**	**Tot. thick. (mm) of discrete seams**			
Line A (bottom)											13	
Line B	3							1,1,1	3		10	
Line C	broken											
Line D	1							1	1		12	
Line E (top)	2							1,1	2		16	
Total	**6**								**6**		**51**	
Total broken thickness (m)	0.67											
No. of metres in box - broken	2.23											
Comments/notes e.g. porosity, stylolite networks												

Discontinuity core log data sheet

Page 26 of 32

Logged by	Orla Hansen
Location	McDonald's Quarry
Date logged	May-07
Borehole number	503
Box number	26
Depth (m)	76.7-79.6
Total thickness in box (m)	2.9
Thickness described (m) if two units in same box	
Geological unit	Otorohanga Limestone
Quarry unit	Sub-economic unit

	Discrete seam thickness (mm)									Diffuse seam (mm)	Subhorizontal stylolite	Subvertical stylolite
Box lines	**1**	**2-4**	**5-7**	**8-10**	**11-13**	**14-16**	**17-19**	**Thicknesses (mm) (discrete seams)**	**Tot. thick. (mm) of discrete seams**			
Line A (bottom)	6	1						2,1,1,1,1,1,1	8		3	
Line B	1	3	1					3,2,3,7,1	16			
Line C	2							1,1	2		4	1
Line D	7							1,1,1,1,1,1,1	7			
Line E (top)	5							1,1,1,1,1	5		10	
Total	**21**	**4**	**1**						**38**		**17**	**1**
Total broken thickness (m)	0.12											
No. of metres in box - broken	2.78											
Comments/notes e.g. porosity, stylolite networks												

Discontinuity core log data sheet

Page 27 of 32

Logged by	Orla Hansen
Location	McDonald's Quarry
Date logged	May-07
Borehole number	503
Box number	27
Depth (m)	79.6-82.4
Total thickness in box (m)	2.8
Thickness described (m) if two units in same box	
Geological unit	Otorohanga Limestone
Quarry unit	Sub-economic unit

	Discrete seam thickness (mm)									Diffuse seam (mm)	Subhorizontal stylolite	Subvertical stylolite
Box lines	**1**	**2-4**	**5-7**	**8-10**	**11-13**	**14-16**	**17-19**	**Thicknesses (mm) (discrete seams)**	**Tot. thick. (mm) of discrete seams**			
Line A (bottom)	6	2						2,2,1,1,1,1,1,1	10			
Line B	8							1,1,1,1,1,1,1,1	8		4	
Line C	4	2						1,1,1,1,2,3	9		3	
Line D	3	2						3,1,1,1	6		5	
Line E (top)	2		2					6,6,1,1	14		5	
Total	**23**	**6**	**2**						**47**		**17**	
Total broken thickness (m)	0.29											
No. of metres in box - broken	2.51											
Comments/notes e.g. porosity, stylolite networks	broken limestone lined with clay											

Discontinuity core log data sheet

Page 28 of 32

Logged by	Orla Hansen
Location	McDonald's Quarry
Date logged	May-07
Borehole number	503
Box number	28
Depth (m)	82.4-85.2
Total thickness in box (m)	2.8
Thickness described (m) if two units in same box	
Geological unit	Otorohanga Limestone
Quarry unit	Sub-economic unit

	Discrete seam thickness (mm)										
Box lines	**1**	**2-4**	**5-7**	**8-10**	**11-13**	**14-16**	**17-19**	**Thicknesses (mm) (discrete seams)**	**Tot. thick. (mm) of discrete seams**	**Diffuse seam (mm)**	**Subhorizontal stylolite**	**Subvertical stylolite**
Line A (bottom)	2							1,1	2	210	2	
Line B	5							1,1,1,1,1	5		4	
Line C	7							1,1,1,1,1,1,1	7		7	
Line D	4	3						2,3,2,1,1,1,1	11		2	
Line E (top)	5	2						3,2,1,1,1,1,1	10		1	1
Total	**23**	**5**							**35**	**210**	**16**	**1**
Total broken thickness (m)	0.35											
No. of metres in box - broken	2.45											
Comments/notes e.g. porosity, stylolite networks	10 cm vertical joint with precipitated calcite, broken limestone lined with clay, sandy											

Discontinuity core log data sheet

Page 29 of 32

Logged by	Orla Hansen
Location	McDonald's Quarry
Date logged	May-07
Borehole number	503
Box number	29
Depth (m)	85.2-88.2
Total thickness in box (m)	3
Thickness described (m) if two units in same box	
Geological unit	Otorohanga Limestone
Quarry unit	Sub-economic unit

	Discrete seam thickness (mm)										
Box lines	**1**	**2-4**	**5-7**	**8-10**	**11-13**	**14-16**	**17-19**	**Thicknesses (mm) (discrete seams)**	**Tot. thick. (mm) of discrete seams**	**Diffuse seam (mm)**	**Subhorizontal stylolite**	**Subvertical stylolite**
Line A (bottom)	3	4						2,2,2,2,1,1,1	11		1	
Line B	6	2						2,2,1,1,1,1,1,1	10		1	
Line C	7	3						2,3,3,1,1,1,1,1,1	15		3	1
Line D	5	2						2,2,1,1,1,1,1	9		2	1
Line E (top)	3	1						4,1,1,1	7	50	7	
Total	**24**	**12**							**52**	**50**	**14**	**2**
Total broken thickness (m)												
No. of metres in box - broken	3											
Comments/notes e.g. porosity, stylolite networks	stylolite feeds from seam											

Discontinuity core log data sheet

Page 30 of 32

Logged by	Orla Hansen
Location	McDonald's Quarry
Date logged	May-07
Borehole number	503
Box number	30
Depth (m)	88.2-91.1
Total thickness in box (m)	2.9
Thickness described (m) if two units in same box	
Geological unit	Otorohanga Limestone
Quarry unit	Sub-economic unit

	Discrete seam thickness (mm)										
Box lines	**1**	**2-4**	**5-7**	**8-10**	**11-13**	**14-16**	**17-19**	**Thicknesses (mm) (discrete seams)**	**Tot. thick. (mm) of discrete seams**	**Diffuse seam (mm)**	**Subhorizontal stylolite**	**Subvertical stylolite**
Line A (bottom)	1	3	2					2,3,2,6,6,1	20		4	
Line B	6							1,1,1,1,1,1	6		7	
Line C	5	1						4,1,1,1,1,1	9		3	1
Line D	6	2						3,2,1,1,1,1,1,1	11		4	1
Line E (top)	4	3						2,4,4,1,1,1,1	14		3	
Total	**22**	**9**	**2**						**60**		**21**	**2**
Total broken thickness (m)												
No. of metres in box - broken												
Comments/notes e.g. porosity, stylolite networks												

Discontinuity core log data sheet

Page 31 of 32

Logged by	Orla Hansen
Location	McDonald's Quarry
Date logged	May-07
Borehole number	503
Box number	31
Depth (m)	91.1-94
Total thickness in box (m)	2.9
Thickness described (m) if two units in same box	
Geological unit	Otorohanga Limestone
Quarry unit	Sub-economic unit

	Discrete seam thickness (mm)									Diffuse seam (mm)	Subhorizontal stylolite	Subvertical stylolite
Box lines	**1**	**2-4**	**5-7**	**8-10**	**11-13**	**14-16**	**17-19**	**Thicknesses (mm) (discrete seams)**	**Tot. thick. (mm) of discrete seams**			
Line A (bottom)	3	4						3,4,3,2,1,1,1	15		10	
Line B	2							1,1	2		23	
Line C	4							1,1,1,1	4		11	
Line D	3							1,1,1	3		11	
Line E (top)	5		2					6,5,1,1,1,1,1	16		8	1
Total	**17**	**4**	**2**						**40**		**63**	**1**
Total broken thickness (m)	0.14											
No. of metres in box - broken	2.76											
Comments/notes e.g. porosity, stylolite networks	intense stylolitisation, bold stylolites											

Discontinuity core log data sheet

Page 32 of 32

Logged by	Orla Hansen
Location	McDonald's Quarry
Date logged	May-07
Borehole number	503
Box number	32
Depth (m)	94-96.9
Total thickness in box (m)	2.9
Thickness described (m) if two units in same box	
Geological unit	Otorohanga Limestone
Quarry unit	Sub-economic unit

	Discrete seam thickness (mm)									Diffuse seam (mm)	Subhorizontal stylolite	Subvertical stylolite
Box lines	**1**	**2-4**	**5-7**	**8-10**	**11-13**	**14-16**	**17-19**	**Thicknesses (mm) (discrete seams)**	**Tot. thick. (mm) of discrete seams**			
Line A (bottom)	3		2	1	1			12,7,7,8,1,1,1	37		2	1
Line B		2	1	2	1			10,3,4,6,13,8,	44			3
Line C	5	3		1				2,2,8,4,1,1,1,1,1	21		7	2
Line D	1	2	2	2				2,5,9,10,7,3,1	37			4
Line E (top)	2			2	2			10,10,12,11,1,1	45		1	2
Total	**11**	**7**	**5**	**8**	**4**				**184**		**9**	**12**
Total broken thickness (m)												
No. of metres in box - broken	2.9											
Comments/notes e.g. porosity, stylolite networks	very sandy box, whole box unoxidised											

Appendix D-4.3. Discontinuity core log summary data including total quarry unit thickness, number of discrete seams per metre, thickness of diffuse seams per metre, and number of stylolites per metre for cores BH501, 502, and 503.

Discontinuity core log summary data

Borehole number	Box number	Depth (m) along hole	Thickness of limestone logged (m)	Geological unit	Quarry unit	Total thickness of discrete seams (mm)	**Per metre (mm)**	Total thickness of diffuse seams (mm)	**Per metre (mm)**	Number of subhorizontal stylolites	**Per metre**	Number of subvertical stylolites	**Per metre**
501	10	35.5-38.3	1.51	Otorohanga Lst	Caprock	22	**15**	40	**26**	0	**0.0**	3	**2.0**
	11-13	38.3-47.6	6.27	Otorohanga Lst	Upper Steel	59	**9**	16	**3**	35	**5.6**	2	**0.5**
	13-17	44.6-59.3	12.37	Otorohanga Lst	Aglime	463	**37**	1450	**117**	5	**0.4**	15	**0.2**
	17-24	56.4-80	18.19	Otorohanga Lst	High Grade	509	**28**	0	**0**	9	**0.5**	12	**0.2**
	24-31	77.1-100.4	21.49	Otorohanga Lst	Lower Steel	218	**10**	0	**0**	40	**1.9**	8	**0.1**
	32-38	100.4-120.9	20.5	Otorohanga Lst	Sub-economic	764	**37**	240	**12**	173	**8.4**	27	**0.1**
502	9-10	23.7-29.5	1.57	Otorohanga Lst	Caprock	8	**5**	244	**155**	3	**1.9**	4	**2.5**
	10-13	26.6-38.1	5.8	Otorohanga Lst	Upper Steel	21	**4**	0	**0**	21	**3.6**	3	**0.5**
	13-17	35.1-49.5	8.47	Otorohanga Lst	Aglime	514	**61**	2612	**308**	6	**0.7**	6	**0.7**
	17-23	46.8-66.8	17.2	Otorohanga Lst	High Grade	384	**22**	56	**3**	20	**1.2**	5	**0.3**
	23-28	63.9-81.3	13.92	Otorohanga Lst	Lower Steel	169	**12**	0	**0**	97	**7.0**	5	**0.4**
	29-39	81.3-112.9	29	Otorohanga Lst	Sub-economic	698	**24**	998	**34**	101	**3.5**	9	**0.3**
503	6-7	18.5-24.4	2.1	Otorohanga Lst	Caprock	15	**7**	470	**224**	0	**0.0**	2	**1.0**
	7-9	21.5-30.2	3.78	Otorohanga Lst	Upper Steel	21	**6**	9	**2**	10	**2.6**	1	**0.3**
	9-13	27.3-42	10.84	Otorohanga Lst	Aglime	401	**37**	1245	**115**	28	**2.6**	13	**1.2**
	13-17	39-53.6	13.47	Otorohanga Lst	High Grade	383	**28**	0	**0**	42	**3.1**	21	**1.6**
	17-23	50.6-70.9	15.43	Otorohanga Lst	Lower Steel	269	**17**	0	**0**	143	**9.3**	12	**0.8**
	23-32	68-96.9	24.22	Otorohanga Lst	Sub-economic	481	**20**	260	**11**	240	**9.9**	19	**0.8**

Apendix D-4.3 Discontinuity core log summary data including quarry unit thickness, number of seams per metre, and percentage of core comprising seams for core BH501, 502, and 503.

Discontinuity core log summary data

Borehole number	Box number	Depth (m) along hole	Thickness of limestone logged (m)	Geological unit	Quarry unit	Number of seams	**Per metre**	% core comprising discrete seams	% core comprising diffuse seams
501	10	35.5-38.3	1.51	Otorohanga Lst	Caprock	7	5	1.5	2.6
	11-13	38.3-47.6	6.27	Otorohanga Lst	Upper Steel	34	5	0.9	0.3
	13-17	44.6-59.3	12.37	Otorohanga Lst	Aglime	171	14	3.7	11.7
	17-24	56.4-80	18.19	Otorohanga Lst	High Grade	232	13	2.8	0.0
	24-31	77.1-100.4	21.49	Otorohanga Lst	Lower Steel	191	9	1.0	0.0
	32-38	100.4-120.9	20.5	Otorohanga Lst	Sub-economic	200	10	3.7	1.2
502	9-10	23.7-29.5	1.57	Otorohanga Lst	Caprock	7	4	0.5	15.5
	10-13	26.6-38.1	5.8	Otorohanga Lst	Upper Steel	17	3	0.4	0.0
	13-17	35.1-49.5	8.47	Otorohanga Lst	Aglime	169	20	6.1	30.8
	17-23	46.8-66.8	17.2	Otorohanga Lst	High Grade	230	13	2.2	0.3
	23-28	63.9-81.3	13.92	Otorohanga Lst	Lower Steel	140	10	1.2	0.0
	29-39	81.3-112.9	29	Otorohanga Lst	Sub-economic	309	11	2.4	3.4
503	6-7	18.5-24.4	2.1	Otorohanga Lst	Caprock	10	5	0.7	22.4
	7-9	21.5-30.2	3.78	Otorohanga Lst	Upper Steel	13	3	0.6	0.2
	9-13	27.3-42	10.84	Otorohanga Lst	Aglime	165	15	3.7	11.5
	13-17	39-53.6	13.47	Otorohanga Lst	High Grade	188	14	2.8	0.0
	17-23	50.6-70.9	15.43	Otorohanga Lst	Lower Steel	152	10	1.7	0.0
	23-32	68-96.9	24.22	Otorohanga Lst	Sub-economic	236	10	2.0	1.1

Appendix D-4-4.A Summary statistics for discrete seams in BH501.

BH501	No. seams	Mean	Median	Mode	Frequency of Mode	Sum	Minimum	Maximum	Std.Dev.	Standard Error
Caprock	7	3.14	3	Multiple	2	22	1	6	2.12	0.80
Upper Steel	34	1.74	1	1	22	59	1	6	1.33	0.23
Aglime	171	2.71	2	1	84	463	1	15	2.70	0.21
High Grade	232	2.19	1	1	124	509	1	12	1.76	0.12
Lower Steel	191	1.14	1	1	176	218	1	6	0.59	0.04
Sub-economic	200	3.82	2	1	95	764	1	18	3.88	0.27

Appendix D-4-4.B Summary statistics for discrete seams in BH502.

BH502	No. seams	Mean	Median	Mode	Frequency of Mode	Sum	Minimum	Maximum	Std.Dev.	Standard Error
Caprock	7	1	1	1	6	8	1	2	0	0.14
Upper Steel	17	1	1	1	13	21	1	2	0	0.11
Aglime	169	3	2	1	67	514	1	15	3	0.21
High Grade	230	2	1	1	156	384	1	14	1	0.09
Lower Steel	140	1	1	1	123	169	1	6	1	0.06
Sub-economic	309	2	1	1	171	698	1	18	2	0.14

Appendix D-4-4.C Summary statistics for discrete seams in BH503.

BH503	No. seams	Mean	Median	Mode	Frequency of Mode	Sum	Minimum	Maximum	Std.Dev.	Standard Error
Caprock	10	2	1	1	9	15	1	6	2	0.50
Upper Steel	13	2	1	1	10	21	1	5	1	0.37
Aglime	165	2	2	1	82	401	1	19	2	0.18
High Grade	188	2	1	1	96	383	1	9	1	0.11
Lower Steel	152	2	1	1	114	269	1	18	2	0.18
Sub-economic	236	2	1	1	166	481	1	13	2	0.15

Appendix E-5.1 Wentworth size scale

	U.S. Standard sieve mesh	Grain diameter (mm)		Phi (ϕ) units	Wentworth size class
GRAVEL	Use wire squares	4096		−12	
		1024		−10	Boulder
		256		−8	
		64	64	−6	Cobble
		16		−4	Pebble
	5	4	4	−2	
	6	3.36		−1.75	
	7	2.83		−1.5	Granule
	8	2.38		−1.25	
	10	2.00	2	−1.0	
SAND	12	1.68		−0.75	
	14	1.41		−0.5	Very coarse sand
	16	1.19		−0.25	
	18	1.00	1	0.0	
	20	0.84		0.25	
	25	0.71		0.5	Coarse sand
	30	0.59		0.75	
	35	0.50	½	1.0	
	40	0.42		1.25	
	45	0.35		1.5	Medium sand
	50	0.30		1.75	
	60	0.25	¼	2.0	
	70	0.210		2.25	
	80	0.177		2.5	Fine sand
	100	0.149		2.75	
	120	0.125	⅛	3.0	
	140	0.105		3.25	
	170	0.088		3.5	Very fine sand
	200	0.074		3.75	
	230	0.0625	1/16	4.0	
SILT	270	0.053		4.25	
	325	0.044		4.5	Coarse silt
		0.037		4.75	
		0.031	1/32	5.0	
		0.0156	1/64	6.0	Medium silt
	Use	0.0078	1/128	7.0	Fine silt
	pipette	0.0039	1/256	8.0	Very fine silt
MUD	or hydrometer	0.0020		9.0	
		0.00098		10.0	Clay
		0.00049		11.0	
		0.00024		12.0	
		0.00012		13.0	
		0.00006		14.0	

Particle size terminology. This figure includes U.S. standard mesh sizes used for sieving samples, and corresponding grain diameter (mm), phi units and Wentworth size classes (right). Sourced from Berkman (2001).

Appendix E-5.2 Cathodoluminescence method

The cathodoluminescence (CL) microscope used was a Nikon Eclipse E400 POL powered by a U-PS power supply unit. The CL unit model used is CITL CL8200 Mk5-1. A Nikon Digital Still camera model DXM1200 is mounted to the microscope connected to a PC to take digital photomicrographs. The figure below shows the CL setup. ACT-1 software was used to produce the photomicrographs.

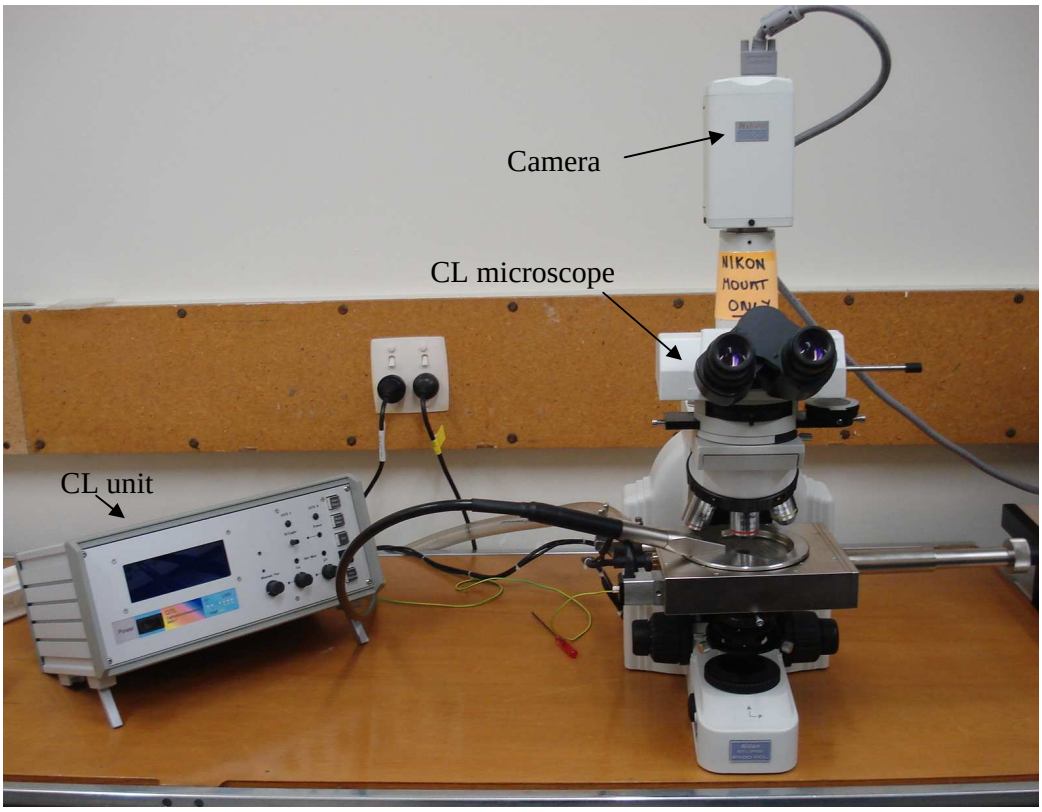

Cathodoluminescent setup at the University of Waikato used for determining mineral type and distribution in polished thin sections.

Appendix E-5.3 Thin section preparation method

Equipment:

- wooden spatula
- plastic containers for mixing
- etching tool to scribe sample number into glass slide
- microscope slides 48 x 28 x 1.35 mm
- glass plate
- carborundum powder grit 600
- diamond lap wheel
- Struers Discoplan – TS
- resin – K142 araldite (A) and hardener (B)
- saw
- hot plate

Sample preparation

1. Each limestone sample was cut using a diamond saw into small blocks approximately 50 x 25 x 20 mm. One surface was then ground smooth using a diamond lap wheel. Blocks were dried on a hot plate over night at 60°C.

2. Each rock block was impregnated using araldite K142 component and a hardener with a mixing ratio of 5 parts component to 1 part hardener. The impregnation resin was mixed on a hot plate at 60°C, spread onto the smoothed block surface (also heated at same temperature) with a spatula, and cured over night at room temperature.

3. To level the surface that was impregnated, each block was polished using water and 600 grit carborundum powder on a glass plate. Each block was then washed in clean water and dried on a hot plate at 60°C over night.

4. Using Hillquist blockmounting resin, components A (component) and B (hardener) were mixed in a ratio of 7 parts component to 3 parts hardener on a hot plate set at 60°C. A small amount was then dropped onto the

prepared block surfaces and spread evenly. Immediately after, a glass slide was placed onto the area that had the resin on it and using light pressure with the finger tips, air bubbles were worked out. After all air bubbles were removed, the blocks were cured, glass slide down, over night.

5. Using a discoplan saw, any excess block was sawn off. The block (attached to the glass slide) was then ground down to standard thin section thickness, approximately 0.03 mm thick on the discoplan. Using an optical microscope, correct thickness was achieved by grinding until quartz grains became yellow under crossed polars, and skeletal fragments became clear enough to identify for standard petrography.

6. Finally, the sample number was etched into the back of each glass slide with a diamond tipped pen.

Appendix E-5.4 Scanning electron microscopy (SEM) method

Sample preparation for SEM

Samples were prepared using the method outlined by Fleger et al. (1993). Each sample was dried and crushed into the size of a small pin head and mounted firmly with tape onto metal (aluminium) holders called stubs. The samples were transferred into a Hitachi Sputter Coater model E1030 to be coated with an electrically conductive substance (i.e. platinum).

The SEM instrument used was a Hitachi Field Emission SEM model S-4100 shown in Figure 1. Three sizes at different magnifications were selected for imaging (i.e. 100 μm, 20 μm, and 6 μm). The best areas to image were large, blocky, flat areas.

Energy dispersive analyser

Energy of the x-rays produced by the sample in the SEM can be analysed EDAX and can provide information about chemical composition of the sample (Fleger et al. 1993). At 20 μm an image was taken to investigate elements present in the samples. To identify elements, three or more locations were chosen on the SEM image to measure elements present. These were then placed in a report using the SEM software and saved.

Figure 1 Hitachi Field Emission SEM instrument model S-1400 at the University of Waikato.

Appendix E-5.5 Wet sieving method

A selection of screens from a standard sieve series was chosen e.g. 2 mm (-1.0 phi), 2.8 mm (-1.5 phi), 4 mm (-2 phi), 5.6 mm (-2.5 phi), 8 mm (-3 phi), 11.2 mm (-3.5 phi), 16 mm (-4 phi), and 22.4 mm (-4.5 phi). Figure 1 shows a schematic of the set up.

1. Samples were soaked in water over night to separate caked lumps and to suspend fine particles.
2. Mount the stack of sieves with a receiver at the bottom onto the sieve shaker. Add sample to the top sieve, secure lid that has the liquid dispersion nozzle which is tightly connected by a tube attached to supply the water. Also ensure that the tube leading out from the receiver is directed into an empty bucket (collector vessel) to collect fines (<2 mm fraction).
3. Turn on the water that is fed through the sieves allowing the water to pass through slowly at a low pressure to avoid loss of sample and sieve damage.
4. Start the sieve shaker, leave on for approximately 5 minutes or when the water passing to the bucket is clear.
5. Stop shaker, allow water to drain, and dismantle sieve stack.
6. Tap the sample retained in each sieve into a pre-weighed tin and put in oven to dry.
7. The fine particles that passed through into the bucket are left over night to settle out of suspension to be later sampled for laser particle size analysis.

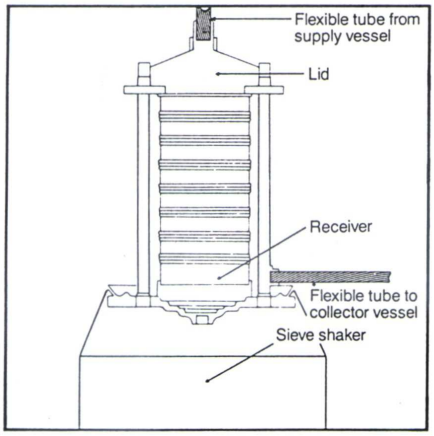

Figure 1 Schematic showing the wet sieve setup including a nest of sieves with a receiver pan at the bottom stacked onto a sieve shaker. The top tube running into the lid supplies the water; the bottom tube transfers fine material to a collector vessel (bucket).

Appendix E-5.6 Laser particle size analysis preparation

The following method is for the preparation of samples for the Malvern-Mastersizer S instrument, adapted from Konert and Vandenberghe (1997).

1. Add 1 teaspoon of sample to a 50 ml beaker and put under fume cupboard. Add 10 ml of 10% hydrogen peroxide (to remove organic matter) to cover sample and stir. Sample will effervesce if organic matter is present.
2. After half an hour check progress and stir sample for effervescence. If there is no reaction organic matter has been efficiently removed. If there is still a reaction move to step 3, if not heat sample on a hot plate to remove excess hydrogen peroxide.
3. Repeat peroxide additions until reaction ceases. Heat beaker gently on a hot plate to speed up reaction and cool slightly before next addition. Organic matter removal is complete when the sample stops effervescing while stirring.
4. Once removal of organic matter is complete, check grain size visually and remove grains larger than 2 mm as the Malvern only measures grains <2 mm in diameter.
5. To remove carbonate, add 25% (1:4) glacial acetic acid to cover sample and wait for reaction to complete. Add more acid if required to remove all carbonate.

Appendix E-5.7 X-ray diffraction results

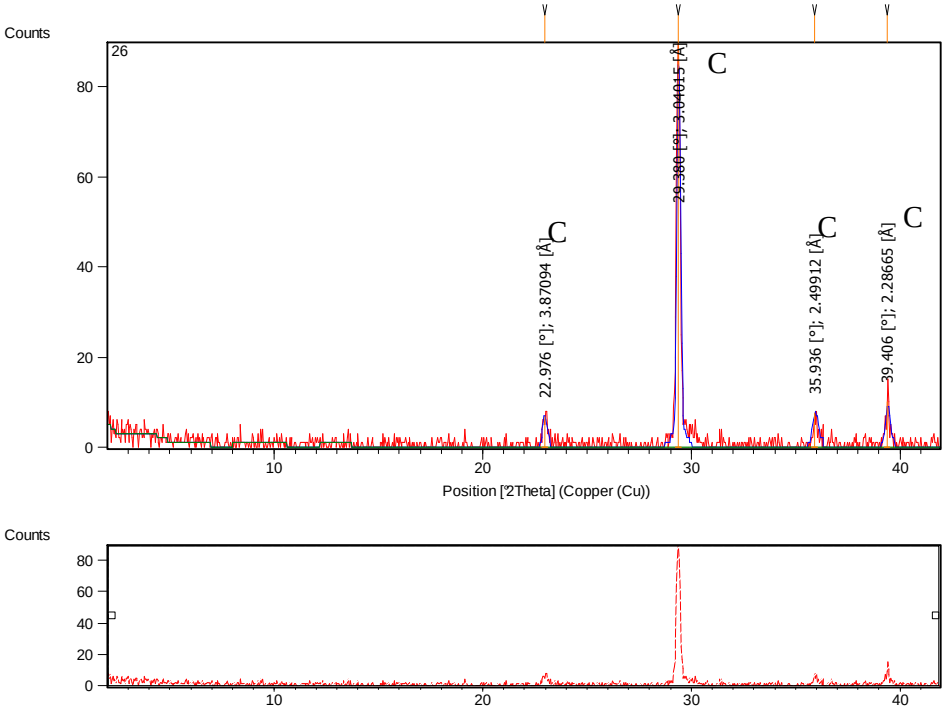

Diffractogram showing XRD results of a sample taken from drill core BH502, box 9 of the Caprock host rock, sample 26. It shows peaks of the mineral calcite (C) which dominates the sample. The lower chart shows the number of counts for each peak corresponding to the above diffractogram.

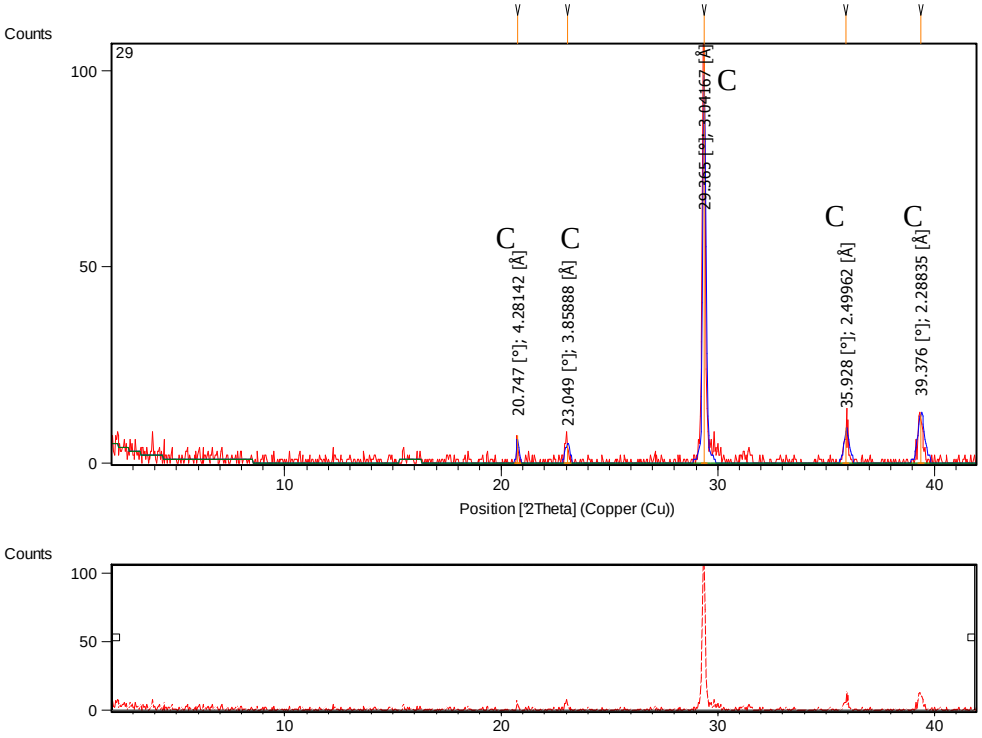

Diffractogram showing XRD results of a sample taken from drill core BH502, box 11 of the Upper Steel host rock, sample 29. It shows peaks of the mineral calcite (C) which dominates the sample. The lower chart shows the number of counts for each peak corresponding to the above diffractogram.

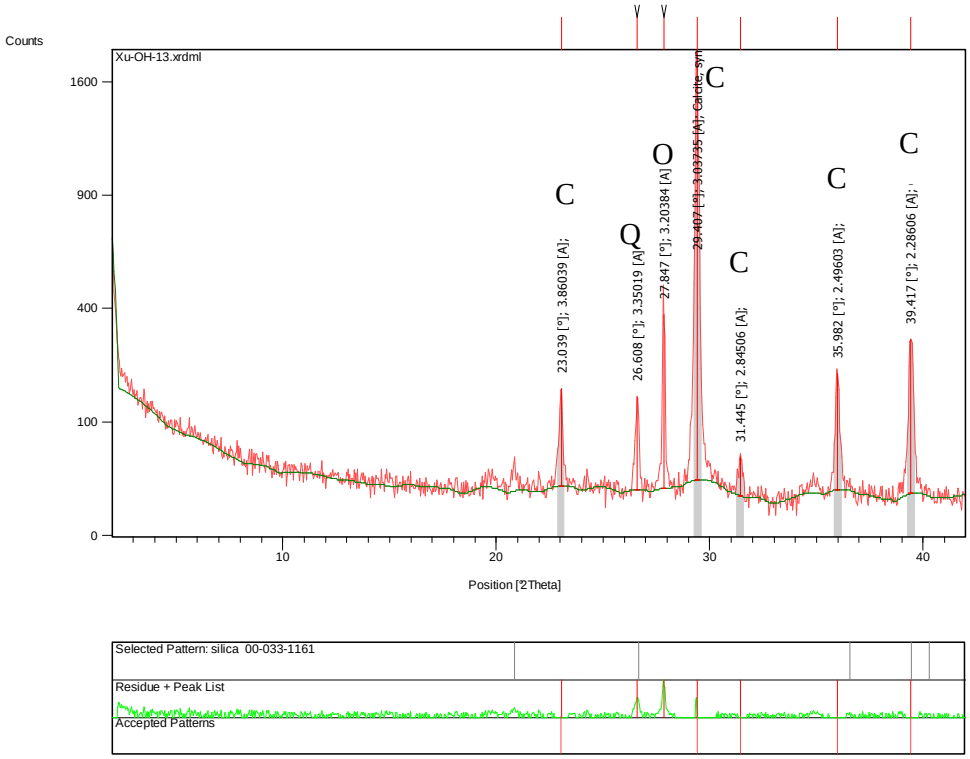

Diffractogram showing XRD results of a sample taken from drill core BH502, box 14 of the Aglime diffuse seam, sample 13. It shows peaks of the mineral calcite (C), oligoclase feldspar (O), and quartz (Q). The lower chart shows the number of counts for each peak corresponding to the above diffractogram.

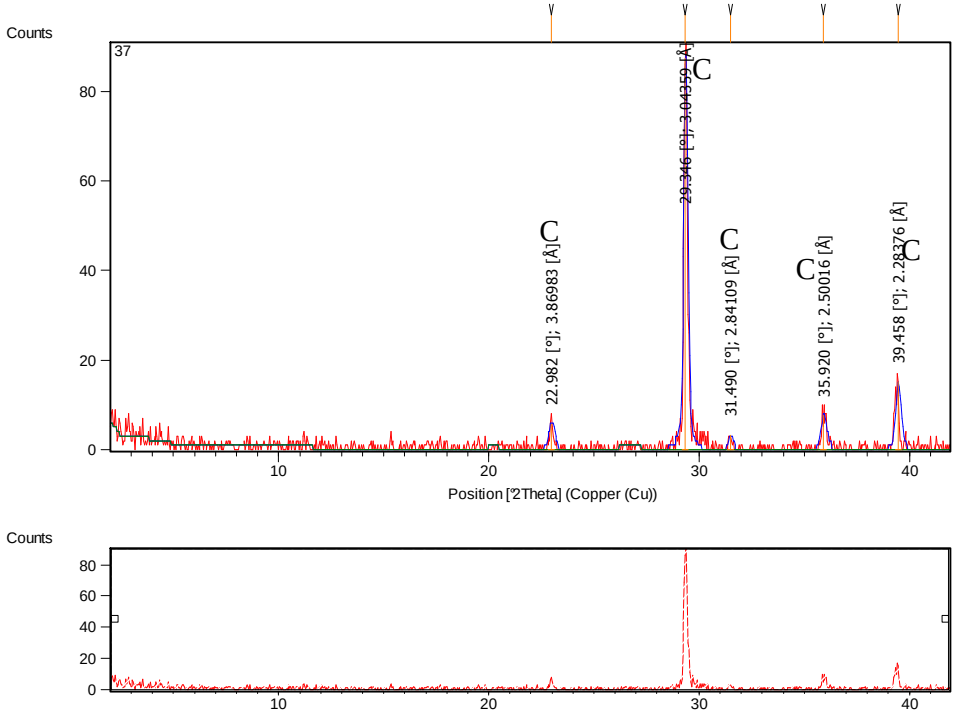

Diffractogram showing XRD results of a sample taken from drill core BH502, box 16 of the Aglime host rock, sample 37. It shows peaks of the mineral calcite (C) which dominates the sample. The lower chart shows the number of counts for each peak corresponding to the above diffractogram.

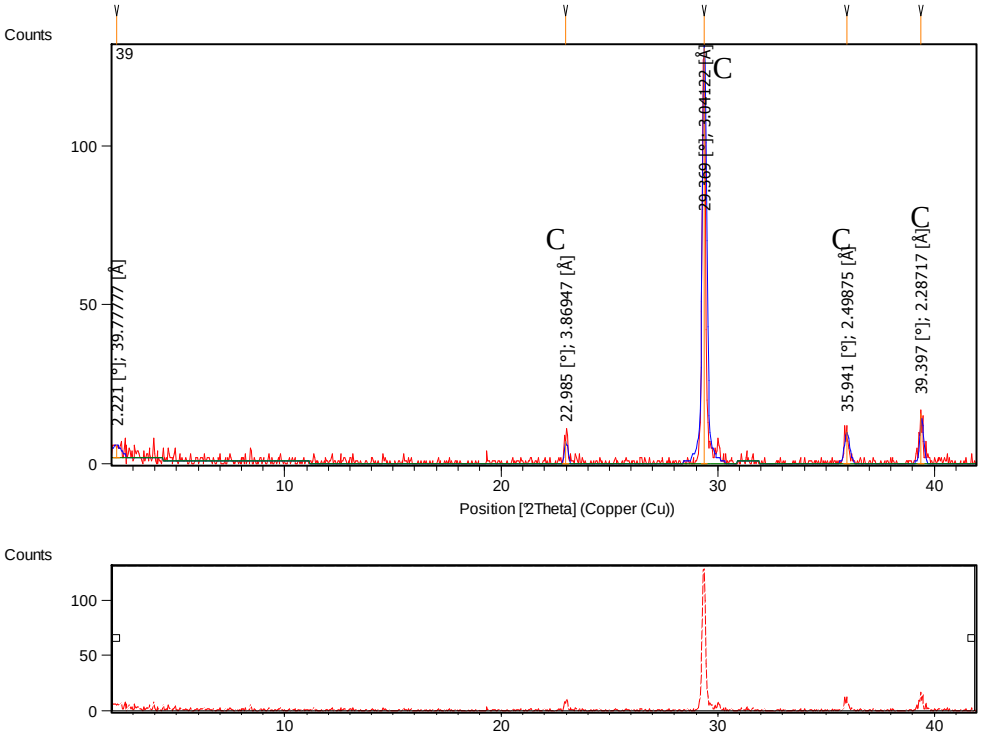

Diffractogram showing XRD results of a sample taken from drill core BH502, box 18 of the High Grade host rock, sample 39. It shows peaks of the mineral calcite (C) which dominates the sample. The lower chart shows the number of counts for each peak corresponding to the above diffractogram.

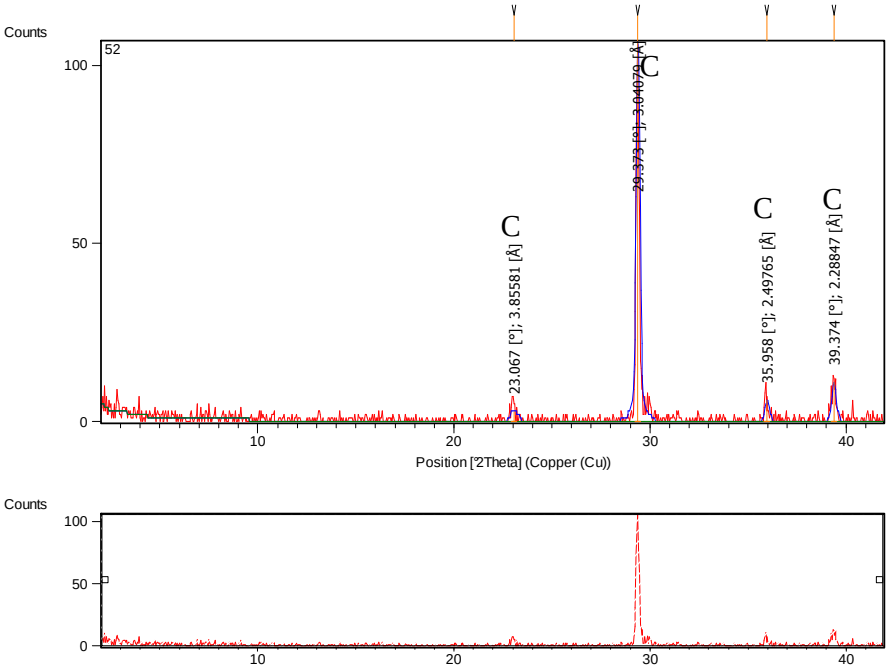

Diffractogram showing XRD results of a sample taken from drill core BH502, box 26 of the Lower Steel host rock, sample 52. It shows peaks of the mineral calcite (C) which dominates the sample. The lower chart shows the number of counts for each peak corresponding to the above diffractogram.

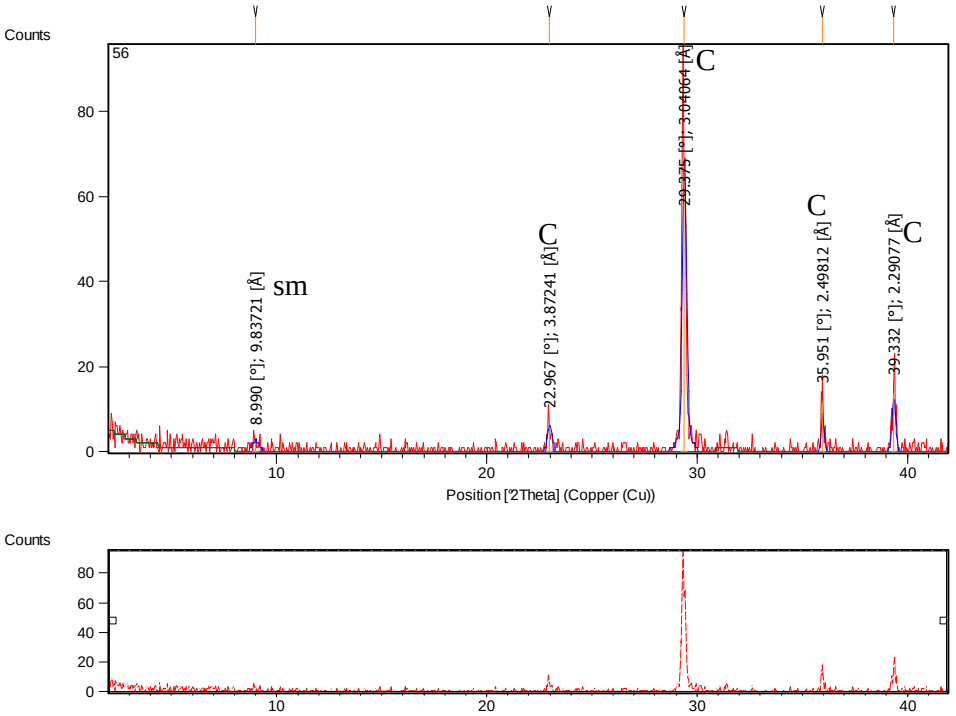

Diffractogram showing XRD results of a sample taken from drill core BH502, box 30 of the Sub-economic host rock, sample 56. It shows peaks of the mineral calcite (C) which dominates the sample, and smectite (sm) (clay). The lower chart shows the number of counts for each peak corresponding to the above diffractogram.

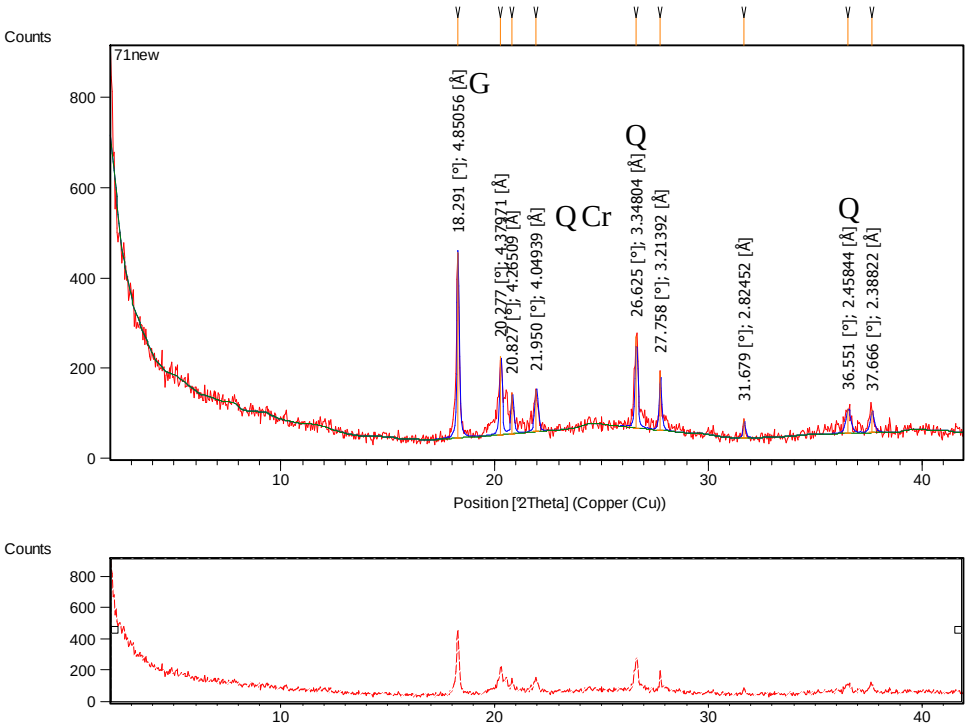

Diffractogram showing XRD results of a sample taken from BH502, box 1 of Kauroa Ash, sample 71. It shows peaks of the minerals gibbsite (G) (clay), smectite (sm) (clay), quartz (Q), and the feldspar cristobalite (Cr). The lower chart shows the number of counts for each peak corresponding to the above diffractogram.

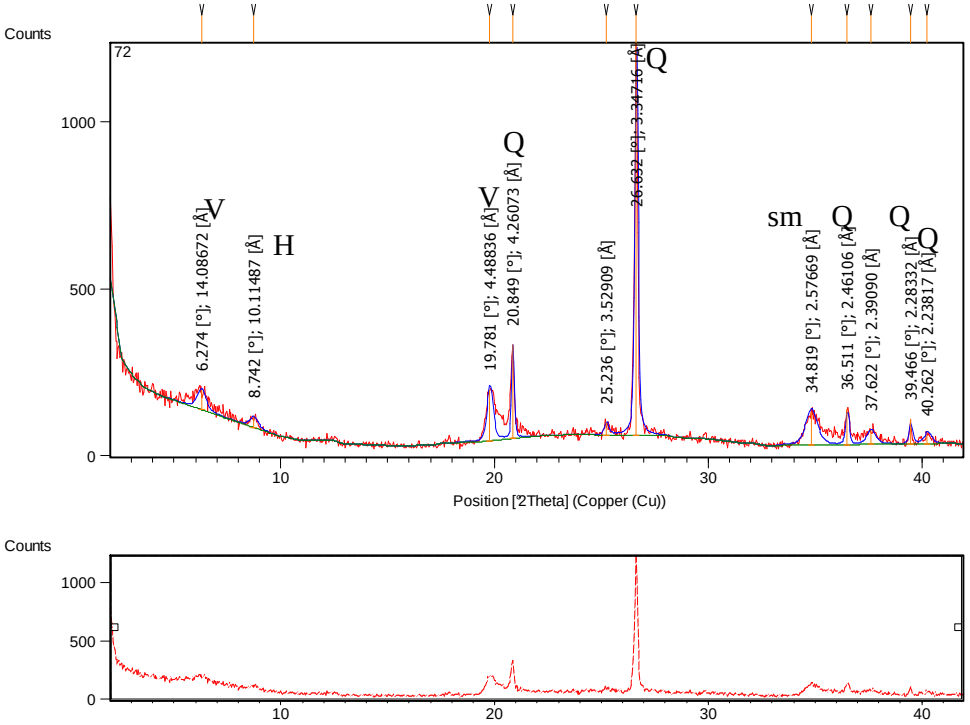

Diffractogram showing XRD results of a sample taken from BH502, box 2 of Kauroa Ash, sample 72. It shows peaks of the minerals halloysite (H) (clay), vermiculite (V) (clay), quartz (Q), and smectite (sm). The lower chart shows the number of counts for each peak corresponding to the above diffractogram.

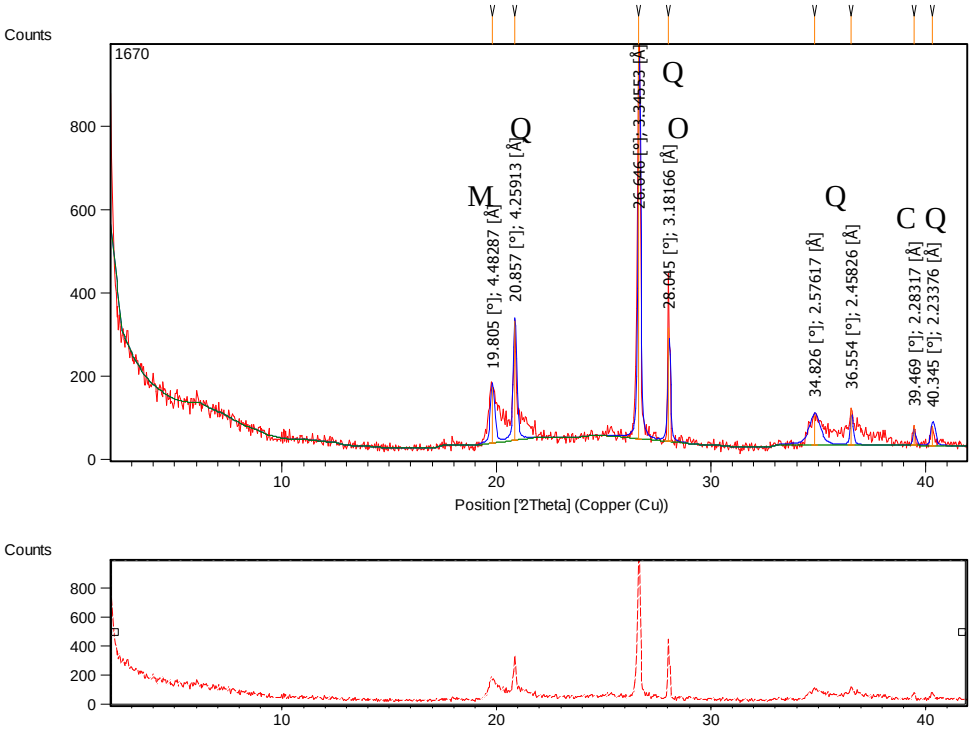

Diffractogram (top) showing XRD results of a sample of Kauroa Ash taken near a limestone outcrop corner of Troopers and Oparure Road, sample 167. It shows peaks of the minerals montmorillonite (M) (clay), calcite (C), quartz (Q), and feldspar oligoclase (O). The lower chart shows the number of counts for each peak corresponding to the above diffractogram.

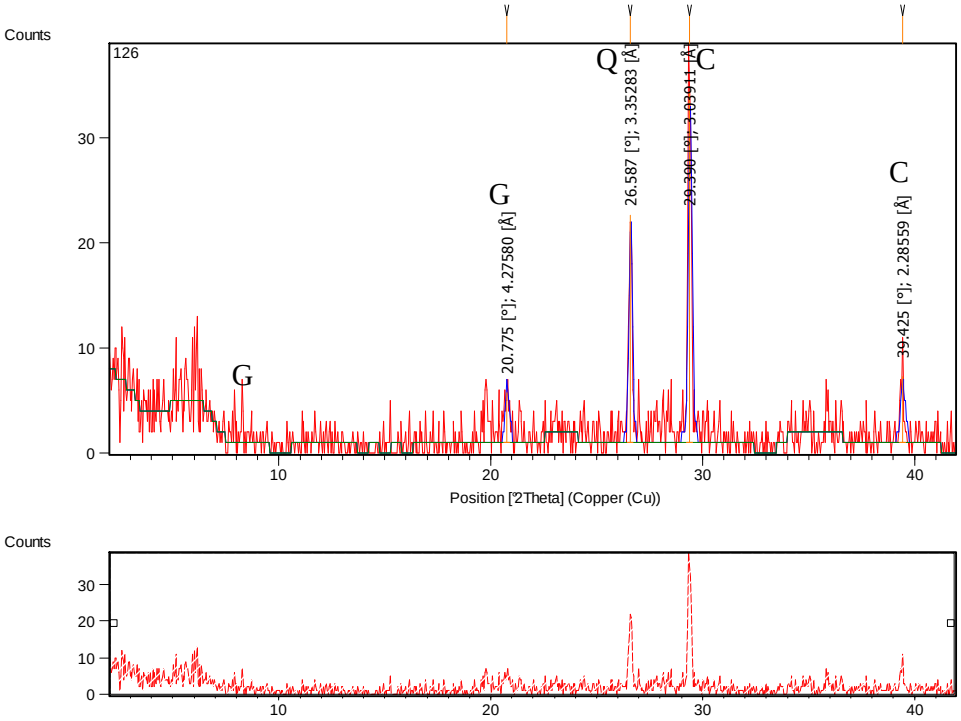

Diffractogram (top) showing XRD results of a sample taken from the Mahoenui Group mudstones, northern face, sample 126. It shows peaks of the minerals gypsum (G), calcite (C), and quartz (Q). The lower chart shows the number of counts for each peak corresponding to the above diffractogram.

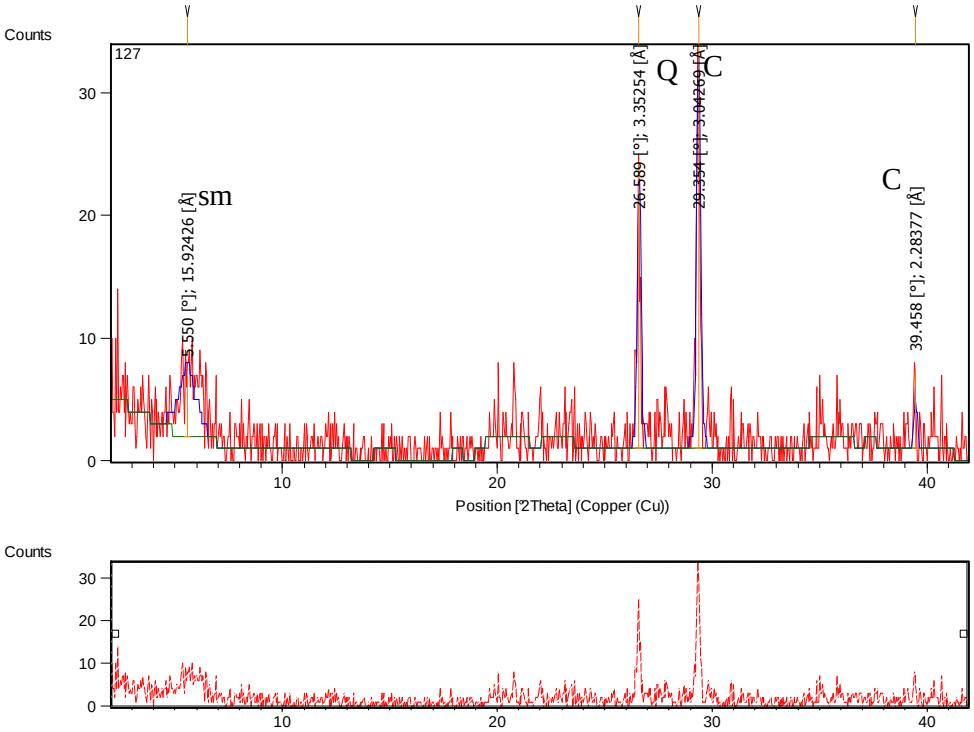

Diffractogram (top) showing XRD results of a sample taken from the Mahoenui Group mudstones, northern face, sample 127. It shows peaks of the minerals smectite (sm) (clay), calcite (C), and quartz (Q). The lower chart shows the number of counts for each peak corresponding to the above diffractogram.

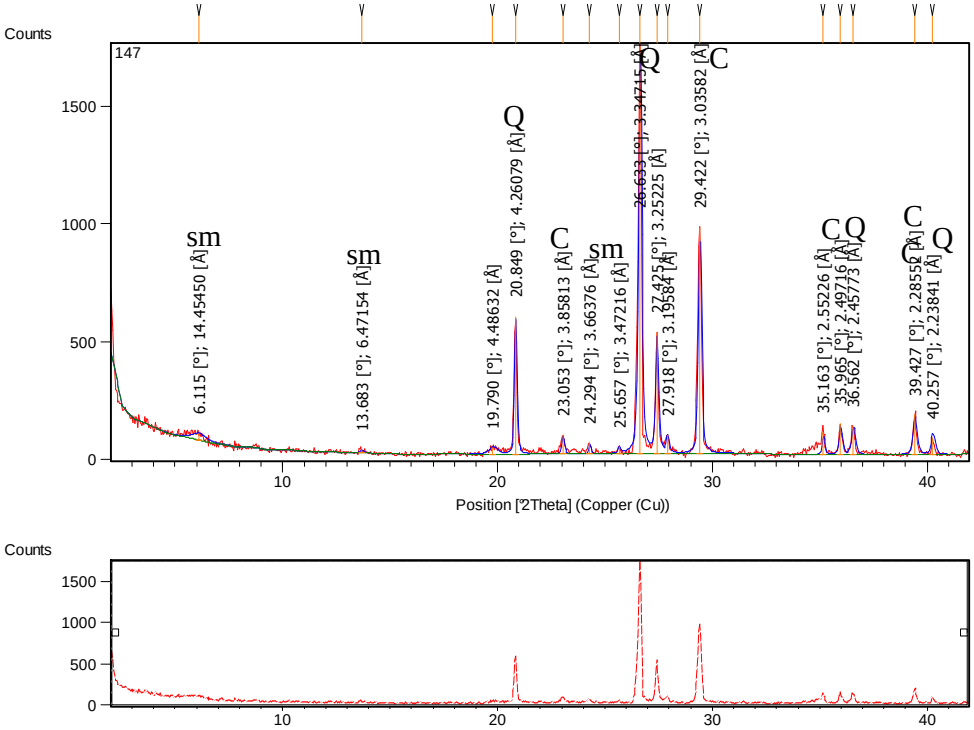

Diffractogram (top) showing XRD results of a sample taken from a discrete dissolution seam on a freshly blasted boulder, Lower Steel, western face, sample 147. It shows peaks of the minerals smectite (sm) (clay), calcite (C), and quartz (Q). The lower chart shows the number of counts for each peak corresponding to the above diffractogram.

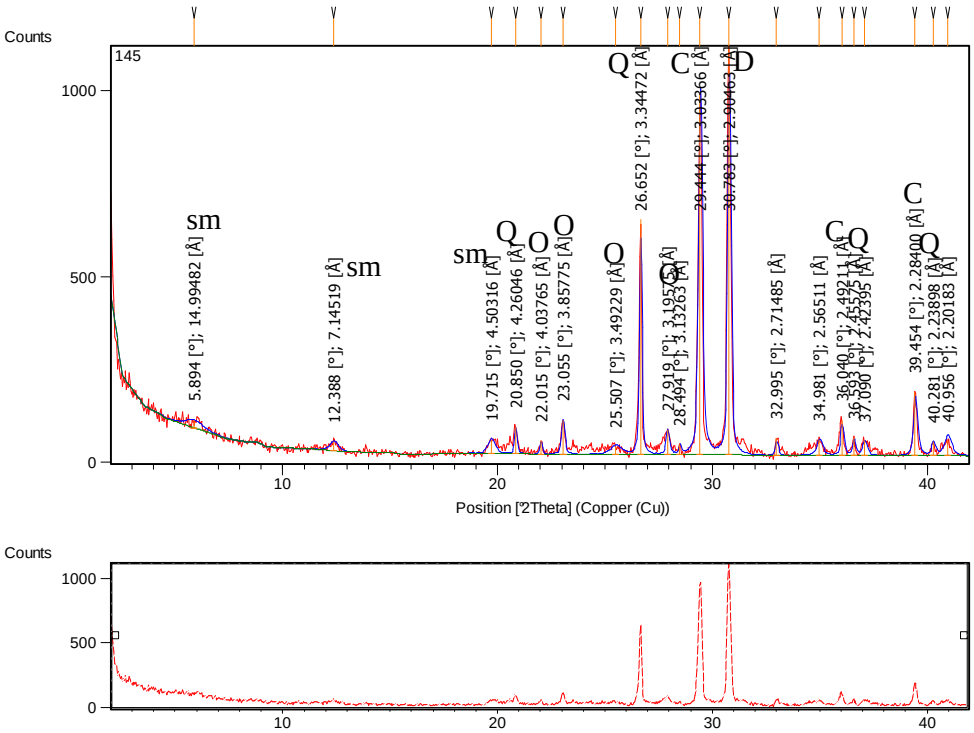

Diffractogram (top) showing XRD results of a sample taken from a discrete dissolution seam on a freshly blasted boulder, High Grade, south western face, sample 145. It shows peaks of the minerals smectite (sm) (clay), calcite (C), dolomite (D), feldspar oligoclase (O), and quartz (Q), and feldspar oligoclase (O). The lower chart shows the number of counts for each peak corresponding to the above diffractogram.

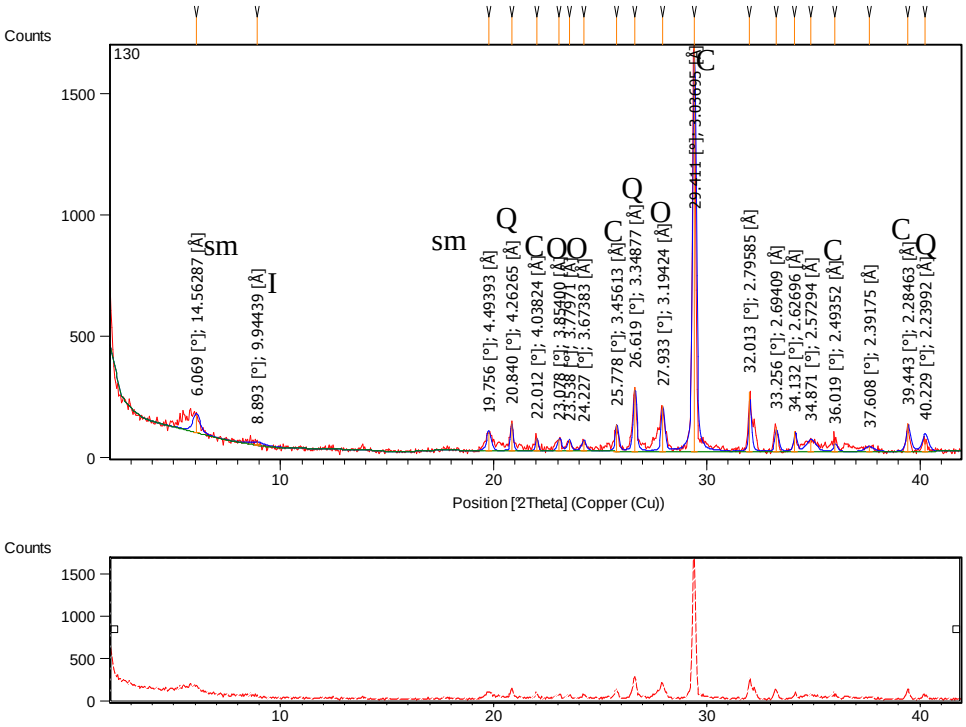

Diffractogram (top) showing XRD results of a sample taken from a diagonal discrete dissolution seam, Upper Steel, northern face, sample 130. It shows peaks of the minerals smectite (sm) (clay), illite (I) (clay), calcite (C), and quartz (Q), and feldspar oligoclase (O). The lower chart shows the number of counts for each peak corresponding to the above diffractogram.

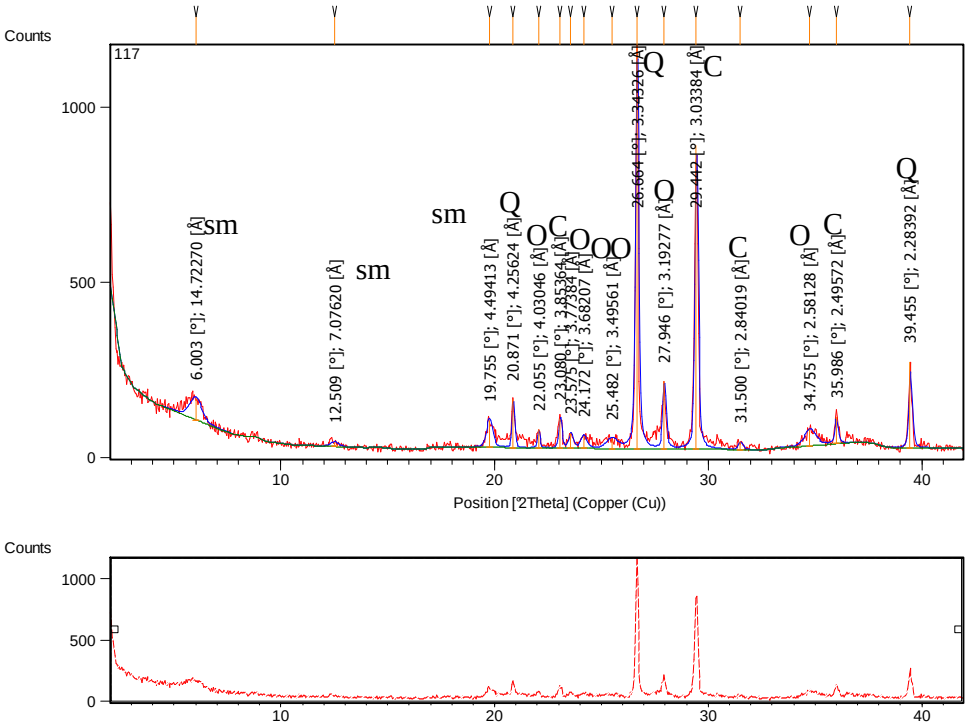

Diffractogram (top) showing XRD results of a sample of a discrete dissolution seam on a boulder, Aglime southern face, sample 117. It shows peaks of the minerals smectite (sm) (clay), calcite (C), and quartz (Q), and feldspar oligoclase (O). The lower chart shows the number of counts for each peak corresponding to the above diffractogram.

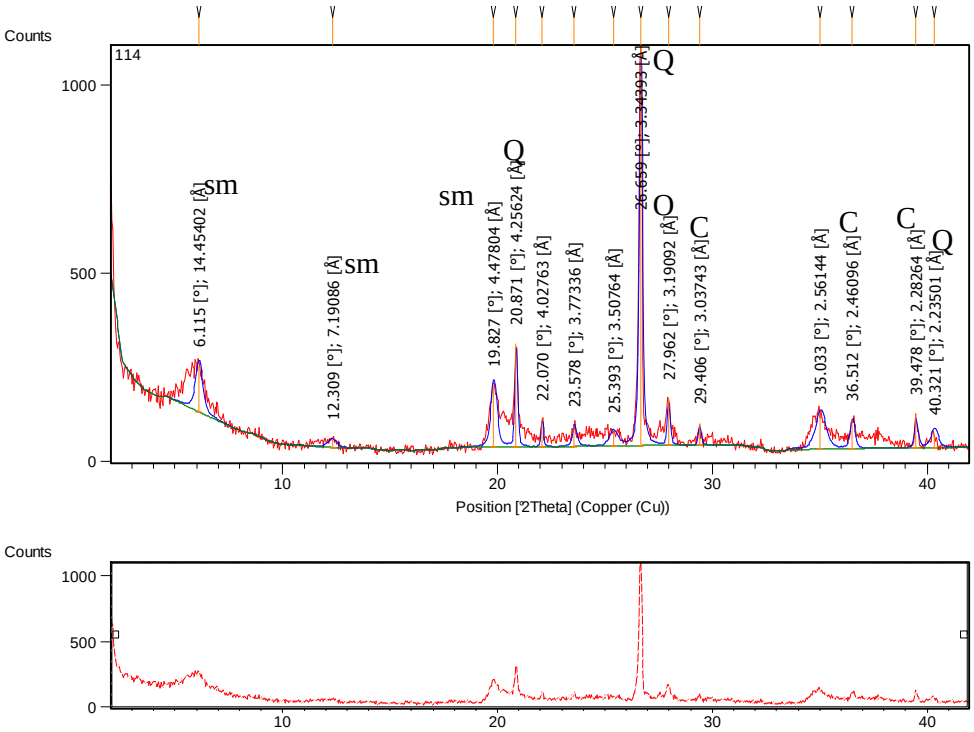

Diffractogram (top) showing XRD results of a sample taken from within a joint zone in the Aglime, southern face, sample 114. It shows peaks of the minerals smectite (sm) (clay), calcite (C), oligoclase (O), and quartz (Q). The lower chart shows the number of counts for each peak corresponding to the above diffractogram.

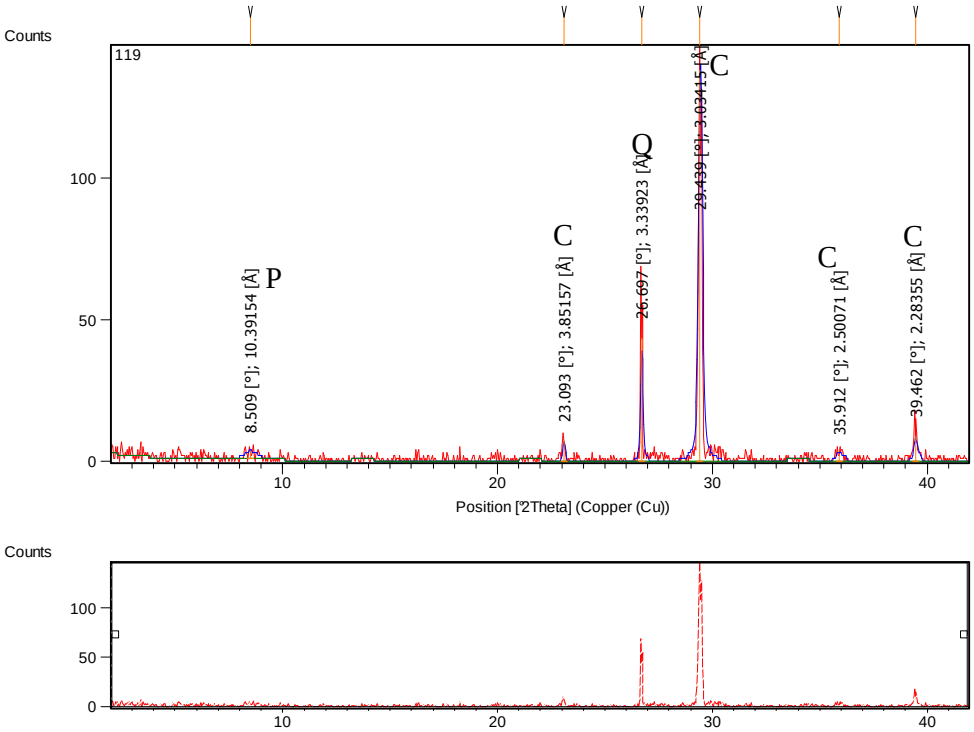

Diffractogram (top) showing XRD results of a sample taken from within a joint in the Aglime, southern face, sample 119. It shows peaks of the minerals palygorskite (P) (clay), calcite (C), and quartz (Q). The lower chart shows the number of counts for each peak corresponding to the above diffractogram.

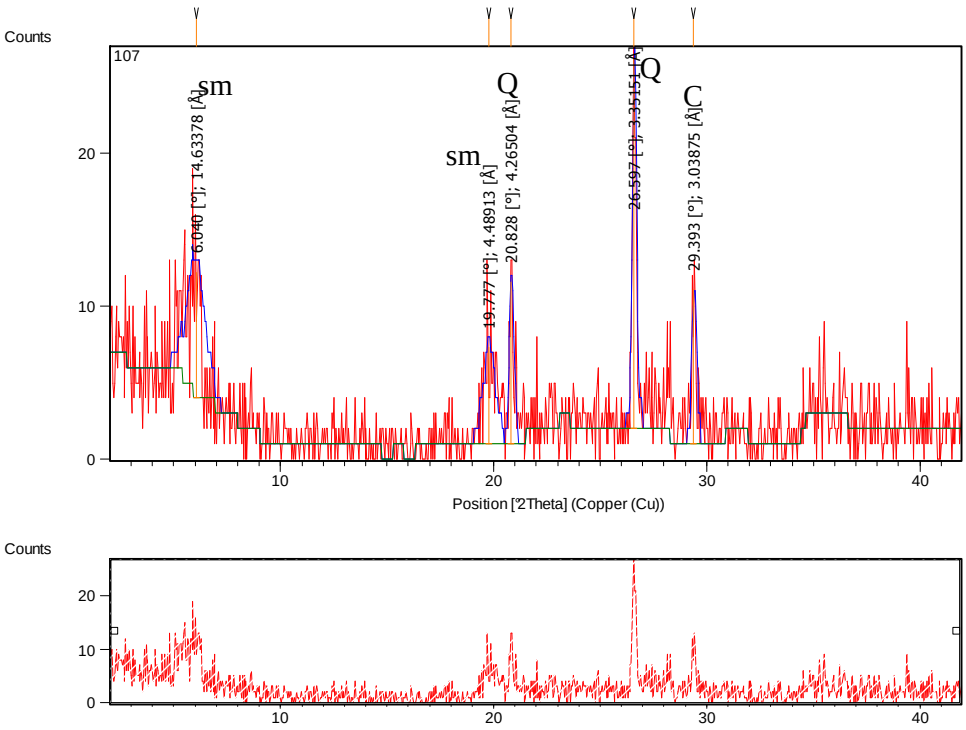

Diffractogram (top) showing XRD results of a sample taken from an exposed joint surface in the High Grade, eastern face, sample 107. It shows peaks of the minerals smectite (sm) (clay), calcite (C), and quartz (Q). The lower chart shows the number of counts for each peak corresponding to the above diffractogram.

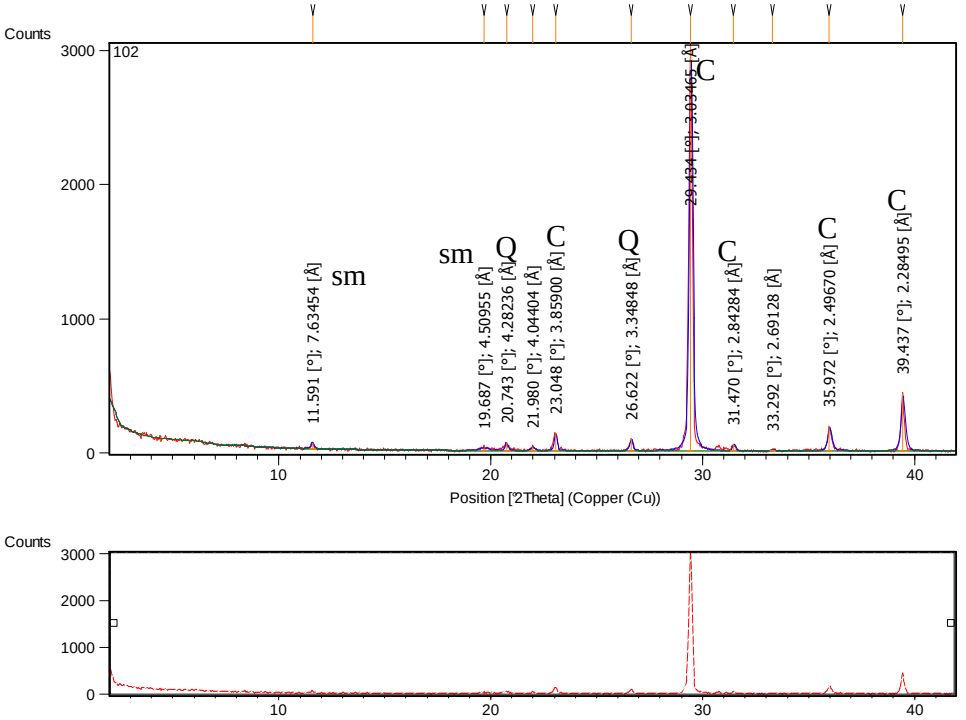

Diffractogram (top) showing XRD results of a sample taken from an exposed joint surface in the Lower Steel, eastern face, sample 102. It shows peaks of the minerals smectite (sm) (clay), calcite (C), and quartz (Q). The lower chart shows the number of counts for each peak corresponding to the above diffractogram.

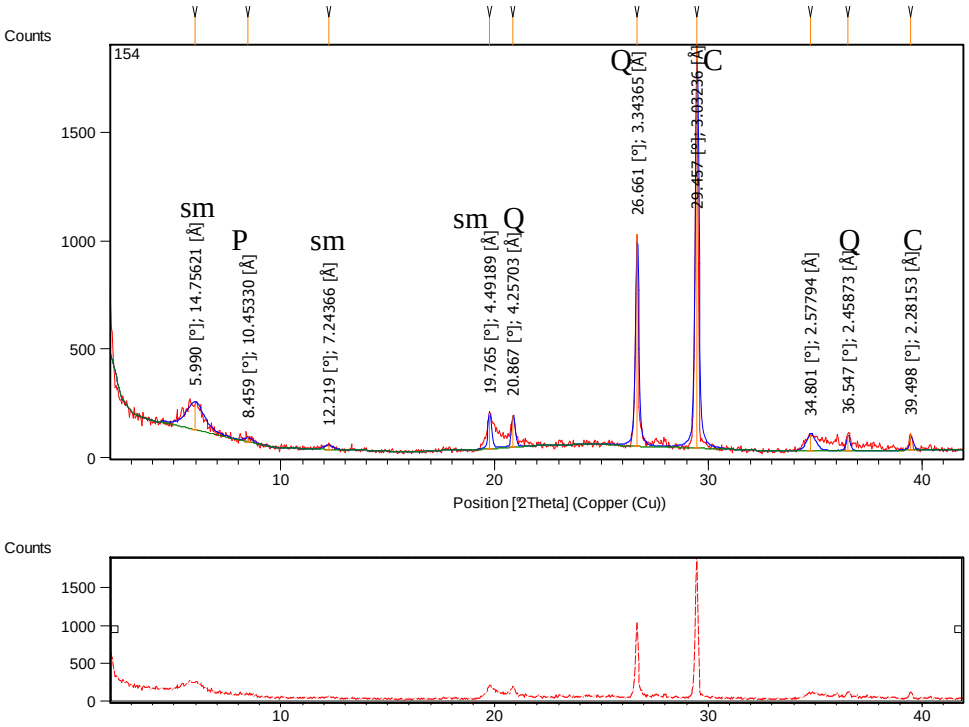

Diffractogram (top) showing XRD results of a sample taken from a joint in the Lower Steel, western face, sample 154. It shows peaks of the minerals smectite (sm) (clay), palygorskite (P), calcite (C), and quartz (Q). The lower chart shows the number of counts for each peak corresponding to the above diffractogram.

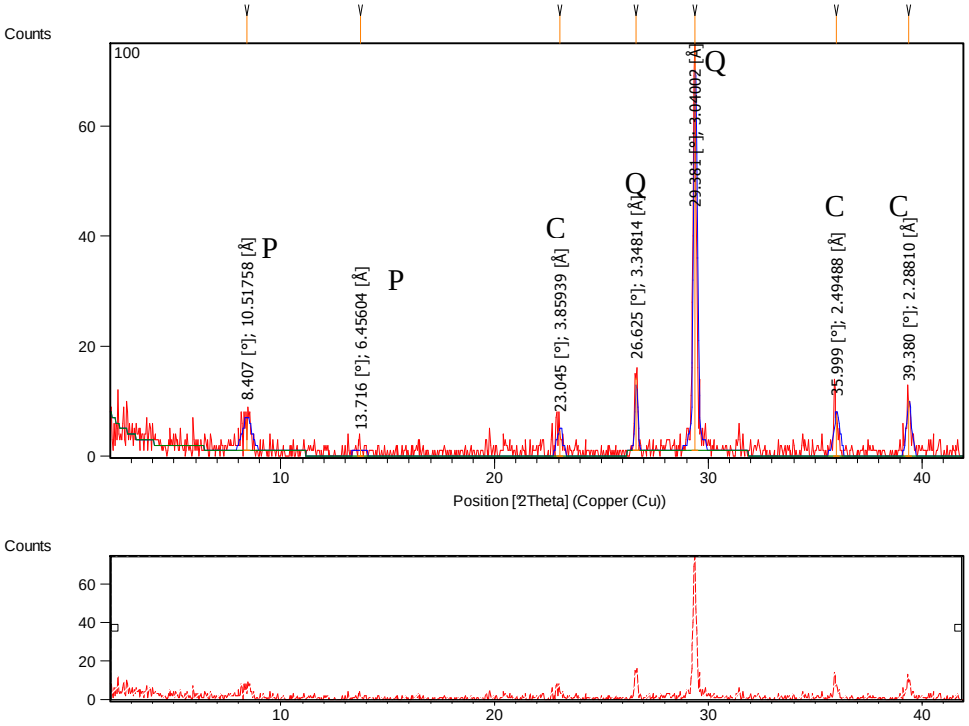

Diffractogram (top) showing XRD results of a sample taken from an exposed joint surface in the Lower Steel, eastern face, sample 100. It shows peaks of the minerals palygorskite (P), calcite (C), and quartz (Q). The lower chart shows the number of counts for each peak corresponding to the above diffractogram.

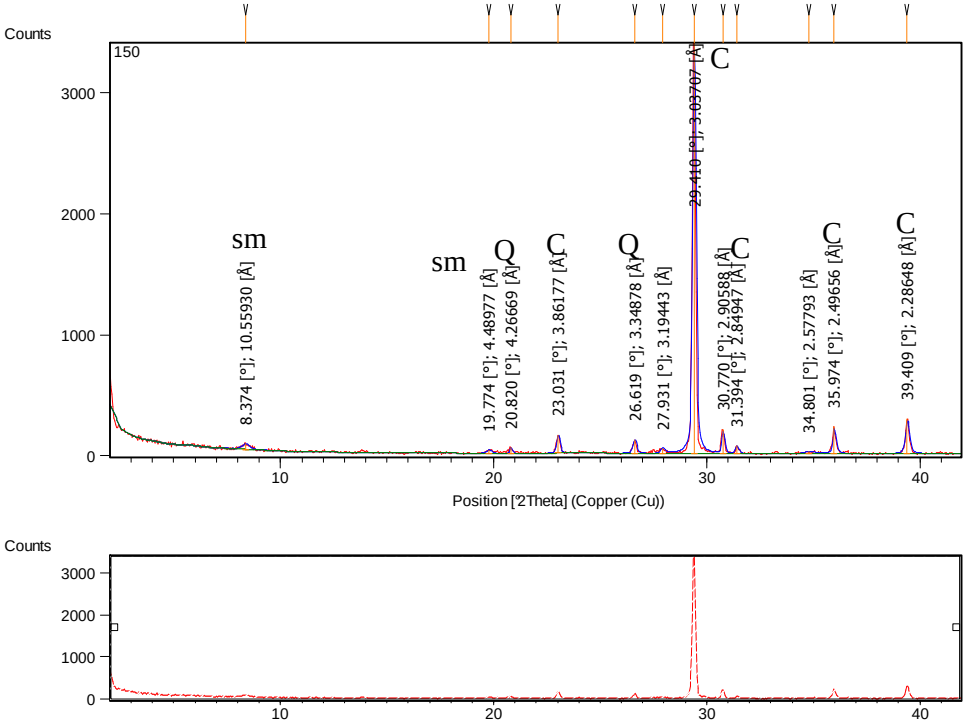

Diffractogram (top) showing XRD results of a sample of surface accumulation, Aglime, old northern face along road to drying plant, sample 150. It shows peaks of the minerals smectite (sm) (clay), calcite (C), and quartz (Q). The lower chart shows the number of counts for each peak corresponding to the above diffractogram.

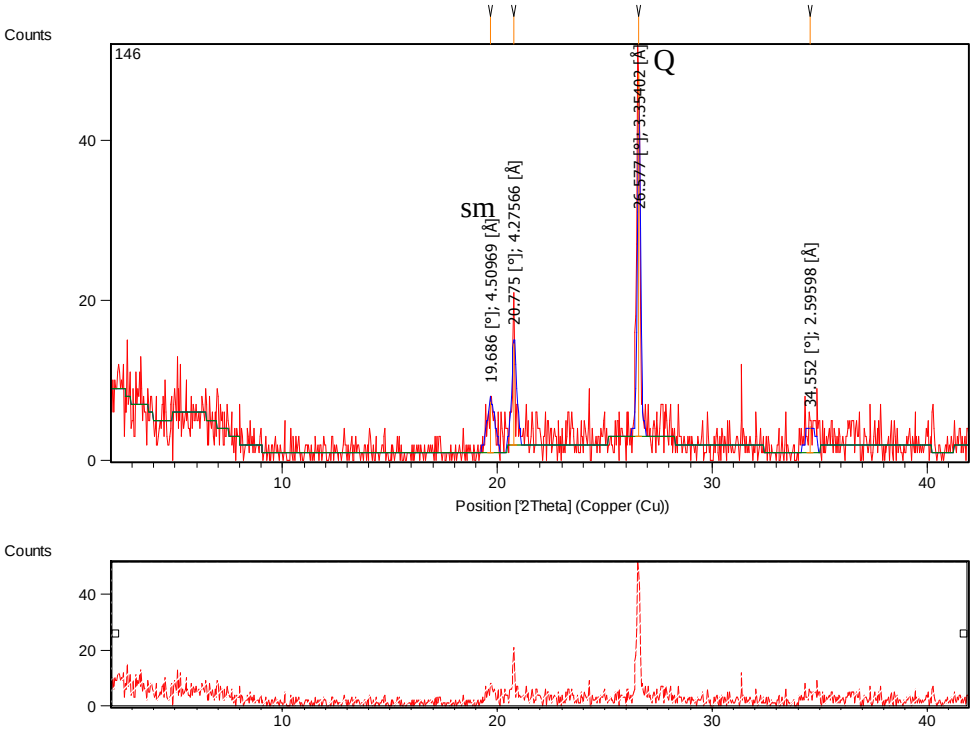

Diffractogram (top) showing XRD results of a sample taken from a limestone cave in the second High Grade bench, western face, sample 146. It shows peaks of the minerals smectite (sm) (clay), and quartz (Q). The lower chart shows the number of counts for each peak corresponding to the above diffractogram.

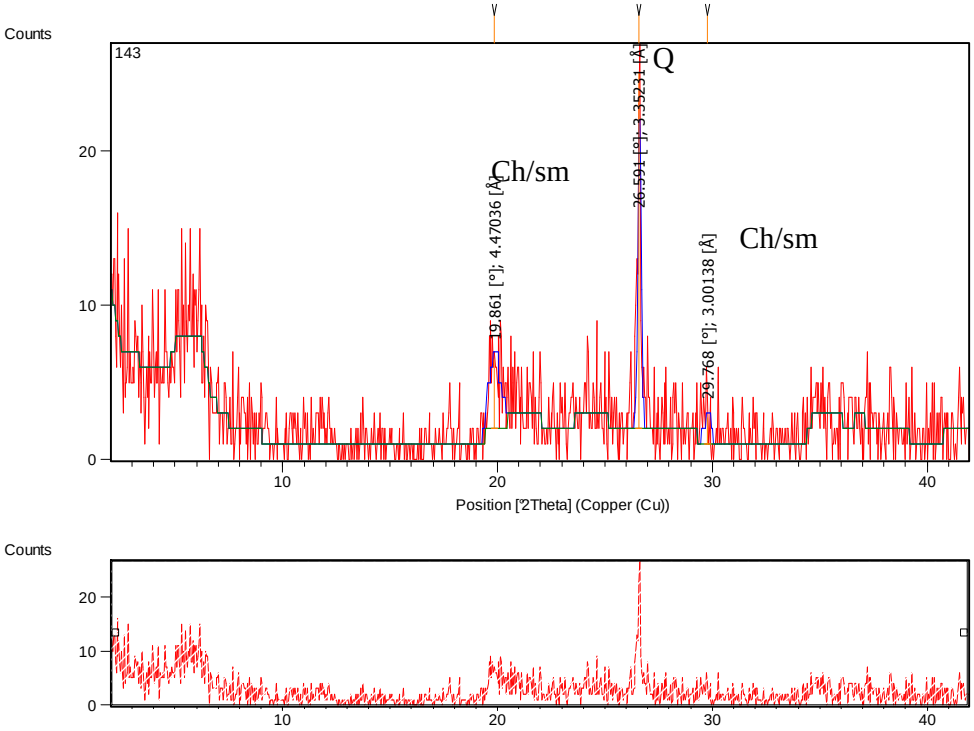

Diffractogram (top) showing XRD results of a sample taken from a limestone cave, Upper Steel, western face, sample 143. It shows peaks of the minerals chlorite/smectite (Ch/sm) (clay), and quartz (Q). The lower chart shows the number of counts for each peak corresponding to the above diffractogram.

Appendix E-5.8 Petrographic data sheets

Petrographic data sheet - McDonald's Lime Quarry 2007			
Sample number		20	
Quarry unit		Caprock	
Analyst		Orla Hansen	
Photomicrographs			
BIOCLASTS	**Total bioclast %**	70	
		%	**Abundance limit**
	Bryozoans	2	some
	Echinoderms	5	some
	Benthic foraminifera	2	some
	Planktic foraminifera	61	abundant
	Bivalves	-	absent
	Pteropods	-	absent
	Gastropods	-	absent
	Calcareous red algae	-	absent
	Barnacles	-	absent
	Porifera	-	absent
	Brachiopods	-	absent
	Corals	-	absent
	Annelids	-	absent
	Other	-	absent
	Modal size 1 (mm)	0.36	
	Modal size 2 (mm)	0.10	
	Grain shape/abrasion	mod abraded	
	Sorting	well	
SILICICLASTS	**Total siliciclast grain %**	30	
		%	**Abundance limit**
	Quartz	-	absent
	Feldspar	-	absent
	Igneous rock fragments	-	absent
	Sedimentary rock fragments	-	absent
	Micas	-	absent
	Pyrite grains	<1	rare
	Pyrite infills	-	absent
	Glauconite pellets	-	absent
	Glauconite infills	-	absent
	Clays	27	very commom
	Modal size 1 (mm)	0.07	
	Modal size 2 (mm)	0.22	
	Grain shape/abrasion	subrounded	
	Sorting	well	
FEATURES	Cements/porosity/fabric	micrite dominated, packed	
	Distribution of Siliciclasts	evenly scattered	
	Oxidation characteristics	oxidised, limonitised	
	Discrete seams - Orientation, thickness (mm), mineralogy, oxidation state	-	
	Diffuse seams - Orientation, pattern, oxidiation state, mineralogy, thickness (mm)	Close to contact with Mahoenui Group, argillaceous	
	Stylolites - Orientation, suture amplitude (mm), mineralogy, oxidation state	-	
	Microstylolites	-	

Petrographic data sheet - McDonald's Lime Quarry 2007			
Sample number		21	
Quarry unit		Caprock	
Analyst		Orla Hansen	
Photomicrographs			
BIOCLASTS	**Total bioclast %**	75	
		%	**Abundance limit**
	Bryozoans	2	some
	Echinoderms	3	some
	Benthic foraminifera	5	some
	Planktic foraminifera	65	abundant
	Bivalves	-	absent
	Pteropods	-	absent
	Gastropods	-	absent
	Calcareous red algae	-	absent
	Barnacles	-	absent
	Porifera	-	absent
	Brachiopods	-	absent
	Corals	-	absent
	Annelids	-	absent
	Other	-	absent
	Modal size 1 (mm)	0.29	
	Modal size 2 (mm)	0.96	
	Grain shape/abrasion	mod abraded	
	Sorting	poorly	
SILICICLASTS	**Total siliciclast grain %**	25	
		%	**Abundance limit**
	Quartz	-	absent
	Feldspar	-	absent
	Igneous rock fragments	-	absent
	Sedimentary rock fragments	-	absent
	Micas	-	absent
	Pyrite grains	<1	rare
	Pyrite infills	<1	rare
	Glauconite pellets	-	absent
	Glauconite infills	-	absent
	Clays	24	common
	Modal size 1 (mm)	0.19	
	Modal size 2 (mm)	0.12	
	Grain shape/abrasion	subrounded	
	Sorting	well	
FEATURES	Cements/porosity/fabric	micrite dom, minor spar, no porosity, open-touching, fractured	
	Distribution of Siliciclasts	scattered, more common within diffuse	
	Oxidation characteristics	oxidised	
	Discrete seams - Orientation, thickness (mm), mineralogy, oxidation state	-	
	Diffuse seams - Orientation, pattern, oxidiation state, mineralogy, thickness (mm)	oxidised, clays, tight fabric	
	Stylolites - Orientation, suture amplitude (mm), mineralogy, oxidation state	-	
	Microstylolites	-	

Petrographic data sheet - McDonald's Lime Quarry 2007			
Sample number		9.1	
Quarry unit		Caprock	
Analyst		Orla Hansen	
Photomicrographs			
BIOCLASTS	**Total bioclast %**	95	
		%	**Abundance limit**
	Bryozoans	75	very abundant
	Echinoderms	10	many
	Benthic foraminifera	3	some
	Planktic foraminifera	5	some
	Bivalves	<1	rare
	Pteropods	-	absent
	Gastropods	-	absent
	Calcareous red algae	-	absent
	Barnacles	-	absent
	Porifera	-	absent
	Brachiopods	-	absent
	Corals	-	absent
	Annelids	-	absent
	Other	-	absent
	Modal size 1 (mm)	1.08	
	Modal size 2 (mm)	0.31	
	Grain shape/abrasion	mod abraded	
	Sorting	well	
SILICICLASTS	**Total siliciclast grain %**	5	
		%	**Abundance limit**
	Quartz	<1	rare
	Feldspar	-	absent
	Igneous rock fragments	-	absent
	Sedimentary rock fragments	-	absent
	Micas	-	absent
	Pyrite grains	-	absent
	Pyrite infills	-	absent
	Glauconite pellets	-	absent
	Glauconite infills	-	absent
	Clays	5	some
	Modal size 1 (mm)	0.29	
	Modal size 2 (mm)	0.14	
	Grain shape/abrasion	subrounded	
	Sorting	poorly	
FEATURES	Cements/porosity/fabric	sparite and micrite, no porosity, open-touching fragments, fractured areas	
	Distribution of Siliciclasts	conc. In stylolites	
	Oxidation characteristics	oxidised, limonitised zooecia	
	Discrete seams - Orientation, thickness (mm), mineralogy, oxidation state	-	
	Diffuse seams - Orientation, pattern, oxidiation state, mineralogy, thickness (mm)	-	
	Stylolites - Orientation, suture amplitude (mm), mineralogy, oxidation state	quartz, vertical	
	Microstylolites	-	

Petrographic data sheet - McDonald's Lime Quarry 2007			
Sample number		9.2	
Quarry unit		Caprock	
Analyst		Orla Hansen	
Photomicrographs			
BIOCLASTS	**Total bioclast %**	89	
		%	**Abundance limit**
	Bryozoans	84	very abundant
	Echinoderms	2*	some
	Benthic foraminifera	<1	rare
	Planktic foraminifera	4	some
	Bivalves	-	absent
	Pteropods	-	absent
	Gastropods	-	absent
	Calcareous red algae	-	absent
	Barnacles	-	absent
	Porifera	-	absent
	Brachiopods	-	absent
	Corals	-	absent
	Annelids	-	absent
	Other	-	absent
	Modal size 1 (mm)	0.72	
	Modal size 2 (mm)	1.30	
	Grain shape/abrasion	mod abraded	
	Sorting	poorly	
SILICICLASTS	**Total siliciclast grain %**	11	
		%	**Abundance limit**
	Quartz	-	absent
	Feldspar	-	absent
	Igneous rock fragments	-	absent
	Sedimentary rock fragments	-	absent
	Micas	-	absent
	Pyrite grains	<1	rare
	Pyrite infills	-	absent
	Glauconite pellets	<1	rare
	Glauconite infills	-	absent
	Clays	10	many
	Modal size 1 (mm)	0.12	
	Modal size 2 (mm)	0.24	
	Grain shape/abrasion	angular	
	Sorting	well	
FEATURES	Cements/porosity/fabric	sparite, micrite, open-touching	
	Distribution of Siliciclasts	scattered	
	Oxidation characteristics	oxidised	
	Discrete seams - Orientation, thickness (mm), mineralogy, oxidation state	-	
	Diffuse seams - Orientation, pattern, oxidiation state, mineralogy, thickness (mm)	? Limonitised over seam, fragmented, fine-grained	
	Stylolites - Orientation, suture amplitude (mm), mineralogy, oxidation state	vertical amp = 1.2 mm	
	Microstylolites	-	

Petrographic data sheet - McDonald's Lime Quarry 2007			
Sample number		23.2	
Quarry unit		Caprock	
Analyst		Orla Hansen	
Photomicrographs			
BIOCLASTS	**Total bioclast %**	90	
		%	**Abundance limit**
	Bryozoans	69	abundant
	Echinoderms	15	common
	Benthic foraminifera	3	some
	Planktic foraminifera	3	some
	Bivalves	-	absent
	Pteropods	-	absent
	Gastropods	-	absent
	Calcareous red algae	-	absent
	Barnacles	-	absent
	Porifera	-	absent
	Brachiopods	-	absent
	Corals	-	absent
	Annelids	-	absent
	Other	-	absent
	Modal size 1 (mm)	0.60	
	Modal size 2 (mm)	0.48	
	Grain shape/abrasion	mod abraded	
	Sorting	poorly	
SILICICLASTS	**Total siliciclast grain %**	10	
		%	**Abundance limit**
	Quartz	-	absent
	Feldspar	-	absent
	Igneous rock fragments	-	absent
	Sedimentary rock fragments	-	absent
	Micas	-	absent
	Pyrite grains	<1	rare
	Pyrite infills	-	absent
	Glauconite pellets	<1	rare
	Glauconite infills	-	absent
	Clays	10	many
	Modal size 1 (mm)	0.26	
	Modal size 2 (mm)	0.19	
	Grain shape/abrasion	angular	
	Sorting	poorly	
FEATURES	Cements/porosity/fabric	no porosity, micrite dom, minor spar, packed	
	Distribution of Siliciclasts	scattered	
	Oxidation characteristics	zooecia limonitised, oxidised	
	Discrete seams - Orientation, thickness (mm), mineralogy, oxidation state	-	
	Diffuse seams - Orientation, pattern, oxidiation state, mineralogy, thickness (mm)	-	
	Stylolites - Orientation, suture amplitude (mm), mineralogy, oxidation state	vertical, amp = 1.7 mm	
	Microstylolites	-	

Petrographic data sheet - McDonald's Lime Quarry 2007			
Sample number		27	
Quarry unit		Caprock	
Analyst		Orla Hansen	
Photomicrographs			
BIOCLASTS	**Total bioclast %**	80	
		%	**Abundance limit**
	Bryozoans	68	abundant
	Echinoderms	5	some
	Benthic foraminifera	2	some
	Planktic foraminifera	5	some
	Bivalves	-	absent
	Pteropods	-	absent
	Gastropods	-	absent
	Calcareous red algae	-	absent
	Barnacles	-	absent
	Porifera	-	absent
	Brachiopods	-	absent
	Corals	-	absent
	Annelids	-	absent
	Other	-	absent
	Modal size 1 (mm)	0.29	
	Modal size 2 (mm)	0.60	
	Grain shape/abrasion	mod abraded	
	Sorting	well	
SILICICLASTS	**Total siliciclast grain %**	20	
			Abundance limit
	Quartz	-	absent
	Feldspar	-	absent
	Igneous rock fragments	-	absent
	Sedimentary rock fragments	-	absent
	Micas	-	absent
	Pyrite grains	<1	rare
	Pyrite infills	-	absent
	Glauconite pellets	<1	rare
	Glauconite infills	-	absent
	Clays 0- clay	19	common
	Modal size 1 (mm)	0.24	
	Modal size 2 (mm)	0.17	
	Grain shape/abrasion	mod abraded	
	Sorting	moderately	
FEATURES	Cements/porosity/fabric	v.muddy, micrite, minor spar, packed	
	Distribution of Siliciclasts	scattered, more common in discrete seam	
	Oxidation characteristics	v.limonitised, oxidised	
	Discrete seams - Orientation, thickness (mm), mineralogy, oxidation state	-	
	Diffuse seams - Orientation, pattern, oxidiation state, mineralogy, thickness (mm)	oxidised clays, argillaceous	
	Stylolites - Orientation, suture amplitude (mm), mineralogy, oxidation state	-	
	Microstylolites	-	

Petrographic data sheet - McDonald's Lime Quarry 2007			
Sample number		10.1	
Quarry unit		Upper Steel	
Analyst		Orla Hansen	
Photomicrographs			
BIOCLASTS	**Total bioclast %**	99	
		%	**Abundance limit**
	Bryozoans	53	abundant
	Echinoderms	45*	very common
	Benthic foraminifera	<1	rare
	Planktic foraminifera	-	absent
	Bivalves	-	absent
	Pteropods	-	absent
	Gastropods	-	absent
	Calcareous red algae	-	absent
	Barnacles	-	absent
	Porifera	-	absent
	Brachiopods	-	absent
	Corals	-	absent
	Annelids	-	absent
	Other	-	absent
	Modal size 1 (mm)	0.84	
	Modal size 2 (mm)	0.36	
	Grain shape/abrasion	mod abraded	
	Sorting	well	
SILICICLASTS	**Total siliciclast grain %**	<1	
		%	**Abundance limit**
	Quartz	-	absent
	Feldspar	-	absent
	Igneous rock fragments	-	absent
	Sedimentary rock fragments	-	absent
	Micas	-	absent
	Pyrite grains	<1	rare
	Pyrite infills	-	absent
	Glauconite pellets	-	absent
	Glauconite infills	-	absent
	Clays	-	absent
	Modal size 1 (mm)	0.19	
	Modal size 2 (mm)	0.14	
	Grain shape/abrasion	angular	
	Sorting	poorly	
FEATURES	Cements/porosity/fabric	slightly porous, spar dom, minor micrite, packed, bioclasts elongated	
	Distribution of Siliciclasts	scattered, or along stylolite	
	Oxidation characteristics	oxidised, minor limonite	
	Discrete seams - Orientation, thickness (mm), mineralogy, oxidation state	-	
	Diffuse seams - Orientation, pattern, oxidiation state, mineralogy, thickness (mm)	-	
	Stylolites - Orientation, suture amplitude (mm), mineralogy, oxidation state	thin vertical stylolite - siliciclasts oxidised	
	Microstylolites	-	

Petrographic data sheet - McDonald's Lime Quarry 2007			
Sample number		10.2	
Quarry unit		Upper Steel	
Analyst		Orla Hansen	
Photomicrographs			
BIOCLASTS	**Total bioclast %**	99	
		%	**Abundance limit**
	Bryozoans	83	very abundant
	Echinoderms	15*	common
	Benthic foraminifera	<1	rare
	Planktic foraminifera	-	absent
	Bivalves	-	absent
	Pteropods	-	absent
	Gastropods	-	absent
	Calcareous red algae	-	absent
	Barnacles	-	absent
	Porifera	-	absent
	Brachiopods	-	absent
	Corals	-	absent
	Annelids	-	absent
	Other	-	absent
	Modal size 1 (mm)	0.48	
	Modal size 2 (mm)	0.72	
	Grain shape/abrasion	mod abraded	
	Sorting	moderately	
SILICICLASTS	**Total siliciclast grain %**	<1	
		%	**Abundance limit**
	Quartz	-	absent
	Feldspar	-	absent
	Igneous rock fragments	-	absent
	Sedimentary rock fragments	-	absent
	Micas	-	absent
	Pyrite grains	<1	rare
	Pyrite infills	-	absent
	Glauconite pellets	<1	rare
	Glauconite infills	-	absent
	Clays	-	absent
	Modal size 1 (mm)	0.19	
	Modal size 2 (mm)	0.14	
	Grain shape/abrasion	subrounded	
	Sorting	poorly	
FEATURES	Cements/porosity/fabric	spar, no porosity, packed bioclasts	
	Distribution of Siliciclasts	scatttered	
	Oxidation characteristics	oxidised	
	Discrete seams - Orientation, thickness (mm), mineralogy, oxidation state	-	
	Diffuse seams - Orientation, pattern, oxidiation state, mineralogy, thickness (mm)	-	
	Stylolites - Orientation, suture amplitude (mm), mineralogy, oxidation state	-	
	Microstylolites	-	

Petrographic data sheet - McDonald's Lime Quarry 2007			
Sample number		10.3	
Quarry unit		Upper Steel	
Analyst		Orla Hansen	
Photomicrographs			
BIOCLASTS	**Total bioclast %**	99	
		%	**Abundance limit**
	Bryozoans	82	very abundant
	Echinoderms	15	common
	Benthic foraminifera	<1	rare
	Planktic foraminifera	-	absent
	Bivalves	<1	rare
	Pteropods	-	absent
	Gastropods	-	absent
	Calcareous red algae	-	absent
	Barnacles	-	absent
	Porifera	-	absent
	Brachiopods	-	absent
	Corals	-	absent
	Annelids	-	absent
	Other	-	absent
	Modal size 1 (mm)	0.48	
	Modal size 2 (mm)	1.20	
	Grain shape/abrasion	mod abraded	
	Sorting	moderately	
SILICICLASTS	**Total siliciclast grain %**	<1	
		%	**Abundance limit**
	Quartz	-	absent
	Feldspar	-	absent
	Igneous rock fragments	-	absent
	Sedimentary rock fragments	-	absent
	Micas	-	absent
	Pyrite grains	<1	rare
	Pyrite infills	-	absent
	Glauconite pellets	-	absent
	Glauconite infills	-	absent
	Clays	-	absent
	Modal size 1 (mm)	0.12	
	Modal size 2 (mm)	0.24	
	Grain shape/abrasion	angular	
	Sorting	poorly	
FEATURES	Cements/porosity/fabric	half porous, half spar, packed stringy squashed bryozoans	
	Distribution of Siliciclasts	scattered	
	Oxidation characteristics	oxidised	
	Discrete seams - Orientation, thickness (mm), mineralogy, oxidation state	small on edge-couple of quartz grains	
	Diffuse seams - Orientation, pattern, oxidiation state, mineralogy, thickness (mm)	-	
	Stylolites - Orientation, suture amplitude (mm), mineralogy, oxidation state	-	
	Microstylolites	-	

Petrographic data sheet - McDonald's Lime Quarry 2007			
Sample number		24.1	
Quarry unit		Upper Steel	
Analyst		Orla Hansen	
Photomicrographs			
BIOCLASTS	**Total bioclast %**	99	
		%	**Abundance limit**
	Bryozoans	87	very abundant
	Echinoderms	7*	many
	Benthic foraminifera	5	some
	Planktic foraminifera	-	absent
	Bivalves	-	absent
	Pteropods	-	absent
	Gastropods	-	absent
	Calcareous red algae	-	absent
	Barnacles	-	absent
	Porifera	-	absent
	Brachiopods	-	absent
	Corals	-	absent
	Annelids	-	absent
	Other	-	absent
	Modal size 1 (mm)	1.32	
	Modal size 2 (mm)	0.72	
	Grain shape/abrasion	mod abraded	
	Sorting	moderately	
SILICICLASTS	**Total siliciclast grain %**	<1	
		%	**Abundance limit**
	Quartz	-	absent
	Feldspar	-	absent
	Igneous rock fragments	-	absent
	Sedimentary rock fragments	-	absent
	Micas	-	absent
	Pyrite grains	<1	rare
	Pyrite infills	-	absent
	Glauconite pellets	<1	rare
	Glauconite infills	-	absent
	Clays	-	absent
	Modal size 1 (mm)	0.12	
	Modal size 2 (mm)	0.26	
	Grain shape/abrasion	subrounded	
	Sorting	poorly	
FEATURES	Cements/porosity/fabric	sparite, no porosity, open fabric	
	Distribution of Siliciclasts	scattered, one small cluster	
	Oxidation characteristics	oxidised	
	Discrete seams - Orientation, thickness (mm), mineralogy, oxidation state	-	
	Diffuse seams - Orientation, pattern, oxidiation state, mineralogy, thickness (mm)	-	
	Stylolites - Orientation, suture amplitude (mm), mineralogy, oxidation state	-	
	Microstylolites	-	

Petrographic data sheet - McDonald's Lime Quarry 2007			
Sample number		24.2	
Quarry unit		Upper Steel	
Analyst		Orla Hansen	
Photomicrographs			
BIOCLASTS	**Total bioclast %**	99	
		%	**Abundance limit**
	Bryozoans	75	very abundant
	Echinoderms	19	common
	Benthic foraminifera	3	some
	Planktic foraminifera	2	some
	Bivalves	-	absent
	Pteropods	-	absent
	Gastropods	-	absent
	Calcareous red algae	-	absent
	Barnacles	-	absent
	Porifera	-	absent
	Brachiopods	-	absent
	Corals	-	absent
	Annelids	-	absent
	Other	-	absent
	Modal size 1 (mm)	1.08	
	Modal size 2 (mm)	3.60	
	Grain shape/abrasion	mod abraded	
	Sorting	poorly	
SILICICLASTS	**Total siliciclast grain %**	<1	
		%	**Abundance limit**
	Quartz	-	absent
	Feldspar	-	absent
	Igneous rock fragments	-	absent
	Sedimentary rock fragments	-	absent
	Micas	-	absent
	Pyrite grains	<1	rare
	Pyrite infills	<1	rare
	Glauconite pellets	-	absent
	Glauconite infills	-	absent
	Clays	-	absent
	Modal size 1 (mm)	0.24	
	Modal size 2 (mm)	0.34	
	Grain shape/abrasion	subrounded	
	Sorting	poorly	
FEATURES	Cements/porosity/fabric	edge porous (open), sparite exclusive	
	Distribution of Siliciclasts	scattered	
	Oxidation characteristics	oxidised	
	Discrete seams - Orientation, thickness (mm), mineralogy, oxidation state	-	
	Diffuse seams - Orientation, pattern, oxidiation state, mineralogy, thickness (mm)	-	
	Stylolites - Orientation, suture amplitude (mm), mineralogy, oxidation state	-	
	Microstylolites	-	

Petrographic data sheet - McDonald's Lime Quarry 2007			
Sample number		24.3	
Quarry unit		Upper Steel	
Analyst		Orla Hansen	
Photomicrographs			
BIOCLASTS	**Total bioclast %**	99	
		%	**Abundance limit**
	Bryozoans	82	very abundant
	Echinoderms	15*	common
	Benthic foraminifera	2	some
	Planktic foraminifera	-	absent
	Bivalves	-	absent
	Pteropods	-	absent
	Gastropods	-	absent
	Calcareous red algae	-	absent
	Barnacles	-	absent
	Porifera	-	absent
	Brachiopods	-	absent
	Corals	-	absent
	Annelids	-	absent
	Other	-	absent
	Modal size 1 (mm)	1.68	
	Modal size 2 (mm)	0.72	
	Grain shape/abrasion	rounded	
	Sorting	poorly	
SILICICLASTS	**Total siliciclast grain %**	<1	
		%	**Abundance limit**
	Quartz	-	absent
	Feldspar (plagioclase)	<1	rare
	Igneous rock fragments	-	absent
	Sedimentary rock fragments	-	absent
	Micas	-	absent
	Pyrite grains	<1	rare
	Pyrite infills	-	absent
	Glauconite pellets	-	absent
	Glauconite infills	-	absent
	Clays	-	absent
	Modal size 1 (mm)	0.34	
	Modal size 2 (mm)	0.24	
	Grain shape/abrasion	angular	
	Sorting	poorly	
FEATURES	Cements/porosity/fabric	porous on one half, sparite Clays tight	
	Distribution of Siliciclasts	scattered	
	Oxidation characteristics	oxidised, limonitised pyrite/glau.	
	Discrete seams - Orientation, thickness (mm), mineralogy, oxidation state	-	
	Diffuse seams - Orientation, pattern, oxidiation state, mineralogy, thickness (mm)	-	
	Stylolites - Orientation, suture amplitude (mm), mineralogy, oxidation state	-	
	Microstylolites	-	

Petrographic data sheet - McDonald's Lime Quarry 2007			
Sample number		25	
Quarry unit		Upper Steel	
Analyst		Orla Hansen	
Photomicrographs			
BIOCLASTS	**Total bioclast %**	98	
		%	**Abundance limit**
	Bryozoans	91	very abundant
	Echinoderms	5*	some
	Benthic foraminifera	-	absent
	Planktic foraminifera	<1	rare
	Bivalves	<1	rare
	Pteropods	-	absent
	Gastropods	-	absent
	Calcareous red algae	-	absent
	Barnacles	-	absent
	Porifera	-	absent
	Brachiopods	-	absent
	Corals	-	absent
	Annelids	-	absent
	Other	-	absent
	Modal size 1 (mm)	1.20	
	Modal size 2 (mm)	0.96	
	Grain shape/abrasion	mod abraded	
	Sorting	moderately	
SILICICLASTS	**Total siliciclast grain %**	2	
		%	**Abundance limit**
	Quartz	-	absent
	Feldspar	-	absent
	Igneous rock fragments	-	absent
	Sedimentary rock fragments	-	absent
	Micas	-	absent
	Pyrite grains	<1	rare
	Pyrite infills	<1	rare
	Glauconite pellets	-	absent
	Glauconite infills	<1	rare
	Clays	-	absent
	Modal size 1 (mm)	0.36	
	Modal size 2 (mm)	0.24	
	Grain shape/abrasion	subrounded	
	Sorting	poorly	
FEATURES	Cements/porosity/fabric	sparite, no porosity, open-touching, fragmented in places	
	Distribution of Siliciclasts	clusters/conc. In stylolites/scattered	
	Oxidation characteristics	limonitised grains and chambers, edges of bioclasts, oxidised	
	Discrete seams - Orientation, thickness (mm), mineralogy, oxidation state	-	
	Diffuse seams - Orientation, pattern, oxidiation state, mineralogy, thickness (mm)	-	
	Stylolites - Orientation, suture amplitude (mm), mineralogy, oxidation state	hori. Oxidised, thinner stylolites branching off main stylolite - limonitised, amp = 1.7 mm	
	Microstylolites	-	

Petrographic data sheet - McDonald's Lime Quarry 2007			
Sample number		30	
Quarry unit		Upper Steel	
Analyst		Orla Hansen	
Photomicrographs			
BIOCLASTS	**Total bioclast %**	98	
		%	**Abundance limit**
	Bryozoans	93	very abundant
	Echinoderms	5*	some
	Benthic foraminifera	<1	rare
	Planktic foraminifera	-	absent
	Bivalves	-	absent
	Pteropods	-	absent
	Gastropods	-	absent
	Calcareous red algae	-	absent
	Barnacles	-	absent
	Porifera	-	absent
	Brachiopods	-	absent
	Corals	-	absent
	Annelids	-	absent
	Other	-	absent
	Modal size 1 (mm)	0.72	
	Modal size 2 (mm)	2.52	
	Grain shape/abrasion	mod abraded	
	Sorting	poorly	
SILICICLASTS	**Total siliciclast grain %**	2	
		%	**Abundance limit**
	Quartz	-	absent
	Feldspar	-	absent
	Igneous rock fragments	-	absent
	Sedimentary rock fragments	-	absent
	Micas	-	absent
	Pyrite grains	<1	rare
	Pyrite infills	<1	rare
	Glauconite pellets	-	absent
	Glauconite infills	-	absent
	Clays	-	absent
	Modal size 1 (mm)	0.36	
	Modal size 2 (mm)		
	Grain shape/abrasion		
	Sorting		
FEATURES	Cements/porosity/fabric	sparite, no porosity, tight	
	Distribution of Siliciclasts	few scattered grains and concentrated in stylolites	
	Oxidation characteristics	oxidised	
	Discrete seams - Orientation, thickness (mm), mineralogy, oxidation state	-	
	Diffuse seams - Orientation, pattern, oxidiation state, mineralogy, thickness (mm)	-	
	Stylolites - Orientation, suture amplitude (mm), mineralogy, oxidation state	three horizontal stylolites, oxidised, avg amp 0.72 mm, clay dominant, very minor quartz	
	Microstylolites	-	

Petrographic data sheet - McDonald's Lime Quarry 2007			
Sample number		32	
Quarry unit		Aglime	
Analyst		Orla Hansen	
Photomicrographs			
BIOCLASTS	**Total bioclast %**	98	
		%	**Abundance limit**
	Bryozoans	87	very abundant
	Echinoderms	<1	rare
	Benthic foraminifera	<1	rare
	Planktic foraminifera	-	absent
	Bivalves	<1	rare
	Pteropods	-	absent
	Gastropods	-	absent
	Calcareous red algae	-	absent
	Barnacles	-	absent
	Porifera	-	absent
	Brachiopods	-	absent
	Corals	-	absent
	Annelids	-	absent
	Other	-	absent
	Modal size 1 (mm)	1.20	
	Modal size 2 (mm)	0.36	
	Grain shape/abrasion	slightly abraded	
	Sorting	poorly	
SILICICLASTS	**Total siliciclast grain %**	2, 70% in seam	
		%	**Abundance limit**
	Quartz	-	absent
	Feldspar	-	absent
	Igneous rock fragments	-	absent
	Sedimentary rock fragments	-	absent
	Micas	-	absent
	Pyrite grains	<1	rare
	Pyrite infills	-	absent
	Glauconite pellets	2	some
	Glauconite infills	<1	rare
	Clays	-	absent
	Modal size 1 (mm)	0.10	
	Modal size 2 (mm)	0.19	
	Grain shape/abrasion	subrounded	
	Sorting	poorly	
FEATURES	Cements/porosity/fabric	micrite in equal amounts to sparite, no porosity, fragmented, packed	
	Distribution of Siliciclasts	scattered or concentrated in seam	
	Oxidation characteristics	oxidised	
	Discrete seams - Orientation, thickness (mm), mineralogy, oxidation state	oxidised, 5 mm thick, 1 mm seam branching off, limonite everywhere, quartz & feldspar dominant, glauconite,	
	Diffuse seams - Orientation, pattern, oxidiation state, mineralogy, thickness (mm)	-	
	Stylolites - Orientation, suture amplitude (mm), mineralogy, oxidation state	-	
	Microstylolites	yes-bryozoans	

Petrographic data sheet - McDonald's Lime Quarry 2007			
Sample number		34	
Quarry unit		Aglime	
Analyst		Orla Hansen	
Photomicrographs			
BIOCLASTS	**Total bioclast %**	98	
		%	**Abundance limit**
	Bryozoans	95	very abundant
	Echinoderms	<1	rare
	Benthic foraminifera	-	absent
	Planktic foraminifera	<1	rare
	Bivalves	<1	rare
	Pteropods	-	absent
	Gastropods	-	absent
	Calcareous red algae	-	absent
	Barnacles	-	absent
	Porifera	-	absent
	Brachiopods	-	absent
	Corals	-	absent
	Annelids	-	absent
	Other	-	absent
	Modal size 1 (mm)	1.20	
	Modal size 2 (mm)	0.55	
	Grain shape/abrasion	slightly abraded	
	Sorting	poorly	
SILICICLASTS	**Total siliciclast grain %**	2	
		%	**Abundance limit**
	Quartz	-	absent
	Feldspar	-	absent
	Igneous rock fragments	-	absent
	Sedimentary rock fragments	-	absent
	Micas	-	absent
	Pyrite grains	1	some
	Pyrite infills	<1	rare
	Glauconite pellets	<1	rare
	Glauconite infills	<1	rare
	Clays	-	absent
	Modal size 1 (mm)	0.24	
	Modal size 2 (mm)	0.10	
	Grain shape/abrasion	angular	
	Sorting	poorly	
FEATURES	Cements/porosity/fabric	minor sparite, major micrite filling zooecia, no porosity, tightly packed, fractured	
	Distribution of Siliciclasts	scattered	
	Oxidation characteristics	unoxidised	
	Discrete seams - Orientation, thickness (mm), mineralogy, oxidation state	-	
	Diffuse seams - Orientation, pattern, oxidiation state, mineralogy, thickness (mm)	-	
	Stylolites - Orientation, suture amplitude (mm), mineralogy, oxidation state	-	
	Microstylolites	-	

Petrographic data sheet - McDonald's Lime Quarry 2007			
Sample number		35	
Quarry unit		Aglime	
Analyst		Orla Hansen	
Photomicrographs			
BIOCLASTS	**Total bioclast %**	99	
		%	**Abundance limit**
	Bryozoans	96	vey abundant
	Echinoderms	<1*	rare
	Benthic foraminifera	-	absent
	Planktic foraminifera	<1	rare
	Bivalves	<1	rare
	Pteropods	-	absent
	Gastropods	-	absent
	Calcareous red algae	-	absent
	Barnacles	-	absent
	Porifera	-	absent
	Brachiopods	-	absent
	Corals	-	absent
	Annelids	-	absent
	Other	-	absent
	Modal size 1 (mm)	1.68	
	Modal size 2 (mm)	0.60	
	Grain shape/abrasion	slightly abraded	
	Sorting	poorly	
SILICICLASTS	**Total siliciclast grain %**	1, 40% in seam	
		%	**Abundance limit**
	Quartz	-	absent
	Feldspar	-	absent
	Igneous rock fragments	-	absent
	Sedimentary rock fragments	-	absent
	Micas	-	absent
	Pyrite grains	<1	rare
	Pyrite infills	<1	rare
	Glauconite pellets	<1	rare
	Glauconite infills	-	absent
	Clays	-	absent
	Modal size 1 (mm)	0.05	
	Modal size 2 (mm)	0.19	
	Grain shape/abrasion	subrounded	
	Sorting	poorly	
FEATURES	Cements/porosity/fabric	Sparite and micrite, no porosity, packed	
	Distribution of Siliciclasts	scattered or concentrated in seam	
	Oxidation characteristics	oxidised, limonitised zooecia	
	Discrete seams - Orientation, thickness (mm), mineralogy, oxidation state	4 mm thick, 2 mm thick, glauconite, clay dominant, minor quartz & feldspar, minor pyrite	
	Diffuse seams - Orientation, pattern, oxidiation state, mineralogy, thickness (mm)	-	
	Stylolites - Orientation, suture amplitude (mm), mineralogy, oxidation state	-	
	Microstylolites	-	

Petrographic data sheet - McDonald's Lime Quarry 2007			
Sample number		11	
Quarry unit		Aglime	
Analyst		Orla Hansen	
Photomicrographs			
BIOCLASTS	**Total bioclast %**	90	
		%	**Abundance limit**
	Bryozoans	86	very abundant
	Echinoderms	<1	rare
	Benthic foraminifera	<1	rare
	Planktic foraminifera	<1	rare
	Bivalves	<1	rare
	Pteropods	-	absent
	Gastropods	-	absent
	Calcareous red algae	-	absent
	Barnacles	-	absent
	Porifera	-	absent
	Brachiopods	-	absent
	Corals	-	absent
	Annelids	-	absent
	Other	-	absent
	Modal size 1 (mm)	1.56	
	Modal size 2 (mm)	0.84	
	Grain shape/abrasion	mod abraded	
	Sorting	poorly	
SILICICLASTS	**Total siliciclast grain %**	2, 60% in seam	
		%	**Abundance limit**
	Quartz	-	absent
	Feldspar	-	absent
	Igneous rock fragments	-	absent
	Sedimentary rock fragments	-	absent
	Micas	-	absent
	Pyrite grains	<1	rare
	Pyrite infills	-	absent
	Glauconite pellets	-	absent
	Glauconite infills	-	absent
	Clays	-	absent
	Modal size 1 (mm)	0.48	
	Modal size 2 (mm)	0.12	
	Grain shape/abrasion	subrounded	
	Sorting	poorly	
FEATURES	Cements/porosity/fabric	sparite, no porosity, minor micrite,	
	Distribution of Siliciclasts	scattered, or conc. In seam	
	Oxidation characteristics	oxidised, rare limonitised pyrite, zooecia limonitised	
	Discrete seams - Orientation, thickness (mm), mineralogy, oxidation state	little seam 1-2 mm thick, quartz - big round crystals .45 mm long, clay, limonite, glauconite	
	Diffuse seams - Orientation, pattern, oxidiation state, mineralogy, thickness (mm)	wispy limonitised bits, quartz in them	
	Stylolites - Orientation, suture amplitude (mm), mineralogy, oxidation state	-	
	Microstylolites	-	

Petrographic data sheet - McDonald's Lime Quarry 2007			
Sample number		12.1	
Quarry unit		Aglime	
Analyst		Orla Hansen	
Photomicrographs			
BIOCLASTS	**Total bioclast %**	95	
		%	**Abundance limit**
	Bryozoans	91	very abundant
	Echinoderms	<1	rare
	Benthic foraminifera	1	some
	Planktic foraminifera	-	absent
	Bivalves	2	some
	Pteropods	-	absent
	Gastropods	-	absent
	Calcareous red algae	-	absent
	Barnacles	-	absent
	Porifera	-	absent
	Brachiopods	-	absent
	Corals	-	absent
	Annelids	-	absent
	Other	-	absent
	Modal size 1 (mm)	0.38	
	Modal size 2 (mm)	1.68	
	Grain shape/abrasion	mod abraded	
	Sorting	poorly	
SILICICLASTS	**Total siliciclast grain %**	host 2-5, 7% in seam	
		%	**Abundance limit**
	Quartz	-	absent
	Feldspar	-	absent
	Igneous rock fragments	-	absent
	Sedimentary rock fragments	-	absent
	Micas	-	absent
	Pyrite grains	2	some
	Pyrite infills	<1	rare
	Glauconite pellets	-	absent
	Glauconite infills	<1	rare
	Clays	-	absent
	Modal size 1 (mm)	0.19	
	Modal size 2 (mm)	0.07	
	Grain shape/abrasion	subrounded	
	Sorting	poorly	
FEATURES	Cements/porosity/fabric	minor spar, micrite dom, no porosity, tight,fragmented	
	Distribution of Siliciclasts	on wispy seams and concentrated in discrete seams, Clayswise scattered in host	
	Oxidation characteristics	lots of limonite, oxidised	
	Discrete seams - Orientation, thickness (mm), mineralogy, oxidation state	thin seams, quartz and limonite concentrated in seams	
	Diffuse seams - Orientation, pattern, oxidiation state, mineralogy, thickness (mm)	-	
	Stylolites - Orientation, suture amplitude (mm), mineralogy, oxidation state	-	
	Microstylolites	-	

Petrographic data sheet - McDonald's Lime Quarry 2007			
Sample number		12.2	
Quarry unit		Aglime	
Analyst		Orla Hansen	
Photomicrographs			
BIOCLASTS	**Total bioclast %**	98	
		%	**Abundance limit**
	Bryozoans	96	very abundant
	Echinoderms	<1	rare
	Benthic foraminifera	<1	rare
	Planktic foraminifera	<1	rare
	Bivalves	<1	rare
	Pteropods	-	absent
	Gastropods	-	absent
	Calcareous red algae	-	absent
	Barnacles	-	absent
	Porifera	-	absent
	Brachiopods	-	absent
	Corals	-	absent
	Annelids	-	absent
	Other	-	absent
	Modal size 1 (mm)	0.96	
	Modal size 2 (mm)	0.72	
	Grain shape/abrasion	slightly abraded	
	Sorting	poorly	
SILICICLASTS	**Total siliciclast grain %**	2, 40% in seam	
		%	**Abundance limit**
	Quartz	-	absent
	Feldspar	-	absent
	Igneous rock fragments	-	absent
	Sedimentary rock fragments	-	absent
	Micas	-	absent
	Pyrite grains	<1	rare
	Pyrite infills	-	absent
	Glauconite pellets	<1	rare
	Glauconite infills	<1	rare
	Clays	-	absent
	Modal size 1 (mm)	0.10	
	Modal size 2 (mm)	0.19	
	Grain shape/abrasion	angular	
	Sorting	poorly	
FEATURES	Cements/porosity/fabric	minor spar, micrite dominated, no porosity, v.packed and fragmented	
	Distribution of Siliciclasts	scattered, or concentrated in seam	
	Oxidation characteristics	unoxidised	
	Discrete seams - Orientation, thickness (mm), mineralogy, oxidation state	4 mm and 1 mm thick, unoxidised, pyrite grains, glauconite, quartz & feldspars	
	Diffuse seams - Orientation, pattern, oxidiation state, mineralogy, thickness (mm)	-	
	Stylolites - Orientation, suture amplitude (mm), mineralogy, oxidation state	glauconite in hori. Stylolite	
	Microstylolites	-	

Petrographic data sheet - McDonald's Lime Quarry 2007			
Sample number		12.3	
Quarry unit		Aglime	
Analyst		Orla Hansen	
Photomicrographs			
BIOCLASTS	**Total bioclast %**	98	
		%	**Abundance limit**
	Bryozoans	95	very abundant
	Echinoderms	1	some
	Benthic foraminifera	1	some
	Planktic foraminifera	-	absent
	Bivalves	-	absent
	Pteropods	-	absent
	Gastropods	-	absent
	Calcareous red algae	-	absent
	Barnacles	-	absent
	Porifera	-	absent
	Brachiopods	-	absent
	Corals	-	absent
	Annelids	1	some
	Other	-	absent
	Modal size 1 (mm)	4.96	
	Modal size 2 (mm)	1.68	
	Grain shape/abrasion	slightly abraded	
	Sorting	poorly	
SILICICLASTS	**Total siliciclast grain %**	2	
		%	**Abundance limit**
	Quartz	-	absent
	Feldspar	-	absent
	Igneous rock fragments	-	absent
	Sedimentary rock fragments	-	absent
	Micas	-	absent
	Pyrite grains	<1	rare
	Pyrite infills	<1	rare
	Glauconite pellets	<1	rare
	Glauconite infills	<1	rare
	Clays	-	absent
	Modal size 1 (mm)	0.05	
	Modal size 2 (mm)	0.17	
	Grain shape/abrasion	angular	
	Sorting	poorly	
FEATURES	Cements/porosity/fabric	minor sparite, micrite, no porosity, packed bioclasts	
	Distribution of Siliciclasts	scattered small ones	
	Oxidation characteristics	oxidised, limonitised zooecia	
	Discrete seams - Orientation, thickness (mm), mineralogy, oxidation state	-	
	Diffuse seams - Orientation, pattern, oxidiation state, mineralogy, thickness (mm)	-	
	Stylolites - Orientation, suture amplitude (mm), mineralogy, oxidation state	-	
	Microstylolites	-	

Petrographic data sheet - McDonald's Lime Quarry 2007			
Sample number		13.1	
Quarry unit		Aglime	
Analyst		Orla Hansen	
Photomicrographs			
BIOCLASTS	**Total bioclast %**	60?	
		%	**Abundance limit**
	Bryozoans	58	abundant
	Echinoderms	<1	rare
	Benthic foraminifera	<1	rare
	Planktic foraminifera	-	absent
	Bivalves	-	absent
	Pteropods	-	absent
	Gastropods	-	absent
	Calcareous red algae	-	absent
	Barnacles	-	absent
	Porifera	-	absent
	Brachiopods	-	absent
	Corals	-	absent
	Annelids	<1	rare
	Other	-	absent
	Modal size 1 (mm)	1.92	
	Modal size 2 (mm)	0.43	
	Grain shape/abrasion	slightly abraded	
	Sorting	poorly	
SILICICLASTS	**Total siliciclast grain %**	30 (whole slide diffuse seam)	
		%	**Abundance limit**
	Quartz	-	absent
	Feldspar	-	absent
	Igneous rock fragments	-	absent
	Sedimentary rock fragments	-	absent
	Micas	-	absent
	Pyrite grains	2	some
	Pyrite infills	-	absent
	Glauconite pellets	<1	rare
	Glauconite infills	-	absent
	Clays - clays	38	very common
	Modal size 1 (mm)	0.19	
	Modal size 2 (mm)	0.07	
	Grain shape/abrasion	angular	
	Sorting	well	
FEATURES	Cements/porosity/fabric	micrite dominated, no porosity, minor sparite, v.tightly packed	
	Distribution of Siliciclasts	scattered, clay concentrated in diffuseness	
	Oxidation characteristics	oxidised, v.limonitised	
	Discrete seams - Orientation, thickness (mm), mineralogy, oxidation state	-	
	Diffuse seams - Orientation, pattern, oxidiation state, mineralogy, thickness (mm)	clay dominant, limonite, minor quartz & feldspar	
	Stylolites - Orientation, suture amplitude (mm), mineralogy, oxidation state	-	
	Microstylolites	-	

Petrographic data sheet - McDonald's Lime Quarry 2007			
Sample number		13.2	
Quarry unit		Aglime	
Analyst		Orla Hansen	
Photomicrographs			
BIOCLASTS	**Total bioclast %**	80	
		%	**Abundance limit**
	Bryozoans	75	very abundant
	Echinoderms	<1	rare
	Benthic foraminifera	<1	rare
	Planktic foraminifera	<1	rare
	Bivalves	<1	rare
	Pteropods	-	absent
	Gastropods	-	absent
	Calcareous red algae	-	absent
	Barnacles	-	absent
	Porifera	-	absent
	Brachiopods	-	absent
	Corals	-	absent
	Annelids	<1	rare
	Other	-	absent
	Modal size 1 (mm)	1.08	
	Modal size 2 (mm)	0.48	
	Grain shape/abrasion	slightly abraded	
	Sorting	poorly	
SILICICLASTS	**Total siliciclast grain %**	40 (whole slide diffuse seam)	
		%	**Abundance limit**
	Quartz	-	absent
	Feldspar	-	absent
	Igneous rock fragments	-	absent
	Sedimentary rock fragments	-	absent
	Micas	-	absent
	Pyrite grains	<1	rare
	Pyrite infills	-	absent
	Glauconite pellets	<1	rare
	Glauconite infills	-	absent
	Clays	-	absent
	Modal size 1 (mm)	0.17	
	Modal size 2 (mm)	0.12	
	Grain shape/abrasion	angular	
	Sorting	poorly	
FEATURES	Cements/porosity/fabric	no porosity, tightly packed fragments, v.fragmented	
	Distribution of Siliciclasts	scattered, mostly concentrated in diffuse seams	
	Oxidation characteristics	oxidised, v.limonitised	
	Discrete seams - Orientation, thickness (mm), mineralogy, oxidation state	-	
	Diffuse seams - Orientation, pattern, oxidiation state, mineralogy, thickness (mm)	limonite, clay, quartz & feldspar, glauconite	
	Stylolites - Orientation, suture amplitude (mm), mineralogy, oxidation state	-	
	Microstylolites	-	

Petrographic data sheet - McDonald's Lime Quarry 2007			
Sample number		13.3	
Quarry unit		Aglime	
Analyst		Orla Hansen	
Photomicrographs			
BIOCLASTS	**Total bioclast %**	95	
		%	**Abundance limit**
	Bryozoans	91	very abundant
	Echinoderms	<1	rare
	Benthic foraminifera	<1	rare
	Planktic foraminifera	<1	rare
	Bivalves	-	absent
	Pteropods	-	absent
	Gastropods	-	absent
	Calcareous red algae	-	absent
	Barnacles	-	absent
	Porifera	-	absent
	Brachiopods	-	absent
	Corals	-	absent
	Annelids	<1	rare
	Other	-	absent
	Modal size 1 (mm)	0.48	
	Modal size 2 (mm)	1.56	
	Grain shape/abrasion	slightly abraded	
	Sorting	poorly	
SILICICLASTS	**Total siliciclast grain %**	5, 60% in seam	
		%	**Abundance limit**
	Quartz	-	absent
	Feldspar	-	absent
	Igneous rock fragments	-	absent
	Sedimentary rock fragments	-	absent
	Micas	-	absent
	Pyrite grains	<1	rare
	Pyrite infills	-	absent
	Glauconite pellets	2	some
	Glauconite infills	<1	rare
	Clays	-	absent
	Modal size 1 (mm)	0.12	
	Modal size 2 (mm)	0.07	
	Grain shape/abrasion	subrounded	
	Sorting	poorly	
FEATURES	Cements/porosity/fabric	micrite dominated, no porosity,	
	Distribution of Siliciclasts	scattered and concentrated along seams and wisps	
	Oxidation characteristics	v.limonitised	
	Discrete seams - Orientation, thickness (mm), mineralogy, oxidation state	-	
	Diffuse seams - Orientation, pattern, oxidiation state, mineralogy, thickness (mm)	meandering wispy seams, quartz & feldspar, clay, limonite	
	Stylolites - Orientation, suture amplitude (mm), mineralogy, oxidation state	-	
	Microstylolites	-	

Petrographic data sheet - McDonald's Lime Quarry 2007			
Sample number		38	
Quarry unit		High Grade	
Analyst		Orla Hansen	
Photomicrographs			
BIOCLASTS	**Total bioclast %**	95	
		%	**Abundance limit**
	Bryozoans	91	very abundant
	Echinoderms	<1	rare
	Benthic foraminifera	<1	rare
	Planktic foraminifera	<1	rare
	Bivalves	<1	rare
	Pteropods	-	absent
	Gastropods	-	absent
	Calcareous red algae	-	absent
	Barnacles	-	absent
	Porifera	-	absent
	Brachiopods	-	absent
	Corals	-	absent
	Annelids	-	absent
	Other	-	absent
	Modal size 1 (mm)	1.44	
	Modal size 2 (mm)	1.68	
	Grain shape/abrasion	mod abraded	
	Sorting	moderately	
SILICICLASTS	**Total siliciclast grain %**	5	
		%	**Abundance limit**
	Quartz	-	absent
	Feldspar	-	absent
	Igneous rock fragments	-	absent
	Sedimentary rock fragments	-	absent
	Micas	-	absent
	Pyrite grains	4	some
	Pyrite infills	<1	rare
	Glauconite pellets	<1	rare
	Glauconite infills	-	absent
	Clays	-	absent
	Modal size 1 (mm)	0.14	
	Modal size 2 (mm)	0.24	
	Grain shape/abrasion	subrounded	
	Sorting	poorly	
FEATURES	Cements/porosity/fabric	sparite, no porosity, micrite?, calcite veins, fractured	
	Distribution of Siliciclasts	scattered	
	Oxidation characteristics	oxidised	
	Discrete seams - Orientation, thickness (mm), mineralogy, oxidation state	-	
	Diffuse seams - Orientation, pattern, oxidiation state, mineralogy, thickness (mm)	-	
	Stylolites - Orientation, suture amplitude (mm), mineralogy, oxidation state	wispy thin, round quartz along it, horizontal, oxidised	
	Microstylolites	-	

Petrographic data sheet - McDonald's Lime Quarry 2007			
Sample number		14	
Quarry unit		High Grade	
Analyst		Orla Hansen	
Photomicrographs			
BIOCLASTS	**Total bioclast %**	95	
		%	**Abundance limit**
	Bryozoans	93	very abundant
	Echinoderms	<1	rare
	Benthic foraminifera	<1	rare
	Planktic foraminifera	<1	rare
	Bivalves	-	absent
	Pteropods	-	absent
	Gastropods	-	absent
	Calcareous red algae	-	absent
	Barnacles	-	absent
	Porifera	-	absent
	Brachiopods	-	absent
	Corals	-	absent
	Annelids	-	absent
	Other	-	absent
	Modal size 1 (mm)	1.68	
	Modal size 2 (mm)	0.72	
	Grain shape/abrasion	slightly abraded	
	Sorting	poorly	
SILICICLASTS	**Total siliciclast grain %**	5	
		%	**Abundance limit**
	Quartz		
	Feldspar	2	some
	Igneous rock fragments	-	absent
	Sedimentary rock fragments	-	absent
	Micas	-	absent
	Pyrite grains	3	some
	Pyrite infills	2	some
	Glauconite pellets	<1	rare
	Glauconite infills	<1	rare
	Clays	-	absent
	Modal size 1 (mm)	0.17	
	Modal size 2 (mm)	0.10	
	Grain shape/abrasion	subrounded	
	Sorting	poorly	
FEATURES	Cements/porosity/fabric	sparite, no porosity, packed fragments	
	Distribution of Siliciclasts	scattered	
	Oxidation characteristics	unoxidised	
	Discrete seams - Orientation, thickness (mm), mineralogy, oxidation state	-	
	Diffuse seams - Orientation, pattern, oxidiation state, mineralogy, thickness (mm)	-	
	Stylolites - Orientation, suture amplitude (mm), mineralogy, oxidation state	-	
	Microstylolites	-	

Petrographic data sheet - McDonald's Lime Quarry 2007			
Sample number		40	
Quarry unit		High Grade	
Analyst		Orla Hansen	
Photomicrographs			
BIOCLASTS	**Total bioclast %**	**96**	
		%	**Abundance limit**
	Bryozoans	93	very abundant
	Echinoderms	<1	rare
	Benthic foraminifera	<1	rare
	Planktic foraminifera	<1	rare
	Bivalves	<1	rare
	Pteropods	-	absent
	Gastropods	-	absent
	Calcareous red algae	-	absent
	Barnacles	-	absent
	Porifera	-	absent
	Brachiopods	-	absent
	Corals	-	absent
	Annelids	-	absent
	Clays	-	absent
	Modal size 1 (mm)	1.32	
	Modal size 2 (mm)	0.72	
	Grain shape/abrasion	mod abraded	
	Sorting	poorly	
SILICICLASTS	**Total siliciclast grain %**	4, 80% in seam	
		%	**Abundance limit**
	Quartz	-	absent
	Feldspar	-	absent
	Igneous rock fragments	-	absent
	Sedimentary rock fragments	-	absent
	Micas	-	absent
	Pyrite grains	3	some
	Pyrite infills	<1	rare
	Glauconite pellets	<1	rare
	Glauconite infills	-	absent
	Clays	-	absent
	Modal size 1 (mm)	0.14	
	Modal size 2 (mm)	0.10	
	Grain shape/abrasion	angular	
	Sorting	poorly	
FEATURES	Cements/porosity/fabric	sparite, no porosity, fractured	
	Distribution of siliciclastics	scattered or concentrated along seam	
	Oxidation characteristics	unoxidised	
	Discrete seams - Orientation, thickness (mm), mineralogy, oxidation state	2 mm thick, diagonal, unoxidised, clay & pyrite, quartz & feldspar	
	Diffuse seams - Orientation, pattern, oxidiation state, mineralogy, thickness (mm)	-	
	Stylolites - Orientation, suture amplitude (mm), mineralogy, oxidation state	horizontal stylolite, pyrite dominated, clay, minor quartz & feldspar	
	Microstylolites	-	

Petrographic data sheet - McDonald's Lime Quarry 2007			
Sample number		40.2	
Quarry unit		High Grade	
Analyst		Orla Hansen	
Photomicrographs			
BIOCLASTS	**Total bioclast %**	**94**	
		%	**Abundance limit**
	Bryozoans	90	very abundant
	Echinoderms	<1	rare
	Benthic foraminifera	<1	rare
	Planktic foraminifera	<1	rare
	Bivalves	<1	rare
	Pteropods	-	absent
	Gastropods	-	absent
	Calcareous red algae	-	absent
	Barnacles	-	absent
	Porifera	-	absent
	Brachiopods	-	absent
	Corals	-	absent
	Annelids	-	absent
	Other	-	absent
	Modal size 1 (mm)	0.72	
	Modal size 2 (mm)	1.56	
	Grain shape/abrasion	mod abraded	
	Sorting	poorly	
SILICICLASTS	**Total siliciclast grain %**	6, 70% in seam	
		%	**Abundance limit**
	Quartz		
	Feldspar	2	some
	Igneous rock fragments	-	absent
	Sedimentary rock fragments	-	absent
	Micas	-	absent
	Pyrite grains	2	absent
	Pyrite infills	<1 infills zooecia	rare
	Glauconite pellets	<1	rare
	Glauconite infills	<1	rare
	Clays	-	absent
	Modal size 1 (mm)	0.12	
	Modal size 2 (mm)	0.168	
	Grain shape/abrasion	angular	
	Sorting	poorly	
FEATURES	Cements/porosity/fabric	sparite, no porosity, slightly packed	
	Distribution of Siliciclasts	scattered or concentrated in seam	
	Oxidation characteristics	unoxidised	
	Discrete seams - Orientation, thickness (mm), mineralogy, oxidation state	3 mm thick, unoxidised, quartz & feldspar, clay & pyrite	
	Diffuse seams - Orientation, pattern, oxidiation state, mineralogy, thickness (mm)	-	
	Stylolites - Orientation, suture amplitude (mm), mineralogy, oxidation state	-	
	Microstylolites	-	

Petrographic data sheet - McDonald's Lime Quarry 2007			
Sample number		15.1	
Quarry unit		High Grade	
Analyst		Orla Hansen	
Photomicrographs			
BIOCLASTS	**Total bioclast %**	97	
		%	**Abundance limit**
	Bryozoans	91	very abundant
	Echinoderms	3	some
	Benthic foraminifera	<1	rare
	Planktic foraminifera	<1	rare
	Bivalves	<1	rare
	Pteropods	-	absent
	Gastropods	-	absent
	Calcareous red algae	-	absent
	Barnacles	-	absent
	Porifera	-	absent
	Brachiopods	-	absent
	Corals	-	absent
	Annelids	-	absent
	Other	-	absent
	Modal size 1 (mm)	1.44	
	Modal size 2 (mm)	0.48	
	Grain shape/abrasion	slightly abraded	
	Sorting	poorly	
SILICICLASTS	**Total siliciclast grain %**	3, 30% in seam	
		%	**Abundance limit**
	Quartz	-	absent
	Feldspar	-	absent
	Igneous rock fragments	-	absent
	Sedimentary rock fragments	-	absent
	Micas	-	absent
	Pyrite grains	3	some
	Pyrite infills	<1	rare
	Glauconite pellets	<1	rare
	Glauconite infills	-	absent
	Clays	-	absent
	Modal size 1 (mm)	0.12	
	Modal size 2 (mm)	0.19	
	Grain shape/abrasion	angular	
	Sorting	poorly	
FEATURES	Cements/porosity/fabric	sparite, no porosity, open-packed fabric	
	Distribution of Siliciclasts	scattered or concentrated in seam	
	Oxidation characteristics	unoxidised	
	Discrete seams - Orientation, thickness (mm), mineralogy, oxidation state	<1 mm thick, unoxidised, seam filled with pyrite, minor quartz & feldspar, clay	
	Diffuse seams - Orientation, pattern, oxidiation state, mineralogy, thickness (mm)	-	
	Stylolites - Orientation, suture amplitude (mm), mineralogy, oxidation state	-	
	Microstylolites	yes	

Petrographic data sheet - McDonald's Lime Quarry 2007			
Sample number		15.2	
Quarry unit		High Grade	
Analyst		Orla Hansen	
Photomicrographs			
BIOCLASTS	**Total bioclast %**	95	
		%	**Abundance limit**
	Bryozoans	92	very abundant
	Echinoderms	<1*	rare
	Benthic foraminifera	2	some
	Planktic foraminifera	-	absent
	Bivalves	<1	rare
	Pteropods	-	absent
	Gastropods	-	absent
	Calcareous red algae	-	absent
	Barnacles	-	absent
	Porifera	-	absent
	Brachiopods	-	absent
	Corals	-	absent
	Annelids	-	absent
	Clays	-	absent
	Modal size 1 (mm)	1.56	
	Modal size 2 (mm)	0.48	
	Grain shape/abrasion	slightly abraded	
	Sorting	poorly	
SILICICLASTS	**Total siliciclast grain %**	5, 20% in seam	
		%	**Abundance limit**
	Quartz	-	absent
	Feldspar	-	absent
	Igneous rock fragments	-	absent
	Sedimentary rock fragments	-	absent
	Micas	-	absent
	Pyrite grains	4-10	many
	Pyrite infills	<1	rare
	Glauconite pellets	<1	rare
	Glauconite infills	<1	rare
	Clays	-	absent
	Modal size 1 (mm)	0.22	
	Modal size 2 (mm)	0.10	
	Grain shape/abrasion	subrounded	
	Sorting	moderately	
FEATURES	Cements/porosity/fabric	sparite, no porosity, fragmented, packed	
	Distribution of siliciclastics	scattered or concentrated in seam	
	Oxidation characteristics	unoxidised	
	Discrete seams - Orientation, thickness (mm), mineralogy, oxidation state	4 mm thick, unoxidised, pyrite dominated, glauconite, quartz & feldspar, clay	
	Diffuse seams - Orientation, pattern, oxidiation state, mineralogy, thickness (mm)	-	
	Stylolites - Orientation, suture amplitude (mm), mineralogy, oxidation state	-	
	Microstylolites	-	

Petrographic data sheet - McDonald's Lime Quarry 2007			
Sample number		15.3	
Quarry unit		High Grade	
Analyst		Orla Hansen	
Photomicrographs			
BIOCLASTS	**Total bioclast %**	97	
		%	**Abundance limit**
	Bryozoans	93	very abundant
	Echinoderms	<1	rare
	Benthic foraminifera	<1	rare
	Planktic foraminifera	<1	rare
	Bivalves	<1	rare
	Pteropods	-	absent
	Gastropods	-	absent
	Calcareous red algae	-	absent
	Barnacles	-	absent
	Porifera	-	absent
	Brachiopods	-	absent
	Corals	-	absent
	Annelids	-	absent
	Other	-	absent
	Modal size 1 (mm)	0.48	
	Modal size 2 (mm)	0.84	
	Grain shape/abrasion	slightly abraded	
	Sorting	poorly	
SILICICLASTS	**Total siliciclast grain %**	3, 30% in seam	
		%	**Abundance limit**
	Quartz	-	absent
	Feldspar	-	absent
	Igneous rock fragments	-	absent
	Sedimentary rock fragments	-	absent
	Micas	-	absent
	Pyrite grains	2	some
	Pyrite infills	<1	rare
	Glauconite pellets	<1	rare
	Glauconite infills	<1	rare
	Clays	-	absent
	Modal size 1 (mm)	0.24	
	Modal size 2 (mm)	0.10	
	Grain shape/abrasion	subrounded	
	Sorting	poorly	
FEATURES	Cements/porosity/fabric	sparite, no porosity, micrite in chambers, packed	
	Distribution of Siliciclasts	scattered or concentrated in seam	
	Oxidation characteristics	unoxidised	
	Discrete seams - Orientation, thickness (mm), mineralogy, oxidation state	4 mm thick, mud sized particles in seam micrite?or clay?, unoxidised, pyrite dominant, quartz & feldspar, clay	
	Diffuse seams - Orientation, pattern, oxidiation state, mineralogy, thickness (mm)	-	
	Stylolites - Orientation, suture amplitude (mm), mineralogy, oxidation state	-	
	Microstylolites	-	

Petrographic data sheet - McDonald's Lime Quarry 2007			
Sample number		15.4	
Quarry unit		High Grade	
Analyst		Orla Hansen	
Photomicrographs			
BIOCLASTS	**Total bioclast %**	98	
		%	**Abundance limit**
	Bryozoans	94	very abundant
	Echinoderms	<1	rare
	Benthic foraminifera	<1	rare
	Planktic foraminifera	<1	rare
	Bivalves	<1	rare
	Pteropods	-	absent
	Gastropods	-	absent
	Calcareous red algae	-	absent
	Barnacles	-	absent
	Porifera	-	absent
	Brachiopods	-	absent
	Corals	-	absent
	Annelids	-	absent
	Other	-	absent
	Modal size 1 (mm)	1.44	
	Modal size 2 (mm)	0.60	
	Grain shape/abrasion	mod abraded	
	Sorting	poorly	
SILICICLASTS	**Total siliciclast grain %**	2, 20% in seam	
		%	**Abundance limit**
	Quartz	-	absent
	Feldspar	-	absent
	Igneous rock fragments	-	absent
	Sedimentary rock fragments	-	absent
	Micas	-	absent
	Pyrite grains	2	some
	Pyrite infills	<1	rare
	Glauconite pellets	<1	rare
	Glauconite infills	<1	rare
	Clays	-	absent
	Modal size 1 (mm)	0.22	
	Modal size 2 (mm)	0.07	
	Grain shape/abrasion	subrounded	
	Sorting	poorly	
FEATURES	Cements/porosity/fabric	sparite, no porosity	
	Distribution of Siliciclasts	scattered or concentrated in seam	
	Oxidation characteristics	unoxidised	
	Discrete seams - Orientation, thickness (mm), mineralogy, oxidation state	5 mm thick, unoxidised, grains packed near seam-more open fabric elsewhere, pyrite, glauconite, quartz & feldspar, clay	
	Diffuse seams - Orientation, pattern, oxidiation state, mineralogy, thickness (mm)	-	
	Stylolites - Orientation, suture amplitude (mm), mineralogy, oxidation state	-	
	Microstylolites	-	

Petrographic data sheet - McDonald's Lime Quarry 2007			
Sample number		43	
Quarry unit		High Grade	
Analyst		Orla Hansen	
Photomicrographs			
BIOCLASTS	**Total bioclast %**	**93**	
		%	**Abundance limit**
	Bryozoans	89	very abundant
	Echinoderms	<1	rare
	Benthic foraminifera	<1	rare
	Planktic foraminifera	<1	rare
	Bivalves	<1	rare
	Pteropods	-	absent
	Gastropods	-	absent
	Calcareous red algae	-	absent
	Barnacles	-	absent
	Porifera	-	absent
	Brachiopods	-	absent
	Corals	-	absent
	Annelids	-	absent
	Other	-	absent
	Modal size 1 (mm)	0.96	
	Modal size 2 (mm)	2.16	
	Grain shape/abrasion	mod abraded	
	Sorting	poorly	
SILICICLASTS	**Total siliciclast grain %**	7, 70% in seam	
		%	**Abundance limit**
	Quartz		
	Feldspar	3	some
	Igneous rock fragments	-	absent
	Sedimentary rock fragments	-	absent
	Micas	-	absent
	Pyrite grains	<1	rare
	Pyrite infills	2	some
	Glauconite pellets	<1	rare
	Glauconite infills	-	absent
	Clays	-	absent
	Modal size 1 (mm)	0.17	
	Modal size 2 (mm)	0.10	
	Grain shape/abrasion	angular	
	Sorting	moderately	
FEATURES	Cements/porosity/fabric	sparite, no porosity,some micrite, fractured	
	Distribution of Siliciclasts	concentrated in seam or scattered/clusters	
	Oxidation characteristics	oxidised - zooecia limonitised	
	Discrete seams - Orientation, thickness (mm), mineralogy, oxidation state	2 mm thick, oxidised, limonite, clay, glauconite, quartz & feldspar dominant	
	Diffuse seams - Orientation, pattern, oxidiation state, mineralogy, thickness (mm)	-	
	Stylolites - Orientation, suture amplitude (mm), mineralogy, oxidation state	-	
	Microstylolites	-	

Petrographic data sheet - McDonald's Lime Quarry 2007			
Sample number		47	
Quarry unit		Lower Steel	
Analyst		Orla Hansen	
Photomicrographs			
BIOCLASTS	**Total bioclast %**	97	
		%	**Abundance limit**
	Bryozoans	94	very abundant
	Echinoderms	2	some
	Benthic foraminifera	<1	rare
	Planktic foraminifera	-	absent
	Bivalves	<1	rare
	Pteropods	-	absent
	Gastropods	-	absent
	Calcareous red algae	-	absent
	Barnacles	-	absent
	Porifera	-	absent
	Brachiopods	-	absent
	Corals	-	absent
	Annelids	-	absent
	Other	-	absent
	Modal size 1 (mm)	1.92	
	Modal size 2 (mm)	1.44	
	Grain shape/abrasion	slightly abraded	
	Sorting	moderately	
SILICICLASTS	**Total siliciclast grain %**	3	
		%	**Abundance limit**
	Quartz	-	absent
	Feldspar	-	absent
	Igneous rock fragments	-	absent
	Sedimentary rock fragments	-	absent
	Micas	-	absent
	Pyrite grains	1	some
	Pyrite infills	<1	rare
	Glauconite pellets	<1	rare
	Glauconite infills	<1	rare
	Clays	-	absent
	Modal size 1 (mm)	0.22	
	Modal size 2 (mm)	0.14	
	Grain shape/abrasion	subrounded	
	Sorting	poorly	
FEATURES	Cements/porosity/fabric	sparite, porous along parts of stylolite, packed	
	Distribution of Siliciclasts	scattered or along stylolite	
	Oxidation characteristics	small limonitised patches or zooecia	
	Discrete seams - Orientation, thickness (mm), mineralogy, oxidation state	-	
	Diffuse seams - Orientation, pattern, oxidiation state, mineralogy, thickness (mm)	-	
	Stylolites - Orientation, suture amplitude (mm), mineralogy, oxidation state	vertical, clay dominant	
	Microstylolites	-	

Petrographic data sheet - McDonald's Lime Quarry 2007			
Sample number		49.1	
Quarry unit		Lower Steel	
Analyst		Orla Hansen	
Photomicrographs			
BIOCLASTS	**Total bioclast %**	97	
		%	**Abundance limit**
	Bryozoans	92	very abundant
	Echinoderms	<1	rare
	Benthic foraminifera	<1	rare
	Planktic foraminifera	<1	rare
	Bivalves	3	some
	Pteropods	-	absent
	Gastropods	-	absent
	Calcareous red algae	-	absent
	Barnacles	-	absent
	Porifera	-	absent
	Brachiopods	-	absent
	Corals	-	absent
	Annelids	-	absent
	Other	-	absent
	Modal size 1 (mm)	0.60	
	Modal size 2 (mm)	1.08	
	Grain shape/abrasion	slightly abraded	
	Sorting	moderately	
SILICICLASTS	**Total siliciclast grain %**	3	
		%	**Abundance limit**
	Quartz	-	absent
	Feldspar	-	absent
	Igneous rock fragments	-	absent
	Sedimentary rock fragments	-	absent
	Micas	-	absent
	Pyrite grains	<1	rare
	Pyrite infills	<1	rare
	Glauconite pellets	<1	rare
	Glauconite infills	<1	rare
	Clays	-	absent
	Modal size 1 (mm)	0.19	
	Modal size 2 (mm)	0.24	
	Grain shape/abrasion	subrounded	
	Sorting	poorly	
FEATURES	Cements/porosity/fabric	micrite, calcite veins, very fragmented	
	Distribution of Siliciclasts	scattered or along stylolite	
	Oxidation characteristics	oxidised	
	Discrete seams - Orientation, thickness (mm), mineralogy, oxidation state	-	
	Diffuse seams - Orientation, pattern, oxidiation state, mineralogy, thickness (mm)	-	
	Stylolites - Orientation, suture amplitude (mm), mineralogy, oxidation state	thin vertical stylolite <1 mm, clay, very minor quartz & feldspar	
	Microstylolites	-	

Petrographic data sheet - McDonald's Lime Quarry 2007			
Sample number		49.2	
Quarry unit		Lower Steel	
Analyst		Orla Hansen	
Photomicrographs			
BIOCLASTS	**Total bioclast %**	96	
		%	**Abundance limit**
	Bryozoans	91	very abundant
	Echinoderms	<1	rare
	Benthic foraminifera	<1	rare
	Planktic foraminifera	<1	rare
	Bivalves	3	some
	Pteropods	-	absent
	Gastropods	-	absent
	Calcareous red algae	-	absent
	Barnacles	-	absent
	Porifera	-	absent
	Brachiopods	-	absent
	Corals	-	absent
	Annelids	-	absent
	Other	-	absent
	Modal size 1 (mm)	1.56	
	Modal size 2 (mm)	0.43	
	Grain shape/abrasion	slightly abraded	
	Sorting	poorly	
SILICICLASTS	**Total siliciclast grain %**	4	
		%	**Abundance limit**
	Quartz	-	absent
	Feldspar	-	absent
	Igneous rock fragments	-	absent
	Sedimentary rock fragments	-	absent
	Micas	-	absent
	Pyrite grains	<1	rare
	Pyrite infills	<1	rare
	Glauconite pellets	<1	rare
	Glauconite infills	-	absent
	Clays	-	absent
	Modal size 1 (mm)	0.12	
	Modal size 2 (mm)	0.10	
	Grain shape/abrasion	subrounded	
	Sorting	poorly	
FEATURES	Cements/porosity/fabric	micrite, no porosity, calcite veins, very	
	Distribution of Siliciclasts	scattered or along stylolite	
	Oxidation characteristics	limonitised zooecia	
	Discrete seams - Orientation, thickness (mm), mineralogy, oxidation state	-	
	Diffuse seams - Orientation, pattern, oxidiation state, mineralogy, thickness (mm)	-	
	Stylolites - Orientation, suture amplitude (mm), mineralogy, oxidation state	hori. Pushed up against bivalve fragment, clay, minor quartz & feldspar, glauconite	
	Microstylolites	-	

Petrographic data sheet - McDonald's Lime Quarry 2007			
Sample number		51	
Quarry unit		Lower Steel	
Analyst		Orla Hansen	
Photomicrographs			
BIOCLASTS	**Total bioclast %**	98	
		%	**Abundance limit**
	Bryozoans	95	very abundant
	Echinoderms	<1	rare
	Benthic foraminifera	<1	rare
	Planktic foraminifera	-	absent
	Bivalves	<1	rare
	Pteropods	-	absent
	Gastropods	-	absent
	Calcareous red algae	-	absent
	Barnacles	-	absent
	Porifera	-	absent
	Brachiopods	-	absent
	Corals	-	absent
	Annelids	<1	rare
	Other	-	absent
	Modal size 1 (mm)	1.68	
	Modal size 2 (mm)	3.12	
	Grain shape/abrasion	slightly abraded	
	Sorting	moderately	
SILICICLASTS	**Total siliciclast grain %**	2, 90% in seam	
		%	**Abundance limit**
	Quartz	-	absent
	Feldspar	-	absent
	Igneous rock fragments	-	absent
	Sedimentary rock fragments	-	absent
	Micas	-	absent
	Pyrite grains	<1	rare
	Pyrite infills	<1	rare
	Glauconite pellets	<1	rare
	Glauconite infills	-	absent
	Clays	-	absent
	Modal size 1 (mm)	0.72	
	Modal size 2 (mm)	0.36	
	Grain shape/abrasion	anhedral-subrounded	
	Sorting	poorly	
FEATURES	Cements/porosity/fabric	sparite, sl packed	
	Distribution of Siliciclasts	clusters assoc. with oxidised material	
	Oxidation characteristics	oxidised along grains and inside chambers	
	Discrete seams - Orientation, thickness (mm), mineralogy, oxidation state	3 mm thick, oxidised, quartz & feldspar dominant - large crystals 0.7 mm long, clay, glauconite	
	Diffuse seams - Orientation, pattern, oxidiation state, mineralogy, thickness (mm)	-	
	Stylolites - Orientation, suture amplitude (mm), mineralogy, oxidation state	-	
	Microstylolites	-	

Petrographic data sheet - McDonald's Lime Quarry 2007			
Sample number		17.1	
Quarry unit		Lower Steel	
Analyst		Orla Hansen	
Photomicrographs			
BIOCLASTS	**Total bioclast %**	**96**	
		%	**Abundance limit**
	Bryozoans	92	very abundant
	Echinoderms	3*	some
	Benthic foraminifera	<1	rare
	Planktic foraminifera	-	absent
	Bivalves	-	absent
	Pteropods	-	absent
	Gastropods	-	absent
	Calcareous red algae	-	absent
	Barnacles	-	absent
	Porifera	-	absent
	Brachiopods	-	absent
	Corals	-	absent
	Annelids	<1	rare
	Clays	-	absent
	Modal size 1 (mm)	0.72	
	Modal size 2 (mm)	1.68	
	Grain shape/abrasion	mod abraded	
	Sorting	poorly	
SILICICLASTS	**Total siliciclast grain %**	4	
		%	**Abundance limit**
	Quartz		
	Feldspar	2/3	some
	Igneous rock fragments	-	absent
	Sedimentary rock fragments	-	absent
	Micas	-	absent
	Pyrite grains	<1	rare
	Pyrite infills	<1	rare
	Glauconite pellets	<1	rare
	Glauconite infills	-	absent
	Clays	-	absent
	Modal size 1 (mm)	0.336	
	Modal size 2 (mm)	0.192	
	Grain shape/abrasion	subrounded	
	Sorting	poorly	
FEATURES	Cements/porosity/fabric	sparite exclusive, open fabric	
	Distribution of siliciclastics	clusters or scattered	
	Oxidation characteristics	oxidised, limonitised areas	
	Discrete seams - Orientation, thickness (mm), mineralogy, oxidation state	-	
	Diffuse seams - Orientation, pattern, oxidiation state, mineralogy, thickness (mm)	-	
	Stylolites - Orientation, suture amplitude (mm), mineralogy, oxidation state	-	
	Microstylolites		

Petrographic data sheet - McDonald's Lime Quarry 2007			
Sample number		17.2	
Quarry unit		Lower Steel	
Analyst		Orla Hansen	
Photomicrographs			
BIOCLASTS	**Total bioclast %**	98	
		%	**Abundance limit**
	Bryozoans	91	very abundant
	Echinoderms	5	some
	Benthic foraminifera	2	some
	Planktic foraminifera	-	absent
	Bivalves	-	absent
	Pteropods	-	absent
	Gastropods	-	absent
	Calcareous red algae	-	absent
	Barnacles	-	absent
	Porifera	-	absent
	Brachiopods		absent
	Corals	-	absent
	Annelids	-	absent
	Other	-	absent
	Modal size 1 (mm)	0.72	
	Modal size 2 (mm)	1.44	
	Grain shape/abrasion	mod abraded	
	Sorting	poorly	
SILICICLASTS	**Total siliciclast grain %**	2, 50% in stylolite	
		%	**Abundance limit**
	Quartz	-	absent
	Feldspar	-	absent
	Igneous rock fragments	-	absent
	Sedimentary rock fragments	<1	rare
	Micas	-	absent
	Pyrite grains	<1	rare
	Pyrite infills	<1	rare
	Glauconite pellets	<1	rare
	Glauconite infills	<1	rare
	Clays	-	absent
	Modal size 1 (mm)	0.48	
	Modal size 2 (mm)	0.19	
	Grain shape/abrasion	angular	
	Sorting	poorly	
FEATURES	Cements/porosity/fabric	sparite, no porosity, open-packed fragments	
	Distribution of Siliciclasts	scattered or clusters	
	Oxidation characteristics	oxidised	
	Discrete seams - Orientation, thickness (mm), mineralogy, oxidation state	-	
	Diffuse seams - Orientation, pattern, oxidiation state, mineralogy, thickness (mm)	-	
	Stylolites - Orientation, suture amplitude (mm), mineralogy, oxidation state	hori. Oxidised, limonite, clay, minor quartz & feldspar, pyrite, glauconite	
	Microstylolites	-	

Petrographic data sheet - McDonald's Lime Quarry 2007			
Sample number		17.3	
Quarry unit		Lower Steel	
Analyst		Orla Hansen	
Photomicrographs			
BIOCLASTS	**Total bioclast %**	96	
		%	**Abundance limit**
	Bryozoans	91	very abundant
	Echinoderms	3	some rare
	Benthic foraminifera	<1	rare
	Planktic foraminifera	-	absent
	Bivalves	<1	rare
	Pteropods	-	absent
	Gastropods	-	absent
	Calcareous red algae	-	absent
	Barnacles	-	absent
	Porifera	-	absent
	Brachiopods	-	absent
	Corals	-	absent
	Annelids	-	absent
	Other	-	absent
	Modal size 1 (mm)	1.32	
	Modal size 2 (mm)	1.20	
	Grain shape/abrasion	mod abraded	
	Sorting	moderately	
SILICICLASTS	**Total siliciclast grain %**	4	
		%	**Abundance limit**
	Quartz	-	absent
	Feldspar	-	absent
	Igneous rock fragments	-	absent
	Sedimentary rock fragments	<1	rare
	Micas	-	absent
	Pyrite grains	<1	rare
	Pyrite infills	<1	rare
	Glauconite pellets	<1	rare
	Glauconite infills	-	absent
	Clays	-	absent
	Modal size 1 (mm)	0.48	
	Modal size 2 (mm)	0.19	
	Grain shape/abrasion	subrounded	
	Sorting	poorly	
FEATURES	Cements/porosity/fabric	sparite, no porosity, open-packed	
	Distribution of Siliciclasts	scattered or conc. In stylolite, clusters	
	Oxidation characteristics	oxidised, filled zooecia	
	Discrete seams - Orientation, thickness (mm), mineralogy, oxidation state	-	
	Diffuse seams - Orientation, pattern, oxidiation state, mineralogy, thickness (mm)	-	
	Stylolites - Orientation, suture amplitude (mm), mineralogy, oxidation state	two hori. Stylolites	
	Microstylolites	-	

Petrographic data sheet - McDonald's Lime Quarry 2007			
Sample number		16	
Quarry unit		Lower Steel	
Analyst		Orla Hansen	
Photomicrographs			
BIOCLASTS	**Total bioclast %**	**97**	
		%	**Abundance limit**
	Bryozoans	92	very abundant
	Echinoderms	5	some
	Benthic foraminifera	<1	rare
	Planktic foraminifera	-	absent
	Bivalves	-	absent
	Pteropods	-	absent
	Gastropods	-	absent
	Calcareous red algae	-	absent
	Barnacles	-	absent
	Porifera	-	absent
	Brachiopods	-	absent
	Corals	-	absent
	Annelids	-	absent
	Other	-	absent
	Modal size 1 (mm)	2.04	
	Modal size 2 (mm)	1.2	
	Grain shape/abrasion	slightly abraded	
	Sorting	poorly	
SILICICLASTS	**Total siliciclast grain %**	3, 80% in seam	
		%	**Abundance limit**
	Quartz	2	some
	Feldspar	-	absent
	Igneous rock fragments	-	absent
	Sedimentary rock fragments	-	absent
	Micas	-	absent
	Pyrite grains	<1	rare
	Pyrite infills	<1	rare
	Glauconite pellets	<1	rare
	Glauconite infills	-	absent
	Clays	-	absent
	Modal size 1 (mm)	0.144	
	Modal size 2 (mm)	0.096	
	Grain shape/abrasion	subrounded	
	Sorting	poorly	
FEATURES	Cements/porosity/fabric	sparite, no porosity, fragmented, packed,	
	Distribution of Siliciclasts	scattered or concentrated in seam	
	Oxidation characteristics	oxidised	
	Discrete seams - Orientation, thickness (mm), mineralogy, oxidation state	1 mm thick, oxidised, limonite, clay, quartz & feldspar, pyrite, glauconite	
	Diffuse seams - Orientation, pattern, oxidiation state, mineralogy, thickness (mm)	-	
	Stylolites - Orientation, suture amplitude (mm), mineralogy, oxidation state	-	
	Microstylolites	-	

Petrographic data sheet - McDonald's Lime Quarry 2007			
Sample number		55	
Quarry unit		Lower Steel	
Analyst		Orla Hansen	
Photomicrographs			
BIOCLASTS	**Total bioclast %**	97	
		%	**Abundance limit**
	Bryozoans	92	very abundant
	Echinoderms	4	some
	Benthic foraminifera	<1	rare
	Planktic foraminifera	-	absent
	Bivalves	<1	rare
	Pteropods	-	absent
	Gastropods	-	absent
	Calcareous red algae	-	absent
	Barnacles	-	absent
	Porifera	-	absent
	Brachiopods	-	absent
	Corals	-	absent
	Annelids	<1	rare
	Other	-	absent
	Modal size 1 (mm)	1.68	
	Modal size 2 (mm)	0.96	
	Grain shape/abrasion	mod abraded	
	Sorting	moderately	
SILICICLASTS	**Total siliciclast grain %**	3, 90% in seam	
		%	**Abundance limit**
	Quartz	-	absent
	Feldspar	-	absent
	Igneous rock fragments	-	absent
	Sedimentary rock fragments	-	absent
	Micas	-	absent
	Pyrite grains	<1	rare
	Pyrite infills	<1	rare
	Glauconite pellets	<1	rare
	Glauconite infills	1	some
	Clays	-	absent
	Modal size 1 (mm)	0.58	
	Modal size 2 (mm)	0.24	
	Grain shape/abrasion	subrounded/anhedral	
	Sorting	poorly	
FEATURES	Cements/porosity/fabric	sparite, no porosity, packed, fractured one end	
	Distribution of Siliciclasts	clusters of limonitised grains/infill	
	Oxidation characteristics	oxidised	
	Discrete seams - Orientation, thickness (mm), mineralogy, oxidation state	1 mm thick, oxidised, diagonal, limonite rich, clay dominant, quartz & feldspar - large crystals	
	Diffuse seams - Orientation, pattern, oxidiation state, mineralogy, thickness (mm)	-	
	Stylolites - Orientation, suture amplitude (mm), mineralogy, oxidation state	<1 mm coming off seam, vertical, clays, quartz & feldspar	
	Microstylolites	-	

Petrographic data sheet - McDonald's Lime Quarry 2007			
Sample number		18.1	
Quarry unit		Lower Steel	
Analyst		Orla Hansen	
Photomicrographs			
BIOCLASTS	**Total bioclast %**	98	
		%	**Abundance limit**
	Bryozoans	91	very abundant
	Echinoderms	5	some
	Benthic foraminifera	<1	rare
	Planktic foraminifera	-	absent
	Bivalves	<1	rare
	Pteropods	-	absent
	Gastropods	-	absent
	Calcareous red algae	-	absent
	Barnacles	-	absent
	Porifera	-	absent
	Brachiopods	-	absent
	Corals	-	absent
	Annelids	-	absent
	Other	-	absent
	Modal size 1 (mm)	1.44	
	Modal size 2 (mm)	0.84	
	Grain shape/abrasion	mod abraded	
	Sorting	moderately	
SILICICLASTS	**Total siliciclast grain %**	2	
		%	**Abundance limit**
	Quartz		
	Feldspar	2	some
	Igneous rock fragments	-	absent
	Sedimentary rock fragments	-	absent
	Micas	-	absent
	Pyrite grains	<1	rare
	Pyrite infills	<1	rare
	Glauconite pellets	<1	rare
	Glauconite infills	<1	rare
	Clays	-	absent
	Modal size 1 (mm)	0.29	
	Modal size 2 (mm)	0.48	
	Grain shape/abrasion	subrounded	
	Sorting	poorly	
FEATURES	Cements/porosity/fabric	sparite, open-sl packed	
	Distribution of Siliciclasts	scattered	
	Oxidation characteristics	oxidised, limonitised in places	
	Discrete seams - Orientation, thickness (mm), mineralogy, oxidation state	-	
	Diffuse seams - Orientation, pattern, oxidiation state, mineralogy, thickness (mm)	-	
	Stylolites - Orientation, suture amplitude (mm), mineralogy, oxidation state	small stylolites	
	Microstylolites	-	

Petrographic data sheet - McDonald's Lime Quarry 2007			
Sample number		18.2	
Quarry unit		Lower Steel	
Analyst		Orla Hansen	
Photomicrographs			
BIOCLASTS	**Total bioclast %**	98	
		%	**Abundance limit**
	Bryozoans	91	very abundant
	Echinoderms	5	some
	Benthic foraminifera	<1	rare
	Planktic foraminifera	<1	rare
	Bivalves	<1	rare
	Pteropods	-	absent
	Gastropods	-	absent
	Calcareous red algae	-	absent
	Barnacles	-	absent
	Porifera	-	absent
	Brachiopods	-	absent
	Corals	-	absent
	Annelids	-	absent
	Other	-	absent
	Modal size 1 (mm)	0.96	
	Modal size 2 (mm)	2.04	
	Grain shape/abrasion	mod abraded	
	Sorting	moderately	
SILICICLASTS	**Total siliciclast grain %**	2, 90% in seam	
		%	**Abundance limit**
	Quartz	-	absent
	Feldspar	-	absent
	Igneous rock fragments	-	absent
	Sedimentary rock fragments	-	absent
	Micas	-	absent
	Pyrite grains	<1	rare
	Pyrite infills	<1	rare
	Glauconite pellets	<1	rare
	Glauconite infills	<1	rare
	Clays	-	absent
	Modal size 1 (mm)	0.29	
	Modal size 2 (mm)	0.60	
	Grain shape/abrasion	subrounded	
	Sorting	poorly	
FEATURES	Cements/porosity/fabric	sparite, no porosity, open-sl packed	
	Distribution of Siliciclasts	scattered or highly conc. In seam	
	Oxidation characteristics	oxidised some areas unoxidised, limonitised zooecia	
	Discrete seams - Orientation, thickness (mm), mineralogy, oxidation state	1.5 mm thick,oxidised, limonitised full of pyrite, clay, quartz & feldspar - huge crystals 0.5 mm long, glauconite	
	Diffuse seams - Orientation, pattern, oxidiation state, mineralogy, thickness (mm)	-	
	Stylolites - Orientation, suture amplitude (mm), mineralogy, oxidation state	vertical stylolite coming off seam, minor quartz, clay	
	Microstylolites	-	

Petrographic data sheet - McDonald's Lime Quarry 2007			
Sample number		18.3	
Quarry unit		Lower Steel	
Analyst		Orla Hansen	
Photomicrographs			
BIOCLASTS	**Total bioclast %**	97	
		%	**Abundance limit**
	Bryozoans	93	very abundant
	Echinoderms	2	some
	Benthic foraminifera	<1	rare
	Planktic foraminifera	-	absent
	Bivalves	-	absent
	Pteropods	-	absent
	Gastropods	-	absent
	Calcareous red algae	-	absent
	Barnacles	-	absent
	Porifera	-	absent
	Brachiopods	-	absent
	Corals	-	absent
	Annelids	<1	rare
	Other	-	absent
	Modal size 1 (mm)	0.96	
	Modal size 2 (mm)	2.88	
	Grain shape/abrasion	mod abraded	
	Sorting	poorly	
SILICICLASTS	**Total siliciclast grain %**	3	
		%	**Abundance limit**
	Quartz	-	absent
	Feldspar	-	absent
	Igneous rock fragments	-	absent
	Sedimentary rock fragments	-	absent
	Micas	-	absent
	Pyrite grains	<1	rare
	Pyrite infills	<1	rare
	Glauconite pellets	<1	rare
	Glauconite infills	<1	rare
	Clays	-	absent
	Modal size 1 (mm)	0.29	
	Modal size 2 (mm)	0.43	
	Grain shape/abrasion	subrounded	
	Sorting	poorly	
FEATURES	Cements/porosity/fabric	sparite, no porosity, open-sl packed	
	Distribution of Siliciclasts	clusters of pyrite or along stylolite, scattered	
	Oxidation characteristics	partly oxidised partly unoxidised	
	Discrete seams - Orientation, thickness (mm), mineralogy, oxidation state	-	
	Diffuse seams - Orientation, pattern, oxidiation state, mineralogy, thickness (mm)	-	
	Stylolites - Orientation, suture amplitude (mm), mineralogy, oxidation state	unoxidised very thin hori., pyrite & clay dominated, glauconite	
	Microstylolites	-	

Petrographic data sheet - McDonald's Lime Quarry 2007			
Sample number		18.4	
Quarry unit		Lower Steel	
Analyst		Orla Hansen	
Photomicrographs			
BIOCLASTS	**Total bioclast %**	97	
		%	**Abundance limit**
	Bryozoans	94	very abundant
	Echinoderms	2	some
	Benthic foraminifera	<1	rare
	Planktic foraminifera	-	absent
	Bivalves	<1	rare
	Pteropods	-	absent
	Gastropods	-	absent
	Calcareous red algae	-	absent
	Barnacles	-	absent
	Porifera	-	absent
	Brachiopods	-	absent
	Corals	-	absent
	Annelids	-	absent
	Other	-	absent
	Modal size 1 (mm)	2.16	
	Modal size 2 (mm)	0.97	
	Grain shape/abrasion	slightly abraded	
	Sorting	poorly	
SILICICLASTS	**Total siliciclast grain %**	3	
		%	**Abundance limit**
	Quartz	-	absent
	Feldspar	-	absent
	Igneous rock fragments	-	absent
	Sedimentary rock fragments	-	absent
	Micas	-	absent
	Pyrite grains	<1	rare
	Pyrite infills	<1	rare
	Glauconite pellets	<1	rare
	Glauconite infills	<1	rare
	Clays	-	absent
	Modal size 1 (mm)	0.36	
	Modal size 2 (mm)	0.24	
	Grain shape/abrasion	subrounded	
	Sorting	poorly	
FEATURES	Cements/porosity/fabric	sparite, no porosity	
	Distribution of Siliciclasts	scattered or along stylolite	
	Oxidation characteristics	oxidised	
	Discrete seams - Orientation, thickness (mm), mineralogy, oxidation state	-	
	Diffuse seams - Orientation, pattern, oxidiation state, mineralogy, thickness (mm)	-	
	Stylolites - Orientation, suture amplitude (mm), mineralogy, oxidation state	hori. Amp = 0.5 mm, clay, big round quartz & feldspar dominant crystals = .48 mm long, glauconite	
	Microstylolites	-	

Sample number		57.2A	
Quarry unit		Sub-economic	
Analyst		Orla Hansen	
Photomicrographs			
BIOCLASTS	**Total bioclast %**	92	
		%	**Abundance limit**
	Bryozoans	85	very abundant
	Echinoderms	2*	some
	Benthic foraminifera	<1	rare
	Planktic foraminifera	<1	rare
	Bivalves	2	some
	Pteropods	-	absent
	Gastropods	-	absent
	Calcareous red algae	-	absent
	Barnacles	-	absent
	Porifera	-	absent
	Brachiopods	-	absent
	Corals	-	absent
	Annelids	2	some
	Other	-	absent
	Modal size 1 (mm)	1.68	
	Modal size 2 (mm)	0.84	
	Grain shape/abrasion	slightly abraded	
	Sorting	poorly	
SILICICLASTS	**Total siliciclast grain %**	8	
		%	**Abundance limit**
	Quartz		
	Feldspar	5	some
	Igneous rock fragments	-	absent
	Sedimentary rock fragments	-	absent
	Micas	-	absent
	Pyrite grains	1	some
	Pyrite infills	2	some
	Glauconite pellets	2	some
	Glauconite infills	<1	rare
	Clays	-	absent
	Modal size 1 (mm)	0.24	
	Modal size 2 (mm)	0.12	
	Grain shape/abrasion	angular	
	Sorting	poorly	
FEATURES	Cements/porosity/fabric	sparite, no porosity, tightly packed,fractured	
	Distribution of Siliciclasts	scattered, patchy pyrite assoc. with bioclasts inside zooecia/chambers	
	Oxidation characteristics	oxidised, filled zooecia	
	Discrete seams - Orientation, thickness (mm), mineralogy, oxidation state	-	
	Diffuse seams - Orientation, pattern, oxidiation state, mineralogy, thickness (mm)	-	
	Stylolites - Orientation, suture amplitude (mm), mineralogy, oxidation state	-	
	Microstylolites	-	

Petrographic data sheet - McDonald's Lime Quarry 2007			
Sample number		57.1B	
Quarry unit		Sub-economic	
Analyst		Orla Hansen	
Photomicrographs			
BIOCLASTS	**Total bioclast %**	93	
		%	**Abundance limit**
	Bryozoans	83	very abundant
	Echinoderms	5*	some
	Benthic foraminifera	<1	rare
	Planktic foraminifera	-	absent
	Bivalves	2	some
	Pteropods	-	absent
	Gastropods	-	absent
	Calcareous red algae	-	absent
	Barnacles	-	absent
	Porifera	-	absent
	Brachiopods	-	absent
	Corals	-	absent
	Annelids	2	some
	Other	-	absent
	Modal size 1 (mm)	1.92	
	Modal size 2 (mm)	0.84	
	Grain shape/abrasion	mod abraded	
	Sorting	poorly	
SILICICLASTS	**Total siliciclast grain %**	7, 50% in seam	
		%	**Abundance limit**
	Quartz		
	Feldspar	3	some
	Igneous rock fragments	-	absent
	Sedimentary rock fragments	-	absent
	Micas	-	absent
	Pyrite grains	<1	rare
	Pyrite infills	2	some
	Glauconite pellets	1	some
	Glauconite infills	<1	rare
	Clays	-	absent
	Modal size 1 (mm)	0.10	
	Modal size 2 (mm)	0.17	
	Grain shape/abrasion	subrounded	
	Sorting	poorly	
FEATURES	Cements/porosity/fabric	sparite, no porosity, slightly open-packed	
	Distribution of Siliciclasts	scattered	
	Oxidation characteristics	oxidised, pyrite oxidised	
	Discrete seams - Orientation, thickness (mm), mineralogy, oxidation state	broken <1 mm seam, oxidised, limonite, clay, rounded glauconite, quartz & feldspars	
	Diffuse seams - Orientation, pattern, oxidiation state, mineralogy, thickness (mm)	-	
	Stylolites - Orientation, suture amplitude (mm), mineralogy, oxidation state	-	
	Microstylolites	-	

Petrographic data sheet - McDonald's Lime Quarry 2007			
Sample number		19.1	
Quarry unit		Sub-economic	
Analyst		Orla Hansen	
Photomicrographs			
BIOCLASTS	**Total bioclast %**	95	
		%	**Abundance limit**
	Bryozoans	92	very abundant
	Echinoderms	2	some
	Benthic foraminifera	<1	rare
	Planktic foraminifera	-	absent
	Bivalves	<1	rare
	Pteropods	-	absent
	Gastropods	-	absent
	Calcareous red algae	-	absent
	Barnacles	-	absent
	Porifera	-	absent
	Brachiopods	-	absent
	Corals	-	absent
	Annelids	<1	rare
	Other	-	absent
	Modal size 1 (mm)	2.16	
	Modal size 2 (mm)	0.72	
	Grain shape/abrasion	mod abraded	
	Sorting	moderately	
SILICICLASTS	**Total siliciclast grain %**	5	
		%	**Abundance limit**
	Quartz	-	absent
	Feldspar	-	absent
	Igneous rock fragments	-	absent
	Sedimentary rock fragments	-	absent
	Micas	-	absent
	Pyrite grains	2	some
	Pyrite infills	1	some
	Glauconite pellets	<1	rare
	Glauconite infills	<1	rare
	Clays	-	absent
	Modal size 1 (mm)	0.53	
	Modal size 2 (mm)	0.19	
	Grain shape/abrasion	subrounded	
	Sorting	poorly	
FEATURES	Cements/porosity/fabric	sparite, no porosity, micrite-fill, calcite veins, open-sl packed	
	Distribution of Siliciclasts	scattered	
	Oxidation characteristics	oxidised	
	Discrete seams - Orientation, thickness (mm), mineralogy, oxidation state	-	
	Diffuse seams - Orientation, pattern, oxidiation state, mineralogy, thickness (mm)	-	
	Stylolites - Orientation, suture amplitude (mm), mineralogy, oxidation state	-	
	Microstylolites	-	

Petrographic data sheet - McDonald's Lime Quarry 2007			
Sample number		19.2	
Quarry unit		Sub-economic	
Analyst		Orla Hansen	
Photomicrographs			
BIOCLASTS	**Total bioclast %**	95	
		%	**Abundance limit**
	Bryozoans	92	very abundant
	Echinoderms	2	some
	Benthic foraminifera	<1	rare
	Planktic foraminifera	-	absent
	Bivalves	-	absent
	Pteropods	-	absent
	Gastropods	-	absent
	Calcareous red algae	-	absent
	Barnacles	-	absent
	Porifera	-	absent
	Brachiopods	-	absent
	Corals	-	absent
	Annelids	<1	rare
	Other	-	absent
	Modal size 1 (mm)	1.44	
	Modal size 2 (mm)	2.64	
	Grain shape/abrasion	slightly abraded	
	Sorting	poorly	
SILICICLASTS	**Total siliciclast grain %**	5, 90% in seam	
		%	**Abundance limit**
	Quartz		
	Feldspar	2	some
	Igneous rock fragments	-	absent
	Sedimentary rock fragments	-	absent
	Micas	-	absent
	Pyrite grains	2	some
	Pyrite infills	<1	rare
	Glauconite pellets	<1	rare
	Glauconite infills	<1	rare
	Clays	-	absent
	Modal size 1 (mm)	0.24	
	Modal size 2 (mm)	0.19	
	Grain shape/abrasion	subrounded	
	Sorting	poorly	
FEATURES	Cements/porosity/fabric	sparite, no porosity, calcite veins, fragmented	
	Distribution of Siliciclasts	scattered or conc. In seam	
	Oxidation characteristics	oxidised	
	Discrete seams - Orientation, thickness (mm), mineralogy, oxidation state	2 mm seam, oxidised, quartz & feldspar dominant, glauconite, clay dominant also, limonite	
	Diffuse seams - Orientation, pattern, oxidiation state, mineralogy, thickness (mm)	-	
	Stylolites - Orientation, suture amplitude (mm), mineralogy, oxidation state	-	
	Microstylolites	-	

Petrographic data sheet - McDonald's Lime Quarry 2007			
Sample number		19.3	
Quarry unit		Sub-economic	
Analyst		Orla Hansen	
Photomicrographs			
BIOCLASTS	**Total bioclast %**	95	
		%	**Abundance limit**
	Bryozoans	91	very abundant
	Echinoderms	2	some
	Benthic foraminifera	<1	rare
	Planktic foraminifera	-	absent
	Bivalves	-	absent
	Pteropods	-	absent
	Gastropods	-	absent
	Calcareous red algae	-	absent
	Barnacles	-	absent
	Porifera	-	absent
	Brachiopods	-	absent
	Corals	-	absent
	Annelids	2	some
	Other	-	absent
	Modal size 1 (mm)	1.20	
	Modal size 2 (mm)	0.72	
	Grain shape/abrasion	mod abraded	
	Sorting	poorly	
SILICICLASTS	**Total siliciclast grain %**	5, 30% in seam	
		%	**Abundance limit**
	Quartz		
	Feldspar	3	some
	Igneous rock fragments	-	absent
	Sedimentary rock fragments	-	absent
	Micas	-	absent
	Pyrite grains	<1	rare
	Pyrite infills	1	some
	Glauconite pellets	<1	rare
	Glauconite infills	<1	rare
	Clays	-	absent
	Modal size 1 (mm)	0.36	
	Modal size 2 (mm)	0.19	
	Grain shape/abrasion	subrounded	
	Sorting	poorly	
FEATURES	Cements/porosity/fabric	sparite, no porosity,open-sl packed	
	Distribution of Siliciclasts	scattered or conc. In seam	
	Oxidation characteristics	oxidised	
	Discrete seams - Orientation, thickness (mm), mineralogy, oxidation state	two 1 mm thick seams, clay, oxidised, glauconite, quartz & feldspar	
	Diffuse seams - Orientation, pattern, oxidiation state, mineralogy, thickness (mm)	-	
	Stylolites - Orientation, suture amplitude (mm), mineralogy, oxidation state	-	
	Microstylolites	-	

Petrographic data sheet - McDonald's Lime Quarry 2007			
Sample number		61	
Quarry unit		Sub-economic	
Analyst		Orla Hansen	
Photomicrographs			
BIOCLASTS	**Total bioclast %**	90	
		%	**Abundance limit**
	Bryozoans	87	very abundant
	Echinoderms	2	some
	Benthic foraminifera	<1	rare
	Planktic foraminifera	<1	rare
	Bivalves	<1	rare
	Pteropods	-	absent
	Gastropods	-	absent
	Calcareous red algae	-	absent
	Barnacles	-	absent
	Porifera	-	absent
	Brachiopods	-	absent
	Corals	-	absent
	Annelids	-	absent
	Other	-	absent
	Modal size 1 (mm)	2.04	
	Modal size 2 (mm)	1.08	
	Grain shape/abrasion	slightly abraded	
	Sorting	poorly	
SILICICLASTS	**Total siliciclast grain %**	3, 30% in diffuse seam	
		%	**Abundance limit**
	Quartz		
	Feldspar	3	some
	Igneous rock fragments	-	absent
	Sedimentary rock fragments	-	absent
	Micas	-	absent
	Pyrite grains	3	some
	Pyrite infills	2	some
	Glauconite pellets	1	some
	Glauconite infills	1	some
	Clays	-	absent
	Modal size 1 (mm)	0.24	
	Modal size 2 (mm)	0.14	
	Grain shape/abrasion	angular	
	Sorting	poorly	
FEATURES	Cements/porosity/fabric	micrite, no porosity, tight, fragmented in places	
	Distribution of Siliciclasts	scattered or conc. In diffuse seam	
	Oxidation characteristics	unoxidised	
	Discrete seams - Orientation, thickness (mm), mineralogy, oxidation state	-	
	Diffuse seams - Orientation, pattern, oxidiation state, mineralogy, thickness (mm)	pyrite along wisps, unoxidised, glauconite, clay, quartz & feldspar dominant	
	Stylolites - Orientation, suture amplitude (mm), mineralogy, oxidation state	-	
	Microstylolites	-	

Petrographic data sheet - McDonald's Lime Quarry 2007			
Sample number		66.1	
Quarry unit		Sub-economic	
Analyst		Orla Hansen	
Photomicrographs			
BIOCLASTS	**Total bioclast %**	95	
		%	**Abundance limit**
	Bryozoans	87	very abundant
	Echinoderms	2	some
	Benthic foraminifera	1	some
	Planktic foraminifera	-	absent
	Bivalves	3	some
	Pteropods	-	absent
	Gastropods	-	absent
	Calcareous red algae	<1	rare
	Barnacles	-	absent
	Porifera	-	absent
	Brachiopods	-	absent
	Corals	-	absent
	Annelids	2	some
	Other	-	absent
	Modal size 1 (mm)	1.56	
	Modal size 2 (mm)	0.84	
	Grain shape/abrasion	mod abraded	
	Sorting	poorly	
SILICICLASTS	**Total siliciclast grain %**	5	
		%	**Abundance limit**
	Quartz		
	Feldspar	3	some
	Igneous rock fragments	-	absent
	Sedimentary rock fragments	-	absent
	Micas	-	absent
	Pyrite grains	1	some
	Pyrite infills	<1	rare
	Glauconite pellets	1	some
	Glauconite infills	<1	rare
	Clays	-	rare
	Modal size 1 (mm)	0.29	
	Modal size 2 (mm)	0.12	
	Grain shape/abrasion	angular	
	Sorting	poorly	
FEATURES	Cements/porosity/fabric	micrite dominated, no porosity,	
	Distribution of Siliciclasts	scattered or along mini stylolite or	
	Oxidation characteristics	unoxidised	
	Discrete seams - Orientation, thickness (mm), mineralogy, oxidation state	-	
	Diffuse seams - Orientation, pattern, oxidiation state, mineralogy, thickness (mm)	-	
	Stylolites - Orientation, suture amplitude (mm), mineralogy, oxidation state	unoxidised, glauconite, minor clay, quartz & feldspar dominant	
	Microstylolites	-	

Petrographic data sheet - McDonald's Lime Quarry 2007			
Sample number		66.3	
Quarry unit		Sub-economic	
Analyst		Orla Hansen	
Photomicrographs			
BIOCLASTS	**Total bioclast %**	95	
		%	**Abundance limit**
	Bryozoans	90	very abundant
	Echinoderms	2	some
	Benthic foraminifera	<1	rare
	Planktic foraminifera	-	absent
	Bivalves	2	some
	Pteropods	-	absent
	Gastropods	-	absent
	Calcareous red algae	<1	rare
	Barnacles	-	absent
	Porifera	-	absent
	Brachiopods	-	absent
	Corals	-	absent
	Annelids	<1	rare
	Other	-	absent
	Modal size 1 (mm)	1.68	
	Modal size 2 (mm)	2.40	
	Grain shape/abrasion	mod abraded	
	Sorting	poorly	
SILICICLASTS	**Total siliciclast grain %**	5	
		%	**Abundance limit**
	Quartz		
	Feldspar	3	some
	Igneous rock fragments	-	absent
	Sedimentary rock fragments	<1	rare
	Micas	-	absent
	Pyrite grains	<1	rare
	Pyrite infills	<1	rare
	Glauconite pellets	<1	rare
	Glauconite infills	<1	rare
	Clays	-	absent
	Modal size 1 (mm)	0.17	
	Modal size 2 (mm)	0.12	
	Grain shape/abrasion	subrounded	
	Sorting	poorly	
FEATURES	Cements/porosity/fabric	sparite, no porosity, fractured edge	
	Distribution of Siliciclasts	conc. Along stylolite	
	Oxidation characteristics	unoxidised	
	Discrete seams - Orientation, thickness (mm), mineralogy, oxidation state	-	
	Diffuse seams - Orientation, pattern, oxidiation state, mineralogy, thickness (mm)	-	
	Stylolites - Orientation, suture amplitude (mm), mineralogy, oxidation state	hori. Stylolite, unoxidised, glauconite, clay, pyrite, minor quartz & feldspar	
	Microstylolites	-	

Petrographic data sheet - McDonald's Lime Quarry 2007			
Sample number		66.4	
Quarry unit		Sub-economic	
Analyst		Orla Hansen	
Photomicrographs			
BIOCLASTS	**Total bioclast %**	96	
		%	**Abundance limit**
	Bryozoans	92	very abundant
	Echinoderms	3	some
	Benthic foraminifera	<1	rare
	Planktic foraminifera	-	absent
	Bivalves	-	absent
	Pteropods	-	absent
	Gastropods	-	absent
	Calcareous red algae	<1	rare
	Barnacles	-	absent
	Porifera	-	absent
	Brachiopods	-	absent
	Corals	-	absent
	Annelids	-	absent
	Other	-	absent
	Modal size 1 (mm)	1.92	
	Modal size 2 (mm)	0.72	
	Grain shape/abrasion	slightly abraded	
	Sorting	poorly	
SILICICLASTS	**Total siliciclast grain %**	4	
		%	**Abundance limit**
	Quartz		
	Feldspar	3-5	some
	Igneous rock fragments	-	absent
	Sedimentary rock fragments	-	absent
	Micas	-	absent
	Pyrite grains	<1	rare
	Pyrite infills	<1	rare
	Glauconite pellets	<1	rare
	Glauconite infills	-	absent
	Clays	-	absent
	Modal size 1 (mm)	0.29	
	Modal size 2 (mm)	0.12	
	Grain shape/abrasion	subrounded	
	Sorting	poorly	
FEATURES	Cements/porosity/fabric	sparite, no porosity, micrite fill in zooecia, sl packed	
	Distribution of Siliciclasts	scattered or conc. In stylolite	
	Oxidation characteristics	unoxidised	
	Discrete seams - Orientation, thickness (mm), mineralogy, oxidation state	-	
	Diffuse seams - Orientation, pattern, oxidiation state, mineralogy, thickness (mm)	-	
	Stylolites - Orientation, suture amplitude (mm), mineralogy, oxidation state	hori. Unoxidised, clay and quartz along stylolite	
	Microstylolites	-	

Appendix E-5.9 Total carbonate and non-carbonate content and bioclast componentry in quarry limestones for BH502. Approx. depth (m) = depth along drill hole.

Quarry unit	Thin section number	Approx. depth (m)	Total $CaCO_3$ %	Total silica %	% Bryozoans	% Echinoderms	% Benthic forams	% Planktic forams	% Bivalves	% Calc. red algae	% Annelids
Caprock	20	25.5	70	30	2	5	2	61	0	0	0
	21	25.8	75	25	2	5	3	65	0	0	0
	9.1	26.2	95	5	75	10	3	5	0.5	0	0
	9.2	26.25	89	11	84	2	0.5	4	0	0	0
	23.2	26.69	90	10	69	15	3	3	0	0	0
	27	26.75	80	20	68	5	2	5	0	0	0
Upper Steel	10.1	28.1	99	1	53	45	0.5	0	0	0	0
	10.2	28.15	99	1	83	15	0.5	0	0	0	0
	10.3	28.2	99	1	82	15	0.5	0	0.5	0	0
	24.1	28.5	99	1	87	7	5	0	0	0	0
	24.2	28.55	99	1	75	19	3	2	0	0	0
	24.3	28.9	99	1	82	15	2	0	0	0	0
	25	34.7	98	2	91	5	0	0.5	0.5	0	0
	30	35.8	98	2	93	5	0.5	0	0	0	0
Aglime	32	37	98	2	87	0.5	0.5	0	0.5	0	0
	34	38.4	98	2	95	0.5	0	0.5	0.5	0	0
	35	39.45	99	1	96	0.5	0	0.5	0.5	0	0
	11	40.2	90	10	86	0.5	0.5	0.5	0.5	0	0
	12.1	41.2	95	5	91	0.5	1	0	2	0	0
	12.2	41.25	92	8	96	0.5	0.5	0.5	0.5	0	0
	12.3	41.3	98	2	95	1	1	0	0	0	1
	13.1	42.8	60	40	58	0.5	0.5	0	0	0	0.5
	13.2	42.85	80	20	75	0.5	0.5	0.5	0.5	0	0.5
	13.3	42.9	95	5	91	0.5	0.5	0.5	0	0	0.5
High Grade	38	50.1	95	5	91	0.5	0.5	0.5	0.5	0	0
	14	52.6	95	5	93	0.5	0.5	0.5	0	0	0
	40	54.8	96	4	93	0.5	0.5	0.5	0.5	0	0
	40.2	54.85	94	6	90	0.5	0.5	0.5	0.5	0	0
	15.1	56.65	97	3	91	3	0.5	0.5	0.5	0	0
	15.2	56.7	95	5	92	0.5	2	0	0.5	0	0
	15.3	56.75	97	3	93	0.5	0.5	0.5	0.5	0	0

Appendix E-5.9 continued.

Quarry unit	Thin section number	Approx. depth (m)	Total $CaCO_3$ %	Total silica %	% Bryozoans	% Echinoderms	% Benthic forams	% Planktic forams	% Bivalves	% Calc. red algae	% Annelids
High Grade	15.4	56.8	98	2	94	0.5	0.5	0.5	0.5	0	0
	43	62.1	93	7	89	0.5	0.5	0.5	0.5	0	0
Lower Steel	47	67.9	97	3	94	2	0.5	0	0.5	0	0
	49.1	70.7	97	3	92	0.5	0.5	0.5	3	0	0
	49.2	70.75	96	4	91	0.5	0.5	0.5	3	0	0
	51	72.6	98	2	95	0.5	0.5	0	0.5	0	0.5
	17.1	73.6	96	4	92	3	0.5	0	0	0	0.5
	17.2	73.65	98	2	91	5	2	0	0	0	0
	17.3	73.7	96	4	91	3	0.5	0	0.5	0	0
	16	74.1	97	3	92	5	0.5	0	0	0	0
	55	76.3	97	3	92	4	0.5	0	0.5	0	0.5
	18.1	77.85	98	2	91	5	0.5	0	0.5	0	0
	18.2	77.9	98	2	91	5	0.5	0.5	0.5	0	0
	18.3	77.95	97	3	93	2	0.5	0	0	0	0.5
	18.4	78	97	3	94	2	0.5	0	0.5	0	0
Sub-economic	57.2A	86.9	92	8	85	2	0.5	0.5	2	0	0.5
	57.1B	86.95	93	7	83	5	0.5	0	2	0	2
	19.1	87.6	95	5	92	2	0.5	0	0.5	0	0.5
	19.2	87.65	95	5	92	2	0.5	0	0	0	0.5
	19.3	87.7	95	5	91	2	0.5	0	0	0	2
	59.4	88.9	94	6	89	3	0.5	0	0.5	0	0.5
	61	91	90	10	87	2	0.5	0.5	0.5	0	0
	66.1	97.5	95	5	87	2	1	0	3	0	2
	66.3	97.55	95	5	90	2	0.5	0	2	0.5	0.5
	66.4	97.6	96	4	92	3	0.5	0	0	0.5	0

Appendix E-5.10 Siliciclastic componentry in quarry limestones for BH502.

Quarry unit	Thin section number	Approx. depth (m)	Quartz & feldspar	Sed. rock frags.	Pyrite grains	Pyrite infills	Glauc. pellets	Glauc. infills	% Clays
Caprock	20	25.5	0	0	3	0	0	0	27
	21	25.8	0	0	0	0.5	0.5	0	24
	9.1	26.2	0.5	0	0	0	0	0	5
	9.2	26.25	0	0	0.5	0	0.5	0	10
	23.2	26.69	0	0	0.5	0	0.5	0	10
	27	26.75	0	0	0.5	0	0.5	0	19
Upper Steel	10.1	28.1	0	0	0.5	0	0	0	0
	10.2	28.15	0	0	0.5	0	0.5	0	0
	10.3	28.2	0	0	0.5	0	0	0	0
	24.1	28.5	0	0	0.5	0	0.5	0	0
	24.2	28.55	0	0	0.5	0.5	0	0	0
	24.3	28.9	0.5	0	0.5	0	0	0	0
	25	34.7	0	0	0.5	0.5	0.5	0	0
	30	35.8	0	0	0.5	0.5	0	0	0
Aglime	32	37	0	0	0.5	0	2	0.5	0
	34	38.4	0	0	1	0.5	0.5	0.5	0
	35	39.45	0	0	0.5	0.5	0.5	0	0
	11	40.2	0	0	0.5	0	0	0	0
	12.1	41.2	0	0	2	0.5	0	0.5	0
	12.2	41.25	0	0	0.5	0	0.5	0.5	0
	12.3	41.3	0	0	0.5	0.5	0.5	0.5	0
	13.1	42.8	0	0	2	0	0.5	0	38
	13.2	42.85	0	0	0.5	0	0.5	0	0
	13.3	42.9	0	0	0.5	0	2	0.5	0
High Grade	38	50.1	0	0	4	0.5	0.5	0	0
	14	52.6	2	0	3	2	0.5	0.5	0
	40	54.8	0	0	3	0.5	0.5	0	0
	40.2	54.85	2	0	2	0.5	0.5	0.5	0
	15.1	56.65	0	0	3	0.5	0.5	0	0
	15.2	56.7	0	0	7	0.5	0.5	0.5	0
	15.3	56.75	0	0	2	0.5	0.5	0.5	0

Appendix E-5.10 continued.

Quarry unit	Thin section number	Approx. depth (m)	Quartz & feldspar	Sed. rock frags.	Pyrite grains	Pyrite infills	Glauc. pellets	Glauc. infills	% Clays
High Grade	15.4	56.8	0	0	2	0.5	0.5	0.5	0
	43	62.1	3	0	0.5	2	0.5	0	0
	47	67.9	0	0	1	0.5	0.5	0.5	0
	49.1	70.7	0	0	0.5	0.5	0.5	0.5	0
Lower Steel	49.2	70.75	0	0	0.5	0.5	0.5	0	0
	51	72.6	0	0	0.5	0.5	0.5	0	0
	17.1	73.6	2	0	0.5	0.5	0.5	0	0
	17.2	73.65	0	0.5	0.5	0.5	0.5	0.5	0
	17.3	73.7	0	0.5	0.5	0.5	0.5	0	0
	16	74.1	2	0	0.5	0.5	0.5	0	0
	55	76.3	0	0	0.5	0.5	0.5	1	0
	18.1	77.85	2	0	0.5	0.5	0.5	0.5	0
	18.2	77.9	0	0	0.5	0.5	0.5	0.5	0
	18.3	77.95	0	0	0.5	0.5	0.5	0.5	0
	18.4	78	0	0	0.5	0.5	0.5	0.5	0
Sub-economic	57.2A	86.9	5	0	1	2	2	0.5	0
	57.1B	86.95	3	0	0.5	2	1	0.5	0
	19.1	87.6	0	0	2	1	0.5	0.5	0
	19.2	87.65	2	0	2	0.5	0.5	0.5	0
	19.3	87.7	3	0	0.5	1	0.5	0.5	0
	59.4	88.9	2	0	1	2	0.5	1	0
	61	91	3	0	3	2	1	1	0
	66.1	97.5	3	0	1	0.5	1	0.5	0
	66.3	97.55	3	0.5	0.5	0.5	0.5	0.5	0
	66.4	97.6	4	0	0.5	0.5	0.5	0	0

Appendix E-5.11 Bioclast and siliciclast shape and modal sizes from thin section study of quarry limestones. Note that (B) = bioclasts and (S) = siliciclasts and that there are two modal sizes for each. Grain size classes are based on the Wentworth scale; fs = fine sand, ms = medium sand, cs = coarse sand, vcs = very coarse sand, g = granule. mod. abraded = moderately abraded, sl. abraded = slightly abraded.

Sample/thin section No.	Quarry unit	BIOCLASTS					SILICICLASTS				
		Bioclast shape	(B)Modal size 1 (mm)	Grain size class	(B)Modal size 2 (mm)	Grain size class	Siliciclast shape	Grain size class	(S)Modal size 1	(S)Modal size 2 (mm)	Grain size class
20	Caprock	mod. abraded	0.36	ms	0.31	ms	subrounded	ms	0.29	0.14	fs
21	Caprock	mod. abraded	0.29	ms	0.96	cs	subrounded	fs	0.19	0.12	fs
9.1	Caprock	mod. abraded	1.08	vcs	0.31	ms	subrounded	ms	0.29	0.14	fs
9.2	Caprock	mod. abraded	0.72	cs	1.3	vcs	angular	fs	0.12	0.24	fs
23.1	Caprock	mod. abraded	0.34	ms	0.72	cs	subrounded	fs	0.19	0.07	vfs
23.2	Caprock	mod. abraded	0.6	cs	0.48	ms	angular	ms	0.26	0.19	fs
27	Caprock	mod. abraded	0.29	ms	0.6	cs	subrounded	fs	0.24	0.17	fs
10.1	Upper Steel	mod. abraded	0.84	cs	0.36	ms	angular	fs	0.19	0.14	fs
10.2	Upper Steel	mod. abraded	0.48	ms	0.72	cs	subrounded	fs	0.19	0.14	fs
10.3	Upper Steel	mod. abraded	0.12	fs	0.24	fs	angular	fs	0.12	0.24	fs
24.1	Upper Steel	mod. abraded	1.32	vcs	0.72	cs	subrounded	fs	0.12	0.26	ms
24.2	Upper Steel	mod. abraded	1.08	vcs	3.6	g	subrounded	g	2.4	0.34	ms
24.3	Upper Steel	mod. abraded	1.68	vcs	0.72	cs	angular	ms	0.34	0.24	fs
25	Upper Steel	mod. abraded	1.2	vcs	0.96	cs	subrounded	ms	0.36	0.24	fs
30	Upper Steel	mod. abraded	0.72	cs	2.52	g	subrounded	ms	0.36	0.24	fs
32	Aglime	mod. abraded	1.2	vcs	0.36	ms	subrounded	vfs	0.1	0.19	fs
34	Aglime	mod. abraded	1.2	vcs	0.55	cs	angular	fs	0.24	0.1	vfs
35	Aglime	sl. abraded	1.68	vcs	0.6	cs	subrounded	cs	0.05	0.19	fs
11	Aglime	mod. abraded	1.56	vcs	0.84	cs	subrounded	ms	0.48	0.12	fs
12.1	Aglime	mod. abraded	0.38	ms	1.08	vcs	subrounded	fs	0.19	0.07	vfs
12.2	Aglime	sl. abraded	0.96	cs	0.72	cs	angular	vfs	0.1	0.19	fs
12.3	Aglime	sl. abraded	0.05	cs	0.17	cs	angular	cs	0.05	0.17	fs
13.1	Aglime	sl. abraded	1.92	vcs	0.43	ms	angular	fs	0.19	0.07	vfs
13.2	Aglime	sl. abraded	1.08	vcs	0.48	ms	angular	fs	0.17	0.12	fs
13.3	Aglime	sl. abraded	0.48	ms	1.56	vcs	subrounded	fs	0.12	0.07	vfs
38	High Grade	mod. abraded	1.44	vcs	1.68	vcs	subrounded	fs	0.14	0.24	fs
14	High Grade	sl. abraded	1.68	vcs	0.72	cs	subrounded	fs	0.17	0.1	vfs
40	High Grade	mod. abraded	1.32	vcs	0.72	cs	angular	fs	0.14	0.1	vfs
40.2	High Grade	mod. abraded	0.72	vcs	1.56	vcs	angular	fs	0.12	0.168	fs
15.1	High Grade	sl. abraded	1.44	vcs	0.48	ms	angular	fs	0.12	0.19	fs

Appendix E-5.11 continued.

Sample/thin section No.	Quarry unit	BIOCLASTS					SILICICLASTS				
		Bioclast shape	(B)Modal size 1 (mm)	Grain size class	(B)Modal size 2 (mm)	Grain size class	Siliciclast shape	(S)Modal size 1	Grain size class	(S)Modal size 2 (mm)	Grain size class
15.2	High Grade	sl. abraded	1.56	vcs	0.48	ms	subrounded	0.22	fs	0.1	vfs
15.3	High Grade	sl. abraded	0.48	ms	0.84	cs	subrounded	0.24	fs	0.1	vfs
15.4	High Grade	mod. abraded	1.44	vcs	0.6	cs	subrounded	0.22	fs	0.07	vfs
43	High Grade	mod. abraded	0.96	cs	2.16	g	angular	0.17	fs	0.1	vfs
47	Lower Steel	slightly abraded	1.92	fs	1.44	vcs	subrounded	0.22	fs	0.14	fs
49.1	Lower Steel	sl. abraded	0.6	cs	1.08	vcs	subrounded	0.19	fs	0.24	fs
49.2	Lower Steel	sl. abraded	1.56	vcs	0.43	ms	subrounded	0.12	fs	0.1	vfs
51	Lower Steel	sl. abraded	1.68	vcs	3.12	g	anhedral	0.72	cs	0.36	ms
17.1	Lower Steel	mod. abraded	0.72	cs	1.68	vcs	subrounded	0.34	ms	0.19	fs
17.2	Lower Steel	mod. abraded	0.72	cs	1.44	vcs	angular	0.48	ms	0.19	fs
17.3	Lower Steel	mod. abraded	1.32	vcs	1.2	vcs	subrounded	0.48	ms	0.19	fs
16	Lower Steel	sl. abraded	2.04	g	1.2	vcs	subrounded	0.14	fs	0.09	vfs
55	Lower Steel	mod. abraded	1.68	vcs	0.96	cs	subrounded	0.58	cs	0.24	fs
18.1	Lower Steel	mod. abraded	1.44	vcs	0.84	cs	subrounded	0.29	ms	0.48	ms
18.2	Lower Steel	mod. abraded	0.96	cs	2.04	g	subrounded	0.29	ms	0.6	cs
18.3	Lower Steel	mod. abraded	0.96	cs	2.88	g	subrounded	0.29	ms	0.48	ms
18.4	Lower Steel	sl. abraded	2.16	g	0.97	cs	subrounded	0.36	ms	0.24	fs
57.2A	Sub-economic	sl. abraded	1.68	vcs	0.84	cs	angular	0.24	fs	0.12	fs
57.1B	Sub-economic	mod. abraded	1.92	vcs	0.84	cs	subrounded	0.1	vfs	0.17	fs
19.1	Sub-economic	mod. abraded	2.16	g	0.72	cs	subrounded	0.53	cs	0.19	fs
19.2	Sub-economic	sl. abraded	1.44	vcs	2.64	g	subrounded	0.24	fs	0.19	fs
19.3	Sub-economic	mod. abraded	1.2	vcs	0.72	cs	subrounded	0.36	ms	0.19	fs
59.4	Sub-economic	sl. abraded	1.8	vcs	1.2	vcs	subrounded	0.36	ms	0.17	fs
61	Sub-economic	sl. abraded	2.04	g	1.08	vcs	angular	0.24	fs	0.14	fs
66.1	Sub-economic	mod. abraded	1.56	vcs	0.84	cs	angular	0.29	ms	0.12	fs
66.3	Sub-economic	mod. abraded	1.68	vcs	2.4	g	subrounded	0.17	fs	0.12	fs
66.4	Sub-economic	sl. abraded	1.92	vcs	0.72	cs	subrounded	0.29	ms	0.12	fs

NB: (B) = bioclast (S) = siliciclast

Appendix E-5.12 Laser particle size results

Malvern data		Samples							
mm		**117**		**146**		**114**		**141**	
Size Low	Phi size	Vol.% In	Cum vol.% In	Vol.% In	Cum vol.% In	Vol.% In	Cum vol.% In	Vol.% In	Cum vol.% In
1	0	0	0	0	0	0	0	0	0
0.84	0.5	0	0	0	0	0	0	0	0
0.71	1	0	0	0	0	0	0	0	0
0.59	1.5	0	0	0	0	0	0	0	0
0.5	2	0	0	0	0	0	0	0	0
0.42	2.25	0	0	0	0	0	0	0	0
0.35	2.5	0	0	0	0	0	0	0	0
0.3	2.75	0	0	0	0	0	0	0	0
0.25	3	0.21	0.21	0	0	0	0	0	0
0.21	3.25	0.4	0.61	0	0	0	0	0.02	0.02
0.177	3.5	0.55	1.16	0	0	0	0	0.32	0.34
0.149	3.75	0.65	1.81	0	0	0	0	1.32	1.66
0.125	4	0.72	2.53	0	0	0	0	2.18	3.84
0.105	4.25	0.76	3.29	0	0	0	0	3.05	6.89
0.088	4.5	0.85	4.14	0.41	0.41	0.01	0.01	3.99	10.88
0.074	4.75	0.96	5.1	1.08	1.49	0.14	0.15	4.49	15.37
0.063	5	1.06	6.16	1.88	3.37	0.27	0.42	4.25	19.62
0.053	5.25	1.4	7.56	3.13	6.5	0.42	0.84	4.16	23.78
0.044	5.5	1.94	9.5	4.71	11.21	0.61	1.45	3.76	27.54
0.037	5.75	2.38	11.88	5.52	16.73	0.77	2.22	2.97	30.51
0.031	6	3.16	15.04	6.51	23.24	1.14	3.36	2.7	33.21
0.0156	6.25	18.93	33.97	26.53	49.77	10.68	14.04	11.95	45.16
0.0078	6.5	19.49	53.46	18.85	68.62	20.1	34.14	16.28	61.44
0.0039	6.75	14.85	68.31	11.01	79.63	21.2	55.34	13.37	74.81
0.002	7	11.15	79.46	7.01	86.64	17.89	73.23	9.35	84.16
0.00098	7.25	7.91	87.37	5.1	91.74	13.41	86.64	6.59	90.75
0.0007	7.5	2.47	89.84	1.77	93.51	3.94	90.58	1.98	92.73
0.00049	7.75	2.51	92.35	1.77	95.28	3.11	93.69	1.8	94.53
0.00024	8	5.47	97.82	3.44	98.72	4.53	98.22	3.55	98.08
0.00012	8.25	2.01	99.83	1.19	99.91	1.6	99.82	1.65	99.73
0.00006	8.5	0.17	100	0.1	100.01	0.19	100.01	0.26	99.99
0.00005	8.75	0	100	0	100.01	0	100.01	0.01	100

Appendix E-5.12 continued.

Malvern data		Samples							
mm		**138**		**143**		**108**		**118**	
Size Low	Phi size	Vol.% In	Cum vol.% In	Vol.% In	Cum vol.% In	Vol.% In	Cum vol.% In	Vol.% In	Cum vol.% In
1	0	0	0	0	0	0	0	0	0
0.84	0.5	0	0	0	0	0	0	0	0
0.71	1	0	0	0	0	0	0	0	0
0.59	1.5	0	0	0	0	0	0	0	0
0.5	2	0	0	0	0	0	0	0	0
0.42	2.25	0	0	0	0	0	0	0	0
0.35	2.5	0	0	0	0	0	0	0	0
0.3	2.75	0	0	0	0	0	0	0	0
0.25	3	0	0	0	0	0	0	0	0
0.21	3.25	0	0	0	0	0	0	0	0
0.177	3.5	0	0	0	0	0	0	0	0
0.149	3.75	0	0	0	0	0	0	0.11	0.11
0.125	4	0	0	0	0	0	0	0.93	1.04
0.105	4.25	0	0	0	0	0	0	1.91	2.95
0.088	4.5	0.25	0.25	0	0	0	0	2.91	5.86
0.074	4.75	0.74	0.99	0	0	0.02	0.02	3.53	9.39
0.063	5	1.13	2.12	0	0	0.2	0.22	3.52	12.91
0.053	5.25	1.68	3.8	0	0	0.56	0.78	3.7	16.61
0.044	5.5	2.41	6.21	0.18	0.18	0.94	1.72	3.73	20.34
0.037	5.75	3.01	9.22	0.99	1.17	1.21	2.93	3.32	23.66
0.031	6	4.04	13.26	1.93	3.1	1.71	4.64	3.71	27.37
0.0156	6.25	23.81	37.07	17.19	20.29	15.47	20.11	18.66	46.03
0.0078	6.5	23.98	61.05	23.91	44.2	25.39	45.5	19.85	65.88
0.0039	6.75	16.77	77.82	20.97	65.17	22.99	68.49	13.95	79.83
0.002	7	11.06	88.88	15.5	80.67	16.11	84.6	9.64	89.47
0.00098	7.25	7.48	96.36	10.27	90.94	10.48	95.08	7.03	96.5
0.0007	7.5	2.35	98.71	2.67	93.61	3.18	98.26	2.26	98.76
0.00049	7.75	1.3	100.01	2	95.61	1.75	100.01	1.24	100
0.00024	8	0	100.01	3.09	98.7	0	100.01	0	100
0.00012	8.25	0	100.01	1.16	99.86	0	100.01	0	100
0.00006	8.5	0	100.01	0.14	100	0	100.01	0	100
0.00005	8.75	0	100.01	0	100	0	100.01	0	100

Appendix E-5.12 continued.

Malvern data		Samples							
mm		**139**		**144**		**72**		**160**	
Size Low	Phi size	Vol.% In	Cum vol.% In	Vol.% In	Cum vol.% In	Vol.% In	Cum vol.% In	Vol.% In	Cum vol.% In
1	0	0	0	0	0	0	0	0	0
0.84	0.5	0	0	0	0	0	0	0	0
0.71	1	0	0	0	0	0	0	0	0
0.59	1.5	0	0	0	0	0	0	0	0
0.5	2	0	0	0	0	0	0	0	0
0.42	2.25	0	0	0	0	0	0	0	0
0.35	2.5	0	0	0.16	0.16	0	0	0	0
0.3	2.75	0	0	1.2	1.36	0	0	0	0
0.25	3	0.31	0.31	2.7	4.06	0.13	0.13	0.24	0.24
0.21	3.25	0.86	1.17	3.42	7.48	0.27	0.4	0.42	0.66
0.177	3.5	1.46	2.63	3.61	11.09	0.32	0.72	0.56	1.22
0.149	3.75	2.09	4.72	3.51	14.6	0.37	1.09	0.66	1.88
0.125	4	2.67	7.39	3.29	17.89	0.49	1.58	0.75	2.63
0.105	4.25	3.04	10.43	3	20.89	0.73	2.31	0.85	3.48
0.088	4.5	3.35	13.78	2.9	23.79	1.17	3.48	1.05	4.53
0.074	4.75	3.45	17.23	2.93	26.72	1.73	5.21	1.3	5.83
0.063	5	3.28	20.51	2.79	29.51	2.2	7.41	1.52	7.35
0.053	5.25	3.52	24.03	3.06	32.57	2.97	10.38	2	9.35
0.044	5.5	3.68	27.71	3.34	35.91	3.77	14.15	2.56	11.91
0.037	5.75	3.25	30.96	3.12	39.03	3.86	18.01	2.73	14.64
0.031	6	3.13	34.09	3.16	42.19	4.11	22.12	3.1	17.74
0.0156	6.25	10.61	44.7	11.86	54.05	15.98	38.1	14.25	31.99
0.0078	6.5	9.73	54.43	11.46	65.51	16.2	54.3	16.65	48.64
0.0039	6.75	10.16	64.59	10.37	75.88	15.75	70.05	16.81	65.45
0.002	7	9.78	74.37	8.2	84.08	12.22	82.27	13.45	78.9
0.00098	7.25	9.39	83.76	6.43	90.51	8.29	90.56	9.8	88.7
0.0007	7.5	3.75	87.51	2.22	92.73	2.42	92.98	3.03	91.73
0.00049	7.75	3.75	91.26	2.04	94.77	2.06	95.04	2.56	94.29
0.00024	8	6.62	97.88	3.56	98.33	3.5	98.54	4.06	98.35
0.00012	8.25	1.97	99.85	1.48	99.81	1.32	99.86	1.46	99.81
0.00006	8.5	0.13	99.98	0.22	100.03	0.16	100.02	0.17	99.98
0.00005	8.75	0	99.98	0.01	100.04	0	100.02	0	99.98

Appendix E-5.12 continued.

Malvern data		Samples							
mm		**71**		**167**		**161**		**163**	
Size Low	Phi size	Vol.% In	Cum vol.% In	Vol.% In	Cum vol.% In	Vol.% In	Cum vol.% In	Vol.% In	Cum vol.% In
1	0	0	0	0	0	0	0	0	0
0.84	0.5	0	0	0	0	0	0	0	0
0.71	1	0	0	0	0	0	0	0	0
0.59	1.5	0	0	0	0	0	0	0	0
0.5	2	0	0	0	0	0	0	0	0
0.42	2.25	0	0	0	0	0	0	0	0
0.35	2.5	0.76	0.76	0	0	0	0	0.31	0.31
0.3	2.75	1.41	2.17	0	0	0	0	1.26	1.57
0.25	3	2.5	4.67	0.22	0.22	0	0	2.67	4.24
0.21	3.25	2.82	7.49	0.42	0.64	0.03	0.03	3.38	7.62
0.177	3.5	2.85	10.34	0.57	1.21	0.08	0.11	3.68	11.3
0.149	3.75	2.78	13.12	0.69	1.9	0.12	0.23	3.72	15.02
0.125	4	2.75	15.87	0.81	2.71	0.14	0.37	3.57	18.59
0.105	4.25	2.76	18.63	0.91	3.62	0.18	0.55	3.21	21.8
0.088	4.5	3.04	21.67	1.05	4.67	0.27	0.82	2.93	24.73
0.074	4.75	3.45	25.12	1.19	5.86	0.45	1.27	2.85	27.58
0.063	5	3.76	28.88	1.29	7.15	0.67	1.94	2.68	30.26
0.053	5.25	4.6	33.48	1.63	8.78	1.07	3.01	3	33.26
0.044	5.5	5.51	38.99	2.11	10.89	1.63	4.64	3.44	36.7
0.037	5.75	5.47	44.46	2.34	13.23	2.03	6.67	3.44	40.14
0.031	6	5.69	50.15	2.79	16.02	2.62	9.29	3.71	43.85
0.0156	6.25	19.34	69.49	13.58	29.6	15.47	24.76	14.59	58.44
0.0078	6.5	12.75	82.24	14.66	44.26	20.82	45.58	12	70.44
0.0039	6.75	8.81	91.05	15.52	59.78	19.81	65.39	9.47	79.91
0.002	7	4.99	96.04	14.41	74.19	14.3	79.69	7.07	86.98
0.00098	7.25	2.02	98.06	11.23	85.42	9.56	89.25	4.7	91.68
0.0007	7.5	0.42	98.48	3.49	88.91	2.86	92.11	1.4	93.08
0.00049	7.75	0.37	98.85	3.09	92	2.45	94.56	1.45	94.53
0.00024	8	0.77	99.62	5.55	97.55	3.99	98.55	3.46	97.99
0.00012	8.25	0.33	99.95	2.19	99.74	1.32	99.87	1.75	99.74
0.00006	8.5	0.05	100	0.26	100	0.12	99.99	0.27	100.01
0.00005	8.75	0	100	0.01	100.01	0	99.99	0.01	100.02

Appendix E-5.12 continued.

Malvern data		Samples							
mm		**152**		**172**		**162**		**171**	
Size Low	Phi size	Vol.% In	Cum vol.% In	Vol.% In	Cum vol.% In	Vol.% In	Cum vol.% In	Vol.% In	Cum vol.% In
1	0	0	0	0	0	0	0	0	0
0.84	0.5	0	0	0	0	0	0	0	0
0.71	1	0	0	0	0	0	0	0	0
0.59	1.5	0	0	0	0	0	0	0	0
0.5	2	0	0	0	0	0	0	0	0
0.42	2.25	0	0	0	0	0	0	0	0
0.35	2.5	0	0	0.01	0.01	0	0	0	0
0.3	2.75	0.3	0.3	0.89	0.9	0.64	0.64	0	0
0.25	3	0.95	1.25	2.23	3.13	2.07	2.71	0.04	0.04
0.21	3.25	1.52	2.77	3.29	6.42	3.26	5.97	1.18	1.22
0.177	3.5	2	4.77	3.98	10.4	4	9.97	2.99	4.21
0.149	3.75	2.28	7.05	4.42	14.82	4.28	14.25	4.73	8.94
0.125	4	2.4	9.45	4.61	19.43	4.05	18.3	5.93	14.87
0.105	4.25	2.34	11.79	4.49	23.92	3.33	21.63	5.83	20.7
0.088	4.5	2.34	14.13	4.4	28.32	2.59	24.22	4.85	25.55
0.074	4.75	2.36	16.49	4.31	32.63	2.34	26.56	3.4	28.95
0.063	5	2.36	18.85	4.02	36.65	2.13	28.69	2.49	31.44
0.053	5.25	2.81	21.66	4.35	41	2.47	31.16	2.13	33.57
0.044	5.5	3.4	25.06	4.74	45.74	3.12	34.28	2.06	35.63
0.037	5.75	3.49	28.55	4.45	50.19	3.47	37.75	2.05	37.68
0.031	6	3.85	32.4	4.51	54.7	4.1	41.85	2.47	40.15
0.0156	6.25	15.94	48.34	15.48	70.18	17.7	59.55	12.83	52.98
0.0078	6.5	14.31	62.65	10.37	80.55	13.64	73.19	13.21	66.19
0.0039	6.75	12.24	74.89	6.81	87.36	9.38	82.57	11.06	77.25
0.002	7	9.97	84.86	4.67	92.03	6.38	88.95	7.63	84.88
0.00098	7.25	7.02	91.88	3.04	95.07	3.95	92.9	4.69	89.57
0.0007	7.5	1.93	93.81	0.9	95.97	1.16	94.06	1.46	91.03
0.00049	7.75	1.63	95.44	0.92	96.89	1.21	95.27	1.63	92.66
0.00024	8	3.1	98.54	2.09	98.98	2.96	98.23	4.25	96.91
0.00012	8.25	1.29	99.83	0.93	99.91	1.52	99.75	2.55	99.46
0.00006	8.5	0.16	99.99	0.11	100.02	0.24	99.99	0.53	99.99
0.00005	8.75	0	99.99	0	100.02	0.01	100	0.02	100.01

Appendix E-5.12 continued.

Malvern data		Samples							
mm		**107**		**166**		**165**		**169**	
Size Low	Phi size	Vol.% In	Cum vol.% In	Vol.% In	Cum vol.% In	Vol.% In	Cum vol.% In	Vol.% In	Cum vol.% In
1	0	0	0	0	0	0	0	0	0
0.84	0.5	0	0	0	0	0	0	0	0
0.71	1	0	0	0	0	0	0	0	0
0.59	1.5	0	0	0	0	0	0	0	0
0.5	2	0	0	0	0	0.08	0.08	0.28	0.28
0.42	2.25	0	0	0	0	0.82	0.9	1.16	1.44
0.35	2.5	0	0	0	0	2.14	3.04	1.76	3.2
0.3	2.75	0	0	0	0	2.31	5.35	1.46	4.66
0.25	3	0	0	0	0	2.67	8.02	1.24	5.9
0.21	3.25	0	0	0	0	2.09	10.11	0.61	6.51
0.177	3.5	0	0	0	0	1.63	11.74	0.36	6.87
0.149	3.75	0	0	0	0	1.59	13.33	0.71	7.58
0.125	4	0	0	0	0	2.05	15.38	1.69	9.27
0.105	4.25	0.55	0.55	0	0	2.83	18.21	3.05	12.32
0.088	4.5	1.42	1.97	0.44	0.44	3.76	21.97	4.57	16.89
0.074	4.75	2.24	4.21	1.23	1.67	4.41	26.38	5.73	22.62
0.063	5	2.85	7.06	1.94	3.61	4.41	30.79	6.11	28.73
0.053	5.25	3.63	10.69	3.02	6.63	4.61	35.4	6.87	35.6
0.044	5.5	4.25	14.94	4.25	10.88	4.8	40.2	7.09	42.69
0.037	5.75	4.15	19.09	4.58	15.46	4.23	44.43	6.25	48.94
0.031	6	4.45	23.54	5	20.46	4.07	48.5	5.88	54.82
0.0156	6.25	19.86	43.4	19.35	39.81	14.25	62.75	17.53	72.35
0.0078	6.5	19.24	62.64	18.19	58	13.18	75.93	11.36	83.71
0.0039	6.75	14.48	77.12	16.9	74.9	10.53	86.46	6.99	90.7
0.002	7	10.31	87.43	12.64	87.54	6.88	93.34	3.56	94.26
0.00098	7.25	6.53	93.96	7.83	95.37	4.28	97.62	1.87	96.13
0.0007	7.5	1.64	95.6	2.1	97.47	1.27	98.89	0.55	96.68
0.00049	7.75	1.3	96.9	1.83	99.3	1.11	100	0.59	97.27
0.00024	8	2.26	99.16	0.71	100.01	0	100	1.45	98.72
0.00012	8.25	0.78	99.94	0	100.01	0	100	1	99.72
0.00006	8.5	0.06	100	0	100.01	0	100	0.28	100
0.00005	8.75	0	100	0	100.01	0	100	0.01	100.01

Appendix E-5.12 continued.

Malvern data		Samples							
mm		**109**		**164**		**168**		**154**	
Size Low	Phi size	Vol.% In	Cum vol.% In	Vol.% In	Cum vol.% In	Vol.% In	Cum vol.% In	Vol.% In	Cum vol.% In
1	0	0	0	0	0	0	0	0	0
0.84	0.5	0	0	0	0	0	0	0	0
0.71	1	0	0	0	0	0	0	0	0
0.59	1.5	0	0	0	0	0	0	0	0
0.5	2	0	0	0	0	0	0	0	0
0.42	2.25	0	0	0	0	0.11	0.11	0	0
0.35	2.5	0	0	0	0	0.67	0.78	0	0
0.3	2.75	0	0	0	0	1.09	1.87	0	0
0.25	3	0	0	0	0	1.45	3.32	0	0
0.21	3.25	0	0	0	0	1.21	4.53	0	0
0.177	3.5	0	0	0	0	1.01	5.54	0	0
0.149	3.75	0	0	0	0	1.09	6.63	0	0
0.125	4	0.61	0.61	0	0	1.57	8.2	0	0
0.105	4.25	2.13	2.74	0	0	2.29	10.49	0	0
0.088	4.5	3.46	6.2	0.01	0.01	3.18	13.67	0	0
0.074	4.75	4.34	10.54	0.64	0.65	3.89	17.56	0	0
0.063	5	4.43	14.97	0.99	1.64	4.14	21.7	0	0
0.053	5.25	4.74	19.71	1.59	3.23	4.78	26.48	0.16	0.16
0.044	5.5	4.75	24.46	2.32	5.55	5.24	31.72	1.28	1.44
0.037	5.75	4.1	28.56	2.76	8.31	4.8	36.52	1.82	3.26
0.031	6	4.1	32.66	3.43	11.74	4.82	41.34	2.65	5.91
0.0156	6.25	16.52	49.18	19.03	30.77	17.56	58.9	17.79	23.7
0.0078	6.5	16.99	66.17	22.02	52.79	15.17	74.07	22.67	46.37
0.0039	6.75	13.74	79.91	18.06	70.85	11.43	85.5	19.69	66.06
0.002	7	9.73	89.64	12.99	83.84	7.28	92.78	14.86	80.92
0.00098	7.25	6.59	96.23	8.43	92.27	4.5	97.28	9.86	90.78
0.0007	7.5	2	98.23	2.26	94.53	1.4	98.68	2.63	93.41
0.00049	7.75	1.77	100	1.78	96.31	1.31	99.99	2.06	95.47
0.00024	8	0	100	2.75	99.06	0	99.99	3.22	98.69
0.00012	8.25	0	100	0.86	99.92	0	99.99	1.17	99.86
0.00006	8.5	0	100	0.07	99.99	0	99.99	0.14	100
0.00005	8.75	0	100	0	99.99	0	99.99	0	100

Appendix E-5.12 continued.

Malvern data		Samples					
		127		126		22	
mm	Phi size	%in vol	%in cum	%in vol	%in cum	%in vol	%in cum
1	0	0	0	0	0	0	0
0.84	0.5	1	1	0.12	0.12	0.07	0.07
0.71	1	1.11	2.11	1.06	1.18	0.98	1.05
0.59	1.5	3.18	5.29	2.81	3.99	3.17	4.22
0.5	2	1.74	7.03	1.62	5.61	1.76	5.98
0.42	2.25	1.95	8.98	1.86	7.47	1.93	7.91
0.35	2.5	6.45	15.43	6.13	13.6	6.38	14.29
0.3	2.75	9.23	24.66	8.69	22.29	9.24	23.53
0.25	3	12.01	36.67	11.02	33.31	11.83	35.36
0.21	3.25	13.83	50.5	11.39	44.7	13.31	48.67
0.177	3.5	18.29	68.79	12.5	57.2	17.99	66.66
0.149	3.75	5.6	74.39	3.81	61.01	5.68	72.34
0.125	4	5.43	79.82	4.02	65.03	5.57	77.91
0.105	4.25	5.42	85.24	4.59	69.62	5.6	83.51
0.088	4.5	4.33	89.57	4.51	74.13	4.48	87.99
0.074	4.75	3.23	92.8	4.19	78.32	3.32	91.31
0.063	5	2.56	95.36	4.26	82.58	2.59	93.9
0.053	5.25	1.75	97.11	3.91	86.49	1.72	95.62
0.044	5.5	1.12	98.23	3.35	89.84	1.06	96.68
0.037	5.75	0.77	99	2.85	92.69	0.7	97.38
0.031	6	0.6	99.6	2.32	95.01	0.71	98.09
0.0156	6.25	0.52	100.12	1.89	96.9	0.81	98.9
0.0078	6.5	0.44	100.56	1.52	98.42	0.62	99.52
0.0039	6.75	0.27	100.83	1.09	99.51	0.36	99.88
0.002	7	0.06	100.89	0.46	99.97	0.12	100
0.00098	7.25	0	100.89	0.002	99.972	0	100
0.0007	7.5	0	100.89	0	99.972	0	100
0.00049	7.75	0	100.89	0	99.972	0	100
0.00024	8	0	100.89	0	99.972	0	100
0.00012	8.25	0	100.89	0	99.972	0	100
0.00006	8.5	0	100.89	0	99.972	0	100
0.00005	8.75	0	100.89	0	99.972	0	100

Appendix E-5.13 Petrographic descriptions of dissolution seams: Results from thin section study of dissolution seams (discrete and diffuse) in quarry limestones. This table includes information such as % silica, % $CaCO_3$ within each seam, seam thickness, and actual percentages of siliciclastic grains (clay, quartz and feldspar, glauconite pellets, and pyrite grains) alongside abundance limits. These limits are abbreviated as ab = absent (0%), r = rare (<1%), s = some (1-5%), m = many (5-15%), c = common (15-25%), vc = very common (25-50%), a = abundant (50-75%), and va = very abundant (>75%). Sample depth = along hole.

Sample number	Sample depth (m)	Quarry unit	%Silica	%$CaCO_3$	Seam thickness (mm)	Seam type	%Clay	Abund.	%Quartz and feldspar	Abund.	%Glauc.	Abund.
32	37	Aglime	70	30	5	discrete	49	vc	20	c	1	s
35	39.45	Aglime	40	60	4	discrete	35	vc	3	s	1	s
11	40.2	Aglime	60	40	1	discrete	40	vc	19	c	1	s
12.1	41.2	Aglime	9	91	2	discrete	5	s	2	s	0	ab
12.2	41.25	Aglime	40	60	4	discrete	10	m	4	s	1	s
13.1	42.8	Aglime	30	70	40	diffuse	25	c	5	s	0	ab
13.2	42.85	Aglime	40	60	40	diffuse	59	a	10	m	1	s
13.3	42.9	Aglime	60	40	40	diffuse	54	a	5	s	1	s
40	54.8	High Grade	80	20	2	discrete	49	vc	20	c	1	s
40.2	54.85	High Grade	70	30	2	discrete	20	c	30	vc	0	ab
15.1	56.65	High Grade	30	70	1	discrete	18	c	2	s	0	ab
15.2	56.7	High Grade	20	80	4	discrete	5	s	7	m	1	s
15.3	56.75	High Grade	30	70	4	discrete	22	c	3	s	0	ab
15.4	56.8	High Grade	20	80	6	discrete	5	s	4	s	1	s
43	62.1	High Grade	70	30	3	discrete	48	vc	20	c	2	s
51	72.6	Lower Steel	90	10	2	discrete	20	c	69	a	1	s
16	74.1	Lower Steel	80	20	1	discrete	64	a	15	m	1	s
55	76.3	Lower Steel	90	10	1	discrete	50	vc	40	vc	0	ab
18.2	77.9	Lower Steel	90	10	1	discrete	45	vc	40	vc	2	s
57.1B	86.95	Sub-economic	50	50	1	discrete	30	vc	15	m	5	s
19.2	87.65	Sub-economic	90	10	1	discrete	57	a	30	vc	3	s
19.3	87.7	Sub-economic	30	70	1	discrete	19	c	10	m	1	s
61	91	Sub-economic	30	70	40	diffuse	0	ab	9	m	1	s

Appendix E-5.13 continued.

Sample number	Sample depth (m)	Quarry unit	%Pyrite grains	Abund.	Grain shape	Grain shape abbrev.	Modal size (mm)	Grain size class
32	37	Aglime	0	ab	subangular	sa	0.200	fs
35	39.45	Aglime	1	s	subrounded	sr	0.100	vfs
11	40.2	Aglime	0	ab	rounded	r	0.250	ms
12.1	41.2	Aglime	2	s	subrounded	sr	0.200	fs
12.2	41.25	Aglime	25	vc	subangular	sa	0.125	fs
13.1	42.8	Aglime	0	ab	subangular	sa	0.125	fs
13.2	42.85	Aglime	0	ab	angular	a	0.075	vfs
13.3	42.9	Aglime	0	ab	subangular	sa	0.075	vfs
40	54.8	High Grade	10	m	subangular	sa	0.150	fs
40.2	54.85	High Grade	20	c	subrounded	sr	0.150	fs
15.1	56.65	High Grade	10	m	subrounded	sr	0.075	vfs
15.2	56.7	High Grade	7	m	subangular	sa	0.100	vfs
15.3	56.75	High Grade	5	m	subrounded	sr	0.175	fs
15.4	56.8	High Grade	10	m	subrounded	sr	0.175	fs
43	62.1	High Grade	0	ab	subangular	sa	0.250	ms
51	72.6	Lower Steel	0	ab	rounded	r	0.750	cs
16	74.1	Lower Steel	0	ab	subangular	sa	0.150	fs
55	76.3	Lower Steel	0	ab	subrounded	sr	0.300	ms
18.2	77.9	Lower Steel	1	s	subangular	sa	0.250	ms
57.1B	86.95	Sub-economic	0	ab	rounded	r	0.250	ms
19.2	87.65	Sub-economic	0	ab	subangular	sa	0.250	ms
19.3	87.7	Sub-economic	0	ab	subangular	sa	0.375	ms
61	91	Sub-economic	5	s	angular	a	0.225	fs

Appendix E-5.13 continued.

Sample number	Sample depth (m)	Quarry unit	Description
32	37	Aglime	Oxidised, 5 mm thick, 1 mm seam branching off, limonite very common, quartz & feldspar dominant, glauconite, clay, minor pyrite
35	39.45	Aglime	4 mm thick, 2 mm thick, glauconite, clay dominant, minor quartz & feldspar, minor pyrite
11	40.2	Aglime	Thin seam 1-2 mm thick, quartz - big round crystals 0.45 mm long, clay, limonite, glauconite
12.1	41.2	Aglime	Thin seams, quartz and limonite concentrated in seams
12.2	41.25	Aglime	4 mm and 1 mm thick, unoxidised, pyrite grains, glauconite, quartz & feldspars
13.1	42.8	Aglime	Clay dominant, limonite, minor quartz & feldspar
13.2	42.85	Aglime	Limonite, clay, quartz & feldspar, glauconite
13.3	42.9	Aglime	Meandering wispy seams, quartz & feldspar, clay, limonite
40	54.8	High Grade	2 mm thick, diagonal, unoxidised, clay & pyrite, quartz & feldspar
40.2	54.85	High Grade	3 mm thick, unoxidised, quartz & feldspar, clay & pyrite
15.1	56.65	High Grade	<1 mm thick, unoxidised, seam filled with pyrite, minor quartz & feldspar, clay
15.2	56.7	High Grade	4 mm thick, unoxidised, pyrite dominated, glauconite, quartz & feldspar, clay
15.3	56.75	High Grade	4 mm thick, mud sized particles in seam micrite?or clay?, unoxidised, pyrite dominant, quartz & feldspar, clay
15.4	56.8	High Grade	5 mm thick, unoxidised, grains packed near seam- more open fabric elsewhere, pyrite, glauconite, quartz & feldspar, clay
43	62.1	High Grade	2 mm thick, oxidised, limonite, clay, glauconite, quartz & feldspar dominant
51	72.6	Lower Steel	3 mm thick, oxidised, quartz & feldspar dominant - large crystals 0.7 mm long, clay, glauconite
16	74.1	Lower Steel	1 mm thick, oxidised, limonite, clay, quartz & feldspar, pyrite, glauconite
55	76.3	Lower Steel	1 mm thick, oxidised, diagonal, limonite rich, clay dominant, quartz & feldspar - large crystals
18.2	77.9	Lower Steel	1.5 mm thick,oxidised, limonitised full of pyrite, clay, quartz & feldspar - huge crystals 0.5 mm long, glauconite
57.1B	86.95	Sub-economic	Broken <1 mm seam, oxidised, limonite, clay, rounded glauconite, quartz & feldspars
19.2	87.65	Sub-economic	2 mm seam, oxidised, quartz & feldspar dominant, glauconite, clay dominant also, limonite
19.3	87.7	Sub-economic	Two 1 mm thick seams, clay, oxidised, glauconite, quartz & feldspar
61	91	Sub-economic	Pyrite along wisps, unoxidised, glauconite, clay, quartz & feldspar dominant

Appendix E-5.14 Sieve results

Sieve data		Samples							
		164		168		107		169	
mm	Phi size	Wt % In	Cum wt% In	Wt % In	Cum wt% In	Wt % In	Cum wt% In	Wt % In	Cum wt% In
32	-5	0	0	0	0	30	30	0	0
22.63	-4.5	17	17	2	2	0	30	7	7
16	-4	15	32	21	23	8	38	15	22
11.31	-3.5	12	44	12	35	2	40	6	28
8	-3	9	53	12	47	3	43	10	38
5.66	-2.5	4	57	9	56	1	44	7	45
4	-2	3	60	6	62	2	46	5	50
2.83	-1.5	2	62	3	65	1	47	3	53
2	-1	1	63	2	67	1	48	2	55
1.41	-0.5	0	63	0	67	0	48	0	55

Sieve data		Samples					
		154		165		109	
mm	Phi size	Wt % In	Cum wt% In	Wt % In	Cum wt% In	Wt % In	Cum wt% In
32	-5	0	0	28	28	0	0
22.63	-4.5	28	28	0	28	0	0
16	-4	0	28	3	31	12	12
11.31	-3.5	6	34	0	31	15	27
8	-3	2	36	0	31	7	34
5.66	-2.5	2	38	0	31	4	38
4	-2	1	39	0	31	4	42
2.83	-1.5	1	40	0	31	2	44
2	-1	0	40	0	31	1	45
1.41	-0.5	0	40	0	31	0	45

Appendix E-5.15 Palygorskite EDAX spectra results

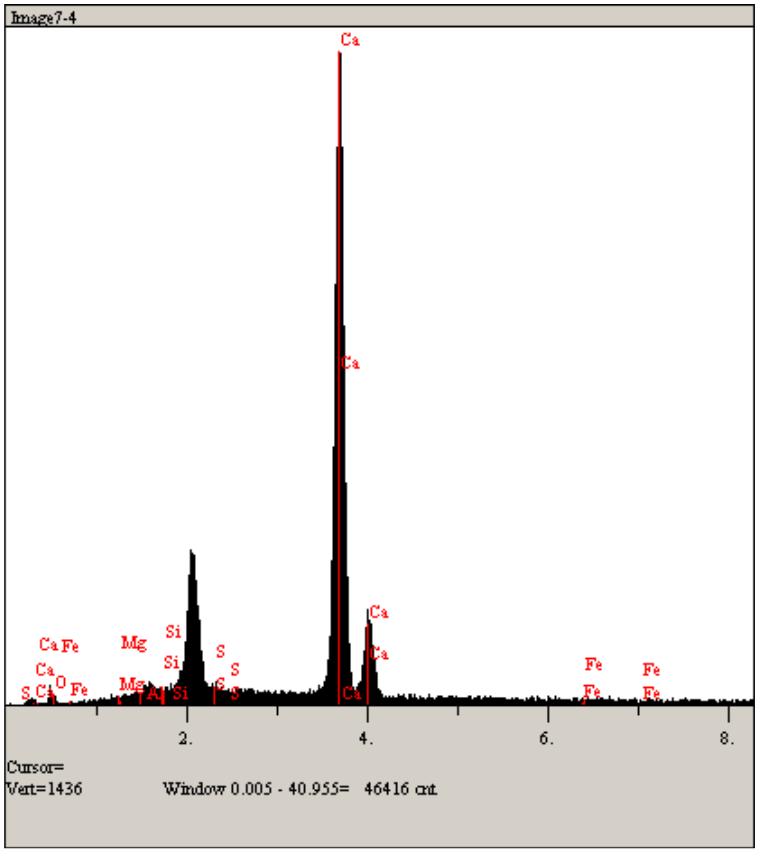

Results from the scanning electron microscope energy dispersive analyser for sample 105 (palygorskite). The main element peaks shown are Ca (calcium), Si (silica), Mg (magnesium), oxygen (O), sulphur (S), and Fe (iron). Sample 105, northern face, Lower Steel.

Appendix E-5.16 Grain size distribution results for discontinuity types

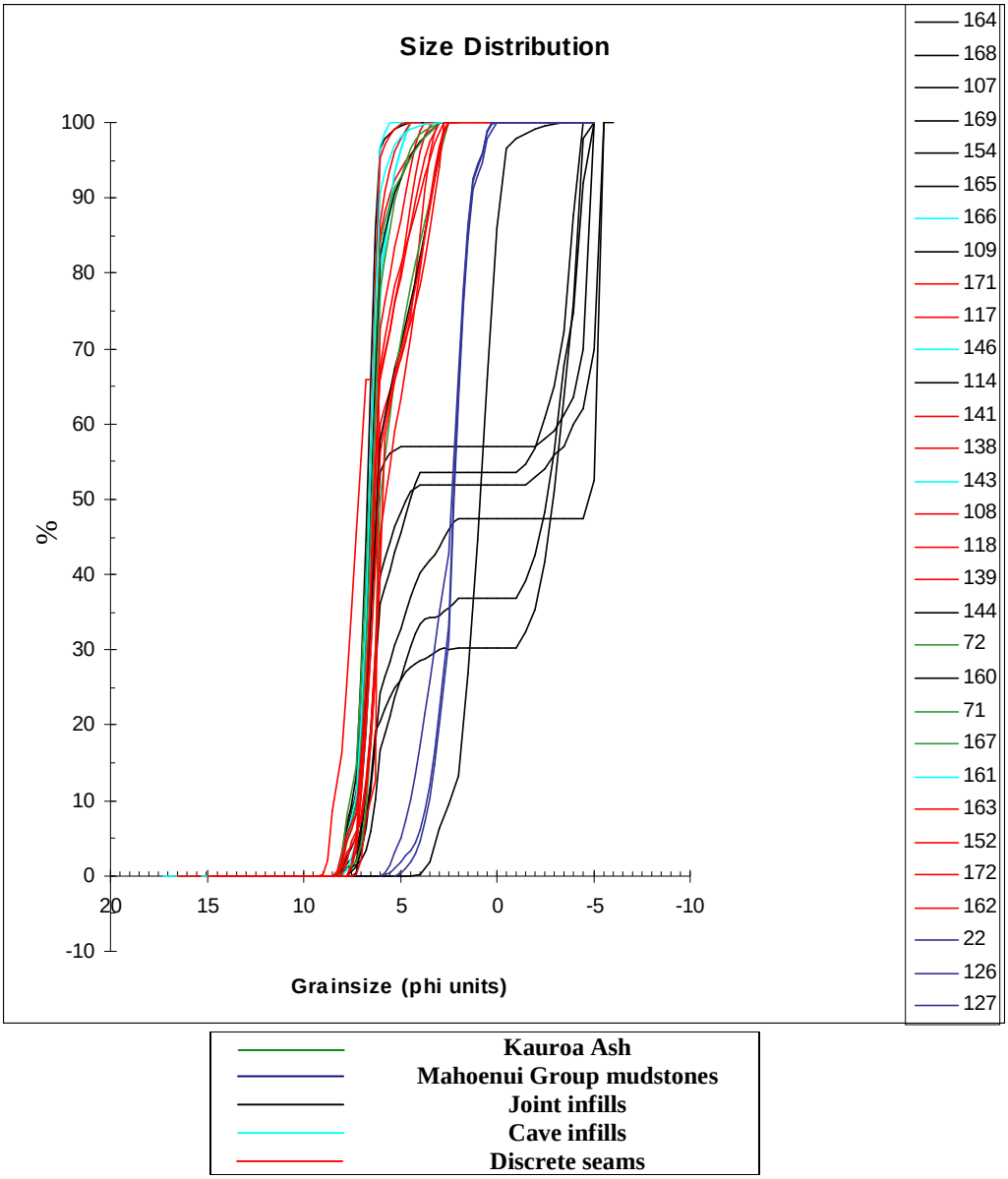

Cumulative graph showing a summary of combined texture (sieve and laser particle size) data including the grain size distribution of Kauroa Ash, Mahoenui Group mudstone, cave, joint, and discrete seam samples. The top figure shows approximately 30 samples across the discontinuity types, the coloured lines next to the sample numbers shown on the right of the figure correspond to the bottom legend. The Kauroa Ash, cave infill, and discrete seams show a unimodal distribution including clay (10 phi) through to medium silt (5 phi) grain sizes, whereas the joint infills show bimodality and are characterised by clay (10 phi) through to pebble (-5 phi) sized grains.

Appendix F-6.1 Acid titration method for %$CaCO_3$ determination

Sample preparation

Grind sample using an agate mortar and pestle/ring mill to a fine powder and oven dry at 110°C. The autotitrator setup is shown in Figure 1.

Method

1. Record weight of 100 ml sized beaker (titration vessel) and tare.
2. Weigh 0.05 g of powdered sample into tared beaker and record weight.
3. Pipette 30 ml of standard HCl solution with a concentration of 0.1M to sample.
4. Place beaker on a hot plate set at 60°C until effervescing (fizzing) stops to ensure reaction is complete. Swirl occasionally to help reaction. At least an hour is advised, however, do not take samples off hot plate until reaction is complete.
5. Cool to room temperature – this is VERY important because temperature affects pH and the auto-titrator works on measuring the pH.
6. Set auto-titrator to method 006.
7. Flush titrator through and check that there are no air bubbles before running sample.
8. Squirt some distilled water over the probe in a beaker (for waste) to clean every time between samples.
9. Lower probes into beaker and make sure the probe is not touching the sides or bottom of the beaker. Ensure the HCl level covers the end properly.
10. Start mixer (line up matching lines drawn in permanent marker)
11. Back titrate with NaOH 0.1M solution.
12. Push start and it shall back titrate NaOH and stop when it is finished – the titre number is read off the top of the print out labeled RS1 (mL).

Formula for % calcium carbonate determination

$CaCO_3$ =

(conc. HCl x volume) – (conc. NaOH x volume titrated) / 2 x (100.09/1000) x (1/sample weight (g)) x 100

HCl = hydrochloric acid
NaOH = sodium hydroxide
100.09 = molecular weight of calcium carbonate

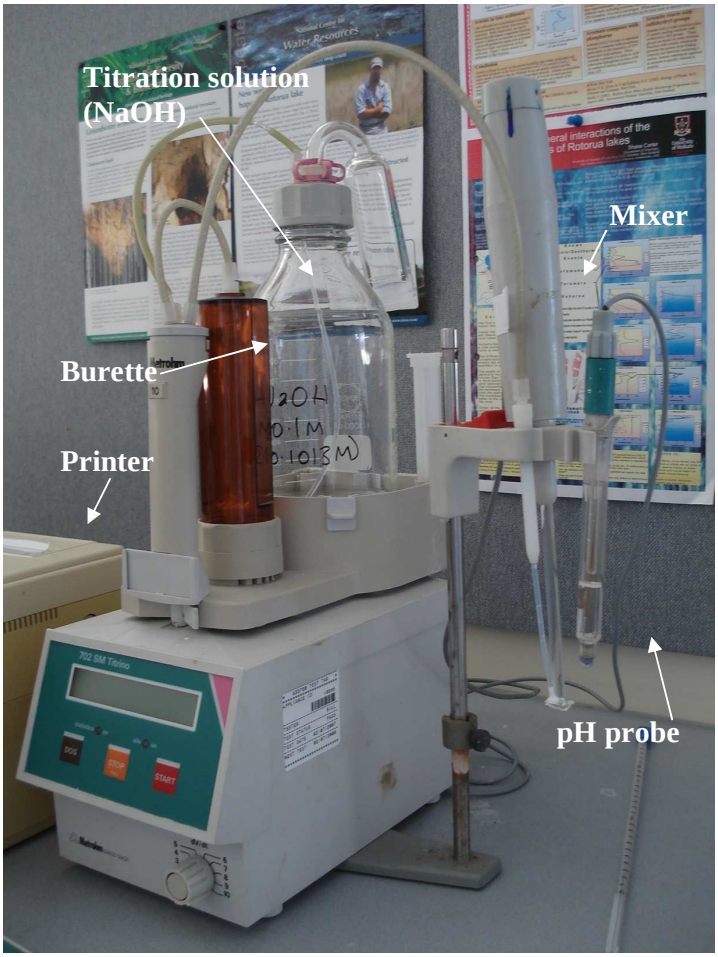

Figure 1 Metrohm Autotitrator, model 702SM Titrino.

Appendix F-6.2 Treatment of errors for acid titration

Measurement errors can be a result of the calibration error (accuracy or tolerance limit) and the reading error (reading accuracy limit) for each piece of equipment used.

To generate errors for the concentrations of the NaOH and HCl, an oxalic acid solution was made up to titrate against the NaOH, which was then titrated against the HCl. Note the total percentage error for the NaOH and HCl are based on previous titrations carried out on similar carbonate samples (pers. Comm. Dabell, 2005). The calculations of each error involved in the acid titration method are as follows:

Oxalic acid		units
Weight	1.2599	g
Molar mass	126.0658	
Moles	0.0100	
Volume	1.0000	l
Concentration	0.0100	mol/l
Errors		
weight		
absolute	0.0002	g
%	0.0159	%
Volume		
absolute	0.4000	ml
%	0.0400	%
Total error	0.0559	%

Total percentage error for NaOH

NaOH		units
Conc Oxalic aid	0.01	mol/l
Volume Oxalic acid	20	ml
Moles of Oxalic acid	0.0002	
moles NaOH = 2x moles Oxalic acid		
therefore moles NaOH	0.0004	
mls NaOH used	4.111	mls
conc NaOH	0.0972999	mol/l
errors oxalic acid %	0.0559	%
volume absolute	0.04	ml
%	0.2	%
burrette absolute	0.02	ml
%	0.4864996	%
Total error for NaOH	0.7424	%

Total percentage error for HCl

HCl		units
Conc NaOH	0.0973	mol/l
volume NaOH	11.361	ml
moles of NaOH	0.001105	
moles NaOH = 1x moles HCl		
therefore moles NaOH	0.001105	
mls HCl used	10	ml

conc		
HCl	0.110542	mol/l
errors		
NaOH		
%	0.7424	%
volume		
absolute	0.04	ml
%	0.4	%
burrette		
absolute	0.04	ml
%	0.352082	%
Total error for		
HCL	1.4945	%

Weight error (balance)

Absolute error in the weight of the sample = ± 0.0002 g

Percentage error in the weight of the sample = $\frac{0.0002}{\text{Sample weight (g)}}$ x 100

= ± *x*%

Volume % for HCl (10 ml pipette)

Absolute volume error in HCl = ± 0.04

Percentage volume error in HCl $= \frac{0.04}{\text{Volume of HCl}}$ x 100

= ± *x*%

Volume % for NaOH (burette)

Absolute volume error in NaOH = ± 0.04

Percentage volume error in NaOH $= \frac{0.04}{\text{Volume titrated}}$ x 100

Appendix F-6.3 Acid titration results for carbonate % determination analyses.

Field sample No. and standards	Quarry unit/sample type	Sample wt. (g)	Conc. HCL (M)	Conc. NaOH (M)	Vol. HCL (ml)	Vol. titre (ml)	Meq of HCL	Moles of CO_3 in sample	Molecular wt. of $CaCO_3$	$\%CaCO_3$	Total % error for HCL	Total % error for NaOH	% Error for wt.	Vol. % for HCL	Vol. % for NaOH	Total % error
9	Caprock	0.0502	0.1024	0.1013	30	21.197	3.072	2	100.09	92.2	1.4942	0.7424	0.3984	0.1333	0.1887	2.9570
27B	Caprock	0.0524	0.1024	0.1013	30	20.704	3.072	2	100.09	93.1	1.4942	0.7424	0.3817	0.1333	0.1932	2.9448
21	Caprock	0.0529	0.1024	0.1013	30	21.261	3.072	2	100.09	86.9	1.4942	0.7424	0.3781	0.1333	0.1881	2.9361
27	Caprock	0.0522	0.1024	0.1013	30	21.736	3.072	2	100.09	83.4	1.4942	0.7424	0.3831	0.1333	0.1840	2.9371
26	Caprock	0.0518	0.1024	0.1013	30	20.791	3.072	2	100.09	93.3	1.4942	0.7424	0.3861	0.1333	0.1924	2.9484
31A	Upper Steel	0.0539	0.1024	0.1013	30	19.824	3.072	2	100.09	98.8	1.4942	0.7424	0.3711	0.1333	0.2018	2.9428
29	Upper Steel	0.056	0.1024	0.1013	30	19.406	3.072	2	100.09	98.9	1.4942	0.7424	0.3571	0.1333	0.2061	2.9332
28	Upper Steel	0.0529	0.1024	0.1013	30	20.103	3.072	2	100.09	98.0	1.4942	0.7424	0.3781	0.1333	0.1990	2.9470
36	Aglime	0.0512	0.1024	0.1013	30	20.694	3.072	2	100.09	95.4	1.4942	0.7424	0.3906	0.1333	0.1933	2.9539
37	Aglime	0.0568	0.1024	0.1013	30	19.728	3.072	2	100.09	94.6	1.4942	0.7424	0.3521	0.1333	0.2028	2.9248
35	Aglime	0.0546	0.1024	0.1013	30	20.111	3.072	2	100.09	94.8	1.4942	0.7424	0.3663	0.1333	0.1989	2.9351
13	Diffuse seam	0.0596	0.1024	0.1013	30	20.439	3.072	2	100.09	84.1	1.4942	0.7424	0.3356	0.1333	0.1957	2.9012
34	Diffuse seam	0.0509	0.1024	0.1013	30	21.546	3.072	2	100.09	87.4	1.4942	0.7424	0.3929	0.1333	0.1856	2.9485
42	High Grade	0.052	0.1024	0.1013	30	20.288	3.072	2	100.09	97.9	1.4942	0.7424	0.3846	0.1333	0.1972	2.9517
39	High Grade	0.0587	0.1024	0.1013	30	18.807	3.072	2	100.09	99.5	1.4942	0.7424	0.3407	0.1333	0.2127	2.9233
41	High Grade	0.0536	0.1024	0.1013	30	20.221	3.072	2	100.09	95.6	1.4942	0.7424	0.3731	0.1333	0.1978	2.9409
46	Lower Steel	0.0584	0.1024	0.1013	30	19.078	3.072	2	100.09	97.6	1.4942	0.7424	0.3425	0.1333	0.2097	2.9221
52	Lower Steel	0.055	0.1024	0.1013	30	19.814	3.072	2	100.09	96.9	1.4942	0.7424	0.3636	0.1333	0.2019	2.9354
48	Lower Steel	0.0509	0.1024	0.1013	30	20.66	3.072	2	100.09	96.3	1.4942	0.7424	0.3929	0.1333	0.1936	2.9565
58	Sub-economic	0.0533	0.1024	0.1013	30	20.348	3.072	2	100.09	94.9	1.4942	0.7424	0.3752	0.1333	0.1966	2.9417
56	Sub-economic	0.0521	0.1024	0.1013	30	20.612	3.072	2	100.09	94.5	1.4942	0.7424	0.3839	0.1333	0.1941	2.9479
60	Sub-economic	0.0577	0.1024	0.1013	30	19.443	3.072	2	100.09	95.6	1.4942	0.7424	0.3466	0.1333	0.2057	2.9223
61	Diffuse seam	0.0519	0.1024	0.1013	30	21.666	3.072	2	100.09	84.6	1.4942	0.7424	0.3854	0.1333	0.1846	2.9399
40% calcite run A	Standard	0.0562	0.1024	0.1013	30	26.226	3.072	2	100.09	37.0	1.4942	0.7424	0.3559	0.1333	0.1525	2.8783
60% calcite run A	Standard	0.0515	0.1024	0.1013	30	24.773	3.072	2	100.09	54.7	1.4942	0.7424	0.3883	0.1333	0.1615	2.9197
80% calcite run A	Standard	0.0515	0.1024	0.1013	30	22.219	3.072	2	100.09	79.8	1.4942	0.7424	0.3883	0.1333	0.1800	2.9383
100% calcite run A	Standard	0.0555	0.1024	0.1013	30	19.702	3.072	2	100.09	97.0	1.4942	0.7424	0.3604	0.1333	0.2030	2.9333
100% quartz run A	Standard	0.0505	0.1024	0.1013	30	30.546	3.072	2	100.09	-2.2	1.4942	0.7424	0.3960	0.1333	0.1310	2.8969
35(1 cm)	Aglime	0.0528	0.1024	0.1013	30	20.616	3.072	2	100.09	93.2	1.4942	0.7424	0.3788	0.1333	0.1940	2.9427
35 (2 cm)	Aglime	0.0559	0.1024	0.1013	30	20.039	3.072	2	100.09	93.3	1.4942	0.7424	0.3578	0.1333	0.1996	2.9273
35 (3 cm)	Aglime	0.0526	0.1024	0.1013	30	20.747	3.072	2	100.09	92.3	1.4942	0.7424	0.3802	0.1333	0.1928	2.9430
35 (top seam)	Discrete seam	0.0569	0.1024	0.1013	30	27.039	3.072	2	100.09	29.3	1.4942	0.7424	0.3515	0.1333	0.1479	2.8694
35 (4 cm)	Aglime	0.057	0.1024	0.1013	30	20.058	3.072	2	100.09	91.3	1.4942	0.7424	0.3509	0.1333	0.1994	2.9202
35 (5 cm)	Aglime	0.0551	0.1024	0.1013	30	20.185	3.072	2	100.09	93.3	1.4942	0.7424	0.3630	0.1333	0.1982	2.9311
35 (6 cm)	Aglime	0.054	0.1024	0.1013	30	20.591	3.072	2	100.09	91.4	1.4942	0.7424	0.3704	0.1333	0.1943	2.9346
35 (7 cm)	Aglime	0.057	0.1024	0.1013	30	19.677	3.072	2	100.09	94.7	1.4942	0.7424	0.3509	0.1333	0.2033	2.9241
35 (middle seam)	Discrete seam	0.0522	0.1024	0.1013	30	28.681	3.072	2	100.09	16.0	1.4942	0.7424	0.3831	0.1333	0.1395	2.8925
35 (8 cm)	Aglime	0.0582	0.1024	0.1013	30	19.71	3.072	2	100.09	92.5	1.4942	0.7424	0.3436	0.1333	0.2029	2.9165
35 (9 cm)	Aglime	0.0537	0.1024	0.1013	30	20.612	3.072	2	100.09	91.7	1.4942	0.7424	0.3724	0.1333	0.1941	2.9364
35 (10 cm)	Aglime	0.054	0.1024	0.1013	30	20.674	3.072	2	100.09	90.6	1.4942	0.7424	0.3704	0.1333	0.1935	2.9338
35 (11 cm)	Aglime	0.0542	0.1024	0.1013	30	20.65	3.072	2	100.09	90.5	1.4942	0.7424	0.3690	0.1333	0.1937	2.9326
35 (12 cm)	Aglime	0.0584	0.1024	0.1013	30	19.682	3.072	2	100.09	92.4	1.4942	0.7424	0.3425	0.1333	0.2032	2.9156
25 (bottom seam)	Discrete seam	0.0573	0.1024	0.1013	30	27.253	3.072	2	100.09	27.2	1.4942	0.7424	0.3490	0.1333	0.1468	2.8657

Appendix F-6.3 continued.

Field sample No. and standards	Quarry unit/sample type	Sample wt. (g)	Conc. HCL (M)	Conc. NaOH (M)	Vol. HCL (ml)	Vol. titre (ml)	Meq of HCL	Moles of CO_3 in sample	Molecular wt. of $CaCO_3$	% $CaCO_3$	Total % error for HCL	Total % error for NaOH	% Error for wt.	Vol. % for HCL	Vol. % for NaOH	Total % error
126	Mahoenui Group	0.0523	0.1024	0.1013	30	26.655	3.072	2	100.09	35.6	1.4942	0.7424	0.3824	0.1333	0.1501	2.9024
127	Mahoenui Group	0.0533	0.1024	0.1013	30	26.679	3.072	2	100.09	34.7	1.4942	0.7424	0.3752	0.1333	0.1499	2.8951
136	Caprock	0.0532	0.1024	0.1013	30	20.171	3.072	2	100.09	96.8	1.4942	0.7424	0.3759	0.1333	0.1983	2.9442
121	Upper Steel	0.0526	0.1024	0.1013	30	20.229	3.072	2	100.09	97.3	1.4942	0.7424	0.3802	0.1333	0.1977	2.9479
123	Upper Steel	0.0569	0.1024	0.1013	30	19.324	3.072	2	100.09	98.0	1.4942	0.7424	0.3515	0.1333	0.2070	2.9284
135	Upper Steel	0.0542	0.1024	0.1013	30	19.813	3.072	2	100.09	98.3	1.4942	0.7424	0.3690	0.1333	0.2019	2.9408
124	Aglime	0.0542	0.1024	0.1013	30	20.227	3.072	2	100.09	94.5	1.4942	0.7424	0.3690	0.1333	0.1978	2.9367
151	Aglime	0.0593	0.1024	0.1013	30	19.249	3.072	2	100.09	94.7	1.4942	0.7424	0.3373	0.1333	0.2078	2.9150
125	Aglime	0.0525	0.1024	0.1013	30	20.699	3.072	2	100.09	93.0	1.4942	0.7424	0.3810	0.1333	0.1932	2.9441
111	High Grade	0.0533	0.1024	0.1013	30	20.308	3.072	2	100.09	95.3	1.4942	0.7424	0.3752	0.1333	0.1970	2.9421
156	High Grade	0.0527	0.1024	0.1013	30	20.336	3.072	2	100.09	96.1	1.4942	0.7424	0.3795	0.1333	0.1967	2.9461
128	High Grade	0.0521	0.1024	0.1013	30	20.180	3.072	2	100.09	98.7	1.4942	0.7424	0.3839	0.1333	0.1982	2.9520
112	Lower Steel	0.0594	0.1024	0.1013	30	18.763	3.072	2	100.09	98.7	1.4942	0.7424	0.3367	0.1333	0.2132	2.9198
153	Lower Steel	0.0555	0.1024	0.1013	30	19.694	3.072	2	100.09	97.1	1.4942	0.7424	0.3604	0.1333	0.2031	2.9334
147	Discrete seam	0.0556	0.1024	0.1013	30	28.049	3.072	2	100.09	20.8	1.4942	0.7424	0.3600	0.1333	0.1426	2.8726
159	Discrete seam	0.0524	0.1024	0.1013	30	27.215	3.072	2	100.09	30.1	1.4942	0.7424	0.3817	0.1333	0.1470	2.8986
138	Discrete seam	0.0562	0.1024	0.1013	30	27.350	3.072	2	100.09	26.8	1.4942	0.7424	0.3559	0.1333	0.1463	2.8721
*139	Leached seam	0.0556	0.1024	0.1013	30	19.711	3.072	2	100.09	96.8	1.4942	0.7424	0.3597	0.1333	0.2029	2.9326
130	Discrete seam	0.0557	0.1024	0.1013	30	27.664	3.072	2	100.09	24.2	1.4942	0.7424	0.3591	0.1333	0.1446	2.8736
110	Discrete seam	0.0596	0.1024	0.1013	30	25.170	3.072	2	100.09	43.9	1.4942	0.7424	0.3356	0.1333	0.1589	2.8644
145	Discrete seam	0.0558	0.1024	0.1013	30	25.146	3.072	2	100.09	47.1	1.4942	0.7424	0.3584	0.1333	0.1591	2.8874
117	Discrete seam	0.0537	0.1024	0.1013	30	27.403	3.072	2	100.09	27.6	1.4942	0.7424	0.3724	0.1333	0.1460	2.8883
141	Discrete seam	0.0584	0.1024	0.1013	30	23.797	3.072	2	100.09	56.7	1.4942	0.7424	0.3425	0.1333	0.1681	2.8805
148	Discrete seam	0.0508	0.1024	0.1013	30	24.103	3.072	2	100.09	62.1	1.4942	0.7424	0.3937	0.1333	0.1660	2.9296
155	Surface accumulation	0.0519	0.1024	0.1013	30	22.823	3.072	2	100.09	73.3	1.4942	0.7424	0.3854	0.1333	0.1753	2.9306
150	Surface accumulation	0.0596	0.1024	0.1013	30	22.244	3.072	2	100.09	68.7	1.4942	0.7424	0.3356	0.1333	0.1798	2.8853
107	Joint infill	0.0503	0.1024	0.1013	30	29.599	3.072	2	100.09	7.3	1.4942	0.7424	0.3976	0.1333	0.1351	2.9027
116	Joint infill	0.0511	0.1024	0.1013	30	20.794	3.072	2	100.09	94.6	1.4942	0.7424	0.3914	0.1333	0.1924	2.9537
119	Joint infill	0.0544	0.1024	0.1013	30	21.277	3.072	2	100.09	84.3	1.4942	0.7424	0.3676	0.1333	0.1880	2.9256
114	Joint infill	0.0529	0.1024	0.1013	30	29.725	3.072	2	100.09	5.8	1.4942	0.7424	0.3781	0.1333	0.1346	2.8826
144	Joint infill	0.0561	0.1024	0.1013	30	21.643	3.072	2	100.09	78.5	1.4942	0.7424	0.3565	0.1333	0.1848	2.9113
102	Joint infill	0.0547	0.1024	0.1013	30	22.485	3.072	2	100.09	72.7	1.4942	0.7424	0.3656	0.1333	0.1779	2.9135
143	Cave infill	0.0515	0.1024	0.1013	30	30.299	3.072	2	100.09	0.3	1.4942	0.7424	0.3883	0.1333	0.1320	2.8903
154	Cave infill	0.0532	0.1024	0.1013	30	29.208	3.072	2	100.09	10.7	1.4942	0.7424	0.3759	0.1333	0.1369	2.8828
146	Cave infill	0.0545	0.1024	0.1013	30	30.616	3.072	2	100.09	-2.7	1.4942	0.7424	0.3670	0.1333	0.1307	2.8676
140	Palygorskite	0.0518	0.1024	0.1013	30	23.292	3.072	2	100.09	68.8	1.4942	0.7424	0.3861	0.1333	0.1717	2.9278
100/101	Palygorskite	0.0590	0.1024	0.1013	30	22.746	3.072	2	100.09	65.1	1.4942	0.7424	0.3390	0.1333	0.1759	2.8848
105	Joint infill	0.0523	0.1024	0.1013	30	20.429	3.072	2	100.09	95.9	1.4942	0.7424	0.3824	0.1333	0.1958	2.9481
100% calcite run B	Standard	0.0574	0.1024	0.1013	30	19.154	3.072	2	100.09	98.7	1.4942	0.7424	0.3484	0.1333	0.2088	2.9272
60% calcite run B	Standard	0.0532	0.1024	0.1013	30	24.122	3.072	2	100.09	59.1	1.4942	0.7424	0.3759	0.1333	0.1658	2.9117
80% calcite run B	Standard	0.0529	0.1024	0.1013	30	22.098	3.072	2	100.09	78.8	1.4942	0.7424	0.3781	0.1333	0.1810	2.9290
100% quartz A	Standard	0.0519	0.1024	0.1013	30	31.261	3.072	2	100.09	-9.1	1.4942	0.7424	0.3854	0.1333	0.1280	2.8832
100% calcite B	Standard	0.0541	0.1024	0.1013	30	21.633	3.072	2	100.09	81.5	1.4942	0.7424	0.3697	0.1333	0.1849	2.9245
80% calcite C	Standard	0.0537	0.1024	0.1013	30	22.217	3.072	2	100.09	76.6	1.4942	0.7424	0.3724	0.1333	0.1800	2.9224
167	Kauroa Ash	0.0515	0.1024	0.1013	30	30.832	3.072	2	100.09	-5.0	1.4942	0.7424	0.3883	0.1333	0.1297	2.8880
hq3a	Caprock	0.0533	0.1024	0.1013	30	22.539	3.072	2	100.09	74.1	1.4942	0.7424	0.3752	0.1333	0.1775	2.9226
hq3b	Caprock	0.0556	0.1024	0.1013	30	19.774	3.072	2	100.09	96.2	1.4942	0.7424	0.3597	0.1333	0.2023	2.9319
71	Kauroa Ash	0.0505	0.1024	0.1013	30	30.617	3.072	2	100.09	-2.9	1.4942	0.7424	0.3960	0.1333	0.1306	2.8966
72	Kauroa Ash	0.0511	0.1024	0.1013	30	30.663	3.072	2	100.09	-3.3	1.4942	0.7424	0.3914	0.1333	0.1305	2.8918

SPECTRACHEM ANALYTICAL

X-RAY FLUORESCENCE ANALYTICAL PROCEDURES FOR MAJOR OXIDE ANALYSIS

1. INITIAL SAMPLE PREPARATION – LIME SAMPLES

The sixty samples were received as pre-ground semi-fine powders. A small number were considered to be fairly coarse and were re-ground in a Zr ring mill.
The samples were oven-dried at 110°C for at least 24 hours prior to the determination of loss on ignition. All remaining material is stored.

2. LOSS ON IGNITION [LOI] DETERMINATION

Oven dried sub-samples of approximately 3g were ignited at 1000°C for 60 minutes.

Following ignition and final weighing, ignited residues were stored at 60°C in air-tight screw-cap vials in readiness for fusion preparation.

LOI calculations from inputted weights were carried out in an Excel database.

3. SAMPLE PREPARATION

- **For Major Oxide Analysis.**

Weighed fractions of ignited sample material were fused with a lithium borate flux in a semi-automated agitating furnace, cast into platinum moulds at 1100°C and air-jet cooled to form glass discs.

Sample fusions were carried out as soon as possible following the determination of ignition loss.

[All geochemical reference standards used for the calibration of individual elements are prepared in exactly the same manner].

4. X-RAY FLUORESCENCE ANALYSIS

- **Instrumentation and Analytical Programs**

Major oxide analyses were carried out using a Siemens SRS3000 wavelength dispersive X-ray spectrometer. The instrument has an automated 90 position sample loader and 3kW Rh anode end window tube.

Automation and all on-line matrix and other inter-element corrections were carried out using the most recent version of Spectra^{plus} software. Measurement times and parameters for major analysis were optimised to lower limits of detection of <0.01%. Results for major oxides are reported to the nearest 0.01%.

- **Standard Reference Materials**

Each of the major oxide analyte lines in the analytical program is calibrated using a combination of matrix-appropriate geochemical SRMs and chemical [synthetic] standards prepared from *Specpure* compounds.

Appendix F-6.5 SpectraChem Analytical XRF report

SPECTRACHEM ANALYTICAL

CLIENT	:	**UNIVERSITY OF WAIKATO**
ADDRESS	:	PRIVATE BAG 3105, HAMILTON
EMAIL	:	koh2@waikato.ac.nz
TEL	:	029 299 0537
ATTENTION	:	ORLA HANSEN **JOB REFERENCE : SA11034**

CLIENT REFERENCE	:	150765
SAMPLE TYPE[S]	:	Limestones / Siltstones - 60 samples.
DATE OF SAMPLE RECEIPT	:	16/07/07 **CONDITION :** DRY POWDERS
ANALYSES CARRIED OUT	:	XRF MAJOR OXIDES
REPORTING BASIS	:	OVEN-DRIED [110℃]

The analytical results presented in this report apply to the sample(s) received by SpectraChem Analytical.

Analysis	***Method used***	***LLD***	***Unit***
LOI	*Ignition loss at 1000 deg.C*	0.01	%
Major oxides	*Borate fusion / X-ray spectrometry*	0.01	%

Comments

Date : 8/1/2007 ***Signed :*** Craig Fraser IANZ Signatory

SpectraChem Analytical Limited : 36 Seaview Rd : Lower Hutt : www.spectrachem.co.nz
P O Box 38-680 Wellington Mail Centre : Tel. 04 589-6333 : Fax. 04 569-6605 : Email. spectra@spectrachem.co.nz

UNIVERSITY OF WAIKATO

JOB REFERENCE : SA11034

X-RAY FLUORESCENCE MAJOR OXIDE ANALYSES

Field sample No.	Fe_2O_3	MnO	TiO_2	CaO	K_2O	SO_3	P_2O_5	SiO_2	Al_2O_3	MgO	Na_2O	LOI	SUM
9	0.58	0.03	0.05	52.45	0.17	0.03	0.11	3.09	0.87	0.75	0.01	41.83	99.96
13	1.04	0.01	0.13	47.00	0.49	0.02	0.06	9.21	2.74	0.89	0.17	38.02	99.78
21	1.57	0.03	0.10	47.99	0.44	0.04	0.20	7.65	1.96	0.96	0.08	38.67	99.69
26	0.61	0.02	0.05	52.19	0.16	0.04	0.11	3.31	0.97	0.81	0.01	41.66	99.93
27	1.40	0.03	0.15	46.02	0.54	0.06	0.21	9.84	2.85	1.08	0.14	37.42	99.74
28	0.05	0.01	0.01	55.51	0.02	<0.01	0.05	0.23	0.06	0.29	<0.01	43.51	99.72
29	0.13	0.01	0.01	54.60	0.06	<0.01	0.09	1.19	0.31	0.38	<0.01	42.83	99.61
31a	0.13	0.01	0.01	54.75	0.04	<0.01	0.06	0.98	0.32	0.39	<0.01	43.07	99.75
34	0.90	0.01	0.09	49.51	0.27	0.82	0.07	6.31	1.88	0.88	0.10	39.05	99.89
35	0.38	0.01	0.03	53.01	0.10	0.38	0.05	2.50	0.78	0.71	0.01	41.97	99.94
36	0.44	0.01	0.04	52.39	0.14	0.44	0.05	2.83	0.90	0.74	0.02	41.75	99.75
37	0.27	0.02	0.03	53.44	0.10	0.02	0.06	2.18	0.62	0.64	0.01	42.45	99.83
39	0.20	0.01	0.01	54.78	0.03	<0.01	0.03	0.76	0.23	0.47	<0.01	43.24	99.78
41	0.27	0.01	0.02	54.16	0.06	0.37	0.04	1.28	0.44	0.57	<0.01	42.73	99.96
42	0.17	0.01	0.01	54.57	0.03	<0.01	0.03	0.98	0.32	0.44	<0.01	43.16	99.71
46	0.12	0.01	0.01	54.91	0.03	<0.01	0.03	0.72	0.23	0.40	<0.01	43.29	99.77
48	0.22	0.01	0.02	54.00	0.06	0.01	0.04	1.37	0.41	0.57	<0.01	42.95	99.66
52	0.19	0.01	0.01	54.15	0.07	0.03	0.03	1.59	0.38	0.53	<0.01	42.87	99.87
56	0.26	0.02	0.02	53.91	0.07	<0.01	0.05	1.54	0.40	0.51	<0.01	42.91	99.68
58	0.44	0.01	0.02	53.96	0.07	0.01	0.06	1.45	0.41	0.54	<0.01	42.85	99.81

LOI = loss on ignition at 1000℃ for 1 hour.
Results are expressed as weight % on oven dried 110℃ basis.

UNIVERSITY OF WAIKATO

JOB REFERENCE : SA11034

X-RAY FLUORESCENCE MAJOR OXIDE ANALYSES

Field sample No.	Fe_2O_3	MnO	TiO_2	CaO	K_2O	SO_3	P_2O_5	SiO_2	Al_2O_3	MgO	Na_2O	LOI	SUM
60	0.18	0.01	0.01	53.95	0.09	0.01	0.05	2.23	0.36	0.43	<0.01	42.51	99.84
61	1.04	0.01	0.10	48.30	0.36	1.01	0.11	7.40	2.06	0.97	0.10	38.33	99.78
100	0.94	0.02	0.07	36.94	0.26	0.26	0.11	20.52	4.33	3.52	0.12	32.89	99.97
102	3.84	0.03	0.08	42.12	0.41	1.32	0.14	14.03	1.84	1.38	0.18	34.45	99.80
107	6.54	0.03	0.64	8.42	1.83	<0.01	0.19	50.76	17.22	2.19	0.38	11.71	99.89
110	5.76	0.06	0.37	26.18	1.68	<0.01	0.37	33.06	7.46	1.59	0.42	22.84	99.79
111	0.19	0.01	0.02	53.70	0.08	0.22	0.03	1.69	0.39	0.85	<0.01	42.74	99.91
112	0.14	0.01	0.01	55.12	0.04	0.02	0.03	0.71	0.18	0.39	<0.01	43.35	99.98
114	6.54	0.05	0.81	1.43	2.19	<0.01	0.18	59.46	18.84	2.81	0.63	6.97	99.91
117	6.82	0.06	0.65	16.59	2.42	<0.01	0.29	41.66	12.03	2.33	0.99	16.10	99.95
118	4.21	0.05	0.48	18.58	1.85	2.51	0.14	36.35	9.81	5.51	1.47	19.02	99.98
119	0.11	0.01	0.01	49.07	0.05	0.12	0.01	7.23	1.48	1.59	<0.01	40.08	99.75
121	0.05	0.01	0.01	55.55	0.02	0.01	0.02	0.28	0.14	0.21	<0.01	43.52	99.82
123	0.15	0.01	0.01	55.09	0.04	<0.01	0.05	0.71	0.25	0.30	<0.01	43.25	99.86
124	0.33	0.01	0.03	53.22	0.11	0.35	0.04	2.00	0.65	0.89	0.01	42.31	99.96
125	0.57	0.01	0.05	51.57	0.16	0.06	0.10	3.51	1.05	1.08	0.04	41.54	99.74
126	4.56	0.05	0.54	21.32	1.83	<0.01	0.17	38.66	10.67	2.00	0.74	19.39	99.92
127	4.65	0.05	0.53	21.72	1.78	2.89	0.13	37.02	10.36	2.04	0.87	17.76	99.81
128	0.24	0.01	0.02	54.04	0.08	0.30	0.05	1.62	0.42	0.57	0.01	42.56	99.92
130	4.73	0.04	0.60	19.57	2.25	<0.01	6.16	39.12	11.82	2.28	1.11	11.60	99.28

LOI = loss on ignition at 1000℃ for 1 hour.
Results are expressed as weight % on oven dried 110℃ basis.

UNIVERSITY OF WAIKATO

JOB REFERENCE : SA11034

X-RAY FLUORESCENCE MAJOR OXIDE ANALYSES

Field sample No.	Fe_2O_3	MnO	TiO_2	CaO	K_2O	SO_3	P_2O_5	SiO_2	Al_2O_3	MgO	Na_2O	LOI	SUM
135	0.08	0.01	0.01	55.39	0.03	0.02	0.02	0.42	0.18	0.27	<0.01	43.44	99.87
138	4.26	0.03	0.55	16.99	2.34	<0.01	0.54	45.11	11.35	1.76	1.70	15.29	99.92
140	0.64	0.02	0.05	38.02	0.20	0.49	0.11	18.86	3.86	3.51	0.02	34.11	99.89
141	3.48	0.03	0.38	24.71	1.48	1.96	0.12	26.73	7.34	6.90	0.78	25.96	99.87
143	8.86	0.05	0.78	1.95	1.86	<0.01	0.36	54.06	21.06	2.07	0.40	8.47	99.91
144	1.14	0.02	0.10	47.33	0.31	0.04	0.09	8.70	2.44	1.02	0.01	38.38	99.59
145	4.86	0.03	0.43	23.57	1.64	4.97	0.33	30.70	7.87	4.30	0.75	20.37	99.82
146	5.57	0.06	0.70	1.04	1.98	<0.01	0.08	61.49	18.64	2.37	1.02	6.88	99.85
147	3.83	0.02	0.28	14.86	2.21	<0.01	0.44	56.67	6.98	0.97	0.78	12.90	99.92
148	3.05	0.04	0.28	35.66	1.03	0.09	0.30	21.96	5.77	1.32	0.26	30.20	99.95
150	1.76	0.02	0.16	40.67	0.57	0.34	0.18	15.08	3.57	2.22	0.21	35.00	99.79
151	0.39	0.01	0.03	52.50	0.14	0.40	0.06	2.64	0.77	0.85	0.05	41.94	99.78
153	0.16	0.01	0.01	54.69	0.05	0.03	0.05	0.90	0.23	0.40	<0.01	43.23	99.75
154	6.44	0.03	0.67	8.91	1.74	<0.01	0.21	49.71	16.87	2.50	0.29	12.57	99.93
155	1.78	0.02	0.20	41.18	0.67	0.86	0.17	12.91	3.72	1.93	0.31	36.04	99.80
156	0.26	0.01	0.02	53.37	0.09	0.31	0.05	1.95	0.48	0.81	<0.01	42.47	99.81
157	0.14	0.01	0.01	54.20	0.06	0.15	0.03	1.44	0.27	0.39	<0.01	42.96	99.67
159	6.99	0.02	0.43	19.05	1.92	<0.01	0.46	42.48	8.30	1.58	1.03	17.45	99.73
HQ3a	2.00	0.03	0.15	43.53	0.64	1.62	0.35	12.09	2.91	1.24	0.29	34.72	99.56
HQ3b	0.29	0.02	0.02	53.97	0.09	0.02	0.13	1.73	0.42	0.50	<0.01	42.66	99.86

LOI = loss on ignition at 1000℃ for 1 hour.
Results are expressed as weight % on oven dried 110℃ basis.

Appendix F-6.6 XRF oxide analyses.

		Major oxides							Minor oxides					
Sample type	Field sample No.	Fe_2O_3	CaO	SiO_2	Al_2O_3	LOI	MgO	Na_2O	MnO	TiO_2	K2O	SO_3	P_2O_5	SUM
Kauroa Ash	502001	9.33	1.23	38.67	27.12	19.29	0.93	0.97	0.08	1.04	0.74	0.14	0.16	99.71
Kauroa Ash	502002	9.59	0.07	29.32	36.01	22.27	0.42	0.13	0.10	1.05	0.25	0.06	0.14	99.43
Kauroa Ash	502003	7.03	<0.01	57.10	21.82	8.84	1.88	<0.01	0.08	0.88	2.01	0.08	0.10	99.82
Mahoenui Gp	126	4.56	21.32	38.66	10.67	19.39	2.00	0.74	0.05	0.54	1.83	0.01	0.17	97.33
Mahoenui	127	4.65	21.72	37.02	10.36	17.76	2.04	0.87	0.05	0.53	1.78	2.89	0.13	94.42
Caprock	HQ3a	2.00	43.53	12.09	2.91	34.72	1.24	0.29	0.03	0.15	0.64	1.62	0.35	96.78
Caprock	9	0.58	52.45	3.09	0.87	41.83	0.75	0.01	0.03	0.05	0.17	0.03	0.11	99.57
Caprock	HQ3b	0.29	53.97	1.73	0.42	42.66	0.50	<0.01	0.02	0.02	0.09	0.02	0.13	99.58
Caprock	21	1.57	47.99	7.65	1.96	38.67	0.96	0.08	0.03	0.10	0.44	0.04	0.20	98.88
Caprock	26	0.61	52.19	3.31	0.97	41.66	0.81	0.01	0.02	0.05	0.16	0.04	0.11	99.56
Caprock	27	1.40	46.02	9.84	2.85	37.42	1.08	0.14	0.03	0.15	0.54	0.06	0.21	98.76
Upper Steel	28	0.05	55.51	0.23	0.06	43.51	0.29	<0.01	0.01	0.01	0.02	<0.01	0.05	99.64
Upper Steel	29	0.13	54.60	1.19	0.31	42.83	0.38	<0.01	0.01	0.01	0.06	<0.01	0.09	99.43
Upper Steel	135	0.08	55.39	0.42	0.18	43.44	0.27	<0.01	0.01	0.01	0.03	0.02	0.02	99.78
Upper Steel	121	0.05	55.55	0.28	0.14	43.52	0.21	<0.01	0.01	0.01	0.02	0.01	0.02	99.75
Upper Steel	31a	0.13	54.75	0.98	0.32	43.07	0.39	<0.01	0.01	0.01	0.04	<0.01	0.06	99.63
Upper Steel	123	0.15	55.09	0.71	0.25	43.25	0.30	<0.01	0.01	0.01	0.04	<0.01	0.05	99.75
Aglime	124	0.33	53.22	2.00	0.65	42.31	0.89	0.01	0.01	0.03	0.11	0.35	0.04	99.42
Aglime	125	0.57	51.57	3.51	1.05	41.54	1.08	0.04	0.01	0.05	0.16	0.06	0.10	99.36
Aglime	35	0.38	53.01	2.50	0.78	41.97	0.71	0.01	0.01	0.03	0.10	0.38	0.05	99.36
Aglime	36	0.44	52.39	2.83	0.90	41.75	0.74	0.02	0.01	0.04	0.14	0.44	0.05	99.07
Aglime	151	0.39	52.50	2.64	0.77	41.94	0.85	0.05	0.01	0.03	0.14	0.40	0.06	99.14
Aglime	37	0.27	53.44	2.18	0.62	42.45	0.64	0.01	0.02	0.03	0.10	0.02	0.06	99.61
High Grade	39	0.20	54.78	0.76	0.23	43.24	0.47	<0.01	0.01	0.01	0.03	<0.01	0.03	99.69
High Grade	111	0.19	53.70	1.69	0.39	42.74	0.85	<0.01	0.01	0.02	0.08	0.22	0.03	99.56
High Grade	156	0.26	53.37	1.95	0.48	42.47	0.81	<0.01	0.01	0.02	0.09	0.31	0.05	99.34
High Grade	128	0.24	54.04	1.62	0.42	42.56	0.57	0.01	0.01	0.02	0.08	0.30	0.05	99.46
High Grade	41	0.27	54.16	1.28	0.44	42.73	0.57	<0.01	0.01	0.02	0.06	0.37	0.04	99.45
High Grade	42	0.17	54.57	0.98	0.32	43.16	0.44	<0.01	0.01	0.01	0.03	<0.01	0.03	99.63
Lower Steel	46	0.12	54.91	0.72	0.23	43.29	0.40	<0.01	0.01	0.01	0.03	<0.01	0.03	99.68
Lower Steel	153	0.16	54.69	0.90	0.23	43.23	0.40	<0.01	0.01	0.01	0.05	0.03	0.05	99.61
Lower Steel	48	0.22	54.00	1.37	0.41	42.95	0.57	<0.01	0.01	0.02	0.06	0.01	0.04	99.53
Lower Steel	157	0.14	54.20	1.44	0.27	42.96	0.39	<0.01	0.01	0.01	0.06	0.15	0.03	99.41
Lower Steel	112	0.14	55.12	0.71	0.18	43.35	0.39	<0.01	0.01	0.01	0.04	0.02	0.03	99.88
Lower Steel	52	0.19	54.15	1.59	0.38	42.87	0.53	<0.01	0.01	0.01	0.07	0.03	0.03	99.71

Appendix F-6.6 continued.

		Major oxides						Minor oxides						
Sample type	Field sample No.	Fe_2O_3	CaO	SiO_2	Al_2O_3	LOI	MgO	Na_2O	MnO	TiO_2	K2O	SO_3	P_2O_5	SUM
Sub-economic	56	0.26	53.91	1.54	0.40	42.91	0.51	<0.01	0.02	0.02	0.07	<0.01	0.05	99.53
Sub-economic	58	0.44	53.96	1.45	0.41	42.85	0.54	<0.01	0.01	0.02	0.07	0.01	0.06	99.65
Sub-economic	60	0.18	53.95	2.23	0.36	42.51	0.43	<0.01	0.01	0.01	0.09	0.01	0.05	99.66
Diffuse seam	13	1.04	47.00	9.21	2.74	38.02	0.89	0.17	0.01	0.13	0.49	0.02	0.06	99.07
Diffuse seam	34	0.90	49.51	6.31	1.88	39.05	0.88	0.10	0.01	0.09	0.27	0.82	0.07	98.63
Diffuse seam	61	1.04	48.30	7.40	2.06	38.33	0.97	0.10	0.01	0.10	0.36	1.01	0.11	98.20
Discrete seam	159	6.99	19.05	42.48	8.30	17.45	1.58	1.03	0.02	0.43	1.92	<0.01	0.46	96.89
Discrete seam	145	4.86	23.57	30.70	7.87	20.37	4.30	0.75	0.03	0.43	1.64	4.97	0.33	92.42
Discrete seam	141	3.48	24.71	26.73	7.34	25.96	6.90	0.78	0.03	0.38	1.48	1.96	0.12	95.91
Discrete seam	147	3.83	14.86	56.67	6.98	12.90	0.97	0.78	0.02	0.28	2.21	<0.01	0.44	96.98
Discrete seam	138	4.26	16.99	45.11	11.35	15.29	1.76	1.70	0.03	0.55	2.34	<0.01	0.54	96.46
Discrete seam	130	4.73	19.57	39.12	11.82	11.60	2.28	1.11	0.04	0.60	2.25	<0.01	6.16	90.23
Discrete seam	110	5.76	26.18	33.06	7.46	22.84	1.59	0.42	0.06	0.37	1.68	<0.01	0.37	97.31
Discrete seam	117	6.82	16.59	41.66	12.03	16.10	2.33	0.99	0.06	0.65	2.42	<0.01	0.29	96.53
Discrete seam	118	4.21	18.58	36.35	9.81	19.02	5.51	1.47	0.05	0.48	1.85	2.51	0.14	94.96
Joint fill	102	3.84	42.12	14.03	1.84	34.45	1.38	0.18	0.03	0.08	0.41	1.32	0.14	97.83
Joint fill	148	3.05	35.66	21.96	5.77	30.20	1.32	0.26	0.04	0.28	1.03	0.09	0.30	98.21
Joint fill	114	6.54	1.43	59.46	18.84	6.97	2.81	0.63	0.05	0.81	2.19	<0.01	0.18	96.69
Joint fill	119	0.11	49.07	7.23	1.48	40.08	1.59	<0.01	0.01	0.01	0.05	0.12	0.01	99.56
Joint fill	144	1.14	47.33	8.70	2.44	38.38	1.02	0.01	0.02	0.10	0.31	0.04	0.09	99.02
Joint fill	107	6.54	8.42	50.76	17.22	11.71	2.19	0.38	0.03	0.64	1.83	<0.01	0.19	97.20
Palygorskite	100	0.94	36.94	20.52	4.33	32.89	3.52	0.12	0.02	0.07	0.26	0.26	0.11	99.26
Palygorskite	140	0.64	38.02	18.86	3.86	34.11	3.51	0.02	0.02	0.05	0.20	0.49	0.11	99.02
Cave infill	143	8.86	1.95	54.06	21.06	8.47	2.07	0.40	0.05	0.78	1.86	<0.01	0.36	96.86
Cave infill	154	6.44	8.91	49.71	16.87	12.57	2.50	0.29	0.03	0.67	1.74	<0.01	0.21	97.29
Cave infill	146	5.57	1.04	61.49	18.64	6.88	2.37	1.02	0.06	0.70	1.98	<0.01	0.08	97.01
Surface accumulation	150	1.76	40.67	15.08	3.57	35.00	2.22	0.21	0.02	0.16	0.57	0.34	0.18	98.51
Surface accumulation	155	1.78	41.18	12.91	3.72	36.04	1.93	0.31	0.02	0.20	0.67	0.86	0.17	97.87

Appendix F-6.7 XRF oxide average values based on the different sample types in Table F-6.6.

	Major oxides							Minor oxides					
Sample type	**Fe_2O_3**	**CaO**	**SiO_2**	**Al_2O_3**	**LOI**	**MgO**	**Na_2O**	**MnO**	**TiO_2**	**K_2O**	**SO_3**	**P_2O_5**	**SUM**
Kauroa Ash	**8.65**	**0.65**	**41.70**	**28.32**	**16.80**	**1.08**	**0.55**	**0.09**	**0.99**	**1.00**	**0.09**	**0.13**	**99.65**
Mahoenui Gp	**6.89**	**32.18**	**57.17**	**10.52**	**28.27**	**3.02**	**0.81**	**0.07**	**0.80**	**2.72**	**1.46**	**0.23**	**145.66**
Caprock	**1.07**	**49.36**	**6.29**	**1.66**	**39.49**	**0.89**	**0.11**	**0.03**	**0.09**	**0.34**	**0.30**	**0.18**	**99.15**
Upper Steel	**0.10**	**55.15**	**0.64**	**0.21**	**43.27**	**0.31**	**<0.01**	**0.01**	**0.01**	**0.04**	**0.01**	**0.05**	**99.73**
Aglime	**0.40**	**52.69**	**2.61**	**0.79**	**41.99**	**0.82**	**0.02**	**0.01**	**0.04**	**0.13**	**0.28**	**0.06**	**99.43**
High Grade	**0.22**	**54.10**	**1.38**	**0.38**	**42.82**	**0.62**	**<0.01**	**0.01**	**0.02**	**0.06**	**0.20**	**0.04**	**99.58**
Lower Steel	**0.16**	**54.51**	**1.12**	**0.28**	**43.11**	**0.45**	**<0.01**	**0.01**	**0.01**	**0.05**	**0.04**	**0.04**	**99.69**
Sub-economic	**0.29**	**53.94**	**1.74**	**0.39**	**42.76**	**0.49**	**<0.01**	**0.01**	**0.02**	**0.08**	**0.01**	**0.05**	**99.69**
Diffuse seams	**0.99**	**48.27**	**7.64**	**2.23**	**38.47**	**0.91**	**0.13**	**0.01**	**0.11**	**0.37**	**0.61**	**0.08**	**98.83**
Discrete seams	**4.99**	**20.01**	**39.10**	**9.22**	**17.95**	**3.02**	**1.00**	**0.04**	**0.46**	**1.98**	**1.05**	**0.98**	**96.78**
Joint infills	**3.54**	**30.67**	**27.02**	**7.93**	**26.96**	**1.72**	**0.29**	**0.03**	**0.32**	**0.97**	**0.26**	**0.15**	**98.59**
Palygorskite	**0.79**	**37.48**	**19.69**	4.09	**33.50**	**3.51**	**0.07**	**0.02**	**0.06**	**0.23**	**0.37**	**0.11**	**99.33**
Cave infills	**6.96**	**3.96**	**55.09**	**18.86**	**9.31**	**2.31**	**0.57**	**0.05**	**0.72**	**1.86**	**<0.01**	**0.22**	**98.03**
Surface accumulations	**1.77**	**40.93**	**13.99**	**3.65**	**35.52**	**2.07**	**0.26**	**0.02**	**0.18**	**0.62**	**0.60**	**0.17**	**98.57**

Appendix F-6.8 Host limestone vs. discrete seams vs. bulk samples

SiO_2	Caprock	Upper Steel	Aglime	High Grade	Lower Steel	Sub-economic
Bulk	5.71	0.93	5.54	2.68	1.97	5.28
Host	6.29	0.64	2.61	1.38	1.12	1.74
Discrete seams	-	42.12	34.91	31.88	49.57	-

Al_2O_3	Caprock	Upper Steel	Aglime	High Grade	Lower Steel	Sub-economic
Bulk	1.57	0.03	1.63	0.72	0.42	0.85
Host	1.66	0.21	0.79	0.38	0.28	0.39
Discrete seams	-	11.58	9.73	7.67	7.64	-

Fe_2O_3	Caprock	Upper Steel	Aglime	High Grade	Lower Steel	Sub-economic
Bulk	1.03	0.14	0.72	0.42	0.30	0.68
Host	1.07	0.10	0.40	0.22	0.16	0.29
Discrete seams	-	4.49	4.84	5.31	5.41	-

CaO	Caprock	Upper Steel	Aglime	High Grade	Lower Steel	Sub-economic
Bulk	49.60	54.30	49.99	52.38	53.16	50.96
Host	49.36	55.15	52.69	54.10	54.51	53.94
Discrete seams	-	18.28	19.96	24.87	16.96	-

LOI	Caprock	Upper Steel	Aglime	High Grade	Lower Steel	Sub-economic
Bulk	40.14	43.20	40.17	42.00	42.67	40.56
Host	39.49	43.27	41.99	42.82	43.11	42.76
Discrete seams	-	13.44	20.36	21.61	15.18	-

MgO	Caprock	Upper Steel	Aglime	High Grade	Lower Steel	Sub-economic
Bulk	0.89	0.39	0.77	0.62	0.52	0.61
Host	0.89	0.31	0.82	0.62	0.45	0.49
Discrete seams		2.02	4.91	2.94	1.27	

SO_3	Caprock	Upper Steel	Aglime	High Grade	Lower Steel	Sub-economic
Bulk	0.71	0.05	0.23	0.30	0.09	0.41
Host	0.30	0.01	0.28	0.20	0.04	0.10
Discrete seams	-	0.01	1.49	2.49	0.01	-

K_2O	Caprock	Upper Steel	Aglime	High Grade	Lower Steel	Sub-economic
Bulk	0.31	0.05	0.28	0.13	0.09	0.21
Host	0.34	0.04	0.13	0.06	0.05	0.08
Discrete seams	-	2.29	1.92	1.66	2.07	-

Na_2O	Caprock	Upper Steel	Aglime	High Grade	Lower Steel	Sub-economic
Bulk	0.12	0.04	0.16	0.11	0.08	0.09
Host	0.11	0.01	0.02	0.01	0.01	0.01
Discrete seams	-	1.41	1.08	0.58	0.90	-

MnO	Caprock	Upper Steel	Aglime	High Grade	Lower Steel	Sub-economic
Bulk	0.04	0.02	0.02	0.01	0.01	0.02
Host	0.03	0.01	0.01	0.01	0.01	0.01
Discrete seams	-	0.03	0.05	0.05	0.02	-

TiO_2	Caprock	Upper Steel	Aglime	High Grade	Lower Steel	Sub-economic
Bulk	0.08	0.01	0.08	0.04	0.02	0.04
Host	0.09	0.01	0.04	0.02	0.01	0.02
Discrete seams	-	0.58	0.50	0.40	0.35	-

P_2O_5	Caprock	Upper Steel	Aglime	High Grade	Lower Steel	Sub-economic
Bulk	0.13	0.05	0.07	0.05	0.04	0.06
Host	0.18	0.05	0.06	0.04	0.04	0.05
Discrete seams	-	3.35	0.18	0.35	0.45	-

Appendix G-7.1

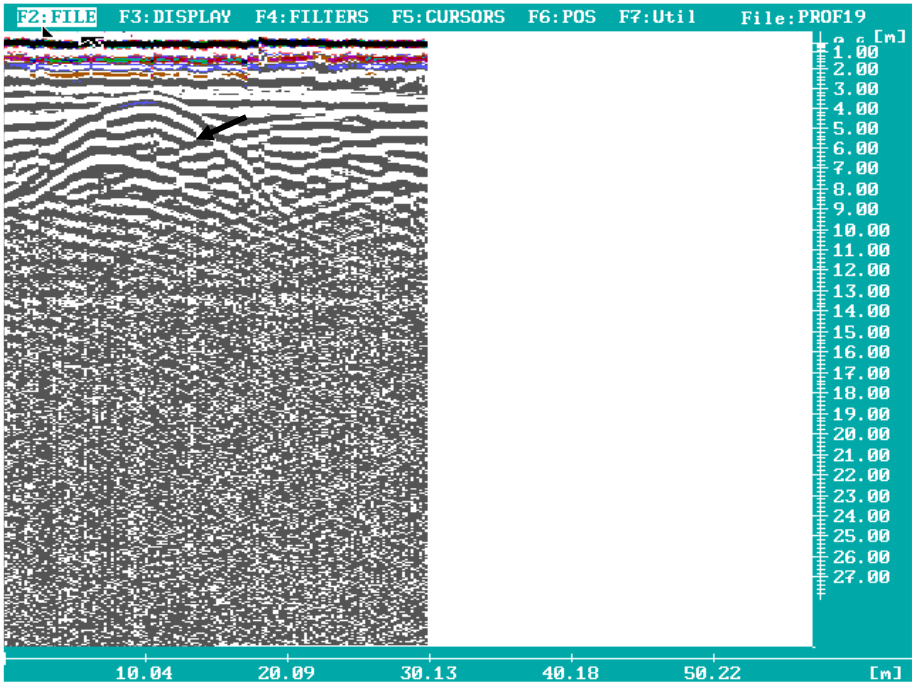

Radar gram of profile 19 trending N-S measured over an observed limestone cave within the second bench of the High Grade unit, western side McDonald's Quarry (2007). A clear reflection of a cave structure is shown by arrow.

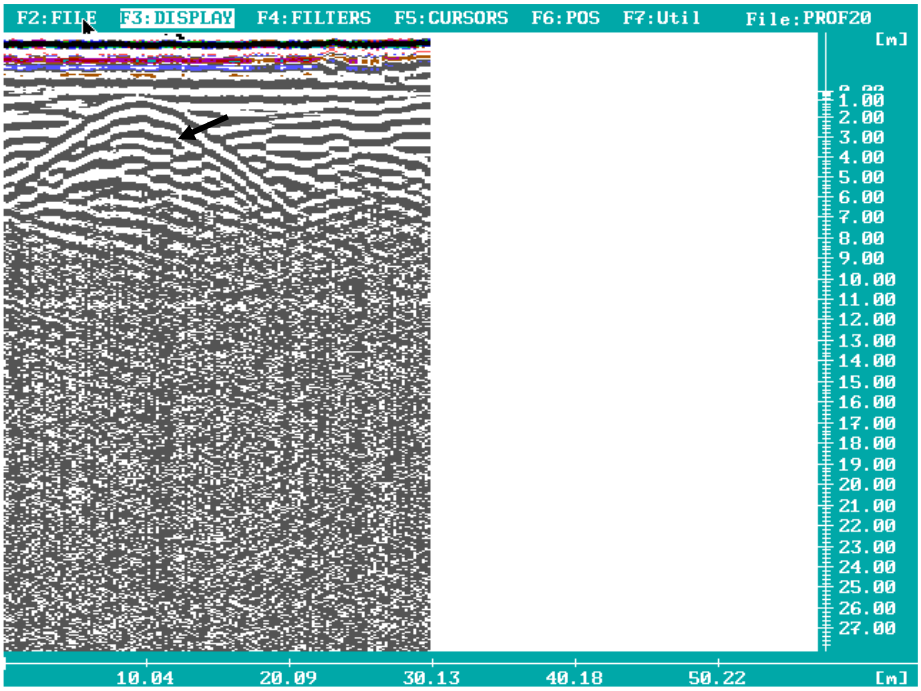

Radar gram of profile 20 trending N-S measured over an observed limestone cave within the second bench of the High Grade unit, western McDonald's Quarry (2007). A clear reflection of a cave structure is shown by arrow.

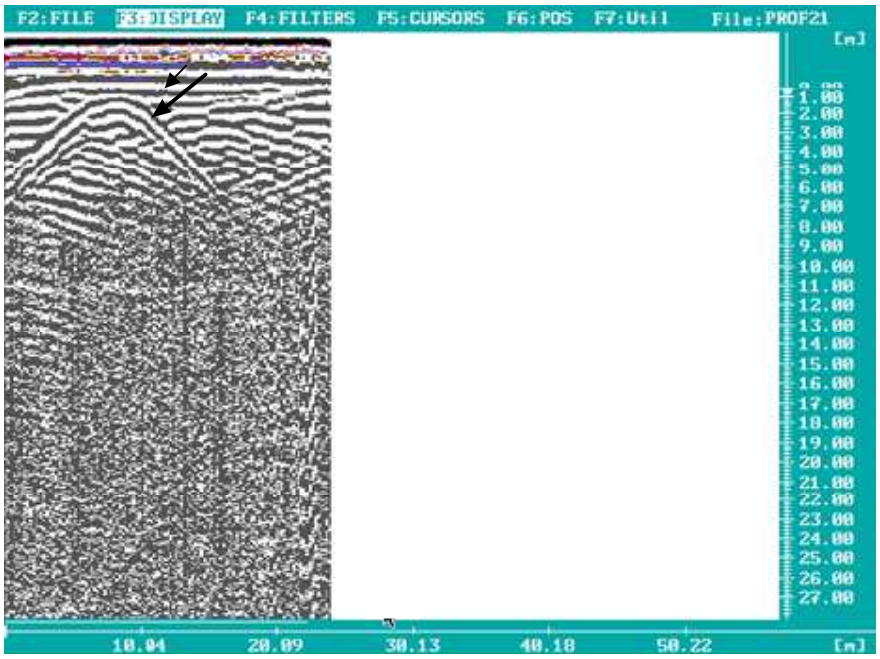

Radar gram of profile 21 trending N-S measured over an observed limestone cave within the second bench of the High Grade unit, western side. A clear reflection of a cave structure is shown by the arrows.

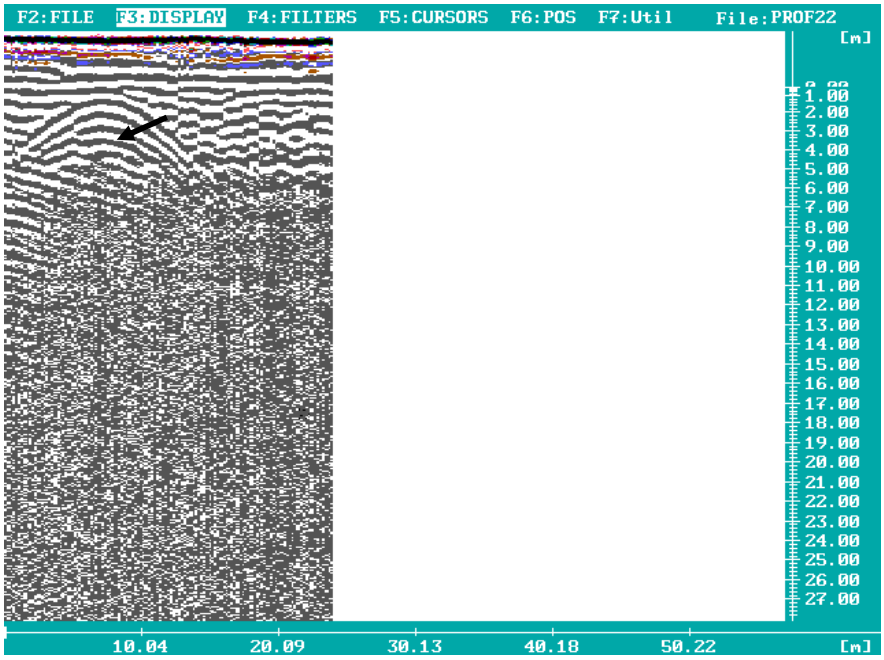

Radar gram of profile 22 trending N-S measured over an observed limestone cave within the second bench of the High Grade unit, western side McDonald's Quarry (2007). A clear reflection of a cave structure is shown by arrow.

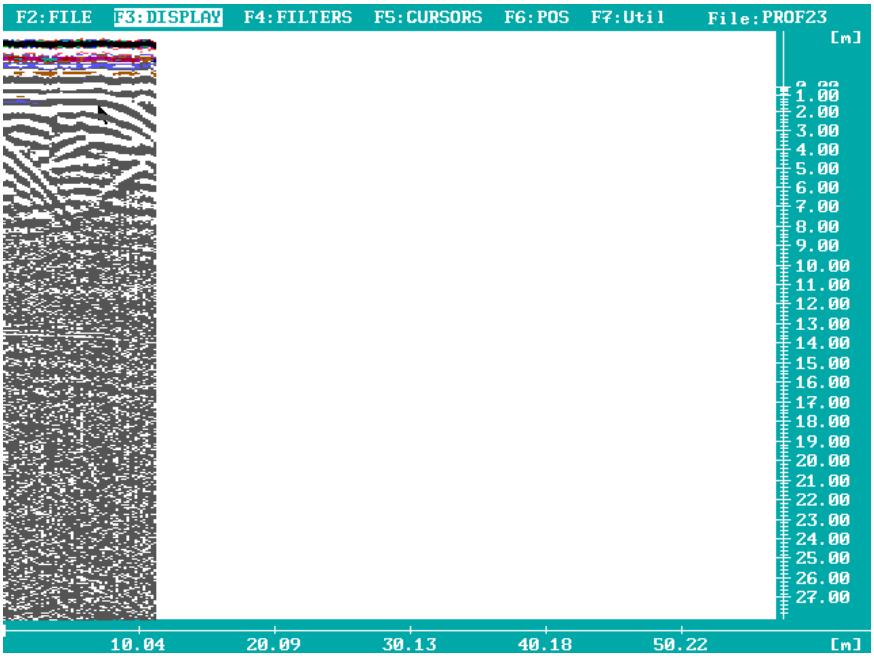

Radar gram of profile 23 trending NNW-SSW measured along the length of an observed limestone cave within the second bench of the High Grade unit, western side McDonald's Quarry (2007).

Radar gram of profile 24 trending NNW-SSW measured along the length of an observed limestone cave within the second bench of the High Grade unit, western side McDonald's Quarry (2007).

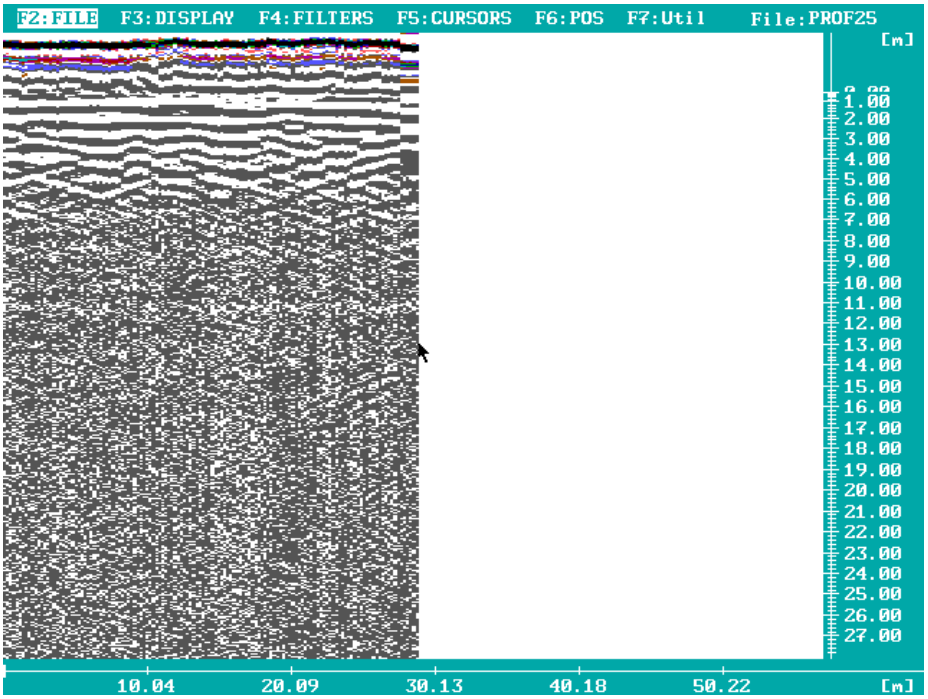

Radar gram of profile 25 trending N-S measured over the second bench of High Grade, western side. No obvious structure appears to be present.

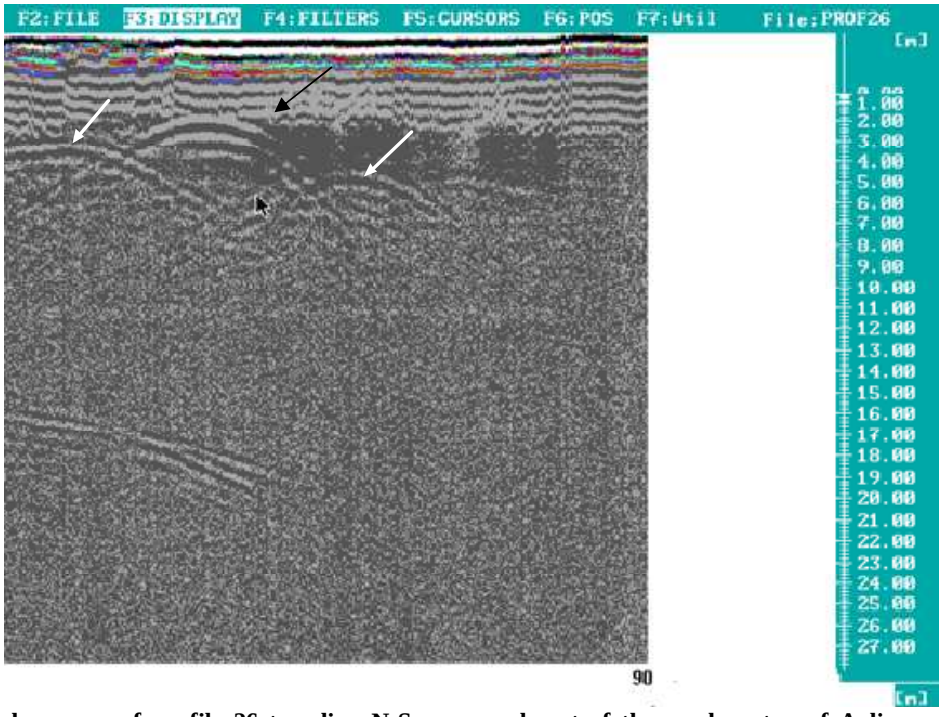

Radar gram of profile 26 trending N-S measured east of the road on top of Aglime unit where a drill hole has intercepted a cavity, western side. The cave observed in the upper bench of the High Grade is approximately 18 m below the transect. The larger black arrow points to a clear reflection indicating a cave structure is present, while the white arrows likely indicate multiples of cave walls. The smaller black arrow is a mouse pointer.

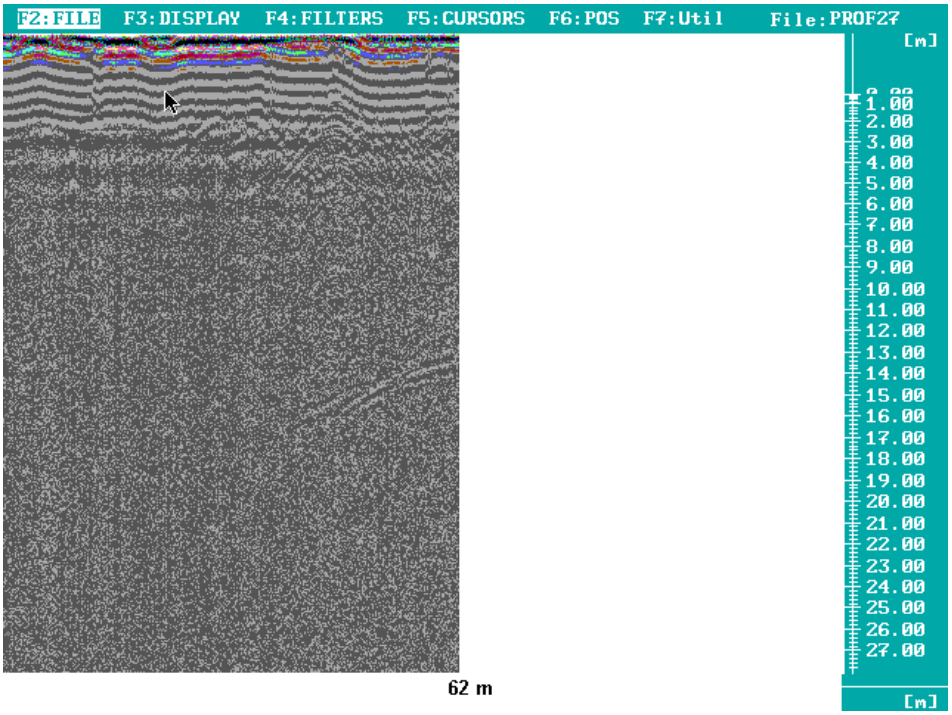

Radar gram of profile 27 trending N-S measured over the west road on top of Aglime unit, western side McDonald's Quarry (2007). The black arrow is a mouse pointer.

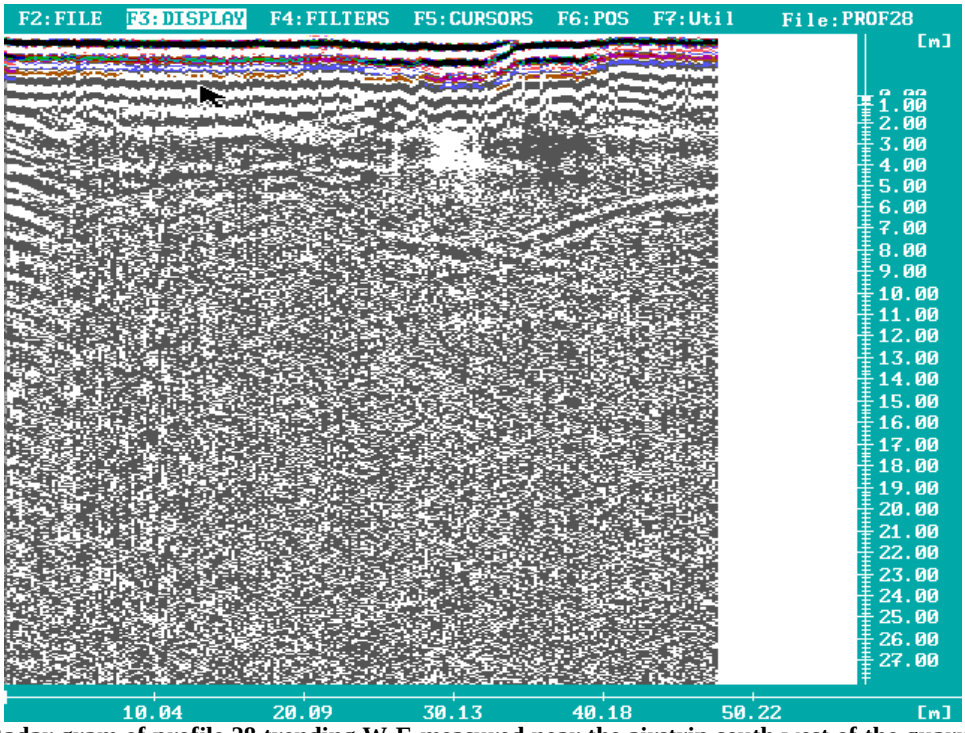

Radar gram of profile 28 trending W-E measured near the airstrip south west of the quarry close to paddock fence. Southern side McDonald's Quarry (2007).

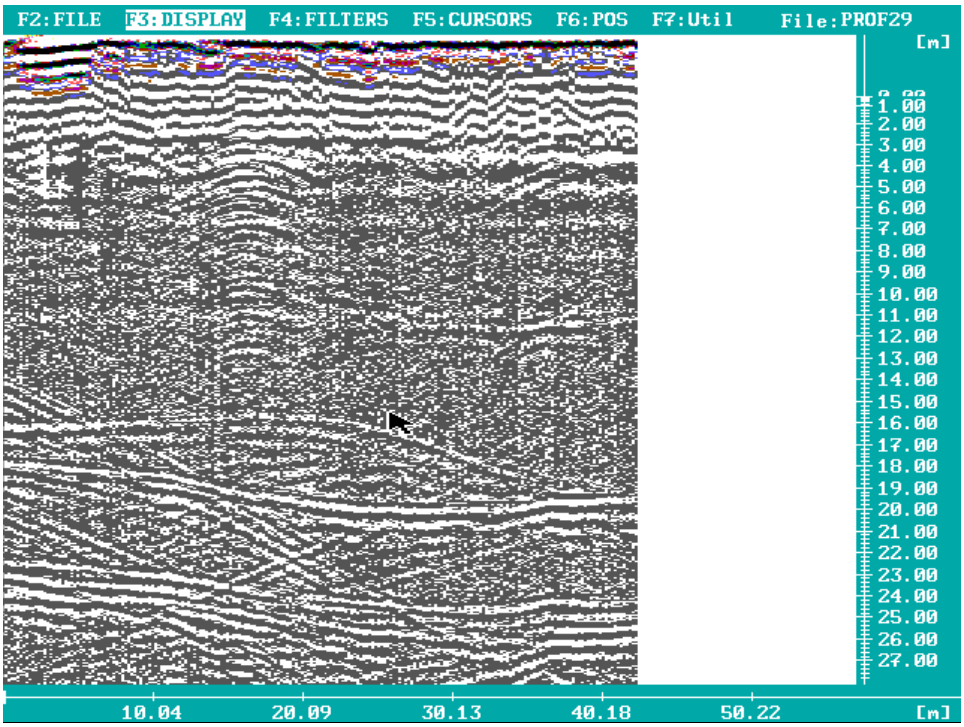

Radar gram of profile 29 trending N-S measured over floor of quarry on top of Sub-economic unit . McDonald's Quarry (2007).

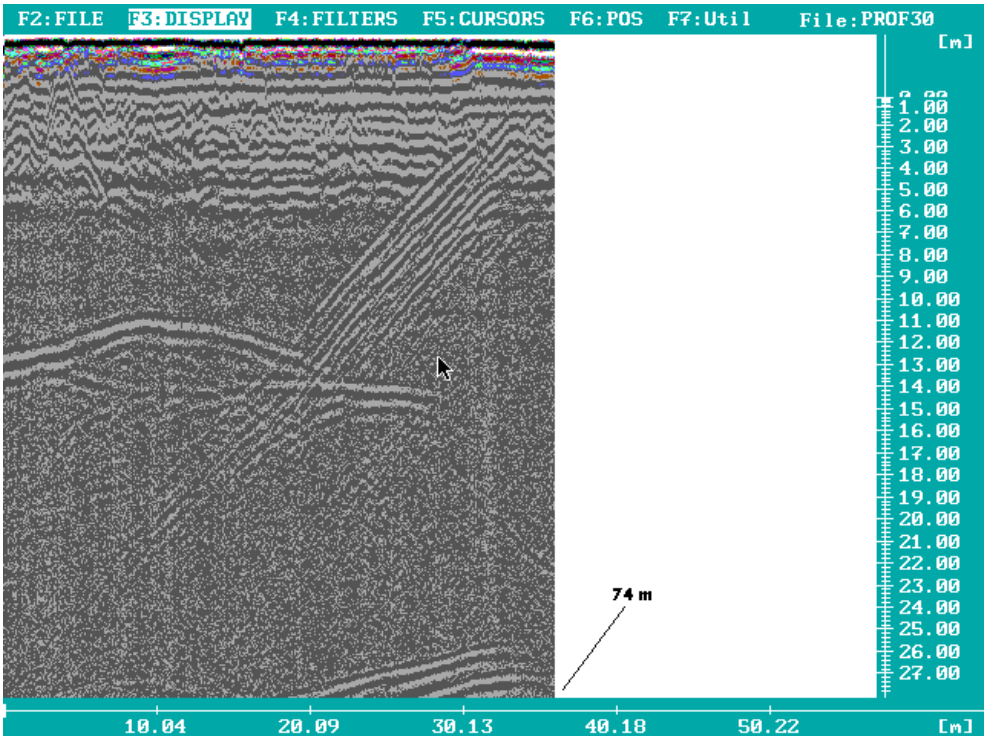

Radar gram of profile 30 trending N-S measured on top of the Lower Steel. To the right of the profile steeply dipping reflectors represent interference caused by a quarry wall and possibly a steel pipe lying on the ground near the end of the transect. The black arrow is a mouse pointer.

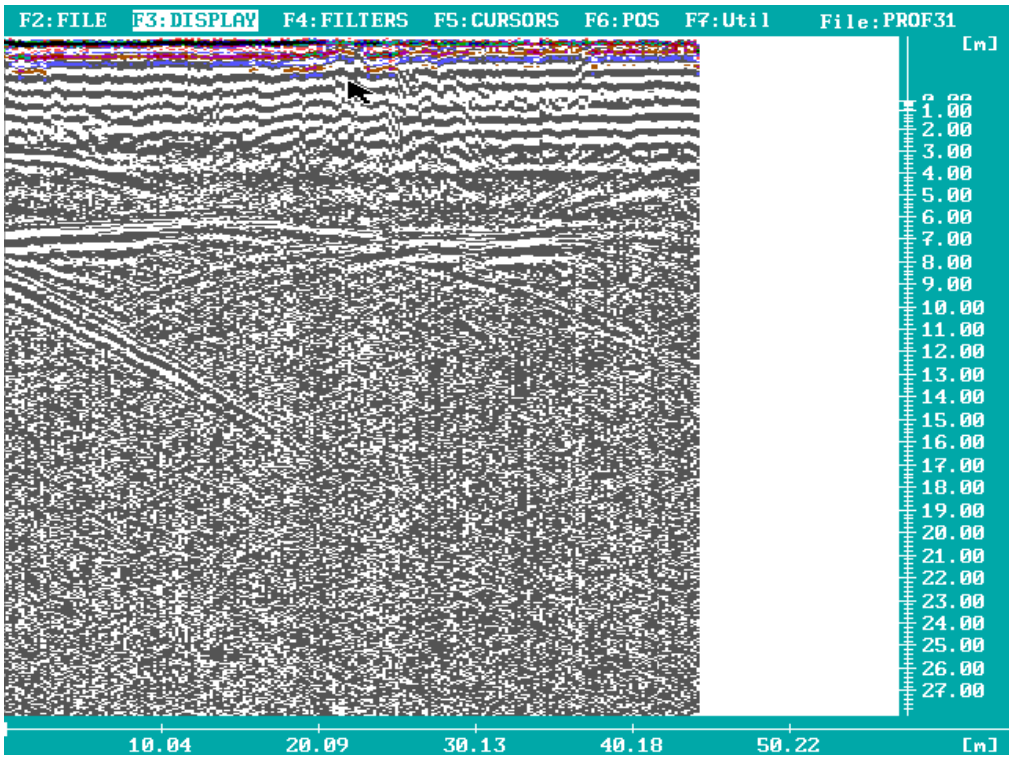

Radar gram of profile 31 trending W-E measured over the top of the second High Grade bench, south side McDonald's Quarry (2007).